Stress and failure analysis of adhesively bonded single lap joints

By

E.F. Karachalios

A thesis submitted to the University of Bristol in accordance with the requirements of Degree of Doctor of Philosophy in the faculty of Mechanical Engineering, May 1999

Summary

The single lap joint (SLJ) is the basic element for many structural bonded joint configurations. Although it is relatively easy to manufacture and test SLJs, the failure and stress analysis of the SLJ configuration is very complex due to the three- dimensional state of stress developing throughout the joint during loading.

In the current work, the SLJ configuration was analysed experimentally and theoretically using the finite element method (F.E.M), both under tensile and bending loading.

Many different parameters, geometric, material and loading, affect the joint strength in different ways. Geometric parameters such as the overlap length, the adherend thickness, and the presence of spew fillets, together with material parameters such as the adherend and adhesive stress-strain behaviour, and also the type of loading (tension or bending) were all investigated in the current work. The effect of inserting artificial defects on the strength and failure mode of the joints was also assessed for a variety of joint configurations.

The mechanisms and modes of failure were observed for different cases, and positions of damage initiation were identified. Failure patterns were correlated with the stress-state in the joints, and also with the associated failure mechanisms. The adhesive "stress whitening" developing at the ends of the overlap was associated with high tensile hydrostatic stresses.

The adherend plasticity was found to dominate failure in many cases. When the adherends deformed plastically there was a limiting strength that the joints could reach which was defined by the yield strength of the adherends, regardless of the adhesive properties or the length of the overlap. When the adherends deformed elastically throughout the loading, a significant strength increase was gained by increasing the overlap length, and the adhesive properties controlled the strength in this case. Thus, it is beneficial for the strength of the joints if the adherends remain elastic throughout loading. For the adhesive material on the other hand, it was found that it is beneficial if some plasticity occurs, especially at high levels of stress. The more strain an adhesive can withstand without failing, the stronger are the joints, provided a high level of stress is

maintained. The shear strength of the adhesives was also found to be very important, especially in joints loaded in tension.

Increasing the adherend thickness results in a linear increase in strength of joints loaded in bending. For joints loaded in tension however, no significant increase in strength is achieved apart from where low yield strength adherends are used.

Experimentally, fillets were not found to affect the strength of the joints.

Failure in an adhesively bonded single lap joint may occur due to either "global" or "local" stresses and strains reaching the limiting values of the adhesive. This depends mainly on the type of loading and the adherend yield strength, but also on the adhesive plastic behaviour. When the adherends deform plastically, or the joint is loaded in bending, then failure is more dominated by local effects. For adherends behaving elastically throughout loading, the adhesive behaviour and the overlap length control whether failure is due to global or to local stresses and strains. The more ductile is the adhesive behaviour and the shorter the overlap length, the more is failure dominated by global effects.

In order to predict joint strength, a failure criterion that takes into consideration all the above parameters must be used. A new failure prediction method was proposed in the form of a flow chart, which consists of several sub-criteria and is capable of predicting the strength of joints in a wide variety of configurations by using the finite element analysis results. The main critical variables controlling strength were found to be the shear strains in the case of tensile loading and the peel strains in the case of loading in bending.

A better understanding of the mechanisms and critical parameters governing failure has been achieved and this can be used to improve the design methodology of bonded joints.

List of Figures

List of Tables

Memorandum

The accompanying dissertation entitled " Stress and failure analysis of adhesively bonded single lap joints" is submitted in support of an application for the degree of Doctor of Philosophy in Engineering at the University of Bristol

The dissertation is based on independent work by the candidate; all contributions from others have been acknowledged fully within the dissertation. The supervisor's contribution was that normally made in a British University.

None of the work described has been, or is being, submitted for any other degree of diploma to this or any other University.

I hereby declare that the above statements are true

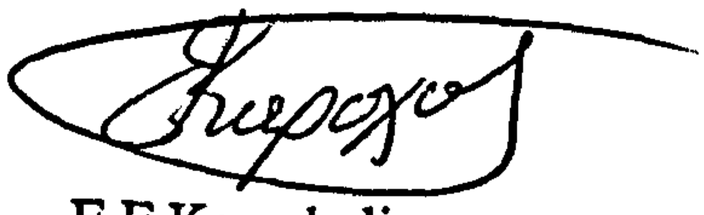

E.F.Karachalios

May 1999

Acknowledgements

I would like to thank Professor R.D. Adams for his supervision and support throughout this work.

I am grateful to Mr. R.G.H Davies for access to the subroutines used in the finite element modelling and many useful discussions both as a friend and in relation to scientific matters. I also wish to thank Dr. F.J. Guild for her support any many useful discussions, as well as the rest of the Composite and Adhesives Group current and past members.

I would also like to thank Mr. D. Jordan and Mr. J. Skinner for producing the adherends and jig for the manufacture of the specimens.

Many thanks go particularly to the Needham and Cooper Foundation for a bursary that generously provided my funding and fees while at Bristol.

Finally, I would like to thank my parents, Fotis and Marina, and also my friends for their encouragement and motivation without which this work would have not been completed.

Chapter 1

1.1 Introduction

Almost every engineering structure is comprised of component pieces, and these usually have to be connected. Mechanical connections, such as screws, rivets and bolts are commonly used to join components. Welding or spot welding and brazing are also used when metallic components are considered. Plastics can also be "welded" together by effectively melting the contacted areas using techniques such as friction welding and laser welding. However there are some cases where neither of the above methods of joining can easily be used. Adhesive bonding is often the only alternative solution in this case. The use of adhesive bonding instead of mechanical fastening has, in many cases, advantages over other techniques of joining but there are also disadvantages.

The **advantages** of adhesive bonding can be summarised in the following:

- More uniform stress distribution, compared with other traditional joining methods such as riveting, spot welding and bolting, thus reducing the stress concentrations
- Longer fatigue resistance as a consequence of the above, and internal vibration damping mechanisms reducing vibrations
- The bonded joint, being continuous, produces a stiffer structure. Alternatively, if the stiffness is not required, the weight of the structure can be reduced while maintaining the required stiffness
- Different materials can be bonded to each other (e.g. composite to metal joining)
- Avoiding heat distortion of the bonded parts as in the case of welding, brazing, and spot welding
- The appearance of the bonded components is smoother (no protruding fasteners such as screws or rivets) which is especially important from the aerodynamic point of view. Designs are also more aesthetically pleasing

- Assembly of bonded components is simplified and can be easily automated compared to traditional methods of joining. No drilling is necessary, no finishing needed, gaps are automatically filled, bonding and sealing at the same operation, number of parts are reduced, weight is reduced, accurate jigging of components is possible. All the above results in cost reduction for the final product.
- The continuous adhesive bond acts as a seal so that the joint and the surrounding metal are less prone to corrosion.
- Thin sheets of materials can be bonded, producing very efficient joints.

Disadvantages of adhesive bonding:

- The relatively low service temperatures over which adhesives can be used limits the number of applications in which adhesive bonding can be applied
- Surface preparation of the components is needed to ensure good bonding and good environmental resistance. Surface treatments can vary from simple solvent degrease and abrasion to very complicated chemical treatments, especially when low surface energy materials are to be bonded
- With most adhesives maximum bond strength is not achieved instantly as with mechanical fastening or welding. Some adhesive formulations require heat (and sometimes pressure) in order to cure, and so develop their strength. That could be a problem for a large structure, and specialised equipment is usually needed (ovens, autoclaves etc).
- Bonded structures are not usually or easily dismantled for in-service repair
- Environmental resistance is another problem as the properties of most adhesives degrade with time if the joint is exposed to harsh environments (e.g. humidity, water powerful solvents)
- There is a lack of non-destructive techniques to identify a badly made joint so the quality of the end product relies heavily on the care taken during the manufacturing process.

There are several types of adhesives available in the market and used by the industry but we will only deal with the so-called *structural adhesives*. These adhesives are generally able to carry significant loads, withstand impacts and work under aggressive environments.

Adhesive bonding seems a very attractive joining technique offering great flexibility to the designer engineer. However designing adhesively bonded joints that could carry significant loads has been encumbered by the lack of a suitable strength predictor. There is no universally applicable failure criterion that can predict failure in a variety of joint configurations (material, geometry, loading). This is because the failure of the bonded joints depends on many different parameters and the way they interact with each other.

There is therefore a need to understand the mechanisms of failure that occur in bonded joints. This will enable accurate strength predictions so that the designer could make use of all the advantages that the adhesives can provide.

Parameters that affect strength must be identified and if possible quantified. Critical variables that control strength must be found, bearing in mind that they could be different depending on the configuration of joint under consideration. The effect of small geometric modifications, such as fillets, rounded corners, on the strength of joints must also be assessed. The overlap length and the adherend thickness are very important geometric variables that could alter the strength of joints and must be investigated. This is very important in the design, especially when an optimum strength to weight ratio is sought, as in cases where weight savings are critical, aerospace and automotive industries.

Another important aspect in the design of bonded joints is the effect of defects (areas of poor bonding) on the strength of the joints. Such areas of poor bonding can be introduced into the bonded component during the manufacturing process. Depending on the configuration (adhesive type, adherend, loading) the effect would be different. Non-destructive methods could be used to evaluate the extent of such debonded areas. Knowing the effect of defects on the strength of various joint configurations will enable us to make predictions for the strength of any defective joint, which is very important for quality control and areas of mass production.

Structures that are adhesively bonded must be designed in such a way so that certain types of loading should be avoided or at least minimised. As a general rule peel and cleavage loads should be avoided. The adhesive should be mainly loaded in shear if optimum strength is required. Adhesives are generally stronger in compression than in tension, and this should be taken into account in the design by using appropriate pressure dependent yield-failure criteria.

There are many different configurations of joints used in practical applications. These could be lap, scarf, T-peel, strap, butt, bevel, or tubular joints as they are usually named in literature (Adams Comyn & Wake 1997). Many of these different joints are used in industry and as standard geometries for testing the adhesive properties under various loading conditions. Combinations of the configurations named above could increase the efficiency of the jointed component but complexity of some designs would also raise the cost of manufacture and analysis.

The configuration of the single lap joint (SLJ) will be used in the current work, as it is simple to manufacture and also is the basis for most joint configurations. Although simple to manufacture, the SLJ is quite complex to analyse. The eccentricity of the load path causes the joint to rotate under load. The materials (both adherends and adhesive) can also deform plastically under load. Poisson's ratio effects will give rise to transverse stresses in both the adhesive and the adherends. As a consequence of all the above a three-dimensional stress state develops throughout the joint. The behaviour of both the adherends and adhesives is important in the strength of the joints so both the adherends and adhesive must be modelled accurately.

Since the SLJ is the basis of most joint configurations, it could therefore be possible to analyse more complex geometries by treating them as a number of single lap joints. Once the stress and strain states have been defined by using appropriate modelling procedures and criteria, then a failure analysis will be needed. The failure criteria must be applicable in a variety of cases and basic material properties (from tensile and shear tests) should be used in the prediction process. Different critical valuès may be used for different cases since there is not a single universally applicable failure criterion. The failure criterion

should be set in such a way that the prediction could be made without knowing a-priori the critical variable causing failure.

Once the strength of joints can be predicted and the fracture processes can be understood, optimisation of joints can be performed without the need for costly and time-consuming experiments, leading to more efficient designs. However, it is believed that the experimental validation and testing will still be needed, as it is an integral part of the design process. It is the amount of testing that will be reduced, speeding up the optimisation processes and reducing the cost.

1.2 Literature review

Several approaches have been made up to now including both experimental and theoretical ones. Experiments on adhesively bonded joints are relatively easy to perform, but performing direct measurements on the adhesive layer is a difficult task, especially when the adhesive is in a very thin film. Furthermore, the results are not accurate at the edges of the joints where the stresses are at a peak and where failure will initiate.

A number of standard testing specimens and techniques have been developed in order to characterise the adhesives mechanical behaviour, such as tests on bulk adhesive specimens, butt joint and thick adherend shear specimens. The background on these is given in section 1.2.1. The majority of tests are either tensile or shear tests. These tests form the basis of any theoretical analysis, as they will provide the basic material properties, like moduli and stress-strain data, as input in the analysis.

Theoretical analysis can be either analytical (1.2.2) or numerical (1.2.3), where the physical problem is described mathematically. The mathematical problem is then solved and a variety of mechanical values (stress, strain, stiffness, energy etc) are calculated in different parts of the geometry of the structure, in order to get a better insight and a more detailed view on the mechanical behaviour of the structure. However, any theoretical analysis needs to be backed up and validated by experimental results. Thus, experimental and theoretical analyses are very closely interconnected. The following sub-sections discuss the background to testing and analysis of adhesively bonded joints.

1.2.1 Experimental techniques

There have been various experimental techniques used for determining the stresses and strains in bonded joints. McLaren & Mac Innes (1958) performed a photoelastic study on a single lap joint. They showed that the highest stresses are near the ends of the overlap of the joint. They found that the position and the magnitude of the stress depended particularly on the contact angle of the adhesive to the adherend. Apart from this effect, the adhesive appeared to be in a state of fairly uniform shear throughout the length of the overlap. The main outcome of their work was the clarification of the significance of bending of the adherends.

Adams *et al* (1973a) used rubber models to represent the adhesive joint behaviour. Hard rubber was used as the adherend and soft foam rubber as the adhesive. The results for the displacements agreed well with the corresponding finite element analysis. By profiling the adhesive layer, and also the adherend ends, they showed that stress concentrations could be removed from the ends of the overlap, as in a scarf joint. They showed that there is significant stress concentration at the adherend corners and that strains across the lap joint exist, due to Poisson's ratio effects.

The Moiré interferometry technique is an established method for measuring surface deformations of both adherends and the adhesive layer. It is an optical technique, which uses the interference of two coherent light beams to measure in-plane surface displacement. The displacement components u and v (recorded as fringe patterns) represent the horizontal and vertical displacement contours, respectively. The in-plane strains can be determined by differentiating the displacement components. Tsai and Morton (1994a, 1995) have used this technique to determine surface deformations of the adherend and the adhesive in a single lap joint configuration. Good correlation was found between experimental and theoretical predictions. Strain gauges were also used in the same investigation in order to assess the adherend bending moment variation by means of monitoring the longitudinal strains at several points of interest. However, because aluminium adherends (that deform plastically) were used, results presented are only for

very low applied loads. Three points along the adherend free length were investigated: (i) near the clamped end, (ii) midway from the clamped end to the overlap end and (iii) very near the overlap end. They showed that the bending moment at the different cross section points examined (i, ii, and iii) increases as the overlap ends are approached. Near the clamped ends there is nearly no bending moment applied while near the overlap ends large moments exist.

As already mentioned, the theoretical approach can be divided in two different categories: the analytical or closed form approach, and the use of numerical methods.

In practice, a joint is subjected to a combination of loads, thermal effects, moisture, fatigue, vibration and impact. Furthermore, a joint is constructed from dissimilar materials, which may deform plastically under load. The geometry of the joint may sometimes be complex. Including all these effects into a set of governing equations would give rise to serious mathematical difficulties. Simplifications and assumptions are inevitable if a solution is to be made. On the other hand numerical methods such as the finite element method have gained acceptance since they can give more complete analyses including several of the above effects. However powerful computers and experienced users are required to program the problem properly and, which is even more important, to interpret the results obtained.

The first aim for all these analyses is to describe the stress and strain state within both the adhesive and adherend as accurately as possible, taking into account the geometry and also the mechanical behaviour of the materials used in the joint configuration. The next step is to develop suitable failure criteria, which would predict the strength of the joints using the calculated stresses and strains.

1.2.2 Analytical solutions

The analysis of stresses and strains in single lap joints started with Volkersen's (1938) shear lag theory. It was assumed that the adherends are simply in tension and the adhesive is in pure shear. Based on these assumptions, Volkersen developed an analytical solution

for the shear stress state of the adhesive. Shearing of the adherends, which is especially important for composites but also for metals, was not taken into account. In single lap joints, adherend bending introduces large peel stresses in the adhesive layer so the adhesive cannot be in pure shear, and the adherends cannot be in simple uniform tension. Initially, this method was supposed to be for single lap joints but, due to the above statement, it is only applicable to double lap joints, where the bending of the adherends is much smaller. Volkersen's solution predicts that shear stresses are maximum at the ends of the overlap, so it fails to satisfy the zero shear stress condition that must exist at the ends of the overlap (free surface, law of complementary shear).

The effect of bending of the adherends was taken into account by Goland and Reissner (1944) to show that peel stresses in the adhesive arise. They developed a set of equations for the calculation of the bending moments at the ends of the overlap. They showed the bending moments are reduced from the initial values due to the rotation of the joint. A bending moment factor was introduced in order to calculate the true bending moment M at the ends of the joint as the load increased. Two types of solution were analysed: one with a very stiff and another one with a very flexible adhesive layer. Shear and normal deformations in the adherends were neglected and peel stresses were assumed to be constant through the thickness of the adhesive layer. As a result the zero-shear stress condition at the ends of the overlap was not satisfied.

The analysis of Renton and Vinson (1977) was concerned with anisotropic materials in order to model composite joints. Adherend bending, together with shear and normal stresses were included. However, there is no coupling between bending-stretching and shearing which is very important in composites. Shear and peel stresses are assumed to be constant across the adhesive thickness. They set the adhesive shear stresses to zero at the ends of the overlap but, as shown by Harris (1983), this violates the stress equilibrium at the adhesive ends. By including transverse normal and shear stresses in the adherends, the peel stresses are significantly reduced. However there is little effect on the shear stresses except for the ends of the overlap.

Allman (1977) included in his analysis the effect of bending, stretching and shearing of the adherends and accounted for the shearing and peeling of the adhesive. He also

accounted for the shear stress free edges with stresses at the edges in equilibrium, because it allowed a linear variation of peel stresses through the adhesive thickness. This is the most realistic analysis done so far including all the factors the other analyses have used. Hart-Smith (1973) developed an equation for determining the bending moment at the edge of the overlap, taking into account the thickness of the adhesive layer. His bending moment equation is less conservative compared to that of Goland and Reissner and it seems it underestimates the bending moment values for long overlaps. Carpenter (1991) reviewed some of the analytical approaches and assessed the effect of various simplification assumptions concerning the behaviour of the adhesive and adherends. It was found that neglecting the adherend shear deformations had only a small effect on the adhesive shear stress distribution, but could affect the adhesive peel stresses by as much as 30%. Zhao (1991) used a procedure combining analytical and numerical methods for the determination of bending moments at the ends of the overlaps for single lap joints. A validation of the theoretical solutions of Goland and Reissner and Hart Smith was carried out by Tsai and Morton (1994b). Comparisons between the analytical solutions and a finite element model that included the geometric non-linear effects were carried out. Their analysis demonstrated the importance of parameters such as the overlap length as well as the free length in the bending moment distribution on a SLJ. It must be mentioned here that the free length, between the different overlap configurations tested must be kept constant in order that comparisons between the different configurations are valid. An improved method of calculating the bending moment factor in SLJ was developed by Oplinger (1994). The analysis appears to provide a more consistent model than that of Goland and Reissner by adding the effects of bond shear strains. However, the effects of the bond thickness deformation were not taken into account and as it is known that could influence the moment distribution along the overlap. There was also no comparison with experimental results to validate the theoretical analysis. The classical theories of Volkersen and Goland and Reissner were used as the basis for the improved theoretical solutions for adhesively bonded single and double lap joints as developed by Tsai, Oplinger and Morton (1998). The adherend shear deformations have been included in the analysis by assuming a linear variation of shear stress (strain) through the thickness of the

adherends. The new solutions provided a better prediction for the adhesive shear distributions and maximum values. The solutions were validated, by comparing with experimental and numerical results. The improved theoretical solutions provide better predictions, especially in the case of adherends of low transverse shear stiffness, such as laminated composites.

Hart-Smith (1981) was among the first to model material non-linearities by using continuum mechanics. To simplify the adhesive behaviour he used a bilinear curve as his elastic-plastic model. The principle is that the area under the curve is equal to that under the true stress strain curve and that the failure stresses or strains are the same for the two curves. It should be noted that only the adhesive elasto-plastic shear properties were considered, the adherends being kept elastic.

Analytical solutions, although relatively easy and cheap to apply, cannot take into account important aspects of real joint design, such as material and geometric non-linearities. As will be shown in the current work, the material and geometric non-linearities play important role in the strength of the joints. It is not possible to deal with complex geometries using analytical solutions. Moreover, the effect of local changes in the geometry of the joints cannot be considered. So inevitably, the use of simple analytical solutions cannot yield the desired accuracy in the calculation of stresses and strains within the adherends and adhesives.

1.2.3 Numerical solutions

With the advent of computer technology, the finite element method became an important tool in stress analysis generally, and the analysis of adhesive joints in particular. Material and geometric non-linearities can be taken into account. Literally any geometric configuration can be analysed and local geometric modifications can be assessed. Complex types of loading and three-dimensional effects can be investigated.

At the early stages of analysis of bonded joints using the finite element method most of the analyses were carried out assuming linear elastic material properties and simple

geometric configurations such as single lap joints with square ends. The aim was to compare the predicted stress distributions with existing analytical solutions.

Peppiatt (1974), investigated the stress distributions in single-lap, butt and tubular lap joints by using the finite difference technique. Two-dimensional models were created, and the materials were taken as linear elastic. The geometric non-linearity of the single lap joint was taken into account, by changing the adherend length of the finite element model. At first, the adhesive layer was treated as having a square edge, and good agreement was found between the finite element stress distributions and appropriate closed form solutions from previous researchers. Adams and Peppiatt (1974) were amongst the first to investigate the effect of a spew fillet in the stress distribution in the adhesive layer using the finite element method. The fillet represents the squeezed adhesive remaining at the ends of the overlap during the manufacture of the joints. It was shown that the fillet significantly modifies the stress field in the highly stressed regions. The deformations predicted theoretically compared well with experimental work carried out on a rubber model, Adams *et al* (1973a). The most significant stresses in the fillet were found to be predominantly tensile and at right angles to the direction of cracks appearing in the fillet at failure. The maximum stresses were found to be at the corner of the "unloaded" adherend.

The importance of taking into account the non-linear behaviour of the adhesive in finite element analyses, was shown by Coppendale (1977). Two different adhesives (a brittle epoxy MY750, and a plasticised epoxy AY 103) were used to make single lap joints. Experimentally, the strength of the joints with the plasticised adhesive were higher, despite the fact that the plasticised adhesive had a lower tensile and shear strength. Using a linear finite element model and a maximum tensile stress criterion the joints with the brittle adhesive were wrongly predicted to give stronger joints. However, when a non-linear analysis and a maximum strain criterion was used, the F.E correctly predicted that the plasticised adhesive should give stronger joints. The use of the non-linear analysis was a significant improvement compared with previous lap joint stress analysis, which assumed linear elastic behaviour of the adhesive. The important conclusion from the above is that structural adhesives should not be assessed merely on the basis of their

strength in tensile or pure shear tests, but the tensile and shear strain to failure is also an important parameter, as will be shown in the current work. Regarding the effects of non-linearity, Harris (1983), pointed out the importance of including both the adhesive and adherend material non-linearity in the F.E analysis. Static tests on lap joints with different yield strengths showed that joints with the lowest strength adherends gave joints with the lowest strength. On impact tests however, the energy absorbed by the joints with lower strength adherends was higher, due to the large plastic deformation of the adherends before failure. Four different adhesives were used in the tests and the ductility of the adhesive was shown to have a positive effect on the strength of lap joints, especially with the high strength adherends. The strength differences between joints with different adhesives were however smaller when the low strength adherends were used. So, the plasticity of the adherends and also the geometric and material non-linearities of both the adherends and adhesive are very important and must be taken into account in the analysis procedures.

Since then, a numerous other researchers, Crocombe (1981), Crocombe and Adams (1981b), Harris and Adams (1984), Adams and Harris (1987), have included the spew fillet geometry in their analysis and also allowed for the non-linear material behaviour to be taken into account. Detailed analysis of the beneficial effect of the spew fillet in reducing the maximum stresses at the ends of the overlap was carried out using models with different degrees of complexity (depending on whether geometric and material non-linearities, for both adherends and adhesives, were taken into account). The large stress and strain concentrations found in the square ended joints were significantly reduced by the introduction of the fillets. It was concluded that some portion of the load is transferred through the fillet and also that the stress concentration effect from the sharp adherend corner is reduced. A corresponding increase in the strength of the joints was therefore predicted due to the addition of the fillets.

The effect of local geometry changes, such as rounding the adherend corner, was investigated in detail by Adams and Harris (1987). Aluminium adherends and a rubber-modified epoxy adhesive were used. Three different joint configurations were compared: sqaure ended joints, filleted joints, and filleted joints with radiused adherend corners. It

was shown that the value of the maximum stress/strain components is highly sensitive to small changes in the degree of rounding and also to the existence of the fillet. Experimental results showed that the strength of the joints was influenced to a smaller degree than the F.E results would suggest. The filleted and radiused joints were found to be the strongest, while the square ended joints were the weakest.

Great attention was therefore given, to the significant theoretical predicted reduction of maximum peel and shear stresses at the ends of the overlap and within the fillet area due to local modifications of the overlap end geometry. This was especially important for joints made of reinforced plastics (carbon or glass) as was shown by Adams and Peppiatt (1977), Adams et al. (1986), Adams (1989). This is because the weakest point in such a configuration was usually the composite adherends (due to the poor through thickness strength of the composites). Different design configurations were tested and analysed theoretically by Adams et al. (1986) and it was found that improvements of up to three times the original strength could be obtained by tapering the adherends and introducing low angle fillets in the joints. The importance of the local geometry and the fillet shape in the strength of the joints is obvious, at least for the case of joints made with composite adherends.

Although the local stress distribution around the ends of the joint was greatly affected by local modifications, such as rounding the adherends or introducing fillets of various geometries, the stress distribution in areas further away from the overlap remained unaffected. This is an important point that many researchers failed to address properly. If the strength of the joints is dominated by such local effects and the associated very high local stresses, then the strength of the joints would be greatly affected. However there is only little experimental evidence showing that great improvements can be achieved by such small-scale modifications, apart from the case where composite adherends were used Adams et al (1986). Some improvements in strength were also noted in Adams and Harris (1987) but not as much as the F.E predictions would suggest. In work carried out by Dorn and Liu (1993), the predicted reduction in stresses by the introduction of fillets was much larger than the corresponding strength improvement observed experimentally on plastic/metal joints. It was also noted by Tsai and Morton (1995) that the very high

(and sometimes physically impossible) stresses in the very localised region around the singularities may not dominate failure initiation. The effect of fillets and the local stress distributions on the overall strength of the joints must be examined further and any theoretical analysis must be validated with appropriate experiments before any conclusions can be drawn. Thus, analyses concerning the effect of different spew geometries in the strength of bonded joints, such as carried out by Lang and Mallick (1998), are therefore not complete as they lack experimental validation and so misleading conclusions can be drawn.

Another reason for concern is the inherent problems associated with the finite element method and the singular points that exist in areas such as around sharp corners or bi-material interfaces. Even if elasto-plastic analyses are carried out, the strain singularity will still exist. As a consequence, the accuracy with which the F.E solution will predict the stresses and strain around the singular points is are greatly dependent on how well the singularity is modelled, i.e. on mesh refinement. Comparisons between different works around such points are difficult and sometimes meaningless, because the predicted maximum values of stress or strain around singular points are greatly dependent on mesh refinement. Furthermore, the very high stress and strain values predicted by the F.E analyses are most of the times physically unrealistic.

However, despite the inherent problem of the singularity, the F.E analysis seems to be able to predict the stress and strain distributions away from these points with reasonable accuracy and for a wide variety of geometric configurations. As an example, the peel test was analysed by Crocombe and Adams (1981a and 1982) while corner joints were analysed by Apalak and Davies (1994). The accuracy depends mainly on how closely the modelling represents the real, physical problem, and how accuratelly any material or geometric non-linearities are modelled. As has been shown by many researchers Coppendale (1977), Crocombe (1981), Harris (1983), Chen (1985), Mallick (1989), it is very important to model both the adhesive and adherend non-linear behaviour in order to obtain realistic results. A better insight about the three-dimensional stress-state in the adhesive was given by Adams and Peppiatt (1973b), Zhao (1991), Richardson (1993), Tsai and Morton (1994a) and Adams and Davies (1996). Analysis showed that there is a

considerable variation of the stresses across the width of the joints. The stress and strains were found to peak in the middle of the width of the joints, where the adhesive is in a condition of plane strain. It was therefore concluded that this is the point where failure initiation is more likely to occur. Comparisons between two- and three-dimensional analysis carried out by Richardson (1993) showed that the two-dimensional analysis results could be improved if modified loads, calculated from the three-dimensional analysis, were applied in the two-dimensional models.

Due to the three dimensional nature of stresses in a joint configuration, the accuracy of the results will also depend on the material model used to describe the adhesive behaviour and whether it accounts for the dependence of yield on the hydrostatic stress component of stress. Most of the analyses on adhesive joints still use the Von Mises yield criterion, due to its robustness and general availability in commercial F.E packages. However, the dependence of the adhesive yield on the hydrostatic stress component must be included in the analysis, as shown by Coppendale (1977), Harris and Adams (1984), Crocombe et al (1995), Adams and Davies (1996), Wang and Rose (1997). This is mainly because the adhesive shear yield behaviour is not adequately described by criteria that are not dependent on the hydrostatic stress component. A typical value for the ratio S of yield in compression to yield in tension ($S=\sigma_{yc}/\sigma_{yt}$), used by many researchers is that of 1.3, typical for epoxy adhesives. However, this value must be calculated by tensile and/or compressive and shear test data for different adhesives, so that the behaviour of the adhesive in shear is adequately described.

The F.E method was also been used by several researchers, Chen (1985), Mallick (1989), Kim et al. (1997), to investigate the effect of residual stresses, resulting from shrinkage or thermal mismatch effects during the fabrication of the joints. A novel apparatus for measuring the adhesive shrinkage was developed by Yu and Adams (1998). Thermal or shrinkage effects have not been taken into account in the current work.

The F.E modelling of bonded joints has also been extensively used as a parametric tool for the investigation of the effects of parameters such as: adherend thickness, overlap length, adherend and adhesive stiffness ratio, adhesive thickness, on the stress distribution in the adhesive layer. Crocombe and Adams (1981b), Dorn and Liu (1993) showed that

the adhesive stresses increase with decreasing modulus ratio ($E_{adher.}$ / $E_{adhes.}$). This was attributed to the effect of the fillet, since as the adhesive modulus increases, so proportionately more load can be transferred through the fillet, thus raising the stress level in these regions and correspondingly reducing the stresses in the overlap region. However, the effect on the strength of the joints cannot be easily quantified and it is very difficult to validate such results experimentally.

As it is known, Goland and Reissner (1944), the overlap length is directly related with the bending moment applied at the edges of the overlap and so should be expected to affect the local stress distributions near the overlap edges. The effect of increasing the overlap length is to decrease both the peel and shear stresses and to result in a more uniform stress distribution along the overlap, as shown by Crocombe and Adams (1981b), Zink et al (1996) and Fargette et al. (1996), in a variety of joint configurations. The overlap length is therefore an important parameter that could affect the strength of joints and needs to be examined for a variety of joint configurations.

Increasing the adherend thickness, results in a decrease in the maximum peel and shear stresses in the adhesive and a more uniform stress distribution along the overlap length, as it was shown by Crocombe and Adams (1981b), Chiu and Jones (1992). However, the effect of adherend thickness on the strength of the joints under different joint and loading configurations (tension or bending) is not yet fully understood and must be examined further.

Most theoretical analyses, Crocombe and Adams (1981b), Chiu and Jones (1992), including the analytical solutions of Volkersen (1938) and Goland and Reissner (1944) predict that, as the adhesive thickness increases, the peak shear stresses decrease. However, experimental evidence concerning the strength of the joints from Grant (1994), Kim et al (1997) show that the strength of the joints decreases with increasing adhesive thickness which is in contrast to the theoretical predictions. Looking at results presented by Chiu and Jones (1992) in more detail, it can be seen that only the peak (near the overlap edge) adhesive shear stresses are increased with decreasing adhesive thickness; the shear stresses in the middle of the overlap being lower for the smaller adhesive thicknesses. Thus, if failure is not dominated by the stress state around the overlap edges,

and areas inside the overlap length need to be taken into account, then the experimentally observed increase in strength as the adhesive thickness decreases can be explained. Crocombe (1989) used the "global yielding" criterion to demonstrate that the strength of the joints increases as the adhesive thickness is decreasing. It was shown by Crocombe (1989), that although yielding of the thinner joints occurs at a lower load than the thicker joints, subsequent spread of the yield zone is faster in the thicker joints, due to the higher constraint imposed in the thinner joint. The global yielding criterion takes into account the whole length of the overlap and this may be a reason why it is able to predict the correct result.

Finite element models of different complexity can therefore be created, taking into account geometric and material non-linearities including any dependence on the type of loading, rate of loading, three-dimensional effects, and local geometric details in the model. The increased complexity of the models will result in a better simulation of the real, physical problem and therefore more accurate prediction of the stress and strain variation in the adhesive and adherends. However, the inherent problem of singularity will still remain. The next step that needs to be taken is failure prediction for the bonded joints. The calculated stresses and strains, together with the material allowable stresses and strains for both the adhesive and adherends, should be combined in a failure criterion in order to predict the strength of the joints. However, this is not a trivial task, because as is known, failure in bonded joints is affected by a variety of parameters (geometric, material, loading) which interact with each other and complicate the prediction process. Indeed, there is no universally applicable failure criterion that could predict the joint strength for a variety of geometric, material and loading configurations.

There are two main approaches followed by researchers as far as the criteria for failure prediction of joints is concerned; the continuum mechanics approach and the fracture mechanics approach. Both methods have their problems and limitations, as will be shown in the next paragraphs.

1.2.3.1 Failure prediction using continuum mechanics principles

In the continuum mechanics approach, the maximum values of stress, strain or strain energy, predicted by the finite element analyses, are usually used in the failure criterion and are compared with the corresponding material allowable values. However, it is known that these maximum predicted values are usually found very near the singular points of the model (sharp corners, bi-material interfaces), and therefore their magnitude depends strongly on how well the stress field around the singularity is modelled (i.e mesh refinement). In order to overcome this problem a common approach used by many researchers is to use the same variables (stress, strain or energy) but this time at some arbitrary distance from the point of singularity, where the stress field is clear of any effects from the singular point. Peppiatt (1974) used a maximum stress criterion to make predictions of joint strength with the materials modelled as linear elastic. Coppendale (1977), found that experimentally a plasticised adhesive gave stronger joints than a brittle adhesive despite the fact that the brittle adhesive had a higher ultimate stress. Using a linear finite element model and a maximum stress criterion, it was wrongly predicted that joints with a brittle adhesive were stronger than joints made with a plasticised adhesive. However, when a non-linear analysis was used in conjunction with a maximum strain criterion, the F.E correctly predicted that the plasticised adhesive should give stronger joints. Crocombe and Adams (1981a), in an elastic analysis of the peel test, stated that initial failure in the adhesive is caused by the adhesive maximum principal stresses reaching a critical level and so a crack is driven towards the interface with the flexible adherend. It was also noted that for a particular adherend and adhesive, failure occurred at a critical bending moment independent of the peel angle. During a later investigation, Crocombe and Adams (1982), an elasto-plastic analysis of the peel test was carried out and failure of the joint was predicted when the effective plastic strain at a critical distance from the crack tip reached a critical level. However, the critical effective plastic strain was effectively calibrated from the analysis for a particular peel angle, and was consequently used to predict the strength of joints at other peel angles. This proved to be successful and reasonable predictions were obtained for the same peel test and different peel angles. However, when the same critical values of effective plastic strain

were used for a different adherend and the same peel geometry, the prediction was not satisfactory and different critical values were needed for the different configuration. This clearly showed some of the weaknesses of that failure prediction method. Harris and Adams (1984), used the maximum principal stress and maximum principal strain, at a short distance from the singular points, to predict the strength of joints made with brittle and ductile adhesives respectively. They argued that although there are points of singular stresses and strains, due to abrupt changes in the geometry and material at the interface, it is unlikely that the maximum conditions exist at the adjacent corner points on the interface, because of the restraining effects of the stiffer adherend. It was concluded that a criterion based on the uniaxial tensile properties of the adhesive, is more applicable than one that is based on the response of the material in pure shear. However, it must be noted here that this will mainly be dependent on the type of loading that the joints are subjected to. In particular, when the adhesive is mainly loaded in shear, as is the case for lap joints loaded in tension, the adhesive critical shear limits can become very important in controlling joint strength, as stated by Chai (1993). In a later work Adams and Harris (1987) used a plastic strain energy density criterion based on the bulk uniaxial tensile properties of the adhesive. They found that by rounding the sharp adherend corner, the effect of singularity is effectively reduced, and the peak stresses were reduced significantly. However, this did not actually solve the problem of having to choose a distance from the singular point because the problem now became that of deciding the degree of rounding that should be applied. In work carried out by Dorn and Liu (1993) on plastic/metal joints, the maximum accumulative effective plastic strain in the critical region (in the plastic adherends) was used as the parameter for strength prediction of these joints. The critical value for failure was effectively calibrated from the F.E results, and was consequently used to carry out predictions for joints with similar geometry and different materials, as adherends and adhesives. Good correlation between F.E predictions and experimental results was obtained. Unfortunately, because failure was within the plastic adherends and not in the adhesive, the application of these results is limited to the certain geometry and materials used. Joint strength predictions for an extended adhesive-adherend sandwich geometry, based on maximum principal stress or strain, and

maximum shear strain, for cleavage and shear type loading respectively have been obtained by Crocombe et al (1990). Zhao (1991) proposed that failure is governed by the "averaged" stresses or strains within a critical distance from the singular points. The critical distance was calculated so that the integral of the stresses, strains or strain energies over a distance, divided by the distance is equal to the corresponding values obtain from uniaxial tensile tests.

The stress (or strain) at a distance criterion was also examined by Crocombe *et al* (1995). Such a criterion requires two parameters to be defined: a critical stress (or strain) and a critical distance ahead of the singular point. However these values need to be calibrated and therefore the criterion is not suitable for design purposes. The values that are usually obtained in order for good correlation to occur do not always relate to the experimentally measured values of stress or strain on the adhesive, as has also been found in the particular publication. The "distance" value usually has no physical meaning.

A review of the most often used failure criteria was presented by McCarthy (1996 a,b) were it was stated that the range of applications of adhesives are still limited due to the lack of consistent test methods, validated test data, and proven failure criteria.

Sometimes, the F.E models created can become very large in terms of the number of elements, in order to model a large structure. This leads to long computation and post processing times. Gaofeng and Crocombe (1996) have proposed an alternative technique to simplify the modelling of joints. Rather than modelling the whole joint (adherends and adhesive) with continuum elements, as is normal practice in two-dimensional analysis, the adherend elements (or part of them) are replaced by beam elements. This is done in order to reduce the computational expense and increase the speed of analysis. Results from the different analysis were compared with the typical two-dimensional continuum F.E results and showed that the simplified models are in reasonable agreement with the continuum models. Some discrepancies were found for the case of more complicated joint designs such as the T-peel type. Although the whole analysis assumed elastic material properties for both the adhesive and adherends, it gives a quick and relatively inexpensive tool for design and parametric study purposes.

The effect of rate of loading has been investigated by many researchers in the past, such as Harris and Adams (1984), Crocombe (1995), Duncan et al. (1998). Rate effects are important in assessing the impact behaviour of adhesive joints. The energy absorption depends mainly on the type of adherend used. Joints made with soft adherends (i.e. mild steel) absorb more energy compared to equivalent joints with stronger (harder) adherends. The yield stress of adhesives seems to increase with increasing loading rate while the strain to failure seems to decrease. Very small differences in the strength of the joints can be observed between the different loading rates. The loading rate effects can be assumed to be not significant, if the joints are tested under quasi-static conditions and the tests are carried out at temperatures well below the glass transition temperature T_g of the adhesive.

From the above discussion, it is clear that strength predictions based on critical values of stress or strain, or even strain energy density at a point or over a critical distance are not suitable for strength prediction. The maximum critical values obtained by the F.E analyses are dependent on the proximity of the critical point from the stress or strain concentrator and therefore on mesh refinement. The critical distances must be usually calibrated from the F.E results, and as a consequence, these critical values obtained can only be used for similar geometric and material configurations. There is usually no physical explanation relating the critical distances with experimental observations.

1.2.3.2 Fracture mechanics approach

In order to overcome some of the problems associated with the continuum mechanics approach, several researchers have proposed using fracture mechanics principles to predict joint failure. The fracture mechanics approach usually assumes the existence of a crack, and evaluates whether the conditions in the structure are suitable for that crack to propagate and cause failure. It must be noted here that most of the specimens tested in the current work failed catastrophically without visible crack growth. In cases where adhesive crack growth was visible, as with the mild or gauge steel joints, this occurred at the very late stages of failure (i.e. just before the final load was reached). It can therefore be said that the failure process is crack initiation controlled and not propagation controlled. The

propagation of cracks, in the fracture mechanics approach, is usually assumed along a predetermined path. This is because the test piece geometries used in such studies are basic geometries, such as the double cantilever beam or cracked lap shear specimen, and the types of loading are usually separated to different modes (typically Mode I, II, III). The adherend materials are also usually assumed as linear elastic. However, in a mixed mode loading condition such as found in structural joint configurations (single or double lap joints, scarf joints, strap joints, T-peel joints with top support, etc) neither the initiation or the propagation of the cracks can be assumed. In general, the areas at which failure initiates, and the direction along which cracks propagate, is dependent on the geometry of the specimen, materials used, and type of loading.

There are two main criteria for fracture. Irwin found that the stress around a crack could be defined by a parameter called the stress intensity factor, K, and stated that failure will occur when the value of K exceeds some critical value K_c. An energy-based criterion was proposed by Griffith, and later by Orowan. They suggested that fracture occurs when sufficient energy is released (from the stress field) by the growth of a crack to supply the requirements of the new fracture surfaces. This approach provides a measure of the energy required to extent a crack over a unit area and is termed fracture energy G_c.

Ripling and Mostovoy (1971) were amongst the first to apply fracture mechanics approach to the failure of adhesive joints. It must be noted that the geometry of most of the specimens used in a fracture mechanics analyses, are that of the double cantilever beam configuration, so are quite different to the geometry of standard joints used in structural applications.

When a joint is tested in a dry environment, failure is expected to be cohesive within the adhesive layer. If, however, moisture is present, the failure locus usually switches from cohesive to the interface. Kinloch (1979) has reviewed the mechanisms of environmental failure and shows the importance of the fracture mechanics method in estimating the service life of bonded structures under crack propagation. In fatigue tests carried out by Gledhill and Kinloch (1976), it was found that there is a critical value of the plastic zone size developed ahead of the crack tip, at which fracture occurs.

The fatigue behaviour of tapered-double cantilever beam specimens both in "dry" and "wet" conditions was investigated by Fernando et al (1996). The fatigue loaded specimens failed at a considerably lower strain energy release rate compared to the value of fracture energy of the adhesive determined from monotonically loaded fracture tests. However there seems to be a threshold value of the applied strain energy release rate below which failures due to cyclic loading do not occur. Similar tests in more hostile environments (humidity, water) further decrease this threshold value. This threshold value has important implications for the design of adhesive joints, as it could be used to rank the fatigue limit behaviour of different adhesive systems and surface pre-treatments and their resistance to hostile environments.

The fracture resistance of a rubber-modified epoxy adhesive has been studied by Kinloch and Shaw (1981) using fracture mechanics analysis. Compact tension and contoured double cantilever beam specimens were used. The plastic flow mechanisms around the crack tip were found to be very important on the material fracture behaviour. It was also found that the fracture behaviour of the joints is strongly dependent on the adhesive bond thickness. An optimum thickness was found at which a maximum fracture toughness is obtained. It was also mentioned that the tensile stress at which a material yields is greater in a triaxial stress field (plane strain) than in a biaxial stress field (plane stress). A more limited degree of plasticity develops at the crack tip in the plane strain case and this results in the fracture toughness in plane strain to be lower than the fracture toughness in plane stress. Comparing the fracture energy obtained from a joint specimen and from a bulk specimen the former value was found to be greater. For very thin bond-lines however, the reverse is usually observed. This was attributed to the varying degree of constraint that the substrates impose when different bond-lines are considered.

A criterion was proposed by Lee (1985) where the adhesive fracture is controlled by the plastic zone developed at the crack tip. Double cantilever beam specimens loaded in Mode I were considered. The main attempt was to determine the plastic zone size as a function of the crack tip stress state because the failure process of a material is critically dependent on the detailed crack tip stress distribution. One of the main problems in determining the fracture toughness of an adhesive material, is that the $G_{IC\ (bulk)}$ of an

unconstrained bulk material is not necessarily the same as the fracture toughness of the same material under different constraint conditions, as in a joint configuration $G_{IC\ (joint)}$. The fracture energy in a joint, $G_{IC\ (joint)}$, was related with adhesive properties such as the yield stress, modulus and fracture energy in bulk, $G_{IC\ (bulk)}$.

Anandarajah et al (1984) also found that there is a strong dependence of the strain energy release rate on the thickness of the adhesive layer used to bond a pair of adherends. It is also mentioned that as a homogeneous material has properties that can be determined by critical strain energy release rates in mode I and II, so does the interface between an adhesive and an adherend. The resistance of an adherend/adhesive interface to crack propagation is strongly dependent on the quality of surface preparation prior to bonding.

Hunston *et al*, (1989) attributed the high mode I fracture energies of structural adhesives to their ability to form large crack tip deformation zones prior to failure. The stress-whitened zone that occurs ahead of the crack tip was used to compare the relative dimensions of the deformation zone between different configurations. In an adhesive joint the size and shape of the deformation zone as well as the nature of the crack tip stress field can be altered by the physical constraint of the adherends and this in turn can change the fracture behaviour of the joint. The deformation zone can be regarded as a mechanism to suppress the onset of rapid crack growth, as the load increases, but the zone must also grow to maintain its effectiveness. The toughness of the material depends on how large this zone can grow before unstable crack propagation initiates.

Chai (1993) used a high magnification video camera to record the evolution of damage at the tip of cracks in adhesive bonds deforming in shear. The End-Notched-Flexure specimen was used and a brittle and a ductile adhesive were tested. An extensive zone of plastic deformation developed ahead of the crack tip prior to fracture. In the brittle adhesive tensile microcracks formed within that zone. The microcracks appeared to grow from the interlayer to the interface and complete bond separation occurred when cracks emanating from adjacent microcracks linked, but this was well before the full yielding capacity of the adhesive could be realised. For the ductile adhesive, on the other hand, cracks always grew from the tip. It is therefore very important to note that the failure mechanisms and patterns could be different depending on the adhesive behaviour (i.e.

ductile or brittle). It was found that for both adhesives, the critical crack tip shear strain increased with decreasing adhesive thickness. This effect was attributed to the decreasing sensitivity of thinner bonds to the presence of flaws. The adhesive shear strain was determined from fine lines scratched on the specimen edge. For a given bondline thickness the critical crack tip shear strain agreed well with the ultimate shear strain of the adhesive determined using the napkin ring shear test. It was therefore concluded that the ultimate shear strain is a key property controlling crack growth. This is a rather important conclusion especially in lap joint configurations loaded in tension where the adhesive experiences high shear strains especially around the overlap edges. The stress field around an interfacial crack in adhesively bonded joints deforming in shear was studied both experimentally and from a large strain, incremental plasticity finite element analysis by Chiang and Chai (1994), (1996), (1998a&b) using the end-notched flexure and end-loaded split test piece geometries. The analysis which considers very large strains and includes the effect of contact and friction between the debonded interfaces showed that although the stresses at the tip is highly triaxial, the deformations are dominated by the shearing component, which is localised at the very edge of the crack tip. The onset of crack growth and the stable interfacial crack propagation that follows are generally reasonably well-governed by the magnitude of the local engineering shear strain at a certain material-specific distance ahead of the crack tip. The development of large voids ahead of the crack tip was attributed to tensile hydrostatic stresses. This damage causes a blunting of the crack tip which temporarily arrests further crack growth. In the current work the stress whitening (probably associated with micro-voiding) occurring near the ends of the joints was also attributed to the large hydrostatic tensile streses developing at the ends of the joints. All these mechanisms occur under very large strains, which is a consequence of the ability of very thin polymeric adhesives to locally sustain very large deformations. As stated by Chiang and Chai (1996), a fracture criterion based on local strains, rather than stresses or strain energy release rates, would be most appropriate for fracture problems involving large deformations. It was also mentioned that, regardless of the specimen geometry, the entire interfacial crack propagation event is controlled by a single parameter - a critical crack tip shear strain. In another publication regarding the

fracture process during shear loading, Chai (1988) concluded that the crack growth occurred when the damage zone in the adhesive became fully developed, the extent of which may exceed by orders of magnitude the adhesive thickness. Observing the fracture process and also the fracture patterns of broken joints (post failure observation), is very important and could lead to very important conclusions correlating certain phenomena with particular areas in the joint as well as particular stress or strain components. Thus, in situ and post failure observations are both very important and should be carried out in order to achieve a complete understanding of the failure process.

Adhesively bonded joints were analysed by Pradhan et al (1995) using the finite element method and the crack closure technique, to compute the strain energy release rate for debonding in cracked lap shear specimens, and thus simulating adhesive failure. Modelling of gradual crack growth was achieved by releasing pairs of nodes on the interfaces. The strain energy release rate was found to decrease with increasing adhesive stiffness, decreasing adhesive thickness and increasing overlap length, for a double lap joint. Also the critical crack length was found independent of the Young's moduli of the constituents (adherends and adhesive).

An analytical model was developed by Daghyani *et al* (1996) to calculate the stress distribution along the bond line of a compact pure shear specimen. The strain energy release rate, G_{II}, in mode II was evaluated as a function of the adhesive bond thickness and results showed that for a given applied load the G_{II} increased gradually with the bond thickness. Comparison between the strain energy release in shear and tension indicates that for different bond thicknesses the joint is at least an order of magnitude tougher in shear than in tension. For rubber modified epoxies, mechanisms such as crazing and void formation followed by shear bands can contribute to increase the fracture energy. Similar mechanisms (such as stress whitening) were observed for some of the adhesives used in the current work, producing higher strength joints. In the absence of these mechanisms, particularly when the adhesive material is suppressed between the adherends, low values of critical energy release rate should be expected. On the other hand, under sliding mode II fracture, shear deformation is the main mechanism to dissipate the energy and therefore a much higher toughness is obtained than mode I.

It is known that the fracture resistance of an adhesive joint, Gc, in general is dependent on the phase angle of loading (ratio of mode I to mode II of loading). A novel load jig is presented in Fernuld and Spelt (1994). The jig was used to generate the fracture envelope (critical energy release rate as a function of the mode ratio) for an epoxy adhesive using double cantilever beam specimens. The critical energy release rate was found to increase with increasing phase angle of loading and G_{IIC} (the critical energy release rate in mode II loading) was found to be approximately three times higher than G_{IC}. The important result was that the measured values of G, were found to be independent of the crack length and also the adherend thickness. Comparisons between the novel testing method and conventional end notch flexure specimens, indicated that there are friction effects in the mode II type loading for the case of the ENF specimens, but these were relatively small. It is also noted by the authors that although models which address the dependence of G_C on the phase angle of loading have been presented in literature, most of them contain many simplifying assumptions, and the only reliable way to characterise the fracture resistance of an adhesive is through testing. The dependence of the critical value of G on the mode of loading could lead to further problems in strength predictions of joints with different geometry or type of loading; the exact phase angle (or loading mode) will not be necessarily known and therefore the value of G_C will also not be defined. In a real structural joint configuration, such as the single lap joint, the mode of loading could also change even during the loading of the specimen, due to the constant rotation of the joint as the load increases. The mode of loading could also change depending on the adherend material behaviour.

An important result regarding the dependence of the critical energy release rate in the mode of failure was presented by Baziard et al (1995), where the failure of an adhesively bonded single lap joint with ceramic adherends was investigated. Both adhesive and cohesive failures were examined by inserting an aluminium foil (representing a defect), in either the adhesive adherend interface, or within the adhesive layer. The critical energy release rate G_{IIC} and critical stress intensity factor K_{IIC} in shear were calculated experimentally for both adhesive and cohesive failures. It was found that the G_{IIC} values, obtained from the cohesive failure of the joint were ten times greater than those

calculated for adhesive failure. This is a very important result, as it implies that different critical values should be used when different failure modes are examined. In the current work it will be shown that the failure mode could be strongly influenced by the behaviour of the adherends. It could be postulated that when failure is more like an adhesive failure, lower adhesive critical values than the ones used in a cohesive failure prediction should be used.

Papini et al (1994 a,b), Fernlund et al (1994) suggested a method for fracture prediction of adhesive joints using the path-independent J-integral for large deformations together with large-deformation beam theory. The adhesive joint is treated as an adhesive sandwich and the reactions acting at the adhesive terminus are determined using large deformation beam theory. Using critical energy release data from a fracture envelope constructed by Fernuld and Spelt (1994), failure predictions for single lap joints were made. It was noted that problems are encountered in the case were adherend yielding was present, so the method is only applicable in the case that the adherends remain elastic. A trial and error procedure is followed, were an estimate load is used to calculate the energy release rate and phase angle (at particular points in the joint) and an iterative procedure is followed until the measured values match the critical values from the fracture envelope. The main problem is that of the mode partitioning in which the relative ratio of mode I to mode II loading must be defined in terms of an equation. Some very interesting results were presented, regarding the effect of the presence of fillets in the strength of the joints. It was found both experimentally and theoretically that there is no effect from the presence of a fillet or a pre-crack in the end of the joints. This is very important and in contrast to the general belief that fillets do actually improve the strength of joints. Fillets are important in certain types of joint geometries (i.e. T-peel joints) and when fibre reinforced plastic (FRP) adherends are used, but this conclusion cannot be generalised for all types of joints and adherend combinations without experimental validation.

Using the same method, Papini et al (1994 a,b) also predicted that the strength of SLJ should increase with increasing adherend thickness. However, this could also depend on other parameters such as the type of loading and also the type of materials used for the adherends. So, the conclusion drawn from Papini et al needs experimental validation,

which was not provided in the publication. Concerning the strength of joints as the overlap length increases, although the strength of the single lap joints was predicted to increase as the overlap length increased, the strength of double lap joints was predicted to be unaffected. This also needs to be validated experimentally for the particular geometry and materials used, as it is not normally seen in practice, unless there is plastic deformation of the adherends. Considering that Papini et al's method is only applicable for elastic adherends, this large variation between the different configurations cannot be predicted.

The validity of different failure criteria for predicting joint strength, of both cracked and un-cracked joints, was investigated by Crocombe *et al* (1995), both theoretically and experimentally. Temperature and strain rate effects as well as the hydrostatic stress effect were taken into account in the analysis. The linear elastic fracture mechanics method was first examined. Using the LEFM approach, the energy release rate (G) was calculated for the different configurations. It was found that G decreases as the crack length decreases and approaches zero for the uncracked configurations. This implies that the strength of the joint should increase as the crack length decreases and that large increases in strength should be observed for very small or uncracked configurations. Experimentally, although it was observed that the strength increases as the crack length decreases, the uncracked configurations did not show large differences, in strength, compared with the cracked configurations with small crack lengths. It was found experimentally that G for mode I loading was higher that G for mixed mode loading. This means that joints loaded in mixed mode should be stronger, which was observed experimentally. It is clear that by using the LEFM method, although reasonable predictions can be made for the cracked configurations, large errors are produced in the prediction of uncracked joint strengths. There is also an added problem, that of the variation of G with the mode mixity. This means that when the type of loading or the geometry of the joint is changed, the G value will also change, which makes it difficult to do predictions for different geometries and loading configurations.

As in the case of failure prediction using continuum mechanics principles, there are some inherent problems when the fracture mechanics approach is used too. Assumptions such as the existence of a pre-crack in the structure are not always valid. Propagation of cracks is usually along a predetermined path that is not always known a priori. There is also a great dependence of critical values such as the critical energy release rate G on the mode of loading but also on the mode of failure too (adhesive or cohesive). Mode partitioning, that is often required when analysing a real structural joint configuration, is not an easy task, apart from simple geometric and loading configurations. Many arbitrary assumptions need to be made when predicting strength of real joint configurations using the fracture mechanics approach. However, the fracture mechanics method needs to be employed in cases where the fatigue and durability performance of the joints is analysed.

1.2.3.3 Damage mechanics approach

As has been seen, most of the problems encountered in the prediction of joint strength are usually associated with treating the effect of singularity and the very high stresses around the crack tips and also the propagation of such sharp cracks. However, many researchers argue that in reality true singular points do not exist, since stresses near the highly stressed areas of the joints are relieved due to zones of local damage, which can show up as micro-voiding, crazing, stress-whitening, etc.

An alternative approach was proposed by Crocombe (1989), known as the global yielding criterion. It applies when a path of adhesive along the overlap region reaches a state in which it can sustain no further significant increase in load. Using the global yield criterion, Crocombe demonstrated why the adhesive strength increases with decreasing adhesive thickness. This is one of the first publications suggesting that failure takes place over a "zone" of "damaged material" rather than at a point. The only limitation of the global yield criterion is that it applies only in lap joints loaded in tension, and thus most of the load in the adhesive is in shear. It is believed that the global yield criterion works only for very ductile adhesive systems. However, this may also depend on the length of the overlap, something that needs to be investigated further. It must also be noted here

that it is very important that the adhesive behaviour is modelled correctly, using a pressure dependent yield criterion, so that the shear behaviour of the adhesive is not underestimated. So, by using a failure criterion such as the global yield criterion the inherent problems with the singularities can be avoided.

Generally speaking, the micro-mechanical processes leading to initiation and propagation of a crack in polymeric materials are not fully understood. It has been proposed by Kinloch and Young (1983), that the crack is initiated in highly strained areas of intersecting shear bands. It also seems that growth of cracks takes place through complicated processes due to extensive plastic flow ahead of the crack tip. Plastic deformations in polymers can take place due to two different mechanisms: shear yielding, (a deviatoric process), and craze yielding, (i.e. formation of microcracks capable of transmitting loads across its faces), a dilatoric process. On the macro-mechanical level these processes lead to permanent deformations and loss of stiffness. As a consequence, the overall response of a damage material volume is characterised by a softening behaviour. A material model including damage reflects the physical processes leading to failure. A continuum damage model for rubber-modified epoxy adhesives was developed by Edlund and Klarbring (1993). The criteria for plastic flow and damage growth were dependent on the hydrostatic stress and isotropic hardening of the material was assumed. The irreversible strain consists of deviatoric part due to plastic flow and damage, and a dilatational part due to damage. Two processes contribute to the increased toughness of rubber modified epoxies. The first process is when the multiaxial state of stress at the crack tip causes failure and void formation in the rubber particles. The second, and more important, energy absorbing process is that of plastic shear flow in the matrix. Extensive, but localised shear yielding takes place in the matrix due to the stress concentration associated with the small particles embedded in the matrix. It was concluded that the corresponding load-bearing capacity of a body (i.e. failure load) can be obtained without the use of a postulated fracture criterion or the explicit assumptions needed in a fracture mechanics approach.

Based on the "damage over a zone" concept, Clark and McGregor (1993) proposed that bonded joint failure should occur when the maximum principal stress calculated over a

finite zone exceeded the ultimate tensile stress of the adhesive. However, the size of the "damaged zone" was effectively calibrated from experiments and the finite element analysis results. Different damage zone sizes are required when different geometric and material combinations are used. The problem associated with this approach is that calibration of the results is needed for a variety of configurations making the method unsuitable for realistic design predictions.

Papini et al (1994 a,b), concluded that, in general, fracture of adhesive joints occurs by the development of a damage zone, rather than by the propagation of a sharp crack. In order for a joint to fracture, the damage zone must first develop to a steady state constant size. Experiments showed that cracking of the adhesive fillet (whenever this is present) is part of the development of this damage zone and does not affect the strength of the joints. For a brittle adhesive it was found that the damage zone development is followed by unstable crack propagation with sudden catastrophic failure. For a more ductile adhesive, the damage zone development is followed by a toughening mechanism with significant amounts of crack growth. It is therefore important to observe how and where in the joints such damage zones develop, as it will help in the failure prediction process.

The stress separation analysis was proposed by Crocombe *et al* (1995), in an attempt to model damage in the adhesive material. The development of a damaged zone in the adhesive was modelled as a line of non-linear springs ahead of the singularity. These springs are not allowed to deform until a certain level of stress is reached. The separation of the springs occurs when a critical displacement is reached and that can be under constant (perfect plastic) or decreasing (softening behaviour) stress. The separation of the initial spring was therefore used as the failure criterion. The method is quite similar to the crack tip opening displacement used in ductile fracture mechanics. The main problem in such an analysis is that the critical displacement must be defined and is dependent on the mode mixity. The separation stress needs to be defined too and must somehow be related with the adhesive properties. Therefore, different critical parameters need to be defined for different types of loading. Also, in order to take the plasticity of the adhesive into account, strain values may be more appropriate than stress values.

Following the above work, Hadidimoud and *et al* (1998) developed strain and stress tripped specially defined non-linear spring elements in order to simulate rupture in adhesive joints. These specially developed elements can be linked with normal continuum elements. The element has an initial stiffness, which changes to either zero or negative when a specified level of strain is reached in the continuum element. The element is finally released when a critical level of energy is absorbed by the spring. Analysis of Compact Tension (CT) specimen showed that there is a high dependence of the strain field on the near tip traction which affects the tripping process of the elements. This methods seems to proved a reasonable means of simulating rupture in adhesive joints, and, as stated by the authors, will be validated further for different geometries and by incorporating more sophisticated material models for the adhesive such as Von Mises and Drucker-Prager.

On the same principle (damage over a zone) Sheppard et al (1998) proposed that failure in an adhesively bonded joint occurs when a damage zone of adhesive at the ends of the overlap reaches a critical size. Failure is predicted when the equivalent Mises strain exceeds the limiting strain of the adhesive over a critical zone. It is quoted that modelling of the adhesive using the Von Mises yield criterion is adequate. However, as has already been discussed, the adhesive shear behaviour can be seriously underestimated if the criterion for modelling the adhesive does not take into account the hydrostatic stress component of stress (as in a pressure dependent yield criterion). Due to the difficulties involved in the calculation of the critical damage zone experimentally, Sheppard et al (1998) effectively calibrate the F.E models in order that a critical damage zone is calculated, and use this critical zone to predict the failure loads of similar joint configurations. The critical damage zone size may be different for a different joint configuration or type of loading, so the applicability of damage zone model over a critical zone is limited. The critical strain limit chosen in the publication probably applies only for the certain configuration tested, since it was chosen arbitrarily purely on the basis that it fitted experimental results best. However, this is a problem that is mainly associated with the uncertainty in the derivation of maximum tensile and shear strains from the corresponding standard tests, and therefore not a deficiency in the model. Although good

correlation between experiments and F.E. predictions was achieved, it seems that the critical values used were obtained through calibration and should therefore not be expected to yield equally good results for a completely different joint configuration (different materials, loading, geometry). The concept of defining failure by a progressively growing damage zone in the adhesive layer, until a critical limit is reached, seems physically correct since failure of the joints usually occurs after some damage in the adhesive has developed (typically seen as a stress whitening area in the adhesive indicating extensive plastic deformation). However, the extent of the damage is very difficult to assess before failure because of its three dimensional nature (and the fact that the adherends are usually not transparent). Also the damage size and location depends on many parameters such as adhesive and adherend plasticity, overlap length, type of loading (tension or bending), adherend thickness and the geometry of the joint in general.

Towse et al (1999) investigated the statistical nature of the material (adhesive) strength. It was found that the strain to failure of an adhesive is a function of the specimen size and the defect spectrum contained within the specimen. This means that smaller specimens should be able to withstand higher strain to failure. As noted by the authors, in order to predict failure in an adhesive joint, it is not enough to know only the level of stress acting in the adhesive, but also the volume of material over which these stresses act. Using a statistical theory proposed by Weibull, the probability of survival of the specimen can be calculated and failure prediction can be carried out. The relevant factors that are needed (characteristic strength and shape factor) are measurable quantities from testing of bulk specimens, so these parameters can be classified as material properties, rather than calibrated properties for a particular geometry. Using this theory, the adhesive is allowed to be very highly stressed (or strained) without failing, providing these very high stresses (or strains) act over a very small volume of material. This way the problem of very high stresses (or strains) around the singular points in an F.E analysis can be bypassed. The criterion proposed appears to have a physical significance, and is able to explain the existence of high localised stresses, without failure occuring. The shear component of stress (or strain) should also be examined as the operator as it has been shown to play important role in shear type loading such as in a single or double lap joint in tension.

Further validation of the model using different adhesive materials, geometries and also type of loading needs to be carried out.

1.2.4 Thesis objectives

From the above review, we can therfore say that the finite element method is capable of describing the stress-state in a bonded joint with reasonable accuracy. If results are to be meaningful and closer to reality, material and geometric non-linearities should be taken into account. It is important for both adherend and adhesive materials to be modelled accurately. For the adhesive material especially, pressure sensitive yield criteria should be used since these take into account the dependence of yield strength on the hydrostatic stress component and the different behaviour in tension and compression. No failure criterion seems to be "universal", such that it will work for different adherend and adhesive materials, different joint geometries and various types of loading. However, it seems that failure criteria based on strain measures rather than stress measures give better results and are more applicable. It appears that rather than trying to concentrate on the singular points at the ends of the joint, failure should be predicted by considering other parts of the overlap too, perhaps the whole overlap in some cases.

In the current thesis both theoretical analysis and experimental measurements on adhesively bonded SLJs will be carried out. Various material and geometric parameters will be investigated. In particular, the effect of adherend and adhesive plasticity will be analysed in detail. The overlap length, adherend thickness and the presence of a fillet will be examined in order to determine their influence on the strength of the joints. Tests for bonded joints will be carried out in both tension and bending. The effect of adding artificial defects on the joint strength will also be investigated for a variety of configurations. Most of the configurations tested experimentally will also be analysed theoretically using the finite element method. The failure mechanisms and modes of failure will be studied for all the different configurations and a failure prediction methodology for the strength of the joints will be proposed.

The objective of this work is to combine analysis and experimental work on adhesive joints (particularly the single lap joint), so as to arrive at a better understanding of why joints break, and to propose design criteria for predicting joint strength.

1.3 Structure of thesis

The thesis is presented in the following chapters:

Chapter 2 - Materials characterisation - Specimen Specification. The specimen specifications and test method for analysis are presented in this chapter along with the equipment used to carry out the tests. Results from material testing (adhesive and adherend) in tension and shear are also presented in this chapter.

Chapter 3 - Tensile tests on SLJ. Results from tensile tests on SLJ are presented in this chapter. The effect of overlap length, adherend and adhesive ductility, and adherend thickness on the strength of SLJ are the parameters that are investigated. Detailed observation on the failure mechanisms and modes of failure for each different configuration are presented.

Chapter 4 - Four-point bend tests on SLJ. Results from four point bend tests on SLJ are presented in this chapter. The effect of adherend thickness and overlap length on the strength of the joints loaded in bending is investigated. The failure mechanisms and modes of failure are also discussed.

Chapter 5 - Joints with artificial defects. The effect of introducing artificial defects on the strength of SLJ is investigated in this chapter. Several overlap configurations are tested. A variety of adhesives and adherends have been used in order to assess the effect on different joint configurations. Tests in both tension and bending are presented.

Chapter 6 - Finite Element Modelling of the Joints. The finite element method was used to analyse the joints theoretically. The analysis procedure considerations, materials modelling, finite element meshes and critical decisions concerning the modelling of the joints are discussed in this chapter.

Chapter 7 - Finite Element Analysis Results. The results from the finite element analysis are presented in this chapter. Detailed stress and strain distribution in the adhesive layer and the adherends are presented for a variety of joint configurations modelled. Some comparisons between the F.E.A and existing closed form analysis is carried out. Correlation between the F.E results and experimental observations and results are also presented.

Chapter 8 - Predictions - Failure Criteria. A new failure prediction methodology for the prediction of joint strength is proposed. Comparisons between the F.E predictions and the experimental results are presented. Suggestions for further work are also presented in this chapter.

Chapter 2

TEST DESCRIPTION - SPECIMEN SPECIFICATION - MATERIALS CHARACTERISATION

2.1 Introduction

The configuration of the single lap joint (SLJ) has been chosen as the test piece geometry in the current work (figure 2.1). It is used in industry for quality assurance and by many researchers because of its simplicity to manufacture and test. However, it should be mentioned here that although simple to manufacture and test, SLJs are quite difficult to analyse. This is mainly due to the non-linear geometric configuration of the joint. The SLJ forms the basis of most possible bonded configurations. Any bonded configuration such as double lap, strap, T- peel, frequently found in literature, could be broken down to a number of single lap joints. It is therefore very important to be able to understand the mechanisms that govern failure in this basic configuration.

Single lap joints were manufactured using a variety of materials as adhesives and adherends. Two types of tests were chosen, tensile tests and four point bend tests, as most of the loadings a component would face in service will be a combination of a tensile load and an applied bending moment. The majority of the specimens were tested to failure. The exception was for a few specimens that were loaded up to the point that some amount of damage was visible. The main reason was to gain more insight in the failure mechanisms and the extent of damage prior to failure. All the tests were conducted at room temperature of approximately 23° C and 50% humidity. At least five specimens were tested for each joint configuration and for the characterisation of the materials (both adherends & adhesives). A total of 44 specimens were tested for the characterisation of the materials (both adherends and adhesives) and approximately 460 specimens were

tested in various joint configurations. Good reproducibility and repeatability was achieved in all tests.

2.2 Specimen specification - dimensions

All the specimens were manufactured in accordance to the ASTM Standards (1982). One of the aims of the current investigation was to assess the effect of the overlap length (l) on the strength and failure of SLJ. Increasing the overlap length reduces the maximum shear and peel stresses and also the average shear stresses in the middle of the overlap region as shown theoretically by Fargette & Gilbert (1996) and Long (1991). Joints with five different overlap lengths were manufactured, ranging from 12.5 mm to 60 mm. End tabs of the same thickness as the adherends were bonded at the ends of the joints as shown in figure 2.1, in order to reduce the eccentricity of the load path. The length of the end tabs was kept constant at 25 mm. The end tabs define the gripping area on the tensile tests. For the case of the four point bend tests, the end tabs play no role at all, since they are far away from the loading positions.

In order to comply with the ASTM standards, the free length, L_f, (figure 2.1) was kept constant at 63.5 mm for all the joint configurations.

As it is well known that increasing the width (b) of the joint leads to a proportional increase in the strength of the joint, a constant width of 24.8 mm was used for all tests.

Another parameter affecting the strength of joints is the glueline thickness (t). This is a parameter of great importance, especially for the manufacturing industries, as it is quite difficult control especially in an industrial scale manufacturing process. Many researchers have tackled the subject. Results presented by Grant (1994) have shown that joint strength should increase as the glueline thickness decreases. Below a certain point of approximately 0.3 mm, no significant changes were noted. Crocombe (1989) has also proved the above theoretically. Lee (1992) found that the torque capacity of a bonded tubular SLJ increases with decreasing adhesive thickness. Based on the above, it was decided to manufacture joints with a glueline thickness of 0.1 mm.

The majority of the joints were manufactured with a full depth fillet (figure 2.1). Some tests were carried out on joints without fillets in order to assess its effect on the strength of the joints. Fillets have been shown by Adams et al (1974), (1981), (1991), Dorn & Liu (1993) to reduce significantly the peak stresses at the ends of the joints. The use of chamfered spacers is one of the most effective ways to control the glueline thickness. The angle of the fillet was chosen to be 45°. All the chamfered spacers were ground to the exact thickness required to produce a glueline thickness of 0.1 mm for every joint.

The majority of the adherends used were 1.6 mm thick. Some tensile specimens were manufactured using 1 mm and 2 mm thick adherends, in order to assess the effect of adherend thickness on the strength of the joints. The specimens tested in the four point bend tests were manufactured using 1.6 mm, 2 mm and 3 mm thick adherends. The thickness of the end tabs was chosen to be the same as that of the thickness of the corresponding adherend in order to reduce the eccentricity of the load path. Thus, joints with 1 mm, 2 mm and 3 mm thick adherends had end tabs 1 mm, 2 mm and 3 mm thick respectively.

Table 2.1 summarises the dimensions of the metal pieces used to manufacture the single lap joints.

All the adherends used to make the joints were machined to a tolerance of ±0.05 mm to the dimensions shown in Table 2.1 from strips of the correct thickness.

Table 2.1 Adherend lengths and total length of joints for the different overlap configurations

Overlap length l (mm)	Adherend length l_a (mm)	Total length of joint l_{tot} (mm)
12.5	101	189.5
20	108.5	197
25	113.5	202
40	128.5	217
60	148.5	237

The jig used to manufacture the joints can be seen in figure 2.2

2.3 Equipment used for experiments

2.3.1 Testing machine

All the specimens were tested on a Zwick universal testing machine, which was annually verified by Zwick to BS EN1002-2: 1992, Class 0.5 for the 100kN range. The machine is interfaced to a computer. It can be manually or computer controlled. Appropriate software (Zwick) was used to capture the data. The output from the load cell is an analogue signal (Volts). As will be explained later (Sect. 2.3.2) this signal was used as an input to another data logging device when strain gauges were used.

Wedge grips were used to clamp the specimens and all tests were displacement controlled. The clamping area was defined as the area covered by the end tabs. As mentioned earlier, apart from a few exceptions, the majority of the joints were tested to failure. The maximum load recorded by the machine was taken as the strength of the joint. The jaws separating speed (test speed) was chosen to be 5 mm per minute for all joint tests to represent quasi-static testing conditions. Failure in the joints occurred in approximately 1-2.5 minutes depending on the configuration.

It is well known Harris (1983), Crocombe (1995), Duncan et al. (1998), that adhesives are strain rate sensitive materials. Apart from the rate of straining applied in a test, the type of adhesive (epoxy, polyurethane, acrylic) as well as the test temperature in comparison to the glass transition temperature, T_g, of the adhesive are very important factors affecting the behaviour of the adhesive. No account was taken for any variations on the rate of straining at different parts of the joint as the load increased during the test. This is a complicated subject not considered here. However it should be mentioned here that epoxies, (the adhesives used in the current investigation), are the least strain rate sensitive of all types of adhesives. Also, all the tests were carried out at room temperature, which is a lot lower than the T_g of the adhesives tested.

The machine by default records the load and the amount of separation of the jaws (cross head displacement), as the tests progress. Unfortunately, this measure is not accurate enough to be used in theoretical calculations. It usually contains components such as slippage between the wedge grips and the specimens, and some amount of stretching of the components of the machine (slack). Also, the length over which the extension is measured is the total length of the joints which is not of any use when local areas of the joint need to be examined. The biggest source of error comes from the way the wedge grips work. They do not grip well at low loads. As a consequence, the displacement measured from the tests will not be used to compare with any theoretical calculation.

2.3.2 Strain gauges - logging devices

Strain gauges were used both in the adherend materials characterisation as well as in the testing of joints. All the strain gauges were purchased from Techni Measure Ltd (TML). Different types of strain gauge were used depending on the material tested and the range of data required, as will be explained later. All the gauges were bonded to the substrate with cyanoacrylate adhesive, as recommended by the manufacturer (TML Strain Gauges). The standard procedure of sanding and etching the adherend surfaces was followed to ensure perfect bonding of the strain gauges.

The commercial program ABAQUS that will be used later for the finite element analyses of the joints requires the material data in true stress versus true strain format. The derivation of such data from nominal or engineering stress and strain is presented in Appendix I. Subsequently, any stress - strain graph presented in this chapter will be in true stress versus true strain format.

A separate computer with an A-D card and the appropriate electronics (strain gauge amplifier FE-254-GA, bridge conditioner FE-492-BBS) manufactured by FYLDE, were used to capture the data. A commercial software package, Lotus 123 was used to write a small program so that the correct amount of information was recorded for each test.

The load signal from the testing machine was always logged together with the strain gauge output in this separate computer to ensure perfect timing in the readings (load - strain).

2.3.3 Video camera - microscopes

A video camera capable of recording at up to 25 frames per second was used to record different configurations of joints while they were tested. The whole event, from initial loading to catastrophic failure, could be then reviewed at a slower speed (usually frame by frame) and useful conclusions could be made. Other researchers Adams & Panes (1994) have used a different approach, loading the specimens in steps, stopping the test, observing the specimen, and repeating that procedure until catastrophic failure occurred. This method was not thought to be appropriate. The advantage of using a video camera is that there is no interference with the experiment, thus minimising any possible errors. Additionally, events that occur at a high speed cannot be caught by the human eye. In some cases, the events were so fast that it was impossible to get any useful information from the recordings. High-speed photography or very high-speed video cameras is a possible solution to that problem. In order to visualise the crack formation better, the surfaces of interest were painted white, using a thin layer of paint. In some cases, marks (black lines) were drawn in the specimens to facilitate making comparative measurements.

Post failure observation of the broken joints (especially the failed bonded surfaces) gave us a better understanding of how joints break. Photographs of the broken surfaces were taken using a still camera. These photographs were then digitised and are presented in several parts of this work. These images will be used to explain the failure mechanisms and modes of failure. It is useful here to define some special terms, such as those shown in figure 2.3, that will be used throughout the following chapters. These terms will be used to locate the exact position in the joint that the images refer to.

In figure 2.3 we can see a three-dimensional view of a single lap joint. Several definitions are given on this schematic. The x-axis runs along the length of the adherends, the y-axis is through the thickness of the joints while the z-axis lies across the width of the joint.

Some of the digitised images that will be presented later on will be side views of the overlap (or parts of it) lying in the xy plane. Perspective views of the joint will usually cover areas around the edge of the overlap including parts of the fillet. All failure patterns of broken joints will show the bonded area (covering the whole overlap or parts of it) which lie on the xz plane. Some images will be presented showing the faces of the fillet covering the whole width of the joint.

Microscopes were used in some cases to observe the failure patterns whenever a more detailed view was needed.

2.4 Testing of joints

The general loading a structural component faces in service can be broken down to a combination of tensile loading and a bending moment. Therefore, two types of test were carried out on the joints, viz tensile tests and four point bend tests.

The majority of joints were tested quasi statically in tension. Four point bend tests were carried out on selected configurations (combination of adherend material, adhesive material and overlap length).

The characteristic value recorded from both the tensile and four point bend tests is the load to failure.

2.4.1 Strain gauging the SLJ

Strain gauges were used in both the tensile and four point bend tests in selected configurations. As will be shown in later chapters, all joint configurations discussed and tested experimentally will be analysed theoretically using the finite element method. There is a need for some means of comparison between the theoretical and experimental results. This can easily be done if a strain measure is available from the experimental

results at some position in the joints. It was decided to use strain gauges placed at some position (defined later in this section) on the adherends. This way, the strain variation as the load increased can be monitored and comparisons with the theoretical predictions can be made.

It is well known that the ends of the overlap are the most stressed parts of the joint. It is important to know the load distribution in that area. The strain gauges were therefore placed near the edges of the overlap at the centre of the width of the joints. Strain gauges were placed at both sides of the adherends and at both ends of the overlap, a total of four strain gauges for each specimen.

By placing strain gauges on each side of the adherends the bending moment distribution can be calculated. The magnitude of the difference in the strain measured between two gauges placed on opposite sides is proportional to the bending moment applied at that section. If there is no difference between the two readings, then that means there is only pure tension with zero bending. In this way, any asymmetry during loading could be recorded, and a better understanding on the distribution of bending moments around the edges of the overlap can be achieved. Numerous researchers, Goland & Reissner (1944), Hart-Smith (1973), Zhao (1991), have published reports on the bending moment distribution around the edges of the overlap. Comparisons with their results will be made in a later chapter.

For the case of the tensile tests, the mid-position of the gauges were placed at a distance of 9 mm from the adherend corner. The gauges were 5 mm long. For the four point bend tests, due to space restriction from the loading rig, the gauges were placed at a distance of 7.5 mm. The exact positioning of the gauges on the adherends can be seen in figure 2.4.

2.5 Materials used - characterisation

2.5.1 Introduction

Steel in three very different conditions of hardness, and four different adhesives were used in order to study the effect of the material properties on the strength and failure of

the joints. Detailed stress-strain data are needed for input in the finite element analyses. Harris (1983) has shown the importance of accurately modelling both the adherend and adhesive material properties. Material properties for both adherends and adhesives were determined experimentally using various standard methods and are presented in the following sub-sections. Tensile tests were carried out for the characterisation of the adherend materials. Tensile and shear tests were carried out for the characterisation of the adhesive materials.

2.5.2 Adherend materials

The main aim of the investigation was to study the effect of adherend plasticity on the strength of the joints made using different adhesives. In order to do so, adherends with different yield behaviour and yield strength were needed. Adherends with three different yield strengths were finally used.

The first set of adherends were made from mild steel. The second and third set were made from high carbon gauge steel in the as-received and heat-treated conditions respectively. Appendix II describes the heat treatment procedure followed to harden the gauge steel adherends and some more information about the composition of the gauge steel. The result was to get three sets of adherends with different hardnesses. It is well known, Pascoe (1978), that there is a direct relationship between the yield strength and the material hardness. The first (mild steel) and second (gauge steel) set of adherends should yield at different stresses while the third set (hardened gauge steel) should remain elastic throughout the loading regime the joints would face.

It is important to know the stress - strain behaviour of the adherends as this will be the input for the material models in the subsequent finite element analysis. Especially important was to record the post-yield behaviour of the mild and gauge steel materials. Tensile tests were carried out on dogbone specimens manufactured from each material. The geometry of the specimens (figure 2.5) is according to the British Standards BS 18 (1987). Specially designed clamps were used to position these specimens on the testing machine.

Strain gauges were used to record the strain in the tensile tests for the adherends. The strain gauges used were special ones (Post - yield type "Y" from TML) capable of recording strains up to 20 %. This was thought to be enough to get information about the yield and post yield behaviour of each kind of steel used, especially for the mild and gauge steels. The gauges were placed at the centre of the specimen, one on each side as can be seen in figure 2.5.

The elastic moduli for each type of metal can easily be derived from the stress strain curves. In addition to the tensile tests, vibration tests were done on each type of steel used as a cross check for the Young's moduli. The results from the two methods were found to agree very well and an average value is presented in table 2.2. More information about the vibration tests can be found in Appendix III.

The Poisson's ratio was assumed ν=0.3 for all types of steel.

2.5.2.1 Mild steel

The stress - strain behaviour of mild steel can be seen on figure 2.6. Mild steel is a very commonly used material. It is quite ductile and the maximum measured strain was approximately 16.5 % at 420MPa. The yield stress for mild steel can be found from the stress strain curve at 200 MPa. At around 269MPa the material behaves as perfectly plastic. After this point the material work-hardens significantly, as can be seen in the stress strain graph (figure 2.6). The strain gauges were capable of measuring strain up to the point shown on the graph. This is thought to be sufficient for the subsequent theoretical analysis that will follow the experimental work. The Young's modulus can be calculated from the graph, E=194 GPa.

2.5.2.2 Gauge steel

Gauge steel is considerably stronger than mild steel, but again quite ductile. Initial yield is reached at 350-400MPa and the maximum measured strain recorded is approximately 9.3 % at 807 MPa, as can be seen from figure 2.7. Similar behaviour to that of mild steel is

observed. After initial yield, the material behaves as perfectly plastic, at around 425 MPa. Gauge steel then work-hardens as can be seen from the stress-strain curve. The Young's modulus can be calculated from the graph, E=205 GPa.

2.5.2.3 Hard steel

Hardened gauge steel, on the other hand, is a very strong material and exhibits a quite brittle behaviour (figure 2.8). It yields at around 1810 MPa and breaks soon after at 2100MPa and only 3 % strain. From now on, the hardened gauge steel will be referred to as hard steel to avoid confusion with untreated gauge steel. The Young's modulus can be calculated from the graph, E=205 GPa.

2.5.2.4 Adherend material comparisons

From the data presented on figures 2.6- 2.8, mild and gauge steel are expected to deform plastically throughout the loading regime of the joints, while hard steel should remain elastic.

In order to make comparisons easier and to get an overall understanding about the differences between the three different types of adherends, the stress-strain curves of all three are presented in the same graph on figure 2.9.

It must be noted here that the gauge and hard steel have exactly the same Young's modulus. Although the hardening treatment (quenching & tempering) changes dramatically the strength and yield behaviour of the steel, the Young's modulus scarcely changes. This was proven experimentally, as the modulus of gauge and hard steel were found to be the same.

Table 2.2 summarises the properties of the adherend materials.

Table 2.2 Basic mechanical properties of adherend materials used

Type of Steel	Yield Stress in tension σ_y (MPa)	Young's Modulus E (GPa)
Mild Steel	200	194
Gauge Steel	319	205
Hard Steel	1810	205

2.5.3 Adhesive materials

Structural adhesives are those adhesives that could be used in a load bearing application. One of the most common type of structural adhesives is the epoxy family. Four different epoxy adhesives were used throughout this investigation. Three out of four are one-part structural epoxies and the fourth is a brittle, two-part epoxy system which was mainly used for comparison reasons, as will be explained in the relevant chapters 3&4. All adhesive systems used require heat to cure and some pressure was applied in the jig during curing. The names and types of adhesives used are summarised in Table 2.3.

Table 2.3 Names and types of adhesives used

Name	Manufacturer	Type
ESP 110	Permabond	Single part epoxy paste
AV 119	Ciba Polymers	Single part epoxy paste
EC 3448	3M	Single part epoxy paste
MY753	Ciba Polymers	Two part epoxy

It is well known, Rabinowitz (1970), Raghava & Caddell (1973a), (1973b), Wronski (1977), that the behaviour of polymeric materials, including adhesives, depends on the type of loading they are subjected to. Different critical values should be expected when an adhesive specimen is loaded in tension, compression or shear. It was therefore decided to carry out tensile and shear tests on the adhesives used. Although it is known that polymeric materials may be rate sensitive, in this work the rate effects will not be taken into account since the adhesives are tested at temperatures well below *Tg*, and are not

very rate-sensitive. In all tests, a monotonic load is applied to failure by displacing the ends of the joints at a constant speed.

In the following subsections, the experimental method chosen and results from tensile and shear tests are presented. Again all the tensile test results are presented in the format of true stress - true strain as required by the finite element program (see Appendix I).

2.5.3.1 ESP 110 adhesive

This is a single-part toughened epoxy paste adhesive, filled with approximately 30 % aluminium powder. It is manufactured and supplied by Permabond Adhesives limited. Its colour is silver grey and it is quite viscous (400,000 cP) at room temperature. The curing schedule is 45 minutes at 150° C.

A 1.4 mm thick sheet of adhesive was cast, producing bulk adhesive rectangular beams. The rectangular beams were machined to produce dogbone specimens same to the ones described in section 2.3.1 (figure 2.5). Clip gauges were used to record the extension on a gauge length of 20 mm. Strain gauges were not used in this case as it is well known that they can locally stiffen polymeric specimens. The bulk specimens were loaded at a cross head displacement rate of 1 mm/min.

A typical stress-strain curve for ESP 110 in tension is presented in figure 2.10. The behaviour is non-linear to failure, which is characteristic of epoxy systems. The distinction between the elastic and the plastic region in the curve is not very clear. Yielding or rather non-linear behaviour in such materials starts at a low load and carries on throughout the loading of the specimen. Some amount of work hardening is present. As can be seen from figure 2.10, ESP 110 has a strain to failure of approximately 3 % and an ultimate strength of approximately 70MPa.

Vibration tests (Appendix III) were carried out on rectangular beams of the adhesive to derive the Young's modulus for ESP 110. The results compare well with the modulus derived from the stress strain curve, E=4.45 GPa.

Shear tests were carried out using the Thick Adherend Shear Test method (TAST), ISO 11003-2. Thick adherend shear specimens were manufactured according to Vaughn & Adams (1996) and the shear properties of the adhesive were then determined. The reader is referred to Vaughn (1997) for further information about the method. The shear stress-strain characteristics of ESP 110 are presented in figure 2.11. The tests were displacement controlled. The shear strain to failure is approximately 15 % and a maximum shear stress recorded is around 48MPa. Some amount of strain softening is visible above 9 % of shear strain. The shear modulus for ESP 110 derived from figure 2.11 was G=1.624GPa.

The Poisson's ratio value for ESP 110 was calculated ν=0.37 using the tensile and shear modulus relationship $E = 2(1+\nu)G$.

Table 2.4 summarises some mechanical properties for ESP 110 adhesive.

Table 2.4 Summary of mechanical properties for ESP 110 adhesive

ESP 110 adhesive properties at room temperature	
Young's modulus E (GPa)	4.45
Shear modulus G (GPa)	1.624
Poisson's ratio ν	0.37
Strain to failure in tension	~ 3 %
Shear strain to failure	~ 15 %

2.5.3.2 AV 119 adhesive

This is a rubber-toughened single-part epoxy. It is manufactured by Ciba Polymers. A curing schedule of 1 hour at 120° C was followed, according to the manufacturers instructions.

Bulk adhesive specimens were used for the tensile tests. The specimens were loaded at a cross head displacement rate of 1 mm/min. Extensometry devices were used to record the extension in this case. Data from the tensile tests were supplied by Dean & Duncan

(1995) and are shown in figure 2.12. The behaviour of this adhesive is non linear up to 5 % strain. The strain to failure for AV 119 is approximately 7-8 % and the maximum stress recorded is about 72MPa. There is some amount of strain softening above 5.6 % strain. There is again no clear point as to where yielding starts to occur. The non-linear behaviour starts at approximately 30.2 MPa, but this does not necessarily mean that permanent plastic deformation has occurred. The Young's modulus determined from the stress strain curve is E=3.022GPa. The Poisson's ratio variation with strain supplied by Dean & Duncan (1995) can be seen in figure 2.13. It can be seen that there is a gradual drop of the Poisson's ratio with increasing longitudinal strain. The value of ν=0.38 is used in the theoretical analyses that will follow.

The butt torsion shear test method was used to derive results for the shear behaviour of AV 119. Data from shear tests were supplied by Thomas & Adams (1996) and are presented in figure 2.14. The shear test was performed under constant rotation rate. The reader is referred to Thomas & Adams (1996) for further information about the method. The maximum shear stress recorded was approximately 49MPa at around 10% shear strain. Above that point some amount of strain softening is visible. The shear strain to failure is approximately 45%.

The shear modulus for AV 119 derived from figure 2.14 is G=1.094GPa.
Table 2.5 summarises some properties for AV 119 adhesive.

Table 2.5 Summary of mechanical properties for AV 119 adhesive

AV 119 adhesive properties at room temperature	
Young's modulus E (GPa)	3.022
Shear modulus G (GPa)	1.094
Poisson's ratio ν	0.38
Strain to failure in tension	~ 7 %
Shear strain to failure	~ 45 %

2.5.3.3 EC 3448 adhesive

This is the last of the structural adhesives used. It is a rubber modified single part epoxy manufactured by 3M. Its colour is off-white and it is very viscous at room temperature. This adhesive is regarded as a top of the range aerospace structural adhesive.

A non-contacting measuring method was used to measure the extension on dogbone shaped bulk adhesive specimens. The method utilises a video camera and appropriate software to track marks on the specimen in real time, as the specimen is loaded. The extension can therefore be calculated and the strain derived. Data from tensile tests and Poisson's ratio variation were supplied by Towse (1997). The tensile stress-strain curve is presented in figure 2.15. The adhesive behaves non-linearly up to approximately 5 %. Then a nearly plastic behaviour follows. There is no strain softening behaviour up to 7 % strain. The maximum stress recorded is 66 MPa and the strain to failure is around 8 %. The Poisson's ratio variation with strain is presented in figure 2.16 and similarly to AV 119 adhesive's behaviour a gradual drop can be seen as the strain increases. The Young's modulus and Poisson's ratio that will be used in the theoretical analysis are E=3.095 GPa and ν=0.4 respectively.

Shear properties for EC 3448 were determined using the butt shear test method. Butt joints were manufactured and the results are presented in figure 2.17. The maximum shear stress recorded is 50.49 MPa. There is no strain softening behaviour up to 45 % shear strain. The shear strain to failure is approximately 50 %. The shear modulus derived from figure 2.17 is G=1.105 GPa.

Table 2.6 summarises some properties for EC 3448 adhesive.

Table 2.6 Summary of mechanical properties for EC 3448 adhesive

EC 3448 adhesive properties at room temperature	
Young's modulus E (GPa)	3.095
Shear modulus G (GPa)	1.105
Poisson's ratio ν	0.4
Strain to failure in tension	~ 8 %
Shear strain to failure	~ 50 %

2.5.3.4 MY753 adhesive

This is a two part epoxy consisting of a liquid epoxy resin MY 753 and a hardener HY 951 (liquid of low viscosity) mixed at a ratio of 100:10 by weight It is an unmodified epoxy and cannot be regarded a structural adhesive, due to its brittle and weak behaviour. Its main usage is for encapsulating electronic circuits and components.

In a similar way to the ESP 110 adhesive, a 1.4 mm thick sheet of adhesive was cast, producing bulk adhesive rectangular beams. The rectangular beams were machined to produce dogbone specimens same to the ones described in section 2.3.1 (figure 2.5). Clip gauges were used to record the extension on a gauge length of 20 mm. Strain gauges were not used in this case as it is well known that they can locally stiffen polymeric specimens. The bulk specimens were loaded at a cross head displacement rate of 1 mm/min.

A typical stress-strain curve for MY753 in tension is presented in figure 2.18. The behaviour is non-linear to failure with a small degree of strain softening at around 3.5% strain. Again the distinction between the elastic and the plastic region in the curve is not very clear. The strain to failure of MY753 is approximately 4 % and the ultimate strength of approximately 48MPa. The Young's modulus is E=1.838 GPa.

The butt torsion shear test method was used to derive results for the shear behaviour of MY753. A typical shear stress-strain for MY753 is presented in figure 2.19. The shear test was performed under constant rotation rate. The maximum shear stress recorded was approximately 33MPa at around 10% shear strain. Above that point some amount of strain softening is visible. The shear strain to failure is approximately 20%.

The shear modulus for MY753 is G=0.670GPa.

The Poisson's ratio value for MY753 was calculated to be 0.37 using the tensile and shear moduli.

Table 2.7 summarises some mechanical properties for MY753 adhesive.

Table 2.7 Summary of mechanical properties for MY 753 adhesive

MY753 adhesive properties at room temperature	
Young's modulus E (GPa)	1.838
Shear modulus G (GPa)	0.670
Poisson's ratio ν	0.37
Strain to failure in tension	~ 4 %
Shear strain to failure	~ 20 %

2.5.3.5 Adhesive comparisons

In order to make comparisons easier, tensile and shear stress-strain curves for all adhesives used will be presented on the same graph in figure 2.20 and figure 2.21 respectively. It is useful to compare the points of maximum stress and the corresponding strains for the different adhesives used. Both tensile and shear properties are important, as will be shown in later chapters.

From the tensile tests we see that ESP 110 does not strain soften at all, and a maximum tensile stress of 70MPa is reached at 3% strain, which is the strain to failure as well. The AV 119 adhesive reaches a maximum tensile stress of 72 MPa at 5.6% strain. The adhesive strain softens slightly after that point and stress drops down to 71MPa at 8.% strain. EC 3448 reaches its maximum tensile stress, 66.00MPa at 7.3% strain. There is a small amount of strain softening after this point with stress drooping down to 65MPa at 8% strain. The MY753 adhesive has a maximum tensile stress of approximately 48 MPa at 3.5% strain and some strain softening can be observed after this point.

From the shear results, ESP 110 adhesive reaches a maximum shear stress of approximately 48MPa at 9% strain. Strain softening is observed just after, and at a maximum strain of 15% the stress has dropped down to 45MPa. AV 119 adhesive

reaches a maximum shear stress of approximately 49MPa at 10% strain and remains almost perfectly plastic up to approximately 18% strain. Strain softening is apparent shortly after, and stress drops down to 45MPa at around 45% strain. EC 3448 adhesive was slightly different. The maximum shear stress reached was 50MPa at 14% strain, and the adhesive remains almost perfectly plastic up to about 50% strain. The MY753 adhesive was considerably weaker in shear compared with the other three structural adhesives reaching a maximum shear strength of approximately 33MPa.

2.6 Conclusions

The range of materials, for adherends and adhesives, as well as the different geometric configurations used to manufacture the SLJ were presented in this chapter. The equipment used for testing the materials as well as the joints was presented.

Tensile data are sufficient for materials used for the adherends. Yield is quite clearly defined and is sharp for the metals. Post yield behaviour is very important, especially for the theoretical analyses.

For the adhesives however, it is important to know both the tensile and the shear behaviour, since these materials behave differently under different loading conditions. Different critical values can be used depending on the type of loading the adhesive is subjected in different joint configurations and loadings. Yield is not clearly defined since these materials yield gradually up to failure. The most critical values for the adhesives are the strain at which maximum stress is achieved as this defines the point where strain softening behaviour starts to occur and of course the strain to failure.

It is very important to notice that all the materials (apart from hard steel) will be expected to behave in a non-linear fashion throughout the loading of the joints. The configuration of the single lap joint is also geometrically non-linear. All these non-linearities must be taken into account in the theoretical modelling of the joints that will follow in a later chapter.

Combinations of all these configurations will be used to manufacture single lap joints. The effect of different parameters such as overlap length, adherend plasticity, adhesive ductility, on the strength of the joints will be investigated in the following chapters.

Chapter 3

TENSILE TESTS ON SINGLE LAP JOINTS

3.1 Introduction

As has been shown in chapter 2, single lap joints with five different overlap lengths, three different kinds of steel adherends and four different adhesive materials were manufactured. It has also been shown that all the materials could behave non-linearly during loading. Harris (1983) was one of the first to investigate the effects of adherend and adhesive plasticity as well as to understand the importance of modelling the non linearities (geometric and material) present in a SLJ configuration. Results from tensile tests carried out on the joints will be presented in this chapter.

Tensile loading of SLJ is the standard method of assessing the strength and load carrying capacity of different adhesives. However, many parameters can affect the results, leading to confusing conclusions.

In service, a structural bonded component will usually carry some combination of a tensile, compressive or shear load and a bending moment. The adhesive will be required to transfer the load between the two (or more) components. Design guidelines suggest that the adhesive should be mainly loaded in shear, avoiding direct tensile and cleavage loads as much as possible.

Many parameters can affect the strength and integrity of the bonded joint. It is necessary to understand how different parameters affect the strength of joints starting with the simplified option of tensile loading in the joints.

However, applying a tensile load at the ends of a single lap joint does not necessarily mean that the adhesive is loaded only in shear. As it will be shown, due to the eccentricity of the load path and the non-linear geometry of the SLJ, the joint is stretched and bent at the same time due to an application of a tensile load at its ends. This complicates the

situation and the adhesive is in a three dimensional stress state, especially at the ends of the overlap.

The aim in this chapter is to identify parameters that could affect the strength of joints and assess the effect of these parameters both qualitatively and quantitatively. This will enable the design of stronger and more efficient joints.

3.2 Experimental variables - configurations

Four different adhesives, five different overlaps and three different types of metal for the adherends were used to manufacture joints that were tested in tension.

The majority of the tests were to failure. Some tests were stopped soon after the first signs of damage had appeared. This was mainly done in order to observe the extent of damage on these particular joints.

The parameters that were investigated in these tests are divided in two main categories: material and geometric parameters. The effect of adherend plasticity and adhesive ductility can be assessed by comparing the different configurations. The term "joint configuration" means a combination of overlap length, adherend thickness, adherend and adhesive materials. The overlap length is a geometric parameter which could also alter the strength and it was a variable in the tests. The adherend thickness is another variable that was also investigated.

When an adhesive joint is manufactured, adhesive is always squeezed out of the ends of the overlap. This forms a fillet, as it is well known, which could have a regular or irregular shape depending on whether appropriate spacers are used. These fillets can be either left on the joint or they could also be removed (before or after the consolidation of the adhesive). If fillets are to be removed, it is generally better to do so before the consolidation of the adhesive. That is because the adhesive still flows, making it easier to remove it. Alternatively, some sort of machining would usually be required (after consolidation) and cracks could be introduced in the bonded area during that process. Machining is much more difficult and it is costly and time consuming.

In this work, as already presented in chapter 2, most of the joints were manufactured with a full depth 45° fillet. This was decided because the process of removing the fillets could introduce damage accidentally and this also introduces an additional step to the whole manufacturing process. On the other hand, irregularly shaped make observations of the failure process difficult and so were avoided. In some configurations, however, it was decided to manufacture joints without fillets in order to assess the effect on the strength of the joints.

Results from the tensile tests on different joint configurations are given below. There are many parameters (either geometric or material parameters) investigated in the current work: overlap length, adherend thickness, adherend and adhesive plasticity, presence of fillet. It was decided to divide the presentation of the results in three main sections depending on the type of adherend used (mild, gauge or hard steel). The effect of all the parameters under investigation on the strength of the joints, and the failure mechanisms associated with each case will be presented in each sub-section. Some of the joints were also strain gauged as explained in section 2.4.1, and results will be presented in these sub-sections.

Tables of results will be presented at the end of the chapter. Tables 3.1, 3.2, 3.3 and 3.4 contain results for the ESP 110, AV 119, EC 3448 and MY 753 adhesive joints. Graphs of strength versus overlap length are presented in figures 3.1, 3.2, 3.3 and 3.4 for the ESP 110, AV 119, EC 3448 and MY 753 adhesives respectively.

3.3 Results for mild steel joints

Mild steel joints were manufactured using two adhesives: ESP 110 and AV 119, in all five different overlap configurations. Joints with mild steel and the MY753 adhesive were also manufactured but only for the 25 mm overlap configuration. This is a total of 11 different joint configurations for joints with mild steel adherends.

3.3.1 Strength results

The results are presented in table 3.1, table 3.2 and table 3.4 for ESP 110, AV 119 and MY753 adhesive respectively. The same results can be found on figure 3.1 and figure 3.2 for the ESP 110 and AV 119 adhesives respectively. It can be seen from the graphs that for both adhesives, as the overlap length increases, the strength of the joint increases. However, a plateau is reached quite quickly and only a small increase in the strength of the joints is achieved for overlaps exceeding the 25 mm. It seems that a further increase in the overlap length would not lead to a further increase in the joint strength. Typical load displacement curves from tests using mild steel adherends can be seen in figure 3.5 for the case of AV 119 adhesive. It is important to repeat here that the displacement measure cannot be taken as an absolute value because, as explained on chapter 2, it contains components such as slippage between the grips and the adherends, and also some straightening of the components of the machine (slack). This is the reason why the first part of the curves shows an increasing slope. As the load increases the grips clamp tighter and the amount of slippage is minimised. This can be seen by the fact that the load displacement curves start to become linear above 4kN load.

At a load of approximately 7-8 kN a slight deviation from linearity starts to occur indicating that the mild steel adherends start to yield.

Joints with longer overlap length are able to extend more. Explanations on the reasons and the way these joints fail will be given at a later section.

It seems the plastic deformation of the adherends controls failure in this case.

Comparison between the two adhesives ESP 110 and AV 119 shows that the AV 119 adhesive gives slightly stronger joints. The differences are, however, very small.

3.3.2 Fillet effect

For the mild steel case, joints without fillets were manufactured for the configuration of 25 mm and 60 mm overlap. The adhesive used was ESP 110. Results from these tests show no apparent differences in strength compared with the filleted joints as shown in

table 3.5. Variations only arise due to experimental scatter. So the presence of a full depth spew fillet does not seem to influence the strength of the joints for this case.

3.3.3 Failure mechanisms - modes of failure

The failure mechanisms were observed by using a video camera, as already explained in section 2.3.3, and also by post failure observation of the joints.

Large plastic deformation of the adherends was obvious for the joints made from mild steel. The experimental results show that joints with longer overlaps are slightly stronger and, as will be shown in the following paragraphs, this altered the failure process in some cases.

As can be seen from figure 2.6, mild steel yields at a low load. After initial yielding, the material behaves initially as perfectly plastic, and then it work hardens until the maximum strength is reached. In a lap joint configuration, the adherends are stretched and bent at the same time. Due to the asymmetry on the load path, the joint tends to rotate around the joint middle. This means that the adherend is under a combination of tensile loading and a bending moment. As is well known, Goland & Reissner (1944), Hart Smith (1973), Zhao (1991) the maximum bending moments will be at the edge of the joints.

Joints with overlaps of up to 25 mm behaved in a similar way while the behaviour of the 40 and 60 mm overlap was slightly different with cracks arising due to Poisson's ratio effects being more visible for the longer overlaps.

The presentation will start with the shorter overlap joints. It is useful to see a typical load displacement curve (figure 3.6), i.e. a 25 mm overlap mild steel joint with the AV 119 adhesive, and explain the process. The initial part of the graph corresponds to the gripping of the specimen (the pressure from the wedge grips is increased as the load increases). As the load in the joint increases there is a point (A - figure 3.6) where the yield stress of the metal is reached at the inner side of the adherend (because the stresses from tension and bending are added). At this point there is no visible damage in the adhesive layer. As the load increases the adherends yield more and a point is reached (B - figure 3.6) where the load displacement curve starts to level off. Because there are four

different parts in the joint where excessive yielding occurs simultaneously (two around the overlap edges and two around the gripping ends), this is why the curve becomes flat. At this point the strain increases dramatically at the area around the corner of the fillet (see figure 3.7) because of the excessive yielding and rotation. The fillet starts to peel off and cracks start to run along the loaded adherend interface as shown schematically in figure 3.7. The load keeps increasing until the cracks in the fillet have reached the overlap edge. This is the point at which the maximum load is recorded. This is another indication that the presence of the fillets is not contributing to the actual strength of the joint. Once the cracks have progressed inside the overlap, the load starts to drop at a slow rate. A stable propagation of cracks follows, until catastrophic failure occurs. The failure is most of the times symmetric with cracks running from both ends of the overlap. Some times asymmetric cracking occurs with cracks running faster from one end of the overlap. This could only be attributed to slight variations in the adherend or adhesive strength between the two ends (uniformity of the adhesive layer, voids, porosity). Catastrophic failure occurs when approximately 10-12 mm of overlap is left (in the middle of the joint).

The final deformation shape of these joints is as shown in figure 3.8 Necking of the adherends was also visible near the edges of the overlap. In figure 3.9 the failure sequences of a mild steel joint are presented. Note that the load starts to drop only after the cracks have reached the overlap edges.

Let us now move on to joints with longer overlap lengths (40 & 60 mm) where the failure modes were slightly different. Experimental results showed that joints with longer overlaps were slightly stronger. Looking now at a typical load-displacement graph (figure 3.10), the initial part of the graph is the same as with the shorter overlaps. Initial yielding occurs at a slightly higher load because the bending moment for the same axial applied load is becoming less as the overlap increases. As the load increases, delaminations of the top edge of the fillet occur and cracks start to run across the width (z-direction) for a short distance (figure 3.11). These cracks are attributed to the Poisson's ratio effect, due to the excessive necking of the adherends near the overlap edges (figure 3.12). At the same time, cracks start to move inwards under the overlap (x-direction). However, the damage

in this case is not the same across the width of the joint. Cracks progress further at the edges of the joint compared to the middle of the width of the joint. This happens because while the bottom adherend (loaded end) starts to neck (deforms along the z-direction) the top adherend (unloaded end) wishes to remain as is (figure 3.12), thus extra shear stresses are generated at the sides of the joint. An ultrasonic c-scan of such a joint (only partially broken) was supplied by Dr. Drinkwater and is presented in figure 3.13. Standard ultrasonic techniques were used to study the reflection of the interfaces in order to create the c-scan. The damage spread has an oval shape showing that there is an asymmetry across the width of the joint. When the cracks have covered the whole width of the joint, then the fillet peels off in a similar manner to the one shown in figure 3.7. Cracks then start to run along the interface from both ends as explained earlier. The main difference in this case with longer overlaps is that once the cracks start to run inside the overlap the load does not start to drop but stays constant until approximately 20-25 mm of overlap is left undamaged. At this point, the load in the joints starts to decrease gradually until sudden failure occurs (again approximately 10-12 mm of overlap left).

In the case of longer overlaps, as the cracks propagate inside the overlap, the point at which maximum bending occurs moves under the overlap. The points where maximum bending occurred initially are now experiencing less bending, as the joint lines up and maximum bending occurs just ahead of the position of the cracks. So the bending moment increases at the fracture point and decreases further behind (away from the fracture point or crack tip). Figure 3.14 and figure 3.15 show the propagation of cracks for the case of a 60 mm overlap mild steel joint. Figure 3.14 is a side view of a joint while figure 3.15 is a detailed perspective view of the area around the overlap edge, where the cracks due to the Poisson's ratio effect become very apparent.

The cracks arising from the effect of Poisson's ratio do not affect the strength of the joints in a direct way since the joints can sustain further load after the initiation of these cracks. These cracks are purely a result of the differential straining (z-direction) between the bottom (loaded end) and top adherend (unloaded end). They are not therefore critical and probably affect strength of the joint only indirectly by providing the path for other cracks

to grow. This could be very important in the case of a brittle adhesive system where crack initiation is usually followed by unstable crack growth.

Joints made of mild steel behaved in a similar way regardless of the adhesive used (ESP 110 or AV 119). The failure mechanisms were the same for both adhesives. Joints with AV 119 were slightly stronger than those with ESP 110 adhesive. That is believed to be because of the higher ductility of the former adhesive, so there is an ability to withstand more adherend deformation. The differences are however small and any differences between the adhesives used are out-shadowed by the plastic deformation of the adherends. This is because of the very high localised strains that the adhesive is subjected to, near the fillet corner. The strains are so localised that any differences between the two adhesives are minimised and eventually the plastic deformation of the steel is what dominates failure.

3.3.4 Strap joints - Poisson's ratio effect

A further investigation on the Poisson's ratio effect was carried out to confirm the above conclusions. The adhesive used in this experiment was ESP 110. Since the situation in a SLJ is quite complex, with the adherends stretching and bending at the same time, it is not easy to distinguish the influence of these parameters unless they are somehow separated. An easy way of separating bending and stretching is to make a "joint" as shown in figure 3.16 (the double strap joint). This joint consists of a continuous piece of metal (centre) and two smaller pieces bonded on each side of it. The effect of bending at the edges of the joint is therefore eliminated. Only stretching and necking of the central adherend and the straps can occur in such a configuration. The results, as expected, showed transverse cracks appearing in the fillets (figure 3.16) similar to the ones described in the SLJ configurations. These cracks then propagate across the width of the joint (z-direction) before they start running along the overlap (x-direction). Perspective views of these joints failing are presented in figure 3.17. This is a demonstration of the effect of transverse straining in the cracking of adhesive bonds. This effect could be of interest for the electronics industry, where brittle adhesives are commonly used to

encapsulate electronic components. Similar conditions may also arise when bonding dissimilar materials. Due to the different coefficient of thermal expansion, similar stress conditions may develop during cooling (shrinkage effects).

3.4 Results for gauge steel joints

Gauge steel joints were manufactured using three adhesives: ESP 110, AV 119 and EC 3448 in all five different overlap configurations. Joints with the MY 753 adhesive were only made in the 25 mm overlap configuration. This is a total of 16 different joint configurations for joints with gauge steel adherends.

3.4.1 Strength results

The results are presented in tables 3.1, 3.2, 3.3 and 3.4 for ESP 110, AV 119, MY 753 and EC 3448 adhesives respectively. The same results can be found on figures 3.1, 3.2 and 3.3 for the three structural adhesives ESP 110, AV 119 and EC 3448 respectively. As the overlap increases the strength of the joints increases, but a plateau is again reached. It seems that further increase in the overlap length would not be of any significant benefit in the strength of the joints. The increase in strength for joints with longer overlaps is now larger compared with that of the mild steel joints.

The three different adhesives give joints of similar strength but with ESP 110 giving the lowest strength. The differences are again not significant and it appears that the adherend plastic deformation still controls failure.

Typical load displacement curves from tests using gauge steel adherends can be seen in figure 3.18 and figure 3.19 for the two different adhesives used. The initial yielding of the gauge steel adherends takes place at approximately 12-13 kN load. The higher strength of the gauge steel adherends in this case increases the strength of the joints almost by a factor of two compared to the mild steel joints (for long overlaps). It is useful to note that

the increase in strength is much more significant for the longer overlaps than for the shorter ones.

3.4.2 Failure mechanisms - modes of failure

Joints made of gauge steel behaved in a quite similar manner to those made with mild steel. Plastic deformation of the adherends was apparent, although much less than for the mild steel. Rotations of the overlap are also smaller in this case. These joints are stronger than the mild steel joints since gauge steel yields at a considerably higher stress.
Joints with different overlap lengths behaved in a similar way, although it must be noted that joints with longer overlaps were stronger.

A typical load-displacement curve for a SLJ made of gauge steel and EC 3448 adhesive is shown in figure 3.20. The initial part of the curve corresponds to the gripping of the specimen in the wedge grips, as in the case of mild steel. A load is reached where there is a slight deviation from linearity in the curve indicating the first signs of yielding in the adherends. At this point, there is no visible damage in the adhesive. Then, as the yielding progresses, there is a point where the curve becomes flat. This is because at this point different parts of the joint start to yield at the same time (two areas around the overlap edges and two areas around the grips). The steel then starts to work harden. At this point there is still no visible damage in the adhesive. A crack then forms through the fillet, as shown in figure 3.21. There is an instant small drop in the load at this point, but the load returns back to the same level almost immediately. This indicates that the fillet does not really contribute to the strength of the joint, since the load is transferred by the area near the edges of the overlap. It does, however, contribute slightly to the stiffness of the joint, thus the instant drop in the load. So this crack through the fillet is not a critical one for the joint strength. It must be noted however that sometimes cracks near the fillet's corner, similar to the mild steel case, were formed. This similarity is because both mild and gauge steel deform plastically but the plastic deformations are less severe for the case of gauge steel.

When the load reaches a maximum, the first cracks are very near the embedded adherend corner and the load suddenly starts to drop. Cracks propagate inside the overlap from both ends, close to the loaded adherend interface and catastrophic failure occurs. The final failure mode is very similar to the failure mode observed for the mild steel joint. Failure was usually symmetric, that is cracks run the same distance from both ends before catastrophic failure occurs. However, there were cases where the pattern was asymmetric, with cracks running more on one side. This is something that cannot be controlled and is attributed to the small variations in the strength of the two adherends or in the uniformity of the adhesive. The cracks will always initiate (and thus run a longer distance) from the side of the less strong adherend. This could be very important in cases where dissimilar adherends are used. The propagation of cracks is much faster compared to the case of mild steel since the whole event (initiation and propagation of cracks, as shown in figure 3.21) happens at a much higher load.

It must be mentioned here that the process of adherend yielding in the SLJ configuration is more complicated than that of the uniaxial test. This is because in a SLJ configuration we have a combination of tension and bending. In addition to that, the load-displacement curves in a SLJ test include all different parts of the joint, that could start yielding at slight different loads (two areas around the overlap edges and two areas around the grips). This is why direct comparisons between the shape of the stress-strain curve in a uniaxial test and the shape of a load-displacement curve in a SLJ configuration cannot be made. However, an explanation about the shape of the load-displacement curve has been given.
Joints with different adhesives behaved in a similar way. Again, the more ductile adhesives gave slightly stronger joints. The differences are again small, indicating that the adherend plastic behaviour still dominates the failure process.

3.4.3. Strain gauging gauge steel joints

In order to get a better understanding about the load and bending moment distribution around the overlap edges, strain gauges were bonded in the joints, as explained in section

2.4.1. Joints with the EC 3448 adhesive were strain gauged for all five overlap configurations.

The use of strain gauges in this case will give us useful information about the strain distribution in the adherends, especially the initiation of yield as well as the post yield behaviour of the joints. The effect of the overlap length could be investigated in more detail.

It is necessary to define some conventions that will be used when referring to the strain gauges. It was shown experimentally that when a lap joint is loaded in tension it will stretch and bend at the same time. As a result, one side of the adherend will initially be in tension while the other one will be in compression. The side that will initially be in tension will be referred to as the inner side and the strain gauge as the inner strain gauge. The other side, initially in compression, will be referred to as the outer side and the outer strain gauge respectively. So, as shown in figure 2.4, strain gauges 1 & 3 are symmetrical (inner) and 2 & 4 are symmetrical (outer).

The results shown in figure 3.22 are for all overlap configurations up to a load level of 10kN. This was done in order to increase the resolution on the graph at low loads, where the initiation of yield is happening.

As can be seen from figure 3.22, results show that for low loads (where the adherends remain elastic), the shorter the overlap the larger is the strain in the inner side of the adherends. The difference between the inner and outer strain gauges is also bigger for shorter overlaps, indicating that the bending moments applied at the ends of the overlap are larger for this case. If the 0.2% strain limit is taken for the adherend as a critical point (where gauge steel starts behaving perfectly plastically), then it is obvious from figure 3.22 that joints with 12.5 mm overlap will start yielding first followed by the 20 mm overlap at a higher axial applied load etc. At this moment the strains in the outer side of the adherends are still elastic and a quite steep strain gradient exists through the thickness of the adherends (the steepest is for the case of short overlaps).

A typical variation of strain in the adherends covering the whole loading range (up to failure) is shown in figure 3.23. After yield has initiated in the inner side of the adherend

the strains in the inner side increase dramatically with only a small increase in load. At the same time the strains start to increase significantly in the outer side. As higher percentage of the cross section enters the plastic zone, there is a point where the outer side of the adherends reaches the limiting values of strain. The cross section is therefore fully plastic at this point and large rotations occur. The strain readings from the two sides of the adherends are becoming equal indicating that the bending moments around the overlap edge (at the position where the gauges are placed) tend to zero due to the formation of the plastic hinge next to the overlap ends. The position where the strain gauges are placed is in a state of pure tension as a plastic hinge is formed very near the edge of the overlap. As the cracks progress inside, the position at which maximum bending occurs moves further inside the overlap (very close to the "crack tip" position). The bending moment distribution around areas where the initial maximum bending moment occurred, (i.e. the edge of the overlap), is gradually reduced as cracks propagate inside the overlap. This holds especially for longer overlaps where cracks propagate for some distance before catastrophic failure occurs.

It is very difficult to make comparison between the different configurations after the inner side of the adherends becomes plastic. Small variations in the behaviour of the metal or the adhesive uniformity cause quite big differences in the readings of the strain gauges for dissimilar cases. Due to these local differences failure is not always symmetrical (as it should be theoretically). This results in differences even between the two overlap ends of the same joint (indicating the asymmetry). For this reason, comparisons of the strain gauge readings between different overlap configurations after the initial yielding are not believed to be useful.

Nevertheless, the point in this case is that the plasticity of the adherends is the cause for all these. For low axial applied loads (where the adherends remain elastic), comparisons can be made for the different overlap configurations. The shorter the overlap, the lower the load at which the inner side of the adherends will yield and the bigger the bending moment is. As the plastic zone increases, then a plastic hinge is formed in all different configurations and strains are localised around the overlap edges.

Although the results and conclusions presented in this section are for gauge steel adherends, they could be applicable for mild steel joints or indeed for any type of adherend that would deform plastically under the same combinations of loading. The only differences would be that the lower the yield stress of the adherend, the lower would be the load at which the bending moments would start decreasing (at the position of the gauges) as the plastic hinges start forming around the overlap edges.

3.5 Results for hard steel joints

Hard steel joints were manufactured using three adhesives: ESP 110, AV 119 and EC 3448 in all five different overlap configurations. Joints with hard steel and the MY 753 adhesive were made for four overlap configurations. This is a total of 19 different joint configurations for joints with hard steel adherends.

3.5.1 Strength results

The results are presented in tables 3.1, 3.2 and 3.3 and 3.4 for ESP 110, AV 119, EC 3448 and MY 753 adhesives respectively. The same results can be found on figures 3.1, 3.2, 3.3 and 3.4 for the four different adhesives respectively.

A different behaviour can be seen for the hard steel joints compared to the mild and gauge steel results presented earlier. The increase in the strength of the joints is almost proportional to the overlap length. There is no definite plateau reached for the long overlaps. However, there is a tendency for a non-proportional increase for very long overlaps (above 40 mm). It seems that further increase in the strength of the joints could be possible by increasing the overlap length, but a limit should be expected because of the adhesive strength.

Comparing the strength of the hard steel joints with the mild and gauge steel ones it is clear that there is some gain for short overlaps, although this is not significant. The gain is much more significant though, for the longer overlaps of 40 mm or 60 mm.

Typical load-displacement curves from tests using hard steel adherends can be seen in figure 3.24 and figure 3.25 for the different adhesives used. As can be seen, the behaviour of the joints is linear to failure.

For the case of hard steel adherends the strength of the joints is different for the three adhesives used. The differences are quite clear compared to the case of mild or gauge steel joints. The MY 753 adhesive gives joints with the lowest strength followed by the ESP 110 and AV 119 adhesives, while the EC 3448 gives the strongest joints. The adhesive ductility is now the parameter governing strength. The comparison of joint strength between hard steel joints and the four different adhesives can be seen in figure 3.26.

An attempt was made to find out whether slightly harder metal adherends would give any stronger joints. A set of adherends was therefore tempered at a lower temperature, resulting in adherends with higher hardness. Joints were then manufactured and tested but results were similar to those of the "less hard" joints. The results can be seen in table 3.6 for two levels of Rockwell hardness.

As it is known, the hardness of a metal is a function of the yield strength. Once the yield strength of the adherends exceeds a certain limit, that would ensure the adherends remain elastic throughout the loading of the joints, then there is no further benefit from trying to increase further the yield strength of the adherends by further hardening. On the contrary, there are some disadvantages in creating very hard adherends. The metal becomes more brittle and more prone to cracking, especially around holes. The specimens become very difficult to grip on the tensile machine as the grips are now as hard as the adherends. Thus, the important point is that the adherends deform elastically throughout loading and not how strong the adherends are. Consequently, using even harder steel as adherends would be of no practical benefit and would not be justified.

It is useful to note here that when the overlap is short, i.e. 12.5 mm, then results from gauge and hard steel are similar. If even shorter overlap lengths are considered, then the strength of the joints is the same regardless of the adherends (mild, gauge or hard). This has been proved experimentally by W. van der Voorden (1995) for overlap lengths up to

5 mm. Thus, the lines shown in figures 3.1-3.4 are only curve fitting lines and are only valid for the range: 12.5-60 mm overlap. As will be discussed in later chapters, this is because for short overlap lengths the strength of the joints is controlled by the average shear stress under the overlap.

3.5.2 Fillet effect

For the hard steel case, joints without fillets were manufactured for the configuration of 25 mm and 40 mm overlap. The adhesive used was ESP 110. The comparison between the joints with and without fillets for this case can be seen in table 3.7.
Results from these tests show no differences in strength compared with the filleted joints. Variations only arise due to experimental scatter. Thus, the presence of a full depth spew fillet does not seem to influence the strength of the joints for this case.

3.5.3 Adherend thickness effect

One of the main advantages of adhesive bonding is the ability to join thin sheets of materials, thus producing efficient joints. The efficiency of a joint is usually defined as the ratio of the joint strength divided by the strength of the weakest of the adherends.

$$\text{Joint efficiency} = (\text{Joint strength}/\text{Strength of weakest adherend})$$

In a lap joint configuration, due to the eccentricity of the load path, the thicker the adherends the larger will be the bending moment induced at the edges of the joint.
An investigation into the effect of adherend thickness on the strength of lap joints was carried out. The 25 mm overlap configuration using hard steel adherends and AV 119 adhesive was chosen. Hard steel was chosen, instead of mild or gauge steel, as the former seems to be the most interesting case, since joint strength is controlled by the adhesive rather than the adherend behaviour. Three different adherend thicknesses were compared: 1, 1.6, and 2 mm. The effect of adherend thickness on the stress distribution on bonded

joints has been also investigated theoretically by Crocombe and Adams (1981), Chiu and Jones (1992) for the thick adherend joint configuration. They found that increasing the adherend thickness results in a reduction of the peak stresses at the edges of the overlap and a more even distribution of the shear stress in the adhesive layer.

Appropriate spacers were used for each configuration so as to keep the adhesive thickness constant at 0.1 mm (as with the results already presented). The free length was also kept constant at 63.5 mm. Joints with full depth fillets were manufactured for each case.

The results are presented in table 3.8 and can be also seen in figure 3.27. It seems that there is only a small difference between the three different cases. The lowest strength was obtained for the case of the 2 mm thick adherends while the highest strength was obtained by using the 1.6 mm thick adherends; the differences are however small. Thus, there seems to be no significant influence on the strength of the joints from the adherend thickness in the case of hard steel joints. As will be explained in later paragraphs, by bonding strain gauges on the adherends more information can be obtained about the load and bending moment distribution around the overlap edges. More conclusions could then be drawn using the additional information concerning the bending moment distribution for the different cases.

It is very interesting, however, to compare the efficiency of these joints. If the yield stress of 1810MPa is taken for the strength of the hard steel joints, then the efficiency can be calculated for each case. The results are shown in figure 3.28 and a linear decrease in the efficiency of the joints can be seen as the thickness of the adherends increases. This is very important when the weight of the bonded structure is of primary consideration, as is usually the case for the automotive or aerospace industry.

3.5.4 Failure mechanisms - modes of failure

For joints made with hard steel there was no plastic deformation of the adherends, and in all configurations, the adherends behaved as linearly elastic materials. The rotations around the edges of the overlap were small compared to the case of mild or gauge steel

joints. However, it is useful to investigate the effect of the bending moments around the overlap edges in the strength of the joints for this case, and also compare the different configurations.

The failure mechanisms in the case of hard steel joints are different to the ones presented previously and this is due to the different behaviour of the adherends.

Slight differences in the failure were noted for the different adhesives used. These differences mainly depend on how brittle or ductile the adhesive is (which is effectively controlled by the stress-strain behaviour and, in particular, the strain to failure of the adhesive). When an adhesive behaves in a brittle manner, then a crack will form and propagate until catastrophic failure occurs. The amount of brittleness of the adhesive will control how "sharp" the crack will be. When the adhesive has the ability to deform plastically then a plastic zone forms ahead of the "crack tip" creating a damaged zone. It has been mentioned by Hunston and Kinloch (1989) that tough materials owe their high fracture energies to their ability to generate crack tip deformation zones of significant size prior to fracture. This damaged zone can be viewed as a mechanism to suppress the onset of rapid crack growth, but the size of the zone must also grow as the load increases in order to maintain its effectiveness. As will be shown in the next paragraphs, and has been also noted by Papini & Fernlund (1994), fracture in modern toughened adhesive joints occurs by the development and propagation of a damage zone, rather than a single sharp crack. This is particularly true for modern toughened adhesives that have the ability to yield at high loads, thus deforming plastically without failing. Out of the four adhesives used in the current work, ESP 110 and MY 753 behaved in a brittle manner while AV 119 and EC 3448 behaved in a more ductile manner. For the case of ESP 110, cracks could be seen forming, while for AV 119 and EC 3448 adhesives, a "stress whitened" damaged area was visible instead of a crack. For the remainder of this section, the term "damage" will be sometimes used instead of "crack", as it describes the situation more realistically.

For joints made with hard steel, damage initiates around the embedded adherend corner (under the overlap) at the centre of the joint (in the width direction). The damage then spreads out to the fillet and inside the overlap. In the case of ESP 110, cracks appear in

the face of the fillet at the centre of the width of the joint, while in the case of AV 119 & EC 3448 the cracks take the form of a stress whitened damaged zone as explained above. Figure 3.29 shows some cracks in the case of ESP 110 adhesive, and figure 3.30 is a schematic of the same process for the more ductile adhesives. The reason why damage initiates at the centre of the width of the joint is attributed to the effect of anticlastic bending, Adams et al. (1996), which is illustrated in figure 3.31. As the adherends start to bend elastically, the middle part of the joint experiences extra through-thickness tensile stresses due to the anticlastic effect, while the edges seem to undergo into compression. It is well known that adhesives are stronger in compression than in tension: as a consequence, the middle of the joint is in a more critical condition.

Different conditions also apply at different parts of the joint. The middle of the joint is in a condition of plane strain while the edges (sides) are in a condition of plane stress. Theoretical analysis done by Heinrich (1997) and Adams *et al* (1998) has shown that in the middle of the joints there exist high hydrostatic tensile components of stress while at the edges high deviatoric components dominate. Consequently, cracks are more likely to develop from the middle part of the joint.

Kinloch and Shaw (1981) found that the fracture toughness G_{IC} in plane strain is less than the G_{IC} in plane stress conditions. The reason is because the tensile stress at which a material yields is greater in a triaxial stress field (plane strain) than in a biaxial stress field (plane stress) and thus in the former a more limited degree of plasticity develops at the crack tip, resulting in G_{IC} (plane strain) < G_{IC} (plane stress). This also suggests that cracks are more likely to form in the middle of the width of the joints.

The damage shown in the fillet face (figure 3.29, 3.30) is a result of the damage that initiates near the adherend embedded corner. Further evidence for that was given by noises emitted from the joints before any visible damage could be seen on the fillet face, something that was observed for hard steel joints with all four different adhesives.

Very useful conclusions were drawn from post failure observation of the broken joints. The broken surfaces were examined visually under a microscope and the patterns were correlated with failure mechanisms.

Three fracture regions have been recognised, for many years, depending on the surface roughness as observed by optical microscopy, Purslow (1986). The *mirror* region is smooth and featureless and normally surrounds the origin of failure and is associated with slow propagation as the incipient damage develops. A smooth matt region called *mist* follows as the fracture accelerates. This changes to *hackle*, a rough-textured surface of rapid damage growth. The speed at which the damage propagates is related to the fracture surface morphology, Roulin-Moloney (1989). The smooth regions correspond to the zone where damage (or cracks) is accelerating. The rough region corresponds to catastrophic failure (very fast damage growth - crack bifurcation). Many of the above features were found in the fractured single lap joints we tested in this investigation.

For the case of the two ductile adhesives there is an area very near the edge of the overlap, and around the embedded adherend corner, where "stress whitening" due to excessive deformation of the adhesive occurs (initiation of damage). This forms a "damaged zone" which spreads inwards through the overlap as the load increases (propagation of damage). At the same time damage spreads into the fillet (stress whitening of the fillet face figure 3.30). The propagation of damage inside the overlap follows a parabolic shape due to the anticlastic bending effect. Damage propagates faster in the centre rather than at the edges of the width of the joint. In the case of ESP 110, this shows up as dark and shiny patterns (figure 3.32) while, in the case of AV 119 & EC 3448, it shows up as a stress whitened area (figure 3.33). Then follows the rough-textured (hackle) area, which corresponds to catastrophic failure (very rapid damage growth). These three regions are not clearly distinguished from each other, but there is a gradual transition from one region to the other.

All joints made of hard steel failed in a catastrophic manner. As already said, noises were emitted in some cases before catastrophic failure, but no cracks were visible (apart from those referred to in figure 3.29) until failure occurred.

By observing the fractured surfaces of the joints, it was noted that the stress whitened area around the adherend embedded corner was bigger for longer overlaps. This means that longer overlaps can sustain more damage at the ends of the joint before catastrophic failure occurs.

Although the typical mode of failure is usually drawn as in figure 3.30, the failure is not interfacial but cohesive failure within the adhesive. Cracks run close to the interface, but adhesive remains bonded to both adherends. There is more evidence for this in areas away from the edges (i.e. closer to the middle of the overlap) where the "hackle region" dominates. Figure 3.34 shows schematically the process of cusp formation, in areas where the adhesive is loaded in shear.

Near the edges of the overlap, damage initially runs closer to the unloaded edge (figure 3.30 III) while, further away, it moves on the loaded adherend side before the "hackle region" is reached where adhesive is left on both sides of the adherends. There must be a strain / stress variation through the adhesive thickness causing this effect. Further evidence for that, will be given in a later chapter.

From results presented in section 3.5.1 it can be seen that the strongest joints in the case of hard steel, were with EC 3448 adhesive followed by AV 119, ESP 110 and MY 753. The increased ductility (strain to failure) is the possible reason for that. Parameters such as strain to failure (both in tension and shear) are critical values that should be looked at when comparing the performance of different adhesives. The maximum shear stress that an adhesive can sustain is another very important parameter controlling strength. More extensive discussion on that subject will follow in the next chapters.

3.5.5 Strain gauging hard steel joints

Joints with EC 3448 adhesive were strain gauged for all five overlap configurations for the case of hard steel adherends. In addition, joints with AV 119 adhesive and the three different adherend thicknesses in the overlap configuration of the 25 mm were also strain gauged.

As has already been shown, the adherends remain elastic throughout the loading of the joints. Therefore, the geometric effect of the overlap length on the load, bending moment distribution can be assessed for the whole loading regime.

The strain gauges used in this case were capable of measuring strains of up to 3 %, which was sufficient for the tests carried out. The gauge length of the strain gauges was 5 mm and they were placed as explained in section 2.4.1, and shown in figure 2.4.

It is important to recall here that the free length of the joints L_f was kept constant for every overlap used as described in section 2.2. This means that comparisons between the different overlap lengths are valid.

Results from experiments for all overlaps and the EC 3448 adhesive are presented in figure 3.35.

The amount of difference between the strain from the inner and outer strain gauge is directly related to the bending moment applied at the particular point of the cross section of the adherend under consideration and the average gives the applied tensile strain. It is obvious from figure 3.35 that for the same axial applied load, joints with longer overlap experience less bending. This is very important in understanding the load and bending moment distribution in single lap joints. This is a purely geometric effect, resulting from changing the length of the overlap, since all the rest of the parameters have been kept the same and there is no adherend plasticity.

A few experiments have been performed using other adhesives, such as ESP 110 and AV 119, to investigate the effect of the adhesive properties on the moment distribution (figure 3.36 and figure 3.37). Results showed that the distribution, for the same overlap, remained the same whatever adhesive used. The only difference in this case is the failure load, which is different, as already shown in section 3.5.1. Some small variations are well within the experimental scatter. The only point where some differences are visible is near the ends of the curves, as failure is approached (especially between EC 3448 and ESP 110). These differences are attributed to the different mechanisms that govern failure in each case. For joints with ESP 110 sometimes cracks were visible before final catastrophic failure of the joints, while in the case of EC 3448 no cracks were visible (as already discussed in section 3.5.4). This different behaviour causes the results to be slightly apart as the failure load is approached for the ESP 110 joints.

The bending moment distribution is therefore mainly affected by the adherend properties, geometric parameters, such as the overlap length, and is independent of the adhesive used. The only point where differences can occur is very near the failure load (the very end of the curves). As long as the load is transferred through the joint, the moment distribution will be governed by the length of the overlap and the properties of the adherend.

It must be mentioned here that all the adhesives compared were epoxy paste adhesives. If a very different type of adhesive (i.e. a much more compliant such as a polyurethane or acrylic) was used then results could be different.

Consequently, experimental strain distribution in the adherends should be the same for all adhesives used up to the failure load for each case.

3.5.6 Adherend thickness effect on strain distribution

It has been shown in the previous section that the bending moment distribution around the edges of the overlap is mainly governed by geometric parameters such as the overlap length and the adherend properties. The same technique will be used to investigate how the thickness of the adherends (for a given overlap length) affects the bending moment distribution and therefore the strength of the joints.

Three different adherend thicknesses were investigated: 1 mm, 1.6 mm and 2 mm. The adhesive used was the AV 119 and the same overlap was chosen: 25 mm. Strain gauges where bonded in similar position as described in section 2.4.1. Results are presented in figure 3.38. Comparisons can be made from the three different configurations. As would be expected, the overall stiffness of the joint increases as the thickness of the adherends increases. The difference between the inner and outer strain gauge readings is proportional to the amount of bending at the edges of the overlap, as has already been mentioned.

If comparisons between the joints with different adherend thicknesses are made it can be seen that the thinner the adherend, the less is the bending moment for a given axial applied load. This could initially lead to the conclusion that the thinner the adherend the

stronger the joint should be, because there is less bending moment at the edges of the overlap. However, the flexural rigidity of the joints should be taken into consideration. The thicker the adherend, the stiffer is the joint in flexure so the local curvature of the adherend is less. That means the adhesive has to deform less at the critical areas around the overlap edges. Thus, there is less peeling load for the thicker adherends and a more uniform shear stress distribution under the overlap.

Furthermore, as it will be shown in a later chapter (5) and also mentioned in section 3.5.4, joint strength is not controlled only by the conditions very near or around the overlap ends. The rest of the overlap should also be taken into account when predicting failure.

3.6 Discussion and conclusions

Results from tensile tests on different configurations of SLJ have been presented in this chapter.

For the case of the mild steel adherends, as the overlap increases there is some increase in strength but a plateau is reached quite quickly. The plastic deformation of the mild steel adherends controls failure. The large plastic deformations and rotations of the metal around the overlap edges introduce very high localised tensile stresses and strains in the adhesive. It is well known that adhesives are not particularly strong in peel so the joints made of mild steel adherends fail at a quite low load. The adhesive capabilities to transfer load have not been used to its full potential since the adhesive is mainly loaded in peel after the initiation of yield in the metal around the overlap ends. The overlap length changes the situation only slightly. As a result of increasing the overlap length, initial yield in the metal occurs at a slightly higher load, thus delaying the initiation of cracks in the adhesive. A 60 mm overlap joint made from mild steel adherends would not be justified since the gain in strength compared to the increase in the component weight and material use is not significant.

When gauge steel adherends are used, a similar situation holds. The strength of the joints increases as the overlap gets longer but again a plateau is reached. This plateau however is at a rather higher load. This is due to the increased yield strength of the gauge steel

compared to that of the mild steel. There some small gain in strength for the short overlaps but this is not significant. For longer overlaps though, a two-fold increase in strength can be seen compared with the mild steel joints. Plastic deformation of the adherends was apparent for this case as well, so again the adhesive capabilities have not been fully used. The behaviour of the adherends is still controlling failure.

In the case of hard steel, the adherends remain elastic. The strength of the joints increases almost linearly as the overlap gets longer and there is no plateau reached up to the 60 mm length tested. There is some gain in strength for the short overlaps (compared to the mild and gauge steel joints), but the significant increase in strength is for longer overlaps. A five-fold increase in strength can be achieved in some cases. The strength of the joint is now controlled by the adhesive, and the load transfer capabilities of the adhesive are now used to its full potential.

When the adherends deform plastically, the steel properties dominate failure, and this is the reason why only small differences in strength can be seen between the different adhesives used. The strength of the adhesive is not so important in this case. Any differences in the adhesive strength are over-shadowed by the plastic deformation of the adherends. This is because of the very high localised strains that the adhesive is subjected to, near the fillet's corner.

When the adherends remain elastic (hard steel case), then differences in strength can be observed between the various adhesives tested. The strongest joints are with the EC 3448 adhesive followed by AV 119, ESP 110 and MY 753. It seems that the more is the ability of the adhesive to yield at high levels of stress, the stronger will the joints be. So, increased ductility at high levels of stress is very important in the classification of adhesives. A very important parameter is also the maximum shear strength of the adhesive. This is why the MY 753 adhesive gives joints with such low strength.

Another important observation from the graphs is that the experimental scatter is significantly bigger for joints with hard steel and longer overlaps. This is because, for the case of hard steel, the strength of the joint is controlled by the adhesive itself. Errors in the preparation of the joints such as air bubbles, inclusions, joint misalignment, glueline thickness, curing schedule, etc. become more important. So it could be said that joints

made from "soft" steel adherends give more consistent strengths compared to those made from "harder" steel adherends. It must be mentioned here that great care was taken both in the preparation and testing of the joints so that the same conditions were met for every specimen tested. The importance of controlling the curing process in the scatter of the results has also been shown by Ikegami et al (1996). This information is particularly useful for industrial scale production where consistency in the strength of a manufactured product without the need for stringent controls is frequently wanted.

Experimental results for joints without fillets have shown that the presence of the fillets does not contribute significantly to the strength of the joints. The same conclusion can be drawn from the observations made during the failure of joints (sections on failure mechanisms: 3.3.3, 3.4.2, 3.5.4). As has been shown theoretically by Adams *et al* (1974), (1987) the fillets modify the stress field in the highly stressed regions of the overlap end. Most of this work, however, concentrated mainly in the distribution of stresses very locally around the edges of the overlap. The influence of local geometry on the strength of joints has been investigated by Adams & Harris (1987). The effect of the fillet in the local stress field is significant, but this does not necessarily mean that these local changes in the stress field will have a significant impact on the strength of the joints. It was also noted by Tsai and Morton (1995) that the very high (and sometimes physically impossible) stresses in the very localised region around the singularities may not dominate failure.

The results presented in this chapter, mainly for the case of the more ductile adhesives, imply that the local variations in the stress and strain distribution should not affect the global strength of the joints. In other words, if failure and strength of the joints is the matter under investigation, areas further away from the overlap ends must be taken into account. In section 3.5.4 it has been shown that a damage zone is formed under the overlap which spreads inwards through the overlap. The adhesive in the middle area of the overlap has been shown to fail mainly in shear (cusp formation). This means that failure of the adhesive bonds is progressive, and the area under the overlap is important in transferring the load and so should be taken into account. Similar conclusions were also drawn by Papini & Fernlund (1994). More data that support the above will be presented

in chapter 5. This conclusion however, cannot be generalised. Composite bonding for example is a completely different case. Work by Adams (1989), Adams *et al* (1986), Kinloch and Kodokian (1992) shows that fillets significantly improve strength in that case. This is due to the different mechanisms (interlaminar failure in the composite) controlling failure for the composite bonding case.

The use of strain gauges in lap joints gave a new insight. The bending moment distribution is very dependent on the length of the overlap. It seems that, when adhesives from the same family (epoxies in the particular case) are compared, there is no significant influence on the bending moment distribution from the behaviour of the adhesive. Thus, it is a geometric effect that changes the stress and strain distribution around the overlap edges. In the case of mild and gauge steel, where yielding in the metal occurs at a low load, the effect is to apply more peel for shorter overlap lengths and thus to initiate failure in the adhesive at a lower load.

For the hard steel joints, where the adherends remain elastic, the bending moment applied for a given axial load becomes much less as the overlap length increases. That means there is less peeling load near the edges and more load is transferred in shear. The area over which the load is distributed increases as the overlap gets longer. The combined effect is to get stronger joints as the overlap increases. The above results could be very useful in the design of bonded composite components, where there is a definite need for reduction of the local peel stresses developing at the edges of the overlap.

Results from the adherend thickness effect showed that the strength of the joints is not much affected, as long as the adherends remain elastic, despite the fact that the bending moment distribution (and thus the stress and strain distribution) around the overlap edges was different for each case. The area under which the load is transferred is the same for all three cases. This implies that the area under the overlap is more important when failure is considered, for the case of elastic adherends, and not the local variation of stress and strain around the ends. The efficiency of the joints is much greater for thin adherends, confirming the great ability of adhesives in joining thin sheets of material.

Clearly, from the design point of view, the most interesting case is when elastic adherends are used, so the adhesive capabilities to transfer load can be used to their full potential.

The mechanisms of failure are different depending on the configuration tested. Different critical areas need to be considered depending on the type of steel used. When "soft" adherends are used (mild and gauge steel), then failure is governed by localised peel mechanisms around the areas where maximum bending occurs, which is due to the large plastic deformations of the steel adherends and the resulting large strains from the rotations. On the other hand, when hard (elastic) adherends are used, failure is dominated by adhesive shear and a large area of the overlap should be taken into account for failure prediction. All this is very important when theoretical predictions for the strength of the joints is the aim.

Table 3.1 Results from tensile testing of SLJs with ESP 110 adhesive

Joints made with **ESP 110** Adhesive		
Overlap Length (mm)	Average Failure Load (kN)	Standard Deviation
Mild Steel Joints		
12.5	7.96	0.116
20	9.72	0.112
25	9.91	0.115
40	10.75	0.127
60	11.23	0.119
Gauge Steel Joints		
12.5	12.07	0.28
20	13.93	1.61
25	17.74	1.04
40	19.73	1.12
60	21.10	0.31
Hard Steel Joints		
12.5	14.82	0.827
20	19.01	0.937
25	23.44	1.05
40	32.39	1.55
60	43.26	1.65

Table 3.2 Results from tensile testing of SLJs with AV 119 adhesive

Joints made with **AV 119** Adhesive		
Overlap Length (mm)	Average Failure Load (kN)	Standard Deviation
Mild Steel Joints		
12.5	9.82	0.87
20	11.54	0.56
25	11.58	0.55
40	12.26	0.31
60	12.06	0.42
Gauge Steel Joints		
12.5	13.30	1.1
20	15.72	0.37
25	18.78	1.14
40	19.18	1.18
60	22.63	0.75
Hard Steel Joints		
12.5	15.01	0.88
20	23.17	1.96
25	30.76	1.59
40	43.09	2.38
60	53.58	3.05

Table 3.3 Results from tensile testing of SLJs with EC 3448 adhesive

Joints made with **EC 3448** Adhesive		
Overlap Length (mm)	Average Failure Load (kN)	Standard Deviation
Gauge Steel Joints		
12.5	15.72	0.96
20	17.71	0.92
25	18.38	0.12
40	19.37	1.32
60	19.52	0.32
Hard Steel Joints		
12.5	15.92	0.98
20	25.28	0.90
25	29.58	2.88
40	46.85	2.25
60	55.72	2.09

Table 3.4 Results from tensile testing of SLJs with MY 753 adhesive

Joints made with **MY753** Adhesive		
Overlap Length (mm)	Average Failure Load (kN)	Standard Deviation
Mild Steel Joints		
25	10.56	0.48
Gauge Steel Joints		
25	10.87	1.98
Hard Steel Joints		
12.5	8.79	1.37
25	13.76	3.06
40	18.80	1.43
60	21.86	1.36

Table 3.5 Results from tensile testing of SLJs with and without fillets using ESP 110 adhesive and mild steel adherends

Mild steel Joints with ESP 110 Adhesive - Fillet Effect				
Overlap Length (mm)	With 45° Fillet		Without Fillet	
	Av. Fail. Load (kN)	St. Deviation	Av. Fail. Load (kN)	St. Deviation
25	9.91	0.115	9.64	0.225
60	11.23	0.119	11.45	0.056

Table 3.6 Results from tensile testing of SLJs with ESP 110 adhesive and hard steel adherends of different hardness

Hard steel Joints with ESP 110 Adhesive - Effect of Hardness				
Overlap Length (mm)	54-56 RC		61-62 RC	
	Av. Fail. Load (kN)	St. Deviation	Av. Fail. Load (kN)	St. Deviation
12.5	14.82	0.827	14.44	1.32
20	19.01	0.937	19.18	0.77
25	23.44	1.05	22.92	1.32
40	32.39	1.55	33.01	1.27
60	43.26	1.65	42.63	2.42

Table 3.7 Results from tensile testing of SLJs with and without fillets using ESP 110 adhesive and hard steel adherends

Hard steel Joints with ESP 110 Adhesive - Fillet Effect				
Overlap Length (mm)	With 45° Fillet		Without Fillet	
	Av. Fail. Load (kN)	St. Deviation	Av. Fail. Load (kN)	St. Deviation
25	23.44	1.05	22.67	1.17
40	32.39	1.55	33.85	1.10

Table 3.8 Results from tensile testing of SLJs with 25 mm overlap, AV119 adhesive and hard steel adherends of different thickness

25 mm overlap Hard Steel joints		
Adherend Thickness (mm)	Average Failure Load (kN)	Standard Deviation
1	27.94	1.06
1.6	30.76	2.96
2	27.5	0.71

Chapter 4

FOUR POINT BEND TESTS ON SINGLE LAP JOINTS

4.1 Introduction

It has been shown in chapter 3 that bending moments play an important role in the strength of joints. It was therefore decided to investigate this further by conducting four point bend tests on SLJ.

Grant (1994) carried out four point bend tests using mild steel adherends and ESP 110 adhesive. Results from this reference show that when the adherends deform plastically, as is the case for mild steel, it is impossible in some cases to fail the joints in a four point bend test. The adherends deform locally around the supporting and loading points making it impossible to apply any significant amount of bending moment at the edges of the joints. The whole failure process is very dependent on the distance between the loading points and the overlap edges. When the loading points are at some distance from the overlap edges, there is small influence from the local deformation of the adherends and it is unlikely to fail the joint. When the distance gets very small (the load application is close to the overlap edge) the influence of the local deformation is great. The adhesive joint will fail without any significant amount of bending is applied to it, due to the large plastic deformations of the metal.

It is obvious that the adherend plastic deformation controls the strength of the joint in this case. No further useful information can be drawn and a way must be found to apply some significant amount of bending moment in the joint without increasing the local peel strains around the overlap edge.

This was the main reason why it was decided to perform four point bend tests on joints made of hard steel adherends. The adhesive chosen was AV 119.

The aim in a four point bend test is to apply a pure bending moment in a part of the specimen that includes the overlap. For the case of joints, the middle section including the overlap, will be in pure bending. However all this simplified approach is only valid for the case of small deflections, as given by Gere and Timoshenko (1987). When the deflections are large compared to the thickness of the adherend, the applied forces and reactions are no longer vertical. This alters the bending moment and induces axial and shear forces in the specimen. As a result of the rotation and slippage (due to friction effects) of the specimen in relation to the supports, the point of application of the applied forces changes as well. In our experiments, deflections of up to 11 mm were recorded. Considering that the loading span varies from 52.5 mm (for the shortest overlap: 12.5 mm) to 100 mm (for the longest overlap: 60 mm) and also the thickness of the adherends (ranging from 1.6-3 mm) these deflections must be considered large.

Some errors in the bending moment calculation will therefore be introduced if the simple theory approach is used.

Wisnom (1990) studied the effects and the errors imposed in the calculations of bending moments when the large deflections are not taken into account. If fixed loading noses are used rather than rollers, then friction may arise. The effect of friction is to reduce the actual bending moment applied to the specimen compared to what simple theory would predict. It was concluded that the combined effect of friction and large deflections can produce an error of the order of up to 5%.

4.2 Experimental variables - test rig

Joints with three different thicknesses of adherend were manufactured and tested in order to investigate the effect of adherend thickness on the strength of joints in bending. The adherend thicknesses used were 1.6 mm, 2 mm, 3 mm. For the case of the 1.6 mm thick adherends three different overlap lengths were tested: 12.5 mm, 25 mm, 60 mm. As it will be shown in the next section (4.3.1) the strength of the joints in bending did not seem to be affected by the overlap length, so it was decided to use only one overlap (25

mm) for the 2 mm & 3 mm thick adherend tests. The glueline thickness was kept constant at 0.1 mm, the same thickness as used for all the tensile tests.

As already mentioned, results from Grant (1994) lead us to the conclusion that the local deformation around the loading and supporting points could seriously affect the results. If comparisons between different geometries are to be valid, then the loading and supporting conditions should be the same for all configurations (figure 4.1). It was therefore decided to load all the joints at a constant distance of 20 mm from the edge of the overlap. The supports were placed at 30 mm distance from the loading points. This was achieved by using a four point bend rig (made of mild steel) with movable loading and supporting pillars as shown in figure 4.1. The noses of the pillars have a radius of 5 mm at the point of contact.

4.3 Results

4.3.1 Overlap length effect

Initially, joints using hard steel adherends of 1.6 mm thickness and AV 119 adhesive were manufactured. Three different overlap lengths where chosen : 12.5 mm, 25 mm, 60 mm to assess whether there is any effect from the overlap length. As mentioned earlier, the loading and supporting positions were kept constant in relation to the edges of the overlap. This was done in order to eliminate any spurious results due to the effects of local deformations around the loading points and around the overlap edges. In a four point bend test, the middle of the joint is under pure bending conditions. However, some amount of axial and shear force is present due to the non - linear effects introduced by the large deflections, as discussed above.

Results are presented in Table 4.1.

Table 4.1 Results form 4 point bending tests on SLJs with 1.6mm thick hard steel adherends, AV 119 adhesive and various overlap lengths

1.6 mm thick Adherend	Average Bending moment at failure (N m)	Standard Deviation
12.5 mm overlap	15.48	0.753
25 mm overlap	16.79	2.26
60 mm overlap	14.16	0.311

As can be seen there is no significant difference between the strength of joints with different overlap lengths in this case. However this is not surprising since the load transfer and rotations of the joint are happening in a very localised area around the edges of the overlap. Therefore, the overlap length is not expected to contribute to the strength of the joints in four point bending.

Typical load displacement curves are presented in figure 4.2. The steel adherends behave linearly elastically and the failure of the joint is catastrophic at the maximum load. As can be seen from figure 4.2, the joints with shorter overlap are slightly stiffer compared to the ones with longer overlap. This is because the distance between the loading points is larger for the longer overlaps as can be seen from figure 4.3.

4.3.3 Adherend thickness effect

Joints with 2 mm and 3 mm thick hard steel adherends were manufactured in order to investigate whether the thickness of the adherend would have a beneficial effect on the strength of the joints. It was concluded from the previous paragraph that the overlap length is not affecting the strength of the joints in bending. Consequently it was decided to use the 25 mm overlap configuration for the joints with thicker adherends. The rest of the geometry of these joints remained similar to the 1.6 mm thick joints. The results are presented in table 4.2.

Table 4.2 Results form 4 point bending tests on SLJs with 25mm overlap, hard steel adherends, AV 119 adhesive and various adherend thicknesses

Adherend thickness (mm)	Average Bending moment at failure (N m)	Standard Deviation
1.6	16.79	2.26
2	22.37	1.97
3	41.69	5.59

The strength of the joints has increased with the increased thickness of the adherends. The flexural rigidity of the joints is increased, and the local curvature around the edge of the overlap is less than in the case of 1.6 mm thick adherend joints. The joints can therefore sustain a higher bending moment before failure.

It can be seen that the strength of the joints in bending is almost linearly dependant on the thickness of the adherend. The thicker the adherend, the stronger the joint would be in bending as can be seen from figure 4.4. It seems that further increase in the strength of the joint in bending could be achieved by increasing the thickness of the adherend. Extensive discussion for the reasons will follow in section 4.3.4.

Typical load displacement curves for the different joint configurations can be seen on figure 4.5. It is obvious that the joint becomes stiffer as the thickness of the adherend increases.

4.3.3. Strain gauging the four point bend joints

Strain gauges were bonded on the adherends in a similar way as described in the tension tests (sections 3.4.3, 3.5.4). As already mentioned in section 2.4.1 the only difference is that because of space restrictions, due to the loading pillars, the strain gauges were placed at a distance of 7.5 mm from the edge of the overlap.

Results are presented in figure 4.6 for the 1.6 mm thick adherends, three different overlap configurations. As can be seen from figure 4.6, there is hardly any difference between the three different configurations other than normal experimental scatter. This leads us to the conclusion that the overlap length is not affecting in any way the load / bending moment distribution in a four point bend test, which confirms why the strength of the joints with different overlaps is also similar.

For the thicker adherend tests, 2 mm and 3 mm, the configuration of 25 mm overlap was chosen. Results for all three thicknesses and 25 mm overlap length are presented in figure 4.7. It is clear that the thicker the adherend, the stiffer the behaviour of the joint becomes and the stronger the joint is in bending.

Symmetry between the strain gauges being in the tension side and those in compression is apparent for every configuration tested (fig. 4.6 & 4.7), which is to be expected for properly calibrated and installed gauges.

4.3.4 Failure mechanisms - modes of failure

Due to the geometry of the lap joint, in a four point bend test, one end of the joint will always be in tension while the other one will be in compression. Since adhesive materials are stronger in compression than they are in tension, failure is always expected to start at the side of the joint that is in tension. In the four point bend tests carried out, there was quite a large amount of deflection exhibited by the adherends, which was however within the elastic limits of the material (hard steel). As a consequence of the large bending of the adherends, the effect of anticlastic bending should be very important in this case.

As expected, failure always starts from the side that was in tension and propagates towards the side that is in compression. The propagation of cracks is very close to the top adherend interface. The process is illustrated in figure 4.8. Damage initiates in the middle of the width of the joint very close to the adherends embedded corner (as in the case of the tension tests) and spreads inside the overlap. Again there is an area very near the adherend embedded corner where adhesive stress whitening is very visible (figures 4.9-

4.11). Damage propagates inside the overlap, forming parabolic shaped cracks, indicating that the anticlastic bending effect is dominating the failure in this case. All the above can be very clearly seen in failure patterns shown in figure 4.9 & figure 4.10. There is always some subcritical damage growth corresponding to the stress whitened area shown in figure 4.10 before catastrophic failure occurs.

Neither the overlap length, nor the different adherend thickness used in the four point bend tests seemed to alter the mode of failure.

There was one case in which the joint failed catastrophically up to a point and some arrest lines were formed. This joint is shown in figure 4.11. The load reached a maximum at which point failure occurred and ran up to the point where the arrest zone is. The load recorded by the testing machine dropped sharply. The joint was still connected by the remainder of the overlap. As the test is displacement controlled the load started to increase in the joint as the loading points kept moving. Before the load reached the previous maximum load, the test was stopped and the test piece was left under a constant load for a few seconds. Catastrophic failure occurred soon after without any further loading applied to the joint. This is an indication that when damage grows subcritically, stress whitening of the adhesive occurs, indicating a slow yielding process. This incident was a one-off event, but it gives useful information about the failure patterns observed in different cases.

Although the joints loaded in four point bending are supposed to be under pure bending (between the loading points), shear forces arise due to the large deflections that occur in such a test. This situation is also enhanced if the friction effects between the loading points and the surface of the specimen are taken into account. In a joint configuration the adhesive layer (relatively low stiffness material) is sandwiched between two metal adherends of comparatively a lot higher stiffness. Due to the large deflections that occur in a four point bend test shear stresses arise in the adhesive layer especially at the edges of the overlap, as illustrated in figure 4.12. These shear stresses are opposite signs at the two overlap ends.

A closer look at the broken surfaces of the four point bend tests showed that cracks in the adhesive layer, which appear a bit further inside the overlap edge, are forming at approximately 35° to the surface of the adherends, depending on the thickness of the adherends. The thinner the adherends, the more is the curvature at the ends of the joints, and the more inclined (larger angles) are the peel loads at the tension side of the joints. So, the thinner the adherends the smaller is the angle at which cracks form in relation to the adherend surface. The direction of maximum principal stresses, which should be at right angles to the cracks, must be at approximately 55°. This is due to the contribution from the peeling stresses introduced by the bending, effectively increasing the angle of the load path. All these, are of course, happening a short distance away from the overlap edge. Very near the overlap edge, we have the stress whitened zone as already seen is figures 4.9, 4.10, and the direction of principal stresses should be at even higher angles. As the load increases, the overlap area tends to bend, as illustrated in figure 4.12, and due to the high difference between the stiffness of the adhesive and the metal adherends shear stresses develop along the overlap. It is believed that the combination of the tensile peel and shear stresses are responsible for the first cracks to appear. After the first crack appears on the tension side of the joint, unstable crack propagation is created leading to the failure patterns shown in figure 4.9, 4.10. Figure 4.13 illustrates the failure mechanism for the case of the four point bend tests in general.

The thinner the adherend, the higher the peel stresses (and the higher the angles of peel) will be at the tension side, where failure initiates. Joints with thicker adherends should therefore be stronger, as a qualitative conclusion. This is in agreement with the results from experiments.

4.4 Discussion and conclusions

The different behaviour of adhesives when loaded in tension or compression is clearly demonstrated in the four point bend tests. Failure always starts at the end where the adhesive is loaded in tension.

The effect of anticlastic bending is clearly demonstrated with the curved cracks appearing in the fractured surfaces.

The length of the overlap has no significant effect on the strength of the joints. This is because the load transfer is happening in a very localised area around the edges of the overlap. Some amount of subcritical damage (corresponding to the stress whitened areas) can always be seen before catastrophic failure occurs.

Four point bend tests showed that joints are capable of withstanding significant amounts of bending moments, typically between 15-30 N m depending on the adherend thickness. Large deformations of the joints occur and the thickness of the adherends strongly affects the strength of the joints. The thicker the adherend, the more bending the joint can withstand. This is directly related to the amount of curvature in the adherends near the overlap edges. Failure will initiate when the amount of curvature is such that the adhesive cannot sustain the strain, especially the through thickness (peel) strains. Grant (1994) has used the term critical bending moment that an adhesive joint can withstand. It seems there is no such thing as critical bending moment for an adhesive since everything depends on the adherend thickness as well. So this term could only be used if similar geometric and material configurations are compared. The local deformation of the adherends around the overlap edges seems to control failure, so the distance of the loading points from the overlap edge is also very important.

Failure in the four point bend tests is governed by peel mechanisms, with the peel and principal stresses and strains around the overlap edge that experiences tension being the critical variables. Failure is more dependent on local stress and strain distributions around the overlap ends compared to the tensile tests where large areas under the overlap must be taken into account, thus the independence of strength on the overlap length for this case.

Chapter 5

JOINTS WITH ARTIFICIAL DEFECTS

5.1 Introduction

Any manufacturing process will inevitably introduce some number of defects in the end product. It is almost impossible to produce an error free joint even under stringent controls. Entrapped air, foreign bodies, grease or dirt create disbonds in the joint. No load can be transferred through areas that are disbonded. Consequently, load has to be transferred through alternative neighbouring paths, increasing the amount of stress in these areas. It is important to know how these defects could affect the strength of the bonded component. Non-destructive techniques capable of identifying defective areas could then be used, and the strength of the defective components could be estimated.

The effect of adding artificial defects on the strength of joints (SLJ), tested in tension and bending, will be investigated in this chapter.

Schonhorn et al (1972) have found that the strength in tension of a single lap joint, containing a brittle adhesive (two-part epoxy: DER332LC), is governed essentially by the leading edges of the joint. In effect, creating a disbond at the centre of the overlap should not alter the strength of the joint significantly. In another publication, Schonhorn et al (1971) concluded that when a relatively flexible adhesive (low-density polyethylene) was used, then the tensile strength of joint is not governed by edge effects but rather by the bonded area. It has to be mentioned here that the terms "brittle" and "ductile" adhesive are very relative. Unless tensile and/or shear data are available, no direct comparisons can be made. Unfortunately, in both the above publications, only maximum limiting values of the adhesive properties used are quoted, so accurate direct comparisons cannot be made. The values quoted for the brittle adhesive was Young's Modulus E=1.59 GPa, fracture strength 63.45 MPa, strain to failure 5%, while for the ductile adhesive E=0.138 GPa.

In both of these published works, aluminium alloy (2024-T3) adherends were used. The yield strength of 2024-T3 aluminium alloy is 330 MPa which is quite similar to that of gauge steel presented in chapter 2. It must be noted however that the aluminium alloy will have a much lower modulus, typically 1/3 that for the steel one. As a consequence, for the same applied stress, the strains in the aluminium adherends will be larger compared to the strains in the gauge steel adherends. It was mentioned in the papers that yielding in the aluminium adherends was apparent in some cases. As we have already shown in chapter 3 the plasticity of the adherends can greatly affect the strength and behaviour of the joints. Spurious results could therefore occur when parameters, such as yielding of the adherends, are not taken into account.

The effect of defects on the strength of joints with various adherend and adhesive materials must therefore be investigated further. Part of this work was done by A. Machon (1998) and H. Knabel (1998), as part of their 3rd year project under the author's supervision.

5.2 Experimental variables - configurations

Modern structural adhesives, such as the ones used in the current work (presented in section 2.3.2) do not fall into either of the two categories mentioned in the introduction (brittle / ductile). The main difference is that most of the structural adhesives used nowadays are toughened. So a similar experimental procedure was carried out to assess the effect of a debond on the strength of SLJ using initially adhesive AV 119. The ESP 110 and the MY 753 adhesives, were used later in selected joint configurations to study the effects of defects when the adhesive is more brittle.

Hard steel was mainly used as the adherends, but gauge and mild steel were also used in some cases in order to prove that results could be significantly altered when the adherends deform plastically. The adherend thickness was 1.6 mm for all cases.

The 25 mm overlap configuration was mainly used although some tests with the 40 mm overlap configuration were also carried out.

The adhesive thickness was kept the same at 0.1 mm as in the tests presented in chapters 3&4. The geometry of the joints was the same as described in chapter 2.

Two types of defects were tried, circular and rectangular. For the rectangular shaped defects, two overlap configurations were tested (25 mm and 40 mm), while for the circular shaped defects only the 25 mm overlap configuration was tested.

The defect is effectively a thin film of Teflon placed in the middle of the overlap, thus creating a disbond of the required size. The rectangular size defects cover the whole width of the joint as can be seen from figure 5.1 The circular defects only cover a portion of the width (depending on the diameter) and the configuration can be seen in figure 5.2. The defect sizes are summarised in the following tables:

Table 5.1 Dimensions of rectangular type defects used

Rectangular shaped defects

R= Rectangular

Overlap	Defect R (I)		Defect R (II)		Defect R (III)	
	% of overlap debonded	Debonded Area (mm^2)	% of overlap debonded	Debonded Area (mm^2)	% of overlap debonded	Debonded Area (mm^2)
25 mm	24	148.8	48	297.6	64	396.8
40 mm	30	297.6	45	446.4	60	595.2

Table 5.2 Dimensions of circular type defects used

Circular shaped defects

C= Circular

25 mm overlap configuration							
Defect C (I)		Defect C (II)		Defect C (III)		Defect C (IV)	
% of overlap debonded	Debonded Area (mm2)	% of overlap debonded	Debonded Area (mm2)	% of overlap debonded	Debonded Area (mm2)	% of overlap debonded	Debonded Area (mm2)
23.43	145.26	27.00	167.41	47.18	292.55	59.10	366.43

The total bondable area for the case of 25mm overlap is 620 mm^2 while that of the 40 mm overlap configuration is 992 mm^2.

5.3 Defective joints - AV 119 adhesive

5.3.1 Joints with hard steel adherends in tension

For the hard steel case both rectangular and circular type of defects were tested. Two overlap configurations, 25 mm and 40 mm, were mainly tested for the rectangular shape defects. Only the 25 mm configuration was tried for the circular shaped defects. The 60 mm overlap configuration was also tested with a medium size [R (II)] rectangular defect only.

Results are presented in figure 5.3 and figure 5.4 (also tables 5.3, 5.4, 5.5 and 5.6) and are compared with joints without any artificial defect (from chapter 3).

It is obvious that the strength of the joints is not governed by edge effects, but rather by the bonded area. There is a slightly non-linear reduction in strength as the size of the defect increases. Both 25 mm and 40 mm overlap configurations follow the same trend and they seem to converge to the point of no strength for 100% of the overlap debonded. The shape of the defect does not seem to affect strength from the comparison between the two types of defects in figure 5.4, but it is only the bonded area that controls strength.

Although there is only one experimental point available for the case of the 60 mm overlap the result clearly indicates that a different situation exists at least for small size defects. When a relatively small part (approximately 20% of the overlap) is removed from the middle of the overlap, the strength of the joint remains unaffected. Thus, for very long overlaps it is only part of the overlap that is effectively carrying the load. This is very important, because it implies that for very long overlaps there must be a part in the middle of the overlap that is still in the elastic state when failure occurs. A limit in the increase in the strength of the joints, as the overlap length increases, must therefore be expected even for joints made with hard steel adherends. For larger defect sizes, a linear decrease in strength should be expected as is the case for the 40 and 25 mm overlap case.

Table 5.3 Results from tensile tests on defective SLJs with 25 mm overlap, hard steel, AV 119 adhesive and rectangular type defects

Hard Steel - AV 119 - 25 mm overlap		
Rectangular defects	Average Failure load (kN)	Standard Deviation
Defect R (I)	25.16	1.33
Defect R (II)	17.97	1.77
Defect R (III)	12.72	0.84

Table 5.4 Results from tensile tests on defective SLJs with 40 mm overlap, hard steel, AV 119 adhesive and rectangular type defects

Hard Steel - AV 119 - 40 mm overlap		
Rectangular defects	Average Failure load (kN)	Standard Deviation
Defect R (I)	36.30	1.06
Defect R (II)	30.82	0.47
Defect R (III)	22.24	0.66

Table 5.5 Results from tensile tests on defective SLJs with 25 mm overlap, hard steel, AV 119 adhesive and circular type defects

Hard Steel - AV 119 - 25 mm overlap		
Circular defects	Average Failure load (kN)	Standard Deviation
Defect C (I)	24.56	0.48
Defect C (II)	23.71	1.37
Defect C (III)	16.82	1.05
Defect C (IV)	14.10	0.22

Table 5.6 Results from tensile tests on defective SLJs with 60 mm overlap, hard steel, AV 119 adhesive and rectangular type defects

Hard Steel - AV 119 - 60 mm overlap		
Rectangular defects	Average Failure load (kN)	Standard Deviation
No defect	53.58	3.05
Defect R (II)	53.14	3.46

5.3.2 Joints with hard steel adherends and in four point bending

Joints with AV 119 adhesive and hard steel with various defect sizes were also tested in four point bending. The configurations tested were those of 25 and 40 mm. The results are presented in tables 5.7 and 5.8, also figures 5.5 and 5.6 for the 25 mm and 40 mm overlap configuration respectively.

Table 5.7 Results from 4 point bend tests on defective SLJs with 25 mm overlap, 1.6 mm thick hard steel adherends, AV 119 adhesive

Defected Area (mm^2)	% of overlap Debonded	Average Failure Load (kN)	Standard Deviation
0	0	1.119	0.151
223.2	36	0.929	0.191
421.6	68	0.959	0.209
520.8	84	0.730	0.110

Table 5.8 Results from 4 point bend tests on defective SLJs with 40 mm overlap, 1.6 mm thick hard steel adherends, AV 119 adhesive

Defected Area (mm^2)	% of overlap Debonded	Average Failure Load (kN)	Standard Deviation
0	0	0.821	0.085
297.6	12	0.743	0.113
595.2	24	1.02	0.057
793.6	32	0.727	0.055

Results show that the defect size is not important in the strength of the joints. This is in agreement with the results obtained from the normal joints of various overlaps in section 4.3.1. This is because failure in the four point bend case is governed by the local stress conditions at the areas around the overlap length, as we have already seen in section 4.3.4

5.3.3 Strain gauging defective joints with hard steel and AV 119 adhesive

Strain gauges were also bonded onto some of the specimens tested in tension (similar procedure to the one described at section 2.4.1) and the results are compared with the normal joints (figure 5.7). As can be seen from figure 5.7, there is no difference between the different configurations other than normal experimental scatter. This means that the distribution of bending moments remains the same for the defective and normal joints. This implies that the bending moment distribution around the overlap edges is mainly dependent on geometric effects (overlap length). This is in agreement with results and conclusions presented in chapter 3. The results also mean that, in the case of hard steel joints, the effect of the bending moment on the strength of the joints is not significant and that failure is not controlled by the local stresses and strains around the overlap edges, but also from the remainder of the overlap.

The above results can be very useful when failure mechanisms are considered and failure criteria are sought for strength predictions of joints.

5.3.4 Joints with mild steel adherends in tension

It has already been shown in chapter 3 that the adherend plasticity strongly affects the strength of joints. It was decided to investigate the effect of adherend plasticity on the strength of defective joints. Joints similar to the ones described in figure 5.1 (with rectangular shaped defects) were manufactured using mild steel adherends, AV 119 adhesive and the 25 mm overlap configuration. Only tensile tests were carried out for this case.

Results from the tensile tests are compared with normal joints and are presented in figure 5.8 and also table 5.9.

As can be seen from figure 5.8, the presence of defects has no effect in the strength of the joints. Only when the defect size exceeds 64% of the total overlap can a slight decrease in

the strength be noticed. It seems that, in this case, the edges of the overlap are the most important part of the joint. Therefore, failure is dominated by edge effects rather than the bonded area.

Table 5.9 Results from tensile tests on defective SLJs with 25 mm overlap, mild steel, AV 119 adhesive and circular type defects

Mild Steel - AV 119 - 25 mm overlap		
Rectangular defects	Average Failure load (kN)	Standard Deviation
Defect R (I)	11.82	0.232
Defect R (II)	11.93	0.308
Defect R (III)	10.89	0.841

It is very interesting to observe the load-displacement curves for the different cases (figure 5.9). A maximum load is reached in each case and the curves then flatten out. The amount of displacement that the joints can sustain without failing is proportional to the amount of adhesive present in the joint (or inversely proportional to the size of the defect). At that point the joints start peeling off under a nearly constant applied load. The more adhesive that exists in the overlap area, the more the joint can extend without failing catastrophically. There is a very important practical aspect behind this observation in the design and safety of bonded structures. Although the ultimate strength of a joint with a large and a small defect will be the same, for the case of mild steel joints, the joint with a smaller defect size will fail in a less catastrophic manner. This could be very important in situations where large damages without total collapse is the designer's aim, such as in crash situations. Although the strength of a joint with a small defect is approximately the same as that for a joint with a larger defect, the energy that the former (small defect) joint can absorb is much greater.

Similar observations were made in chapter 3 for mild steel joints with increasing overlap length. Some similarities exist between these cases and results presented by Crocombe & Adams (1981), (1982) regarding the peel test, where propagation of failure occurred at a critical bending moment applied for a particular adherend and adhesive.

So, the plasticity of the adherends could seriously alter the results. Effects such as this should be taken into account before conclusions about the effect of defects on joints are made. Schonhorn et al (1972), showed that the strength of a SLJ in tension is governed by the leading edges of the joint. These results could arise because the adherend materials they used could deform plastically throughout the loading regime of the joints and not because of the adhesive properties.

5.3.5. Joints with gauge steel adherends in tension

In the work published by Schonhorn et al, the adherends material used has similar yield strength to the gauge steel used in the current work. It was decided to manufacture joints with circular defects so that more direct comparisons could be made. Two sizes of defects were chosen this time, defect C (I) & C (III) from table 5.2. Only tensile tests were carried out. Results can be found in table 5.10 and are compared with those of the normal joints in figure 5.10.

Table 5.10 Results from tensile tests on defective SLJs with 25 mm overlap, gauge steel, AV 119 adhesive and circular type defects

Gauge Steel - AV 119 - 25 mm overlap		
Circular defects	Average Failure load (kN)	Standard Deviation
Defect C (I)	18.88	0.11
Defect C (III)	16.78	0.58

In all the tests carried out there was evidence of adherend plastic deformation, as in the case of mild steel. As can be seen, the behaviour of the joints is similar to that of the mild steel adherends. The effect of adding a debond in the middle of the joint has only a small effect on the strength of the joints. It is quite clear that the strength of the joints is controlled by edge effects rather than by the bonded area for this case. When the defect size is less than 30-40 % of the total overlap, then the reduction in strength is not

significant. Some reduction in strength will only be achieved if the defect size is much larger, above 50% of the overlap. The plasticity of the adherends must again be the main reason for that behaviour.

5.3.6 Failure mechanisms - modes of failure

For joints with mild and gauge steel, plastic deformation of the adherends was apparent, as in the case of normal joints discussed in chapter 3. The failure mechanisms and modes of failure were also the same. Plastic deformation of the adherends is again the dominant factor for failure.

The mechanisms of failure for the hard steel defective joints were similar to the normal joints discussed in chapter 3. Stress whitening of the adhesive occurs again at the edges of the overlap, and a rougher texture (hackle) appears near the areas where the artificial defect is (that is for circular defects in which case adhesive is still present at the centre of the overlap). For the joints with rectangular defects the hackle area appears next to the defect areas. As can be seen from the results presented in section 5.3.1 and figure 5.3 for the case of hard steel joints, it seems that load is not only carried by the edges of the overlap. The middle part of the overlap is also important, giving the almost linear decrease in strength as the defect size increases. The adhesive limiting values, which control failure, must be exceeded over a large area of the overlap (sometimes the whole area, depending on the overlap) for failure to occur.

For many years, researchers, such as Hein and Erdogan (1971), Delale (1984), Groth (1988), and Weissberg (1992) have addressed theoretically the importance of stress and strain singularities on bi-material interfaces such as found in bonded joints. In a real situation, however, singular points such as sharp corners do not exist. Furthermore, experimental evidence shows that although locally the stresses and strains may become singular, there is no real effect on the overall strength of joints. The influence of local geometry on the strength of bonded joints has also been studied by Harris (1987). It was concluded that local changes in the geometry around singular points, such as sharp corners, reduce the peak values of stresses, which may lead to strength improvement.

Results presented in this section however, seem to contradict the above. It seems that the local peaking of stresses at the edges of the overlap is not what controls failure. Otherwise, joints with large or small defects should give the same strength for the case examined (hard steel adherends). Local peaks of stresses will exist under the overlap, especially near the edges, but their effect on the strength of the joints may not be always significant, as seen in the case of tensile loaded hard steel joints. The effect of the singularity seems to become less important in this case, and values further away from the corners should be taken into account.

Global yield as a failure for bonded joints was proposed by Crocombe (1989). Failure is predicted when a part of the adhesive along the overlap region reaches the state in which it can sustain no further significant increase in applied load. As mentioned by the author, the method works well when the loading is a shear type one.

Results presented in this chapter show that a similar failure criterion should be applied in the case of hard steel joints loaded in tension. As more and more of the middle part of the joint is lost (increasing defect size), then more load has to be transferred by the remaining overlap and a point is reached where catastrophic failure occurs. The failure process must be as follows, illustrated in figure 5.11. Initially, as the joint is loaded, most of the load is transferred through the ends of the joint. Gradually the volume of material which is around this area enters the yield zone (i.e. this volume of material starts to yield, and the effective modulus of the material drops as defined by the stress strain characteristics of the adhesive material). At the same time, the material away from the overlap edges has different properties, since the loading conditions are not the same as further inside the overlap. Due to the lack of homogeneity of the material properties under the overlap, the load transfer is now happening further inside the overlap, where the adhesive material is stronger. The volume of the material around the overlap edges reaches a point where it is yielding extensively and doesn't contribute to the strength of the joint, the joint being held by the remainder of the overlap. This process continues until the critical limits of the adhesive material are exceeded for the majority or the whole length of the overlap. Tsai and Morton (1995) have also commented on the stress singularity and they concluded that an approach based on average stress value, rather than the very high localised stresses

around the singular points, may be one alternative to guide engineering design. Further investigation on the above will follow in the theoretical analysis chapters.

From post failure observation of the hard steel joints (section 3.5.4), we have seen that the middle part of the overlap is dominated by the "hackle area". This pattern (hackle), is typical of the shear mode of failure, indicating that the critical shear values control failure in that area (away from the overlap edges). So, in any theoretical analyses, the adhesive limiting values must be exceeded over a large volume of material (possibly the whole of the overlap length) for failure to occur.
The above analysis could be an explanation, as to why the strength of the joints decreases almost linearly with increasing defect size.

5.3.7 Discussion and conclusions from the AV 119 adhesive joints

It is very interesting to plot the results from all different adherend configurations on the same graph (figure 5.12.). We can clearly see that results from different configurations converge to the same values as the defect size becomes very big (approx. above 65% of the total bondable area). This is in effect an inversion of what we get if we plot the strength of the joints as the overlap increases (chapter 3). It is now clear how the adherend properties affect the joint strength in a defective and normal joint configuration. When hard steel is used, there is an almost linear decrease (slightly non linear). In the case of gauge steel, there is no significant effect up to the point that the defect size is approximately 40% of the total area, for the 25 mm overlap joints. When the defect size gets bigger, then a non linear decrease in strength should be expected. For joints with mild steel, a similar behaviour is seen. The joint strength is not affected up to the point where the defect size becomes approximately 50% of the total length (for a 25 mm overlap), where a non linear decrease in the joint strength is apparent.

The rate at which the joint strength is decreasing is largely dependent on the behaviour of the adherends. The higher rate is for the hard steel, followed by the gauge and mild steel.

This is equivalent (but in reverse order) to the "plateaus" we have seen in the case of mild and gauge steel for increasing overlaps in chapter 3.

These results imply that for the case of hard steel, the stress distributions throughout the joint is such that load is transferred through the whole overlap length. This means a fairly even distribution of load transfer along the overlap length. This is why any defect present in the middle of the joint will have a direct influence on the strength of the joints. On the other hand, when gauge or mild steel joints are concerned, the stress distribution is such that more load is transferred through the ends of the overlap. So, there is a less even distribution of load transfer along the overlap in this case. This is because of the large rotations and plastic deformations that occur at the ends of the overlap. Thus, the middle of the overlap becomes less important, since most of the load is now transferred by the ends of the overlap, once the adherends start to yield extensively around the overlap ends. A defect in the middle of the overlap area now will not alter the strength of the joints significantly, since not much load is transferred through that area of the joint.

5.4 Defective joints with ESP 110 adhesive in tension

A more brittle, but still strong structural adhesive, was used next in order to assess the effects of debonds on the strength of joints for this case. The ESP 110 adhesive was used this time in the 25 mm overlap configuration and hard steel adherends.

Rectangular type defects of four different sizes were used. Results are presented in table 5.11 and also Figure 5.13.

Table 5.11 Results from tensile tests on defective SLJs with 25 mm overlap, hard steel, ESP 110 adhesive and circular type defects

Defected Area (mm^2)	% of overlap Debonded	Average Failure Load (kN)	Standard Deviation
99.2	16	22.91	0.53
148.8	24	21.87	0.43
248	40	18.82	0.76
372	60	14.61	1.48

The behaviour of these joints is different to that of joints made with the AV 119 adhesive. For small size defects (approximately 16% of the overlap) the strength of the joints is not significantly affected. For larger size defects the strength decreases in almost a linear fashion with increasing defect size.

So, in the case of a more brittle adhesive, such as the ESP 110, the edges of the joint are becoming more important compare to a more ductile adhesive. However the bonded area is still important too, especially as the defect size get larger.

5.5 Defective joints with MY 753 adhesive in tension

Joints with the MY 753 adhesive were then manufactured. As it has already been stated in chapter 2 this is not a structural adhesive in the actual sense, since it is quite brittle and considerably weaker than the other three adhesives used in the current work. These tests will provide information as to how the adhesives behaviour could alter the dependence of joints strength on the defect size, for different cases. Only the 25 mm overlap configuration was chosen and the shape of the defects was circular in this case (as shown in figure 5.2). Two different sizes of defects were chosen; that of C(I) and C(III) shown in table 5.2. Some more comparisons between the current work and results published by Schonhorn et al (1972) can now be made.

5.5.1 Joints with hard steel adherends

Results for the case of hard steel adherends are presented in table 5.12 and figure 5.14. Due to the very brittle nature of the adhesive, the experimental scatter was quite big. That was something that could not be controlled. Nevertheless, results from figure 5.14 show that as the defect size gets larger, the strength of the joints is decreasing only slightly. It seems that with the very brittle adhesive systems, the strength of the joint is governed mostly by the leading edges of the joint, rather than the bonded area. It must be noted here

that the strength of these joints is considerably less compared to the corresponding joints made with the AV 119 or ESP 110 adhesive.

Table 5.12 Results from tensile tests on defective SLJs with 25 mm overlap, hard steel, MY753 adhesive and circular type defects

Hard Steel - MY753 - 25 mm overlap		
Circular defects	Average Failure load (kN)	Standard Deviation
Normal	13.81	2.29
Defect C (I)	10.38	2.24
Defect C (III)	8.62	1.08

These results seem to be in agreement with results published by Schonhorn et al. (1972) where it was stated that for a brittle adhesive system the strength of the joints is controlled by edge effects. It seems that as the adhesive becomes more brittle and weaker, the edges of the joint become more and more important.

5.5.2 Joints with gauge steel adherends

Similar joints as in section 5.5.1 were manufactured, only this time the adherends were made of gauge steel. Results for this case can be found in table 5.13 and figure 5.15

Table 5.13 Results from tensile tests on defective SLJs with 25 mm overlap, gauge steel, MY753 adhesive and circular type defects

Gauge Steel - MY753 - 25 mm overlap		
Circular defects	Average Failure load (kN)	Standard Deviation
Undefective	10.87	1.98
Defect C (I)	10.74	2.14
Defect C (III)	9.63	1.81

The situation this time is only slightly different; again there seems to be a limited effect of the defect size on the strength of the joints. The strength of the joints reduces slightly as

the defect size increases, but the reduction is much less compared with the case where hard steel adherends were used. Only for defect sizes covering more than 40-50% of the overlap there is some significant reduction in strength. The strength of the joints is again governed by edge effects rather than by the bonded area. The combination of a "soft" adherend with a brittle adhesive enhances the edge effect and the bonded area is not as important in this case. The same conclusion was drawn in section 5.3.5 for the more ductile adhesive (AV 119) with gauge steel adherends.

5.5.3 Joints with mild steel adherends

Mild steel adherends were used this time to manufacture joints similar to the ones described in the previews sections 5.5.1,5.5.2. Results are presented in table 5.14 and also figure 5.16.

Table 5.14 Results from tensile tests on defective SLJs with 25 mm overlap, mild steel, MY753 adhesive and circular type defects

Mild Steel - MY753 - 25 mm overlap		
Circular defects	Average Failure load (kN)	Standard Deviation
Undefective	10.57	0.48
Defect C (I)	10.29	0.09
Defect C (III)	10.1	0.33

It seems there is again only a small effect in the strength of the joints with increasing defect size. For small defect sizes (up to approx. 50% of the bonded area) the decrease in strength is small. However, a more sharp drop in strength should be expected as the defect size exceeds 70-80% of the area. Strength seems to be controlled by the edges of the joint although the area becomes important for very large defect sizes. Similar observations have been made for the case of AV119 adhesive with mild steel.

5.5.4 Failure mechanisms - modes of failure

For mild and gauge steel joints, plastic deformation of the joints was again apparent. The resulting failure mode was the same as described in sections 3.3.3 & 3.4.2 for the mild and gauge steel respectively. Due to the plastic deformation of the adherends around the overlap edge, failure is again dependent on the local stress / strain field around these areas. Failure happens progressively although a lot faster compared to the case of the toughened adhesives. This is due to the reduced resistance of this particular adhesive to withstand crack propagation.

For the hard steel case, there were also some signs of damage prior to failure, although failure was more catastrophic. In chapter 3 (section 3.5.2) a conclusion was made that the fillet does not contribute to the strength of the joints and that failure must initiate near the adherend embedded corner, spreading inwards through the overlap and out to the fillet face.

In figure 5.17, the process of failure initiation and propagation of damage in the fillet can be seen. This is a detailed view of the fillet face (see also figure 2.3 for definition of viewed area). Since the adhesive is transparent, it is possible to observe happenings inside the fillet. A small area of delamination, a thin light area (initial "damage") next to the unloaded adherend's edge can be seen, figure 5.17 (I). As the load increases, this delamination (or damage) grows in size without a crack appearing through the fillet, until catastrophic failure occurs. This is because the load is mainly transferred by areas that are near the ends of the overlap and under the overlap rather than by the area covered by the fillet. This observation is in close agreement with the conclusion made in chapter 3 indicating that failure is dominated by the areas under the overlap and not so much by the local stress and strain distribution in the fillet.

5.5.5. Conclusions from MY 753 adhesive joints

It is easier to compare results from the three different adherend configurations, (mild gauge and hard), by plotting the results on the same graph (figure 5.18). There are no

significant differences between the strength of joints made of different adherends. Normally, we should expect joints with hard steel to be the strongest, followed by the gauge and mild steel. This pattern does not exist and the differences are rather small, especially compared to the experimental scatter. The reason for this is clearly that the adhesive is weak and brittle in behaviour, and especially the low shear strength of the adhesive.

When the adhesive has a low shear strength and behaves in a brittle manner (such as untoughened epoxies), then small differences should be expected by using different adherend materials.

Strength is governed mostly by edge effects, and not the total bonded area. When adherends deform plastically (mild and gauge steel) the edge effect is more enhanced. The size of the defect should be larger than 40-50% of the total overlap before any significant reduction in strength can be seen.

5.6 Conclusions from tests on defective joints

Three different adhesives and three different types of steel were used to manufacture single lap joints in a variety of configurations with artificial defects. Comparisons between the different adhesives and the same overlap and adherend configuration can be seen in figures 5.19, 5.20 and 5.21 for hard, gauge and mild adherend joints.

When a toughened structural adhesive is used, then different levels of joint strength can be achieved, depending on the properties of the adherend material. An almost linear decrease in joints strength, as the defect size increases, is observed for the case of hard steel adherends. When gauge or mild steel are used, then a non linear decrease in strength is observed. For small defect sizes there is no significant effect. But as the size of the defect gets bigger, then a more rapid decrease in the strength of the joints is apparent. Failure is dominated by edge effects for the case of mild and gauge steel (when the defect size is small). The area is important only when the defect size becomes very big (more than 40-50% of the total area). When hard steel is used, then failure is governed by the bonded area, rather than edge effects, regardless of the size of the defect. However if the

overlap becomes very long (i.e. 60 mm), then a small size defect may not affect the strength of the joint (as it would do with a shorter overlap). When the overlap becomes very large, then some area in the middle of the overlap should be expected to remain elastic before catastrophic failure, and therefore should not contribute to the strength of the joint.

The situation is slightly different when the adhesive is more brittle. For hard steel adherends the reduction in strength, as the defect size increases, is not proportional for small defect sizes, indicating that the edges of the joint become more important. The more brittle the adhesive becomes, the more is the edge effect enhanced.

For a brittle adhesive with gauge or mild steel adherends the situation is the same as the one with a ductile adhesive. Failure is dominated by edge effects because the plasticity of the adherends controls failure. Some dependence on the bonded area exists, but only for larger defects.

In the case where failure is dominated by the bonded area, the shape of the defect makes no difference to the strength; all that matters is the size of the bonded area.

Useful conclusions can be drawn for the mechanism of load transfer through the overlap. It seems that, when the adherends remain elastic and the adhesive is ductile, load is transferred from the middle of the overlap as well as the ends. When the adherends remain elastic but the adhesive is brittle, then more load is transferred through the ends of the overlap than through the middle, making the ends of the joint more important.

In chapter 3 it has been shown that the bending moment distribution around the overlap edges is an important parameter for joints loaded in tension. Results from this chapter imply that bending moment alone cannot be used to predict failure, and other parameters should be taken into account at the same time. This is because although the variation of bending moment is the same for joints with different size defects (for the same geometric configuration), the strength of the joints is different. So, areas further away from the overlap edges need to be considered for the case of hard steel joints loaded in tension.

In four point bending loading on the other hand, the edges of the joints are only important, for a ductile adhesive and hard steel adherends. The strength of the joints is controlled by edge effects.

As we have demonstrated, the effect of defects on the strength of the joints is not controlled by the adhesive properties only, as concluded by Schonhorn et al (1971), (1972). The properties of the adherends must be taken into account, as well as the size of the defect (compared to the total bonded area). A better understanding on the failure and strength of defective joints has been achieved. This is very important in practical applications where non-destructive techniques could be applied to identify the defect size and the strength of the defective component could then be calculated.

For the case of the MY 753 adhesive due to its brittle and weak nature the effect of the adherend properties in the strength the joints is much less pronounced. Hard, gauge and mild steel give joints of similar strength in contrast to what happens in the case of a structural adhesive such as AV 119, ESP 110 or EC 3448.

Chapter 6

FINITE ELEMENT MODELLING OF THE JOINTS

6.1 Introduction

The increasing availability of computers and the development of computer technology has resulted in the finite element method (F.E.M) becoming the most popular and powerful method for analysing structures theoretically. The F.E.M can be used to model virtually any joint configuration. Small-scale geometry can be taken into account as well as geometric and material non-linearities. Detailed results can be obtained which could give very interesting information about local stress distributions in adhesive joints. Two-dimensional analysis is usually relatively inexpensive and fast to obtain. Three-dimensional analysis however, although very computationally expensive, gives a more realistic representation.

Adams and Peppiatt (1974) were among the first to use the finite element method to assess the stress distribution in adhesive joints. Adams and Coppendale (1978) used the F.E. method to analyse butt joints loaded in tension and torsion. Crocombe and Adams (1981a) investigated the effect of the spew fillet on the strength of SLJ for a range of geometric and material parameters using linear elastic F.E. The geometric non-linearities of the peel test were taken into account by Crocombe and Adams (1981b) in an elastic analysis. Material non-linearities were added in a later publication Crocombe and Adams (1982). Harris and Adams (1984) analysed the SLJ including both geometric and material non-linearities.

Chiang and Chai (1994), Crocombe *et al* (1995) used the finite element method and fracture mechanics principles to study cracked joint configurations.

Zhao (1991), Tsai and Morton (1994) carried out three-dimensional analyses on both single and double lap joints and it was therefore possible to study the widthwise variations on different stress components. Adams and Davies (1996) perfomed 3-D

analysis on bonded joints with composite adherends, giving further insight on the transverse (across the width) variation of stresses.

However, it must be mentioned here that results from finite element analyses must be interpreted with great care since effects from the element selection, mesh refinement or decisions in the analysis procedure, boundary conditions and materials modelling could seriously alter the results.

6.2 General considerations on the F.E

A commercial finite element package was used throughout the current work in the theoretical analysis carried out. There are several important decisions to be made before theoretical models are developed. Some of the main issues that have to be addressed first are areas such as: 2-D or 3-D analysis, suitable material models, appropriate analysis procedures, appropriate selection of elements. Two-dimensional analyses were mainly carried out in this work. Some three dimensional analyses have also been carried out in order to investigate effects across the width of the joints. Three-dimensional analysis, although more accurate, is very computationally expensive and time consuming. For this reason, the use of 3-D analysis can be implemented for limited cases only.

In the next subsections, some discussion over the decisions made concerning the above will be presented.

6.3 Material modelling considerations

In the current work, it has been assumed that the materials will deform in a linear elastic manner until a point is reached where the stress state is such that yielding initiates and plastic flow occurs. In the linear region, the theory of linear elasticity using Hooke's law is valid. In the non-linear region, the theory of plasticity must be used.

As has been shown in Chapters 2-5, all the materials (both adhesives and adherends) used in the current work can undergo some degree of plastic deformation. The only exception for the materials considered here is the hard steel adherends that remain elastic

throughout the loading regime of the joints tested. The importance of both the adhesive's and the adherend's plastic deformation in the strength of the joints has been addressed in Chapters 2-5. It is therefore necessary to model the behaviour of both adherends and adhesives as accurately as possible, especially the post yield behaviour.

For finite element analysis the following three concepts from the theory of plasticity must be understood. The first is the yield criterion, which relates the onset of yielding to the stress state. The second concept is the flow rule, which relates the stress increments, strain increments and the state of stress in the plastic range. The third concept is the hardening rule. This describes how the "yield surface" grows and moves as the plastic strains accumulate.

6.3.1 Adherend material modelling

The yielding of metals is usually assumed to be independent of the state of hydrostatic stress and dependent purely on the deviatoric stress state in the material. Yielding is only dependent on the shearing of the material. So, for the case of modelling the metal adherends, the classic Von Mises yield criterion available in ABAQUS was used. Yielding is dependent only on the second invariant of the deviatoric stress tensor:

$$\sigma_{yt} = \sqrt{\frac{1}{2}\left[(\sigma_1 - \sigma_2)^2 + (\sigma_2 - \sigma_3)^2 + (\sigma_3 - \sigma_1)^2\right]} = \sqrt{3J_2} \qquad \textbf{Eqn. 6-1}$$

Where σ_i are the principal stresses, σ_{yt} is the yield stress in tension and J_2 is the second deviatoric stress invariant.

The independence of yield on the hydrostatic stress component means that the yield behaviour in tension and compression is the same.

As has already been seen in Chapter 2, all the metals tested strain harden after initial yield. That means the yield stress is not constant and this must be taken into account. The isotropic hardening rule was chosen for this case. This is generally considered to be a

suitable model for problems in which the plastic straining goes well beyond the incipient yield state (ABAQUS) or for problems involving large strains (Rice 1975).

The material properties of the metal adherends have been taken to be independent of the rate of straining. The rate independent metal plasticity model in ABAQUS uses associated flow. Associated flow means that the direction of the plastic flow is the same as the direction of the normal to the yield surface at the point of yield.

Plastic deformation is assumed to take place under constant volume conditions (i.e. the material is nondilational) and the Poisson's ratio approaches the value of 0.5 as plastic deformation accumulates.

The finite element modelling of the behaviour of mild and gauge steel behaviour can be seen in figures 6.1 and 6.2 respectively.

6.3.2 Adhesive material modelling

The yield in polymeric materials, including adhesives, is known to be pressure dependent. This means the yield behaviour is different in tension and compression.

The yield behaviour of adhesives is also very dependent on temperature and the rate of load application. As all tests were carried out at room temperature conditions, there is no account taken for temperature dependence in the modelling. Also, the properties of the adhesives have all been taken to be independent of the rate of straining. This is a simplifying assumption which was felt to be suitable for the type of adhesives (epoxies) used in the current work, as they are the least strain rate sensitive type of adhesives and also for the type of testing, which involved quasi-static loading.

This pressure dependence of the adhesive materials means that yielding is dependent on both the deviatoric and the hydrostatic stress components. These components of stress can be derived from the overall stress state with the hydrostatic component producing purely volumetric deformation and the deviatoric component producing shear deformation.

If one considers an arbitrary stress state (figure 6.3) presented by point P that lies in the principal stress space, then the vector (OP) which represents this stress state can be decomposed into two components: OA that lies along the hydrostatic axis (hence

hydrostatic component of stress) and AP that lies in a plane normal to the hydrostatic axis known as the deviatoric plane (hence the deviatoric stress component). If the general state of stress is such that it lies off the hydrostatic axis, then there will be some amount of deviatoric stress present. At a particular combination of these stresses (depending on the yield criterion) the material will yield. This can be graphically represented in the principal stress space by a surface, such that yield is predicted if a point lies outside it. The next two figures represent yield surfaces, which are dependent (figure 6.4) and independent (figure 6.5) of the hydrostatic component of stress respectively.

There are two pressure-dependent yield criteria in the literature which are related to the yield of polymers. These are the Drucker- Prager (Drucker 1952) and the Raghava (Raghava 1973a&b). These two yield criteria are described by the following equations respectively:

$$\sigma_{yt} = \frac{\sqrt{3}(S+1)}{2S}\sqrt{J_2} + \frac{(S-1)}{2S}I_1 \qquad \text{Drucker-Prager} \qquad \textbf{Eqn. 6-2}$$

$$S\sigma_{yt}^2 = 3J_2 + (S-1)\sigma_{yt}I_1 \qquad \text{Raghava} \qquad \textbf{Eqn. 6-3}$$

where I_1 is the first invariant of the stress tensor and is defined in terms of the principal stresses as: $I_1 = \sigma_1 + \sigma_2 + \sigma_3$, and S is the ratio of yield stress in compression to the yield stress in tension corresponding to the same equivalent plastic strain. The Drucker-Prager criterion was initially proposed for soil mechanics applications while the Raghava criterion was developed especially for polymers.

When a pressure-dependent yield criterion such as the Raghava criterion is used the yield surface is a paraboloid in the principal stress space. In simple terms, this means that as the hydrostatic tensile stress increases then the amount of additional deviatoric stress needed to cause yield decreases in terms of a paraboloid law. To make things clearer, if the linear Drucker-Prager model was used then the amount of additional deviatoric stress needed to

cause yield would decrease in terms of a linear low, as the hydrostatic tensile stress increased.

In the ABAQUS finite element software, both equations 6-2 & 6-3 are available as the linear and exponent Drucker-Prager criteria. Charalambides and Dean (1997) have developed a method to calculate the yield parameters when tensile and shear stress-strain data are available.

Davies (1997 and 1999) developed a subroutine that could be implemented in ABAQUS to simulate the Raghava yield criterion. This model requires the elastic parameters such as Young's Modulus E and Poisson's Ratio ν, the hardening curve (stress vs. corresponding plastic strain) and the yield parameter S. This subroutine, provided by Davies (1997 and 1999) was used to describe the behaviour of the adhesives used in the current work.

It must be mentioned here that the Raghava criterion and the Exponent Drucker-Prager criterion available in ABAQUS are very similar. Equation 6-3 (Drucker-Prager Exponent model) is presented in a different way in the ABAQUS manuals:

$$aq^b - p = p_t \qquad \textbf{Eqn. 6-4}$$

where a and b are material parameters that are independent of plastic deformation and p_t is a hardening parameter that represents the hydrostatic tensile strength of the material. The other terms in Eqn 6-4 are the equivalent pressure stress p and Mises equivalent stress $q=\sigma_{yt}$ defined as:

$$p = -\frac{1}{3}(\sigma_1 + \sigma_2 + \sigma_3) \qquad \textbf{Eqn. 6-5}$$

$$q = \sqrt{3J_2} \qquad \textbf{Eqn. 6-6}$$

Thus, the Drucker-Prager exponent model in ABAQUS (Eqn. 6-4) can be fitted to the Raghava criterion (Eqn. 6-3) if the two equations are rearranged and equal terms are equated. The Raghava criterion is a quadratic surface in the principal stress space so parameter b=2 for the Exponent Drucker Prager model. The following relationships stand:

$$a = \frac{1}{3(S-1)\sigma_{yt}} \qquad \textbf{Eqn. 6-7}$$

$$p_t = \frac{S\sigma_{yt}}{3(S-1)} \qquad \textbf{Eqn. 6-8}$$

Figure 6.6 is a schematic of the yield surface in the meridional plane (p-q) for the case of the Exponent Drucker-Prager or the Raghava model, where the horizontal axis corresponds to the hydrostatic axis and the vertical axis represents the deviatoric axis. It is important to mention here that ABAQUS defines the pressure stress (or hydrostatic stress) with a minus (-) sign for tension, and a plus (+) sign for compression. Thus, a stress state equal to $-p_t$ corresponds to a pure hydrostatic tension condition.

The adhesives used in the current work behave in a non-linear fashion, as already presented in Chapter 2, which is typical behaviour for epoxies. Yield in metals is usually very sharp and is associated with irreversible damage in the material (permanent plastic deformation). The definition of yield in polymers is quite different. Initial yield comes at a very low stress, but this yielding is not necessarily associated with irreversible damage in the adhesive. Young and Lovell (1991) state that the exact position of the yield point is very difficult to define and so define yield as the maximum point on the stress-strain curve. Raghava and Caddell (1973) have proposed the 0.3% yield offset as the definition of yield in polymers. Towse (1998) has also found thàt no irreversible damage occurs in the EC3448 epoxy adhesive below approximately 2% applied strain. For that particular adhesive, this value of strain corresponds to approximately the same level of stress as

defined by the 0.3% Raghava offset. In the finite element simulations, the stress-strain curve of the adhesives has to be input in terms of true stress-true strain data. Although yield in the adhesives does not occur at the point where deviation from linearity occurs, the initial input point in the finite element data that defines the plastic behaviour of the material was chosen to be a small value, typically 25-30MPa. This was done in order to simulate the behaviour of the adhesives more accurately.

It is quite clear from the stress strain curves presented in chapter 2 that there is significant hardening subsequent to initial yield. Isotropic hardening was chosen for the modelling of the hardening behaviour. Isotropic hardening has also been shown by Richardson (1993) to model the behaviour of polymeric adhesives accurately. A schematic diagram of isotropic hardening for the exponent model in the meridional plane can be seen in figure 6.7.

In this material model, it has been assumed that the direction of the plastic flow is the same as the direction of the normal to the yield surface at the point of yield, Davies (1997 and 1999). This is called associated flow and has been used previously by Crocombe (1981) to describe the behaviour of adhesives. According to the ABAQUS manuals, models with associated flow are accurate when the loading is monotonic and there are no sudden changes of the direction of plastic straining.

6.4 Verification of the Raghava material model

The standard procedure of using a single element model to verify the behaviour of the model under different loading conditions was followed. Tensile, compressive and shear loading were applied in a single solid element and the response in tension, compression, and shear can therefore be verified. Experimental results are only available for tensile and shear tests. Results for compression loading are those derived from the F.E simulation.

The experimental tensile data are used as input for the material behaviour. The value used for the yield parameter S is the important parameter that affects the behaviour of the material in compression and shear. In the case were there is no dependence in the

hydrostatic component of stress, the value of S=1 and the Raghava model becomes the Von Mises criterion. The main problem when using the Von Mises criterion is that the shear behaviour of the material is always under estimated ($\tau_{yield} = \frac{1}{\sqrt{3}}\sigma_{yield}$). By choosing the appropriate value of S for each different adhesive, the shear behaviour can be matched. It is very important to match the behaviour of the adhesive in shear, especially in a single lap joint configuration since there is a large volume of material (middle of the overlap) that is predominantly loaded in shear.

A trial and error procedure was followed in order to define the S value for each adhesive material. The S values used are summarised in table 6.1.

Table 6.1 Values of yield ratio S derived from single element models

Adhesive	$S = \sigma_{yc} / \sigma_{yt}$
ESP 110	1.40
AV 119	1.35
EC 3448	1.55
MY753	1.37

For the four adhesives used in the current work the verification of the adhesive material model can be seen in figures 6.8, 6.9, 6.10, 6.11

It is clear that the Von Mises material model (S=1) would not describe the behaviour of the material in shear adequately. The finite element model assumes that as soon as the stresses reach a plateau level there is no more increase in stress as the load increases. This is the meaning of the arrows in the graphs.

6.5 Analysis procedures considerations

The configuration of the single lap joint is geometrically non-linear. Experimental results from Chapters 2-5 have shown that large rotations and large strains occur during the deformation of the joints. Non-linear incremental analysis was therefore performed.

In ABAQUS there is a choice to define the problem as a "small displacement" or "large displacement" to take into account large rotations or displacements that could occur in the deformation of the joints. When the NLGEOM (non-linear geometry) parameter is omitted, then the elements are formulated in the reference (original) configuration, using original nodal coordinates. The errors in such an approximation are of the order of the strains and rotations compared to unity. When the large displacement effect is taken into account (by including the NLGEOM parameter) then the elements are formulated in the current configuration using current nodal positions.

The non-linear effects were taken into account for every analysis performed in the current work as it was found that the results when using the geometrically linear analysis (NLGEOM parameter not included) were considerably different to the ones where a geometrically non-linear analysis was carried out.

6.6 Element formulation

Fully integrated solid quadrilateral 8-noded elements were used throughout the majority of the 2-D models. Some 6-noded triangular elements were used in areas of mesh refinement and around the fillets. For the three-dimensional analysis, 20 noded (brick elements) and 15 noded (wedge elements) solid elements where used.

As has been shown in Chapters 3-5, strain gauges were bonded to some joint configurations in order to get a better understanding about the load and bending moment distribution around the overlap edges. The strain gauges were placed in the middle of the width of the joint. The conditions prevailing in that position are plane strain conditions. The model should therefore be one that represents these conditions as close as possible. Ideally one should perform 3-D analysis where all the degrees of freedom are active and thus the body is not constrained in any direction. However, as we have mentioned earlier, three-dimensional analyses are computationally very expensive. In a 2-D analysis, some assumptions and simplifications can be made. The problem is then reduced to a two dimensional one of either plane stress or plane strain.

A plane stress (PS) formulated solution should be rejected since it is more representative of the case when only the edges of the joint are analysed. ABAQUS offers two more alternatives:

- plane strain (PE) formulation of the elements, where the strains in the width direction (ε_{zz}) are assumed to be zero
- generalised plane strain (GPE) formulated elements, where the strains in the width direction (ε_{zz}) are assumed to be a non zero constant.

In reality, the stressed body is free to deform in any direction. We have also shown that strains in the width direction, arising from the Poisson's ratio effects, are sometimes significant in joint failure modes (case of 60 mm mild steel joints - Poisson's ratio cracks). If the plane strain formulation were to be used, then the elements would become stiffer, due to the extra constraint that is imposed by setting the ε_{zz} strain equal to zero. With the generalised plain strain formulated elements, where ε_{zz} is assumed to be a non-zero constant, the situation is closer to reality. Thus, the generalised plane strain formulation was decided to be used for all the joints modelled. In some cases, analysis using the two different formulations (PE and GPE) were compared and results showed that the behaviour of the joints was indeed stiffer for the plane strain (PE) formulation, than results obtained by the generalised plane strain (GPE) formulation. Generalised plane strain formulated elements were used throughout the two dimensional analysis.

6.7 Finite element mesh

Part of the finite element mesh used in the analyses can be seen in figure 6.12. Three elements through the adhesive thickness were used. The mesh was consistent around the edges of the overlap for all the different overlaps modelled. This was thought necessary so as to make more valid comparisons between different overlaps. Any differences that could arise due to mesh density variation between different models are, in this way, eliminated.

6.8 Boundary conditions - load application

The boundary conditions used in the finite element analysis can be seen in figure 6.13. For the case of the tensile loaded joints, one end of the joint was fully constrained (both D.O.F : u_1, u_2 were constrained). The load was applied at the other end as a uniform pressure at the element faces. This end was also constrained in the 2-direction. The constraints cover a length of 25 mm which corresponds with the gripping area of the specimens.

For the case of joints tested in four point bending, the boundary conditions applied can be seen in figure 6.14. Concentrated loads were applied at the appropriate nodes (corresponding to the experimental loading span). The nodes that serve as "supports" were constrained only in the 2-direction. This was done because during the experiment some sliding (between the specimen and the rollers) always takes place. In order to avoid rigid body movement in the F.E analysis, a single node in the centre of the overlap was constrained in the 1- direction. The joint is free to rotate around the supports (as is observed during the experiments). If the "support" nodes were pinned (constrained in both directions 1&2) the result would be to over-constrain the joint, introducing axial loads that could invalidate the results.

6.9 Three dimensional analysis

Three-dimensional analysis, although it gives a better understanding about the behaviour of case being analysed, is computationally expensive. It is therefore very difficult to analyse many different cases. Only one configuration was chosen to be analysed in three dimensions.

The advantage of three-dimensional analysis is that the model is closer to reality, especially in terms of constraints imposed in the two-dimensional models. Simplifying assumptions that are often applied in a two-dimensional analysis (plane strain, generalised plane strain or plane stress) are not needed for the three-dimensional analysis

and the models are less constrained. In addition, width-wise effects can only be taken into account in a three-dimensional analysis.

Due to the symmetry of the joint in the width direction (z-direction), only half the model needs to be analysed. All the nodes along the middle of the width of the joint are constraint in the z direction, but are free to move in the x and y directions. The boundary conditions and load applied can be seen in figure 6.15 and are similar to the ones applied in the two dimensions.

6.10 Conclusions

The finite element method is a very versatile and powerful method for theoretical analysis. However, the analyst must be very careful during the creation of the model so that the correct analysis procedures are chosen to describe the situation as close to reality as possible. Particular attention should be paid in the modelling of the materials used and also the applied boundary conditions used.

A commercial finite element code ABAQUS was used for the analysis of the joints. Non-linear, large displacement static analyses have been carried out.

Material non-linear behaviour was taken into account for both the adherends and adhesives by using appropriate material models available in ABAQUS. The adhesives were modelled by using a subroutine developed by Davies (1997 and 1999), which simulates the Raghava pressure dependent yield criterion.

The geometric non-linearity of the single lap joint will be taken into account for all the analyses.

The majority of the analyses were two-dimensional, with generalised plane strain formulated elements. Some three-dimensional analyses were also carried out in order to get a better insight about the width-wise variation of stresses and strains in the joints.

Appropriate boundary conditions were used for each case so as to simulate the conditions met by the griping and loading of the joints during testing.

The finite element mesh used was consistent around the edges of the overlap for all the different cases modelled.

Chapter 7

FINITE ELEMENT RESULTS

7.1 Introduction

Results from the finite element analysis will be presented in this chapter. Qualitative and quantitative observations regarding the variation of critical variables in the adhesive layer or the adherends will be made. Detailed stress and strain variations along the overlap length will be used in order to make strength predictions for the different joint configurations.

However, before any predictions can be made, suitable failure criteria must be defined. The failure criteria must be in line with experimental observations and also the strength of the materials for both adhesives and adherends. A failure criterion must also be physically meaningful and applicable in a variety of cases.

As has already been shown in the previous chapters, different joint configurations (overlap length, adherend material, adhesive material, loading type, geometry) behave in completely different ways. The failure mode depends on the materials used as well as the overlap length and the type of loading. The location of critical areas in the joint, where failure initiates, depends on the properties of materials, the geometry of the joint and the type of loading. Therefore, it is probably unlikely that a single failure criterion that would be applicable in all different cases, can be defined. The use of a combination of criteria depending on the conditions of the configuration under investigation is more likely to predict failure in a wider variety of configurations.

It is very important to identify critical variables that control failure so that these can be used in the failure criteria.

7.2 Variation of strain in the adherends between F.E and experiments

The single lap joint configuration is a non-linear geometric configuration due to the eccentricity of the load path. The overlap area of the joint will rotate under load as has already been mentioned in previous chapters, and a combination of a tensile load and a bending moment will be imposed at the edges of the overlap. The load and bending moment distribution in the crucial areas (such as the ends of the overlap), are obviously very important since these will affect the stress and strain distributions inside the overlap area where the stresses peak in the adhesive layer.

It has been shown experimentally that the strength of the joints is very much affected by changes in the overlap length. It is important to assess the effect of the overlap in the stress and strain distribution around the overlap ends where the stresses should reach a maximum.

The finite element model will be used to predict the strain variation in the adherends at the positions where the strain gauges were bonded in the experiments. This longitudinal strain variation is directly related to the bending moment applied in that section of the adherend.

It is very important to compare the finite element and experimental results for the variation of strain in the adherends before any detailed stress or strain variations in the adhesive are looked at. This will ensure that the model is constrained in the correct way (load application and boundary conditions). The finite element model will therefore be able to correctly predict the load and bending moment distribution around the overlap edges.

Several joint configurations will be compared both in tension and four point bending loading.

7.2.1 Joints with hard steel adherends in tension

Experimental results on the strain variation in the adherends for joints with hard steel in tension have been presented in chapter 3, figures 3.35-3.38, for various joint configurations. Joints with hard steel adherends and the EC 3448 adhesive at five different overlap configurations were modelled and the results for the predicted variation of longitudinal strain in the adherends from the F.E analysis are shown in figure 7.1. The strain results calculated from the F.E analysis are the average strain over the area that the strain gauges cover (centre of the gauge is 9 mm from the overlap edge). Two strain variations are presented for each overlap case (inner and outer side of the adherends as defined in section 3.4.5 and shown in figure 2.4).

The comparison between the experimental values and the F.E predictions for this case is shown in Figure 7.2. The correlation is very good up to the failure load for all overlap configurations.

F.E analysis correctly predicts that for a given axial applied load, the bending moment is less for joints with longer overlaps.

In Chapter 3, experimental results showed that the effect of the adhesive material on the strain variation in the adherends is very small, because results from joints with different adhesives were very similar. It is therefore very useful to examine the F.E predictions for the strain variation in the adherends when different adhesives are used.

Comparisons of the strain variation in the adherends between different adhesives and the 25 mm overlap configuration can be seen in figure 7.3. F.E results predict that the adhesive behaviour does not alter the bending moment distribution, which is in agreement with what was observed experimentally (figures 3.36 &3.37). Only very minor differences can be observed for the range of adhesives tested. This is because the bending moment distribution is mainly dependent on the geometry of the joints (overlap length in particular) and of course the adherend properties. Some very small decrease in the F.E predicted bending moment can be seen for the case of MY 753 adhesive is probably due to the slightly lower stiffness of that adhesive.

The adherend thickness is also another variable that affects the bending moment distribution around the overlap edges. Comparisons between experimental results, for the configuration of 25 mm overlap, AV 119 adhesive and different adherend thicknesses, and the F.E predictions can be seen in figure 7.4. As can be seen, the correlation is very good for all cases and the F.E results predict that the thinner the adherends the less is the applied bending moment at the edges of the joint for a given applied load.

It is also very important to note here, that the variation of bending moment was the same for joints with various sizes of defect (for a given overlap length), as has already been shown in figure 5.7.

It can be therefore concluded that for the range of structural adhesives tested and modelled in the current work, the bending moment distribution around the overlap edges is mainly dependent on geometric quantities such as the adherend thickness and the overlap length.

The most important conclusion however is that the bending moment at the edge of the overlap cannot be a critical parameter affecting failure, for the case where the adherends behave elastically. This is because joints with different applied bending moments fail at approximately the same applied tensile load (i.e. : AV 119 joints and 3 different adherend thicknesses). Also joints with the same applied bending moment fail at considerably different loads (i.e. : AV 119 joints with various defect sizes and a given overlap length). Therefore, the bending moment is important in the sense that it will alter the local stress and strain variation around the overlap but not important in determining or affecting the failure load of the joints, at least for the case that the adherends remain elastic. It must be noted here that the situation is quite different for situations in which low yield strength adherends are used, since the amount of bending applied at the overlap edges will define the load at which yielding initiates in the adherends and will therefore affect failure.

7.2.2 Joints with hard steel adherends in four point bending

In a similar way to the tensile loaded cases, comparison between experimental and F.E results for the case of four point bending tests will be presented in this section.

Comparison of the experimental and F.E results for the 25 mm overlap with AV 119 adhesive and three different adherend thicknesses can be seen in figure 7.5. The correlation is very good for all the configurations examined.

7.2.3 Joints with gauge steel adherends in tension

As has already been shown experimentally, joints with gauge and mild steel adherends behave in a different way. This is due to the plastic deformation of the steel adherends that occurs before the adhesive layer starts to fracture.

Comparison between experiments and the finite element prediction for the case of gauge steel adherends and EC 3448 adhesive can be seen in figures 7.6 , 7.7, 7.8,7.9 and 7.10 for the five different overlap (12.5, 20, 25, 40 and 60 mm) configurations respectively. This time, the correlation is good up to the point that gross yielding occurs in the adherends. As can be seen in figures 7.6-7.10 there are two experimental curves for each joint. These are from the four different gauges measuring strains at symmetric positions as already presented in figure 2.4. Yield in the two different adherends, making up the joint, will not necessarily occur at the same load due to small variations in the properties between the adherend pieces. As soon as one end of the joint starts to yield, more load will be transferred through that end causing the readings of the gauges on that side to increase abruptly. On the other overlap end, the opposite situation occurs and strains increase at a much slower rate. This usually causes asymmetric cracking in the joints which has been observed in several of the tests.

As has been shown in figure 3.22, the overlap length affects the load at which this initial yield will take place. If for example, a 0.2 % strain limit is taken as the initial yield point for gauge steel, then yield in a short overlap joint will occur at a lower applied load compared to a longer overlap joint.

At low applied loads, where the adherends remain elastic, a similar situation to the one with the hard steel joints exists. The shorter the overlap, the larger is the predicted bending moment for a given applied load. This means that initial yield in the adherend will occur at a lower applied load for a short overlap than for a long overlap. As the load

keeps increasing, the F.E predicts that the bending moment applied at this section of the adherend will start to decrease and the strains on the opposite face of the adherend will converge to the same value. Initially, the inner side of the adherends cross section will yield first. As the load increases, the yielded zone spreads through the thickness of the adherends, and also further away from the overlap ends. A global yielding condition is reached through the adherend cross section when the strains in the opposite sides read the same value. This is the condition where a plastic hinge forms in the adherends and the joint is near its failure load. Above this load the correlation between experiments and F.E prediction is not good.

Nevertheless, results from the F.E can quite accurately predict the load at which the plastic hinge will start to form which could be used as a conservative, but not unreasonable, strength prediction for the joints.

An F.E analysis was performed where the adhesive layer was substituted by the properties of gauge steel, thus creating a "solid gauge steel SLJ". The results (variation of strain in the adherends) from the "solid gauge steel joint" are compared with a normal joint in figure 7.11. As can be seen, there are only very small differences indicating that the bending moment variation in the edges of the joint is mainly a geometric effect.

7.2.4 Comparison of F.E bending moment results with closed form solutions

In the previous sections, it has been shown how important is the overlap length and the adherend thickness, in the bending moment distribution around the overlap ends. Several approaches have been adopted by researchers such as Goland and Reissner (1944), Hart-Smith (1973), and Zhao (1991) in the calculation of bending moments. These analytical solutions assume that the materials behave in a linear elastic manner throughout loading and geometric non linearities are not accounted for. Such methods could not accurately predict joint strength, but provide an inexpensive alternative to estimate the stress distribution around the critically stressed areas. These stress predictions, combined with simple mechanics and strength of materials theories, could give some fairly quick and

easy estimates for joint strength. This is especially useful in the case of mild and gauge steel, where the initiation of yield in the metal can be calculated by such theories and a conservative estimate obtained for the joint strength.

The finite element models for the case of elastic adherends, presented in the previous sections, have shown very good agreement with experimental results. These results can therefore be used to assess the different analytical methods of calculating the bending moments at the edges of the overlap. Comparisons between the approaches of Goland and Reissner, Zhao, and Hart-Smith will be presented here in order to decide which method is the most accurate. Comparisons will only be made for the hard steel joints loaded in tension for all overlap and adherend thickness configurations.

Appendix IV describes the equations used for each different approach. Using these equations from Appendix IV, we can then calculate the bending moment factors and consequently the bending moments for each case. In all these types of analytical solution the presence of a spew fillet cannot be taken into account. The fillets were removed from the corresponding F.E analysis (i.e. square ended joints) so that the comparisons are valid.

Results are compared in figure 7.12. The results presented are for AV 119 adhesive with 1.6 mm thick hard steel adherends.

As can be seen from the graphs, all the methods seem to give reasonable predictions for short overlaps. Hart-Smith's solution seems to be closer to the F.E results with Goland & Reissner's and Zhao's solution overestimating the bending moments. As the overlap gets longer, the variations become clearer. For very long overlaps, such as 60 mm, Hart-Smith's solution underestimates the bending while Goland & Reissner's solution grossly overestimates, and Zhao's solution is the closest.

It is clear that as the overlap length increases the bending moment at the edge decreases. For long overlaps, such as 60 mm, a plateau seems to be reached and the bending moment tends asymptotically to a maximum value.

Similar comparisons for the case of 25 mm overlap and different adherend thicknesses can be seen in figure 7.13. All the methods seem to correctly predict the general variation of strain with load, Hart-Smith's solution being closer to reality at high applied loads. Goland & Reissner's solution overestimates the bending as does Zhao's solution.

7.3 Variation of hydrostatic and deviatoric stress components

Since the adhesives were modelled using the Raghava pressure dependent yield criterion the main variables examined in the current analysis are the variation of the hydrostatic stress (p) and deviatoric stress (or Mises stress) (q) components. These two components of stress combined in the yield criterion will eventually define yield in the adhesive and ultimately failure. The hydrostatic component of stress is mainly associated with pure volumetric deformation of the material while the deviatoric component is associated with shearing or yielding of the material.

The main results presented in this section will be the variation of p and q along the overlap length at different levels of loading. Since the geometry of the single lap joint is symmetric, results will only be plotted for half the overlap length. The only exception will be for results on joints loaded in four point bending. Results for this case must be plotted for the whole overlap so as to see the effect of tension and compression on the stress distribution.

The results are presented for two different interfaces (the "loaded" and "unloaded" interfaces) along the overlap length. A definition of the term "loaded" and "unloaded" interface is given in figure 7.14. It must be reminded here that the sign of the hydrostatic stress component is negative for tension and positive for compression.

7.3.1 Results for various configurations of hard steel joints in tension

The variation of the hydrostatic and deviatoric stress components at different levels of applied load for AV 119 adhesive at three different overlap configurations can be seen in Figures: 7.15, 7.16, 7.17, 7.18, 7.19, 7.20, 7.21, 7.22, 7.23, 7.24, 7.25 and 7.26. Similar variations were obtained for joints with different adhesives.

As it can be seen from figures 7.15, 7.16, 7.19, 7.20, 7.23 and 7.24, there is an area under the overlap very close to end of the joint where the adhesive is under hydrostatic tension (negative hydrostatic stress). Further inside the overlap, a larger area exists where the

adhesive is under hydrostatic compression. It must be reminded here that due to the dependence of the yield criterion on the hydrostatic component of stress, higher levels of deviatoric stresses are required in order to cause yield in the presence of hydrostatic compressive stresses. The opposite effect is happening when there are tensile hydrostatic stresses present. Thus, yield is "suppressed" under hydrostatic compression and is "encouraged" under hydrostatic tensile conditions.

There is some variation of the hydrostatic stress through the thickness of the adhesive layer, especially very close to the overlap ends where hydrostatic stresses reach a maximum. The highest hydrostatic stresses are closest to the corner of the unloaded interface. However, it must be noted here that there is a significant "singularity" effect from the presence of the sharp corner in the unloaded interface, which artificially increases the stresses and strains even further. Thus, the peak values of stress and strain in this region are very much mesh dependent and should therefore be treated with care. In these areas of the joint, the load from one adherend to the other is mainly carried by tensile stresses. Further away from the overlap edges, the hydrostatic stresses decrease so that near the middle of the overlap, the values are very small.

The variation of the deviatoric or Mises stresses is, however, different as can be seen in figures 7.17, 7.18, 7.21, 7.22, 7.25 and 7.26. For a low applied load, the Mises stresses peak at the overlap edge. As the load increases, the peak is shifted further away from the overlap edge, to inside the overlap. The Mises stresses are also quite high in the middle of the overlap. This is a clear indication that in a tensile test the load is carried from the majority of the overlap and not only by the ends of the overlap. This is in very close agreement with experimental observations from tests with defective joints, where as the defect size increased there was an almost linear decrease in the strength of the joints (figures 5.3 and 5.4).

The above conclusion, together with the fact that the hydrostatic stresses are quite low around the middle of the overlap, means that this area of the joint is mainly loaded in shear.

It is very interesting to note that for loads near the experimental failure load the Mises stresses in the middle of the overlap are quite low for a long overlap configuration. The

same thing is not observed for shorter overlaps. This implies that for joints with very long overlaps (such as 60 mm for the current work) there is an area in the middle of the overlap that remains elastic up to the failure load of the joint. This part of the joint (in the middle of the overlap) is not expected to contribute to the strength of the joint. This has been proven experimentally as shown in section 5.3.1 (table 5.6), where the strength of a 60 mm overlap joint with AV 119 and hard steel remained unaffected by the presence of a 12 mm long defect in the middle of the overlap. Thus, although the strength of joints increases with increasing overlap length (for the case that the adherends remain elastic) there must be a limit of that increase (even for joints with hard steel) for very long overlaps. Such a limit will be defined by the adhesive's behaviour and the geometry of the joint. Failure of joints with very long overlaps must occur because some limiting critical value (either stress or strain) is exceeded somewhere near the highly stressed areas such as the ends of the overlap.

If a comparison between the hydrostatic stress variation for different overlap lengths is made, it can be seen that, as the overlap length increases, the areas that are mainly loaded in shear also increase. In other words, there is a larger proportion of the overlap that is mainly loaded in shear for a long overlap than for a short one.

The area where hydrostatic tensile stresses appear is always confined to the ends of the overlap. It extends typically for 1-1.5 mm from the edge of the overlap for different overlap lengths (figures 7.15, 7.16, 7.19, 7.20, 7.23 and 7.24). This means that the hydrostatic stresses are very localised and are introduced mainly by the rotation and bending of the adherends around the overlap edges. This can be observed for all the different overlaps as well as for different adhesives.

7.3.2 Results for various configurations of hard steel joints in four point bending

Joints were also modelled in four point bending for the AV 119 adhesive, 25 mm overlap and three different adherend thickness configurations. The variation of the hydrostatic and deviatoric stress components along the overlap and at different load levels are presented

in figures 7.27, 7.28, 7.29, 7.30, 7.31, 7.32, 7.33, 7.34, 7.35, 7.36, 7.37, and 7.38 for different configurations.

In a four point bend test, because of the geometry of the SLJ, one end will be loaded in tension while the other will be in compression. Results are this time plotted along the whole of the overlap in order to demonstrate the differences between the end in tension and that in compression.

The differences are clearly shown in the hydrostatic stress variation (figures 7.27, 7.28, 7.31, 7.32, 7.35 and 7.36). High tensile hydrostatic stresses develop in the left part of the joint (part in tension) while high compressive hydrostatic stresses develop on the opposite side (part in compression). The hydrostatic tensile stresses are again very much confined to the ends of the overlap, as was the case for the tensile tests. As the load increases however, the area under hydrostatic tension is slightly increased. It is also interesting to note that, further away from the edges of the joint, the sign of the hydrostatic component of stress reverses. So, near the tension side, some part of the overlap is predicted to be in compression while near the compression side some part of the joint is expected to be in tension.

The Mises stresses peak near the ends of the overlap, and the maximum occurs in the compression side (figures 7.29, 7.30, 7.33, 7.34, 7.37 and 7.38). As the load increases, the peak in the tensile side shifts towards the inside of the overlap.

However, there is a quite steep decrease in the Mises stresses as we move inside the overlap. The stresses reduce to nearly zero in the middle of the overlap. This is in contrast to what has been observed for the tensile tests, where the Mises stresses were quite high even in the middle of the overlap.

The hydrostatic stresses in the middle of the overlap are also very close to zero as was the case for joints loaded in tension. This clearly indicates that in the case of a joint loaded in bending, most of the load is carried in tension / compression by the ends of the joint. The middle of the overlap is not very highly loaded and should therefore not be expected to contribute much to the strength of the joints. This conclusion is also in very close agreement with experimental results from defective joints loaded in bending (figures 5.5 and 5.6). It seems that in the case of a joint loaded in bending only the ends of the overlap

are important in carrying the load. It must also be recalled here that, since adhesives are, in general, stronger in compression than they are in tension, it is the end in tension that would be the critical one, and where failure should be expected to initiate. This has also been observed experimentally as has been mentioned in section 4.3.4.

If a comparison between the different adherend thicknesses for the same applied load is made, it can be seen that the peak stresses are lower for the thicker adherend case. As a result, joints with thicker adherends should be expected to be stronger.

As can be seen from the graphs, the hydrostatic tensile stresses are confined to the ends of the joints and the hydrostatic stresses decrease to nearly zero, regardless of the thickness of the adherends. The variation of Mises stresses also follows the same trend regardless of the thickness of the adherends, with Mises stresses peaking slightly further inside the overlap and decreasing to zero towards the middle of the overlap.

It is only the peak stresses, that occur very near the overlap ends, which are affected by the adherend thickness. The differences in the stress variation get smaller as we move towards the middle of the overlap.

It is quite clear that it is mainly the edges of the overlap that carry the load regardless of the thickness of the adherends.

7.3.3 Correlation of hydrostatic and deviatoric stress variation with experimental observations

Several observations have been made during the testing of the joints and have already been presented in chapters 3-5. One very important feature seen in joints with "ductile" adhesives was the stress whitening observed at the very ends of the overlap. The area where this stress whitening occurs corresponds very closely with the areas that the F.E analysis predicts are under high hydrostatic tension.

Certain polymers, particularly in the glassy state, are capable of undergoing a localised form of plastic deformation known as "crazing", Young and Lovell (1991). This is found to take place only when there is an overall hydrostatic tensile stress and the formation of crazes causes the material to undergo a significant increase in volume. The crazes usually

appear as crack-like entities which are formed perpendicular to the maximum principal stress direction. Crazes are usually regions of cavitated polymer and not cracks in the real sense, although cracks which lead to eventual failure of the specimen usually nucleate within pre-existing crazes. Crazes are generally very small but can be seen by the naked eye because they are less dense than the undeformed matrix and so reflect and scatter light. The presence of hydrostatic tension produces dilation of the material which helps open up voids in the structure and aids the formation of crazes.

For joints loaded in four-point bending, it has been shown that one end of the joint is loaded in tension while the other is in compression. Experimentally, it has been observed that the areas where stress whitening occurs are only the ones when the joint is in tension. The hydrostatic stresses are also confined to the edges of the joint for the case of joints loaded in four point bending.

Thus, the conclusion is that the stress whitened areas found in the joints must be associated with the areas that are under hydrostatic tension. A similar process to craze yielding as described in the previous paragraph must be the dominant yield or failure mechanism in areas of hydrostatic tension. The F.E correctly predicts that the areas of hydrostatic tension in the joint are very localised and are confined to the ends of the overlap as has been observed in the experiments.

Finite element analysis predicts that further away from the overlap ends the adhesive is subjected to hydrostatic compressive stresses as well as to deviatoric or Mises stresses. Epoxy adhesives, such as the ones used in the current investigation, are generally thought of as being brittle materials but they are capable of displaying a considerable amount of ductility when deformed under the influence of an overall hydrostatic compressive stress, Young and Lovell (1991). This process of yielding is called shear yielding. As noted by Young and Lovell (1991), the process of shear yielding in epoxies is found to be homogeneous; the specimens undergo uniform deformation with no evidence of any localisation. Once a small region starts to undergo shear yielding, it will continue to do so because it has a lower flow stress than the surrounding, relatively undeformed, regions. As mentioned by Blanchard et al. (1996), shear yielding of the adhesive appears to be the dominant energy dissipation mechanism in cases were the glueline is thin. Shear yielding

must be the dominant mechanism describing the damage process in areas further away from the overlap ends where the stress conditions are a combination of hydrostatic compression and Mises stresses.

For the case of joints loaded in tension, the hydrostatic stresses fall to very small values, around zero, near the middle of the overlap, as predicted by F.E. The Mises stresses, which are associated with the shearing of the material, are quite high in the same region. The F.E therefore predicts that the adhesive is mainly loaded in shear in those regions. Experimental observations on the surface failure patterns in these regions (rough textured areas, hackles, cusps as in figure 3.33 and 3.34) agree with the above, since the formation of cusps is closely associated with catastrophic failure in shear.

On the other hand, for joints loaded in bending, the failure patterns appearing in the middle of the overlap are different (no rough textured areas such as hackles and cusps) and this is because the Mises stresses in this case are very small values around zero.

7.3.4 Three-dimensional effects on the variation of hydrostatic and deviatoric stress components.

The configuration of hard steel, 25 mm overlap and AV 119 adhesive was chosen to be analysed in three dimensions. Contour plots of the variation of the hydrostatic and deviatoric stress component across the width of the joint are presented in figures 7.39, 7.40 and 7.41.

As has been shown from the two-dimensional F.E analysis the region of tensile hydrostatic stress is confined near the ends of the overlap. The same result can be seen in figures 7.39 and 7.40 across the width of the joints, where the hydrostatic tensile stresses (negative stresses in the legend) are confined to approximately 1 mm from the edge of the overlap. Experimentally, the stress-whitened areas appearing very near the overlap edges have been shown to form a parabolic ("finger nail") pattern (figures 3.32, 3.33, 4.9-4.11). This is also predicted by the F.E results, with areas that are under hydrostatic tension forming an elliptical pattern, which peaks in the middle of the width of the joint. This "finger nail" pattern is attributed to the anticlastic bending effect and also to the

difference between areas being under plane stress (edges of the joint) or plane strain conditions (middle of the width of the joint). Kinloch *et al.* (1981) studied the fracture resistance of a rubber-modified epoxy and concluded that the fracture toughness of an adhesive under plane strain conditions is lower than the fracture toughness under plane stress conditions. This could be another explanation as to why a crack may form in the middle of the width of the joint first, as seen in figure 3.29.

Further inside the overlap, there is a larger region of hydrostatic compression. The peak of hydrostatic compression occurs at the edges of the joint. The Mises stresses peak, on the other hand, occurs at the edge of the joint and slightly further away from the overlap ends (figure 7.41). This is probably because the tensile stress at which a material yields is greater in a triaxial stress field (plane strain) than a biaxial stress field (plane stress), as stated by Kinloch *et. al.* (1981). The region where the peak occurs is also broader compared to the tensile hydrostatic stress peak.

The above results indicate that the middle of the width of the joint is much more likely to fail first due to the higher tensile hydrostatic stress component. According to the predicted results, the region where failure should initiate must be in the middle of the width of the joint, very near to the unloaded adherend corner where the highest tensile hydrostatic stresses occur.

7.4 Initiation and growth of yield zone in the adherends for mild and gauge steel joints

As has been shown in chapter 3, extensive plastic deformation of the adherends occurs before catastrophic failure of the joint for the case of mild and gauge steel. Contour plots of the Mises stresses in the adherends are presented in figures 7.42, 7.43, 7.44, 7.45, 7.46, for the EC 3448 adhesive and gauge steel and figures 7.47, 7.48, 7.49, 7.50, 7.51 for the AV 119 adhesive and mild steel respectively. The adhesive elements have been removed from the contour plots for clarity, and also only a part of the whole joints is shown, see figure 7.42. The initiation and growth of the yield zone in the adherends can be seen from these graphs as the load increases for different overlap configurations. The Mises stresses

are directly related to the level of yield in the adherends which is very closely related with the failure of these type of joints (gauge and mild steel joints). The critical level of stress for mild steel was chosen between 250-270 MPa. This corresponds to the plateau seen in the stress strain curve of mild steel after initial yield. Similarly, the critical stress level for gauge steel is defined between 420-440 MPa. As the load increases, more and more of the cross-sectional area reaches and exceeds the critical level of stress. The initiation of yield happens at different load levels for different overlaps because of the different applied bending moments. Joints with shorter overlaps are predicted to yield at a lower load.

Looking at an experimental load-displacement curve for the case of mild and gauge steel joints (figures 3.5 & 3.19) there is a load level at which a "knee" occurs, and the overall stiffness of the joints decreases dramatically. At this load level (which is approximately around 80% of the failure load) the strain in the adherends increases dramatically and yielding spreads quickly across the adherend cross section. An unstable situation starts to develop above that level and failure of the joints usually occurs at a slightly higher load.

It is very interesting to see the load at which the F.E predicts the initiation of this "knee" in the load-displacement curve. In figures 7.52 and 7.53, the F.E predicted load-displacement curves for mild and gauge steel joints are presented. In the same graphs, a "solid specimen" is also presented which corresponds with a SLJ in which the adhesive has been replaced with mild or gauge steel. This "solid specimen" will effectively define the upper limit in strength for any given lap joint geometry and a particular material for adherends, which could be a very useful "tool" in the design process of bonded joints.

It is very clear that the load at which this knee occurs is not dependent on the adhesive properties, but only on the geometry of the joint and the properties of the adherends. This is also true experimentally since joints with mild steel fail at approximately the same load level regardless of the adhesive used. The same is true for gauge steel joints.

The F.E prediction for the "knee" initiation is approximately at 10-11kN for mild steel joints and around 17-18kN for gauge steel joints. Both predictions are very close to the experimentally measured failure loads.

It is interesting to investigate what would be the effect of increasing the adherend thickness in the case of a joint made with mild steel by using the F.E to calculate the load

at which a "knee" would occur in the load-displacement curve. Finite element models for joints with mild steel adherends, the AV 119 adhesive and four different adherend thicknesses (1, 1.6, 2 and 3 mm thick adherends) were created. The predicted results are compared in figure 7.54. As can be seen from the graph, the load at which the "knee" occurs is predicted to increase almost linearly with increasing adherend thickness. Although the eccentricity of the load path increases, as does the applied bending moment at the edge of the overlap, the cross sectional area of the adherend also increases too, thus making the adherend more resistant to bending. As a result, the yielding in the adherends should occur at a higher applied load, as the thickness of the adherends increases. As a consequence of that, the strength of the joints should also increase as predicted by the F.E. results. However, it must be noted here that there would be a limit to the increase in strength for larger adherend thicknesses because the adhesive material will reach its critical limits (as happens in the case of hard steel joints).

It is quite clear that the plastic deformation of the adherends will be the critical factor defining the failure load for joints made with mild and gauge steel and the adhesive materials used in the current work. The finite element analysis is able to give a conservative limit of the strength of the joints simply by defining the load at which a "knee" can be observed in the load-displacement curves of the joints. The failure in joints made of mild or gauge steel is dominated more by high local stresses and strains around the overlap ends, which are induced by the large plastic deformations occurring in the adherends.

7.5 Strain variation in the adhesive layer

7.5.1 Joints with hard steel loaded in tension

In a single lap joint under tensile loading, although there is some "peeling" load at the edges of the overlap due to the rotation of the joint, high shear strains develop under the overlap which could be associated with the failure of the joints.

Thus, it is rather important to look at the variation of the shear strains in the adhesive layer. The variation of shear strains along the overlap for joints with the EC 3448 adhesive and hard steel can be seen in figures 7.55, 7.56, 7.57, 7.58, 7.59, 7.60, 7.61, 7.62, 7.63,and 7.64.

As can be seen from the graphs the maximum shear strains occur at the unloaded interface corner. The values that these strains reach are extremely high in some cases and there are no experimental values indicating that this particular adhesive (EC 3448) could reach such a high strain to failure. However, these high values act on a very small volume of material and also are very close to the sharp adherend corner which is a singular point in the model. It is believed that high strains may be developed around the unloaded interface corner (this is where damage is expected to initiate) but not as high as those predicted by the F.E analysis. These very high predicted strains are believed to be because of mathematical reasons around the singular point of the sharp corner. Consequently, such very high predicted values should be treated with care if they are used in any calculations for strength prediction.

Shear strains on the loaded interface on the other hand, peak further inside the overlap as the load increases. So, there is a variation of shear strain across the adhesive layer thickness.

The peak shear strain, for the unloaded interface, always occurs at the embedded adherend corner, regardless of the overlap length or the applied load on the joint (figures 7.56, 7.58, 7.60, 7.62 and 7.64) and is highly influenced by the singular effect that the sharp corner produces.

The peak shear strain for the loaded interface, on the other hand, seems to shift further inside the overlap as the load increases. Furthermore, the peak values of strain along the loaded interface are also unaffected by any singularity effects. At loads near the experimental failure load, the peak occurs at a smaller distance (from the edge of the overlap) for a short overlap than for a longer one (figures 7.55, 7.57, 7.59, 7.61, and 7.63). This could be an indication that joints with longer overlaps can accommodate larger amounts of "damage" before catastrophic failure occurs. These high shear strains, on the loaded interface, appear to act over a considerably larger volume of material

compared to the high shear strains acting on the unloaded interface. It is known that the condition where very high stresses (or strains) act over a small volume of material is less critical than the condition where lower stresses (or strains) act over a larger volume of material. Thus, it seems that the peak shear strains along the loaded interface could be used to define the failure of the joints.

The shear strains from both interfaces tend to converge to the same value at a distance further away from the edge of the overlap, indicating that the variation of shear strain across the thickness of the joints is decreasing as we move inside the overlap. This is another indication that the adhesive is subjected to a more uniform shear stress field as we move towards the middle of the overlap. That is again in agreement with experimental observations on the surface failure patterns in these regions (rough textured areas, hackles, cusps as in figure 3.33 and 3.34) since the formation of cusps is closely associated with shear failure.

7.5.2 Joints with hard steel loaded in four-point bending

When a lap joint is loaded in four point bending, there are significantly higher "peel" loads than in the case of a lap joint loaded in tension. Thus, in the case of four point bending it is useful to look at the peel strains acting at adhesive layer. The variation of peel strain along the overlap for the case of AV 119 adhesive and hard steel adherends can be seen in figures 7.65, 7.66, 7.67, 7.68, 7.69, and 7.70.

Very high values of strain are again predicted for the unloaded interface near the sharp corner and a sharp strain variation across the adhesive thickness is apparent. These high strain values however, should be treated with care for the same reasons given in the previous section concerning the shear strains (singularity effect).

It is very important to note that the strain variation at the two overlap ends is not anymore symmetric. Much higher strains are predicted for the tensile loaded end of the joint (left part of the graphs with the negative co-ordinate values for distance). This because the adhesives are modelled using the Raghava pressure dependent yield criterion so the behaviour of the adhesive in tension and compression is quite different (see figures 6.8-

6.11). This is a very important point in the F.E results since it can be concluded that failure will always start from the tensile loaded end of the joint. This result would not be possible to obtain if a yield criterion that is not dependent on the hydrostatic component of stress was used.

It is very clear that only the very edge of the joint is highly strained; the peel strains for the remaining of the overlap (as we move towards the centre of the overlap) are very small. This means that not the whole overlap is important in carrying the load in a joint loaded in bending. Only the areas around the overlap edges are important for the strength of the joints and especially the end loaded in tension, which is in very close agreement with experimental results obtained from defective joints loaded in bending as has already been shown in figures 5.5 and 5.6.

As a result, failure in the case of four-point bend loading should occur due to local strains becoming critical.

Comparing now the peel strain variation between joints with different adherend thickness (figures 7.65-7.70) it can be seen that, for the same applied load, the peak peel strain becomes smaller as the adherend thickness increases. The F.E prediction indicates that the strength of joints loaded in bending should increase with increasing adherend thickness, which is what has been observed experimentally.

7.6 Effect of loading and adherend thickness on principal stress vector direction

The maximum principal stress vectors are plotted for the 25 mm overlap, hard steel and AV 119 joint configuration in tension, in figures 7.71, 7.72 and 7.73 for the 1 mm, 1.6 mm and 2 mm adherend thickness respectively.

As has already been seen (section 7.2.4), due to the non-linear geometry of the joint, some bending will be introduced in the joint in a tensile test. The maximum principal stresses lie at angles of approximately 45° in areas away from the overlap ends. However, near the end of the overlap and especially on the unloaded interface the principal stress vectors are

at slightly larger angles. As has been shown in figure 7.13 the thinner the adherends, the smaller the bending at the ends of the overlap, for the same tensile applied load. This is the reason why the principal vectors lie at a slightly smaller angle for the 1 mm thick adherend case. It is clear that most of the load is transferred in shear from the majority of the overlap.

Similar plots are presented in figures 7.74, 7.75 and 7.76 for the 25 mm overlap, hard steel AV 119 joint configuration in four point bending, for the 1.6 mm, 2 mm and 3 mm adherend thickness respectively. It is quite clear that the direction of the principal vectors is at considerably higher angles, compared with the case of tensile loading. Comparing between the different adherend thicknesses, in the four point bend case, it can be seen that the thinner the adherends, the higher is the angle that the principal vectors lie. This is because as the adherends get thinner, the local curvature (due to bending) gets larger. It must be noted of course that, results for the four point bending case are at different applied loads, which correspond to the failure loads for each different case (1.6 mm, 2 mm or 3 mm thick adherends). Most of the load is transferred through the ends of the overlap in transverse tension (through the adhesive thickness), for the case of a joint loaded in bending.

7.7 Conclusions

Results from the finite element analysis have been presented in this chapter. The variation of stress and strain values along the overlap length has been presented for a variety of cases. The finite element predictions are consistent with experimental behaviour reported in previous chapters for a variety of cases. Parameters and conditions that could affect the failure load have been identified for the different cases. It seems that different critical values and different methodologies must be followed, in order to predict the failure load of the joints in the variety of cases examined. This must be seriously taken into account in the development of any failure criterion.

Chapter 8

FAILURE CRITERIA - PREDICTIONS

8.1 Introduction

The stress and strain distributions in single lap joints of different configurations and for different types of loading have been presented in the previous chapter. Once the stress and strain distributions have been defined, then a failure analysis is needed. Appropriate failure criteria must be applied in order to make predictions for the strength of the joints.
It is well known from literature that there is currently no universally applicable failure criterion that can predict failure for a variety of different cases (different material combinations, different geometries, different types of loading). As presented in Chapter 1, criteria based on a critical value of stress, strain or strain energy have been used in the past by several researchers such as Coppendale (1977), Crocombe and Adams (1982), Harris and Adams (1982), Chen (1985), Zhao (1991), Dorn and Liu (1993). Criteria based on fracture mechanics principles were proposed by Kinloch and Shaw (1981), Lee (1985), Hunston et al (1989), Papini et al (1993), Chiang and Chai (1994), Fernlund et al (1994), Crocombe *et al* (1995). Criteria based on "damage zone in the adhesive layer" were proposed by Crocombe (1989), Edlund and Klarbring (1993), Clark and McGregor (1993), Papini et al (1994), Crocombe *et al* (1995), Hadidimound and Crocombe (1998), Sheppard et al (1998), Towse et al (1999).
Different cases must be treated in different ways in order to achieve useful results that could improve the design of bonded joins. Parameters that affect failure must be identified and, wherever possible, quantified. Guidelines that would assist engineering design will be proposed in this chapter. These design rules and guidelines could then be used to predict the safe working loads in bonded structures. The usual alternative is costly and time-consuming experiments.

8.2 Failure criteria and associated problems

Once the stress distribution in the joint has been determined, appropriate failure criteria must be devised in order to predict the strength of the bonded component.

There are several parameters that can affect the failure of joints. The are also several ways in which a joint could fail. The behaviour of both the adherends and the adhesive, as well as the geometry of the joint and the type of loading, can alter the mechanisms and mode of failure, as has been shown in chapters 3-5. All the above parameters must be taken into account before any attempts to predict failure are made.

Failure of a bonded component will occur either in the adhesive (cohesive failure) or in the adherend, or at the interface (adhesive failure). Even if appropriate surface preparation procedures have been followed, then failure at or close to the interface may occur, but at least it will not be due to poor bonding. A typical example of a failure that occurs near the adherend-adhesive interface (usually the oxide layer) but is not due to poor surface preparation are the joints with mild or gauge steel. The interface in practice is not flat and there are areas where both adhesive and adherend material are present, making the analysis quite complicated. Since the purpose of this interlayer is to transfer normal and shear loads between the adherend and adhesive, the modelling of this type of failure should only consider failure in shear and normal directions, as stated by McCarthy (1996a).

In a single lap joint configuration, failure in the adherend is more common when the adherends are made out of weaker or very brittle materials, such as perspex or glass. Failure within the adherend is also very common in cases where composite (i.e. fibre reinforced plastics) adherends are used. Failure usually occurs due to delamination of the ply closest to the adhesive, due to the low through-thickness strength of the composite. In order to improve the strength of such joints, the stress and strain concentrations near the overlap edges should be reduced by introducing adhesive fillets or altering the adherend geometry near the overlap ends (i.e. chamfers) as shown by Adams (1989). When metallic adherends are used, such as steel or aluminium, the yield stress and strain values

of the metal will determine whether some plastic deformation in the metal will occur before the failure of the joint. If the metal yields at low strain and low stress (as does mild steel), then plastic deformation in the adherends should be expected. If, on the other hand, the metal yields at considerably higher stress (as does heat treated "hard" steel), then adherend plasticity should not be expected.

Failure within the adhesive layer (as happens in the hard steel joints) is the most common type of failure. When using the continuum mechanics approach for predicting stresses and strains, most of the failure criteria use some peak value of stress or strain at a point or over a distance. It is generally believed that failure in the joint will occur when the strain in the adhesive layer reaches a critical level defined by the adhesive material stress-strain properties. It has been shown by many researchers in the past that predicted strains at critical areas can become, in theory, infinite due to strain concentrating effects such as sharp corners. This causes problems in the application of a simple maximum value of strain at a point as the failure criterion, since this value depends on the proximity of the point under consideration to the strain concentrator. Such a criterion is not physically meaningful and requires the use of pre-determined distances. These distances however, are usually determined through calibration, and are not necessarily the same for different joint configurations. Thus, different critical distances must be used, depending on the geometry, materials and loading, which makes the criterion not very useful for general design purposes.

A decision must therefore be made as to whether critical values of stress or strain will be used in the failure analysis. Many researchers, Coppendale (1977), Crocombe and Adams (1982), Adams and Harris (1987), Dorn and Lieu (1993), chose strains as the critical variable to use in the failure predictions. However, there are problems associated with the selection of the critical value of strain for the comparison. The usual procedure is to use the strain to failure from a tensile or shear test as the critical value of strain.

Odom et al (1992) showed that the strain to failure of a specimen is very closely related to the size of the specimen tested; similar results were found by Towse (1997), Towse *et al* (1998). It was shown that the strain to failure of an adhesive tested in tension is very

dependent on the minimum flaw size found in a specimen. The smaller the size of the specimen tested, the larger was the recorded strain to failure. Thus, large variations in the tensile strain to failure can be recorded, depending on the size of specimen used.

Regarding shear data of adhesives, Vaughn (1998) found that the maximum shear strain to failure is very dependent on small local variations in the geometry (such as the presence of spew fillets) on the TAST specimen. Also, by comparing results from different standard methods of testing (TAST, butt joints in torsion), large variations in the shear strain to failure can be recorded depending on the method used. The variation between different methods or slightly different geometries could give differences of the order of 50 %. On the other hand, the experimental scatter in the strength of the joints is nothing like as big. The experimental scatter for SLJs is much less than the scatter obtained from tensile or shear tests carried out to derive the stress-strain properties of the adhesives. It is therefore difficult to choose a critical value when the numbers are not consistent. Great care must be taken in the selection of a variable that is so much dependent on the specimen geometry or type of test as a critical value, since the selection of that value could seriously alter the prediction results.

Another problem is that the standard testing methods for obtaining adhesive properties, are usually obtained by performing tests on bulk specimens, or on joint configurations. The strain to failure of an adhesive could be different in the two configurations because of the highly constrained conditions imposed on the adhesive when it is in a joint (thin layer) configuration. It must be noted here that in an adhesive joint, the adhesive is constrained by the adherends and will therefore be able to undergo much larger local stresses than it can possibly do in a bulk configuration. When a test is carried out on a bulk specimen, failure will usually initiate around the areas where some voids or defects are present. The stresses and strains will therefore concentrate around that point and premature failure of the specimen is quite likely, as there are no alternative routes for transferring the load. On the other hand, in a joint configuration, the situation is not as sensitive to the presence of a small defect, as there are alternative routes for the transferring of the load from the one adherend to the other. Tests on bulk specimens should therefore be expected to be more prone to premature failure than tests on joint configurations.

As an example, results presented by Adams and Thomas (1996) on bulk torsion and butt torsion joints show that although the shape of the curves and maximum stress is quite similar for both types of test, the strain to failure is quite different. The butt joint specimens were found to break at a larger strain to failure compared to the bulk specimens. The problem lies in the difficulty of manufacturing bulk specimens without introducing defects, and also the fact that the strength of a bulk specimen is more sensitive to the existence of such defects than a joint specimen.

Also, from the results presented by Towse (1998) and Vaughn (1998) the shape of the stress-strain curves is consistent up to the point that stresses reach a maximum and the curves start to level off. It seems that the maximum tensile or shear stress recorded in the experiments is consistent, and it is not affected by either the geometry, the size of the specimen, or by the test method. The variation found in the maximum or plateau stress in both tensile and shear tests is fairly small and is not sensitive to small variations in geometry or different types of testing. The strain to failure values however, are dependent on local geometric variations (for the case of joint testing) Vaughn (1998), and the size of the specimens (for the case of bulk testing) Towse (1998).

Experimentally critical values of stress (maximum or plateau stress) might appear to be more consistent than critical values of strain (strain to failure in shear or tension) and should therefore be in favour. However, a criterion based on some critical value of strain, is more physically meaningful for a material that exhibits large plastic deformations, such as several of the adhesives used in the current work.

8.3 Towards a new failure criterion

In general, the behaviour of epoxies can be described schematically as in figure 8.1. In region (I), the adhesive behaves in a non-linear elastic fashion. At slightly higher stresses, the adhesive starts to behave plastically and a maximum stress level is reached. Some strain softening usually occurs, and most experimental values stop just beyond this point. This is because most of the tests performed are displacement control tests and as soon as the specimen starts to neck and separate, there is usually an abrupt drop in load which is

not possible to be recorded with accuracy. This is happening mainly due to the general inability of epoxies to form a stable neck. It can be postulated that the curves could show a further drop in stress with increasing strain and final failure could occur at a higher strain. This postulation mainly applies in the microscopic scale and corresponds to the stress whitening state of the adhesive. The idealised behaviour of the adhesive (which is normally used in the F.E modelling) is as shown in figure 8.1 (region III) where the strains are increasing and a constant stress level in maintained.

At a high applied load, some part of the joint (such as in the middle of the overlap) may still be in the elastic state, region (I). Nearer to the overlap edges, the adhesive would be in the plastic range, region (II). Very close to the ends of the joint and around the areas of high stress and strain concentration, such as the unloaded adherend corner, the adhesive may reach region (III). The adhesive may "fail" locally in a microscopic level (areas of stress whitening) but this does not necessarily mean that a physical crack can grow and propagate in the joint so as to cause catastrophic failure. In the F.E models normally used, it has been noted that there exists a region very near the sharp corner of the unloaded adherend where values of strain reach extremely high values, mainly due to the idealised modelling behaviour and also due to the concentrating effect of the sharp corner. These very high strain values are, in some cases, physically meaningless, in the sense that they are much higher than the adhesive strain limits as defined by tensile or shear tests. In reality, such sharp corners do not exist; but, even so, some small volume of the adhesive may well be beyond the critical limits (such as defined by uniaxial tests) on the unloaded interface, although not at the high strain levels predicted by the F.E.

In a single lap joint configuration, the fact that the adhesive around the unloaded interface corner has exceeded the adhesive strain limits does not necessarily mean that failure of the joint will occur. This is because the load can be transferred by alternative routes, further inside the overlap. As the load increases, another strain peak occurs in the loaded interface (as shown in chapter 7, figures 7.55-7.64) and a new damaged zone starts to develop at the loaded interface. As long as this volume of "damaged" material does not extend to the other interface side (loaded interface) the load can still be carried around that small damaged zone. However, when the critical values of strain are exceeded on the

loaded interface, then a physical crack can appear and propagate in an unstable manner causing catastrophic failure. Thus, when the limiting values of strain are exceeded at the loaded interface, catastrophic failure is expected to occur. Failure in this case appears to be controlled by local mechanisms (i.e. strains becoming critical) around the overlap ends. More extensive discussion will follow in section 8.3.2

For joints with low yield strength adherends, such as mild and gauge steel, it seems that the plastic deformation of the steel controls failure. Experiments show that the strength of joints with mild (or gauge) steel and different adhesives and different overlap lengths is approximately the same. The finite element prediction for the "solid specimen" presented in chapter 7 (figures 7.52, 7.53) shows that even a "solid" mild or gauge steel SLJ would result in a joint of similar strength. Moreover, experimental results on defective joints using mild or gauge steel adherends (chapter 5, figures 5.8, 5.10, 5.15, 5.16) showed that the strength of the defective joints was approximately the same as that of the non-defective joints. There was again a strong influence on the strength from the adherend plastic deformation. The plastic deformation of the steel adherends should be looked at in more detail, and adherend yielding could therefore be used to predict failure in this type of joint. Failure in this case appears to be controlled by local mechanisms.

When a ductile adhesive and hard steel adherends are used, and especially when short overlaps are considered, a global yielding condition develops in the joint. The whole of the overlap is now responsible for transferring the load, as has been shown by experiments on defected joints (figures 5.3, 5.4), because the strength of the joints decreases almost linearly as the size of the defects increases. Failure of these joints appears to be controlled not by local conditions becoming critical (i.e. strains becoming critical around the overlap ends) but rather by more global mechanisms.

For longer overlaps and more brittle adhesives, or for joints loaded in bending, there is usually a large area in the middle of the overlap that remains lightly loaded, and therefore it is often elastic, so the global yield failure criterion cannot be applied. In these cases, the

whole overlap is not responsible for carrying the load and failure occurs due to adhesive strains locally exceeding the adhesive limits. In these cases, some critical value of strain, either in shear or tension, must be exceeded in the highly loaded regions of the joint for failure to occur. Failure is now controlled by local mechanisms.

As it has been shown in this section, and has also been proven experimentally, failure might occur due to either local, or more global conditions becoming critical. Experimentally, it has been shown that different joint configurations fail in different modes, and therefore, different critical variables control failure in different cases. The aim is to apply a failure criterion which could predict failure in as many different configurations as possible without it being necessary to know *a priori* the critical variable to be used. This way, criteria that use some critical value of strain or stress at a distance, and which therefore require calibration can be avoided. For design purposes, a failure criterion that would work for a wide variety of cases should be composed of a series of sub-criteria that would be interconnected in such a way that the selection of the appropriate sub-criterion should come out of the analysis in a form of a flow chart.

8.3.1 Definition of failure due to global yielding

As has been shown in Chapter 6, the adhesives used in the current work have been modelled using the pressure dependent yield criterion, as proposed by Raghava. The Raghava yield criterion is described by equation 6.3.

$$S\sigma_{yt}^2 = 3J_2 + (S-1)\sigma_{yt}I_1 \qquad \text{Eqn. 6.3}$$

Equation 6.3 can be rewritten in terms of the hydrostatic (p) and deviatoric (q) or Mises stress components, as has already been shown in Chapter 6 :

$$aq^b - p = p_t \quad \text{Eqn. 6.4}$$

Where $b=2$ (quadratic yield surface), a and p_t are given by:

$$a = \frac{1}{3(S-1)\sigma_{yt}} \qquad \text{Eqn. 6.7}$$

$$p_t = \frac{S\sigma_{yt}}{3(S-1)} \qquad \text{Eqn. 6.8}$$

The yield surface is therefore a function of the hydrostatic stress (p), the deviatoric stress (q), the yield parameter (S), and the yield stress of the adhesive (σ_{yt}). If the combination of p, q, S, σ_{yt} is such that the function given in Eqn. 6.4 becomes greater than zero, the material is outside the yield surface and is above its initial yield state. If the yield function (Eqn. 6.4) is exactly zero, the material is on the yield surface and is currently yielding; if it is below zero, the material is inside the yield surface and no yield is occurring.

The yield parameter has already been defined in Chapter 6 for every adhesive used in the current work. For any combination of (p) and (q) and for a given yield stress (σ_{yt}) for a particular adhesive, it is possible to calculate the parts of the joint that have exceeded the yield limits as calculated by the Raghava criterion. Global yield is defined as the condition at which the whole of the overlap has exceeded the yield limits.

As has already been shown in Chapter 2, the adhesives used in the current work behave in a very non-linear fashion, which is typical behaviour for epoxies. Yield in metals is usually very sharp and is associated with irreversible damage in the material (permanent plastic deformation). The definition of yield in polymers is quite different. "Apparent yield" comes at a very low load, but this is not necessarily associated with irreversible damage in the adhesive (i.e. permanent plastic deformation). The "true" yield point is usually at quite high levels of stress. Young and Lovell (1991) state that the exact position of the yield point is very difficult to define and so define yield as the maximum point on the stress strain curve. Raghava and Caddell (1973) have proposed the 0.3% yield offset as the definition of yield in polymers. Towse (1998) has found that no irreversible damage occurs in the EC3448 epoxy adhesive below approximately 2% applied strain. This value of strain corresponds to approximately the same level of stress as defined by the 0.3% Raghava offset. It is therefore very important to define the stress level at which permanent plastic deformation in the adhesives occurs, and to use that as the yield stress in the calculation of the conditions of global yielding.

Ideally, repeated tests at progressively increasing levels of load followed by full unloading of the specimens could define this "true" yield point experimentally. As there are no experimental data of that type, except for the EC 3448 adhesive, it was decided that the yield point would be defined by using the 0.3% yield offset as defined by Raghava and Caddell (1973).

Alternatively, if such data are not available or there is a range of values to choose from, and therefore some uncertainty in the exact value to choose, this value can be "calculated" from a combination of experiments and F.E analysis. This value can then be used to predict the failure load of different joint configurations of the same adhesive.

The concept of global yielding could be schematically drawn as in figure 8.2. The thick lines, above the idealised stress strain curve, represent the condition of the adhesive along the overlap length at different levels of loading. At medium applied loads, some part of the overlap is outside the yield surface but there are still parts in the middle of the overlap that have not yet yielded. With further increase in the applied load, more parts of the overlap become yielded. At the same time, some stress whitening may occur at the very edge of the overlap (part of the curve is in region III), but the limiting values of strain in the loaded interface have not yet reached the critical limits. A point is reached when the whole of the overlap becomes yielded, and there is no part of the overlap in the elastic region (I). An unstable situation is reached and immediate failure occurs.

The global yielding criterion effectively means that the whole of the overlap is responsible for transferring the load. Experimentally, it was proven (Chapter 5) that such a situation can occur with some of the adhesives tested in the current work. The strength of joints with hard steel and defects loaded in tension was found to decrease almost linearly with increasing defect size (figures 5.3, 5.4).

In a more general case (with other types of adhesive and different material for adherends), it is the relative strength between the adherends and adhesive that would define whether the joint will fail due to global yielding. As was shown in Chapter 5, global yielding does not occur when mild steel adherends are used. If, however, a much weaker adhesive was used (such as a polyurethane adhesive), then global yielding could occur, even for joints

with low yield metallic adherends. On the other hand, the more brittle the adhesive used, the more unlikely it would be for the joint to fail due to global yielding.

The overlap length could also influence the situation. As was shown in Chapter 5, the strength of the 60 mm overlap long joints with hard steel and AV 119, was unaffected by the presence of a 12 mm size defect (see Table 5.6). This means that as the overlap length increases, there is a limit above which global yielding is no longer the cause for failure of the joint.

It can be said therefore that, in general, the global yielding failure criterion usually applies in joints with relatively short overlaps or when the adhesive behaviour is ductile and the adherends remain elastic. However, it must be noted again that with certain combination of adherend and adhesive materials (i.e. low yield adherends and low shear strength ductile adhesive) global yield could still be the dominant mechanism controlling failure.

8.3.2 Definition of failure due to local strains exceeding limiting values

The concept of failure due to local strains exceeding the limiting values of strain of the adhesive can be schematically illustrated in figures 8.3 , 8.4 and 8.5.

The highest stresses as predicted by F.E will always be on the unloaded adherend interface near the adherend corner. These predicted values of strain are extremely high due to the concentration effect from the presence of the sharp corner. The area (or volume) of material that these very high strains act over is also very small.

At low applied loads (fig. 8.4 (I)), most of the load is transferred through the ends of the overlap. As the load increases, plasticity occurs in the adhesive, especially around the unloaded interface corner and high shear strains start to develop, fig. 8.4 (II). The load is still transferred from the ends of the overlap, but some load transfer is now happening further inside the overlap. The shading of the lines represents the proportion of load carried (i.e. the thinner the line the less is the load passing through that area). At even higher loads fig. 8.4 (III), the strains at the unloaded interface exceed the limiting values for the adhesive, and stress whitening or micro-voiding may occur around that area due to

the very large shear strains developing around the unloaded adherend corner. Because more load is now transferred further inside the overlap, the shear strains start to build up on the loaded interface and the strains peak further inside the overlap as the load increases. When the strains in the loaded interface exceed the adhesive limiting values fig. 8.4 (IV), a crack can develop and catastrophic failure occurs.

It is interesting to note that the strain peak predicted by F.E. (see figures 7.55, 7.57, 7.59, 7.61, 7.63, 7.65, 7.67, 7.69) on the loaded interface, is only mildly affected by the singularity effect from the sharp corner.

Failure of the joint is predicted when the critical strain (shear strain ε_{12} or peel strain ε_{22}) on the loaded adherend interface reaches the strain limits of the adhesive in shear or tension. It is not necessary to know which of the two variables (ε_{12} or ε_{22}) would be the critical one, since this will mainly depend on the relative ratio of tension and bending applied in the joint. When a SLJ is loaded in tension, most of the load is transferred in shear through the overlap and some peel load is also present at the ends of the overlap, which is, however, small. Thus if the joint is mainly loaded in tension, then the shear strains should be expected to be controlling failure. If on the other hand the joint is mainly loaded in bending, then the peel strains should be expected to be the critical variable. It is very important to remind us here that bending and tension cannot be separated in a SLJ configuration. Thus, tensile loading of a SLJ will inevitably introduce some bending in the joint and so both shear and peel strains will be present. Similarly, in a pure bending test (such as the four-point bending test), shear stresses and strains will also be introduced apart from the peel ones.

In sections 8.2 and 8.3, the problem of defining limiting values of strain (strain to failure in tension or shear) from a standard tensile or shear test has been addressed. The experimental variation obtained from different standard tests, or even from the same test by changing the local geometry of the specimen, is significant. Additional problems are created from the specimen size effect in tensile tests. It is difficult to select a single value for the shear or tensile strain to failure from such a broad range.

Results from the lap shear tests (such as those presented in chapters 3-5) on the other hand do not show such a large scatter. The value of strain to failure (in either shear or tension) must be more consistent than what is obtained from a standard tensile or shear test.

In cases that there is a range of values to choose from (due to the experimental scatter), this critical value of failure strain (in tension or shear) can be "calculated" from a combination of testing and F.E analysis. Since failure is due to local strains becoming critical, a long overlap joint (i.e. 60 mm) is chosen. This is because it has been shown that long overlap joints usually fail because local strains become critical and not due to global yielding. The experimental failure load of this joint is applied in the corresponding F.E model, and the maximum predicted shear strain at the loaded interface is obtained. This value will now be used as the critical shear strain limit in the strength prediction for joints with the particular adhesive in any other different configuration (i.e. shorter overlap or different adherend thickness).

A similar procedure can be followed in a four point bending case, where again it has been proven experimentally that failure is due to local strains becoming critical. The experimental failure load from a joint configuration (i.e. 2 mm thick adherends) is applied in the corresponding F.E model, and the maximum predicted peel strain at the loaded interface is obtained. This value will now be used as the critical peel strain limit, in the strength prediction for joints with the particular adhesive in any other different configuration (i.e. different adherend thickness or different overlap).

These "calculated" critical strains should, however, lie within the experimental scatter for a particular adhesive. These values need only be calculated once, and they may then be used in the strength prediction of any joint configuration with this particular adhesive.

It can generally be said that failure due to local strains in the joint exceeding the adhesive strain limits usually applies in cases where failure is controlled by the local strain field. This is usually the case for joints with long overlaps; joints with brittle adhesives, and joints that are loaded in bending.

8.3.3 Definition of failure due to adherends becoming plastic

When the adherends become plastic, a situation similar to the one described in section 7.4 develops. Very high localised strains develop at the edges of the joint due to the excessive plastic deformation of the adherends and a small increase in load results in very large increases in local strain. An unstable condition is created and there is a limiting load above which the overall stiffness of the joints decreases dramatically as has been presented in figures 7.52 and 7.53.

Most finite element programs experience convergence difficulties when this unstable situation develops in the model. As a result, a cutback in the increment size is necessary and the analysis proceeds very slowly. From the engineering point of view, the extra information that might be obtained by letting the analysis continue by applying higher loads is not very useful compared with the computational expense, since the load carrying capacity of the joints has been reached. It is therefore not unreasonable to attempt to define the failure load of these types of joints as the load at which this unstable situation occurs (dramatic decrease in the overall stiffness of the joint or "knee" in the load displacement curve). It is very important to point out that even the "solid specimen" F.E prediction follows the same trend and the "knee" occurs at approximately the same load as with the adhesive joints. This could be used to define an upper strength limit for the particular geometric design under consideration.

It is very important to remind us here that the great influence of the adherend plastic deformation on the strength of the joints has been observed experimentally for a variety of joint configurations. It is clear from results involving mild (or gauge) steel (Chapter 3) that neither the adhesive's ductility nor the overlap length has any significant influence in the strength of the joints. The same effect was also observed for defective joints (Chapter 5) with mild (or gauge) steel. Also, results from private communication with Mr. F. Kadioglou, on a parallel project within the University of Bristol, were found to be in agreement with the above argument. Joints of the same geometry and the same mild steel adherends but with a different, more ductile adhesive (SBT from 3M) were found to be only marginally stronger in tension compared to the AV 119 joints. Despite the fact that

the SBT adhesive has a considerably larger strain to failure than the AV 119 adhesive, the joint strength is still dominated by the adherend plasticity.

This means that regardless of the adhesive performance (within the structural adhesive range) the strength of the joints will be dominated by the yield strength of the adherends. Failure due to adherend yielding could be applied to any type of adherend that yields at low strains (below 1%) and at low applied stress, such as aluminium alloys, "soft" steel and similar materials.

8.4 Proposed failure prediction methodology

As has been explained in the previous sections, different critical variables appear to be necessary when different configurations are analysed. Since the mechanisms that govern failure in each case are different, a variety of steps needs to be taken in order to predict failure in different joint configurations.

A failure criterion should be applicable to as many different joint configurations as possible using the basic material properties of the constituent materials.

Parameters that need to be known and which will be used as input in the F.E analysis include:

- Basic material properties, such as Young's modulus E, and Poisson's ratio ν, in tension for both the adherends and adhesives used.
- Stress-strain data in tension for both adherends and adhesives and especially the data describing the post yield behaviour of the materials
- Stress-strain data in shear, shear modulus G, for the adhesives including the post yield behaviour.
- The definition of a yield point for each adhesive to be used in the global yield criterion. Note that for an epoxy adhesive the yield point is not necessarily within the proportional limit of the tensile stress strain curve, but is usually found at a higher level of stress and corresponds with the point at which permanent plastic deformation occurs in the adhesive.

- The yield parameter S must be defined for each adhesive using the tensile and shear or compressive data.
- The geometry and appropriate boundary conditions representing the type of test and loading.
- The limiting values of strain that the adhesive can withstand in tension and shear must also be known so that they can be used in the failure criterion.

When all these parameters are known, the strength of the joints can be calculated by using the flow chart shown in figure 8.6.

The first thing that needs to be checked is whether a global yielding condition has been reached throughout the adhesive layer. If the answer is yes, then the strength of the joint can be calculated based on the global yield concept using the Raghava criterion as described in section 8.3.1. That could be the case for a low strength, high ductility adhesive (such as polyurethane type or similar) even with low strength adherends (mild or gauge steel). This also applies to short overlap cases or especially when high strength (elastic) adherends are used. This criterion will probably not be applicable in configurations with long overlaps or joints with brittle adhesives.

If global yield in the adhesive does not occur, then the next point to check is whether extensive yield in the adherends is likely to have occurred. If that is the case, then a conservative estimate for the strength of the joints can be calculated by using the load-displacement curves of the overall joint. The load at which the overall stiffness of the joint starts decreasing dramatically defines the strength of the joints in a conservative way. An upper limit on the strength of joints based on the same geometry and adherend yield can be obtained by analysing a "solid specimen". As has been shown in figures 7.52 and 7.53, the F.E predicted load at which the "knee" in the load-displacement curve occurs, is only slightly higher for the "solid specimen", than it is for the same adhesive joint specimen. This is an inexpensive method of carrying out parametric studies on geometric factors that could influence the strength of the joints. Geometric optimisation of a joint type can therefore be achieved without the need for very complicated analysis.

This type of criterion obviously applies to joints with adherends that yield at low stress levels and very low strains (typically 0.1-0.5%) such as mild, gauge steel or aluminium.

If the above two criteria are not met, then failure will occur when local values of strain in tension or shear reach the limiting values that the adhesive can withstand. From the reasons given in sections 8.3 and 8.3.2, maximum values along the "loaded" interface need only be considered. If the peak value of peel strain (ε_{22}) or shear strain (ε_{12}) exceeds the limiting values of strain in tension and shear respectively, then failure is predicted due to these local strains.

When the SLJ is loaded in tension, and high strength adherends are used, the load transfer happens through the majority of the overlap, as has been shown experimentally from tests on the defective joints (Chapter 5). Most of the load is transferred in shear through the adhesive layer, although some direct (ε_{11}) and peel (ε_{22}) strains are present around the edges of the overlap, although these are small in value. So, in this case (SLJ loaded in tension) the critical value controlling failure is the shear strain (ε_{12}). Chai (1993), has also concluded that the ultimate shear strain is a key property controlling crack growth.

On the other hand, when the SLJ is loaded in bending (as in the four point bending tests), most of the load is carried by the very ends of the joint in direct tension through the adhesive thickness. The shear strains are also high near the overlap ends, but the critical value of strain in this case is the peel strain (ε_{22}) due to the way the load is applied.

In a general loading situation, the proportion of load applied in shear and bending is not known *a priori*; whichever of the two critical variables (ε_{12}) or (ε_{22}) exceeds the limiting values first, is the one that will define the failure load. As has been explained in section 8.3.2 it is the relative ratio of tension and bending applied in the joint that will define which variable, (ε_{12}) or (ε_{22}), will be the critical.

8.5 Strength predictions

The strength of the joints can now be predicted using the method presented in section 8.4. The most interesting case of all the different joint configurations examined in the current work is the one where the adherends remain elastic throughout loading (hard steel adherend joints), because the adhesive is used to its full potential. Most of the predictions will therefore be for the case of hard steel joints. Predictions for mild and gauge steel will also be carried out using the F.E predicted load-displacement curves for these joints.

It is necessary now to define the limiting values of strain for each adhesive as well as the yield stress to be used in the global failure criterion. These values will be defined from experimental data available for the adhesives, presented in chapter 2. In some cases, however, some of the critical values will be calculated using a combination of F.E analysis and experimental results, as explained in sections 8.3.1 and 8.3.2.

The limiting values of strain or stress that will be used in the failure predictions are summarised in the following table.

Table 8.1 Critical variables used in the F.E strength predictions for the different adhesives

Adhesive	Yield stress σ_{yt} (MPa)	Max. Shear Strain ε_{12}	Max. Tens. Peel Strain ε_{22}
EC 3448	50	50%	8%
AV 119	50	45%	7%
ESP 110	45	15%	3%
MY753	38	20%	4%

8.5.1 Hard steel joints

For the hard steel joints, the correlation between finite element predictions and experiments can be seen in figures 8.7, 8.8, 8.9, 8.10, 8.11 and 8.12 for the different adhesives and joint configurations tested.

As can be seen, the correlation is generally very good and the failure prediction methodology appears to give good results in a variety of joint configurations (with different adhesive properties, geometry of the joint, and loading).

8.5.1.1 Tensile tests

For joints with the EC 3448 adhesive in tension (figure 8.7), failure due to global yielding occurs for overlaps up to 25 mm. The critical variable for longer overlaps (40 mm and 60 mm) is the shear strain ε_{12}.

For joints with AV 119 in tension (figure 8.8), the same situation exists. Joints with overlaps up to 25 mm fail due to global yielding and failure in longer overlaps is dominated by shear strains along the loaded interface. For joints with AV 119 and different adherend thicknesses (figure 8.9), failure is predicted due to global yielding too, and F.E predicts a very small increase in strength in joint strength as the thickness of the adherends increases. The predicted increase is rather small, but the correlation is still quite good. It must be noted here that this result only applies for cases that the adherends remain elastic. If mild or gauge steel adherends were used, then increasing the adherend thickness would result in an increase in the joint strength (because of the increased load at which adherend yielding would occur).

For ESP 110 joints in tension (figure 8.10) failure due to global yielding occurs for joints up to 20 mm overlap. The critical variable dominating failure for longer overlaps is again shear strain.

A similar situation exists for the MY753 adhesive in tension (figure 8.11). Failure is due to global yielding for the case of 12.5 mm overlap, but longer overlap joints fail due to high local shear strains.

As can be seen from the above results for structural adhesives and a relatively short overlap in single lap shear, failure is dominated by global yielding. This means that the whole of the overlap is involved in transferring the load, as has also been shown experimentally in the case of AV 119 joints with defects. As the overlap gets longer however, failure is not any more due to global yielding, but due to high local shear strains. This is because a critical overlap length is reached at which some part in the middle of the overlap does not contribute to the strength of the joint (as shown for a 60 mm overlap AV 119 joint with defects in section 5.3.1, Table 5.6). As the adhesive's

behaviour becomes more brittle, then the conditions at the edges of the joint becomes more and more important and failure is dominated by local shear strains near the ends of the overlap. This is because as the adhesive gets more brittle, it cannot withstand the high shear strains that develop around the ends of the overlap, as discussed in section 8.4.2 (figure 8.4). Plasticity of the adhesive cannot spread under the whole of the overlap, because the critical strain limits at the overlap ends are exceeded first.

8.5.1.2 Bending tests

The prediction for the AV 119 joints loaded in bending, is presented in figure 8.12. The F.E analysis correctly predicts an almost linear increase in the strength of the joints as the adherend thickness increases. Results from an extension of the current work by Long (1999) also showed that the joint strength continues to increase linearly with adherend thickness, for joints with adherends of up to 8 mm thick. The critical variable dominating failure for the case of joints loaded in bending is the peel strain ε_{22}. The joints are predicted to fail when ε_{22} reaches a critical level of strain on the loaded interface. For a joint loaded in bending, only the very ends of the joint are important in transferring the load, so failure is always dominated by local tensile peel strains. This is agreement with experimental results from Chapters 4 and 5, where it was shown that neither the overlap length nor the defect size, influences the strength of the joints in bending. Results from private communication with Mr. F. Kadioglou, on a parallel project within the University of Bristol, were found to be in agreement with the above argument. Joints of the same geometry and adherend materials but with a different, more ductile adhesive (SBT from 3M) were found to be stronger in bending compared to the AV 119 joints. The SBT adhesive is considerably weaker in shear but has a much higher strain to failure in tension. The superior performance of the SBT joints in bending can therefore be attributed to the higher strain to failure of the SBT adhesive in tension, which controls failure in this type of loading configuration.

8.5.2 Mild and gauge steel joints

For joints with mild and gauge steel adherends, experimental results showed that the strength of the joints becomes dominated by the mechanical properties of the adherends, for all but very short overlaps. This is the reason why all adhesives seem to give joints of approximately similar strength. It is therefore not unreasonable to predict the strength of the joints based on the adherend yield behaviour. A conservative estimate for the strength of the joints can be obtained from the overall load-deflection curve of the different joint configurations as already explained in section 8.3.3. The comparison for mild and gauge steel joints can be seen in figures 8.13 and 8.14 respectively, for several adhesives.

Failure in the case of mild and gauge steel joints is dominated by local strains at the very edge of the overlap. This is where the rotation and the large plastic deformations of the steel occur, leading to stable crack growth very close to the loaded adherend interface. The fact that the strength of joints with mild or gauge steel is dominated by local effects (the very localised adherends yielding and the corresponding very high local strains) is in close agreement with experimental result for the defective joints (Chapter 5). It is very clear that when mild or gauge steel are used as the adherends, only the very ends of the overlap are involved in the transfer of load and joint strength is independent of defect size.

8.6 Final points

The single lap joint, although simple in geometry, is quite a difficult joint to analyse. Predicting the failure load of a single lap joint in a variety of configurations is not an trivial task. Many parameters affect the strength and usually in different ways. Geometric and material non-linearities complicate the situation even further.

The failure prediction must be a multiple stage method since failure can occur in different ways depending on the configuration of the joint under consideration. A failure prediction

methodology has been presented in this chapter which predicts the strength of a variety of joint configurations. Predictions are in good agreement with experimental results.

A failure prediction envelope is presented in figure 8.15. For short overlaps, failure is dominated by global yielding in the adhesive layer, as indicated by the blue line. The extent of this line mainly depends on the ductility of the adhesive used. If the adhesive is ductile, then this method of prediction will probably be valid for longer overlaps too. If the adhesive is brittle however, global yielding as a failure criterion will only be applicable for short overlaps, if at all. It should not, of course, be forgotten that the results depend on the adherend material and the geometry of the joint too. It is important to note here that the global yielding line defines an upper limit for the strength of any configuration.

The yellow line represents a limit in strength imposed by the adherend yield. Joints with different adhesives and different overlaps are expected to fail at approximately the same load. Theoretically, more ductile adhesives should give slightly stronger joints. Joints with longer overlaps should also be slightly stonger due to the smaller bending being present in this case. Differences should, however, be small.

When the adherends remain elastic and the overlap is long, failure is not necessarily governed by global yield in the adhesive, but may be due to local high strains reaching the limiting values of the adhesive. This type of failure is represented by the solid red line in figure 8.15 for the case of a ductile adhesive. When the adhesive becomes brittle, the effect is a strength reduction as represented by the red dashed line.

The effect of increasing the adherend thickness is different depending on whether the failure is due to "local" or more "global" phenomena. So, for the case of a joint loaded in bending (where failure is due to local high strains) the effect will be an increase in strength. For a joint in tension, with elastic adherends and a ductile adhesive, (where failure is due to global yielding) the effect on strength will be minimal. If, however, the adherends were made of mild steel, then the strength of the joint would increase since the yielding of the adherends would happen at a higher load, as predicted by F.E in figure 7.54.

Tests on joints with defects gave very useful information on whether failure is dominated by the "local" (areas close to the overlap ends) or "global" (the whole of the overlap) stress and strain field. The results were again strongly influenced by the adherend behaviour as well as by the adhesive behaviour. It was found that when high strength (elastic) adherends and a relatively ductile adhesive were used, the strength of the joints decreased almost linearly with increasing defect size. When the adherends were mild or gauge steel however (which could yield under the applied loads before the adhesive would fail), the strength was nearly unaffected by the presence of defects and failure is dominated by the "local" stresses and strains. In cases where a more brittle adhesive is used, failure tends to be more "local" dominated. Similarly, for joints loaded in bending, it was shown that failure is controlled by the ends of the overlap. There is no effect in the strength of the joints in bending from the size of defects.

In order to improve joint strength, a number of parameters needs to be considered. Both the behaviour of the adhesive and adherend must be taken into account. Geometric variations in the joint will result in different results depending on the adherend and adhesive materials properties as well as the type of loading.

It is beneficial for the strength of the joints if the adherends remain elastic throughout loading. For the adhesives, on the other hand, it is beneficial if some plasticity occurs, especially at high levels of stress. The more strain an adhesive can withstand without failing, the stronger are the joints, provided a high level of stress is maintained; otherwise failure will occur due to the global yielding phenomena at a quite low load. For an adhesive to be strong, it should be able to yield progressively at high levels of stress and reach high levels of strain without failing. When the SLJs are loaded in tension most of the load is carried through shear in the adhesive. Thus, the adhesive behaviour in shear is also very important, especially when the load in the joint is predominantly tensile. What is equally important is that the shear behaviour of the adhesive is modelled correctly in the theoretical analysis. This can only be achieved by using a pressure dependent yield criterion, otherwise the behaviour of the adhesive can be seriously under estimated (see figures 6.8-6.11 comparison between the Raghava and Mises modelling). The higher the

maximum shear stress and shear strain that the adhesive can withstand, the stronger will be the joint strength.

A better understanding of the failure and the mechanisms that govern the strength of the single lap joints has been achieved. A multi-stage failure criterion for the prediction of strength has been proposed. This will enable a better and more efficient design of bonded joints, and what is more important is that predictions become more reliable.

8.7 Future work

Further validation of the failure criterion must be carried out, especially in other configurations such as the double lap joint, T-peel joint, and double strap joint. The validity of the criterion should also be tested for further adhesive and adherend configurations, covering a wider range of parameters.

It is also important to develop new methods of obtaining more consistent results for the adhesive properties, especially properties such as strain to failure in tension and shear. It seems that the current methods allow for a large variations in the measured values of such quantities. As has been shown in section 8.3, some of these critical parameters can be calculated by using a combination of experimental results and F.E analysis, something that should be validated further for a wider variety of configurations.

It is rather important to develop a method of determining the yield stress of adhesives with accuracy. This yield point should not be taken as the point where the adhesive starts to behave in a non-linear fashion, but as the point at which permanent plastic deformation occurs. This is because most of the adhesive materials behave in a non-linear elastic manner followed by non-linear plastic range.

Manufacturing joints with artificial defects gives a good indication of the sensitivity of failure to "local" or "global" phenomena and should be carried out using a variety of adhesives and joint configurations.

Observing the failure process *in-situ* with high speed video cameras or other methods such as non-destructive techniques will give more insight on how failure initiates and propagates in the joint before catastrophic failure.

Non-contact measurement methods for the derivation of adhesive properties in bulk should be employed whenever possible.

APPENDIX I

Derivation of True stress - True strain

Material test data are commonly supplied using values of nominal stress and strain. However, the stress strain data for the materials modelling, in the finite element analysis, must be supplied as true stress - true strain.

Considering the incompressible nature of plastic deformation (constant volume during plastic flow), then :

$$l_0 A_0 = lA \qquad \text{(Eq. I-1)}$$

where A_0, l_0 are the original cross-sectional area and length of the specimen and A, l are the current cross sectional area and length.

The following expression relates the current cross sectional area to the original:

$$A = A_0 \frac{l_0}{l} \qquad \text{(Eq. I-2)}$$

Substituting A into the definition of true stress σ_{true} we get:

$$\sigma_{true} = \frac{F}{A} = \frac{F}{A_0}\frac{l}{l_0} = \sigma_{nom}\left(\frac{l}{l_0}\right) \qquad \text{(Eq. I-3)}$$

but,

$$\frac{l}{l_0} = 1 + \varepsilon_{nom} \qquad \text{(Eq. I-4)}$$

so eventually the relationship between true stress and nominal stress and strain is:

$$\sigma_{true} = \sigma_{nom}(1 + \varepsilon_{nom}) \qquad \text{(Eq. I-5)}$$

The relationship between true and nominal strain is given:

$$\varepsilon_{true} = \ln(1 + \varepsilon_{nom}) \qquad \text{(Eq. I-6)}$$

APPENDIX II

Hardening of Gauge Steel Adherends.

The gauge steel used is a special alloy steel suitable for hardening. Its structure is such that the hardening of the metal is not happening in the surface only. Typical analysis of the composition from the data sheet : C.95, Mn.1.2, Cr.50, W.50, V.15.

According to the manufacturer, different levels of hardening can be achieved depending on the procedure followed, especially the tempering session. A tempering session of 1h at 350°C was chosen for our case. The whole treatment was done using available equipment at the University of Bristol. The procedure is as follows:

- The specimens are put in the oven for 2-3 minutes at 810 °C until a uniform temperature is reached within them.
- Quench immediately in oil, by immersing the specimens along their length. Care was taken to immerse the specimens as fast as possible so as to have a minimal amount of heat loss.
- A tempering session of 1hour at 350° C follows to achieve the required properties.
- Specimens are then left to cool down to room temperature.
- The hardness of each specimen is measured on a Vickers Hardness Testing Machine to ensure repeatability.

APPENDIX III

Vibration tests

Vibration tests were carried out on rectangular beams of materials used as a cross check in the calculation of the Young's modulus of the materials tested.

Dynamic methods for the determination of material properties such as the Young's moduli are quite simple and reliable. For a free - free beam vibrating at its fundamental frequency we have:

$$f_{nl} = A_1 \frac{ah}{l^2} \qquad \text{(Eq. III-1)}$$

where A_1 is a constant depending on the mode shape of vibration and is equal to 1.027 for the fundamental mode.

a is the velocity of sound

h is the thickness of the beam

l is the length of the beam

$$a = \sqrt{\frac{E}{\rho}} \qquad \text{(Eq. III-2)}$$

where E is the Young's Modulus

and ρ is the density

so finally we get:

$$E = \frac{f_{nl}^2 l^4 \rho}{A_1^2 h^2} \qquad \text{(Eq. III-3)}$$

Experiments done on rectangular beams of material vibrating in its first (fundamental) mode usually experience sharp resonance so the Young's modulus can be calculated with quite good accuracy.

APPENDIX IV

Bending moment calculations

Goland and Reissner (1944) were among the first to determine the importance of bending moments in the strength of the joints. They developed analytical expressions for the calculation of the bending moments at the edges of the overlap. Other researchers like Hart-Smith (1973) and Zhao (1991) followed with similar approaches. In the next paragraphs the equations used to derive the bending moments for each case will be given and comparisons could then be made between the different approaches and the predictions obtained in the current work by using the finite element method. The aim is to assess the range of validity for the different methods, as these methods provide a relatively easy an inexpensive way for calculating the bending moments at the edges of the joint and can be used as a useful design tool.

Goland and Reissner's derivation

The formulas developed by Goland and Reissner for the calculation of bending moments at the edge of the overlap are as follows:

$$M_{GR} = \frac{1}{2} T k_{GR} t \qquad \text{(Eq. IV-1)}$$

where k_{GR} is the bending moment factor and is defined by Goland and Reissner:

$$k_{GR} = \frac{\cosh u_2 c}{\cosh u_2 c + 2\sqrt{2}\sinh u_2 c} \qquad \text{(Eq. IV-2)}$$

u_{2c} is defined as:

$$u_2 c = \sqrt{\frac{3(1-\nu^2)}{2}} \frac{c}{t} \sqrt{\frac{P}{E}} \qquad \text{(Eq. IV-3)}$$

where T is the applied tensile load per unit width

P is the applied tensile stress in the adherends

E is the Young's modulus of the adherends

ν is the Poisson's ratio of the adherends

c is half the overlap length

t is the thickness of the adherends

Zhao's derivation

As part of his thesis Zhao (1991) developed the following expressions for the calculation of the bending moments per unit width at the edge of the overlap.

$$M_{Zhao} = \frac{1}{2} T k_{Zhao} t \qquad \text{(Eq. IV-4)}$$

k_{Zhao} is the bending moment factor which is defined by Zhao as:

$$k_{Zhao} = \frac{1}{1+\zeta c} \qquad \text{(Eq. IV-5)}$$

where ζ is defined as:

$$\zeta = \sqrt{\frac{T}{D}} \qquad \text{(Eq. IV-6)}$$

D is the flexural rigidity of the adherends

$$D = \frac{Et^3}{12(1-\nu^2)} \qquad \text{(Eq. IV-7)}$$

Hart-Smith's derivation

The formula developed by Hart-Smith (1973) is very similar to that of Zhao's but includes the adhesive thickness

$$M_{HS} = \frac{1}{2} T k_{HS} (t + t_\alpha) \qquad \text{(Eq. IV-8)}$$

where t_α is the adhesive's thickness

the bending moment factor defined by Hart-Smith:

$$k_{HS} = \frac{1}{1 + \zeta c + \frac{\zeta^2 c^2}{6}} \qquad \text{(Eq. IV-9)}$$

REFERENCES

ABAQUS Finite element software, Version 5.6, Hibbitt, Karlsson & Sorensen, Inc. 1080 Main Street, Pawtucket, RI 02860-4847

Adams R.D., Strength predictions for lap joints, Especially with Composite Adherends, A Review, J. Adhesion, Vol. 30, pp. 219-242, 1989

Adams R.D., Atkins R.W., Harris J.A., Kinloch A.J., Stress analysis and failure properties of carbon-fibre-reinforced-plastic/steel double-lap joints, J.Adhesion, Vol. 20, pp. 29-53, 1986

Adams R.D., Chambers S.H., Peppiatt N.A., Rubber model for adhesive lap joints, PJA Del Strother, Journal of strain analysis, Vol. 8, No 1, 1973a

Adams R.D., Comyn J. and Wake W.C., Structural adhesive joints in enginnering, 2nd edition, 1997

Adams R.D., Coppendale J., Peppiatt N.A., Stress analysis of axisymmetric butt joints loaded in tortion and tension, Journal of strain analysis, Vol. 13, No. 1, pp. 1-10, 1978

Adams R.D., Davies R.G.H., Strength of joints involving composites, Journal of adhesion. Vol. 59, no 1-4, pp. 171-182, 1996

Adams R.D., Gregory D.A., Panes G.A., The effect of three dimensional stress state on the failure of single lap joints, Mulhouse France, Euradh 1994

Adams R.D., Guild F.J., Heinrich J., Grochowski C., Perret P., The mechanics of failure of single lap adhesive joints, 21st Annual Meeting of the Adhesion Society, Savannah, Georgia, pp. 212-214, February 1998

Adams R.D., Harris J.A., The influence of local geometry on the strength of adhesive joints, Int. J. of Adhesives, Vol. 7, No. 2, pp. 69-80, April 1987

Adams R.D., Karachalios V.F., W.K.L van der Voorden, The effect of adherend plasticity and overlap length on the failure of single lap joints, Euradh '96, Adhesion '96, Cambridge UK, 3-4 Sept. 1996

Adams R.D., Peppiatt N.A., Effect of Poisson's ratio strains in adherends on stresses of an idealised lap joint, J. Strain Analysis Vol. 8, pp. 134-139, 1973b

Adams R.D., Peppiatt N.A., Stress analysis of adhesive bonded lap joints, Journal of strain analysis, Vol. 9, No. 3, pp. 185-196, 1974

Adams R.D., Peppiatt N.A., Stress analysis of lap joints in fibre reinforced composite materials, Fibre Reinforced Materials, Institution of Civil Engineers, London, pp. 39-49, 1977

Adams R.D., Thomas R., Test methods for determining shear property data for adhesives suitable for design, MTS Adhesive project 1, Part 2, Report No 7, March 1996

Allman D.J., A theory for the elastic stresses in adhesive bonded lap joints, Quarterly J Mechanics and Applied Maths. XXX Part 4, pp. 415-436, 1977

Anandarajah A., Vardy A.E., Mode I and II fracture of adhesive joints, J. of Strain Analysis, Vol. 19, No.3, pp. 173-183, 1984

Apalak K.M., Davies R., Analysis and design of adhesively bonded corner joints: fillet effect, Int. J. of Adhesion & Adhesives, Vol. 14, No. 3, 1994

ASTM Standards Part 22, D 1002, pp. 260-264, 1982

Baziard Y., El Abdi R., Amara D., Petit J.A., Levallois F., Study of critical failure parameters for an adhesive-bonded single lap joint with ceramic adherends, Int. J. Adhesion & Adhesives, Vol. 15, pp. 155-160, 1995

Blanchard C., Chateauminois A., Vincent L., A new testing methodology for the assessment of fatigue properties of structural adhesives, Int. J. of Adhes. & Adhesives, Vol. 16, No 4, pp.289-299, 1996

British Standards BS 18 Tensile testing of metals (including aerospace materials) 1987

Carpenter W.C., A comparison of numerous lap joint theories for adhesively bonded joints, J. Adhesion, Vol. 35, pp. 55-73, 1991

Chai H., Chiang M.Y.M., A crack propagation criterion based on local shear strain in adhesive bonds subjected to shear, J. Mech. Phys. Solids, Vol. 44, No. 10, pp. 1669-1689, 1996

Chai H., Chiang M.Y.M., A finite element analysis of interfacial crack propagation based on local shear, Part-II Fracture, Int. J. Solids Structures, Vol. 35, No 9-10, pp. 815-829, 1998b

Chai H., Observation of deformation and damage at the tip of cracks in adhesve bonds loaded in shear and assessment of a criterion for fracture, Int. J. of Fracture, Vol. 60, pp. 311-326, 1993

Chai H., Shear fracture, Int. J. of Fracture, Vol. 37, pp. 137-159, 1988

Charalambides M.N., Dean G.D., Constitutive models and their data requirements for use in Finite element Analysis of adhesives under impact, Project PAJ2, Report No 2, NPL Report CMMT(A)59, April 1997

Chen Z., The failure and fracture analysis of adhesive bonds, PhD Thesis, Univ. of Bristol 1985

Chiang M.Y.M., Chai H., A finite element analysis of interfacial crack propagation based on local shear, Part-I near tip deformation, Int. J. Solids Structures, Vol. 35, No 9-10, pp. 799-814, 1998a

Chiang M.Y.M., Chai H., Plastic deformation analysis of cracked adhesive bonds loaded in shear, Int. J. Solids Structures, Vol. 31, No 18, pp. 2477-2490, 1994

Chiu W.K., Jones R., A numerical study of adhesively bonded lap joints, Int. J. Adhesion&Adhesives, Vol. 12, No 4, Oct. 1992

Clark, J.D., McGregor I.J., Ultimate tensile stress over a zone: A new Failure Criterion for adhesive joints, J. Adhesion, Vol. 42, pp.227-245, 1993

Coppendale J., Stress and failure analysis of adhesive joints, PhD Thesis, Univ. of Bristol 1977

Crocombe A.D., The non-linear stress and failure analysis of adhesive tests, PhD Thesis, Univ. of Bristol 1981

Crocombe A.D., Global yielding as a failure criterion for bonded joints, Int. J. of Adhesion & Adhesives, Vol. 9 No 3, pp. 145-153 July 1989

Crocombe A.D., Modelling and predicting the effects of test speed on the strength of joints made with FM73 adhesive, Int. J. of Adhesion and Adhesives, Vol. 15, pp. 21-27, 1995

Crocombe A.D., Adams R.D., Peel analysis using the finite element method, J.Adhesion, Vol. 12, pp. 127-139, 1981a

Crocombe A.D., Adams R.D., Influence of spew fillet and other parameters on the stress distribution in the single lap joint, J.Adhesion, Vol. 13, pp. 141-155, 1981b

Crocombe A.D., Adams R.D., An elasto-plastic investigation of the peel test, J.Adhesion, Vol. 13, pp. 241-267, 1982

Crocombe A.D., Bigwood D.A., Richardson G., Analysing structural adhesive joints for failure, Int. J. of Adhesion & Adhesives, Vol. 10, No 3, pp. 167-178 July 1990

Crocombe A.D., Richardson G., Smith P.A., A unified approach for predicting the strength of cracked and non-cracked adhesive joints, J. Adhesion, Vol. 49, pp. 211-244, 1995

Dagyani H.R., Ye L., Mai Y.W., Evaluation of mode II fracture energy of adhesive joints with different bond thickness, J. Adhesion, Vol. 56, pp. 171-186, 1996

Davies R.G.H., Development of an adhesive material model within ABAQUS, IACS Report No. 31, Issue 1, July 1997

Davies R.G.H, The properties of adhesives at elevated temperatures and the effect on predicted joint strength, PhD Thesis, University of Bristol, Dept. of Mech. Eng. 1999

Dean G.D., Duncan B.C., Tensile behaviour of bulk specimens of adhesives, MTS Adhesive project 1, Report No 3, May 1995

Delale F., Stress singularities in bonded anisotropic materials, Int. J. of Solids and Structures, Vol. 20, No. 1, pp. 31-40, 1984

Dorn L., Liu W., The stress state and failure properties of adhesive bonded plastic /metal joints, Int. J. Adhesion & Adhesives, Vol. 13, No 1 Jan. 1993

Drucker D.C., Prager W., Soil Mechanics and Plastic Analysis or Limit Design, Vol. 10, No. 2, pp. 157-165, 1952

Duncan B.C., Dean G.D., Prediction of the performance of adhesives under impact loading, SAE V Bristol, pp. 274-277, 1-3 April 1998

Edlund U., Klarbring A., A coupled elastic -plastic damage model for rubber-modified epoxy adhesives, Int. J. of Solids Structures, Vol. 30, No. 19, pp. 2693-2708, 1993

Fargette B., Gilbert Y., Rimlinger L., Comparison between Experimental and theoretical analysis of stress distribution in adhesively bonded joints, J. Adhesion, Vol. 59, pp. 159-170, 1996

Fernando M., Harjoprayitno, W.W., Kinloch A.J., A fracture mechanics study of the influence of moisture on the fatigue behaviour of adhesively bonded aluminium-alloy joints, Int. J of Adhesives and Adhesion, Vol. 16, No. 2, pp.113-119, 1996

Fernlund G., Papini M., McCammond D., Spelt J.K., Fracture load predictions for adhesive joints, Composite Science and Technology, Vol. 51, pp. 587-600, 1994

Fernlund G., Spelt J.K.., Mixed mode fracture characterisation of adhesive joints, Composite Science and Technology, Vol. 50, pp. 441-449, 1994

FYLDE Electonic Lab. Ltd, Preston, Lancs. PR1 2XQ, England

Gaofeng W., Crocombe A.D., Simplified F.E modelling of structural adhesive joints, Computers and Structures, Vol. 61, No. 2, pp. 385-391, 1996

Gere J.M., Timoshenko S.P., Mechanics of Materials, 3rd Edition, Chapman and Hall U.K, 1987

Gledhill R.A., Kinloch A.J., Polymer, Vol. 17, p. 727, 1976

Goland M., Reissner E., The stresses in cemented joints, Journal of applied mechanics, March 1944

Grant L., The characterisation of adhesive joints found typically in the automotive industry, PhD Thesis, Univ. of Bristol 1994

Groth H.L., Stress singularities and fracture at interface corners in bonded joints, Int. J. Adhesion& Adhesives, Vol. 8, No. 2, pp. 107-113, April 1988

Hadidimoud S., Crocombe A.D., Richardson G., Use of local damage model to determine rupture, Euradh 98-WCARP-1, Garmisch-Partenkirchen/Germany, pp. 219-221, Sept. 6-11, 1998

Harris J.A., Non linear analysis and testing of adhesive joints under impact and quasi static loading , PhD Thesis, Univ. of Bristol 1983

Harris J.A., Adams R.D., Strength prediction of bonded SLJ by the non-linear finite element methods, Int. J. Adhesion & Adhesives, Vol. 4, No. 2, April 1984

Harris J.A., Adams R.D., An assessment of the impact performance of bonded joints for use in high energy absorbing structures, Proc. Inst. Mech. Engrs. Vol 199, No. C2, pp. 121-131, 1985

Hart-Smith L.J., Adhesive bonded single lap joints, NASA Report CR-112236,CR-112237, Langley Research Center, 1973

Hart-Smith L.J., Stress Analysis - a continuum mechanics approach, Developments in Adhesives - 2, Appl. Sci. Pub., pp. 1-44, 1981

Hein V.L., Erdogan F., Stress Singularities in a two-material wedge, Int. J. of Fracture Mechanics, Vol. 7, No.3, pp. 317-330, Sept. 1971

Heinrich J. Failure of adhesive joints caused by the combination of hydrostatic and deviatoric stresses, Final Year Project, University of Bristol, 1997

Hunston D.L., Kinloch A.J., Wang S.S., Micromechanics of fracture in structural adhesive bonds, J. Adhesion, Vol. 28, pp. 103-114, 1989

Ikegami K., Fujii T., Kawagoe H., Kyogoku H., Motoie K., Nohno K., Sugibayashi T., Yoshida F., Benchmark tests on adhesive strengths in butt, single and double lap joints and double-cantilever beams, Int. J. of Adhesion and Adhesives, Vol. 16, pp. 219-226, 1996

ISO 11003-2 Structural adhesives - Determination of shear behaviour - Part 2: Thick adherend tensile test method 1993

Kim Y.G., Lee S.J., Lee D.G., Jeong K.S., Strength analysisi of adhesively bonded tubular SL steel-steel joints under axial loads considering residual thermal stresses, J. Adhesion, Vol. 60, pp. 125-140, 1997

Kinloch A.J., Interfacial fracture mechanical aspects of adhesive bonded joints - A review, J. Adhesion, Vol. 10, pp. 193-219, 1979

Kinloch A.J., Kodokian G., The design of double overlap joints using thermoplastic composites, J. Adhesion, Vol. 37, No. 1-3, pp. 33-45, 1992

Kinloch A.J., Shaw S.J., The fracture resistance of a toughened epoxy adhesive, J. Adhesion, Vol. 12, pp. 59-77, 1981

Kinloch A.J., Young R.J., Fracture behaviour of polymers, Elsevier Applied Science Amsterdam, 1983

Knabel H., The effect of artificial defects on the strength and failure of single lap joints, Final Year Project, University of Bristol, Dept. of Mech. Eng. 1998

Lang T.P., Mallick P.K., Effect of spew geometry on stresses in single lap adhesive joints, Int. J. of Adhesion & Adhesives, Vol. 18, pp. 167-177, 1998

Lee S.J., Lee D.G., Development of a failure model for adhesively bonded tubular single lap joint, J. Adhesion, Vol. 40, pp.1-14, 1992

Lee S.M., An in situ failure model for adhesive joints, J. Adhesion, Vol. 18, pp. 1-15, 1985

Long C., The strength of adhesively bonded SLJs in bending, Final Year Project, Univ. of Bristol, Dept. of Mech. Eng. 1999

Long R.S., Static strength of adhesively bonded ARALL-1 joints, J. of Composite Materials, Vol. 25, April 1991

Lotus 123 User's Manuals

Machon A., The strength of single lap joints with artificial defects, Final Year Project, Univ. of Bristol, Dept. of Mech. Eng. 1998

Mallick V., Stress analysis of metal / CFRP adhesive joints subjected to the effects of thermal stresses, PhD Thesis, Univ. of Bristol 1989

McCarthy J., Failure modes and criteria-Some conclusions, Euradh '96 Conference proccedings, Cambridge 1996a

McCarthy J., Quasi static failure criteria for adhesive joints based upon advanced analyses, MTS Adhesives Project 2, Report No. 6, Annex 4, 1996b

McLaren A.S., MacInnes I., The influence on the stress distribution in an adhesive lap joint of bending of the adhering sheets.. British Journal of applied physics, Vol. 9 Feb.1958

Odom E.M., Adams D.F., Specimen size effect during tensile testing of an unreinforced polymer, J. of Materials Science, Vol. 27, pp. 1767-1771, 1992

Oplinger D.W., Deformation and stress analyses of double-lap adhesive joints with laminated composite adherends, The SEM VIII International Congress, Nasville, Tennessee, 1996

Oplinger D.W., Effects of adherend deflections in single lap joints, Int. J. Solids Structures, Vol. 13, No. 18, pp. 2565-2587, 1994

Papini M., Fernlund G., Spelt J.K., Effect of crack-growth mechanism on the prediction of fracture load of adhesive joints. Composites Science and Technology, Vol. 52, pp. 561-570, 1994b

Papini M., Fernlund G., Spelt J.K., The effect of geometry on the fracture of adhesive joints, Int. J. of Adhesion and Adhesives, Vol. 14, No.1, 1994a

Pascoe K.J., An introduction to the properties of engineering materials, 3rd Edition 1978

Peppiatt N.A., Stress analysis of adhesive joints, PhD Thesis, Univ. of Bristol 1974

Pradhan S.C., Iyengar N.G.R., Kishore N.N., Finite element analysis of crack growth in adhesively bonded joints, Int. J. of Adhesion and Adhesives, Vol. 15, pp. 33-41, 1995

Purslow D., Matrix fractography of fibre reinforced epoxy composites, Composites, Vol. 17, No 4 pp. 289-303, Oct. 1986

Rabinowitz S., Ward I., Parry J., The effect of hydrostatic pressure on the shear behaviour of Polymers, J. of Materials Science, Vol. 5 pp. 29-39, 1970

Raghava R., Caddell R., A macroscopic yield criterion for crystalline polymers, Int. J. Mech. Sci., Vol. 15, pp. 967-974, 1973a

Raghava R., Caddell R., The macroscopic yield behaviour of polymers, J. of Materials Science, Vol. 8, pp. 225-232, 1973b

Renton W.J., Vinson J.R., Analysis of adhesively bonded joints between panels of composite materials, J.Appl. Mechanics,Trans. ASME, pp. 101-106, March 1977

Rice J.R., Constitutive Equations in Plasticity (Edited by A.S.Argon), MIT Press, Cambridge, MA, USA, 1975

Richardson G., An investigation of interfacial failure of adhesive joints, PhD Thesis, Univ. of Surrey 1993

Ripling E.J., Mostovoy S., Corten H., Fracture mechanics : A tool for avaluating structural adhesives, J. Adhesion, Vol. 3, pp. 107-123, 1971

Roulin-Moloney A.C., Fractography and failure mechanisms of polymers and composites, Elsvier Science Publishers Ltd, 1989

Schonhorn H., Ryan F.W., Wang T.T., Effects of bonding defects on shear strength in tension of lap joints having brittle adhesives, Journal of applied Polymer Science, vol. 16, pp. 1901-1909, 1972

Schonhorn H., Ryan F.W., Wang T.T., Effects of symmetrical bonding defects on tensile shear strength of lap joints having ductile adhesives, Journal of applied Polymer Science, vol 15, pp. 1069-1078, 1971

Sheppard A., Kelly D., Tong L., A damage zone model for the failure analysis of adhesively bonded joints, Int. J. of Adhesion & Adhesives, Vol. 18, pp. 35-40, 1998

Towse A., Measurement of mechanical properties of 3M EC 3448 adhesive at different specimen sizes, Report No. 51, Issue No. 2, November 97, Univ. of Bristol, Dept. of Aeronautical Engineering 1997

Towse A., Potter K., Wisnom M.R., Adams R.D., Specimen size effects in the tensile failure strain of an epoxy adhesive, J of Materials Science, Vol. 33, pp. 4307-4314, 1998

Towse A., Potter K.D., Wisnom M.R., Adams R.D., The sensitivity of a Weibull failure criterion to singularity strength and local geometry variations, Int. J. of Adhesion & Adhesives, Vol. 19, pp. 71-82, 1999

Tsai M.Y., Morton J., Three-dimensional deformations in a single-lap joint, J. of Strain Analysis for engineering design, Vol. 29, No. 2, pp. 137-145, 1994a

Tsai M.Y., Morton J., An evaluation of analytical and numerical solutions to the single lap joint, Int. J. of Solids Structures, Vol. 31, N0 18, pp. 2537-2563, 1994b

Tsai M.Y., Morton J., An experimental investigation of non-linear deformations in single lap joints, Mechanics of materials, Vol. 20, pp. 183-194, 1995

Tsai M.Y., Oplinger D.W., Morton J., Improved theoretical solutions for adhesive lap joints, Int. J. Solids Structure, Vol. 35, No. 12, pp.1163-1185, 1998

Vaughn L.F., Adams R.D. "Test methods for determining shear propertiy data for adhesives suitable for design, MTS Adhesives Project 1, Part 3, Report No.8, March 1996

Vaughn L.F., Measurment of basic mechanical properties of adhesives for design use, PhD thesis, Univ. of Bristol, Dept. of Mech Eng., April 1998

Volkersen, Die Nietkraftveteilung in zugbanspruchten Nietverbindungen mit konstanten Laschquerschnitten. 15 Lufthrtforschung, 1938

Voorden W.K.L., Adhesively bonded single lap joints - The influence of the overlap length and adherend plasticity, Final year project, Univ. of Bristol, Dept. of Mech. Eng., April 1995

Wang C.H., Rose L.R.F., Determination of triaxial stresses in bonded joints, Int. J. of Adhesion and Adhesives, Vol. 17, pp. 17-25, 1997

Weissberg V., Arcan M., Invariability of singular stress fields in adhesive bonded joints, Int. J. of Fracture, Vol. 56, pp.75-83, 1992

Wisnom M.R., Limitations of linear elastic bending theory applied to four point bending of unidirectional carbon fibre-epoxy, 31st Structures, Structural Dynamics and Materials Conference, Long Beach California, April 1990

Wronski A., Pick M., Pyramidal yield criteria for epoxides, J. of Materials Science, Vol. 12, pp. 28-34, 1977

Young R.J., Lovell P.A., Introduction to Polymers, 2nd Ed. Chapman & Hall 1991

Yu H., Adams R.D., An improved dilatometer for the measurement of adhesive shrinkage, SAE V, Bristol, pp. 237-242, 1-3 April 1998

Zhao X., Stress and failure analysis of adhesively bonded joints, PhD Thesis, Univ. of Bristol, 1991

Zink A.G., Davidson R.W., Hanna R.B., Finite element modelling of double lap wood joints, J. Adhesion, Vol. 56, pp. 217-228, 1996

Zwick Testing Machines Ltd., Southern Avenue, Leominster, Herefodshire HR6 0QH

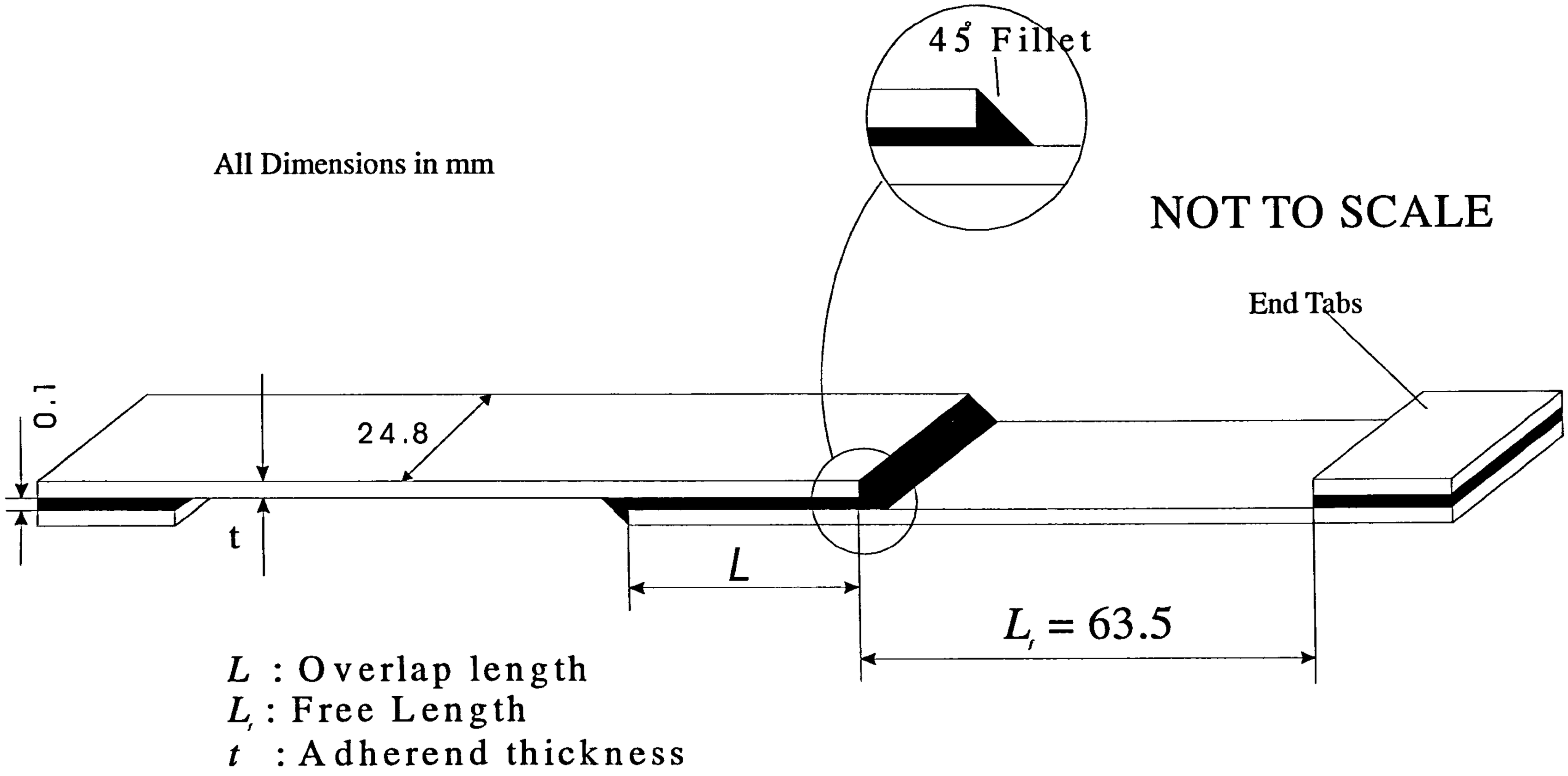

Figure 2.1 Schematic and dimensions of a single lap joint

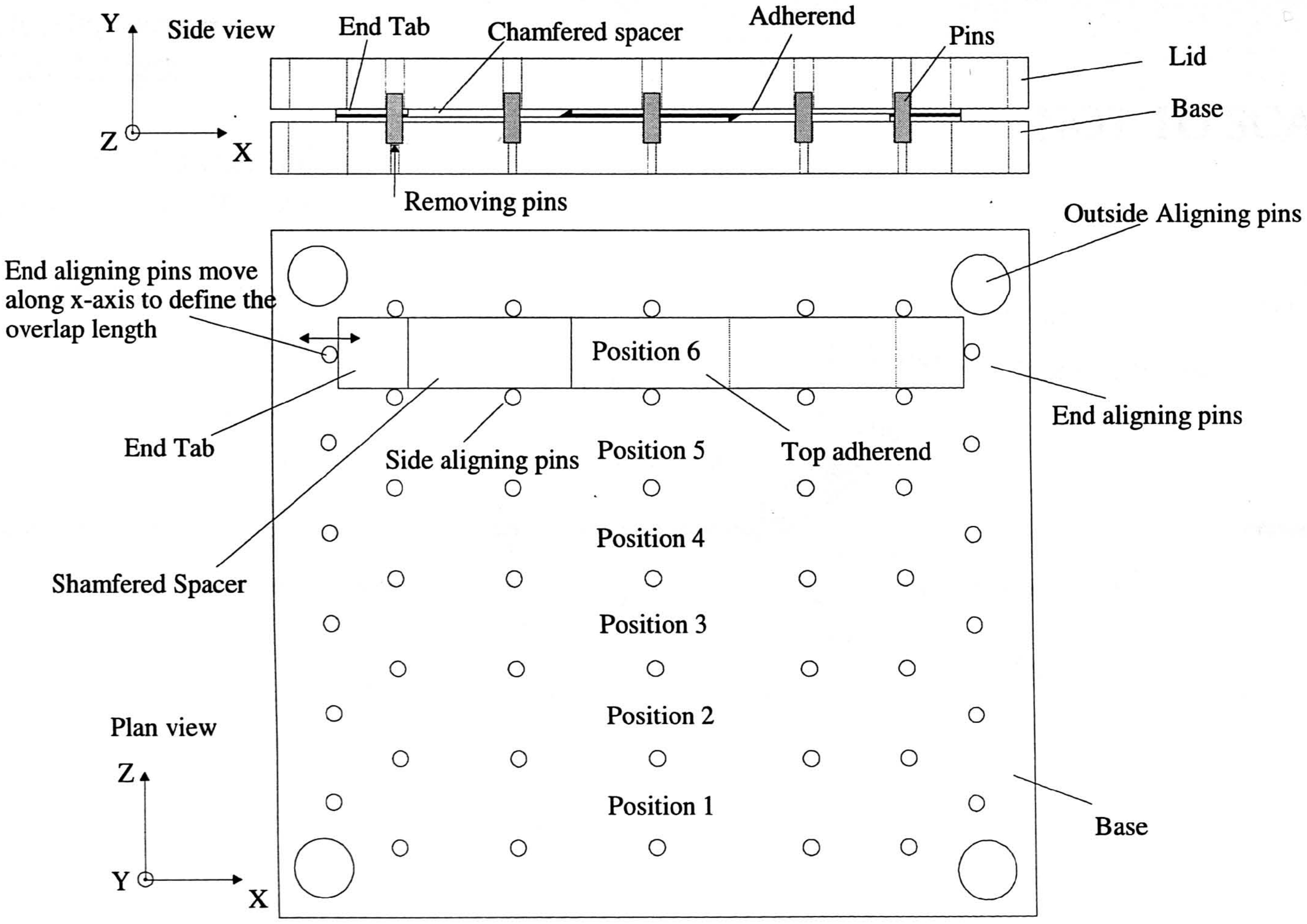

Figure 2.2 Metal jig used to manufacture the SLJ

L : Overlap length
L_r : Free Length
b : width
t : thickness of adherend
t_a : thickness of adhesive

Side view : xy plane
Failure patterns : xz plane

NOT TO SCALE

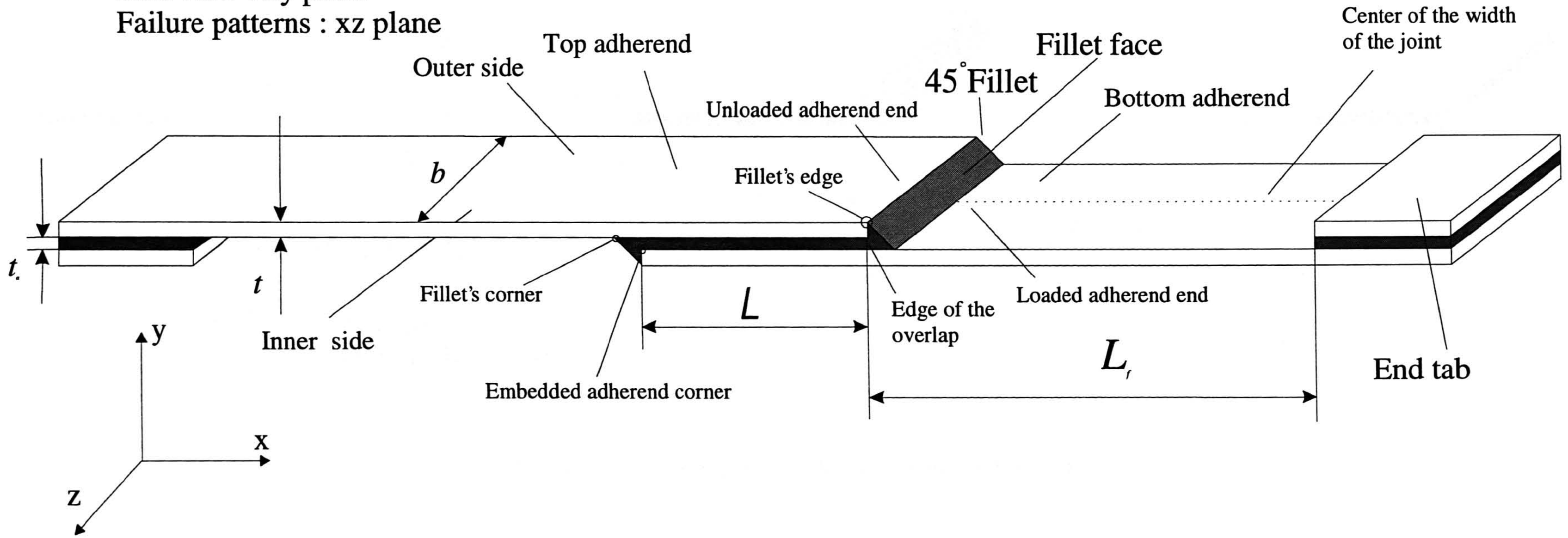

Figure 2.3 3-Dimensional view of a single lap joint - naming definitions and conventions for parts of the joint

Dimensions in mm

L : Overlap length

L_r : Free Length

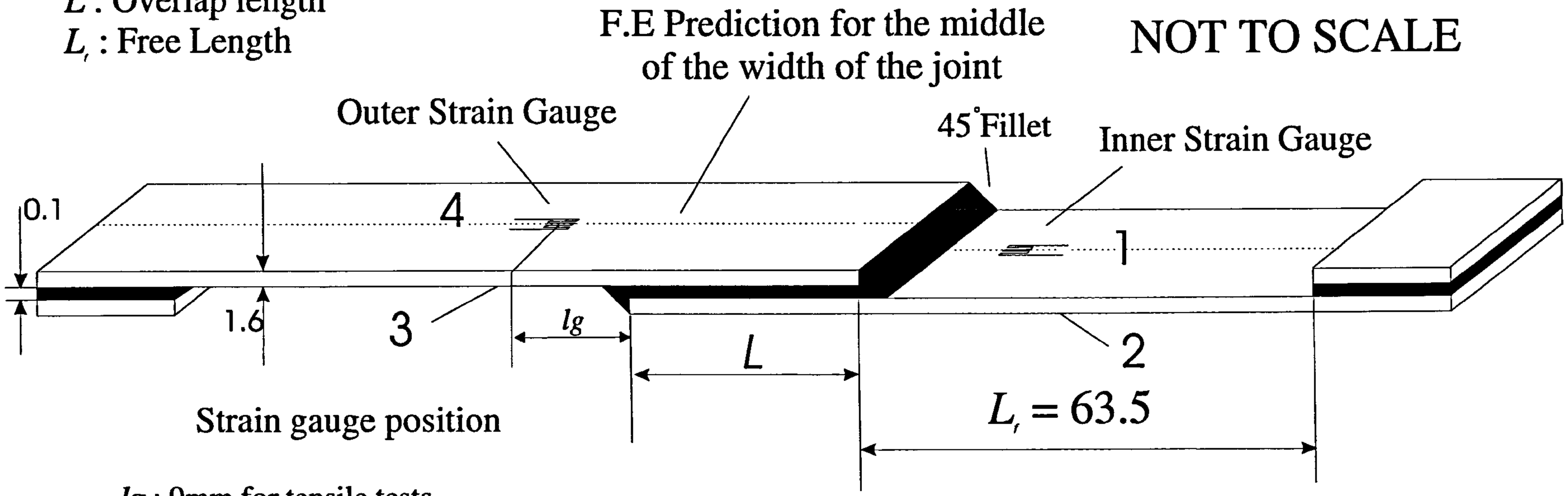

Strain gauge position

lg : 9mm for tensile tests
7.5mm for four point bend tests

Figure 2.4 Strain gauge position on single lap joints

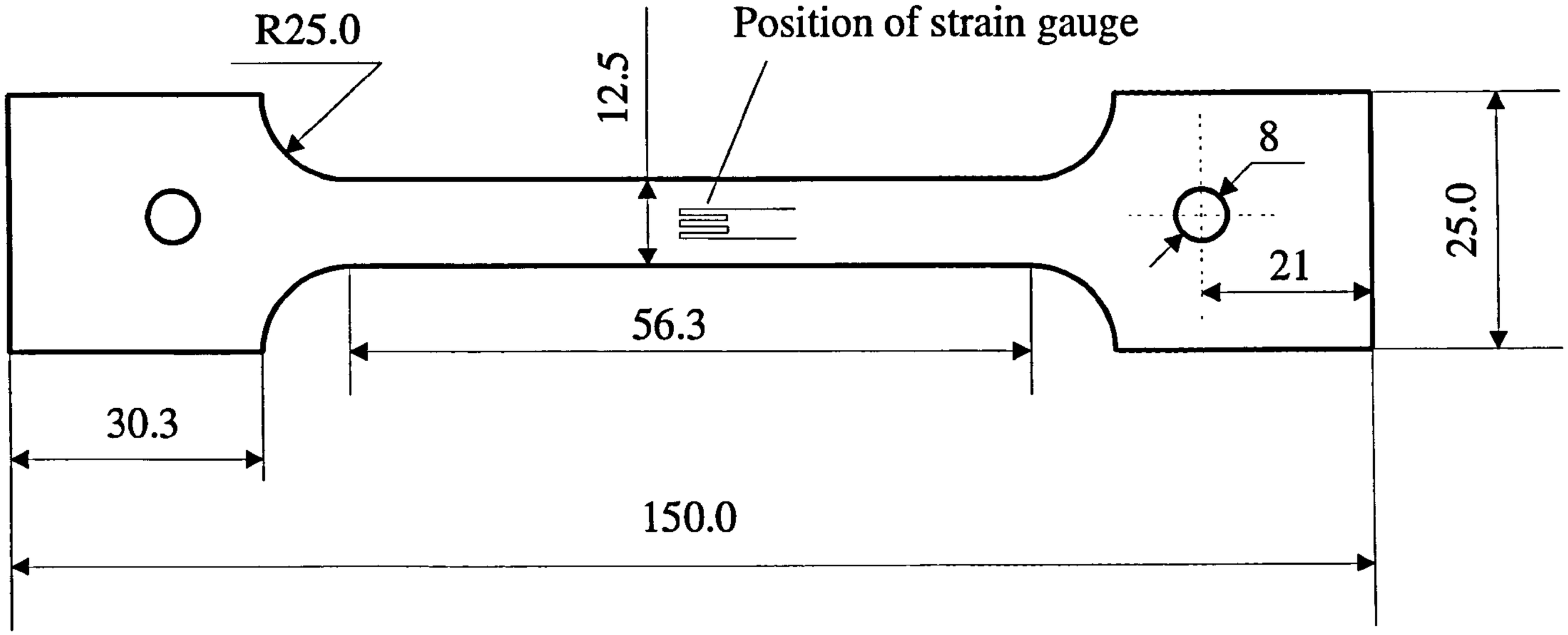

Figure 2.5 Dogbone specimen used for the derivation of stress-strain curves in tension

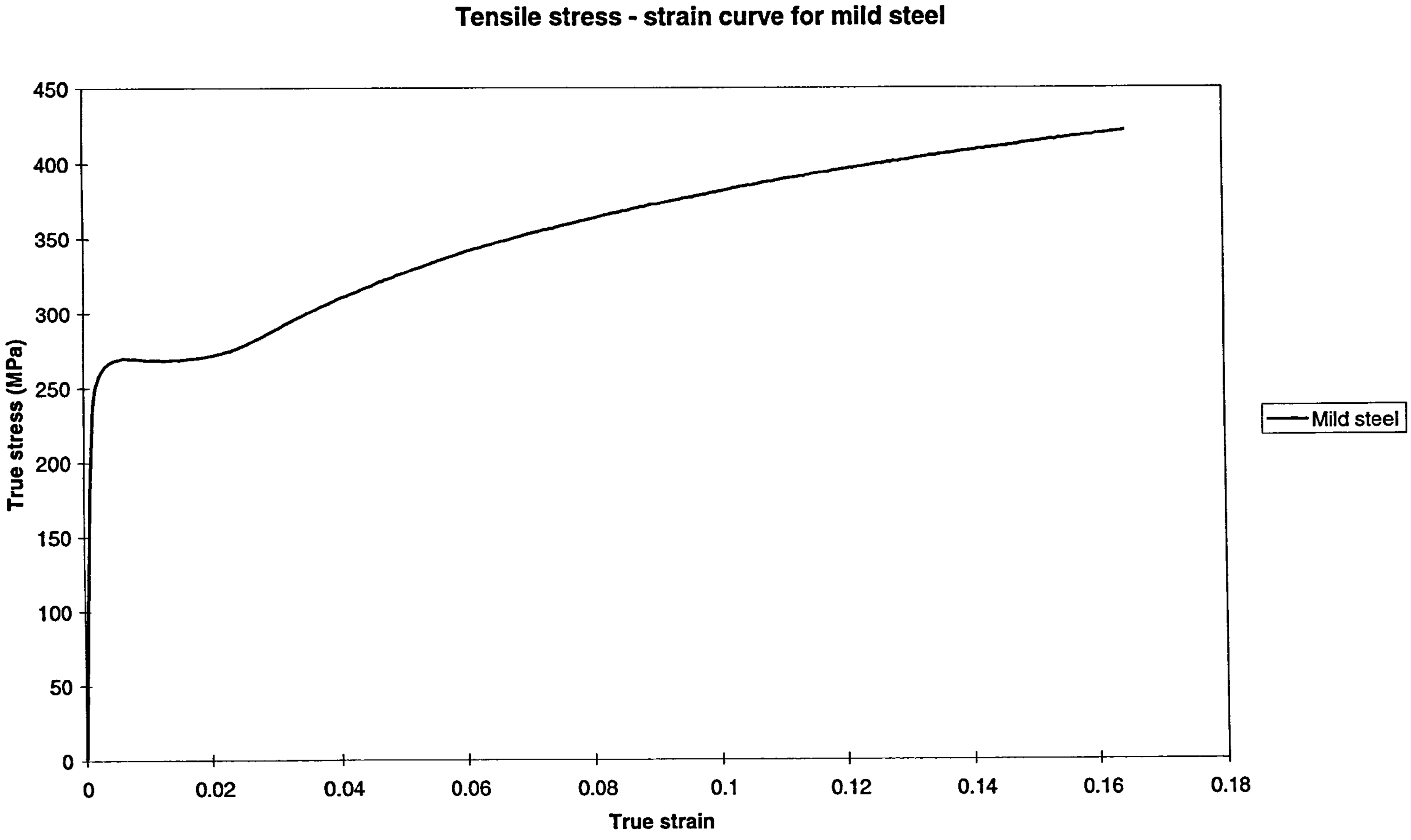

Figure 2.6 Tensile stress-strain curve for mild steel

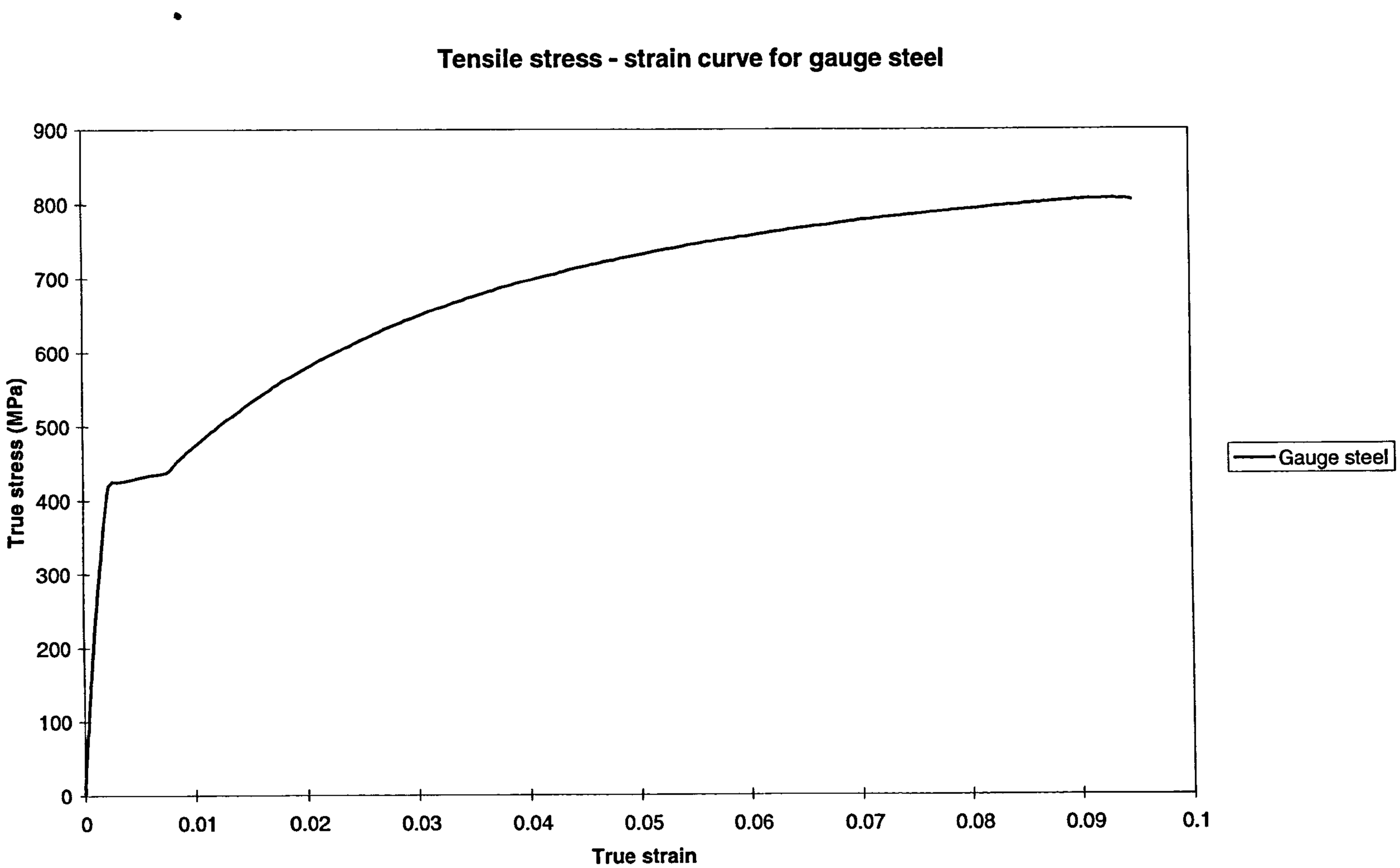

Figure 2.7 Tensile stress-strain curve for gauge steel

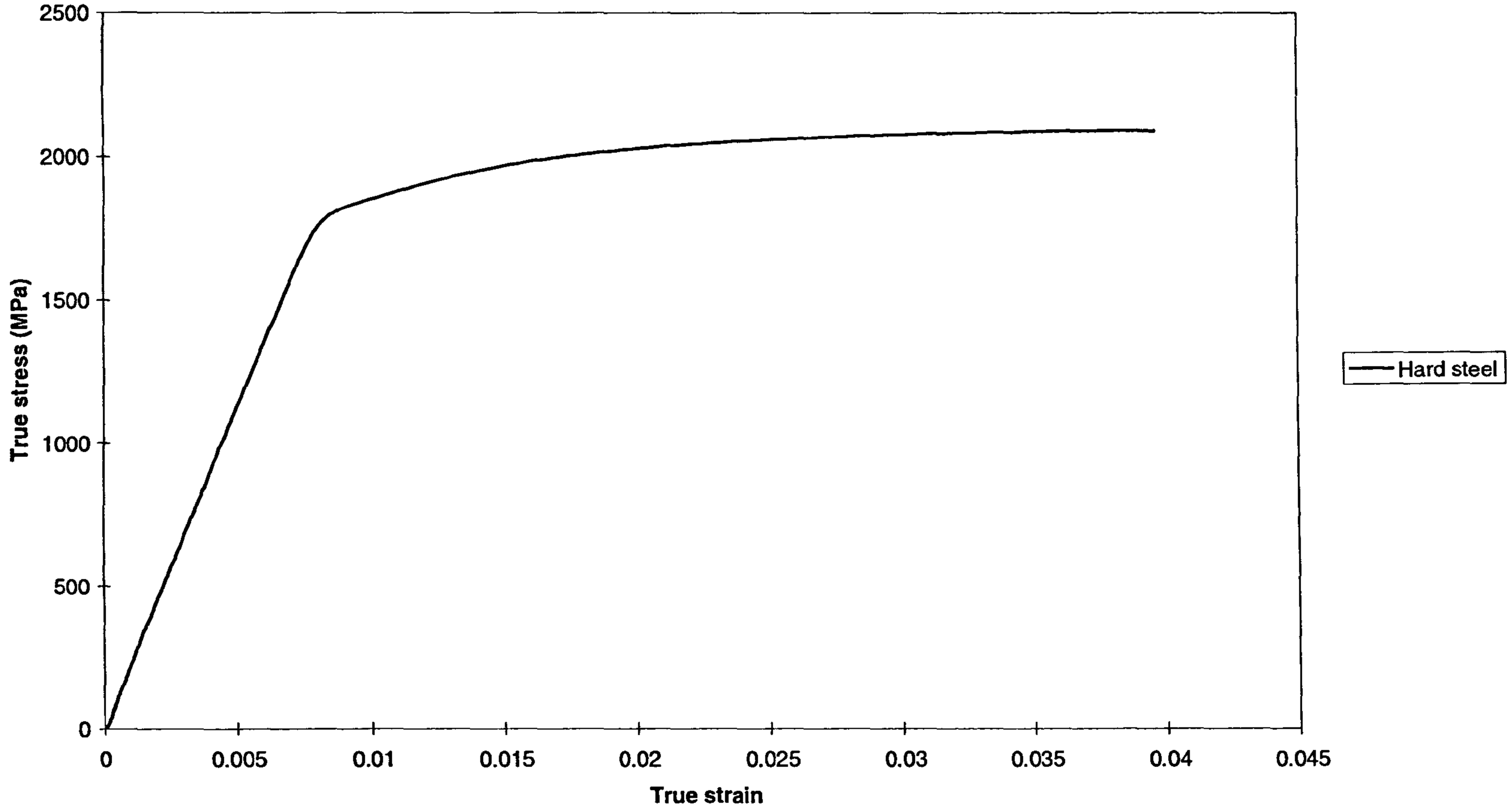

Figure 2.8 Tensile stress-strain curve for hard steel

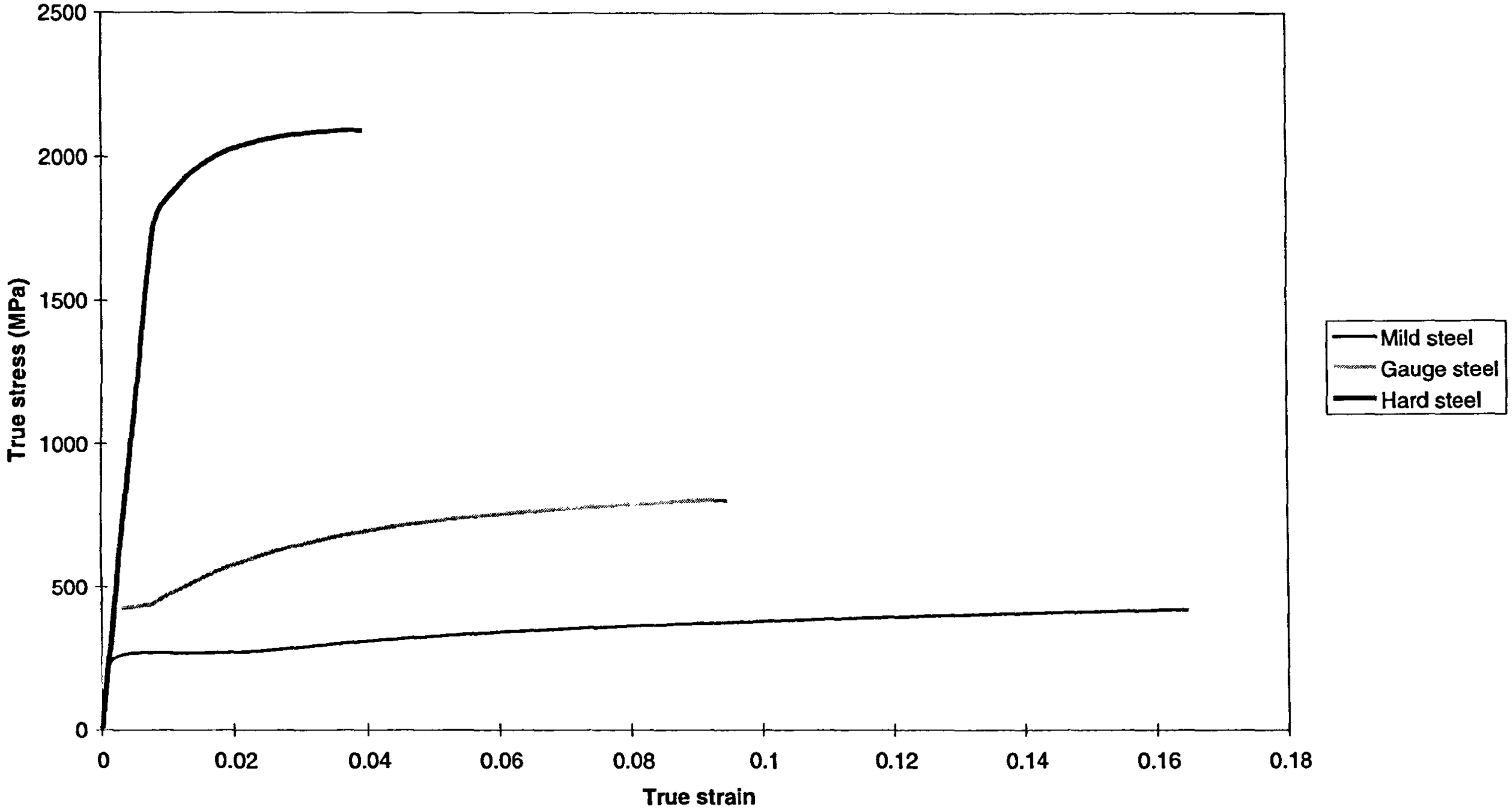

Figure 2.9 Comparison of tensile stress-strain curves for different steel adherends used

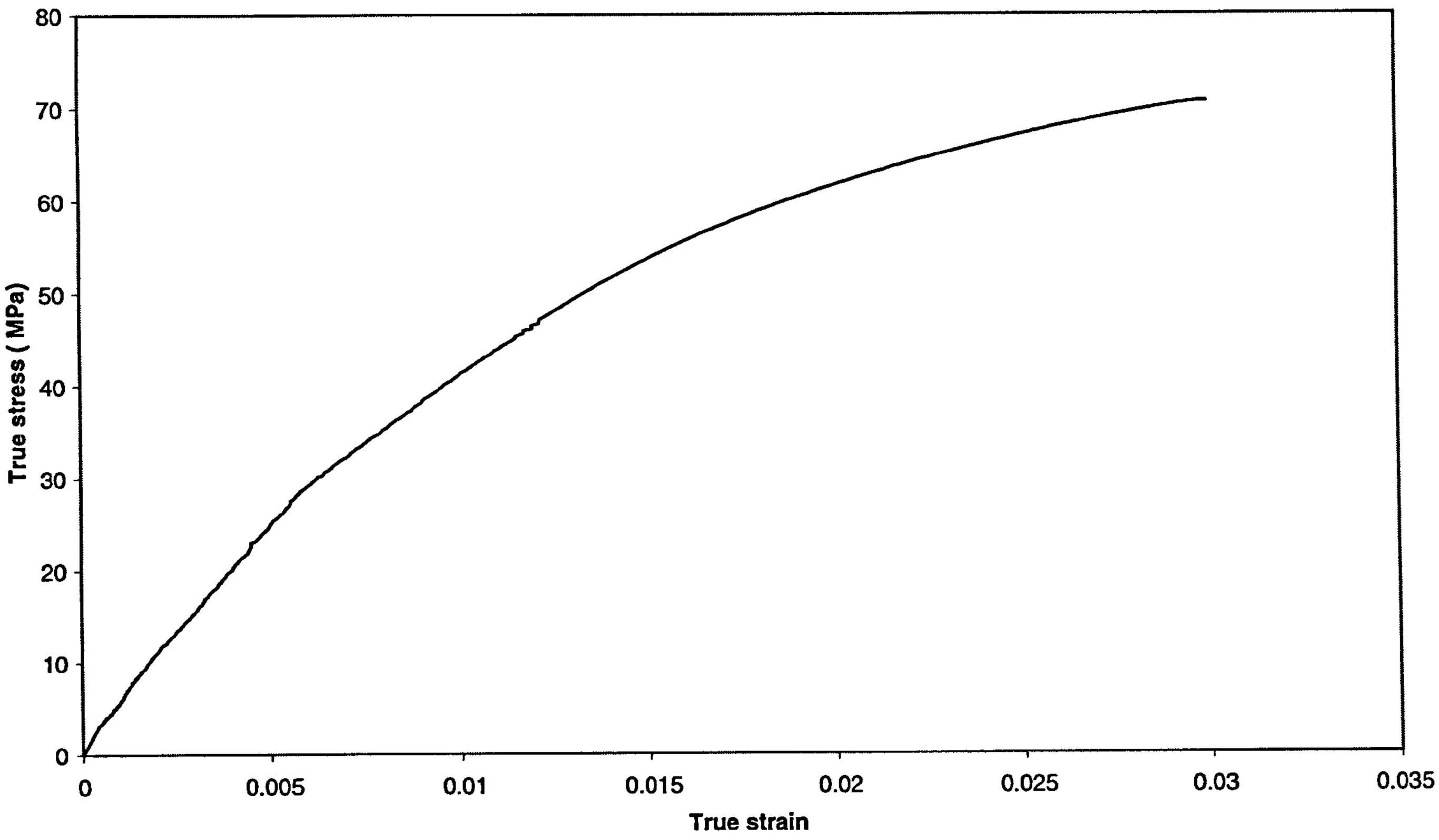

Figure 2.10 Tensile stress-strain curve for ESP 110 adhesive

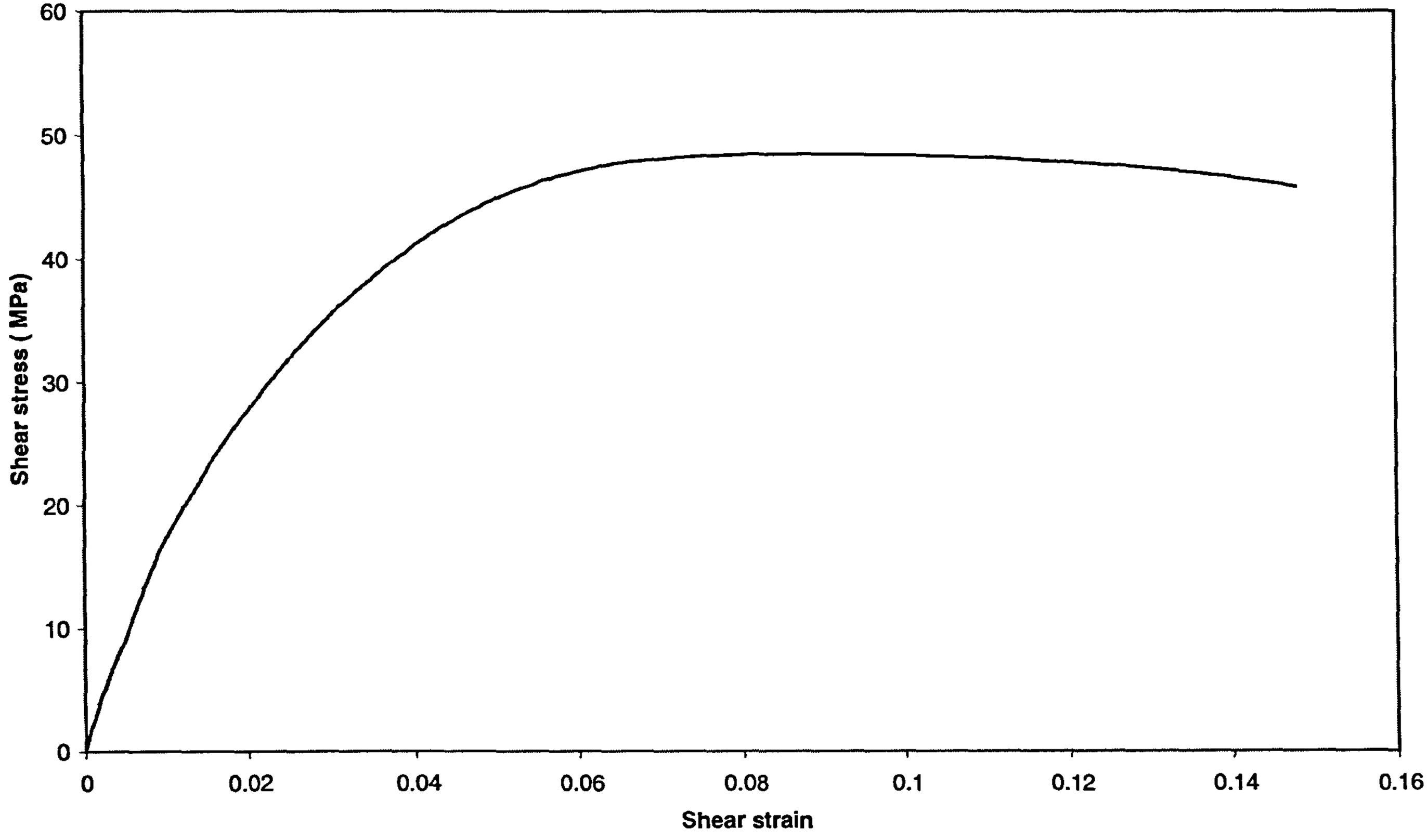

Figure 2.11 Shear stress-strain curve for ESP 110 adhesive

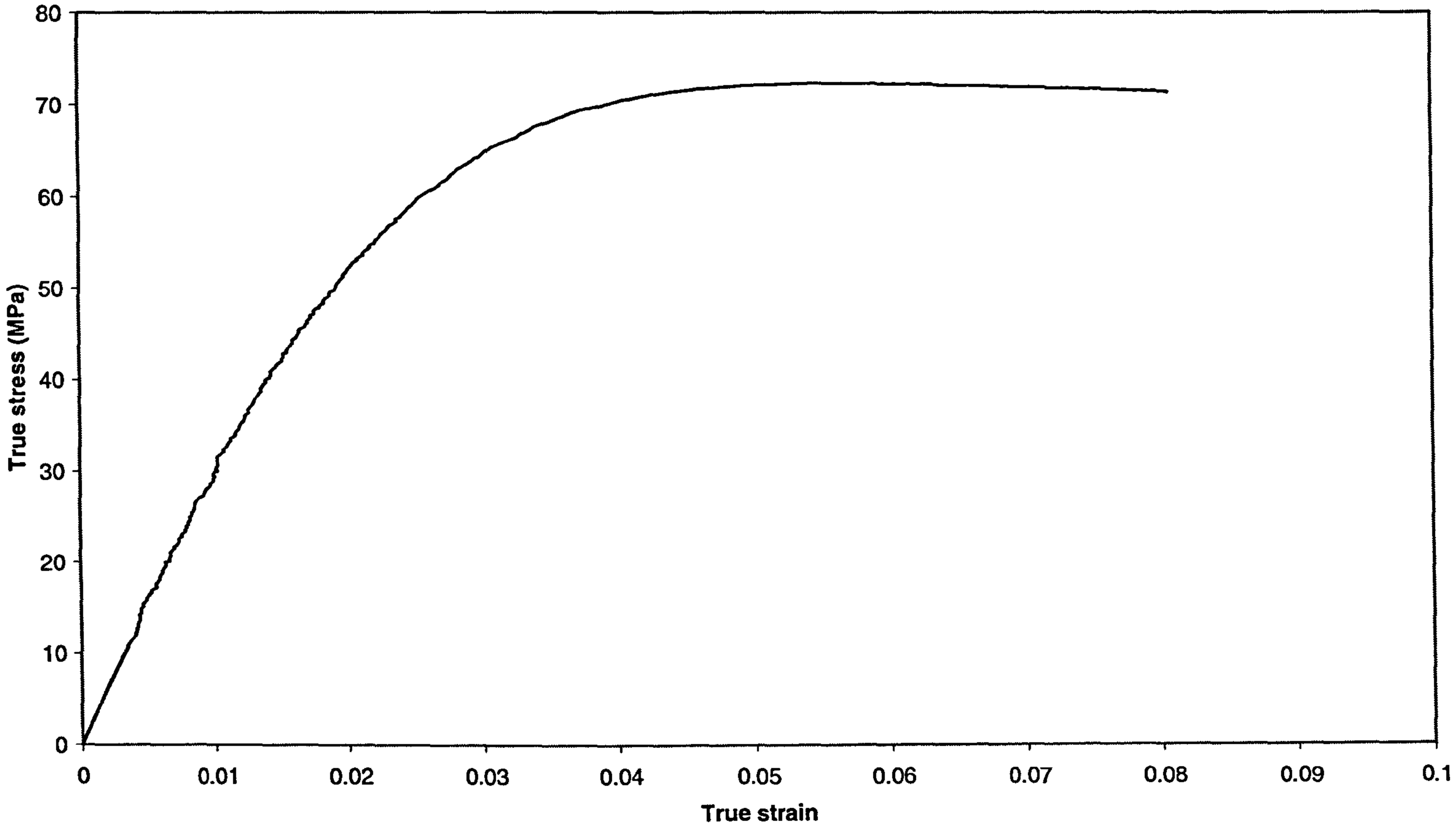

Figure 2.12 Tensile stress-strain curve for AV 119 adhesive

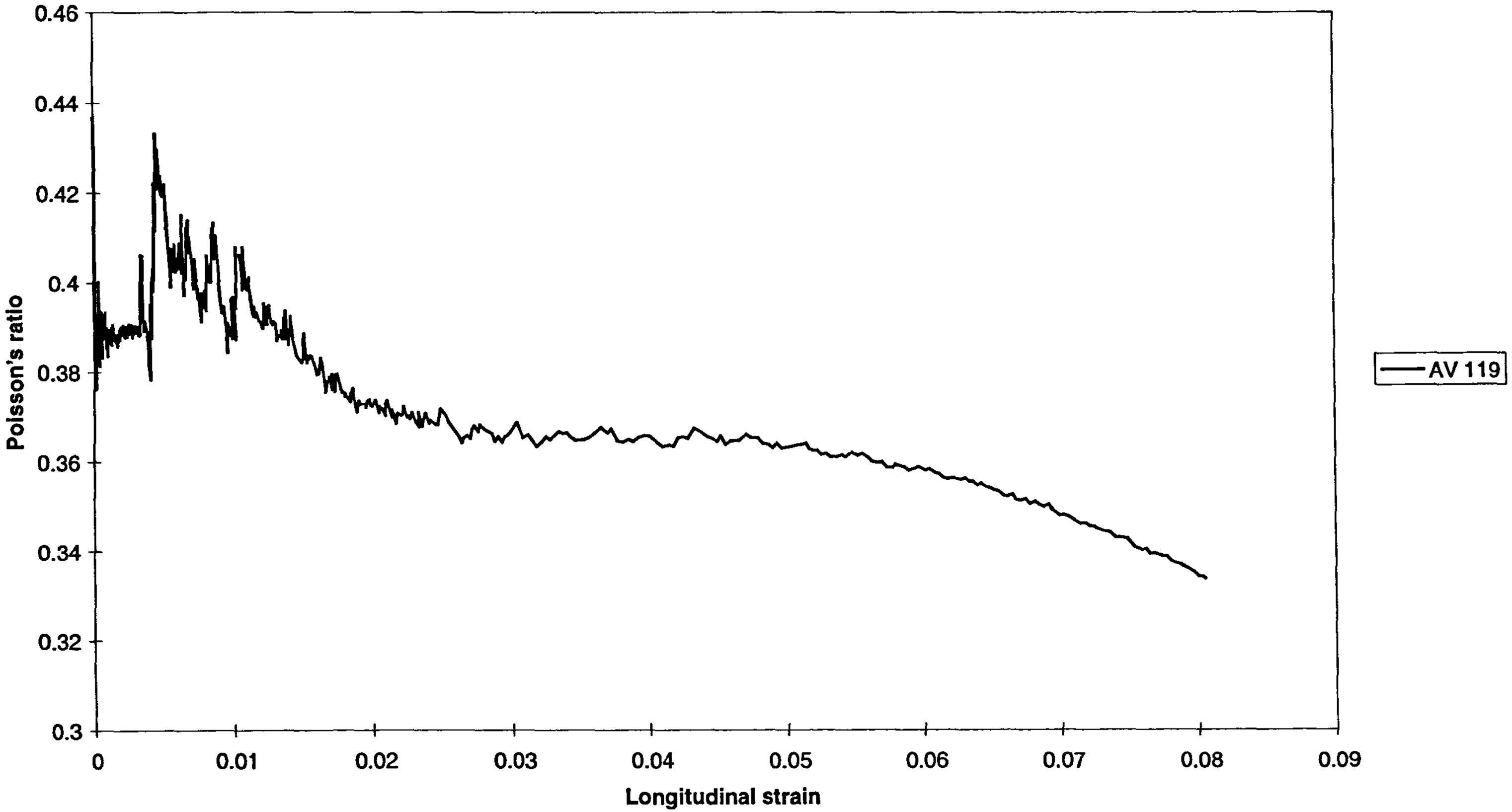

Figure 2.13 Variation of Poisson's ratio for AV 119 adhesive with strain

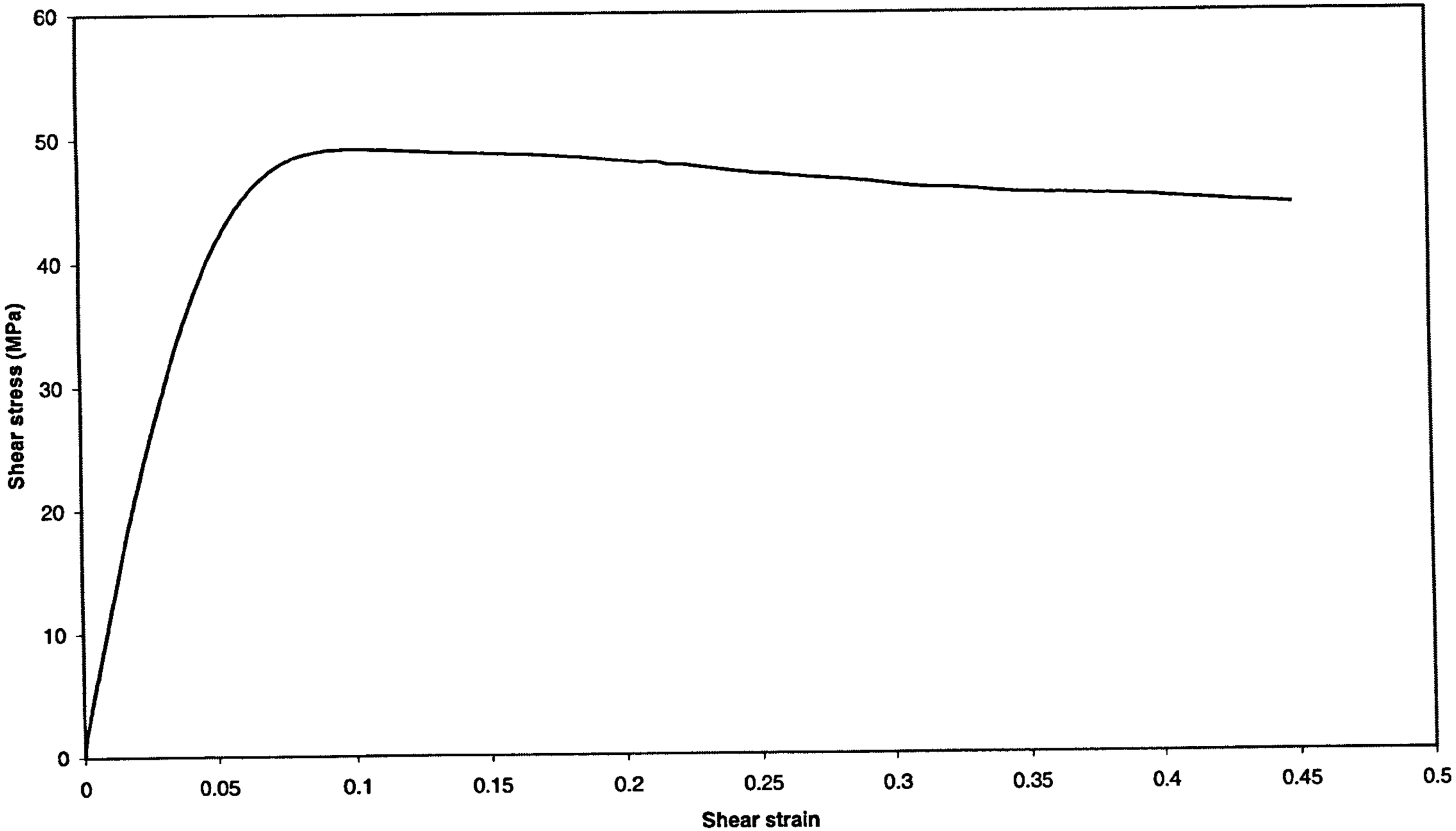

Figure 2.14 Shear stress-strain curve for AV 119 adhesive

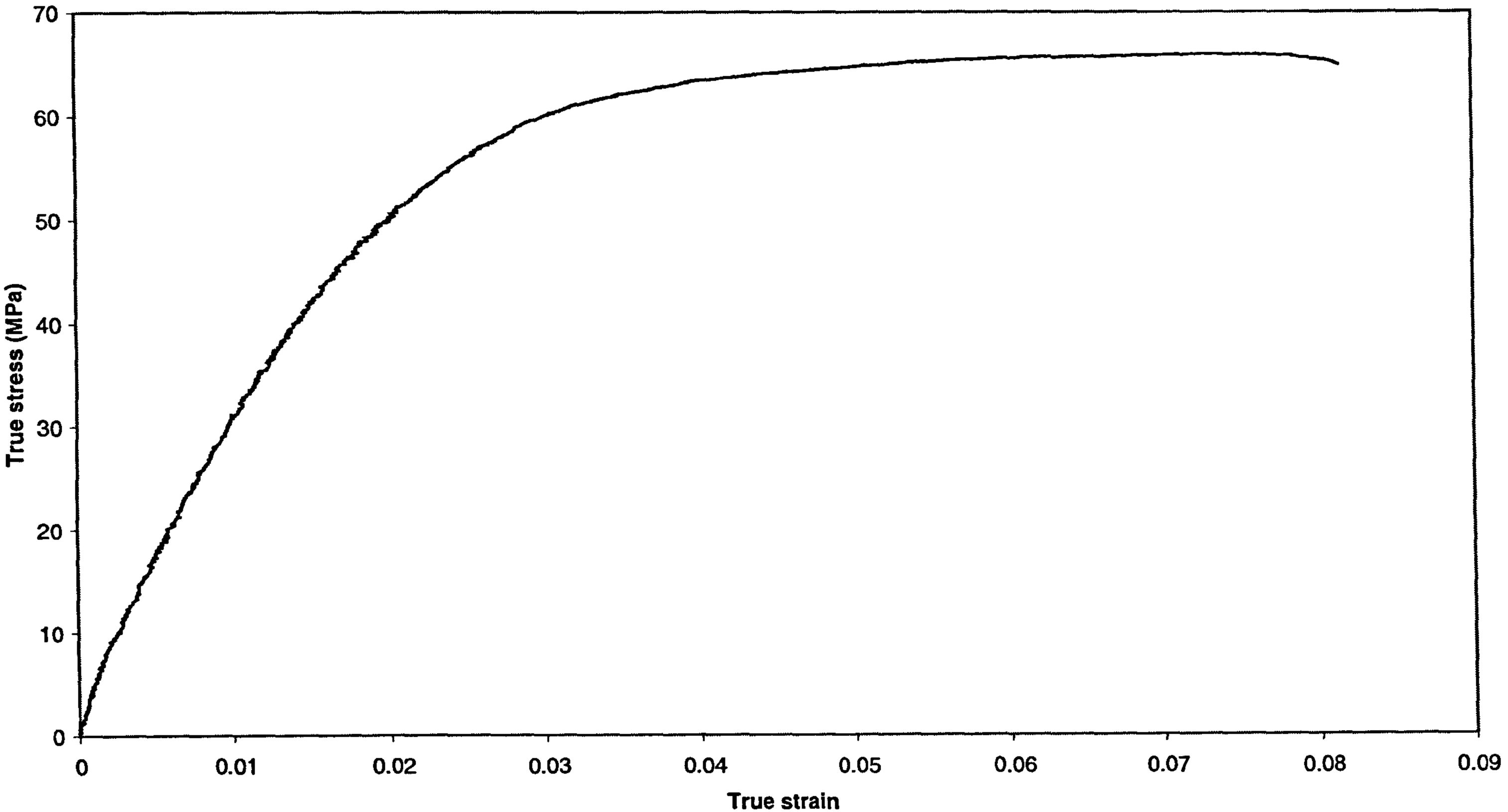

Figure 2.15 Tensile stress-strain curve for EC 3448 adhesive

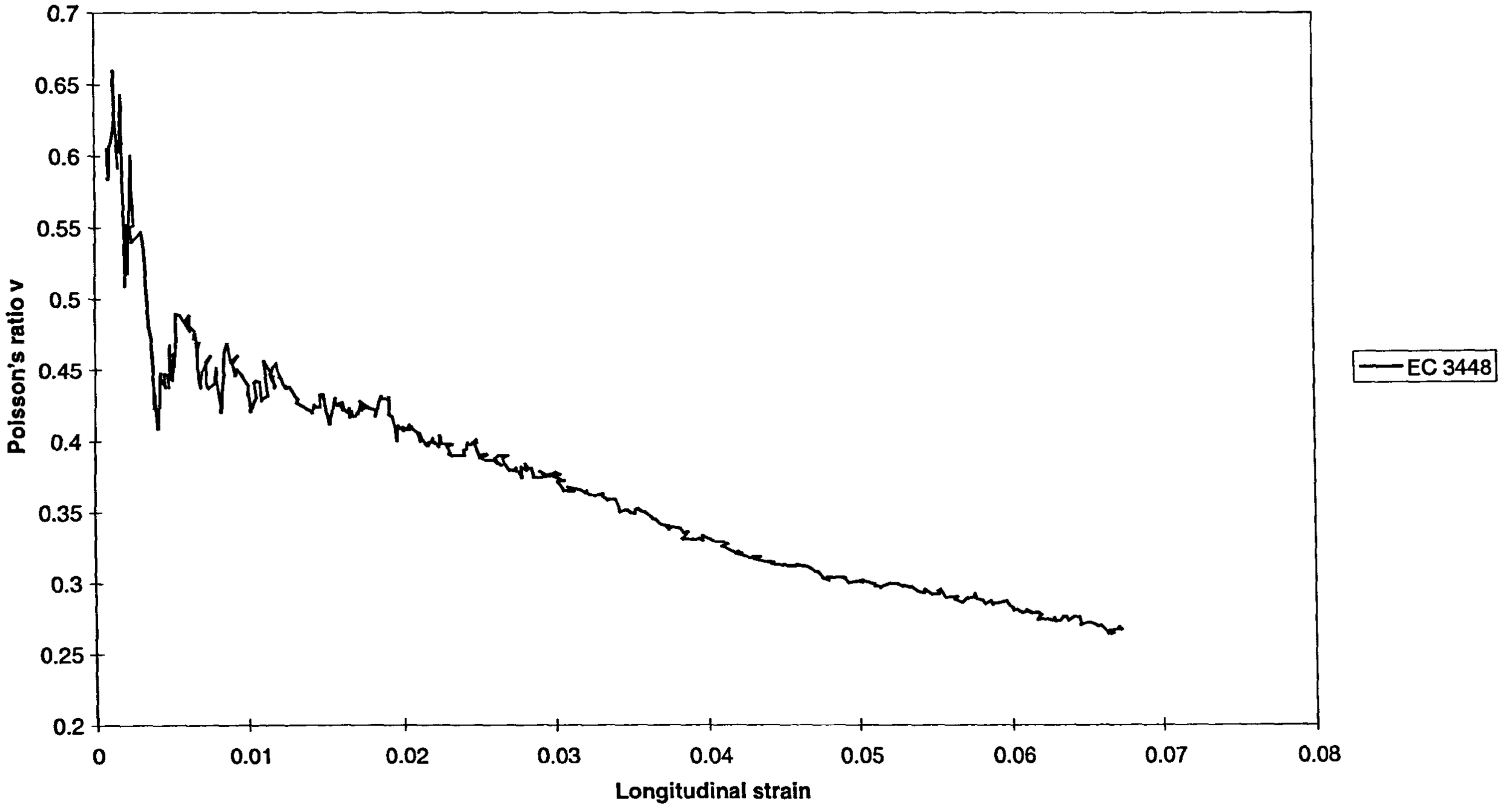

Figure 2.16 Variation of Poisson's ratio for EC 3448 adhesive with strain

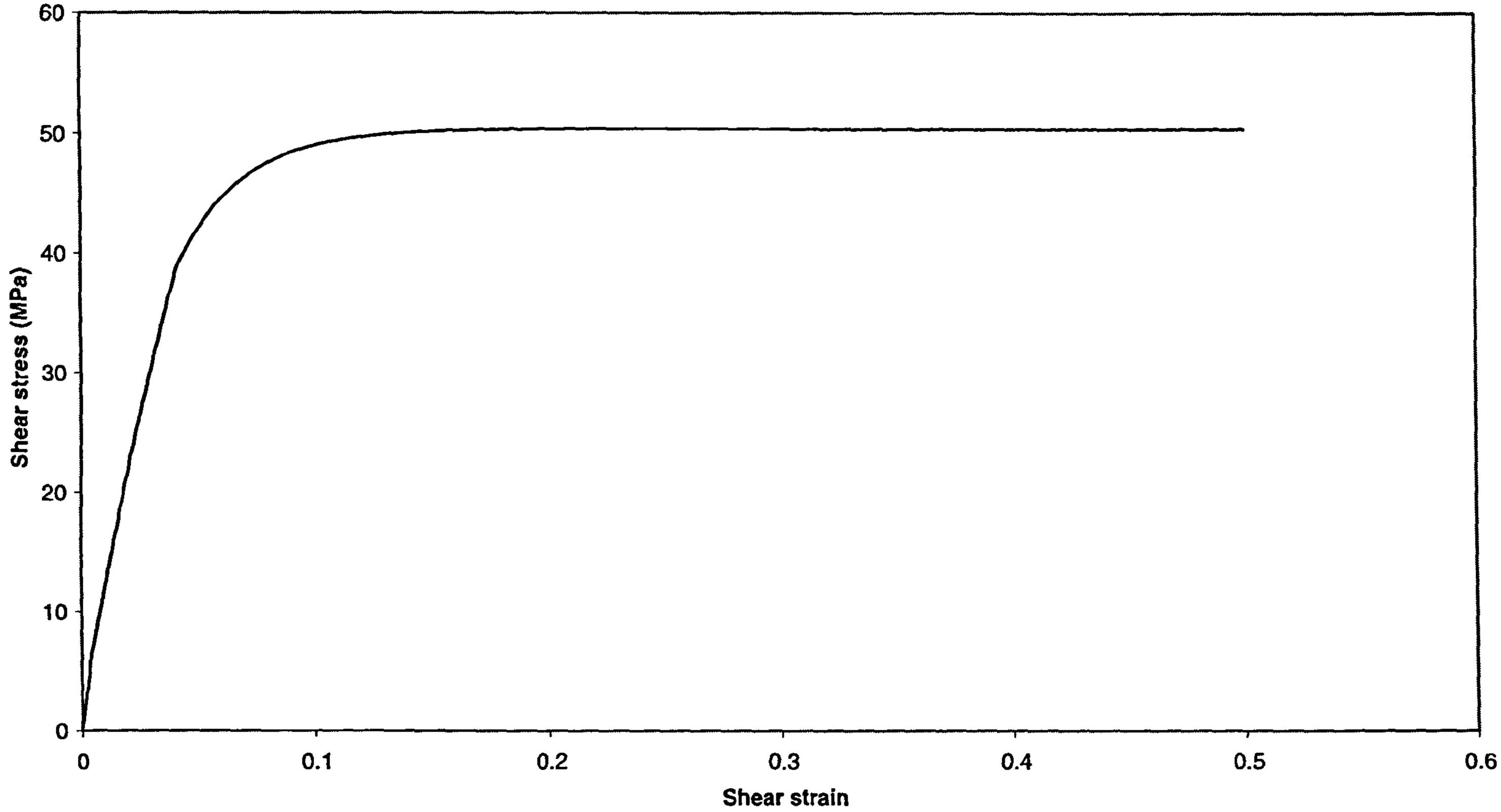

Figure 2.17 Shear stress-strain curve for EC 3448 adhesive

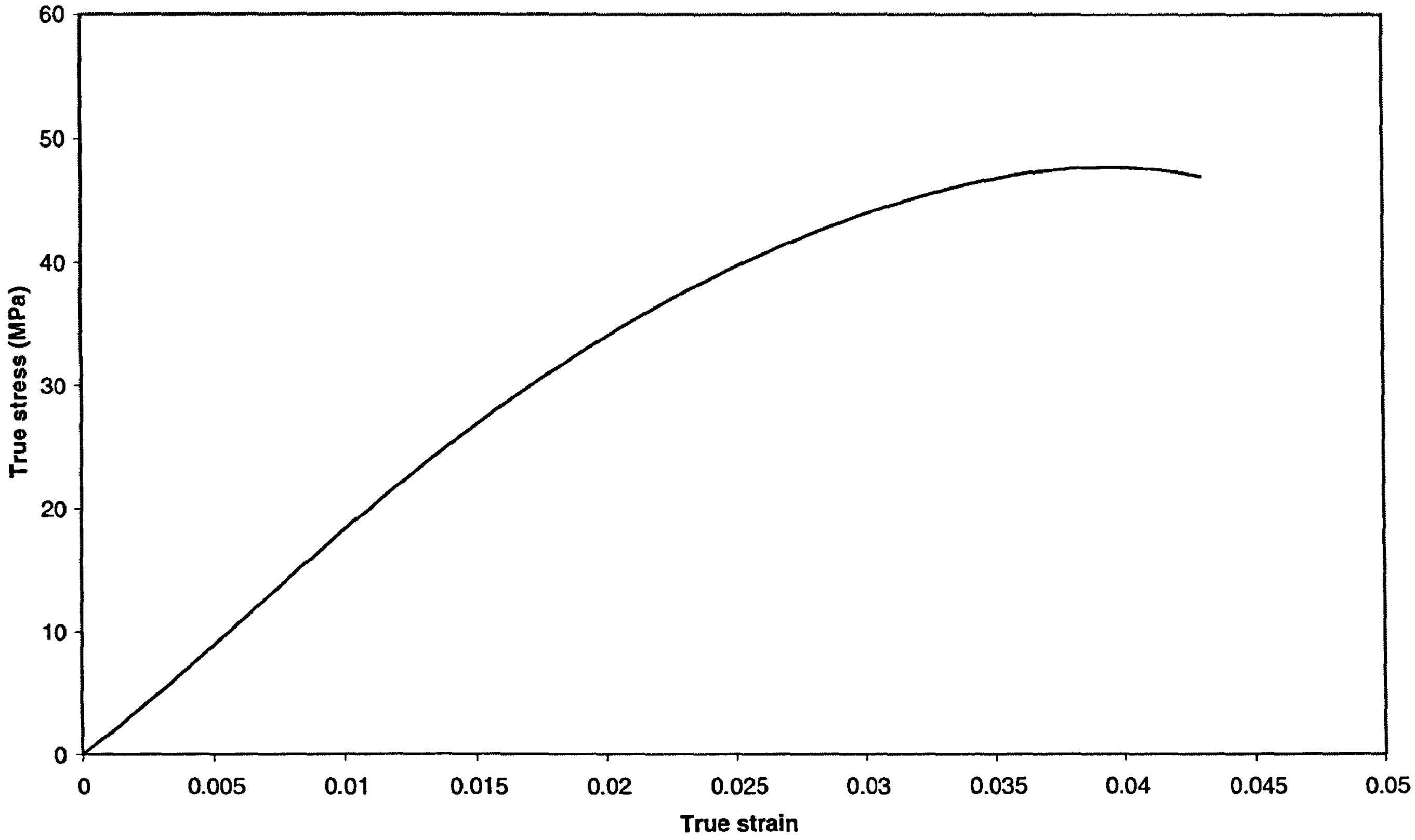

Figure 2.18 Tensile stress-strain curve for MY753 adhesive

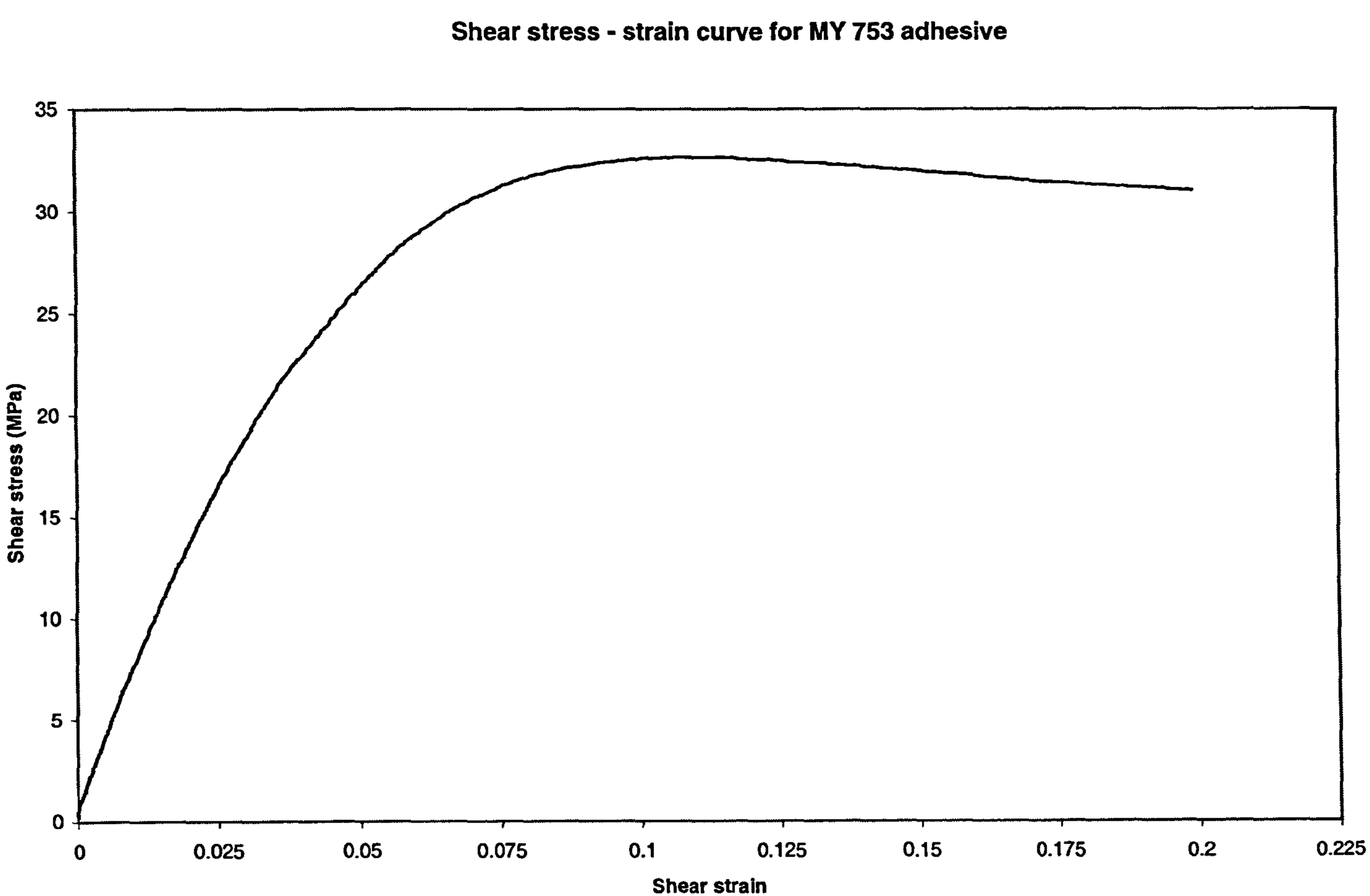

Figure 2.19 Shear stress-strain curve for MY 753 adhesive

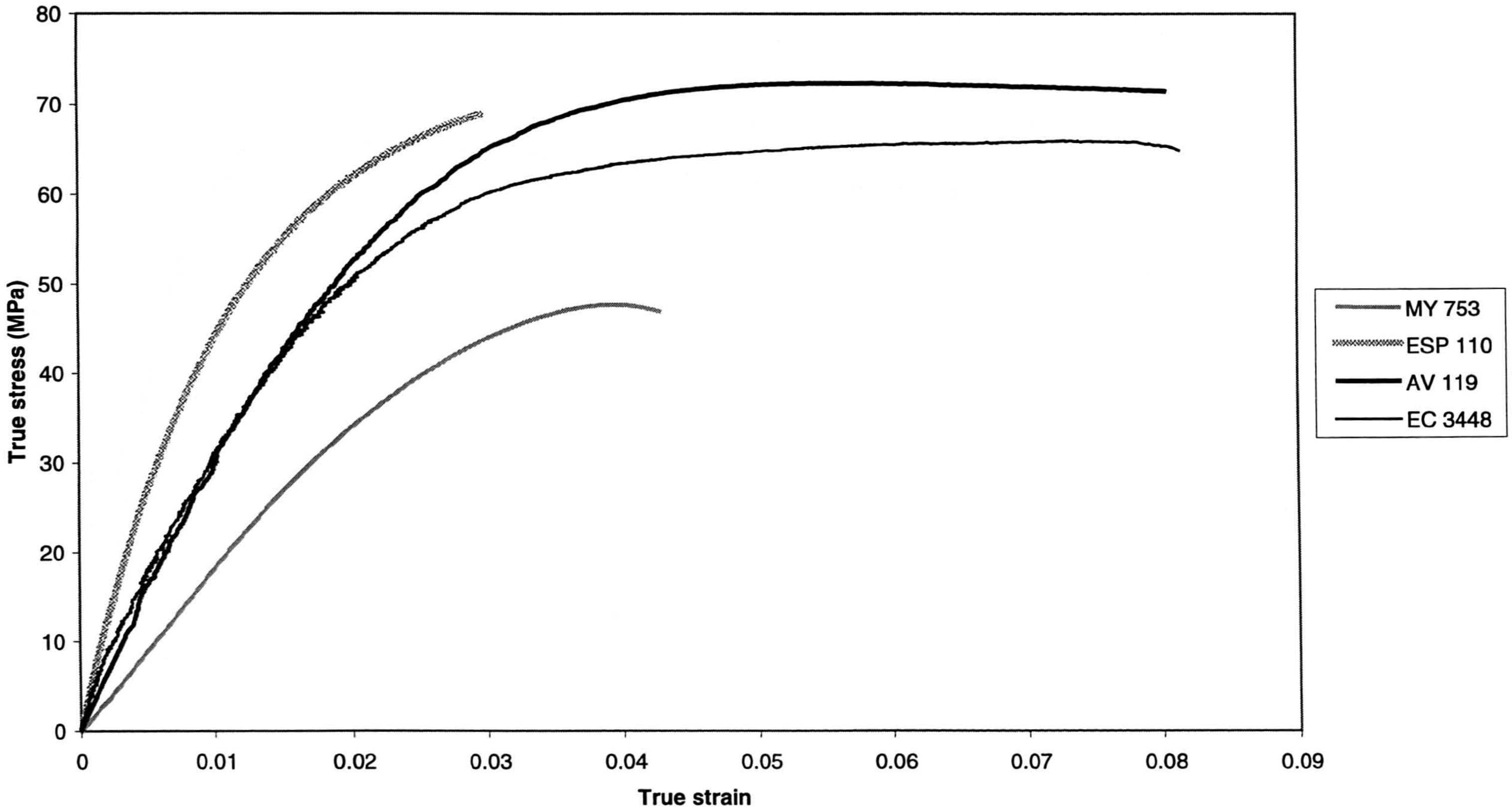

Figure 2.20 Comparison of tensile stress-strain curves for all the adhesives used

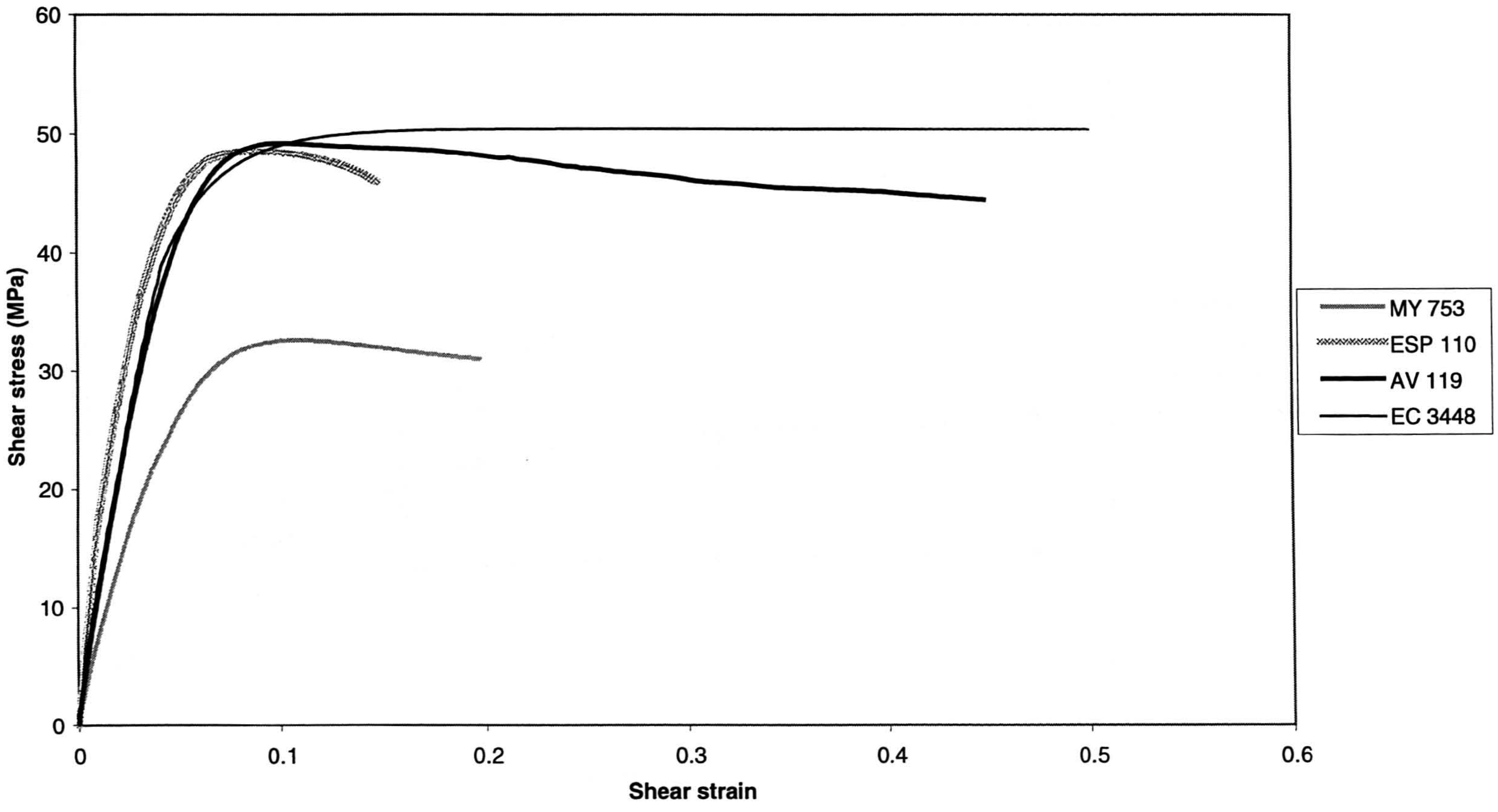

Figure 2.21 Comparison of shear stress-strain curves for all the adhesives used

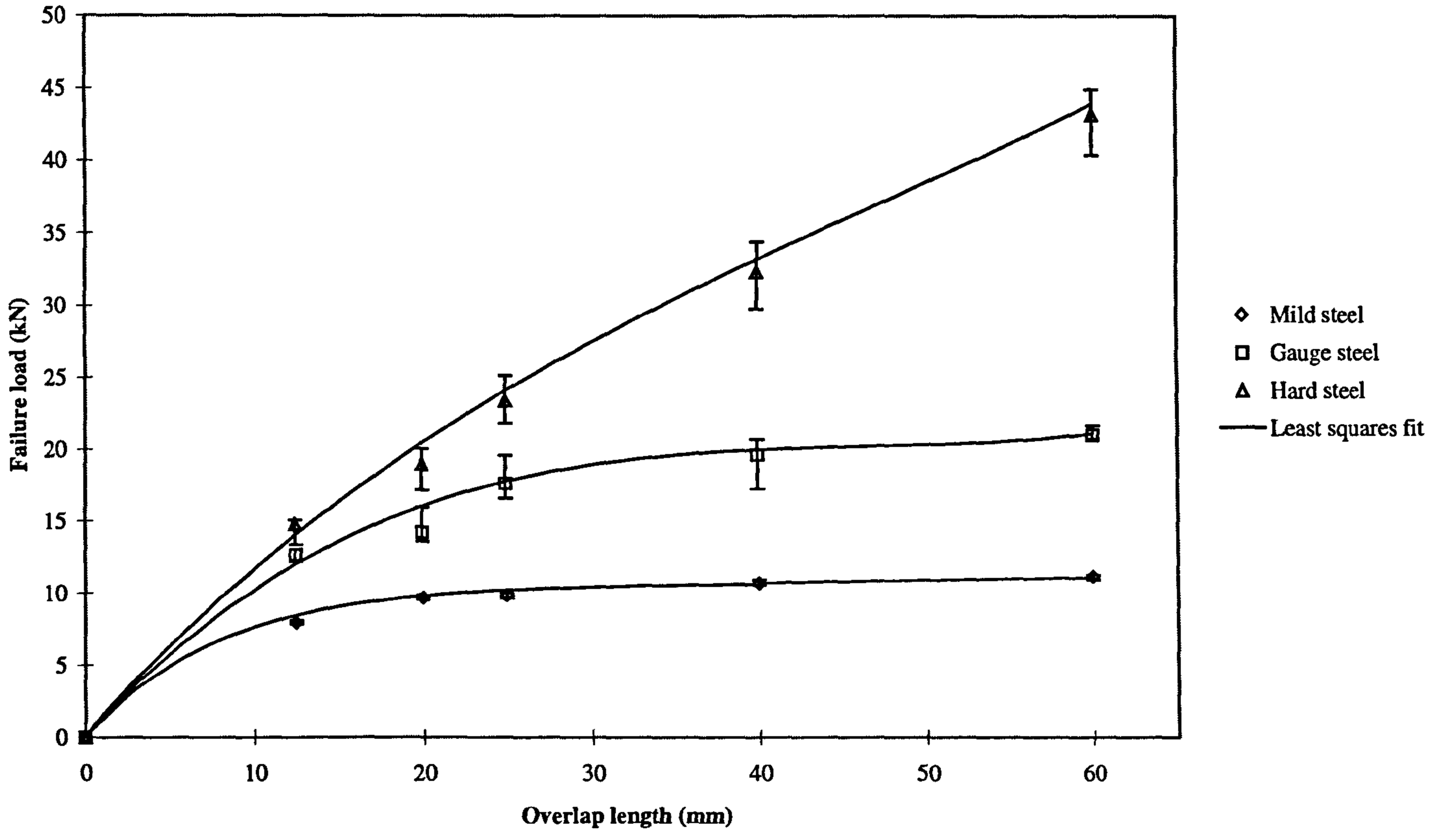

Figure 3.1 Strength of SLJs in tension vs. overlap length for ESP 110 adhesive and different adherend materials

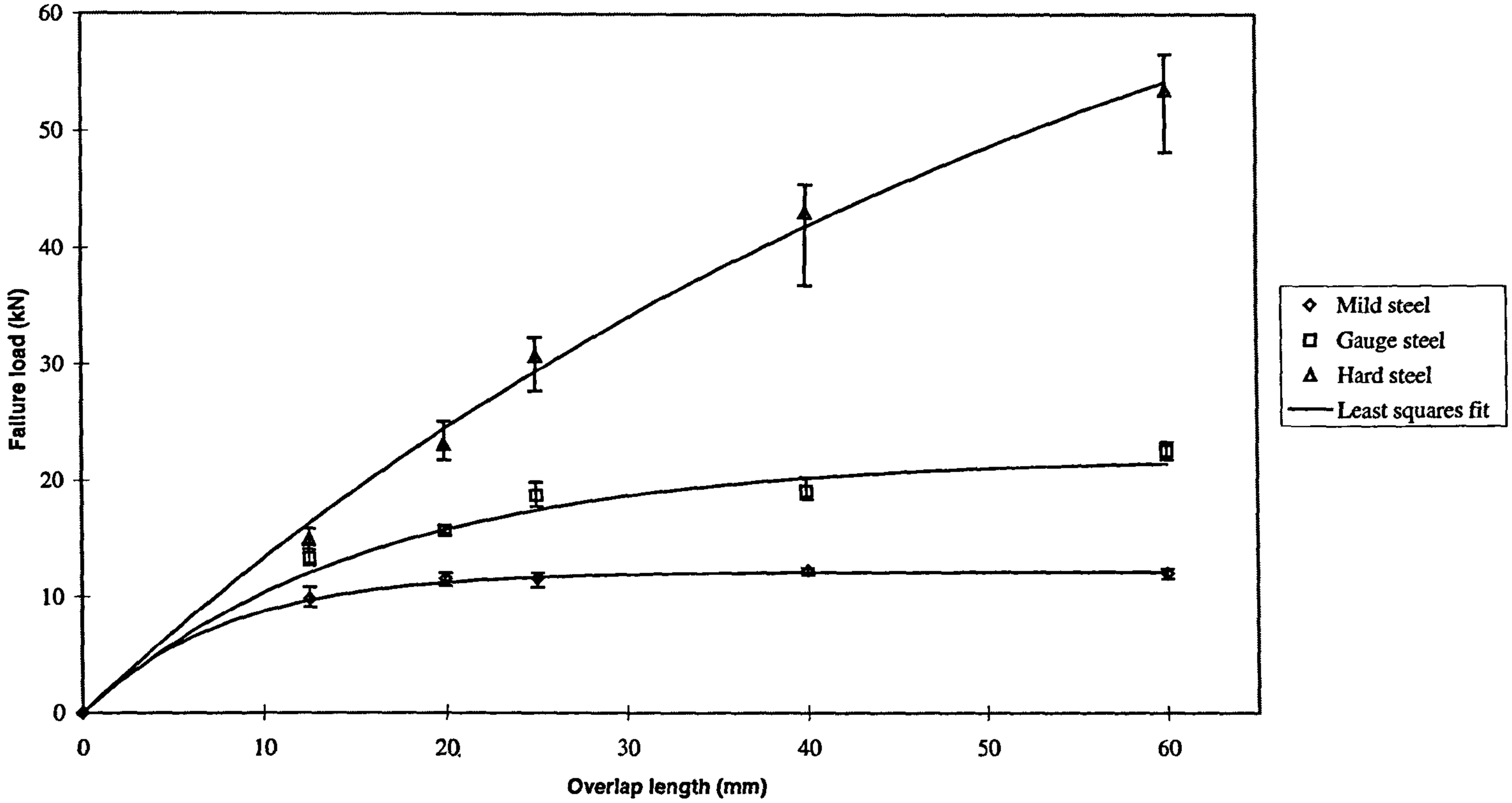

Figure 3.2 Strength of SLJs in tension vs. overlap length for AV 119 adhesive and different adherend materials

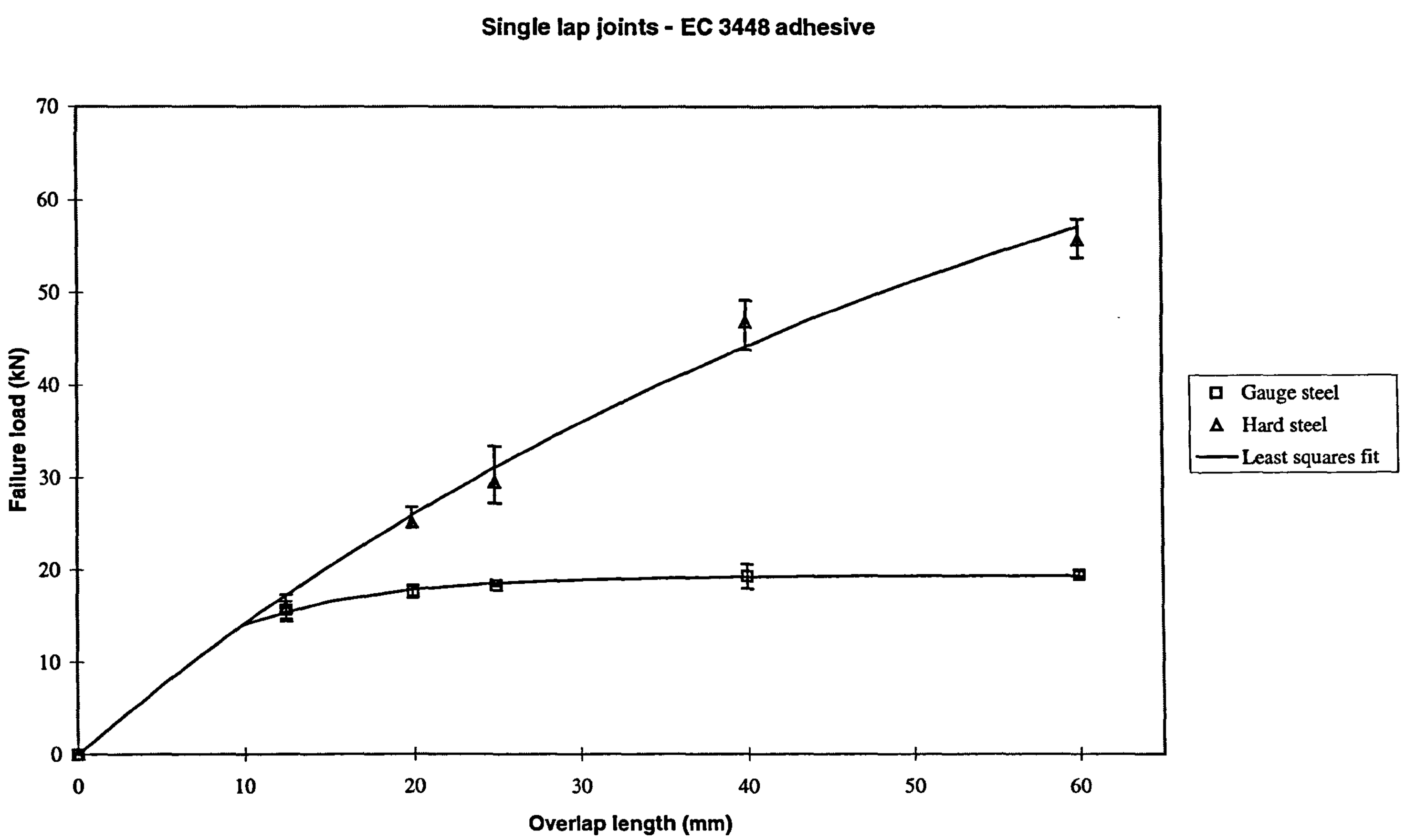

Figure 3.3 Strength of SLJs in tension vs. overlap length for EC 3448 adhesive and different adherend materials

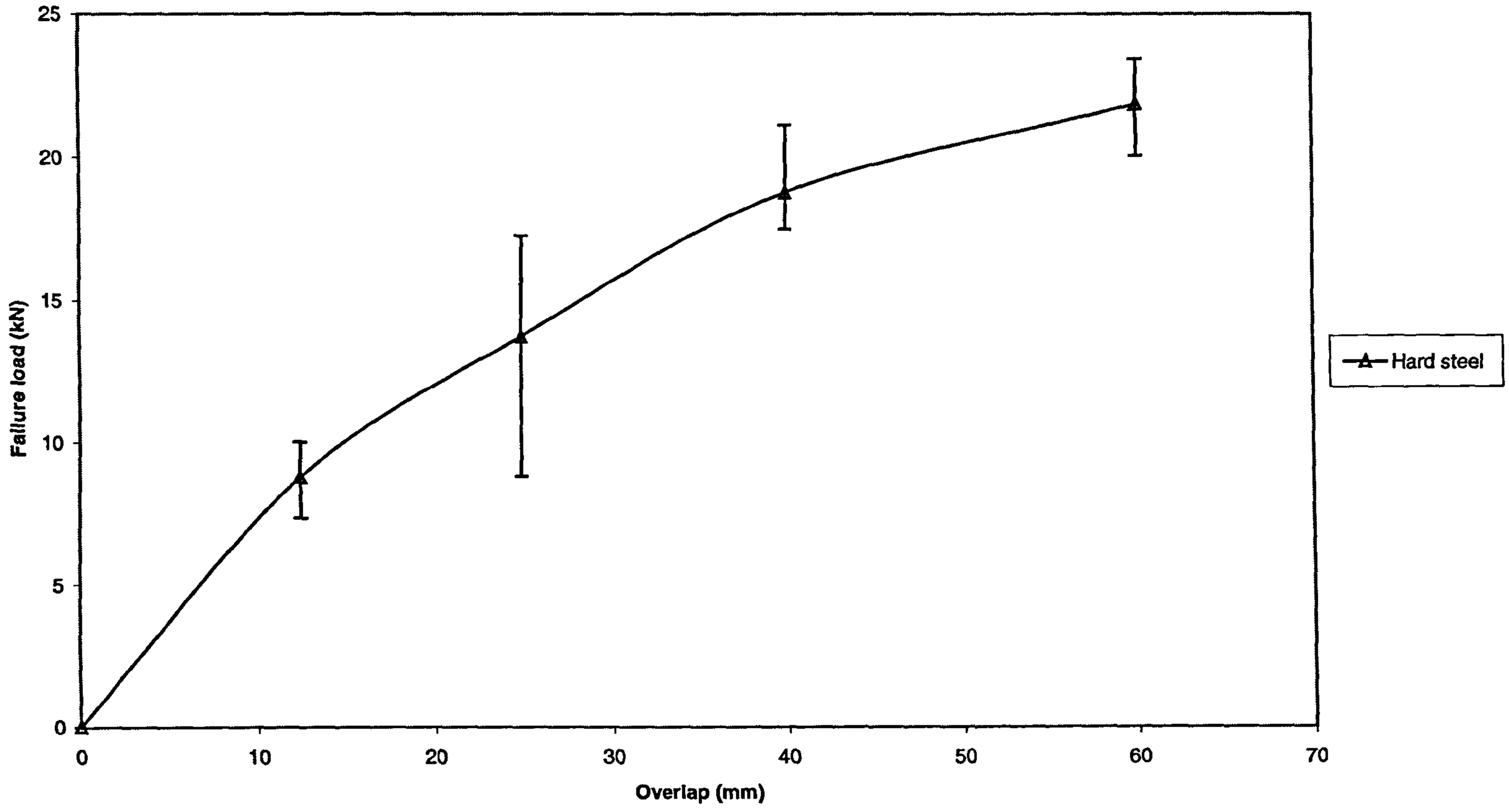

Figure 3.4 Strength of SLJs in tension vs. overlap length for MY 753 adhesive and hard steel adherends

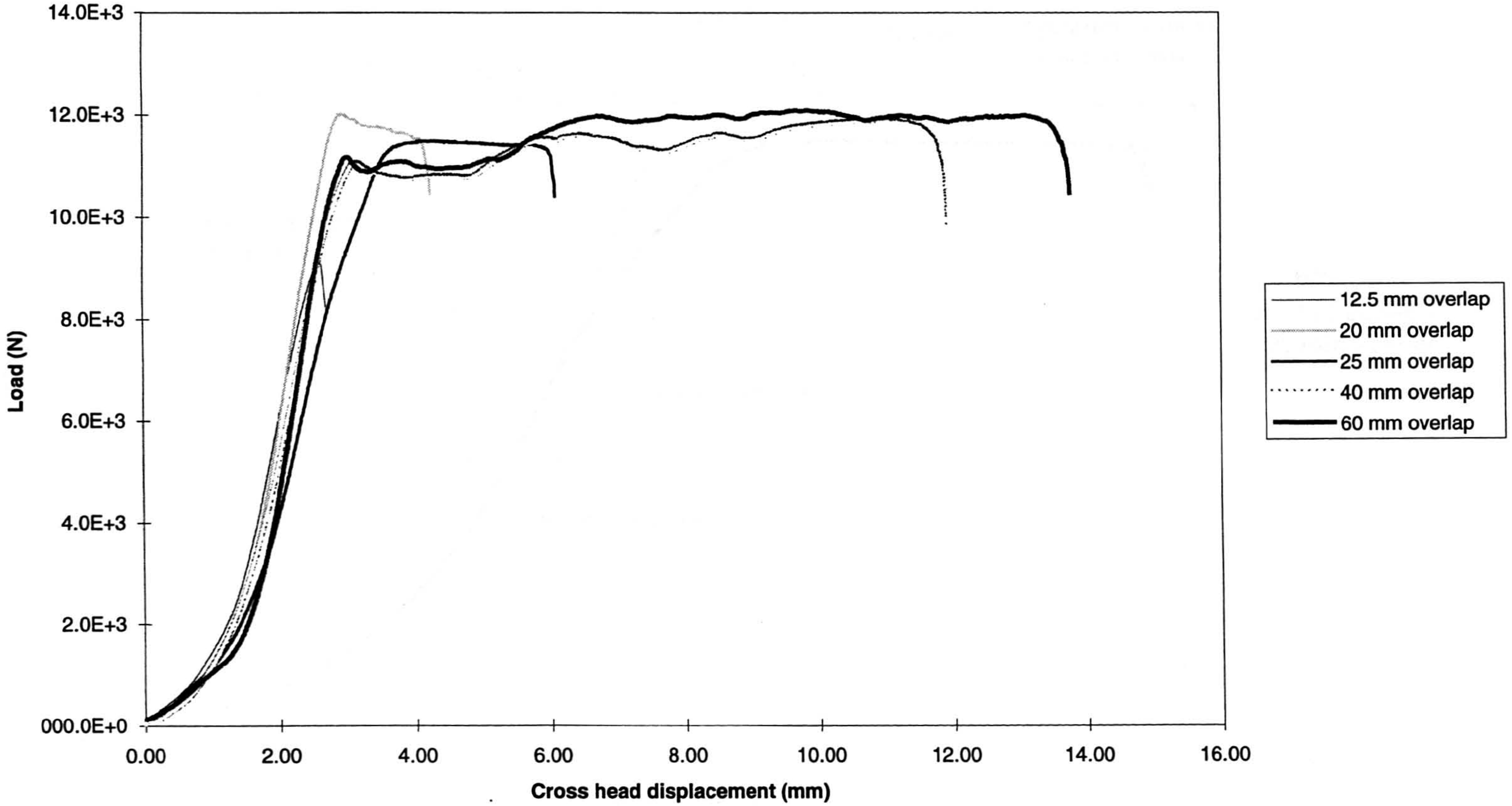

Figure 3.5 Load-displacement curves for SLJs with AV119 adhesive - mild steel adherends and various overlaps

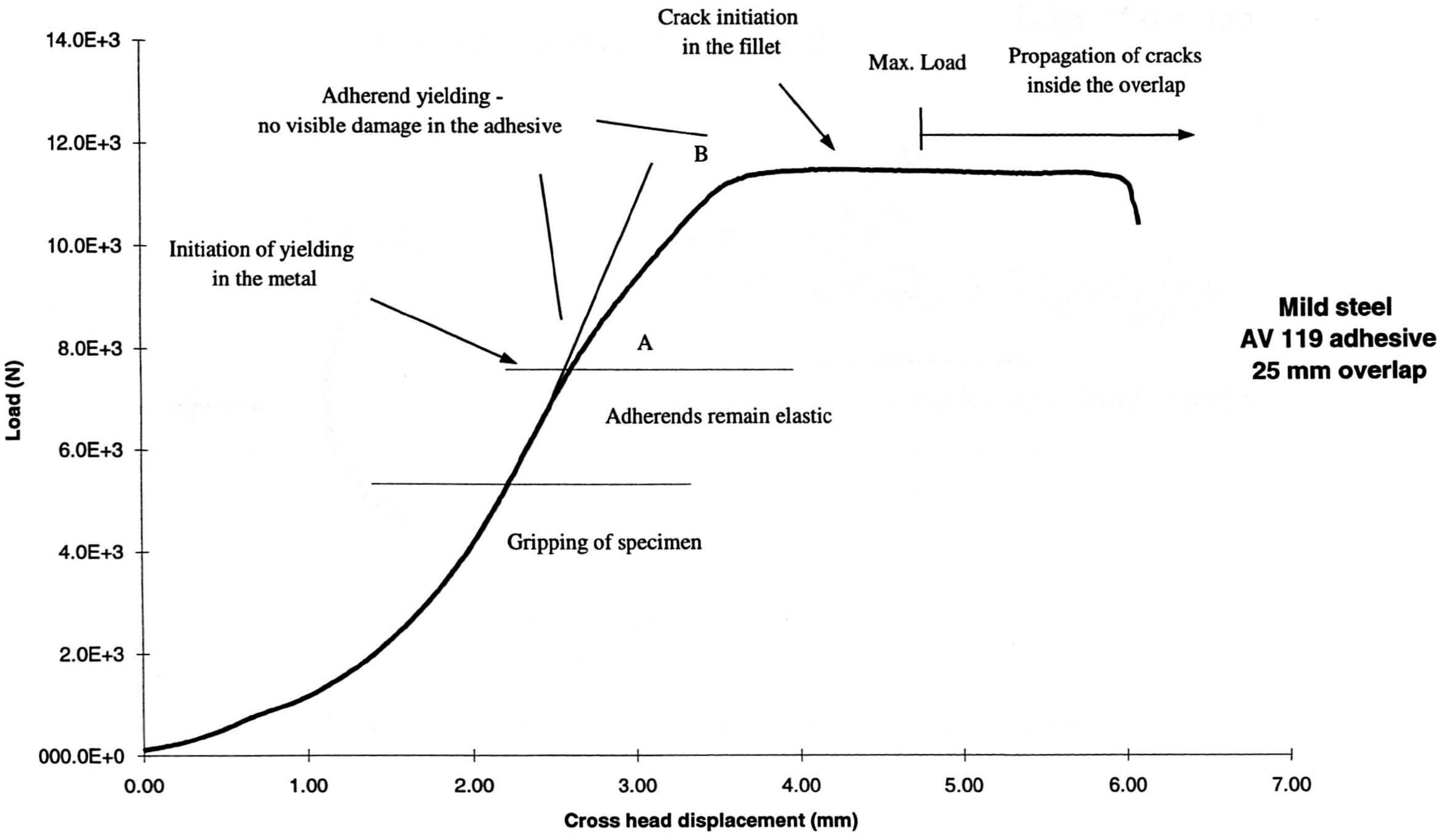

Figure 3.6 Load-displacement curve for SLJ with AV119 adhesive - mild steel adherends and 25 mm overlap

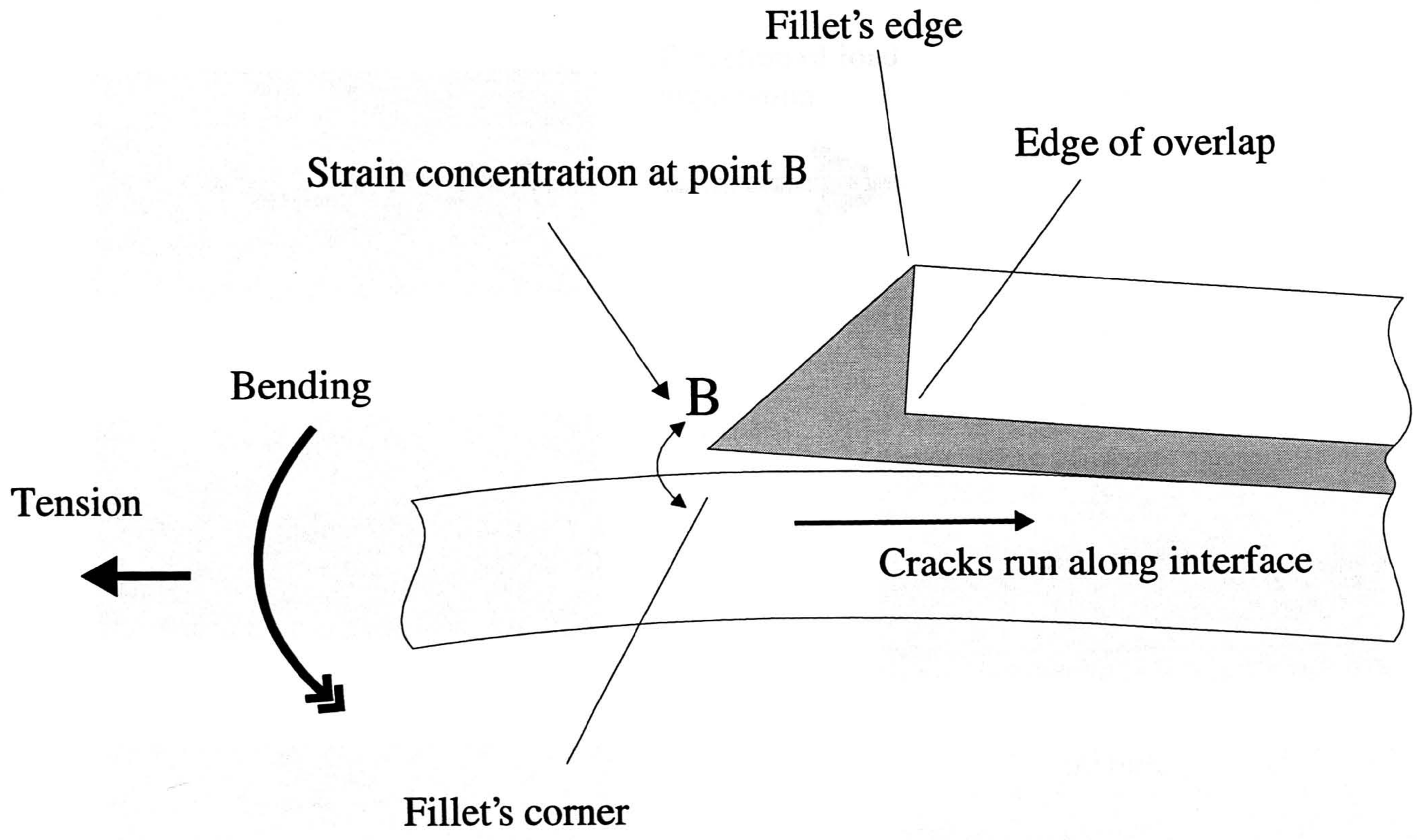

Figure 3.7 Mode of failure for joints with mild steel adherends

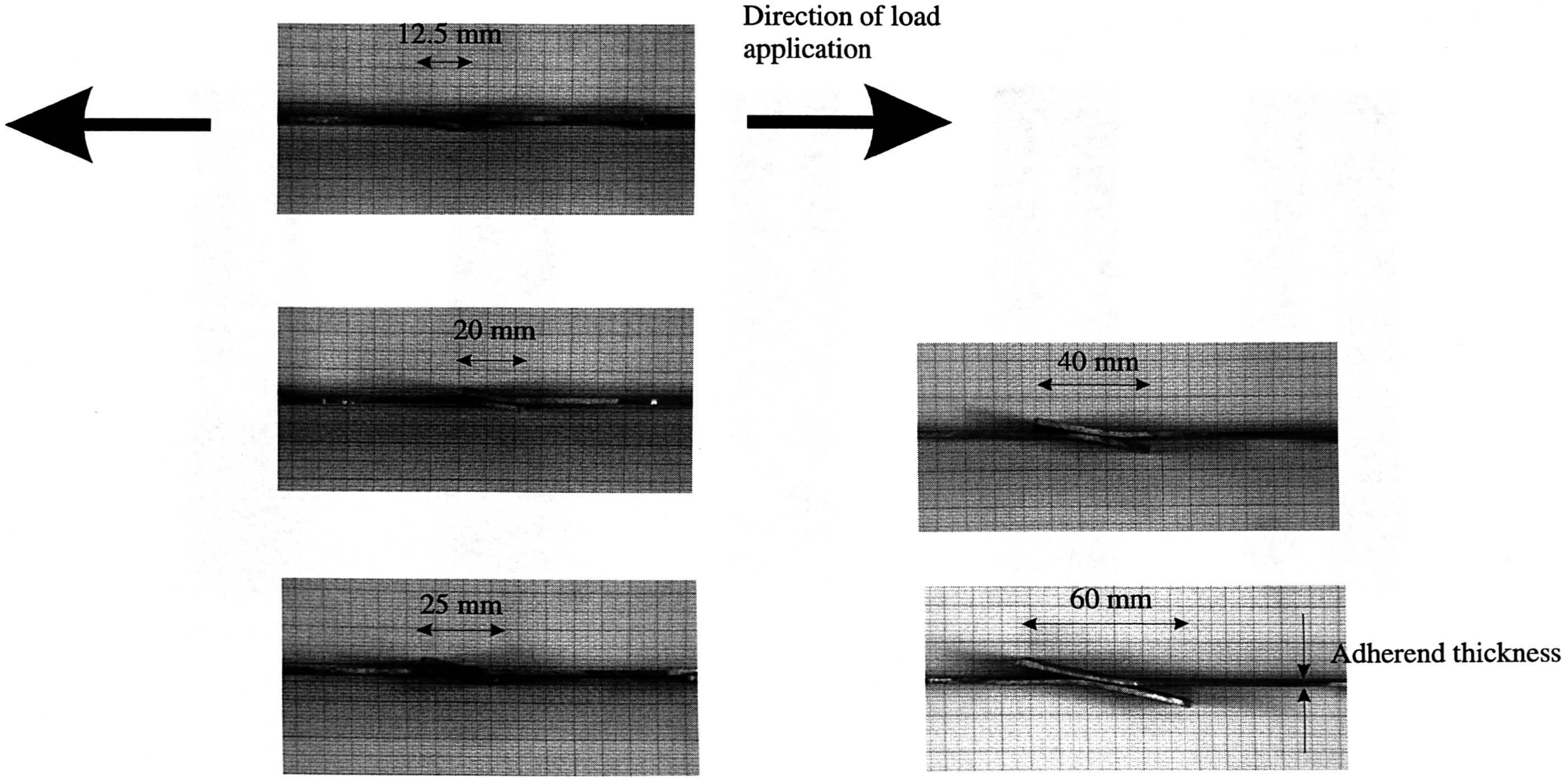

Figure 3.8 Final Deformed shapes of mild steel joints, AV 119 Adhesive (Only part of the total length of the joints is shown)

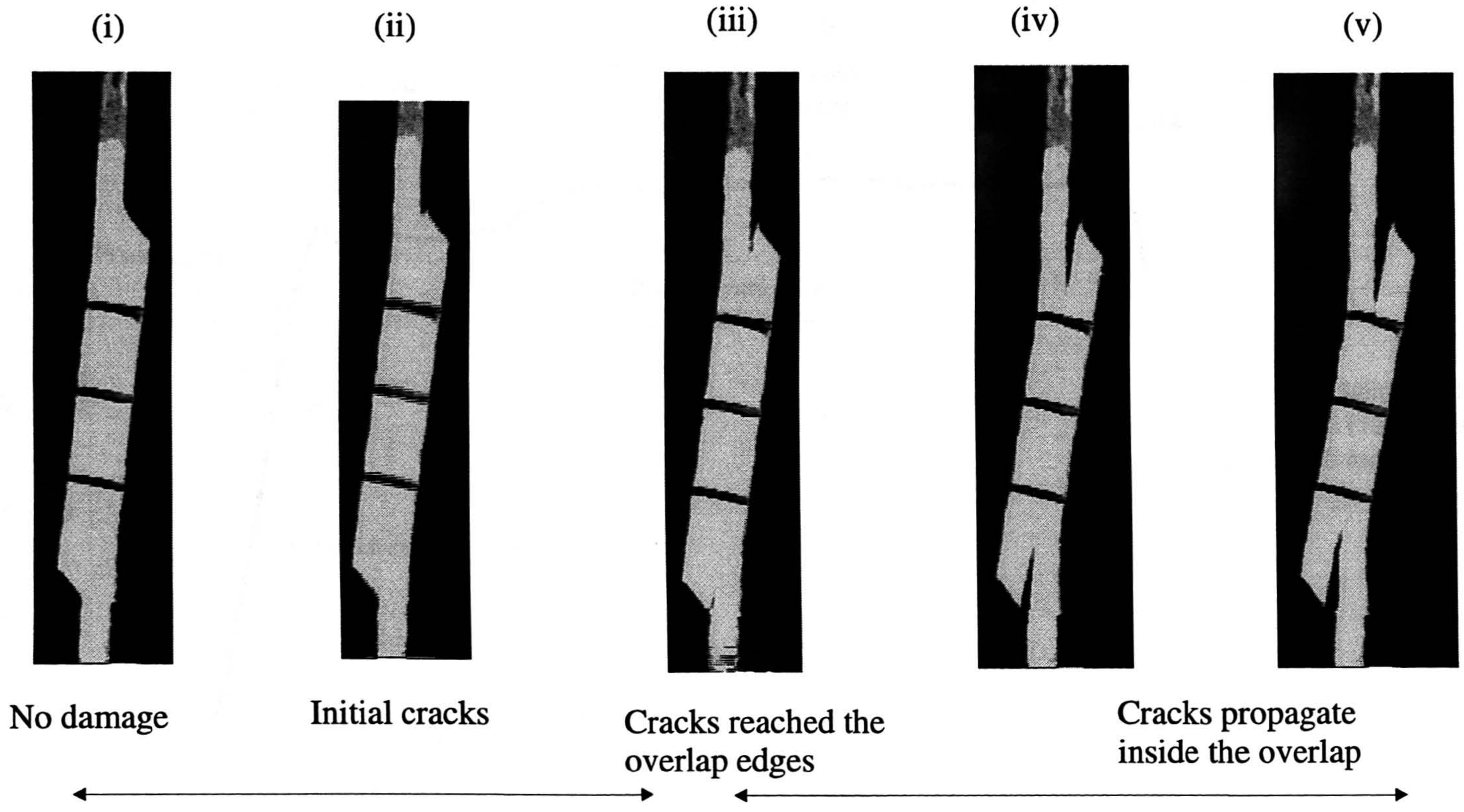

Figure 3.9 Failure propagation on a mild steel joint - AV 119 adhesive - 20 mm overlap

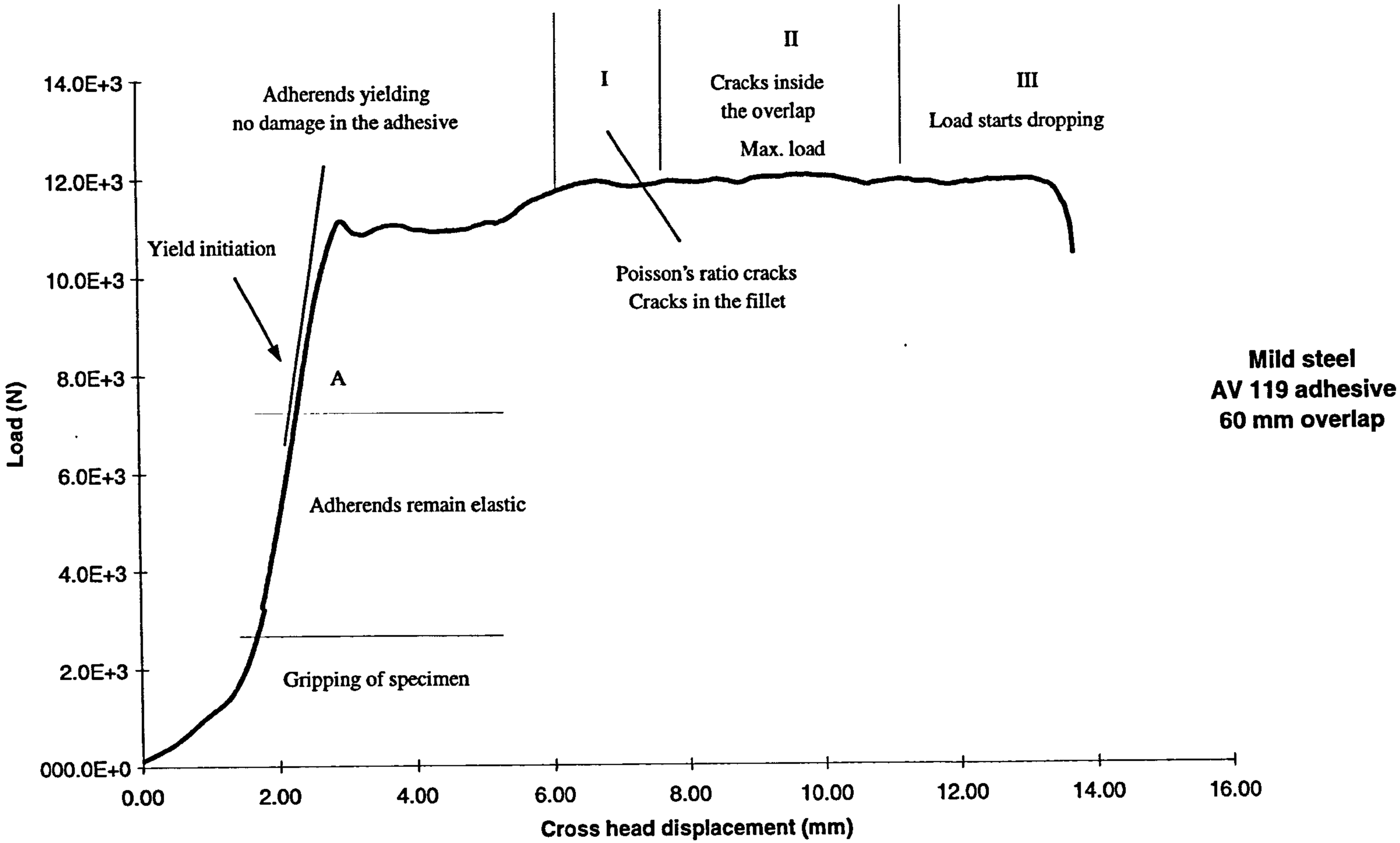

Figure 3.10 Load-displacement curve for SLJ with AV119 adhesive - mild steel adherends and 60 mm overlap

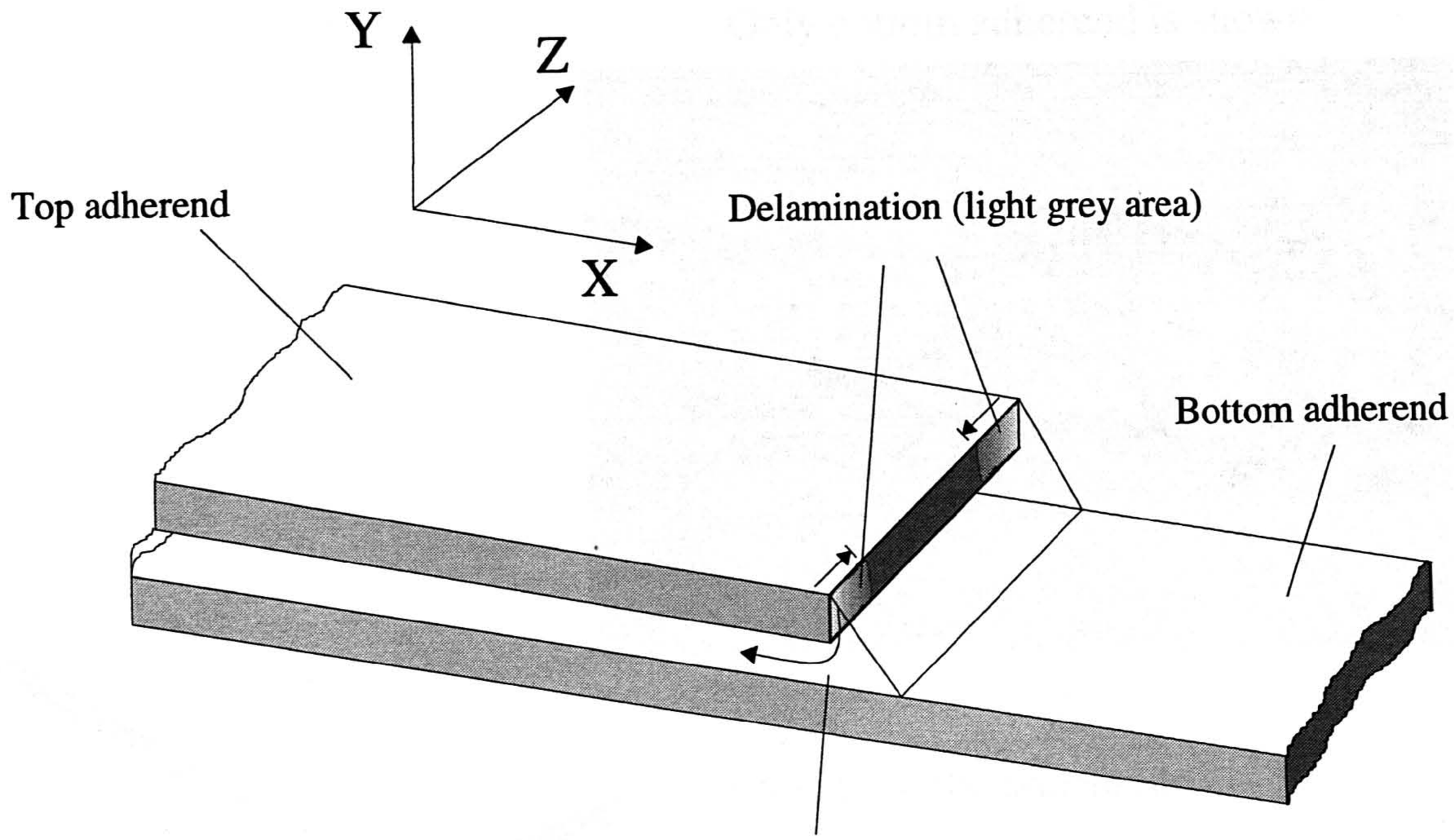

Figure 3.11 Mode of failure for mild steel joints - long overlaps

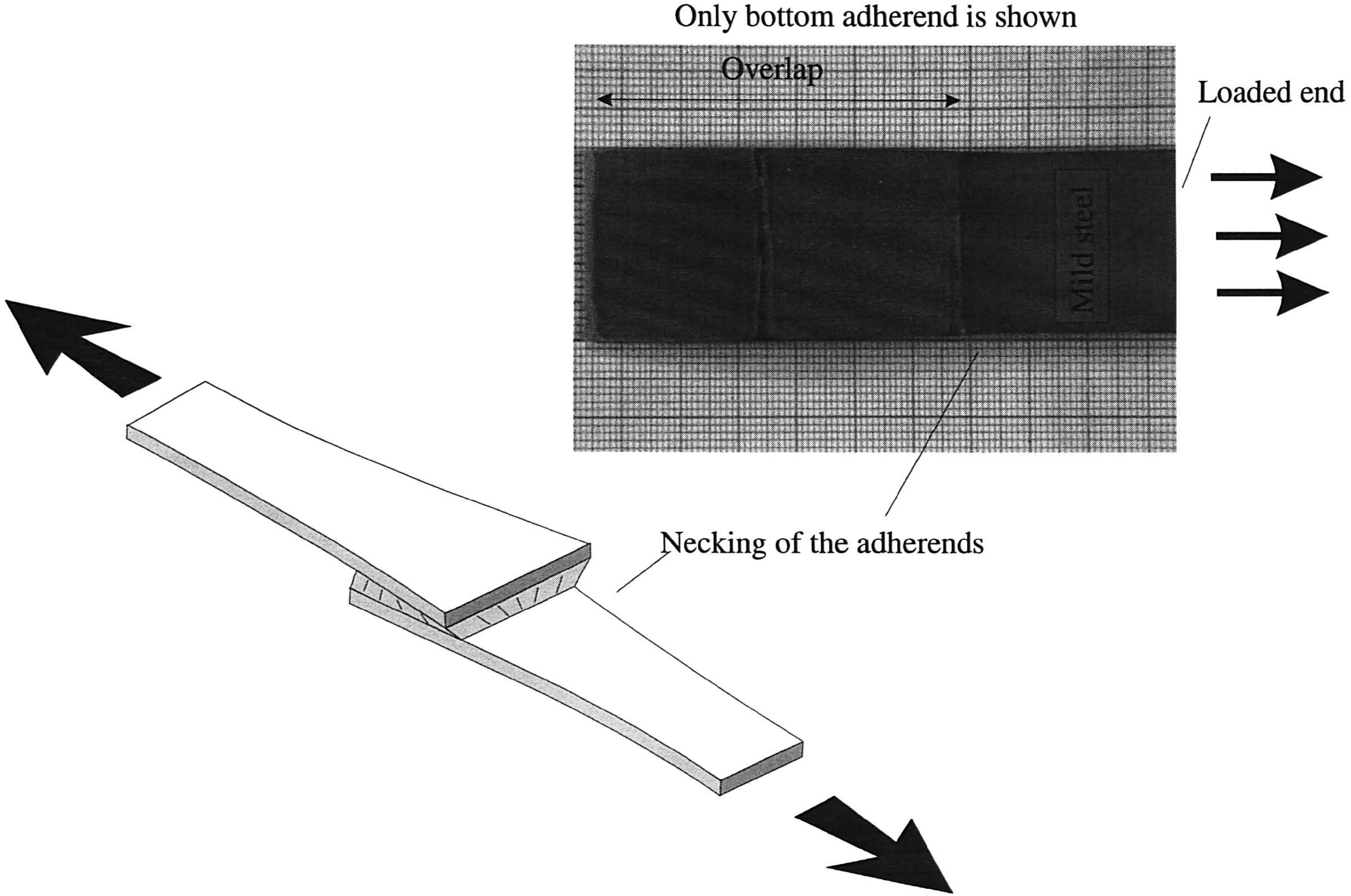

Figure 3.12 Transverse deformations on a SLJ loaded in tension

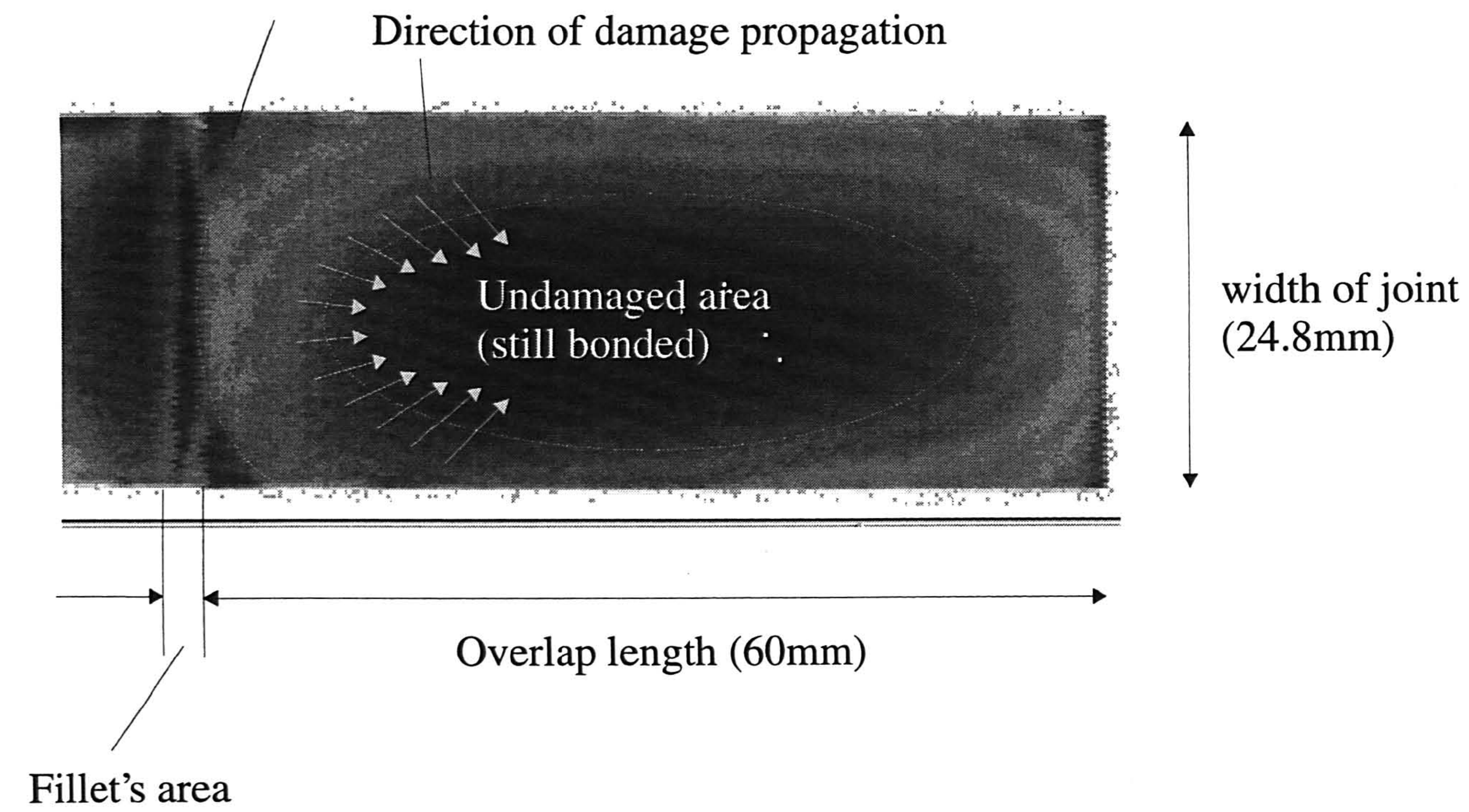

Figure 3.13 Variation of damage under the overlap for 60mm mild steel joint C-Scan

Figure 3.14 60 mm overlap joint with mild steel - ESP 110 adhesive - sequence of failure from initiation of cracks to catastrophic failure (i) - (v)

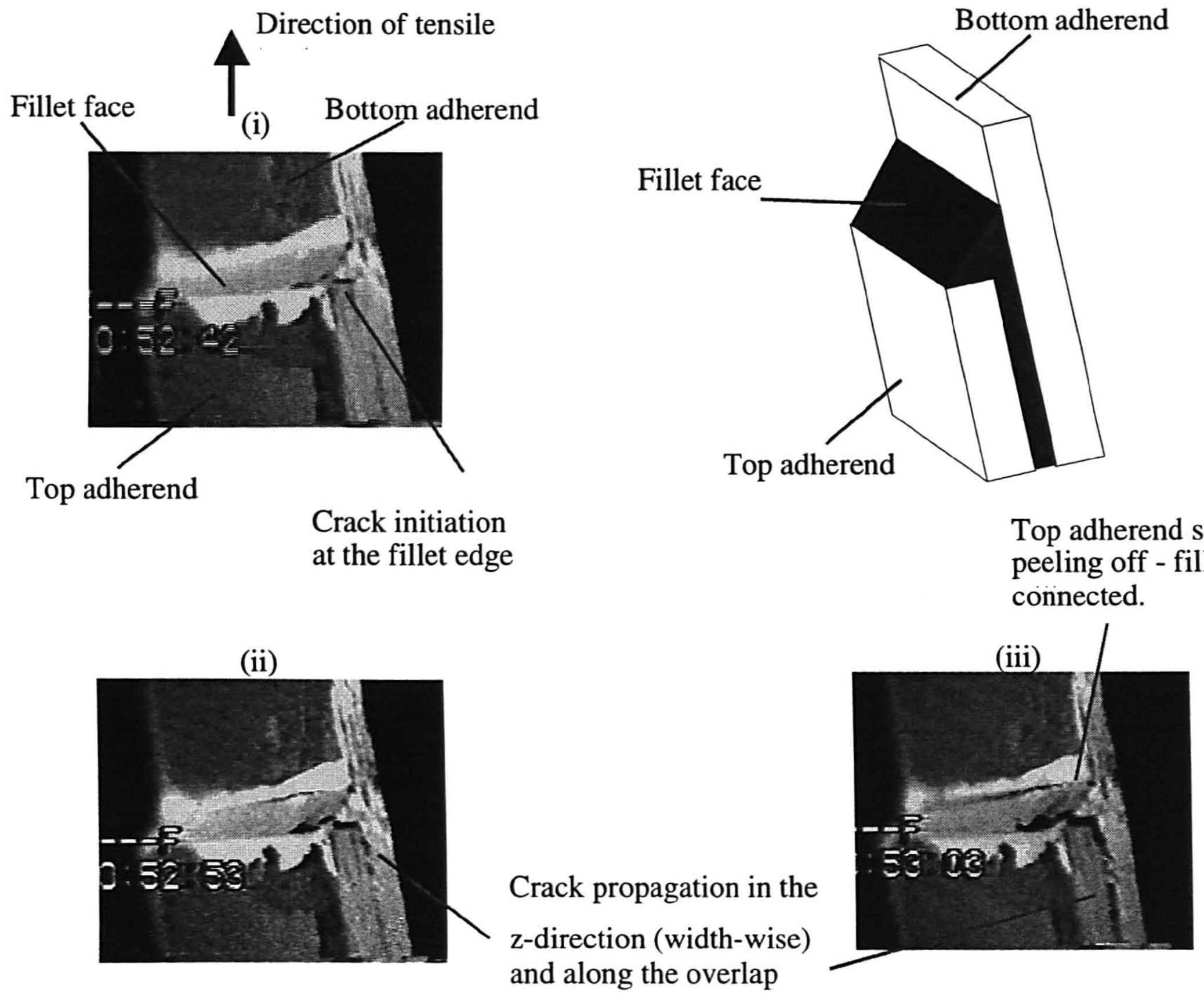

Figure 3.15a Failure of 60 mm mild steel joints in tension. Initiation and propagation of cracks (i)-(vii) - ESP 110 adhesive

(iv)

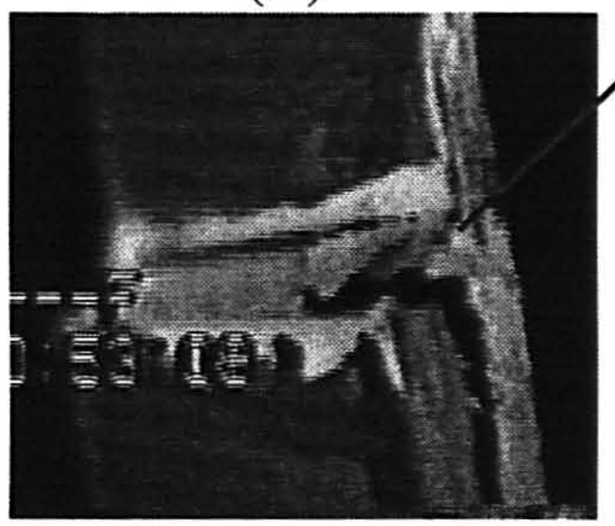

Top adherend starts peeling off - fillet still connected.

(v)

Fillet is peeled off from the bottom adherend.

Failure spans the whole width of the joint. Cracks propagate along the overlap (x-direction).

(vi)

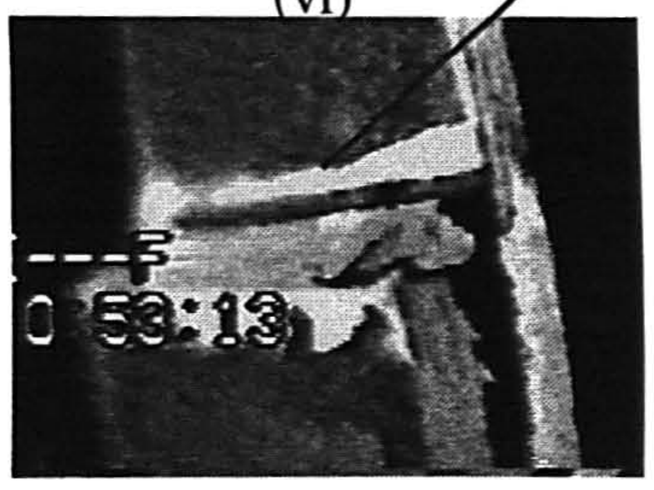

(vii)

Final state before catastrophic failure

Figure 3.15b Failure of 60 mm mild steel joints in tension. Initiation and propagation of cracks (i)-(vii) - ESP 110 adhesive

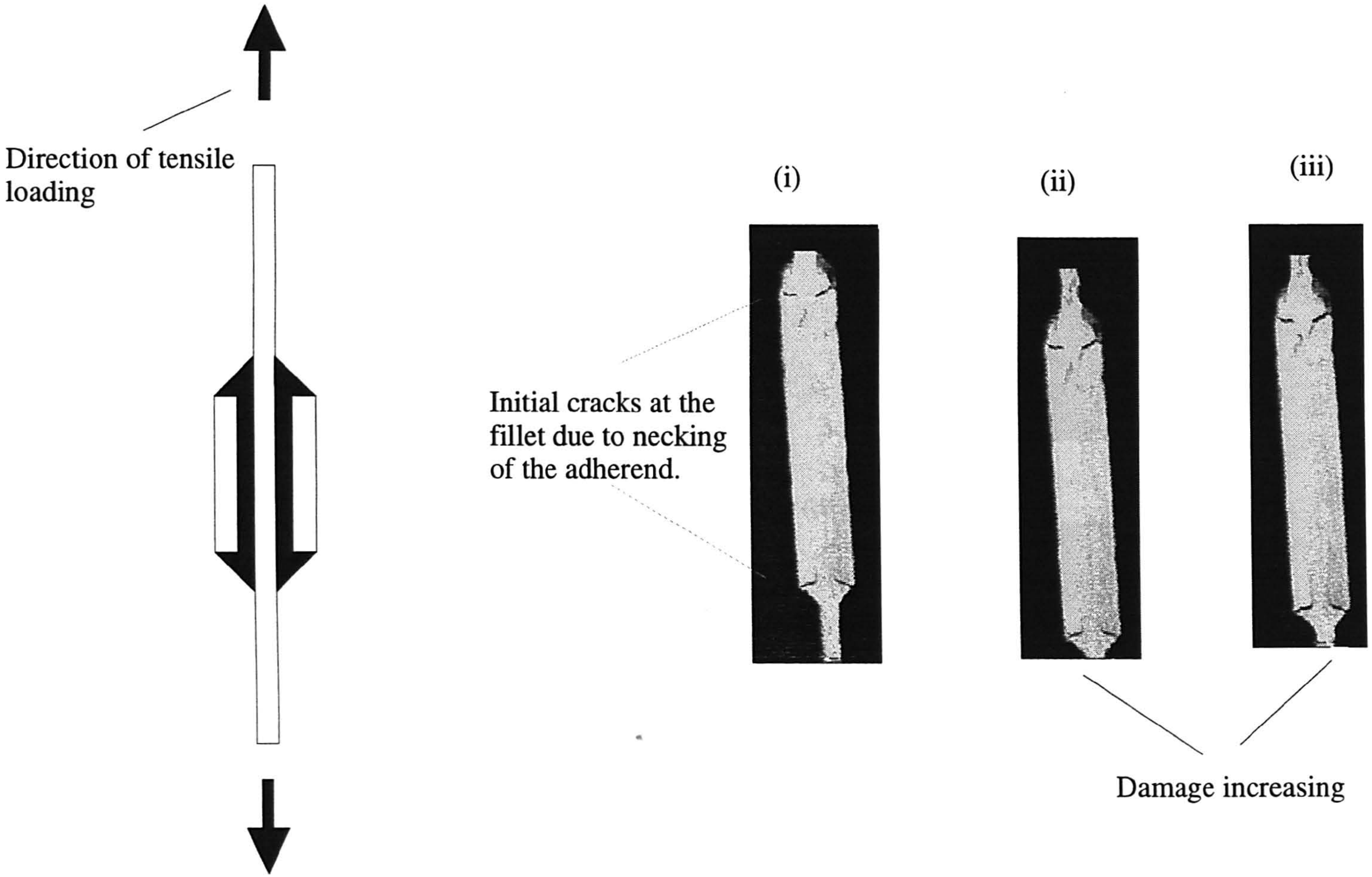

Figure 3.16 Bonded doublers - initiation of cracks due to Poisson's ratio effect - mild steel adherends - ESP 110 adhesive - failure propagation (i) - (iii)

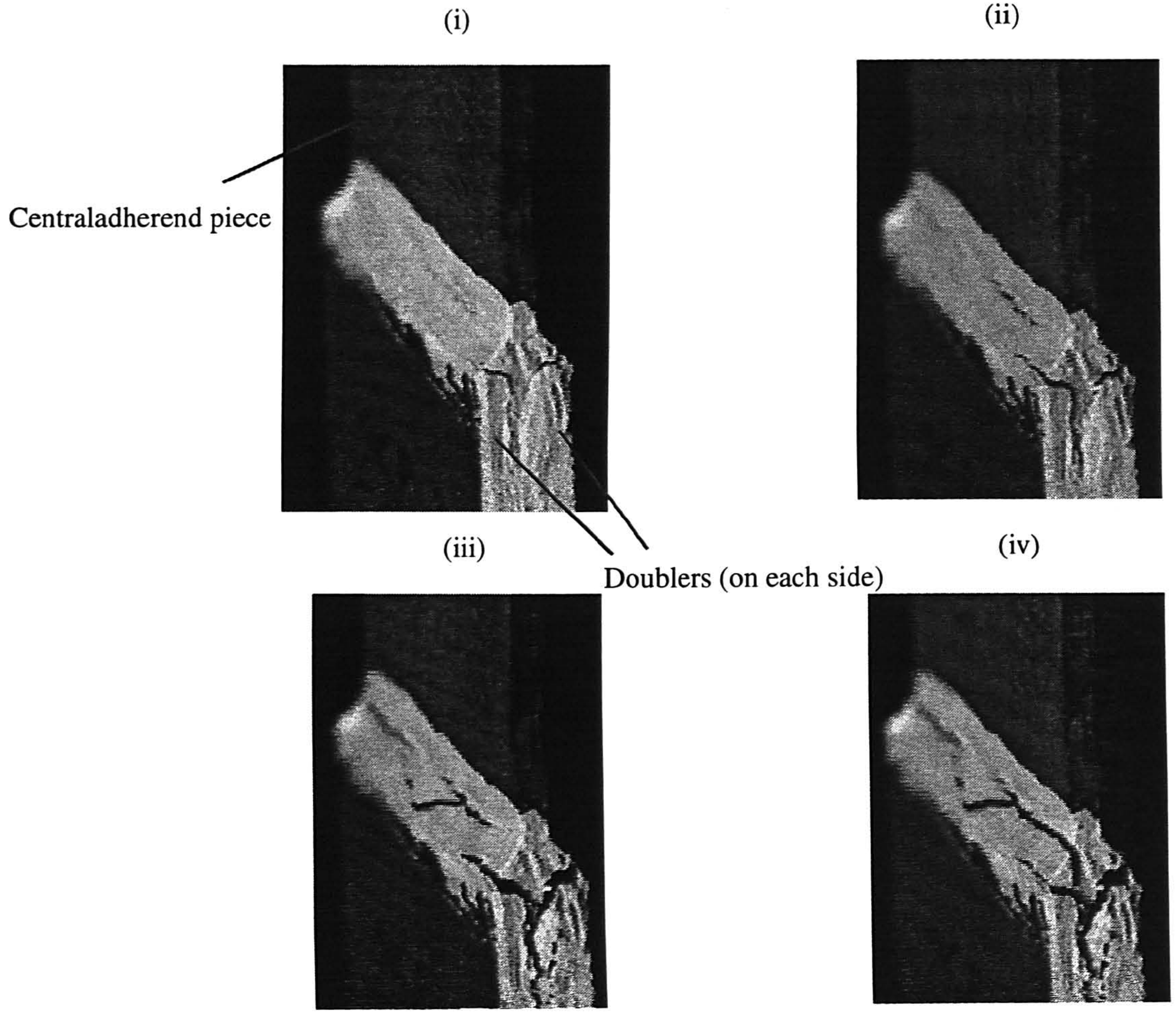

Figure 3.17 Initiation and propagation of damage (i)-(iv) in bonded doublers - mild steel adherends - ESP 110 adhesive - detailed view of fillet's corner

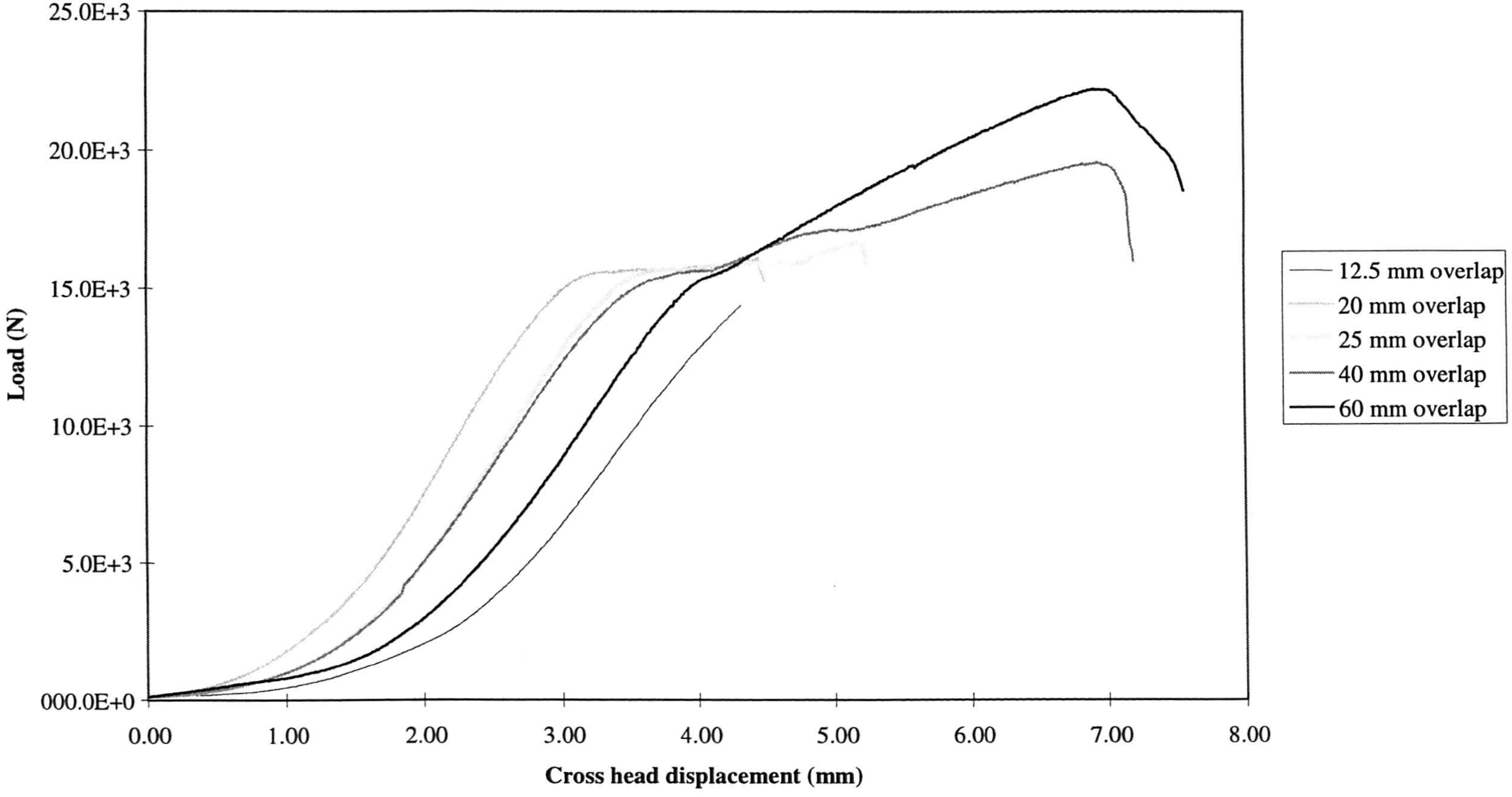

Figure 3.18 Load-displacement curves for SLJs with AV119 adhesive - gauge steel adherends and various overlaps

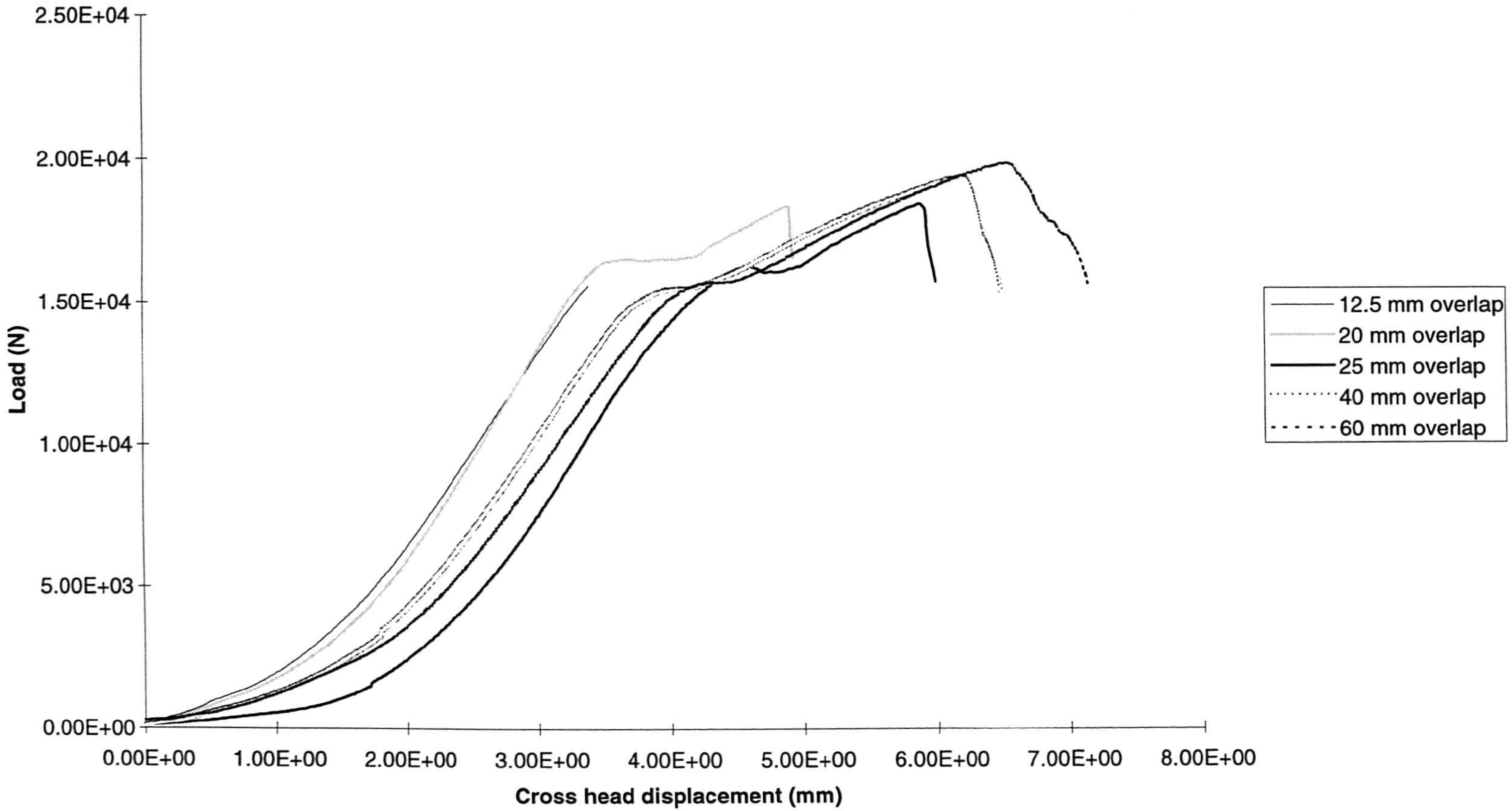

Figure 3.19 Load-displacement curves for SLJs with EC 3448 adhesive - gauge steel adherends and various overlaps

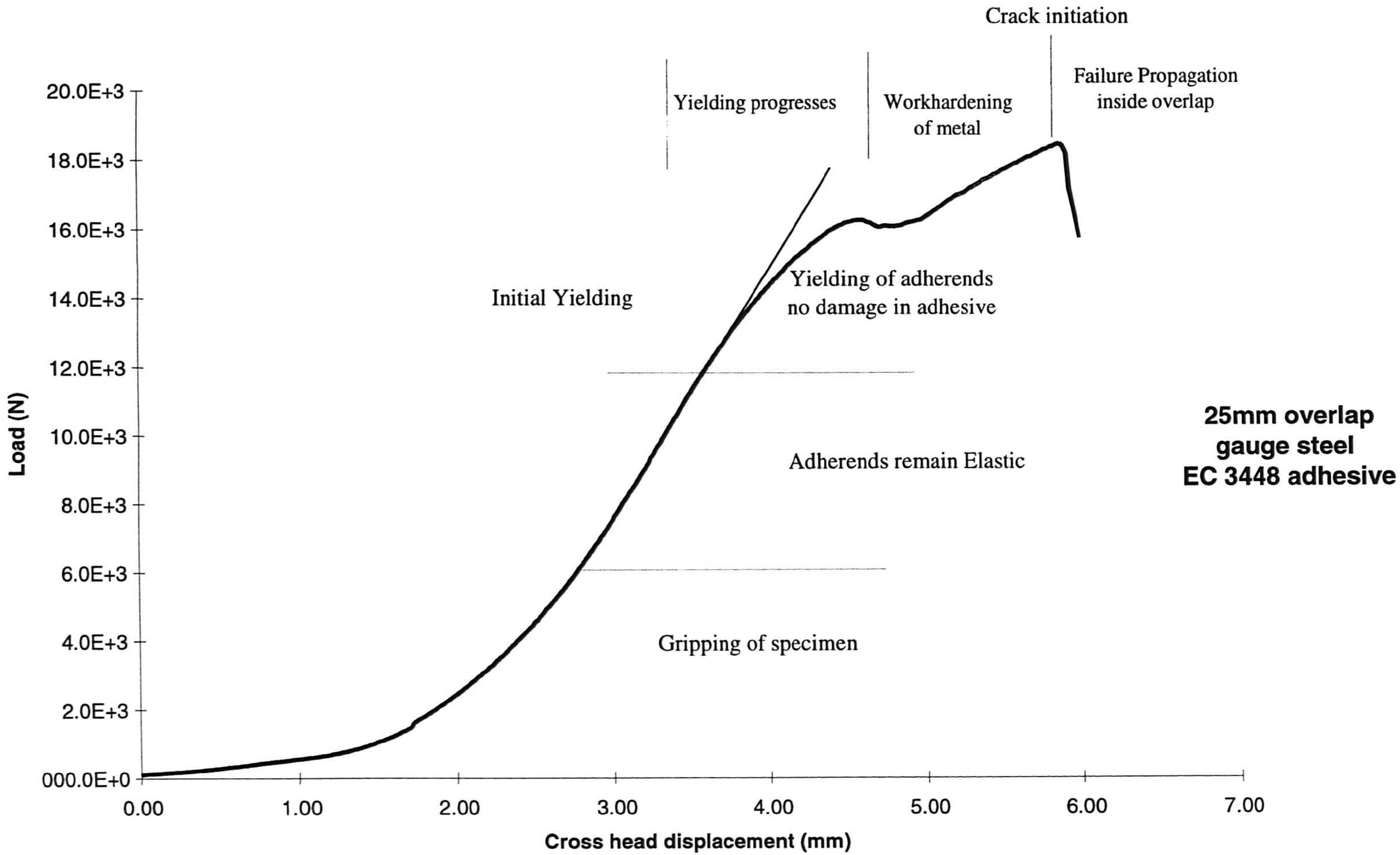

Figure 3.20 Load-displacement curves for SLJ with EC 3448 adhesive - gauge steel adherends and 25 mm overlap

Gauge steel joint - AV 119 adhesive - 25 mm overlap

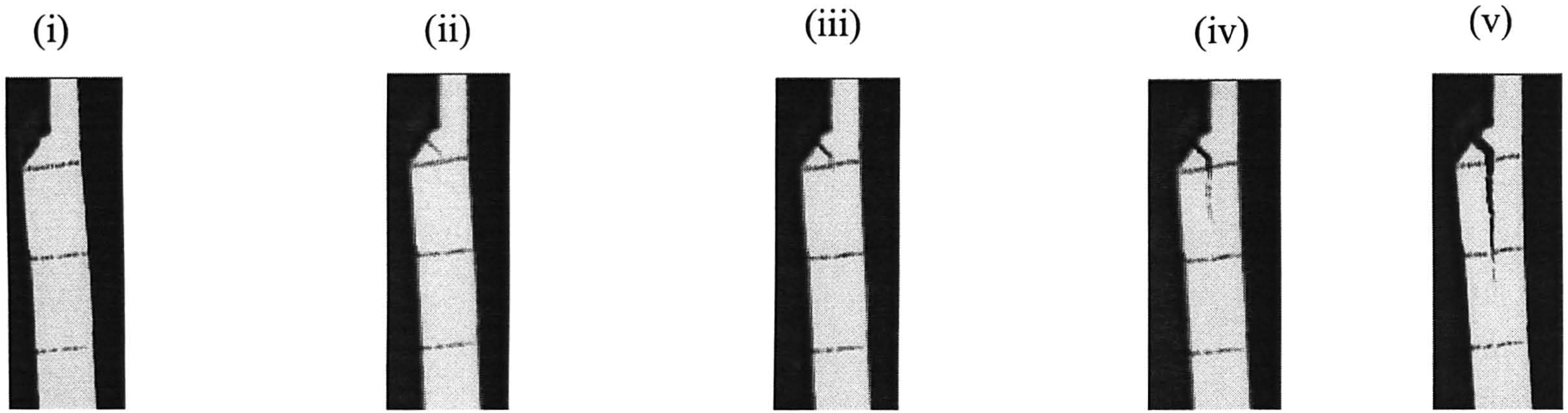

Figure 3.21 Failure propagation for a gauge steel joint - AV 119 adhesive - 25 mm overlap (only approximately half the overlap shown in the frames)

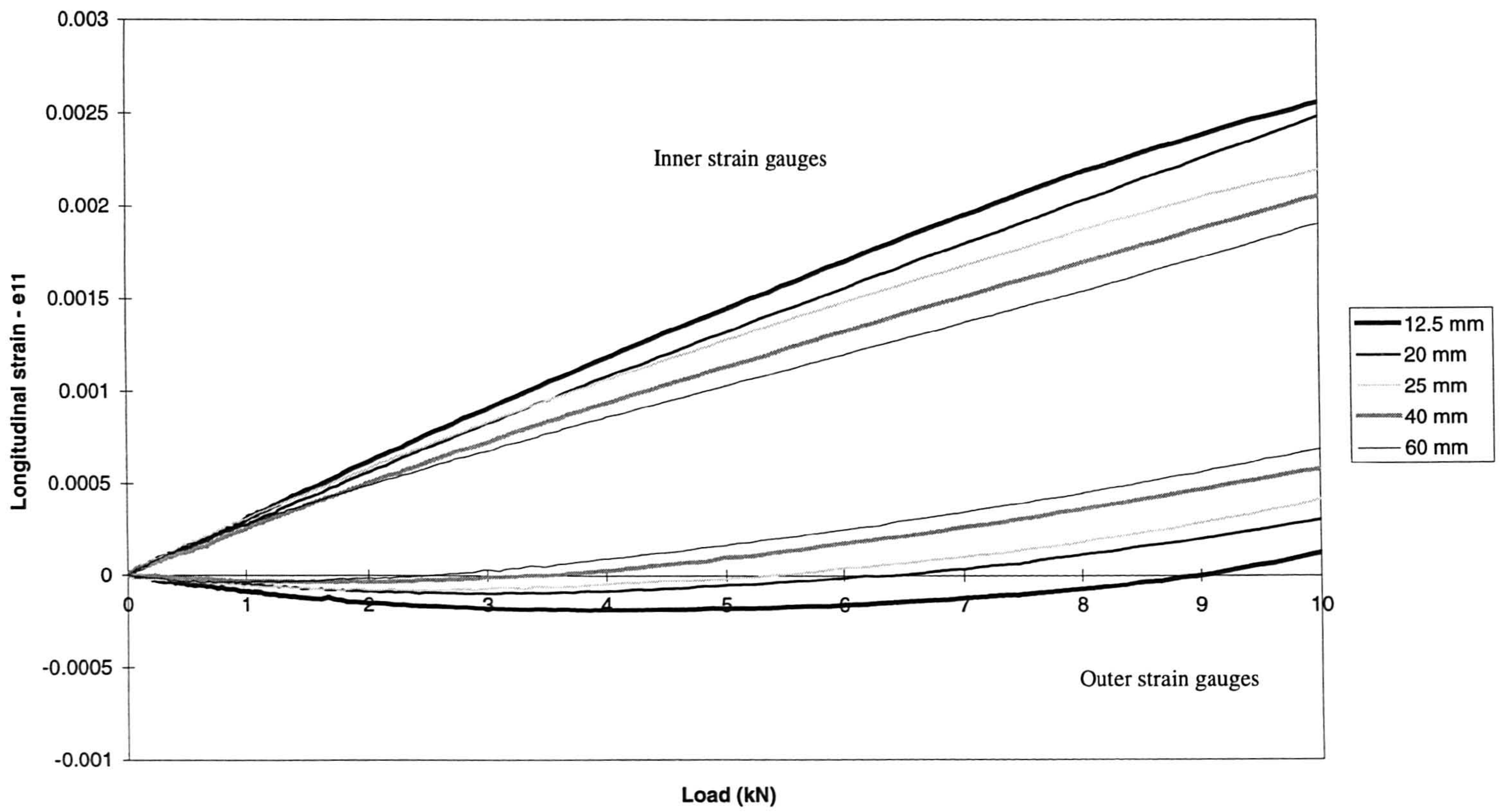

Figure 3.22 Variation of longitudinal strain in the adherends with load for gauge steel - EC 3448 adhesive SLJs - various overlap lengths at low applied loads

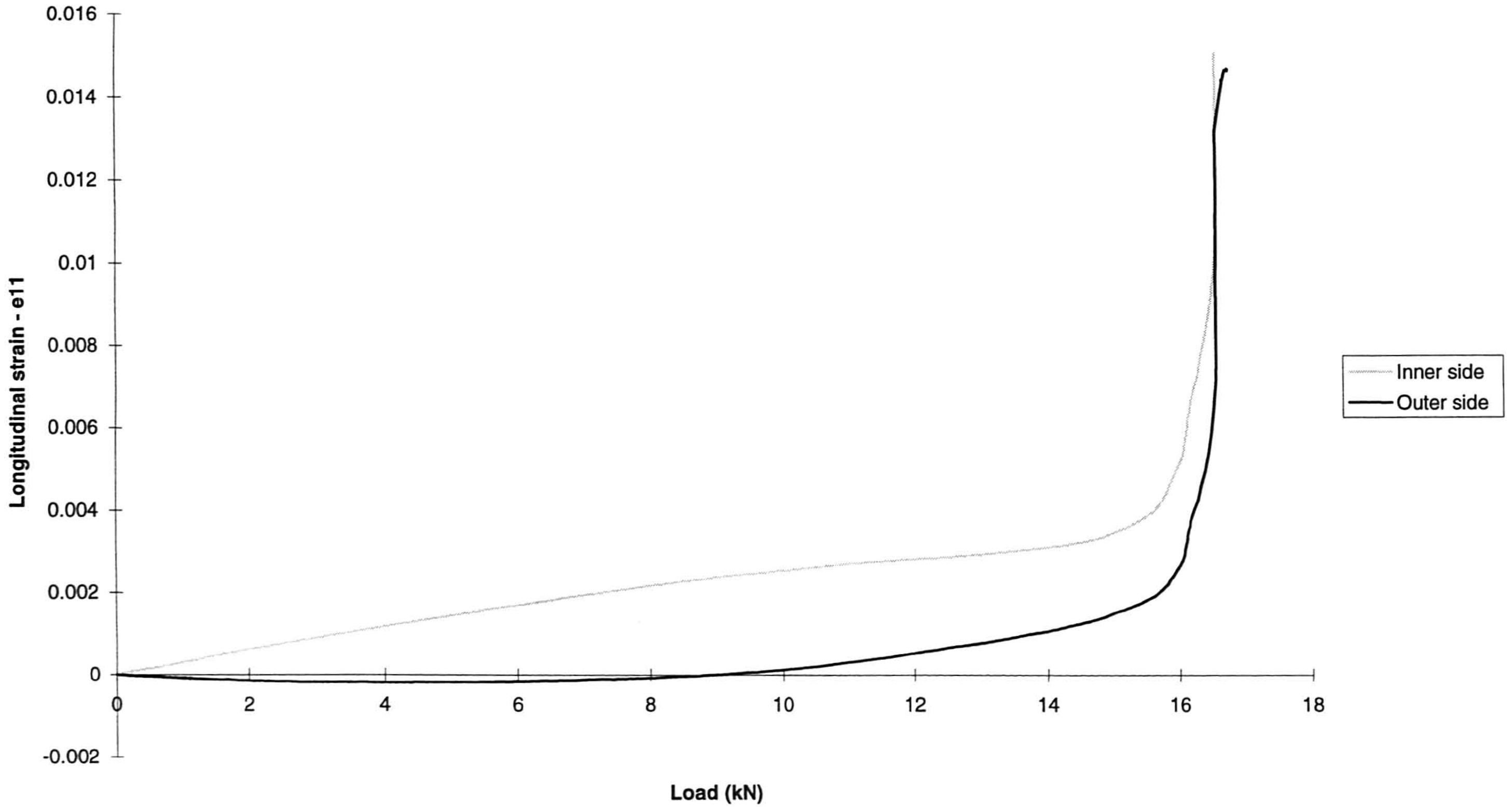

Figure 3.23 Variation of longitudinal strain in the adherends with load for a 12.5 mm overlap length SLJ - gauge steel - EC 3448 adhesive

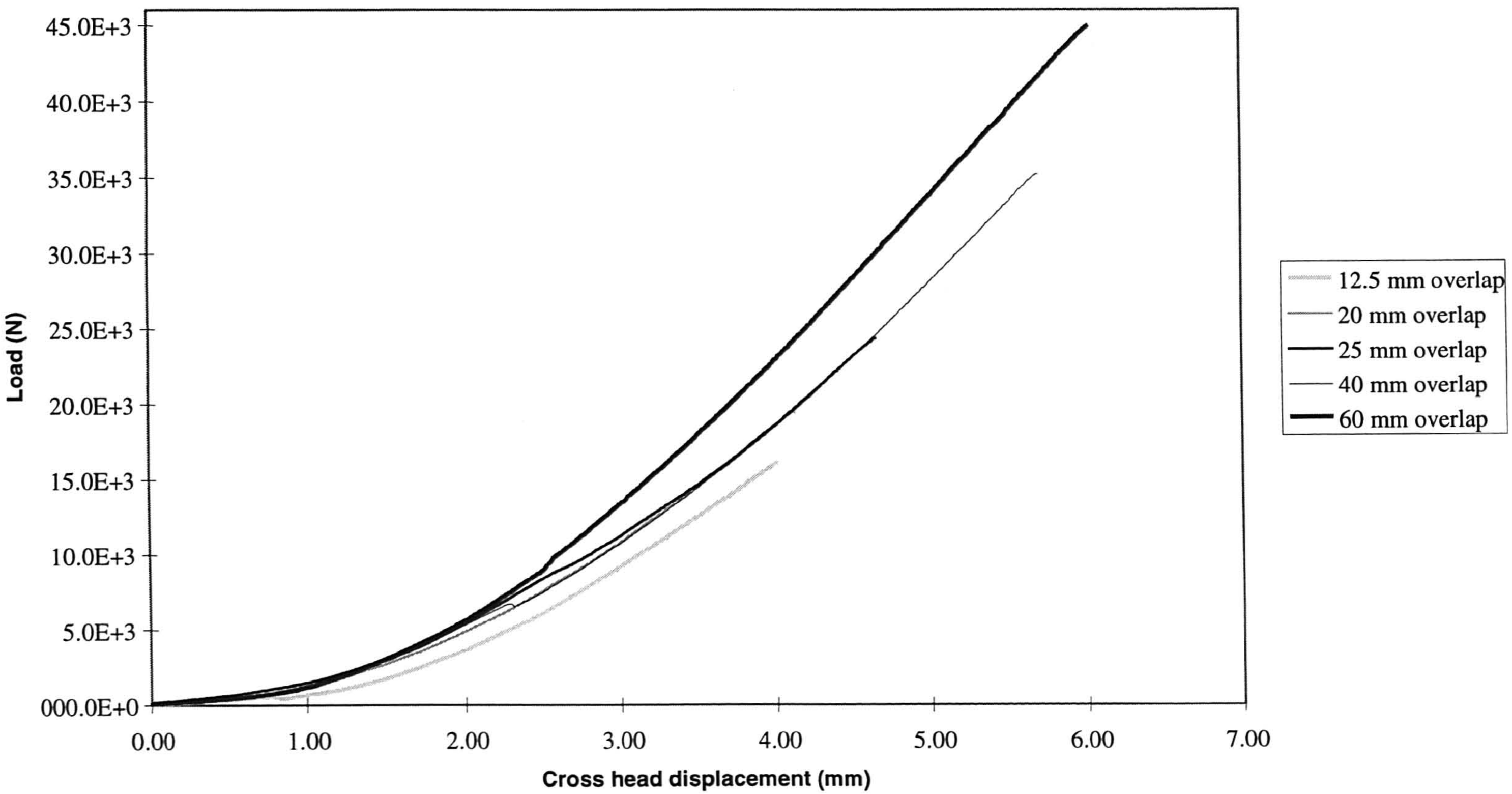

Figure 3.24 Load-displacement curves for SLJs with ESP 110 adhesive - hard steel adherends and various overlaps

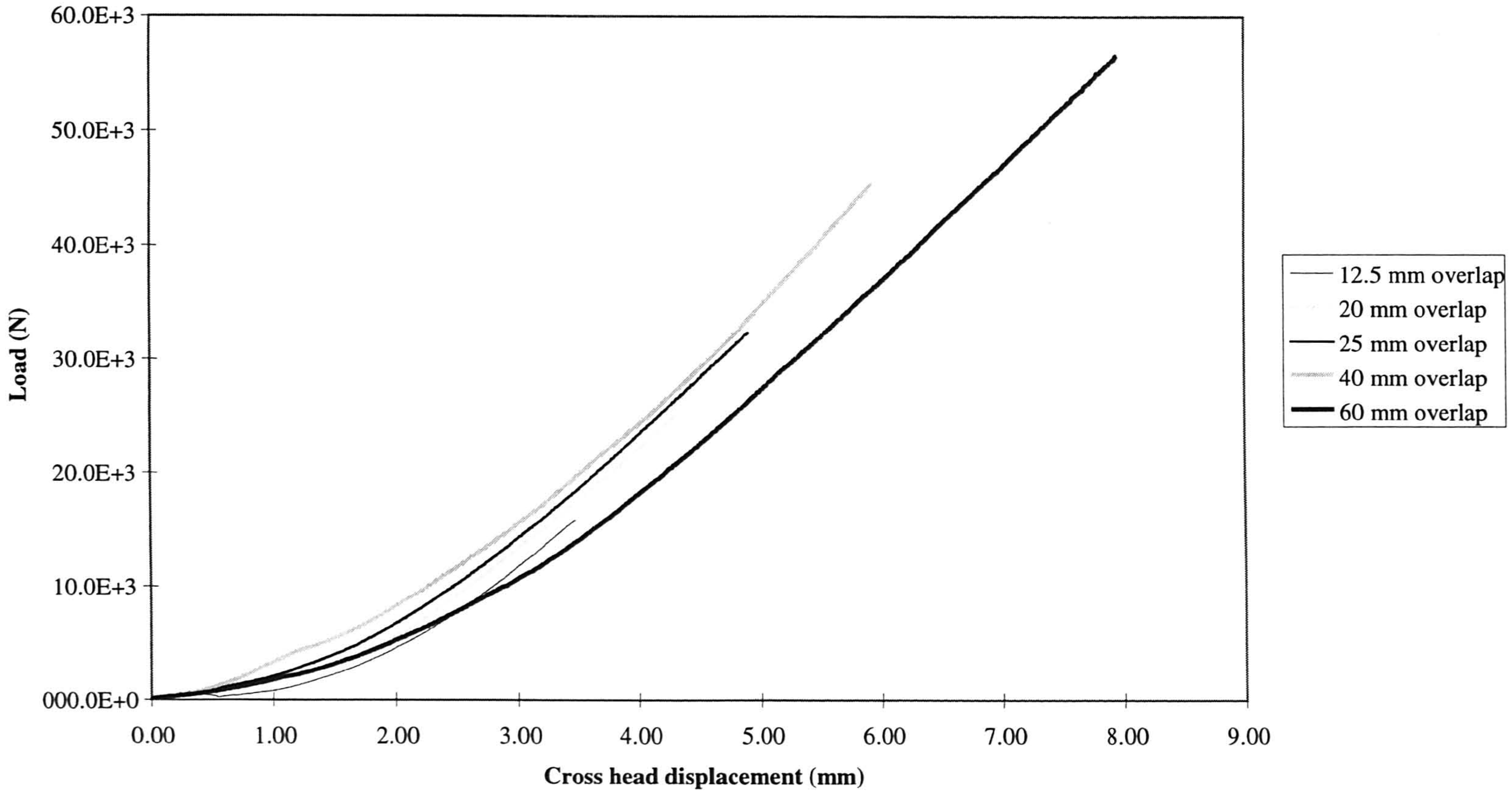

Figure 3.25 Load-displacement curves for SLJs with AV 119 adhesive - hard steel adherends and various overlaps

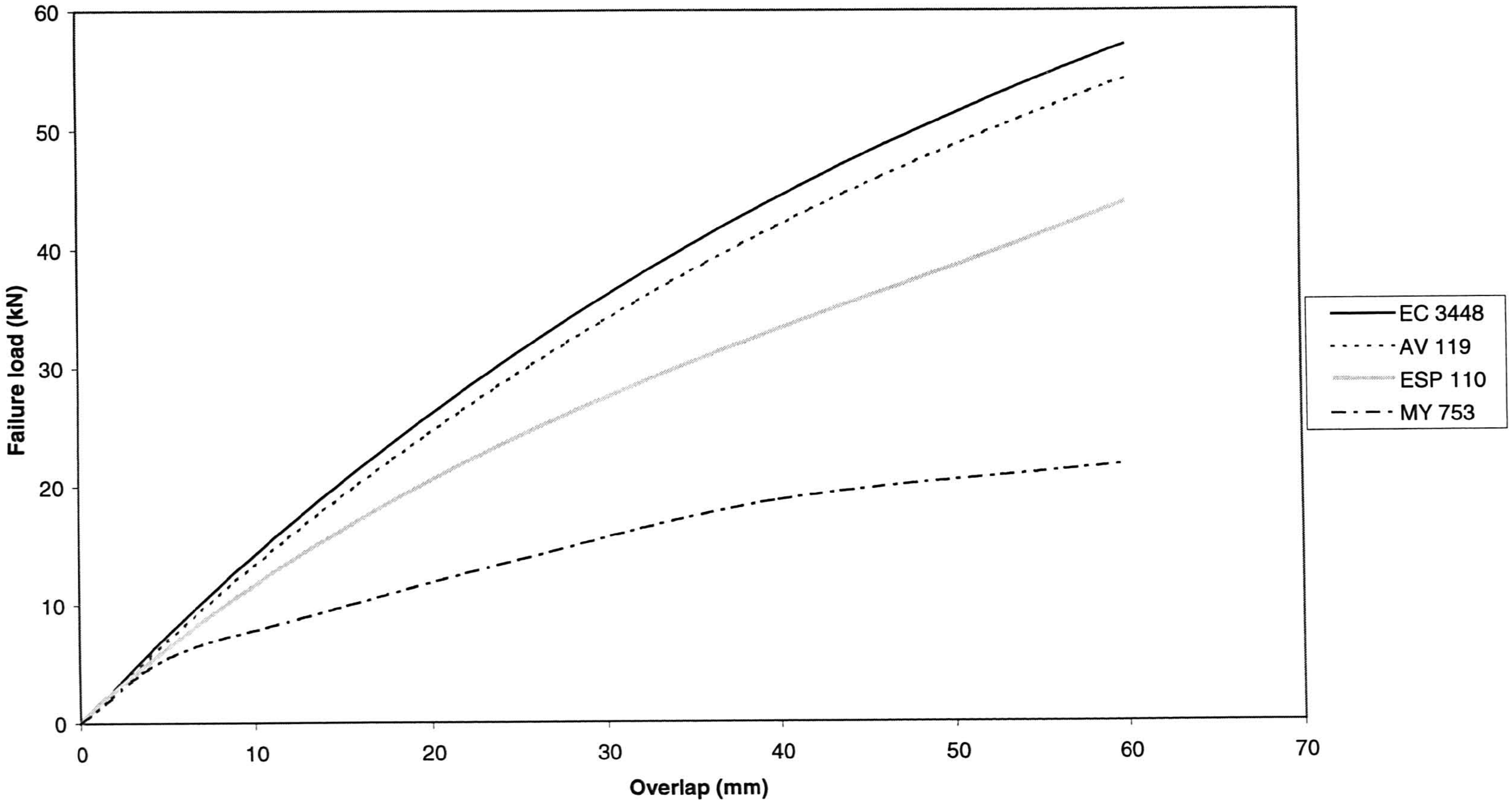

Figure 3.26 Comparison of mean failure load vs. overlap length for joints with hard steel adherends and different adhesives

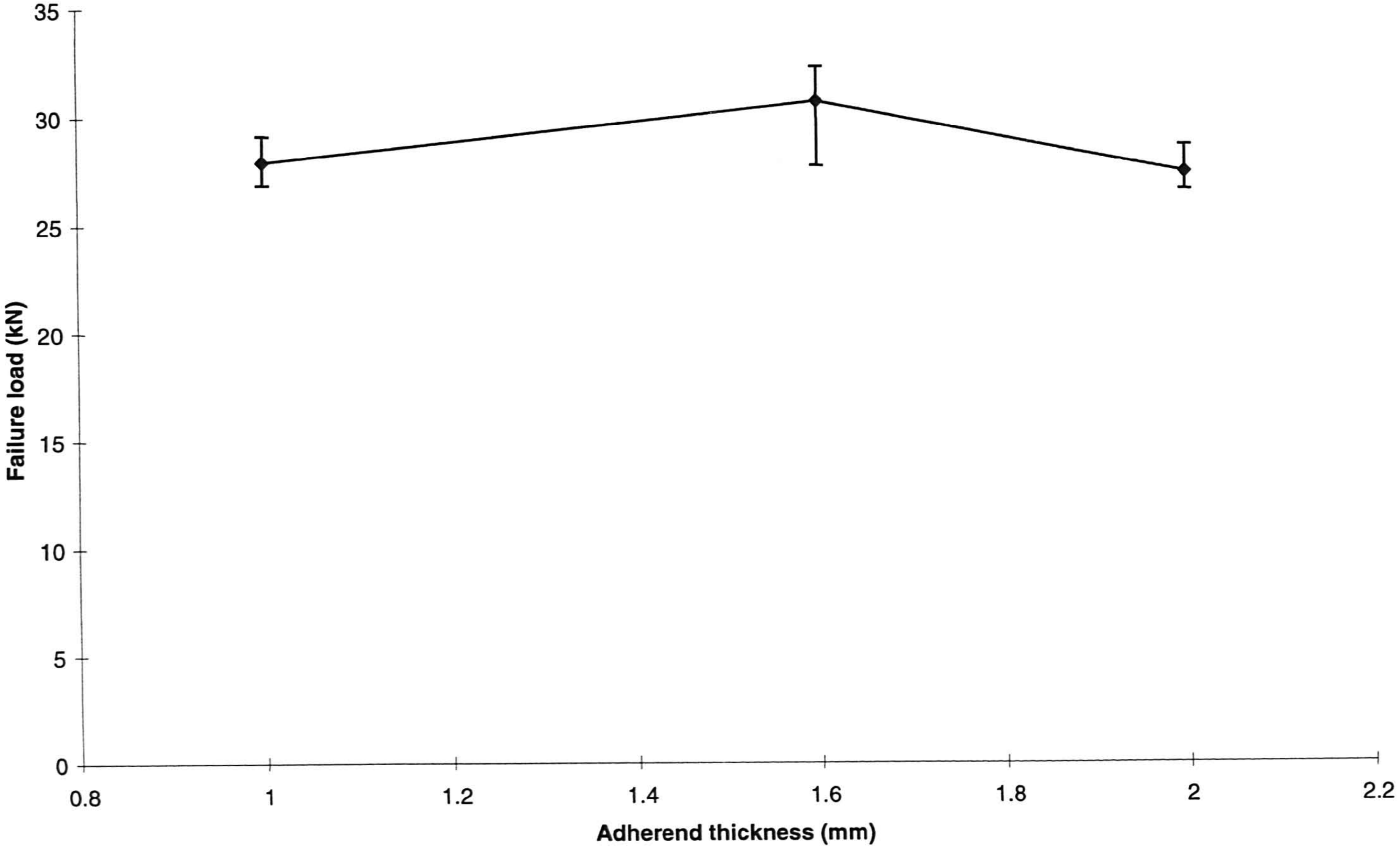

Figure 3.27 Variation of strength of SLJ in tension vs. adherend thickness for hard steel - 25 mm overlap - AV 119 adhesive

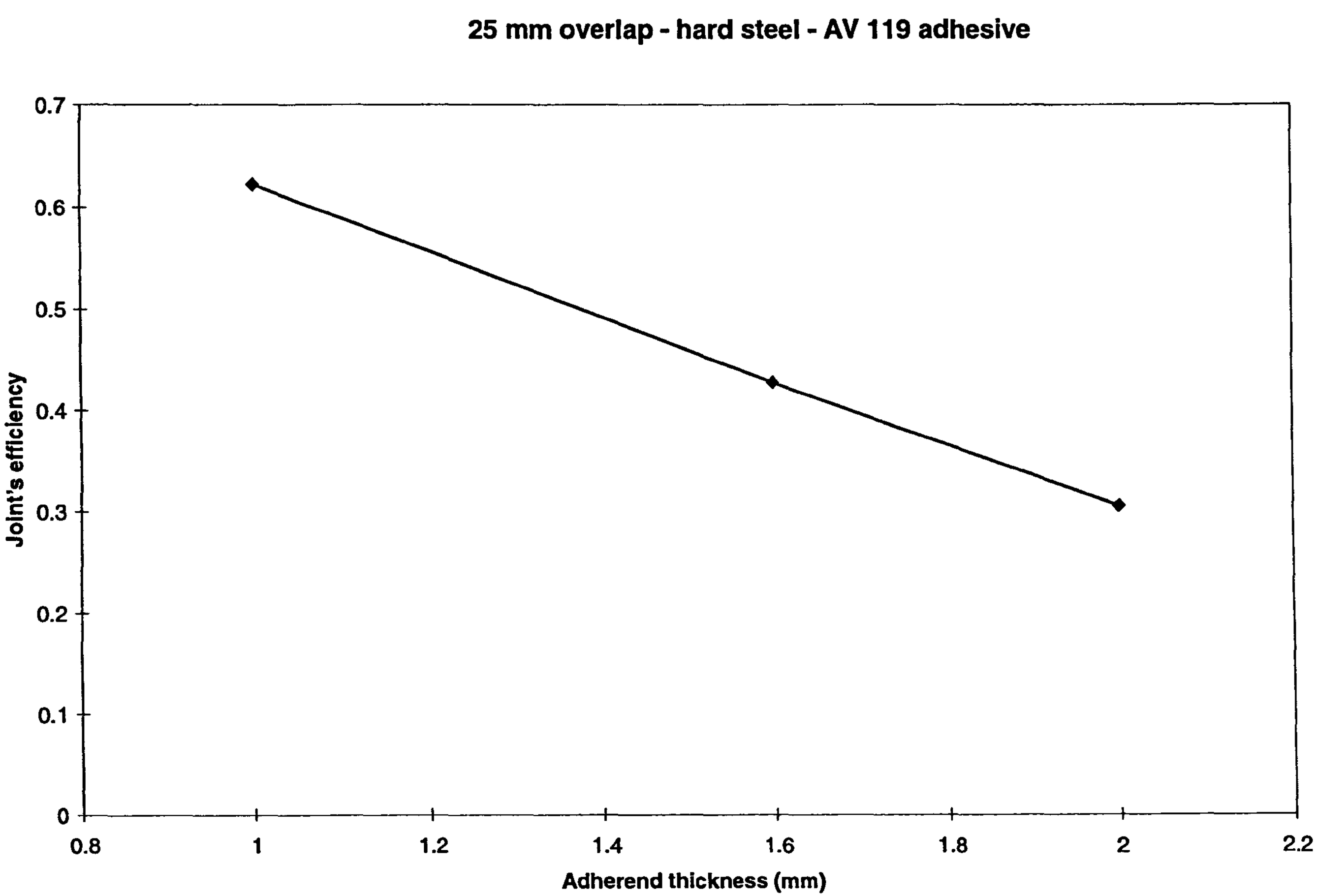

Figure 3.28 Comparison of joint's efficiency vs. adherend thickness for joints with hard steel - 25 mm overlap - AV 119 adhesive

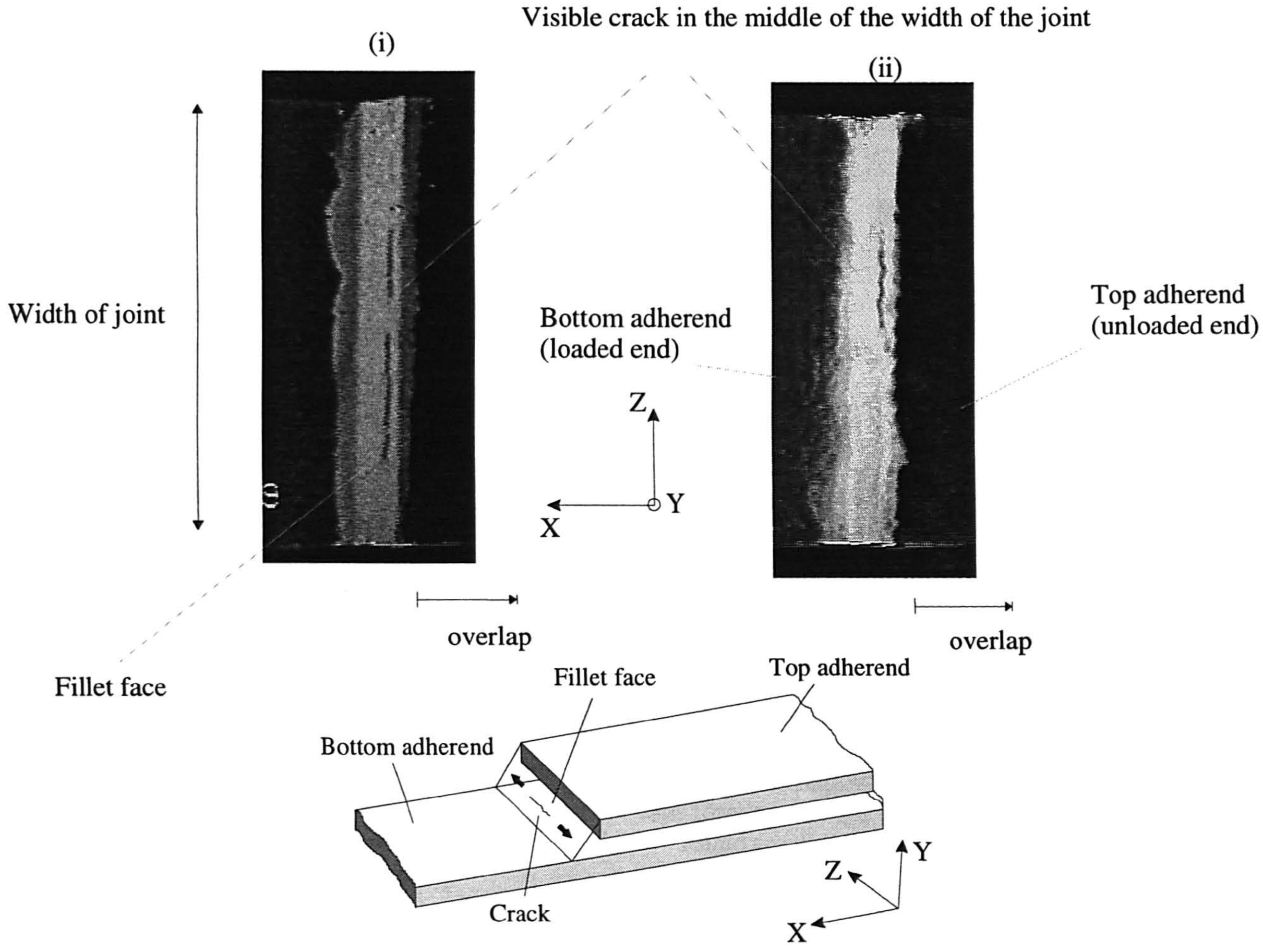

Figure 3.29 40mm (i) &25mm(ii) overlap joints with hard steel - detailed view of fillet's face - ESP 110 adhesive - initiation of cracks in the centre of the width of the joint due to anticlastic bending effect

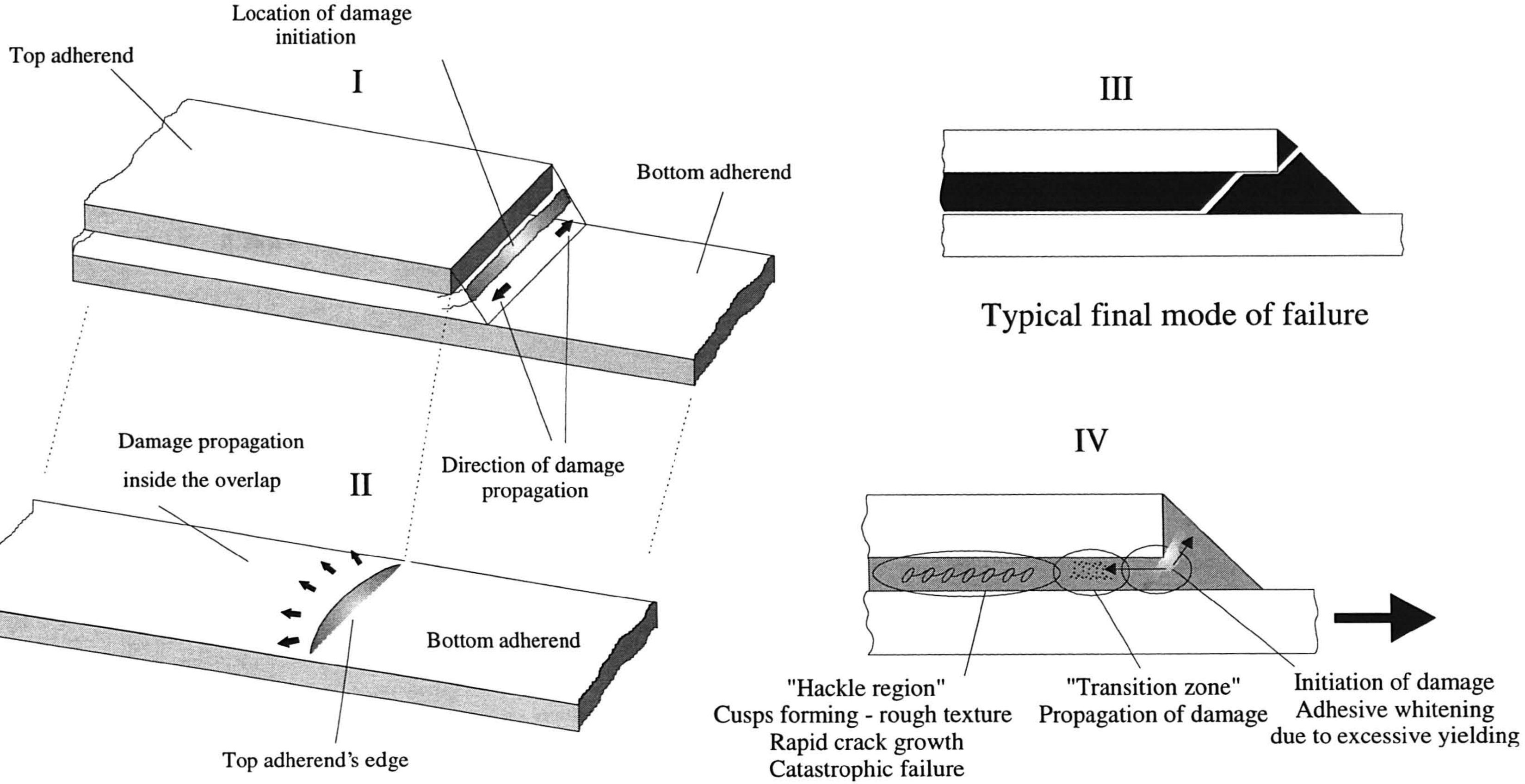

Figure 3.30 Description of failure mechanisms for hard steel - ductile adhesive configuration

Anticlastic bending

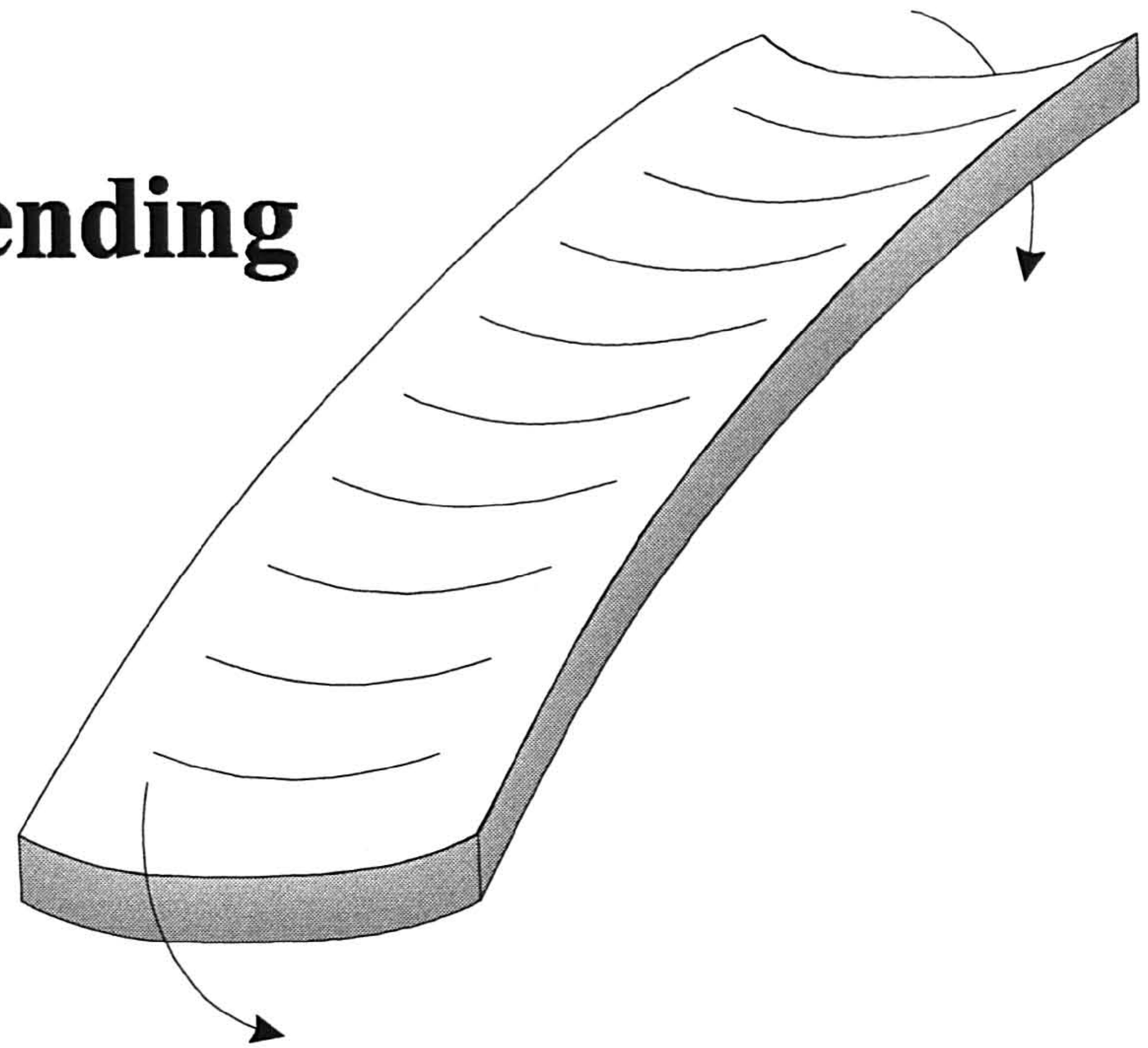

Figure 3.31 Illustration of anticlastic bending effect

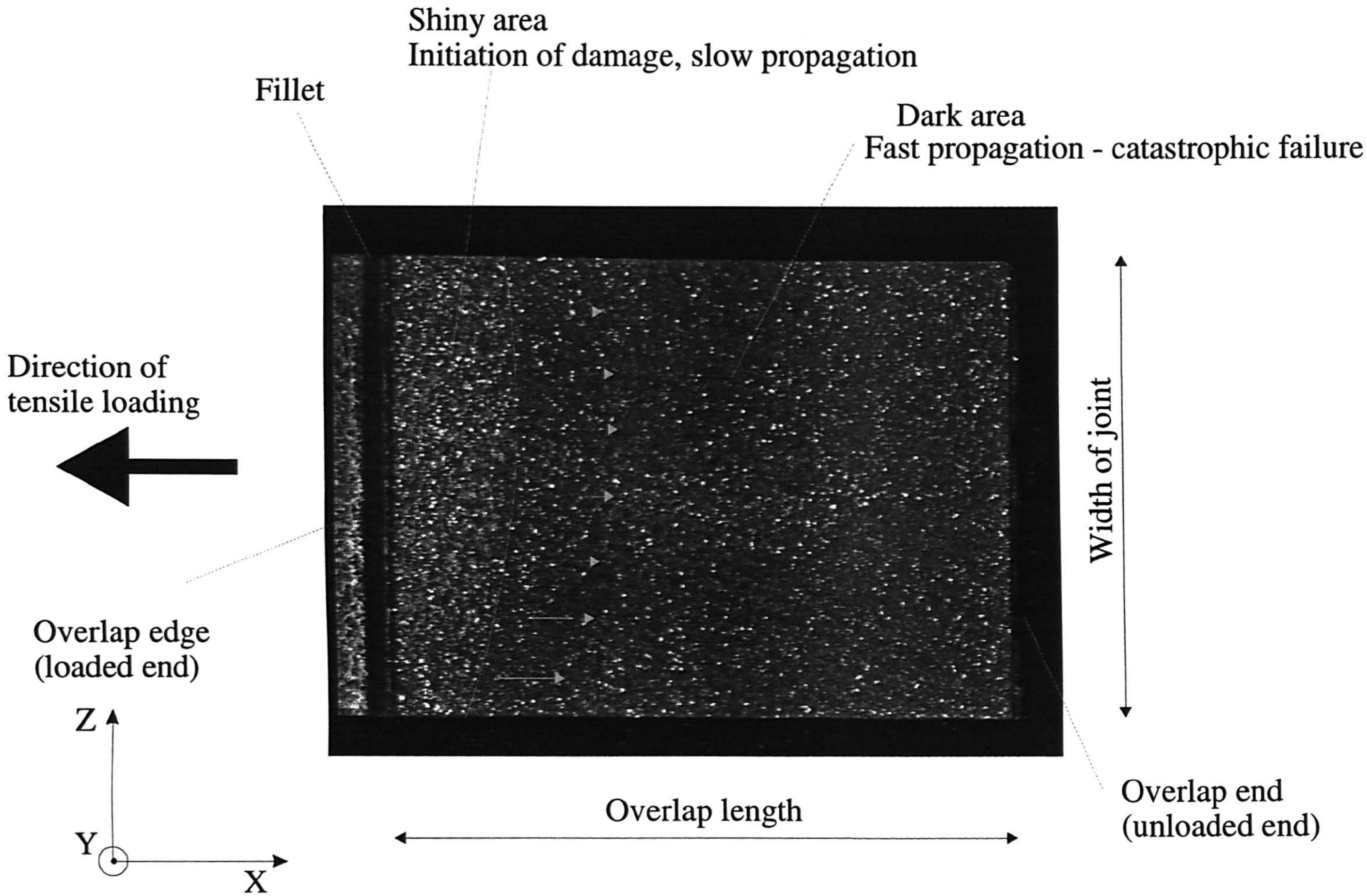

Figure 3.32 40 mm joint in tension - hard steel adherend - ESP 110 adhesive - dark and shinny areas indicating curved crack fronts due to anticlastic bending effect

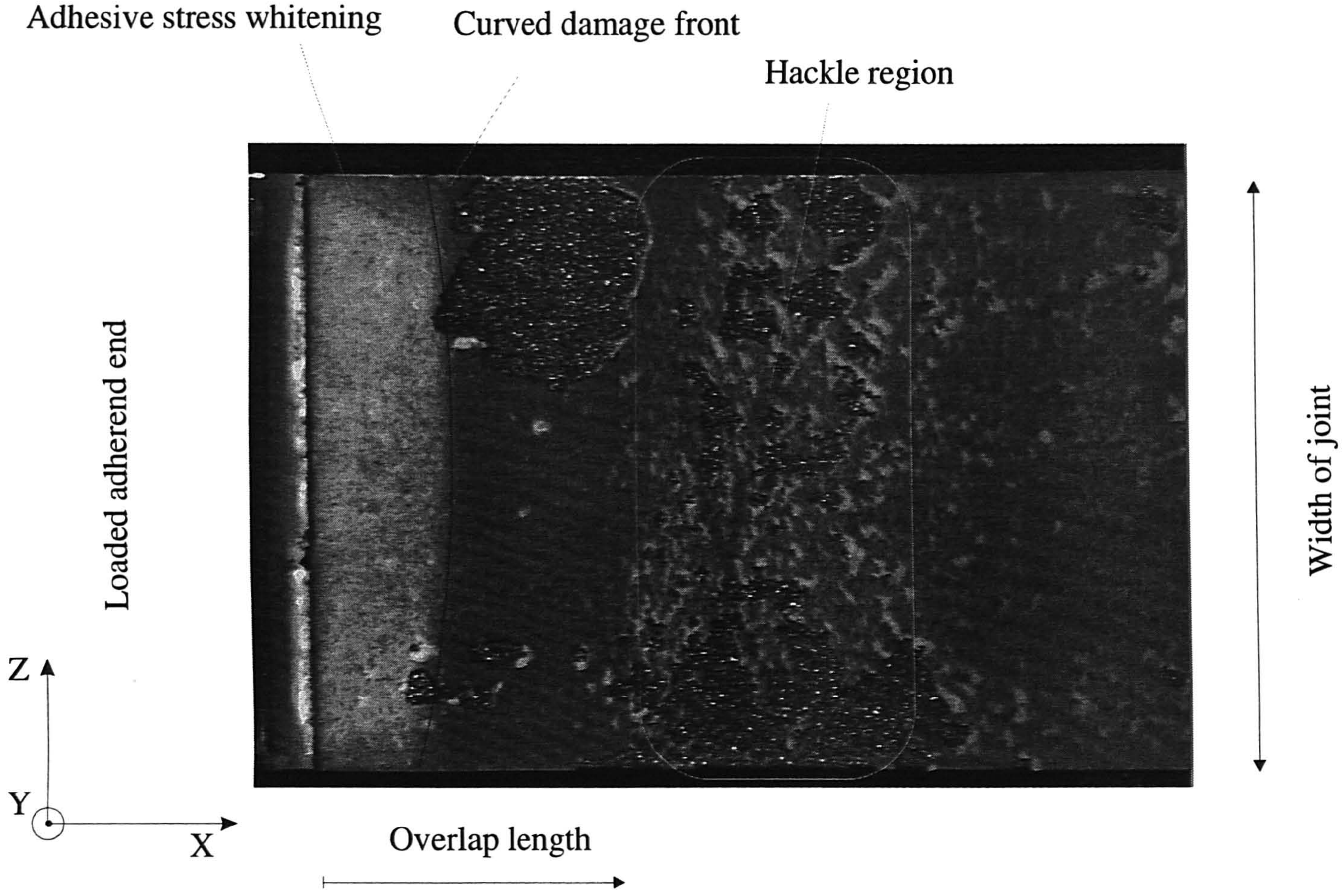

Figure 3.33 Failure pattern of a 60 mm overlap hard steel joint with AV 119 adhesive

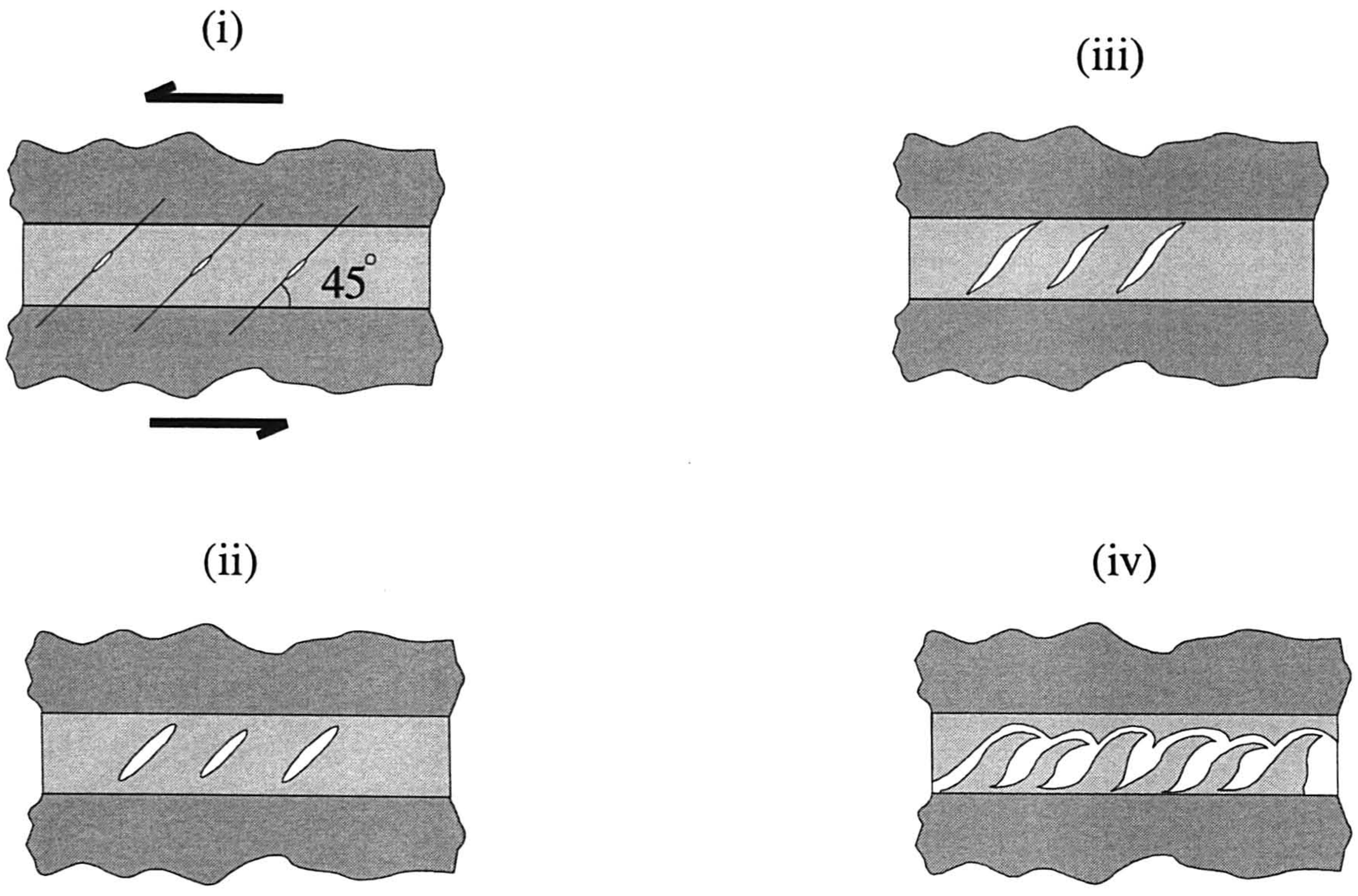

Figure 3.34 Shear failure of adhesive and formation of cusps - rough textured area corresponding to hackle region

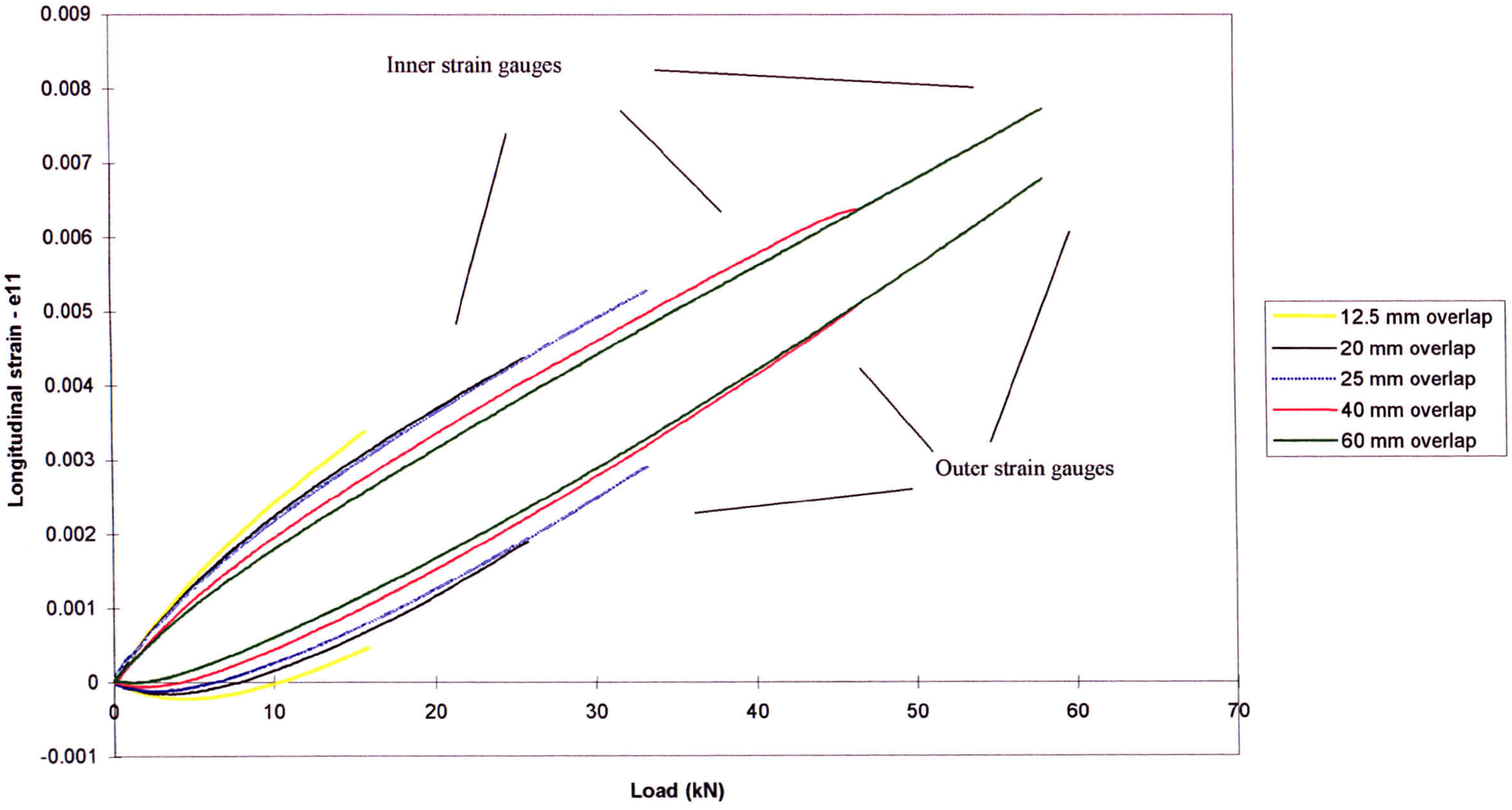

Figure 3.35 Variation of longitudinal strain in the adherends with load for hard steel - EC 3448 adhesive SLJs - various overlap lengths

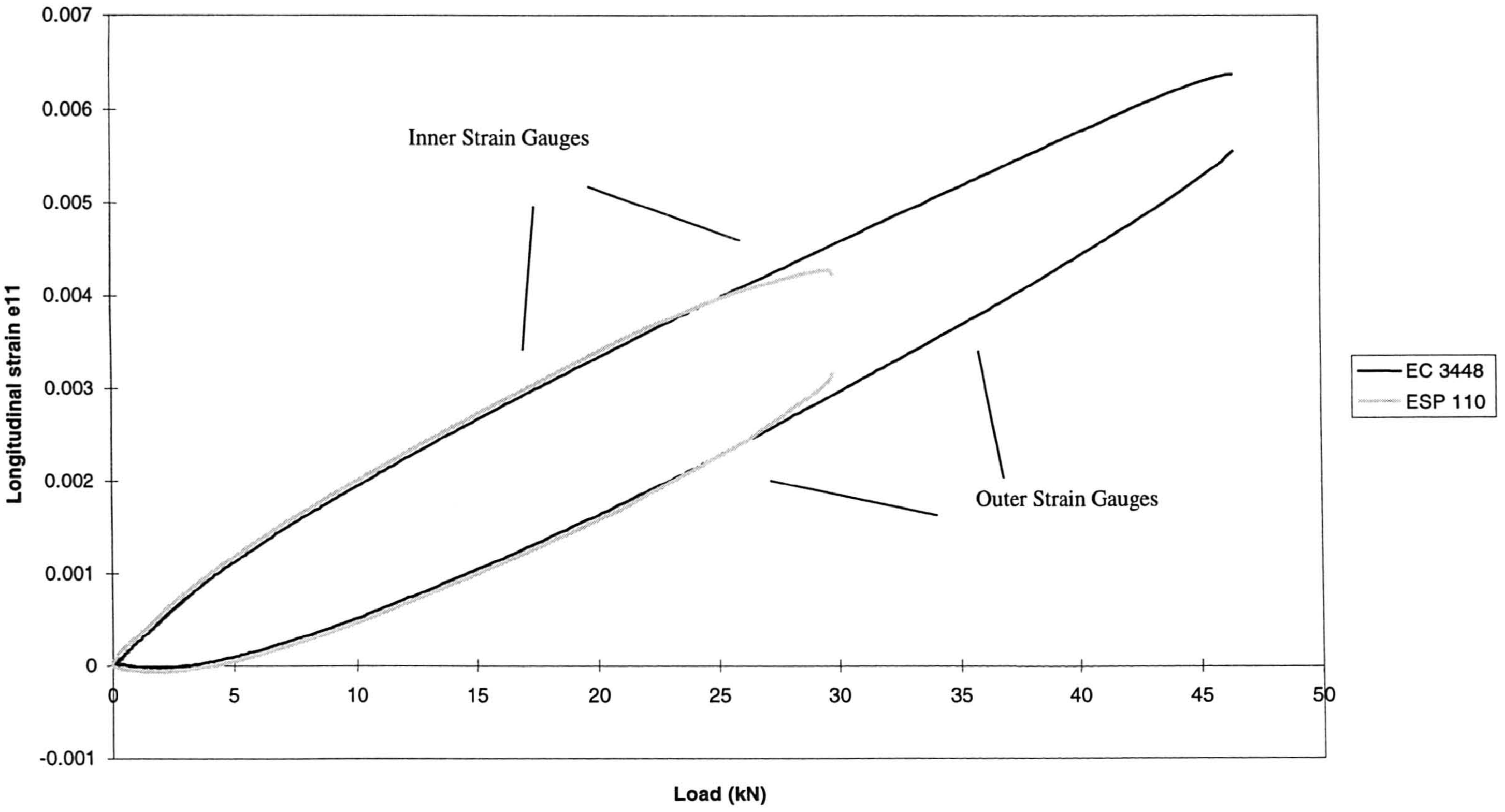

Figure 3.36 Comparison of longitudinal strain in the adherends with load for hard steel - 40 mm overlap - EC 3448 and ESP 110 adhesive SLJs

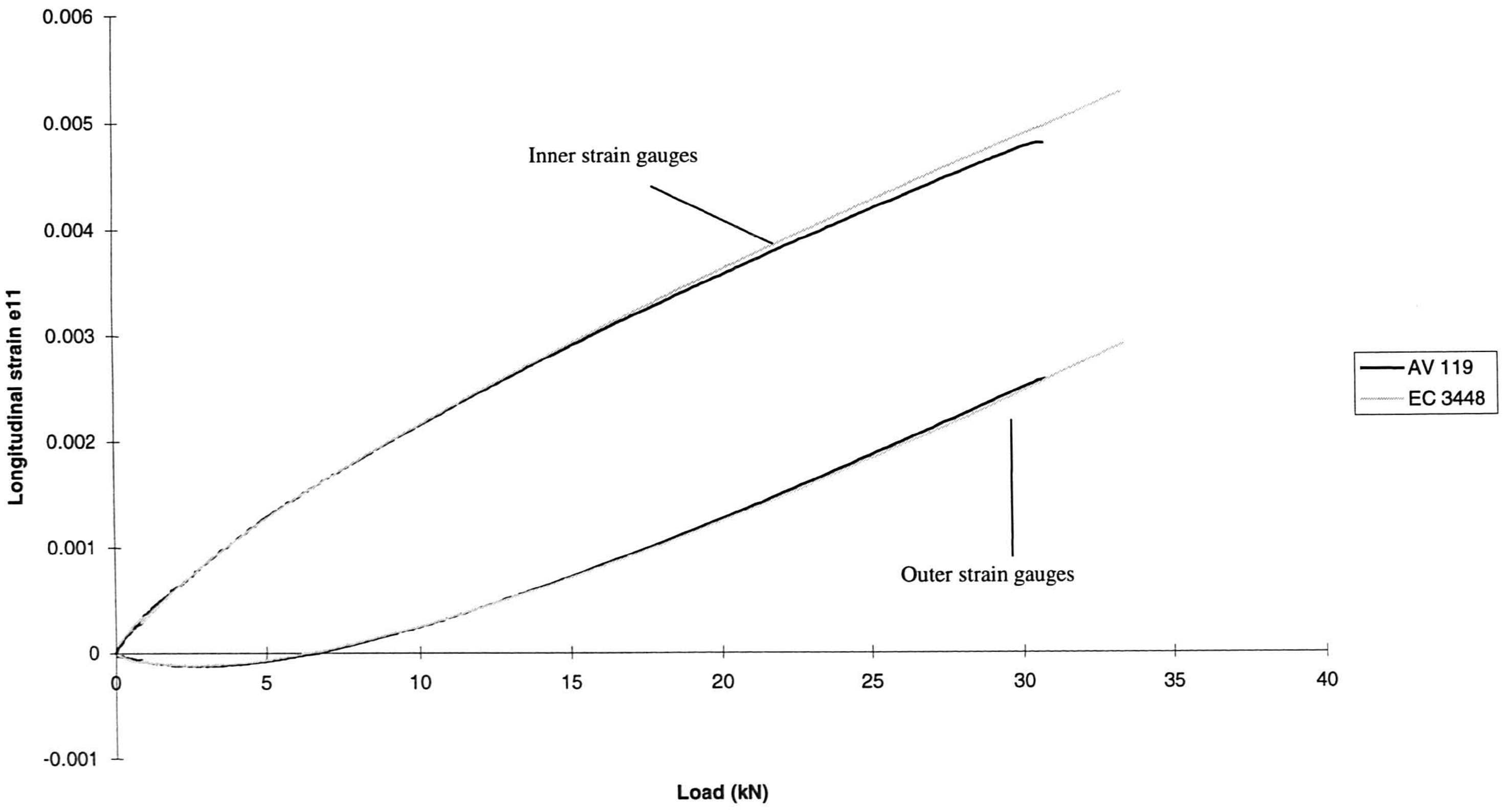

Figure 3.37 Comparison of longitudinal strain in the adherends with load for hard steel - 25 mm overlap - EC 3448 and AV 119 adhesive SLJs

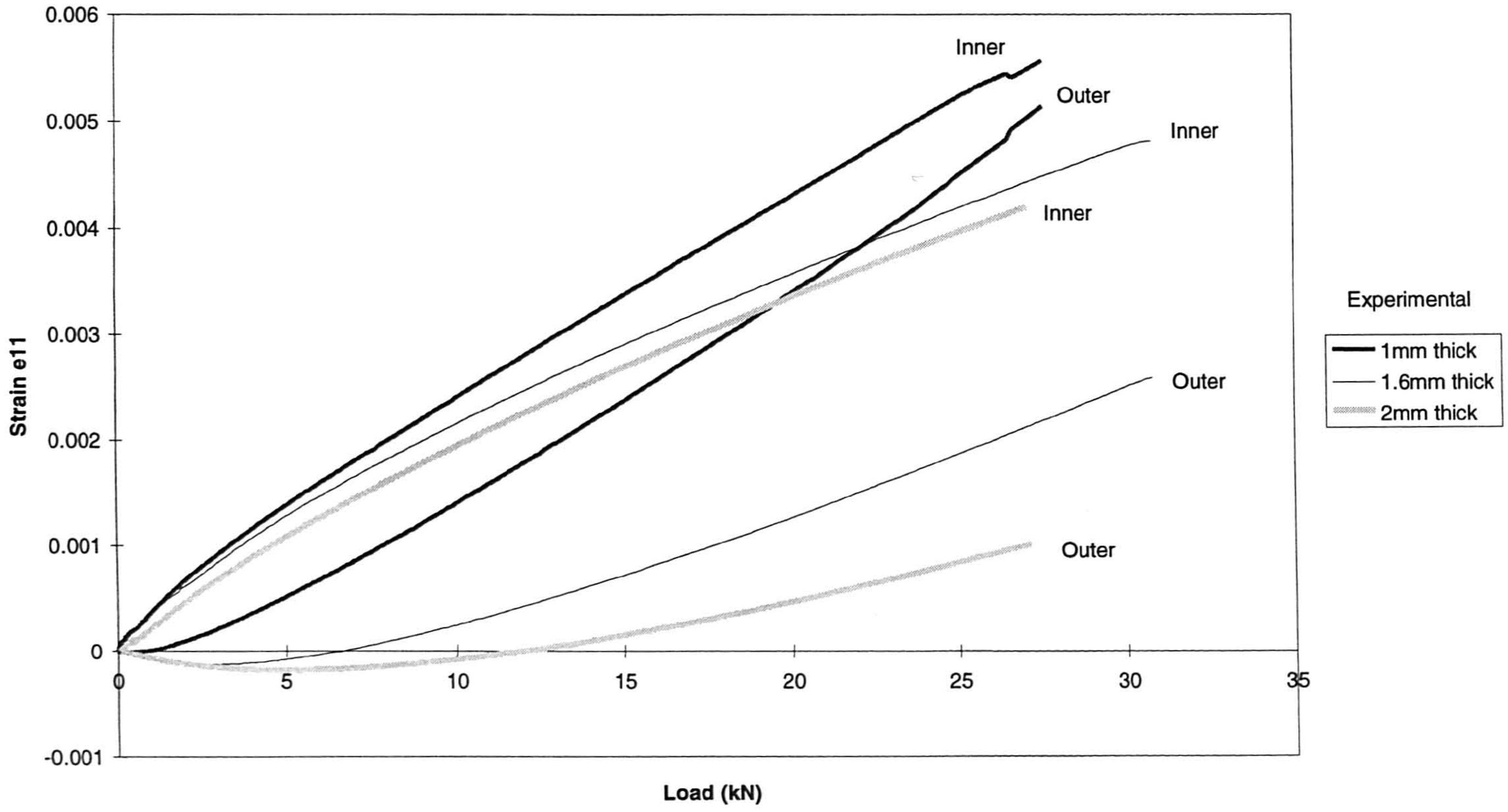

Figure 3.38 Comparison of longitudinal strain in the adherends with load for hard steel - 25 mm overlap - AV 119 adhesive - different adherend thicknesses

Four point bend rig

NOT TO SCALE

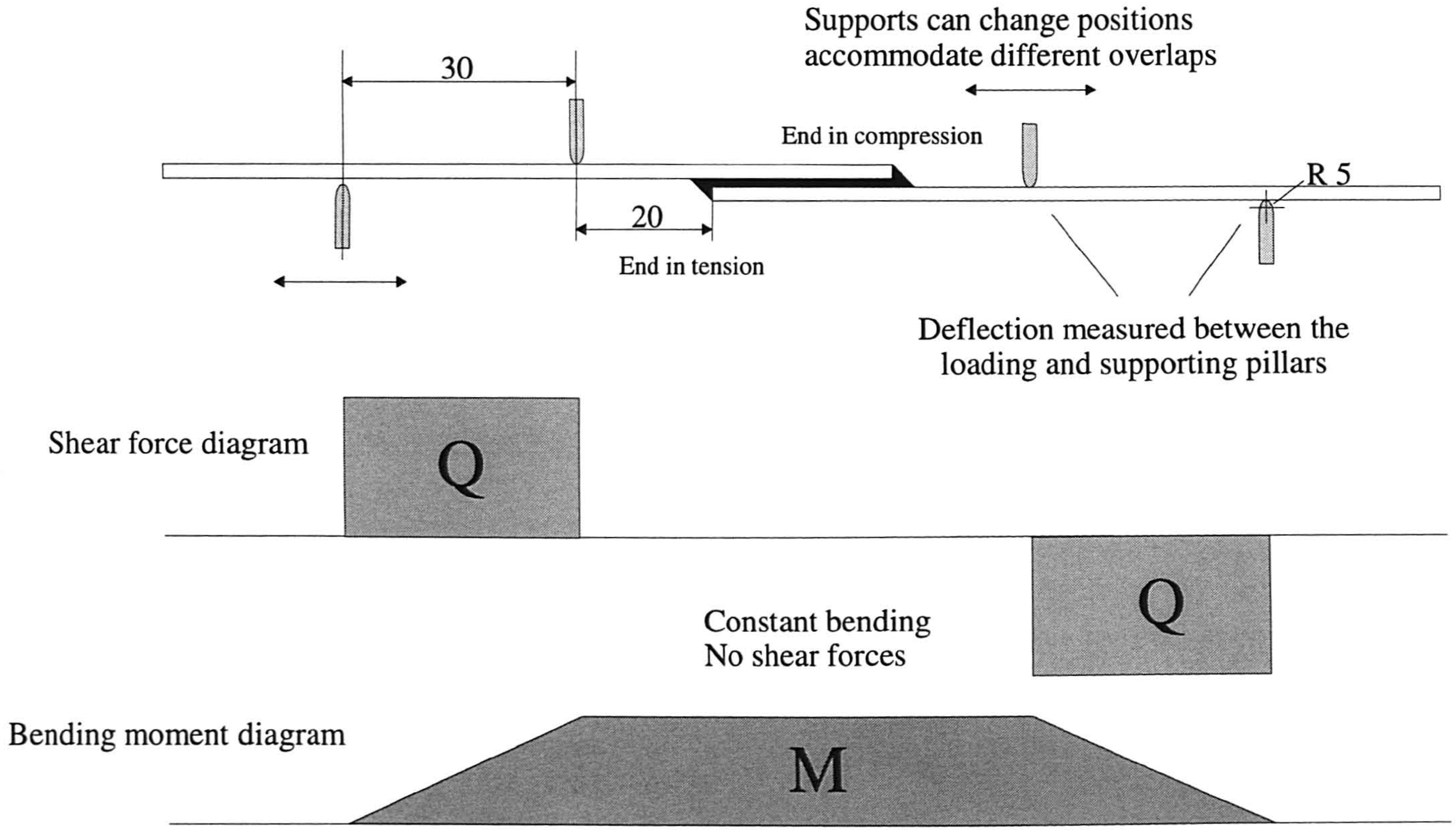

Figure 4.1 Four point bend rig test configuration. Dimensions in mm

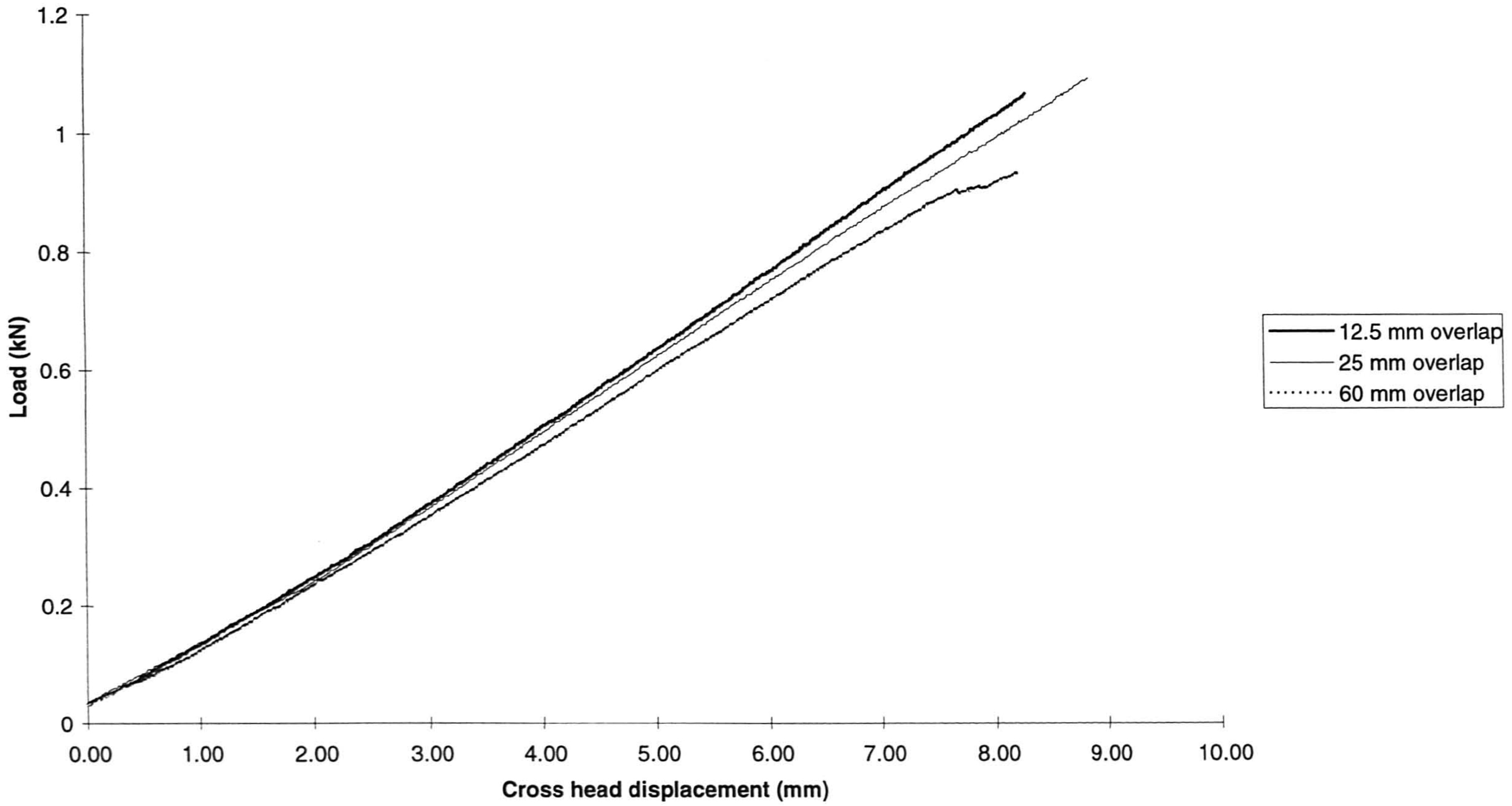

Figure 4.2 Load Displacement curves for hard steel SLJs with AV 119 adhesive and various overlaps under 4 point bending

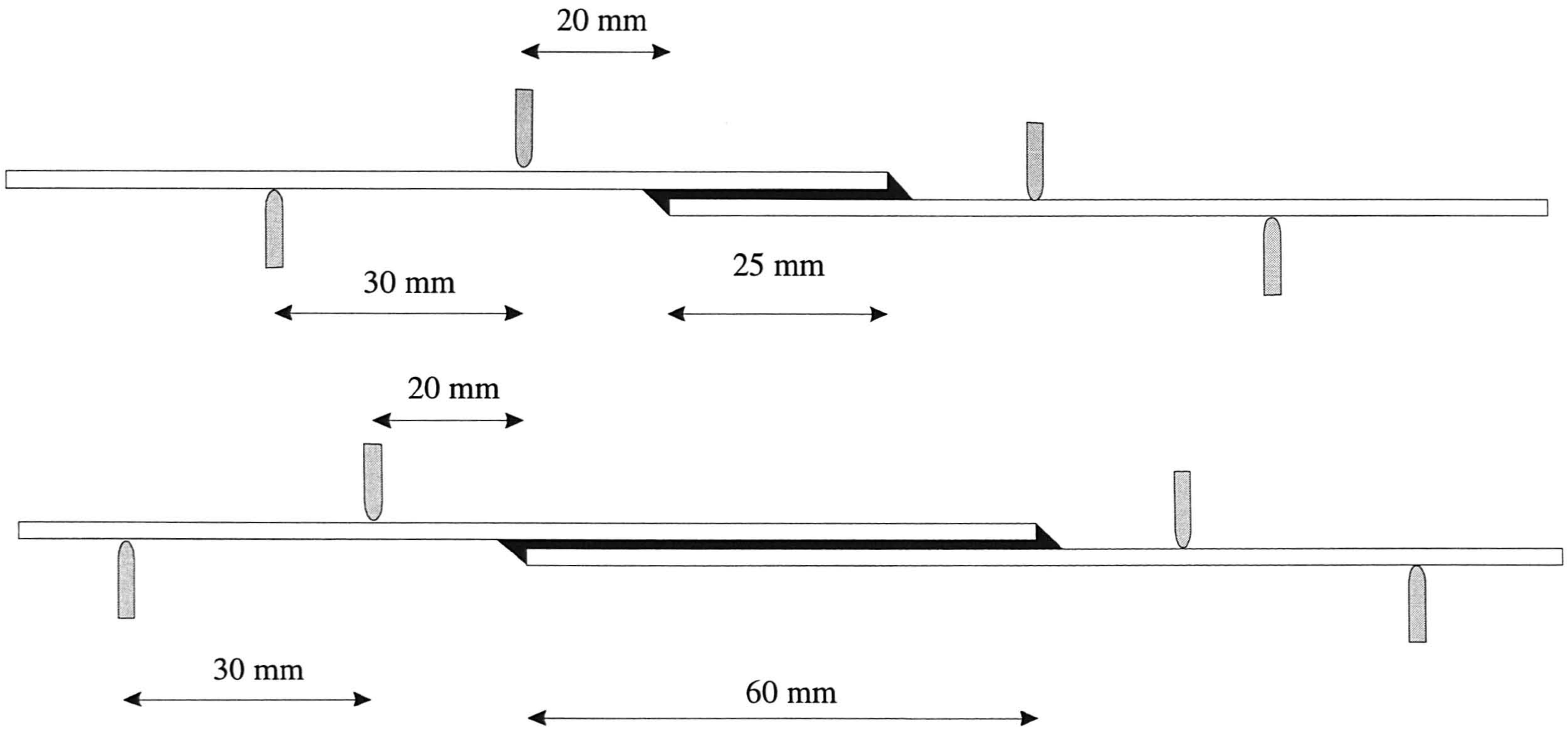

Figure 4.3 Loading configuration for joints with different overlap under four point bending

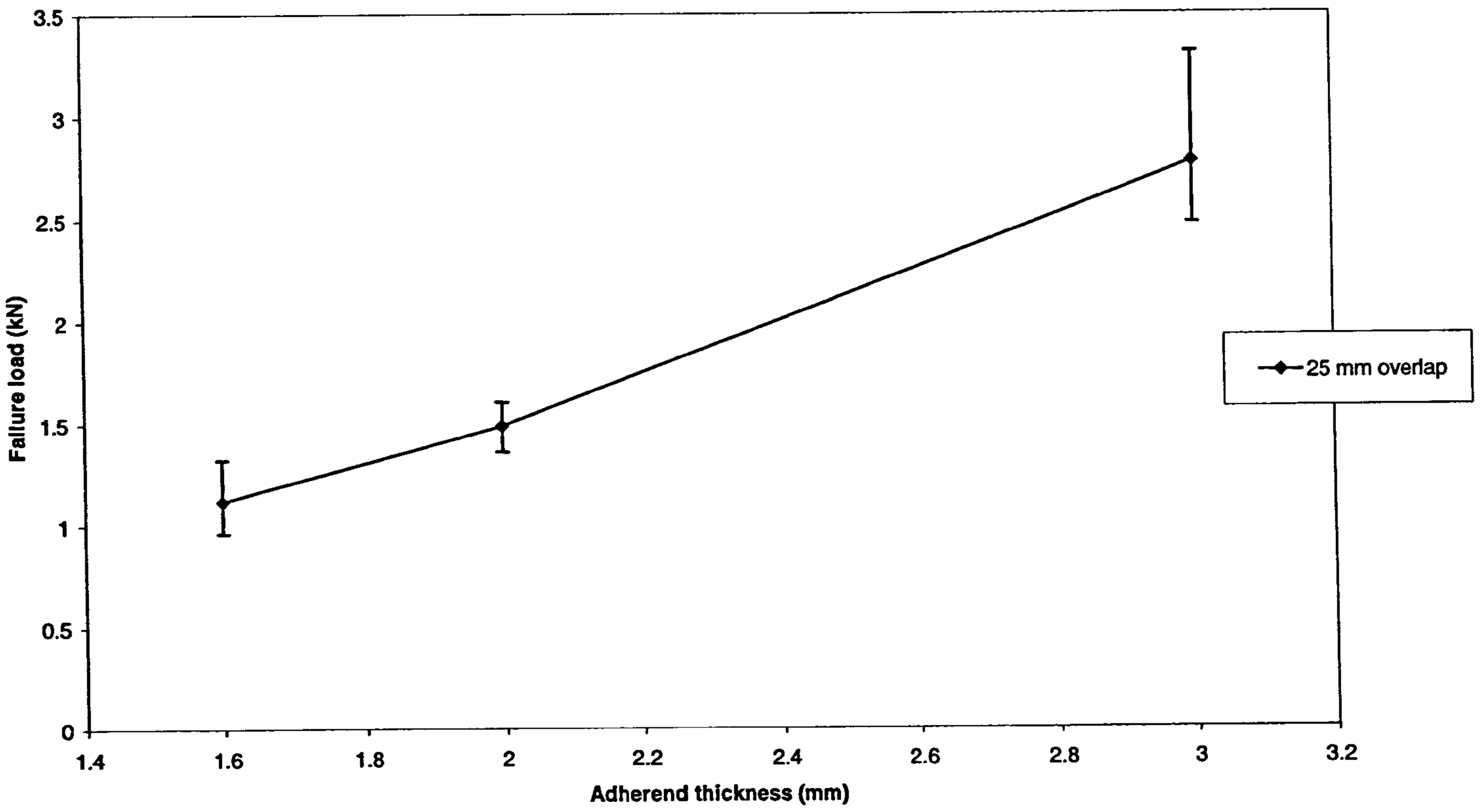

Figure 4.4 Failure load vs. adherend thickness for 25 mm overlap hard steel SLJs with AV 119 under four point bending

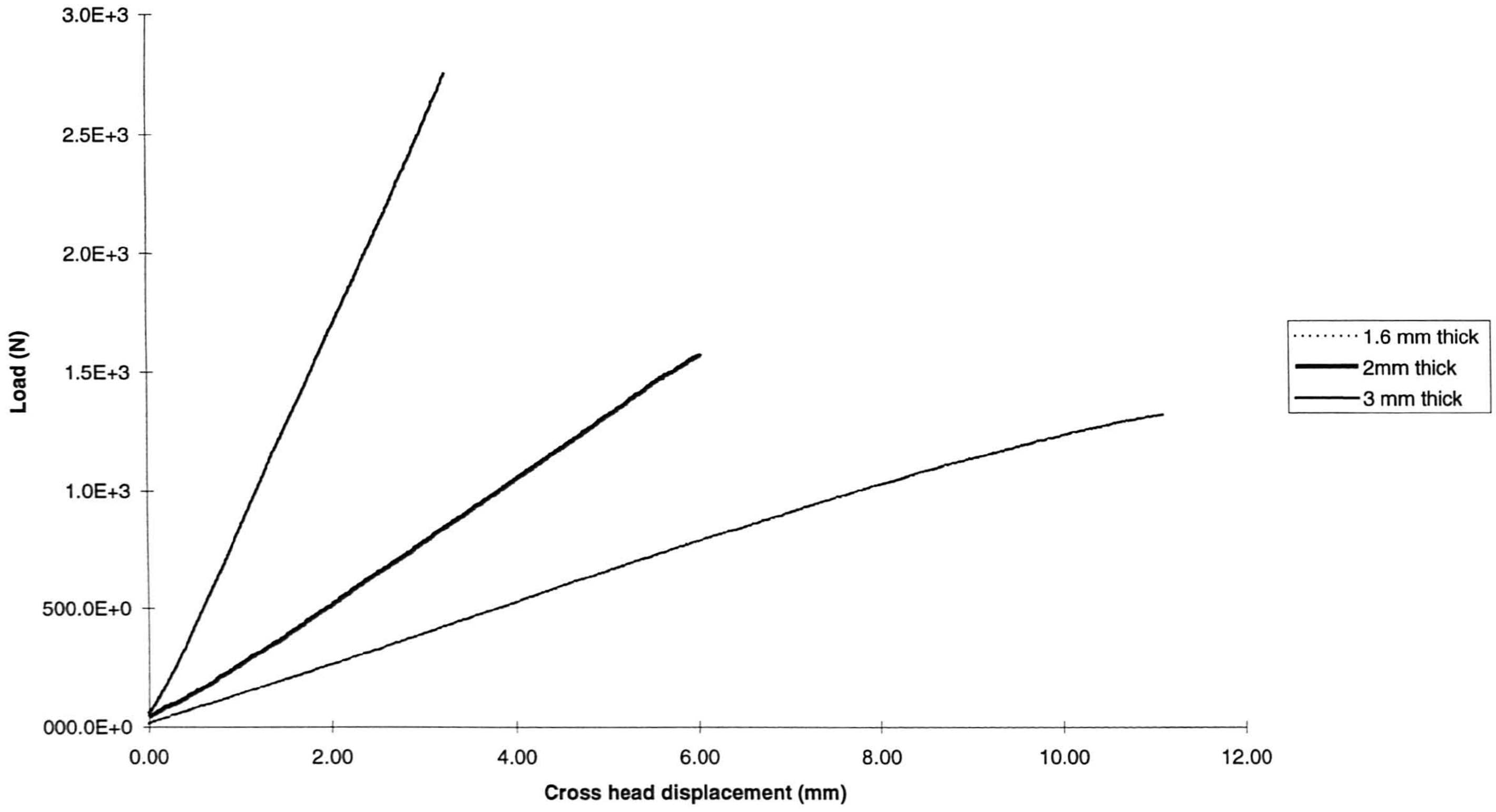

Figure 4.5 Load-Displacement curves for 25 mm overlap hard steel adherends, AV 119 adhesive for various adherend thicknesses under four point bending

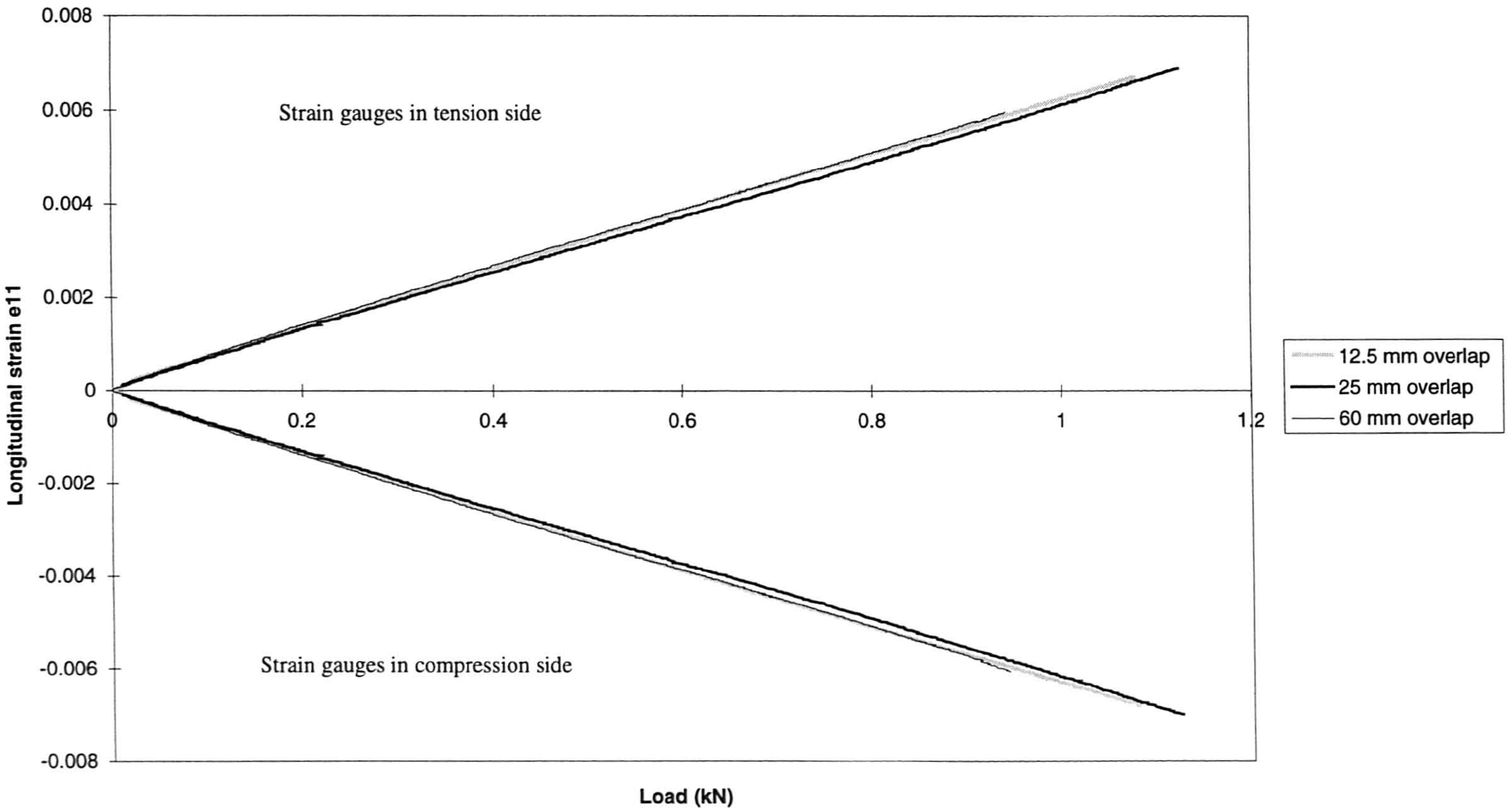

Figure 4.6 Longitudinal strain variation in the adherends for hard steel SLJs with AV 119 adhesive and various overlaps under 4 point bending

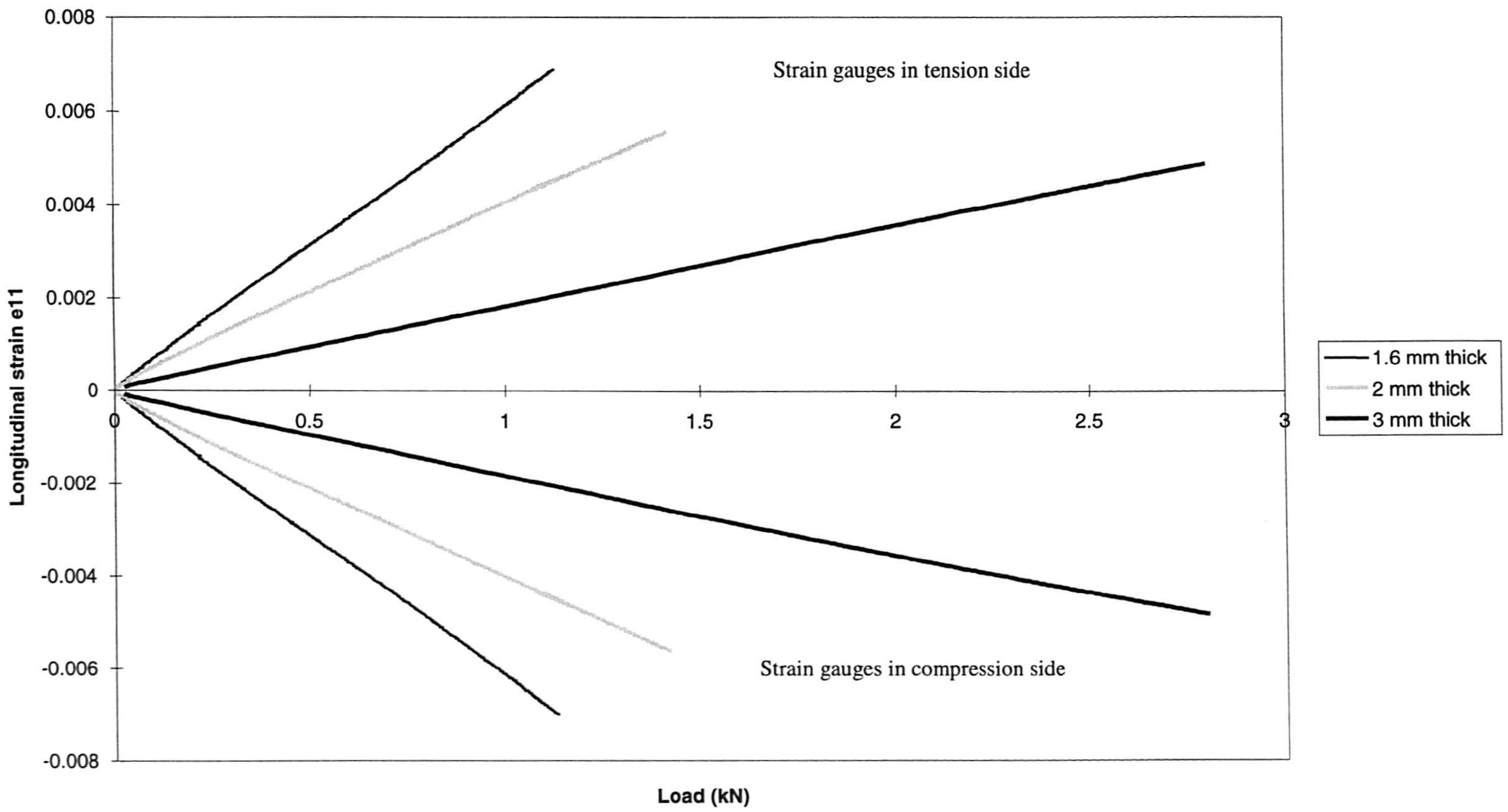

Figure 4.7 Longitudinal strain variation in the adherends for 25mm overlap, hard steel SLJs with AV 119 adhesive and various adherend thicknesses under 4 point bending

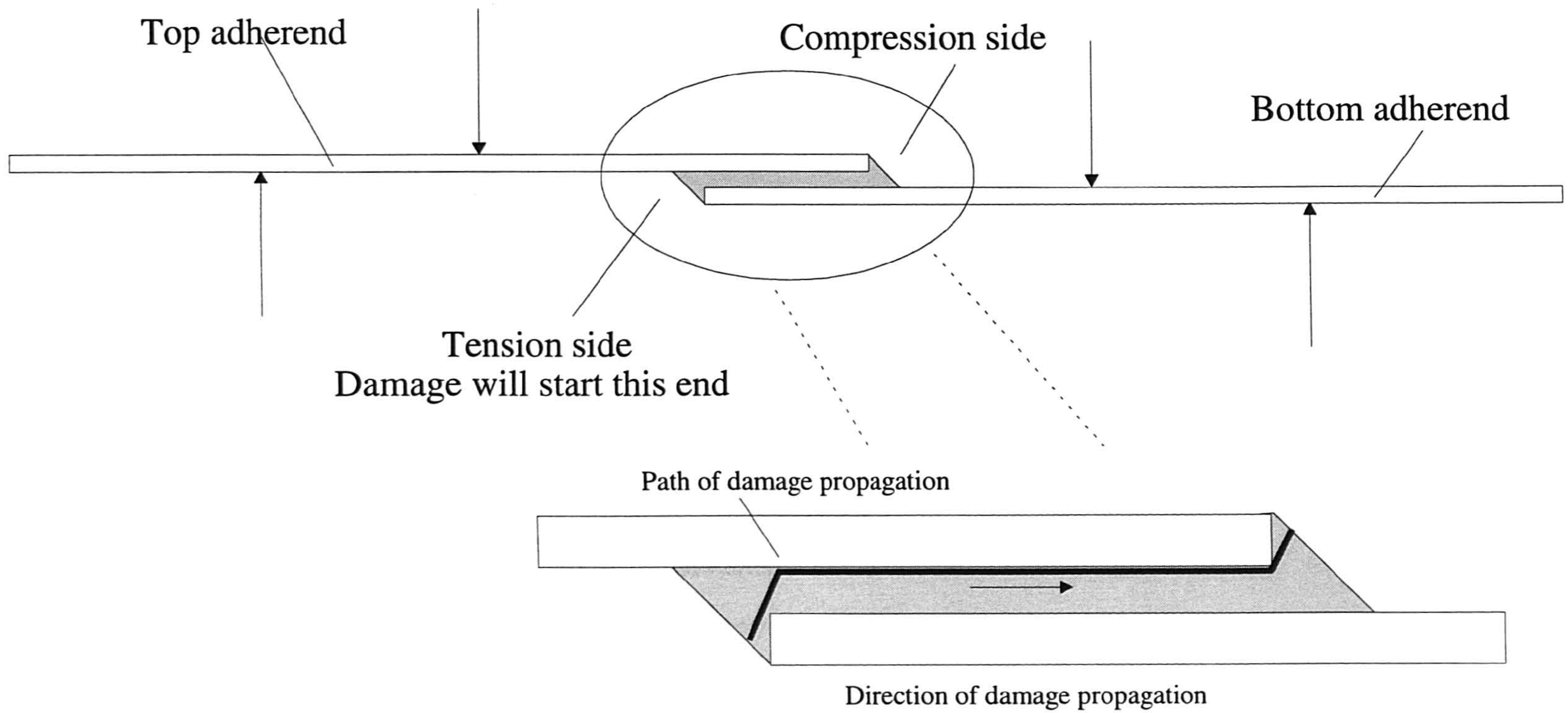

Figure 4.8 Failure mode for a 4 point bend test - asymmetric failure pattern

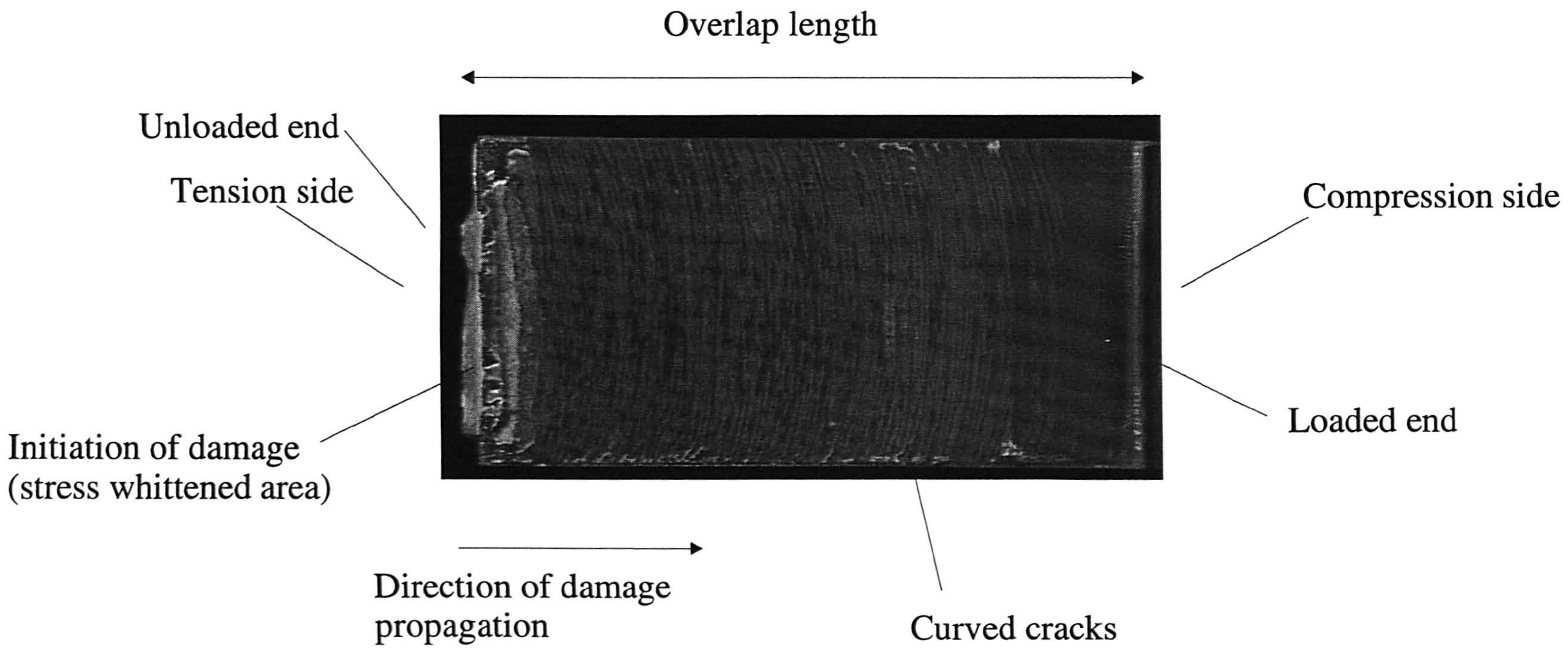

Figure 4.9 4 point bend test - 60 mm overlap - hard steel - AV 119 adhesive - failure pattern revealing curved cracks in the propagation of damage.

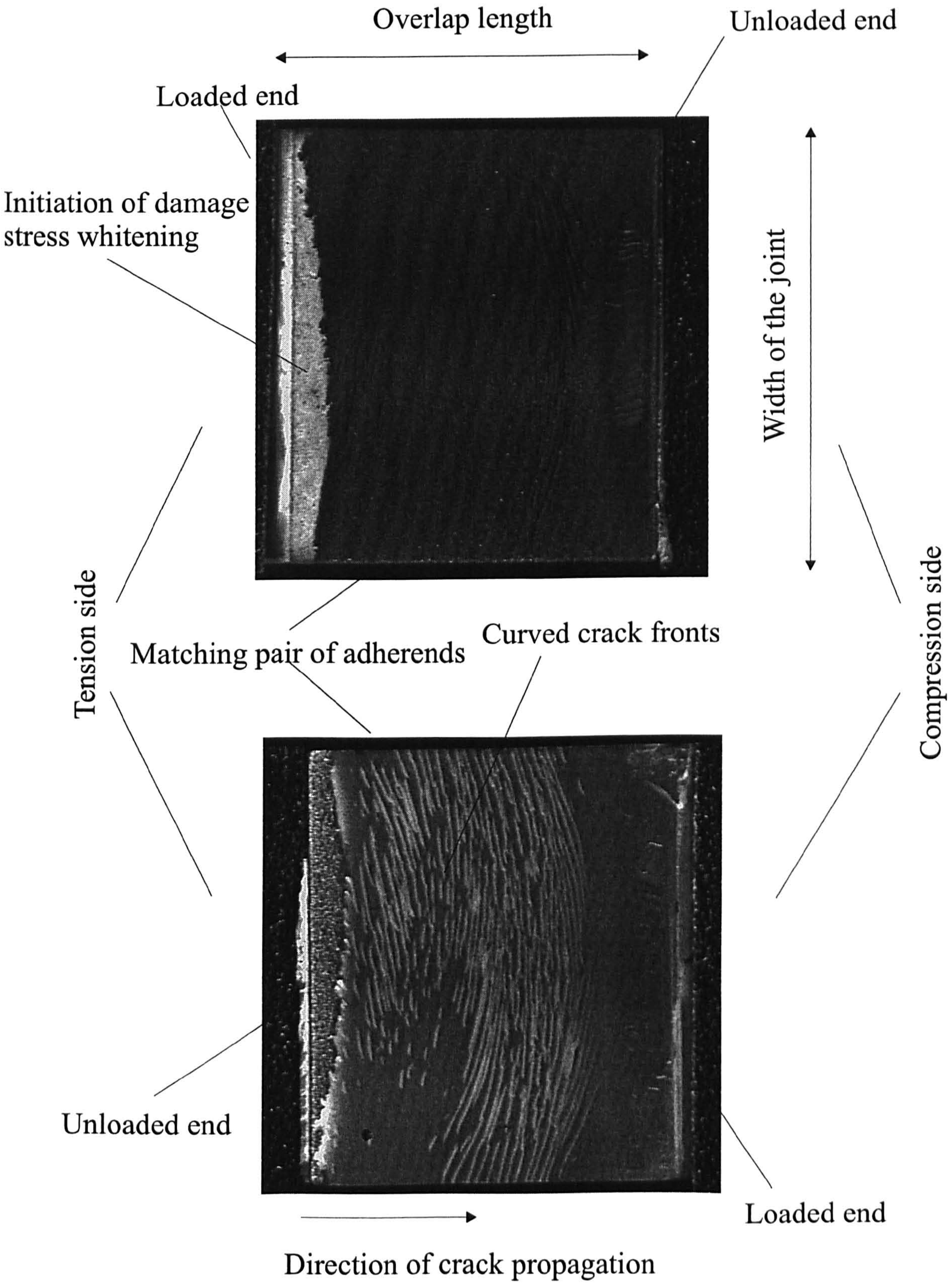

Figure 4.10 Failure pattern from a 4 point bend test - 25 mm overlap - hard steel - AV 119 adhesive - curved crack fronts due to anticlastic bending effect.

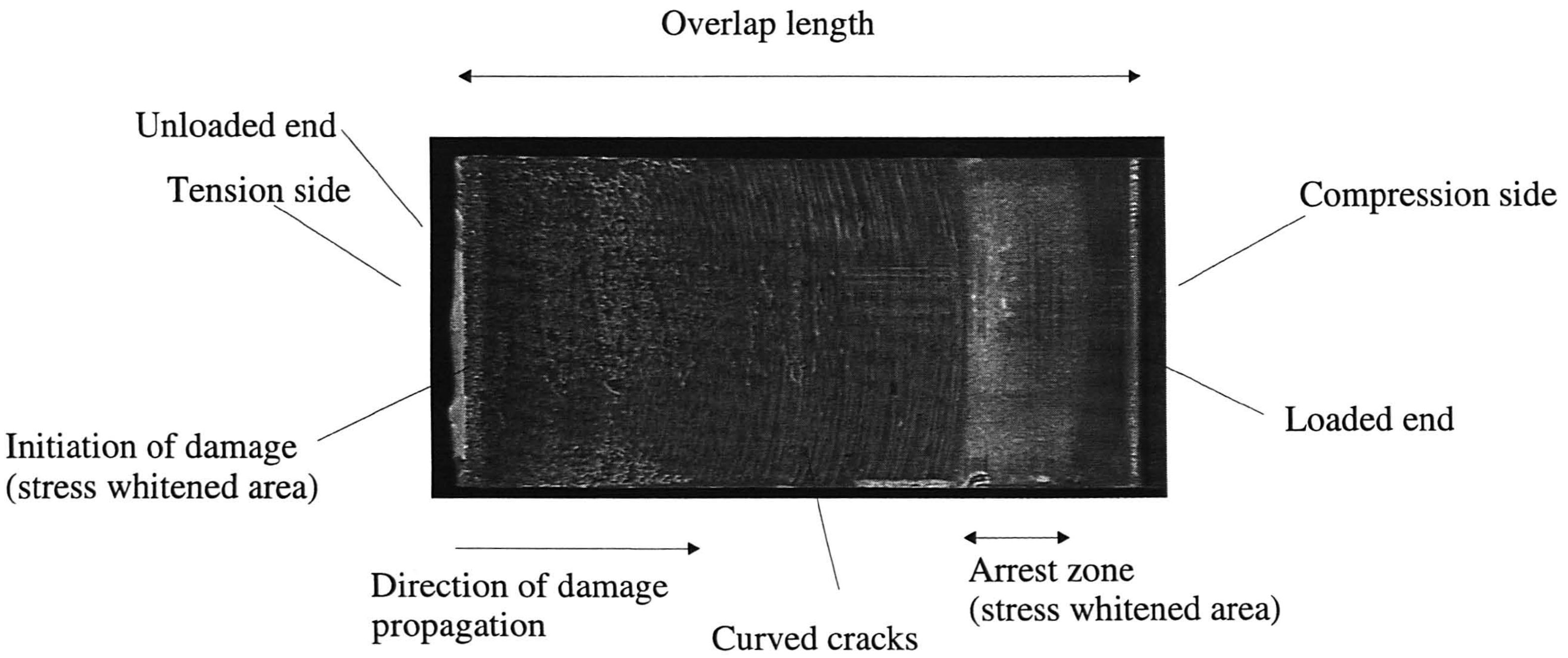

Figure 4.11 4 point bend test - 60 mm overlap - hard steel - AV 119 adhesive - failure pattern revealing curved cracks and arrest lines in the propagation of damage.

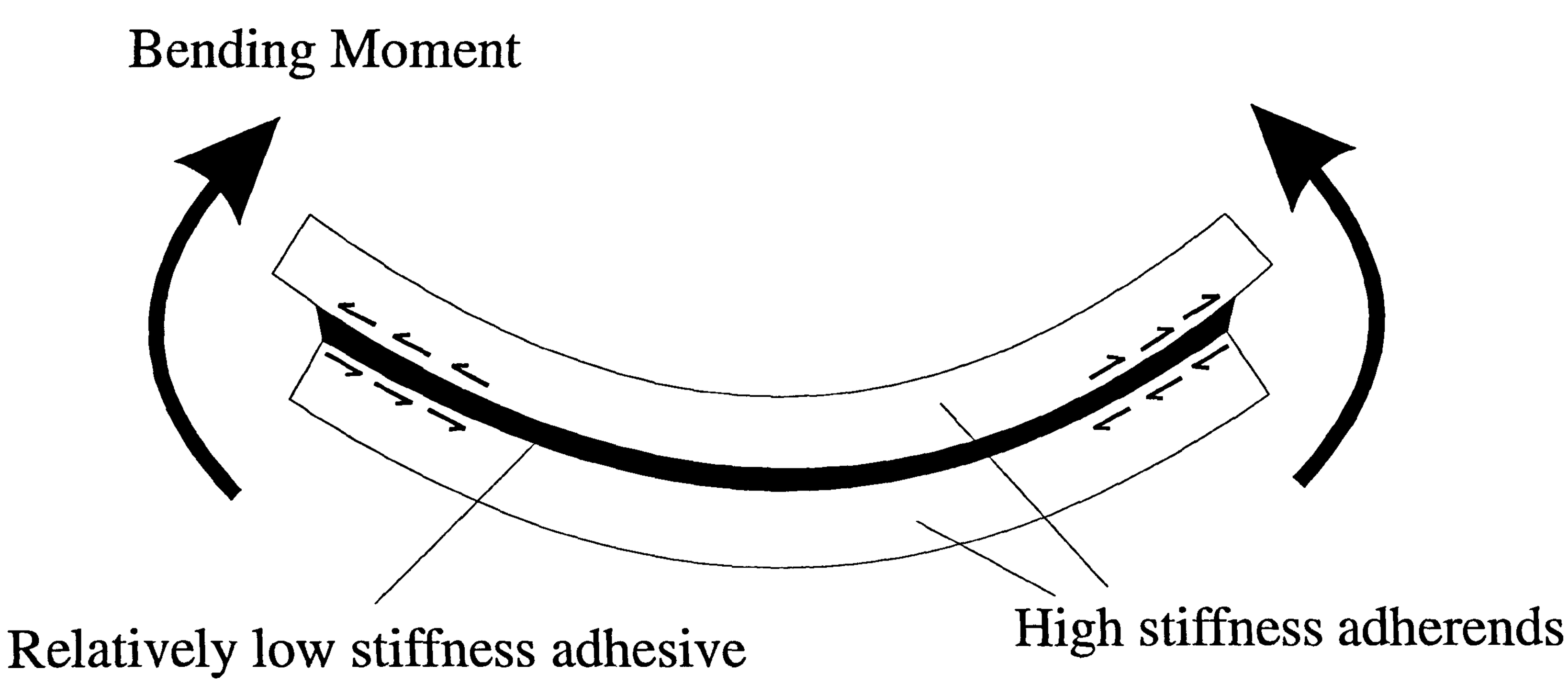

Figure 4.12 Shear stresses in the adhesive layer due to large stiffness differences between adherends and adhesive and large deflections experienced in the 4 point bend tests

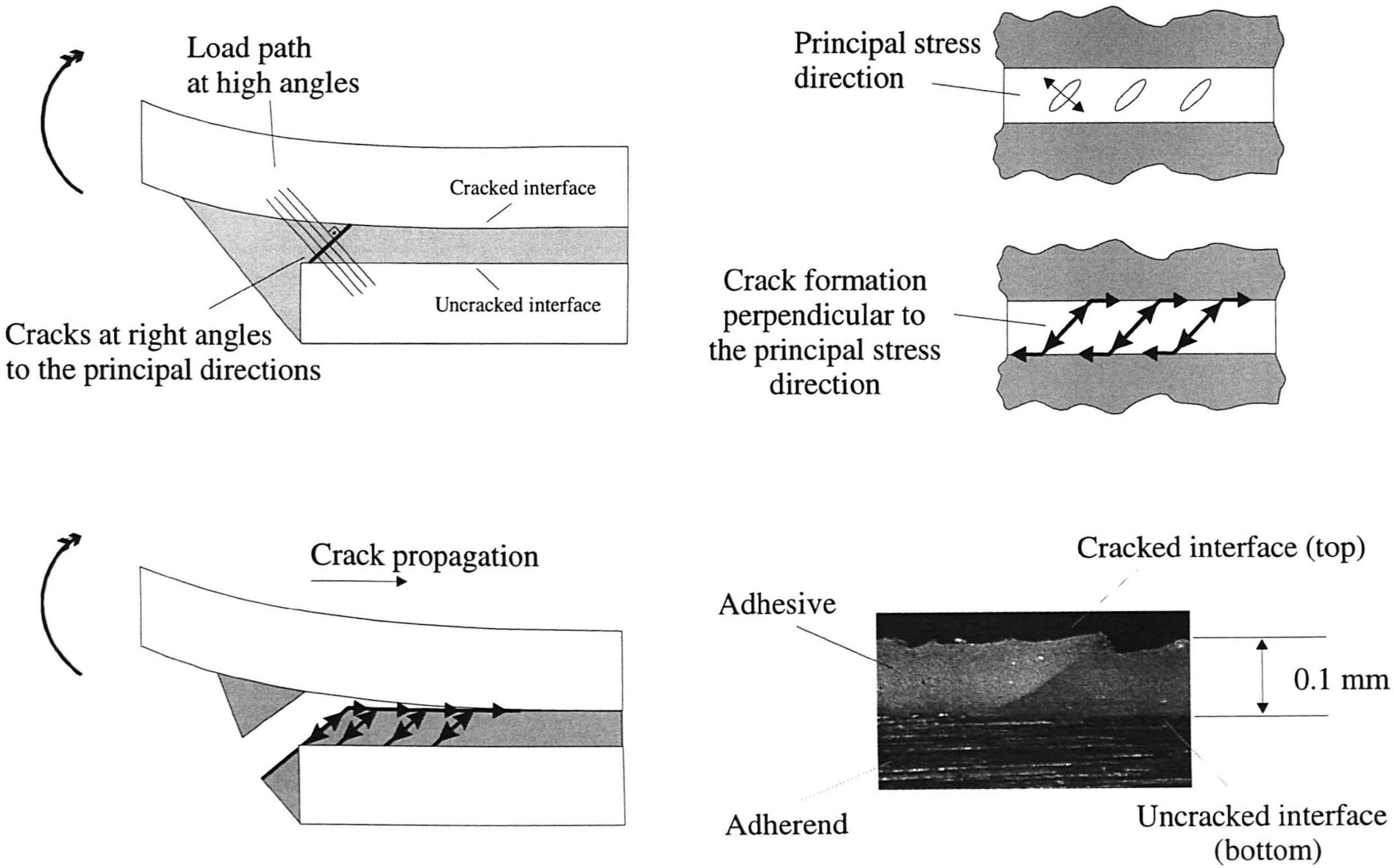

Figure 4.13 Failure mechanism in a four point bend test - hard Steel and AV 119 adhesive

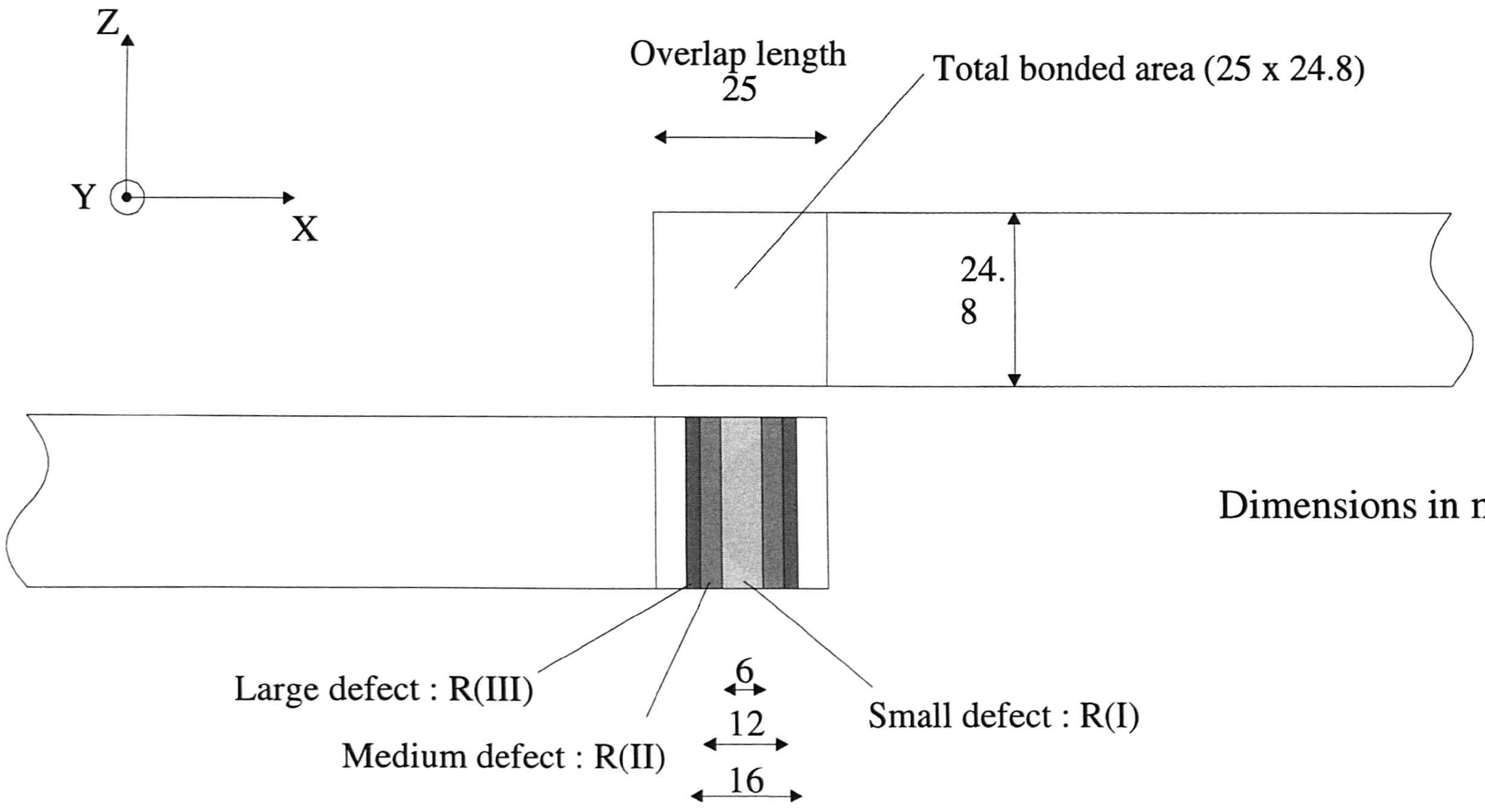

Figure 5.1 Sizes and placement of rectangular defects on single lap joints

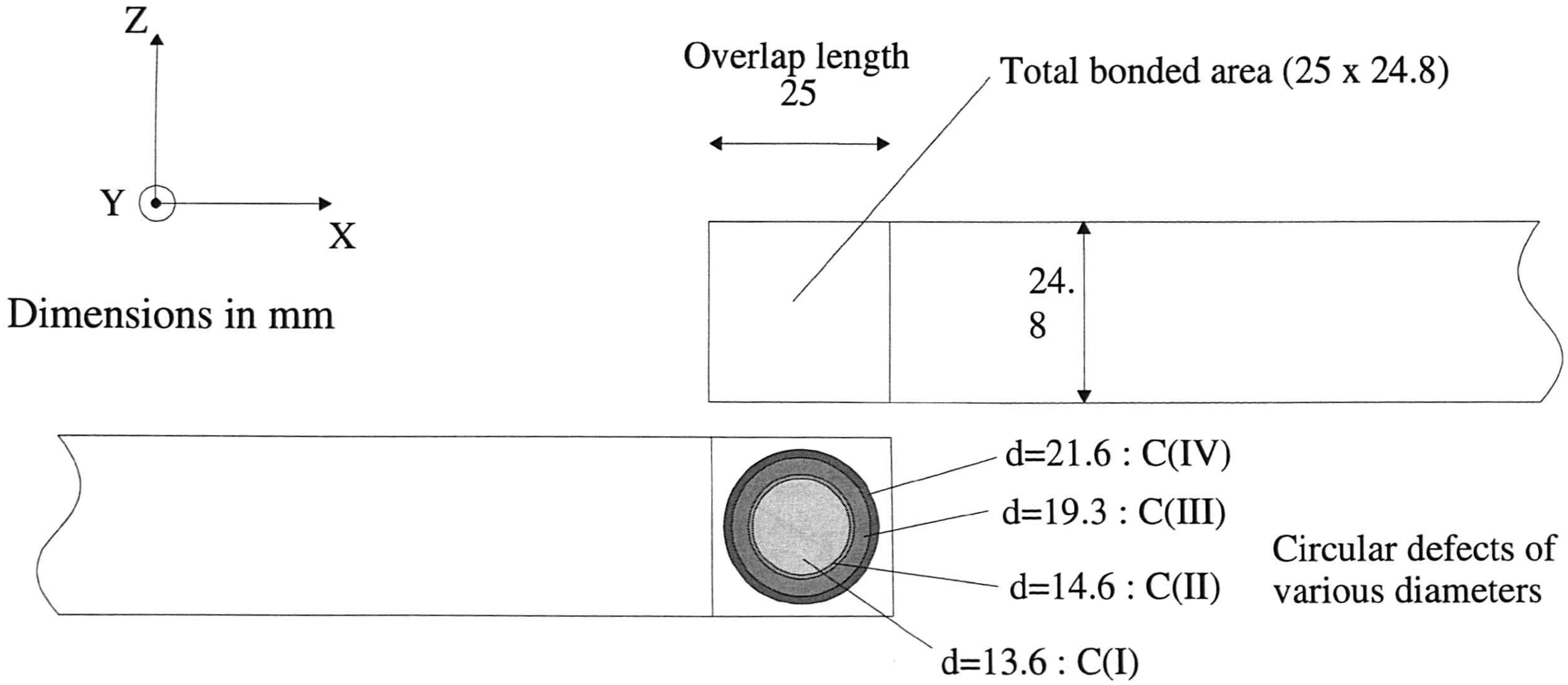

Figure 5.2 Sizes and placement of circular defects on single lap joints

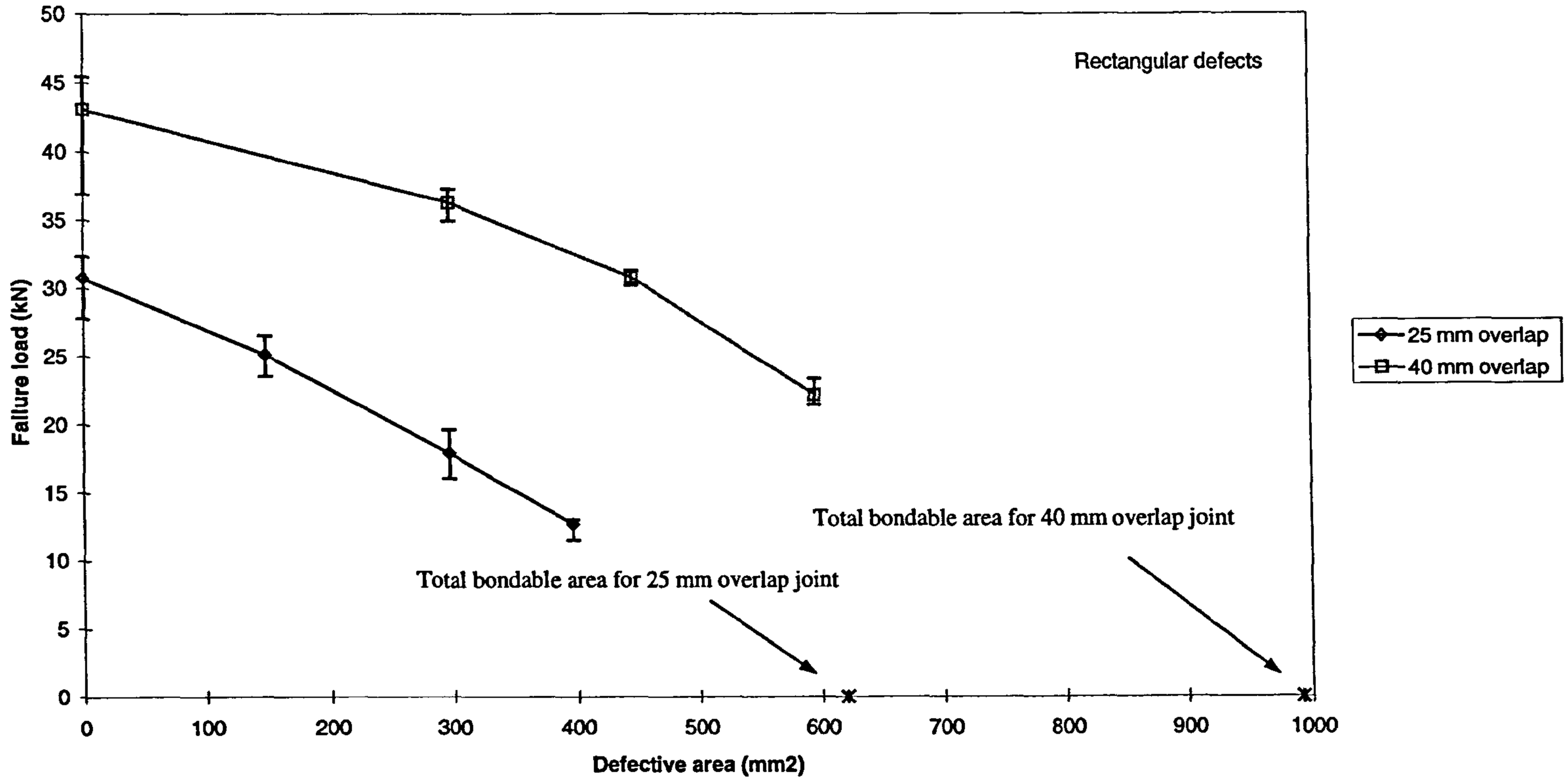

Figure 5.3 Variation of strength vs. defect size for 25 mm and 40 mm hard steel SLJs with AV 119 adhesive and rectangular defects under tensile loading

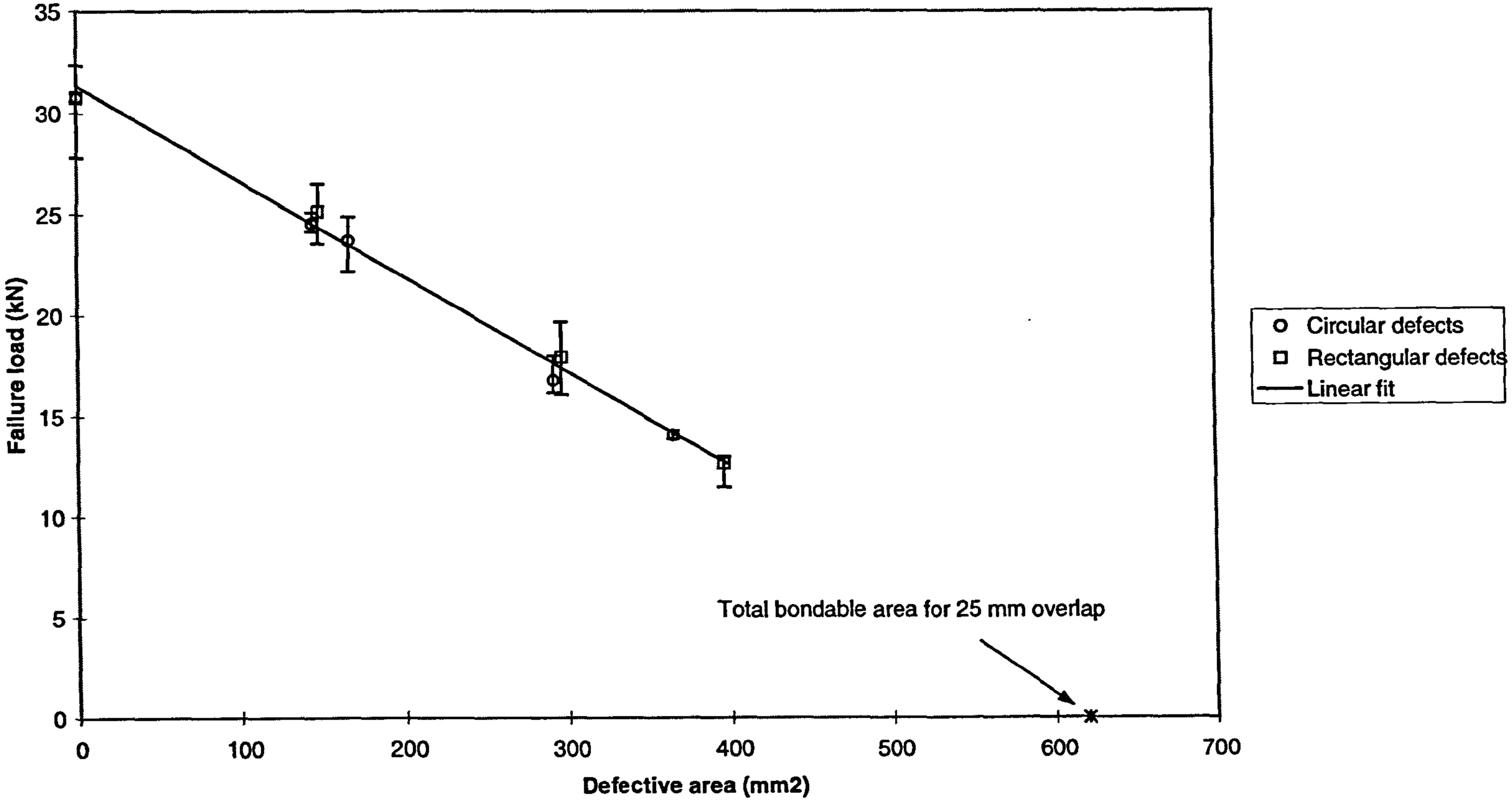

Figure 5.4 Comparison of strength vs. defect size for 25mm overlap hard steel SLJs with AV 119 adhesive and Rectangular or Circular defects under tensile loading

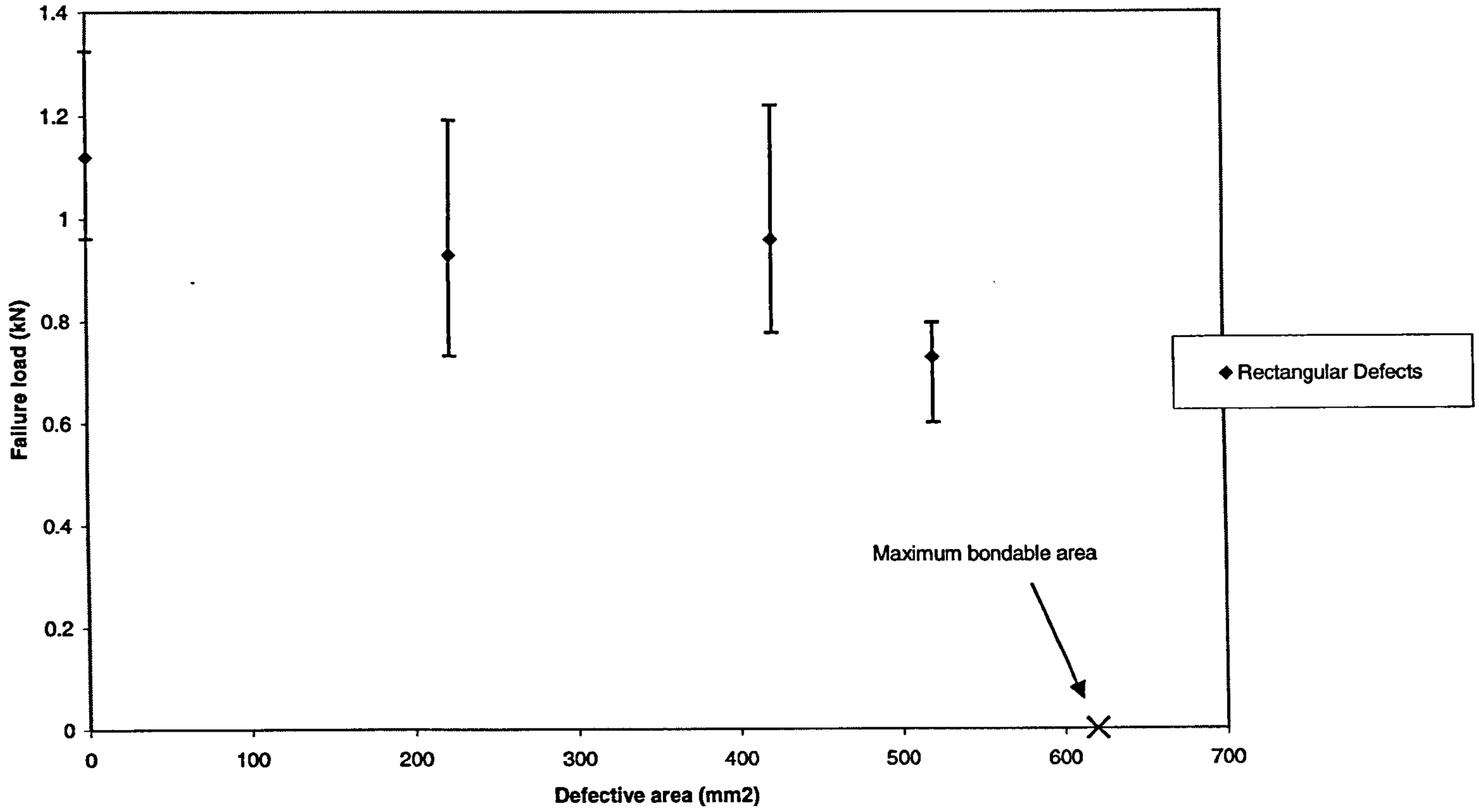

Figure 5.5 Variation of strength vs. defect size for 25 mm overlap hard steel SLJs with AV 119 adhesive and rectangular defects under 4 point bending

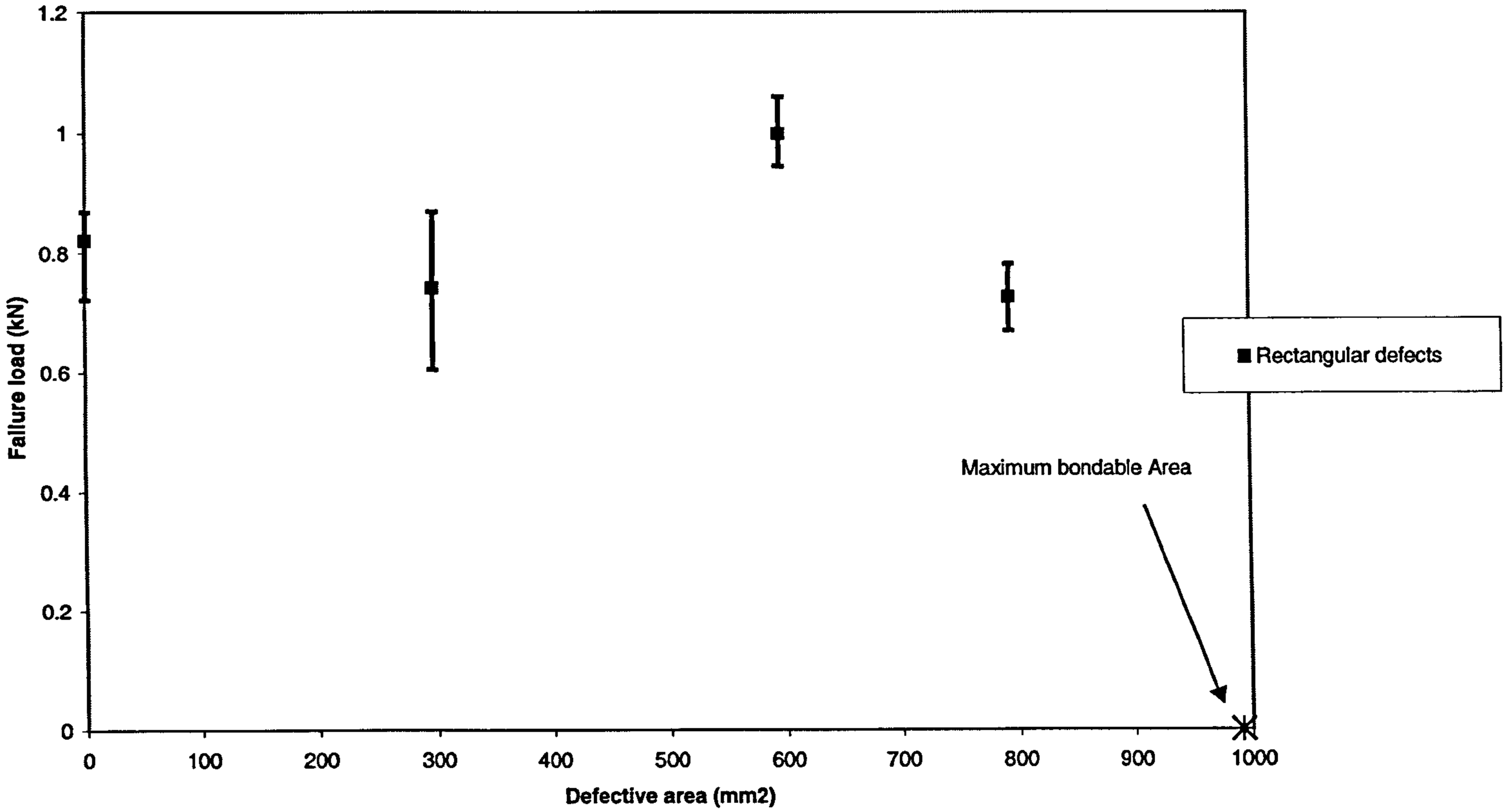

Figure 5.6 Variation of strength vs. defect size for 40 mm overlap hard steel SLJs with AV 119 adhesive and rectangular defects under 4 point bending

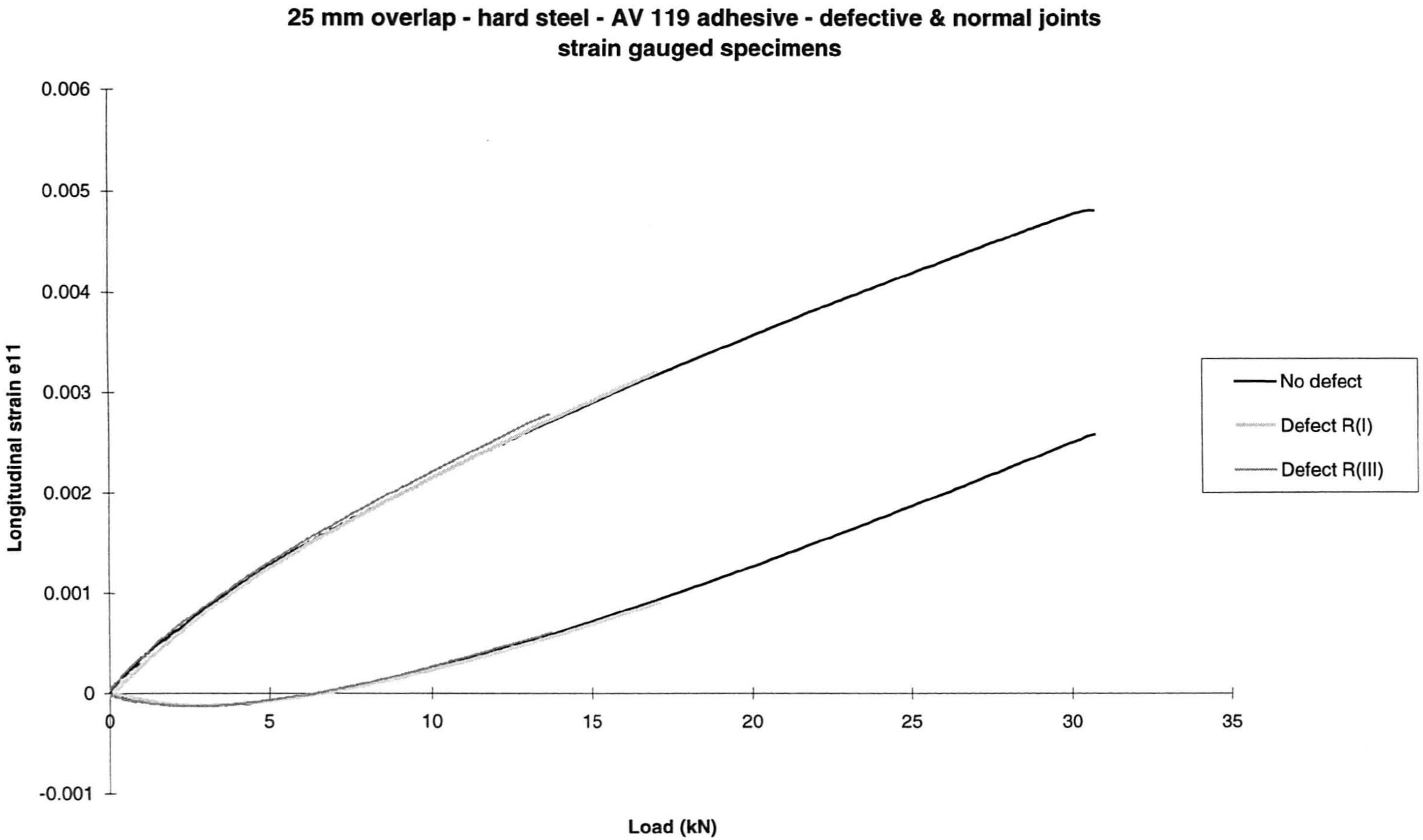

Figure 5.7 Comparison of longitudinal strain in the adherends for 25 mm overlap hard steel SLJs with AV 119 adhesive and various defect sizes

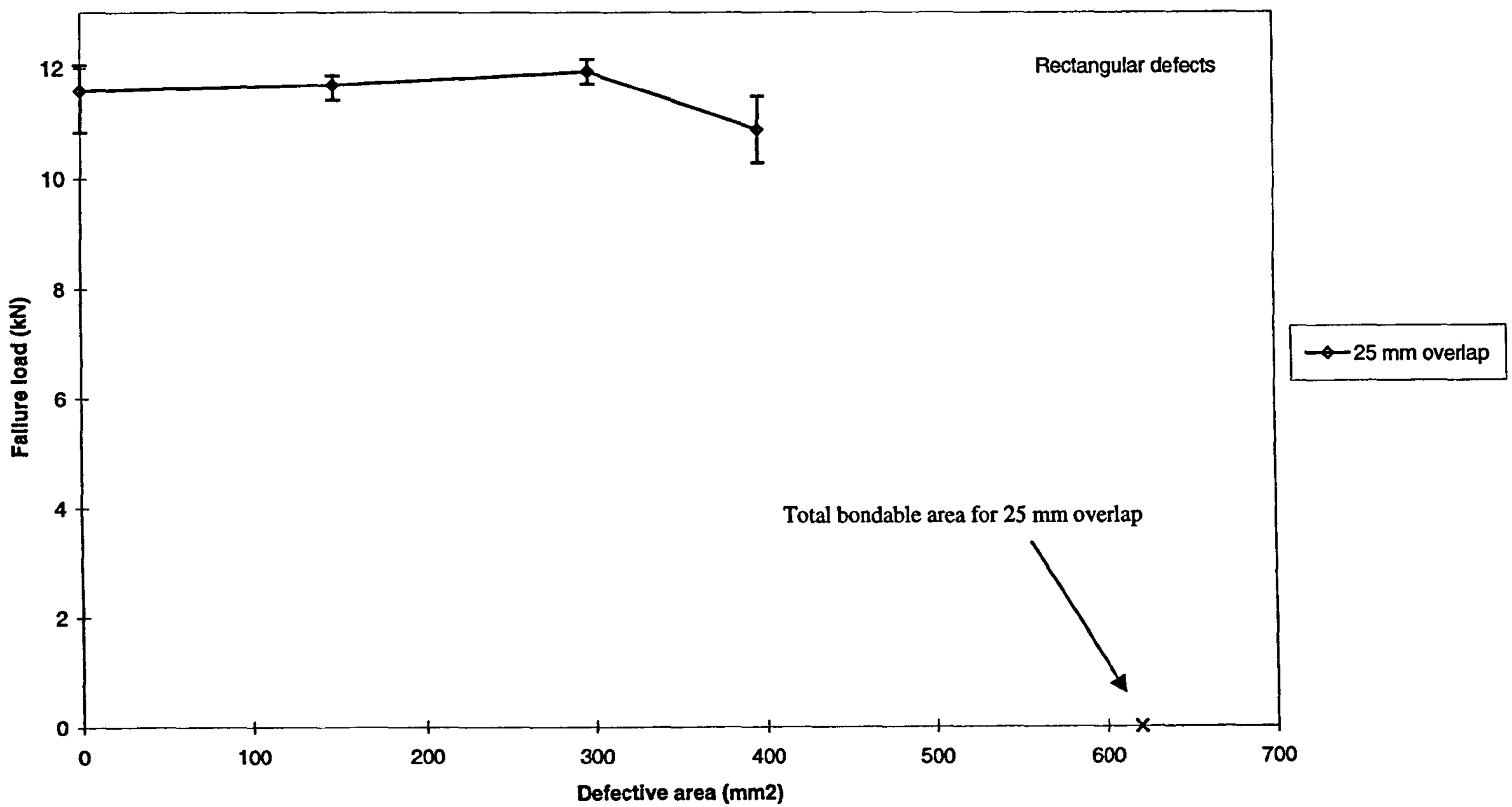

Figure 5.8 Variation of strength vs. defect size for 25 mm overlap mild steel SLJs with AV 119 adhesive and rectangular defects under tensile loading

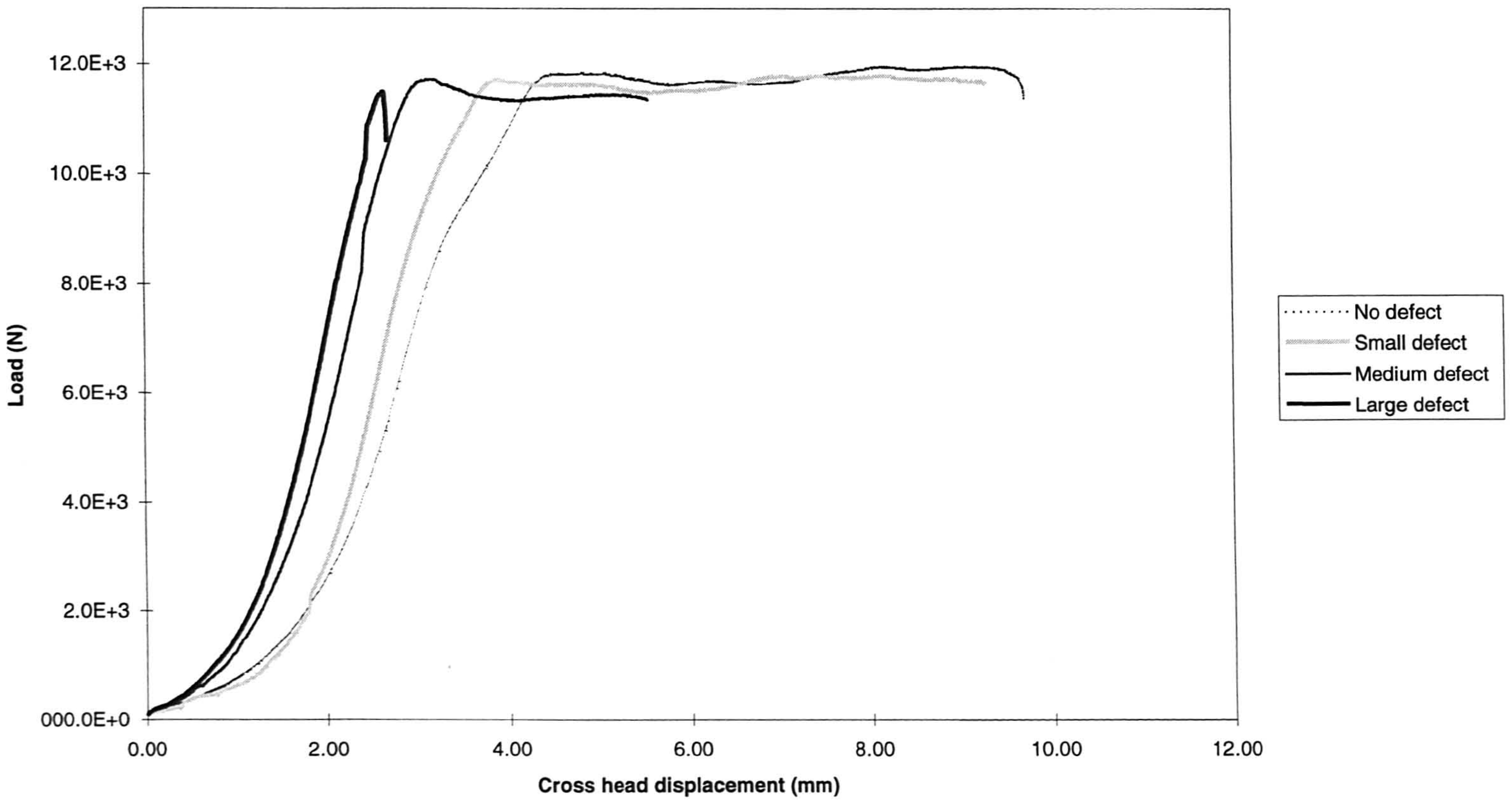

Figure 5.9 Load - displacement curves for 25 mm overlap mild steel SLJs with AV 119 adhesive and various defect sizes under tensile loading

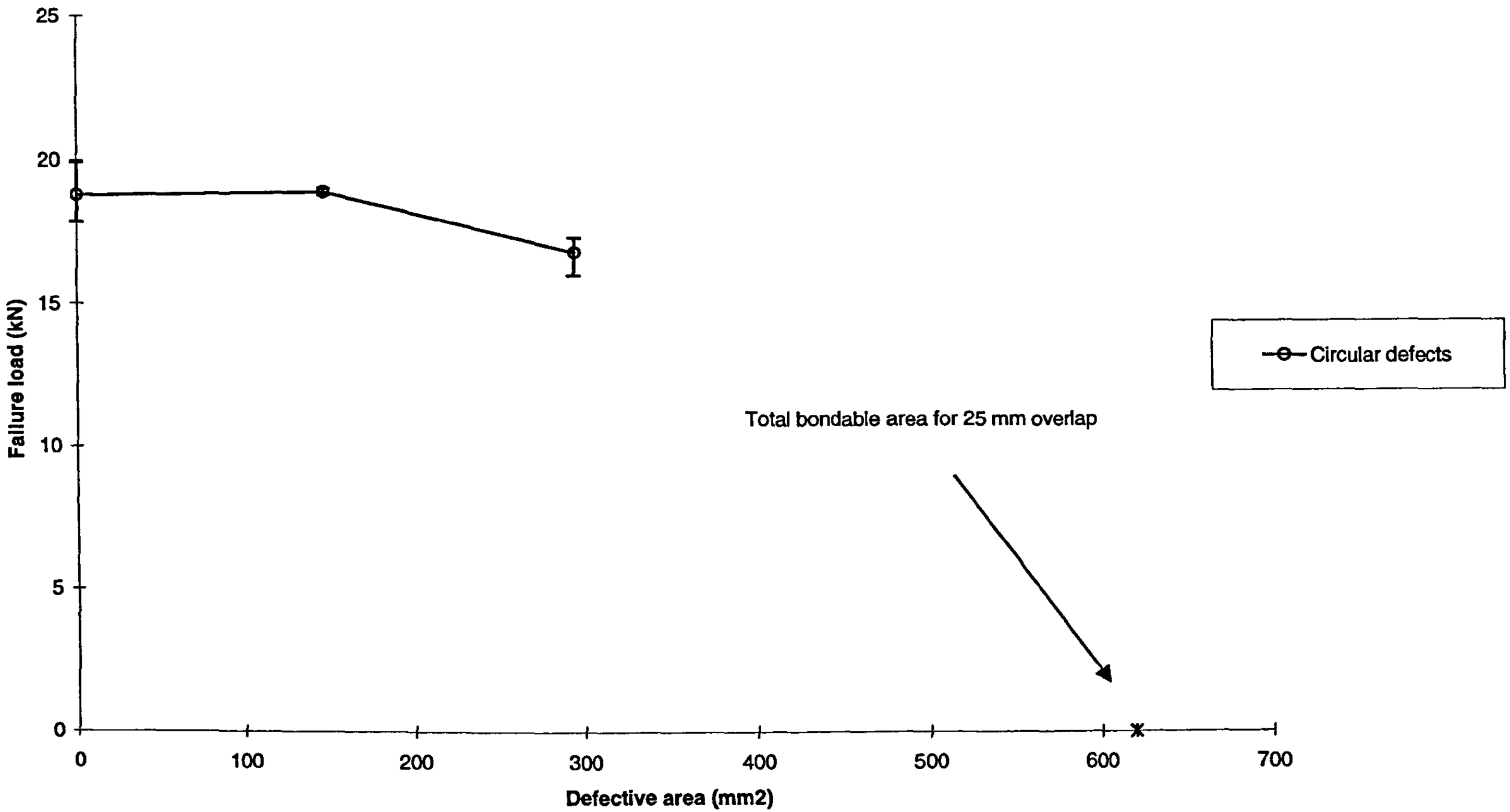

Figure 5.10 Variation of strength vs. defect size for 25 mm overlap gauge steel SLJs with AV 119 adhesive and circular defects under tensile loading

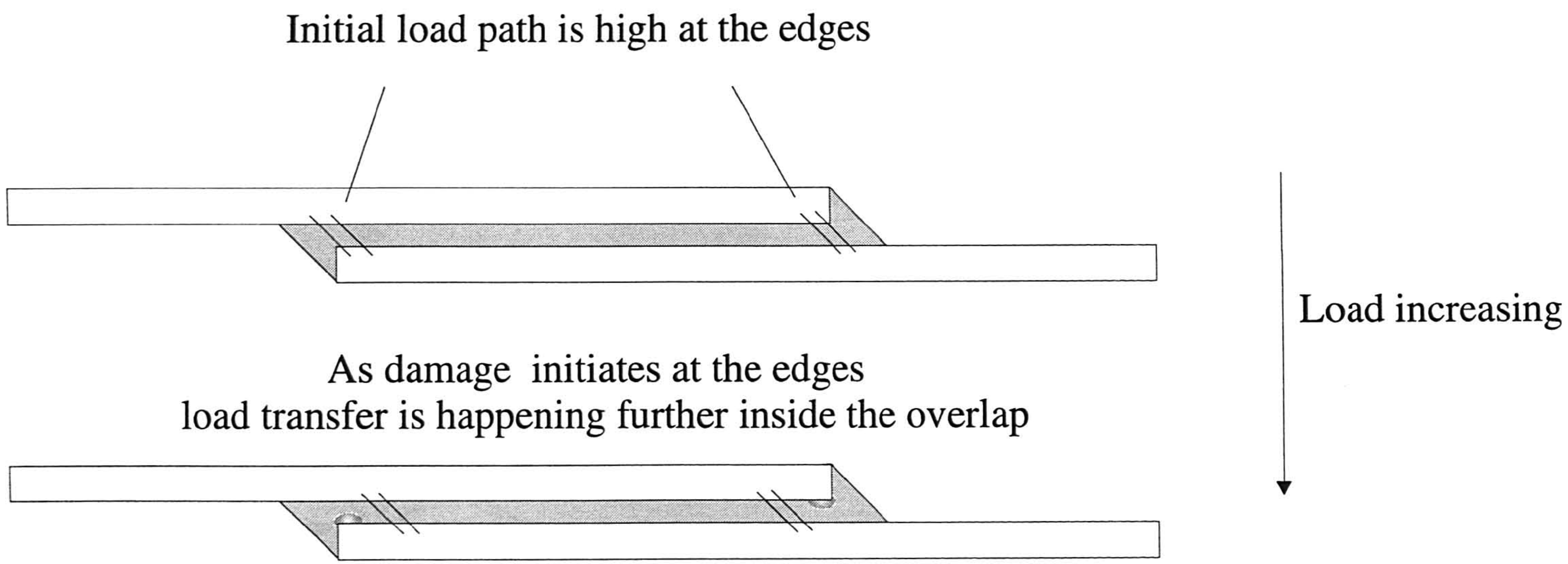

Figure 5.11 Failure process in the hard steel configuration

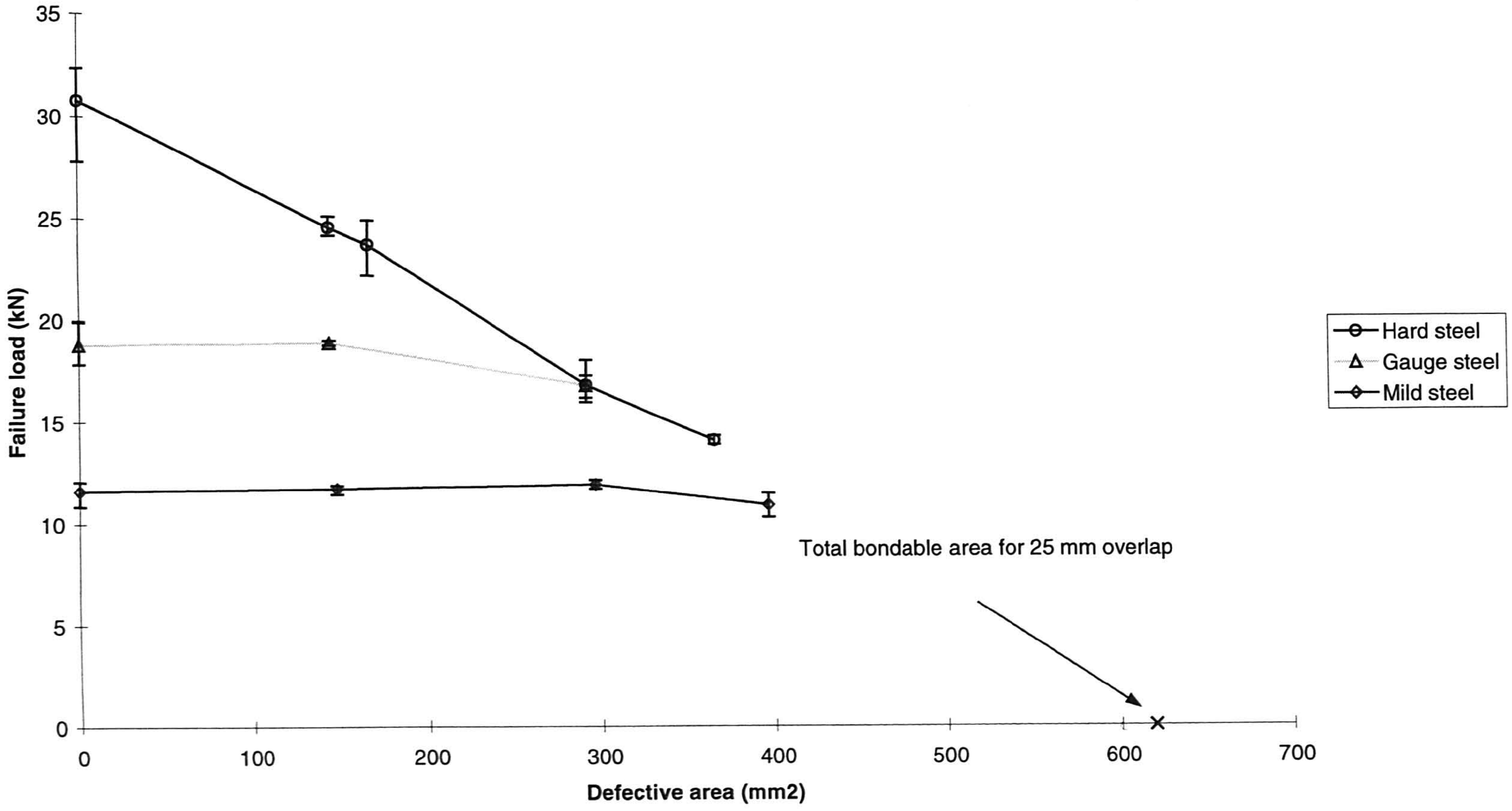

Figure 5.12 Variation of strength vs. defect size for SLJs with AV 119 adhesive and rectangular defects under tensile loading

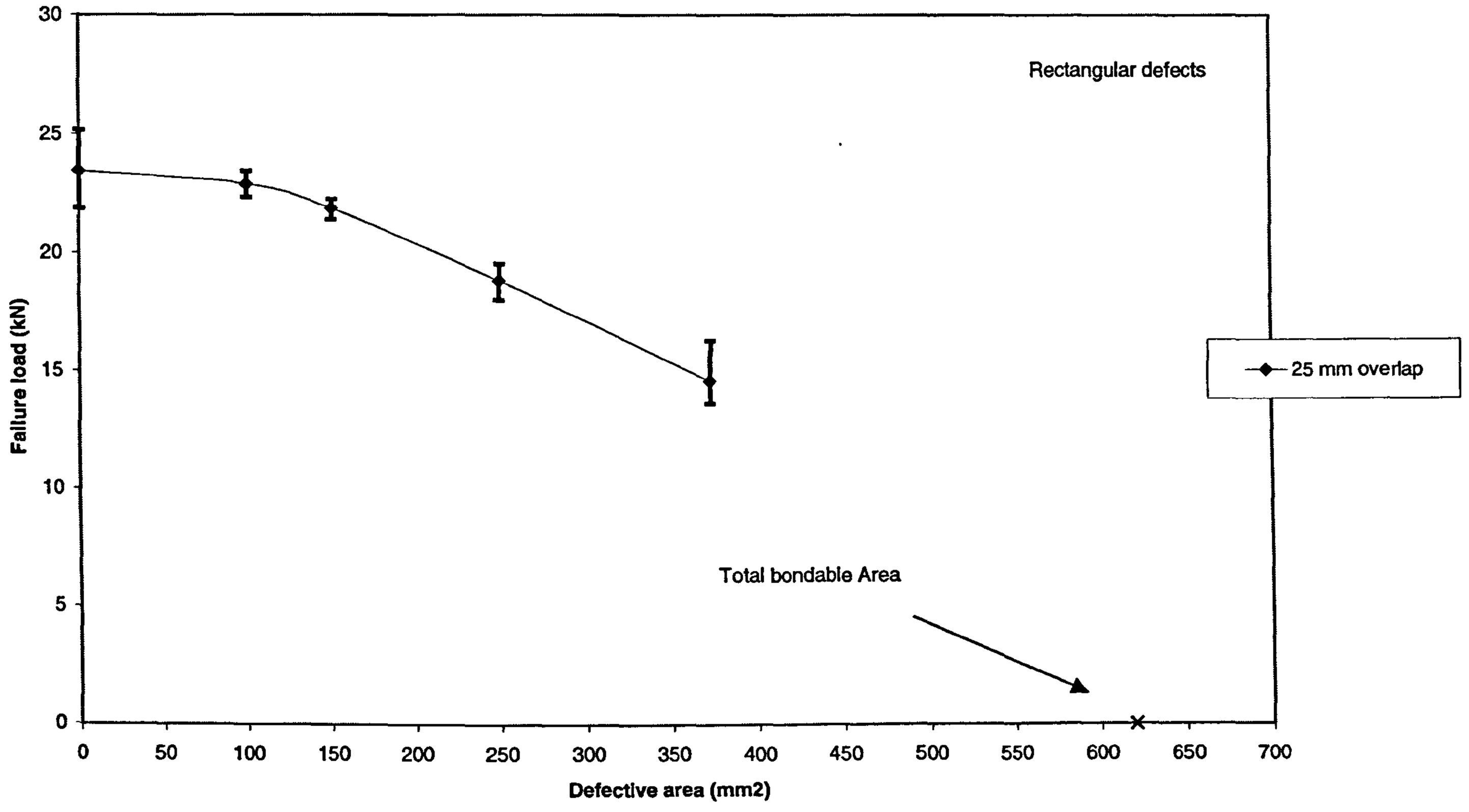

Figure 5.13 Variation of strength vs. defect size for 25 mm overlap hard steel SLJs with ESP 110 adhesive and rectangular defects under tensile loading

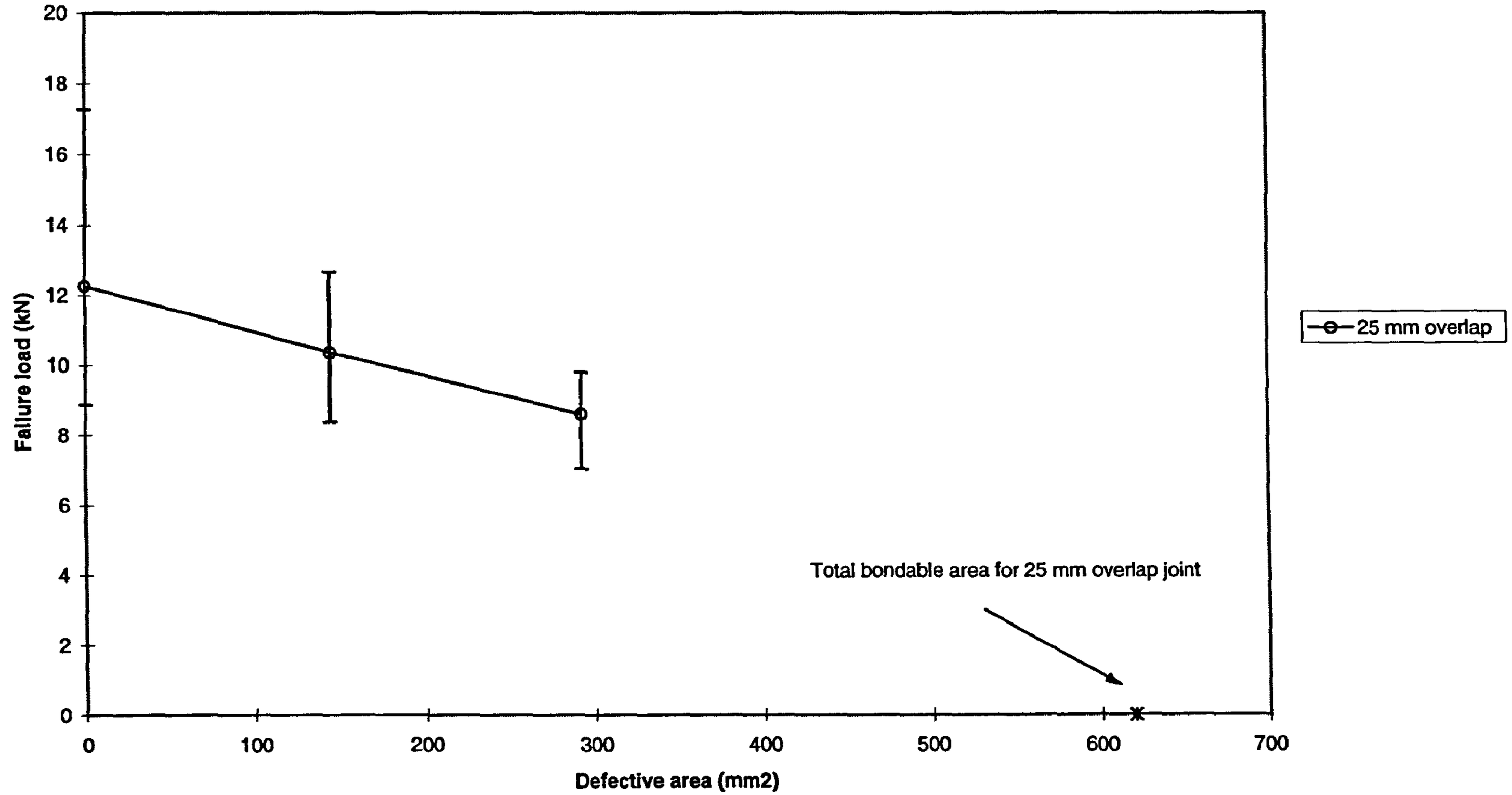

Figure 5.14 Variation of strength vs. defect size for 25mm overlap hard steel SLJs with MY753 adhesive and circular defects under tensile loading

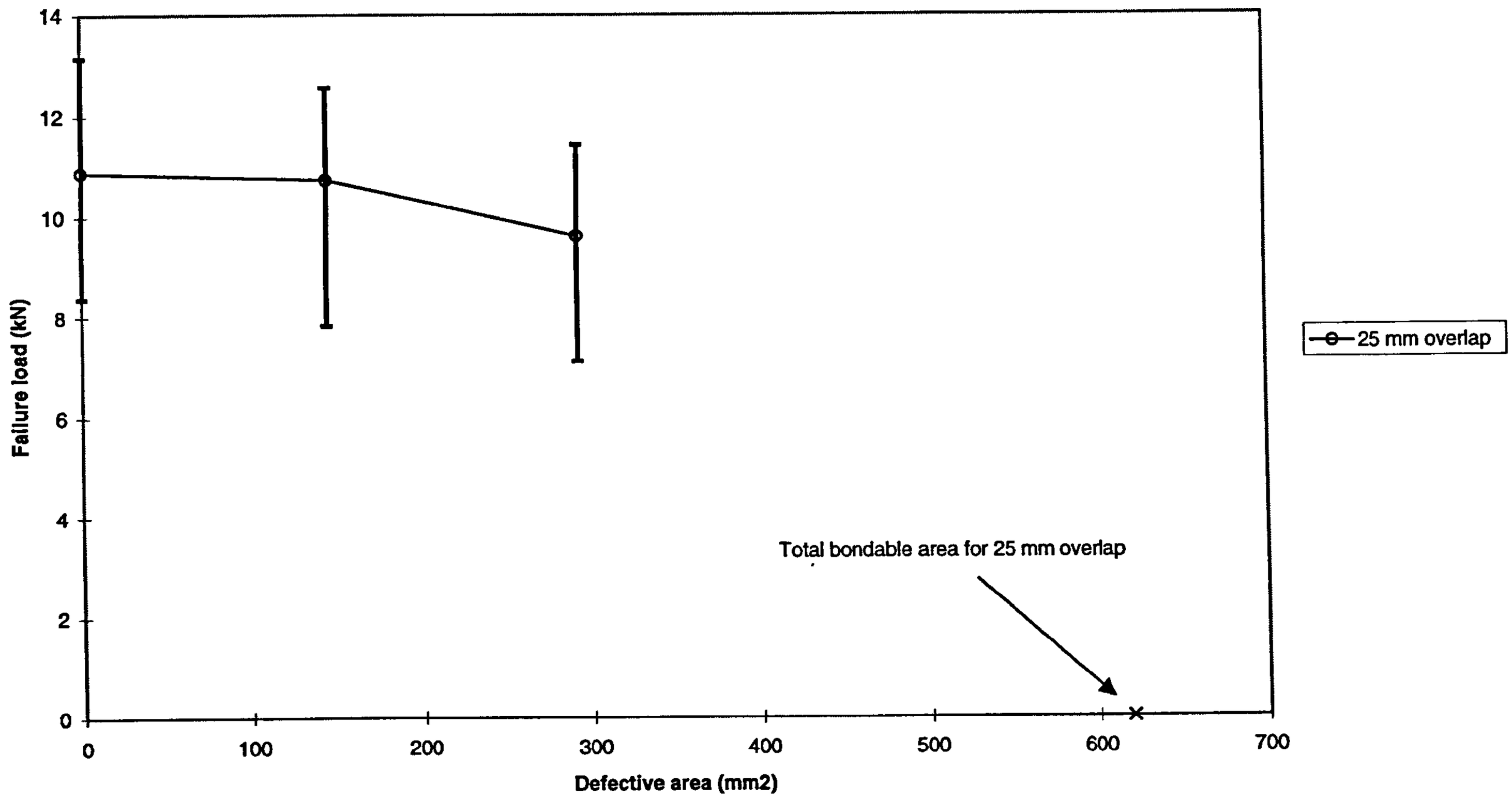

Figure 5.15 Variation of strength vs. defect size for 25 mm overlap gauge steel SLJs with MY753 adhesive and circular defects under tensile loading

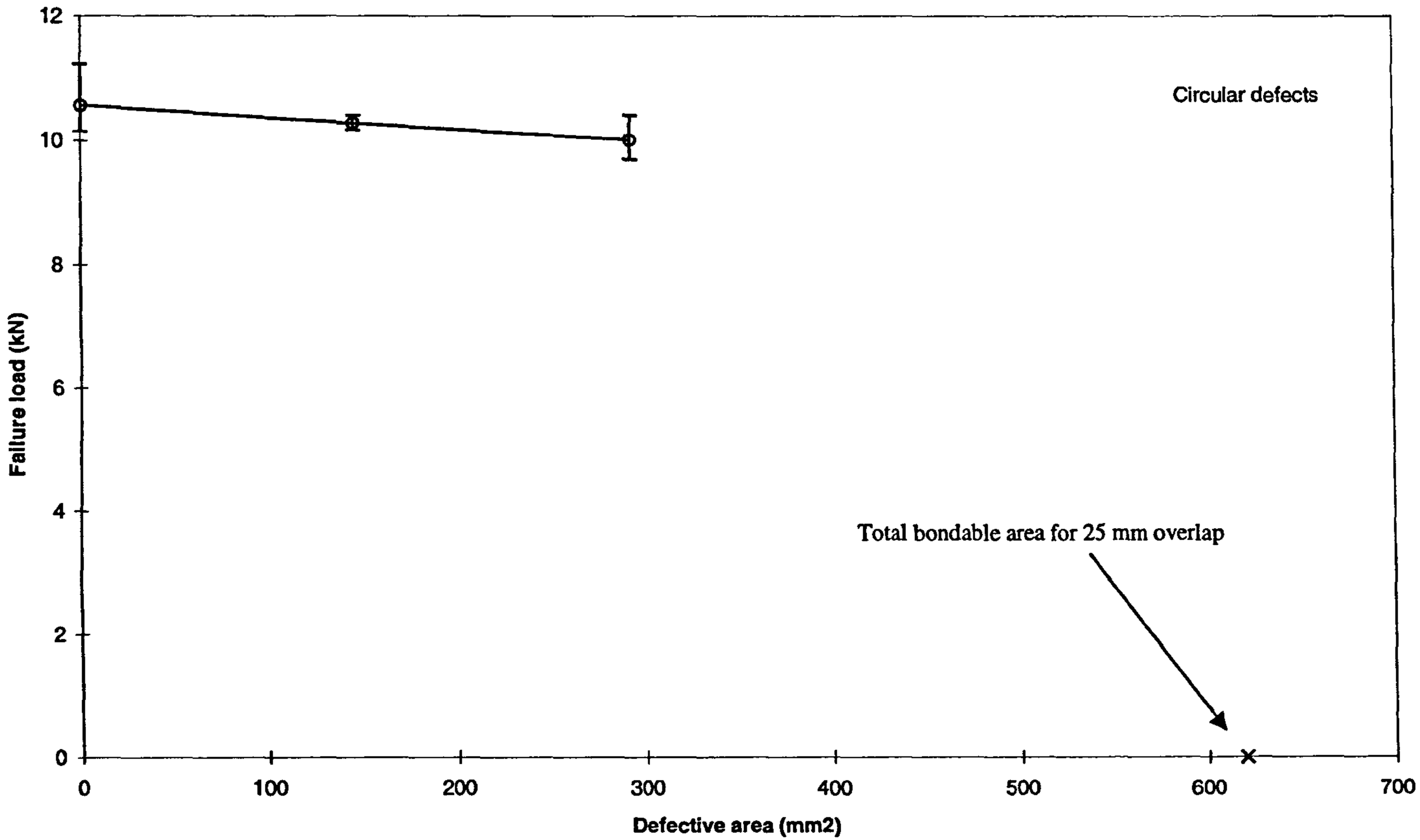

Figure 5.16 Variation of strength vs. defect size for 25 mm overlap mild steel SLJs with MY753 adhesive and circular defects under tensile loading

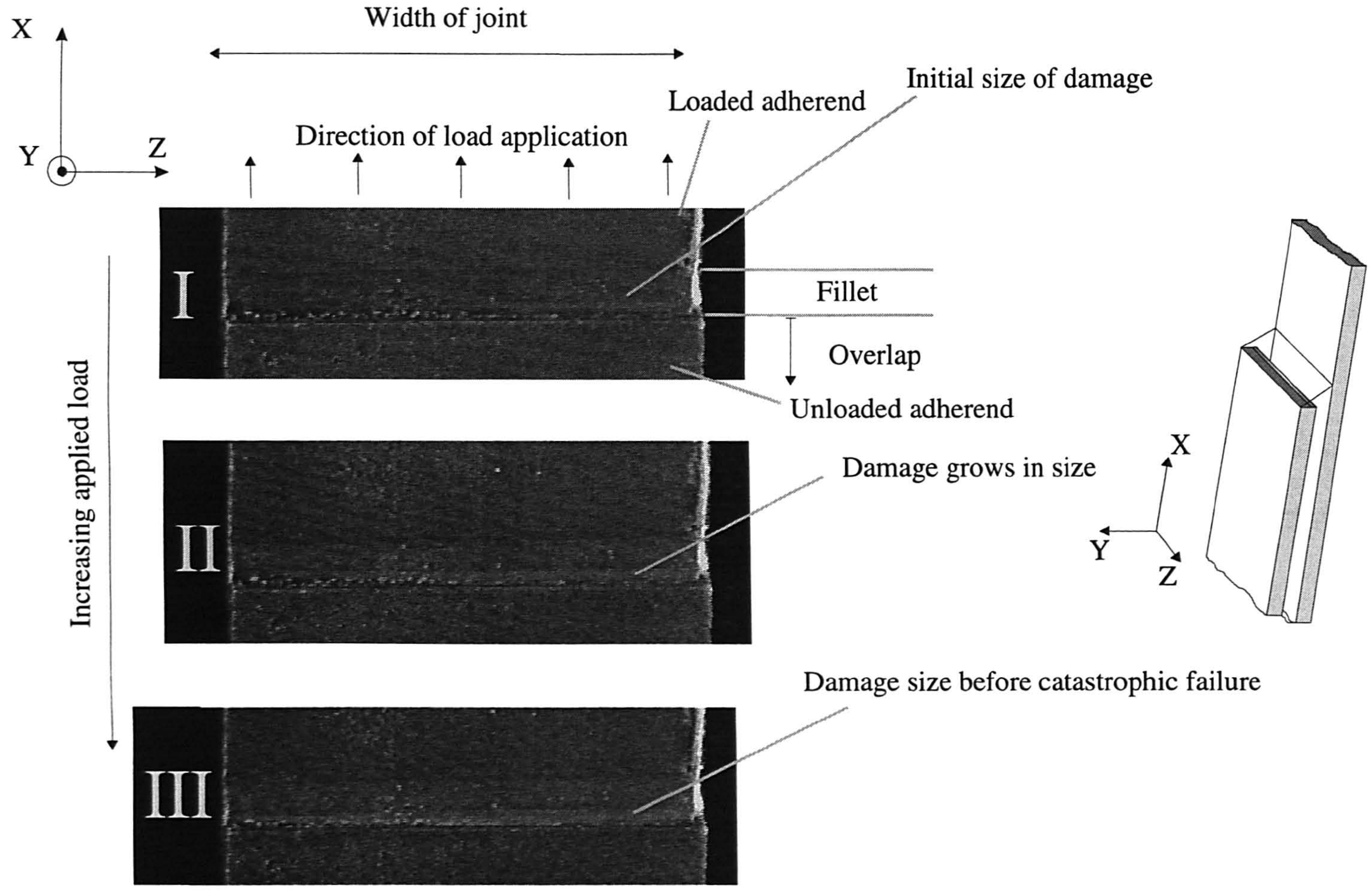

Figure 5.17 25 mm overlap joints with hard steel and MY 753 adhesive - detailed view of fillet face - damage growth next to adherends embedded corner - no visible cracks in the fillet.

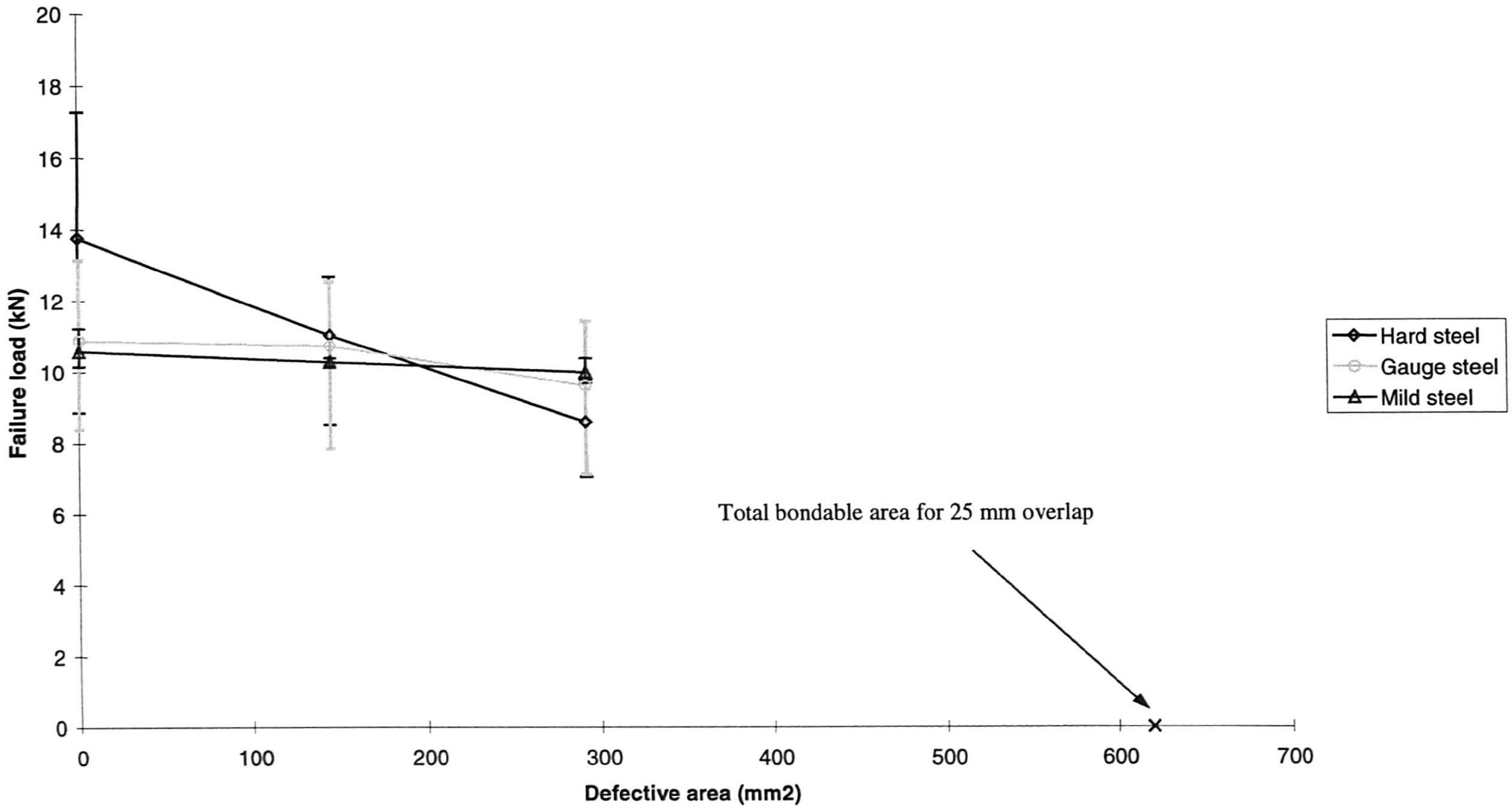

Figure 5.18 Variation of strength vs. defect size for SLJs with MY 753 adhesive and circular defects under tensile loading

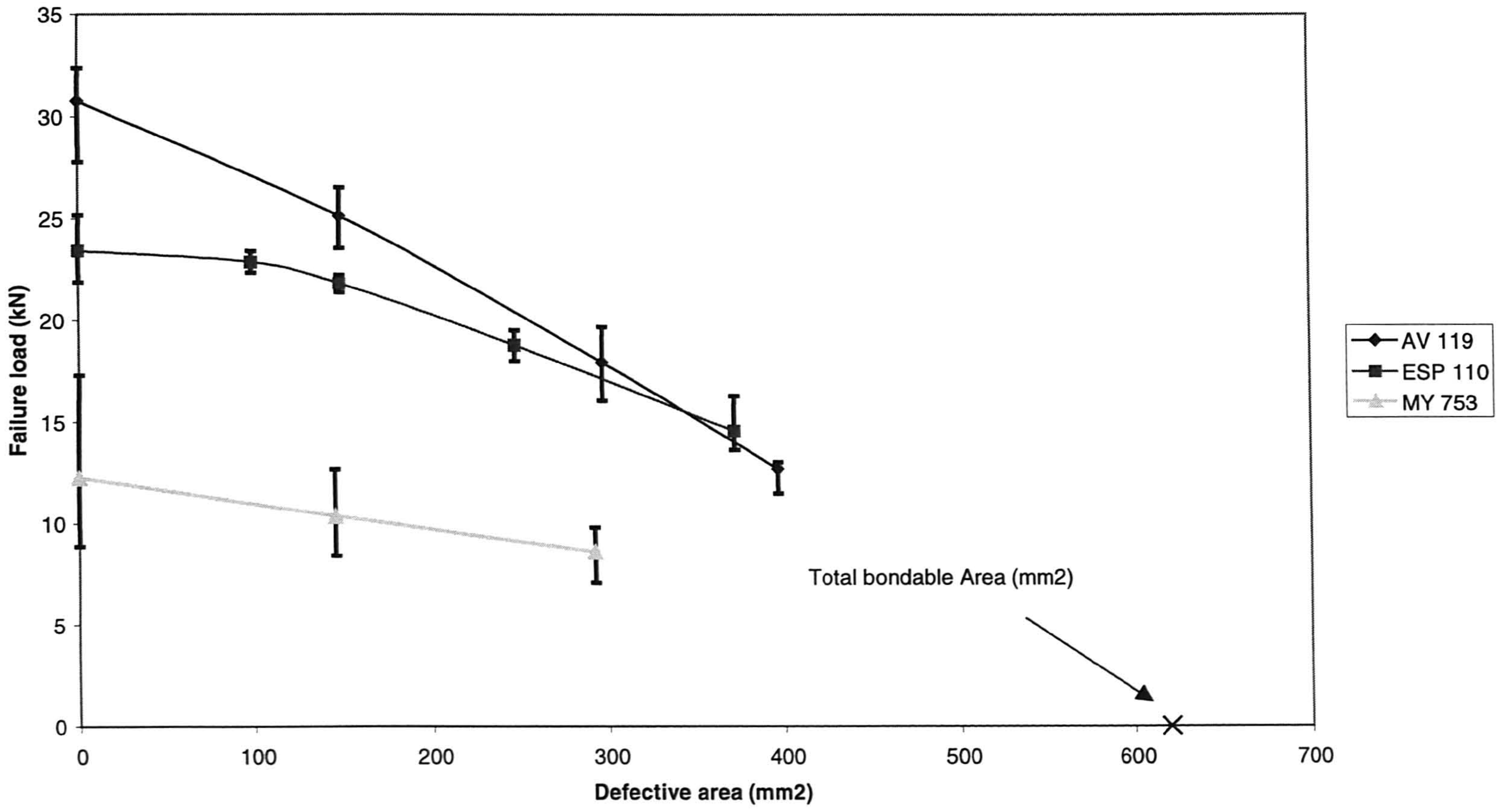

Figure 5.19 Variation of strength vs. defect size for 25 mm overlap hard steel SLJs for various adhesives under tensile loading

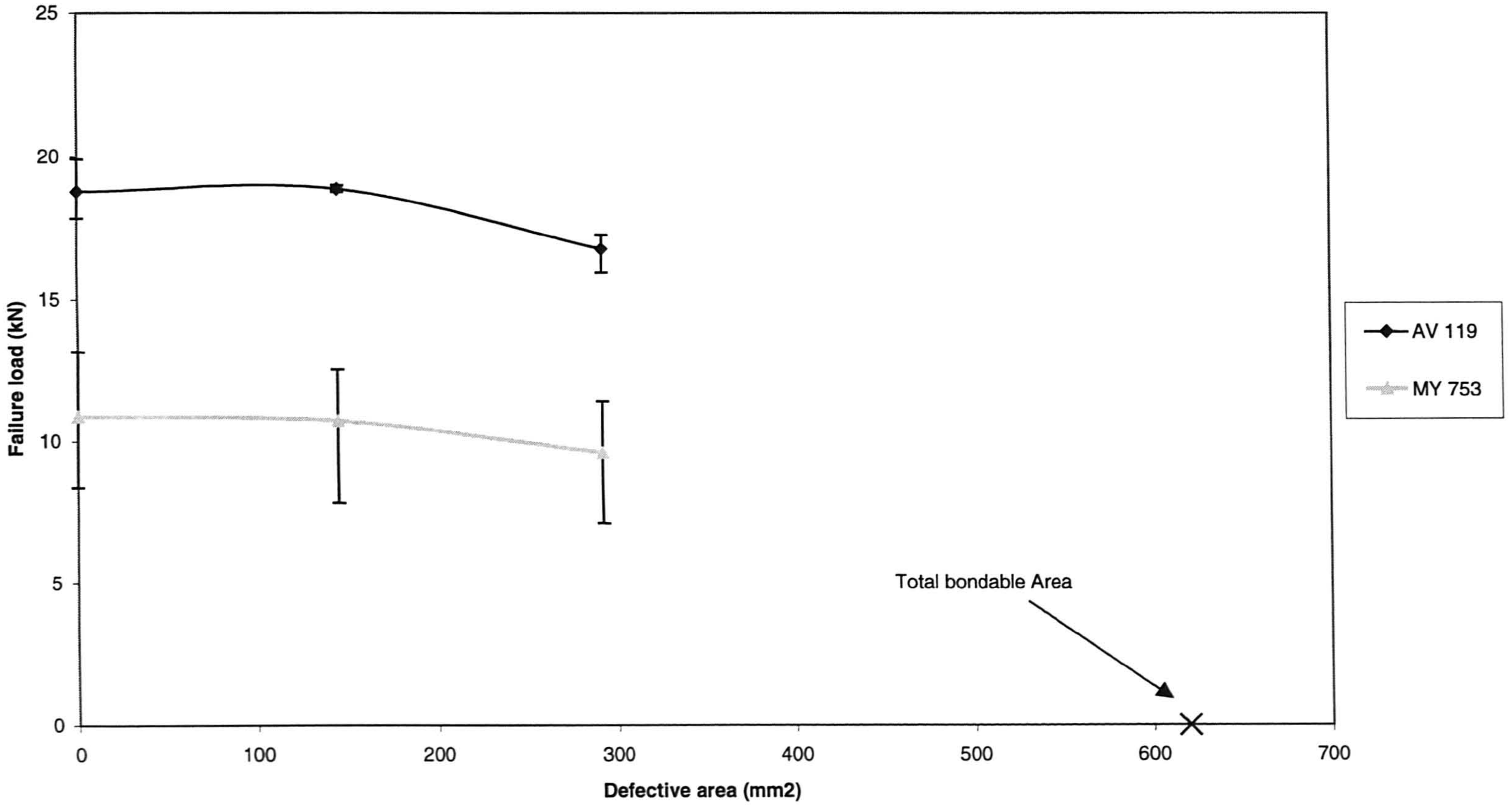

Figure 5.20 Variation of strength vs. defect size for 25 mm overlap gauge steel SLJs for various adhesives under tensile loading

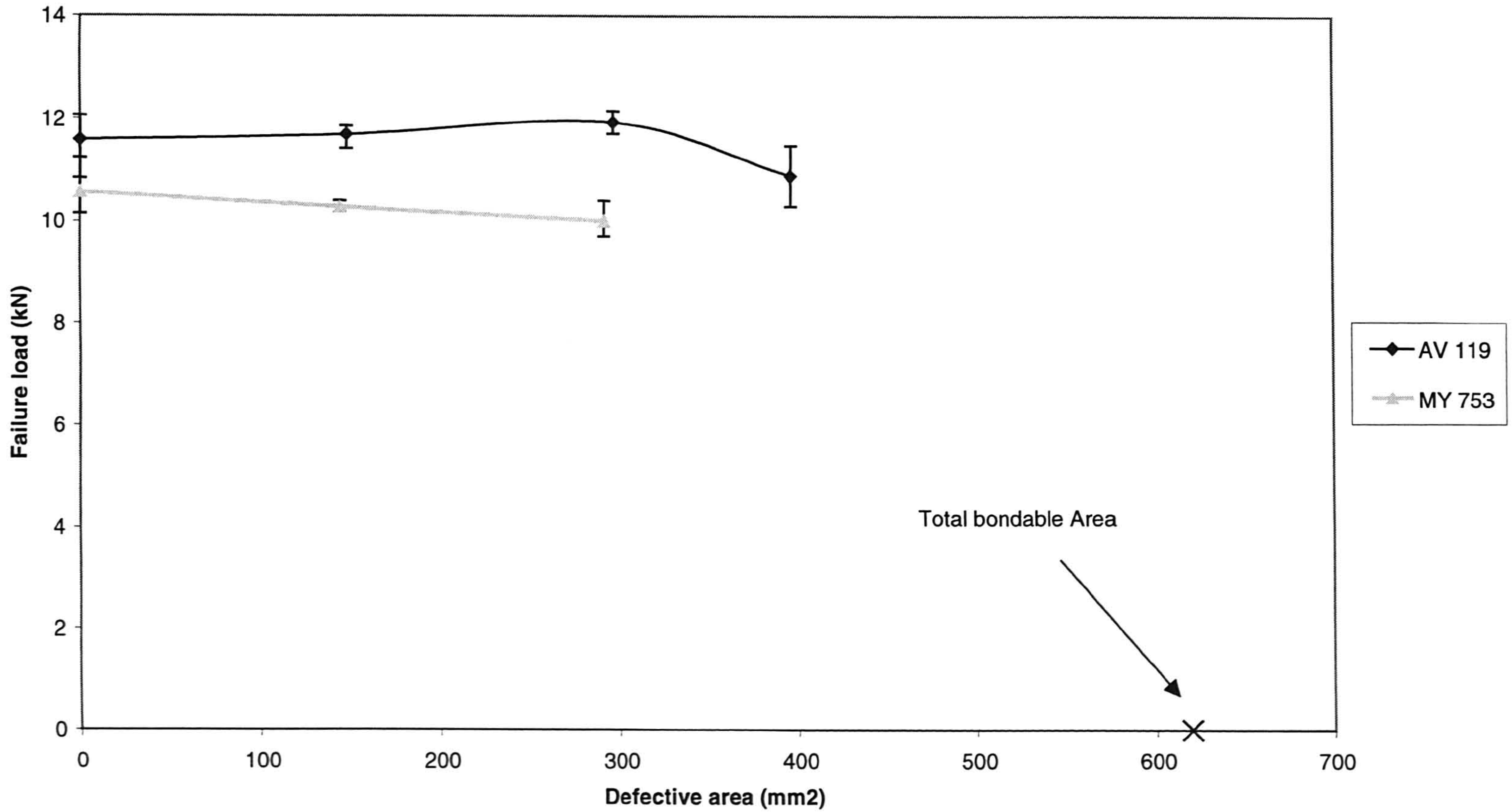

Figure 5.21 Variation of strength vs. defect size for 25mm overlap mild steel SLJs for various adhesives under tensile loading

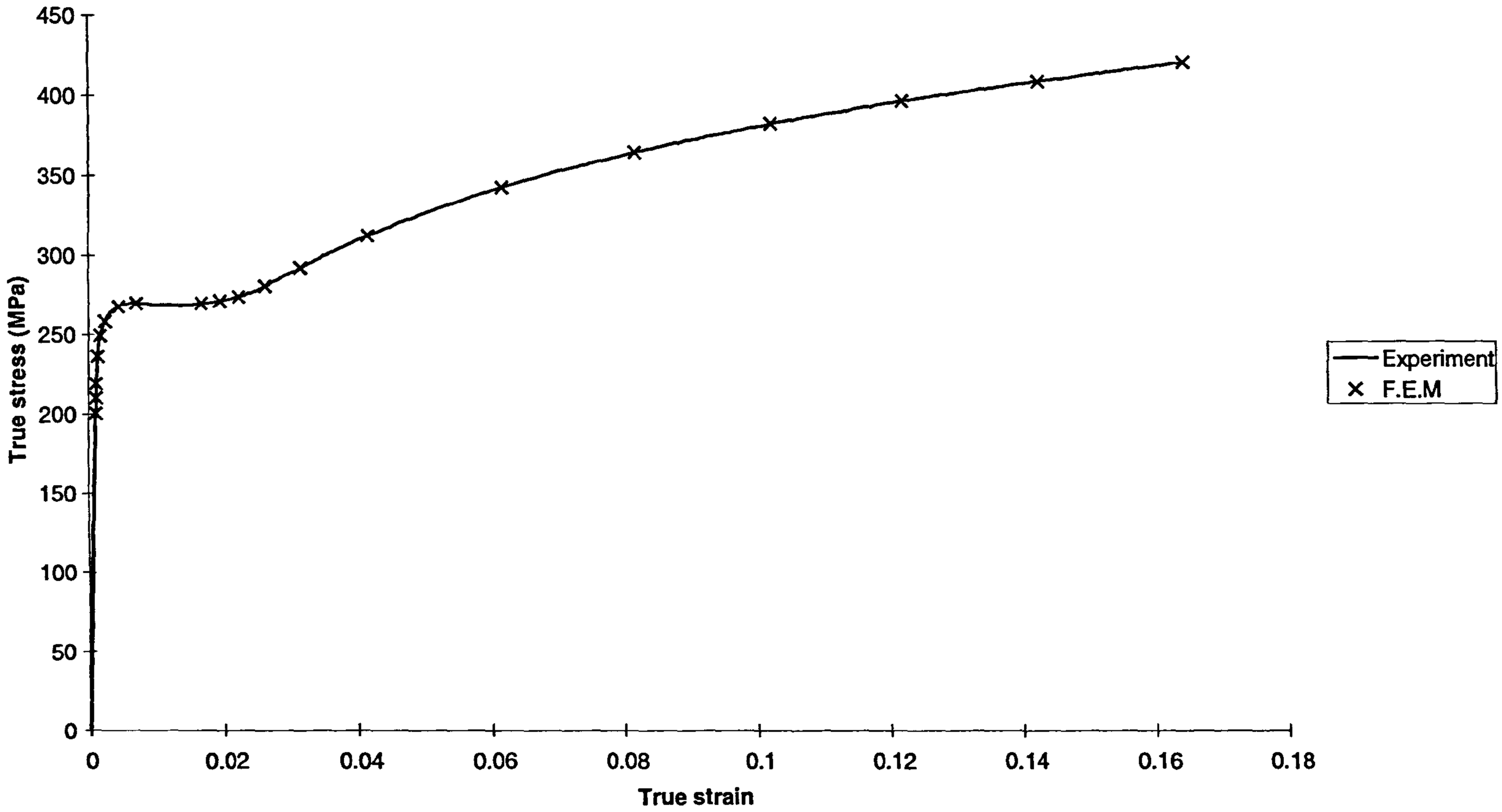

Figure 6.1 Material modelling used in the F.E for mild steel

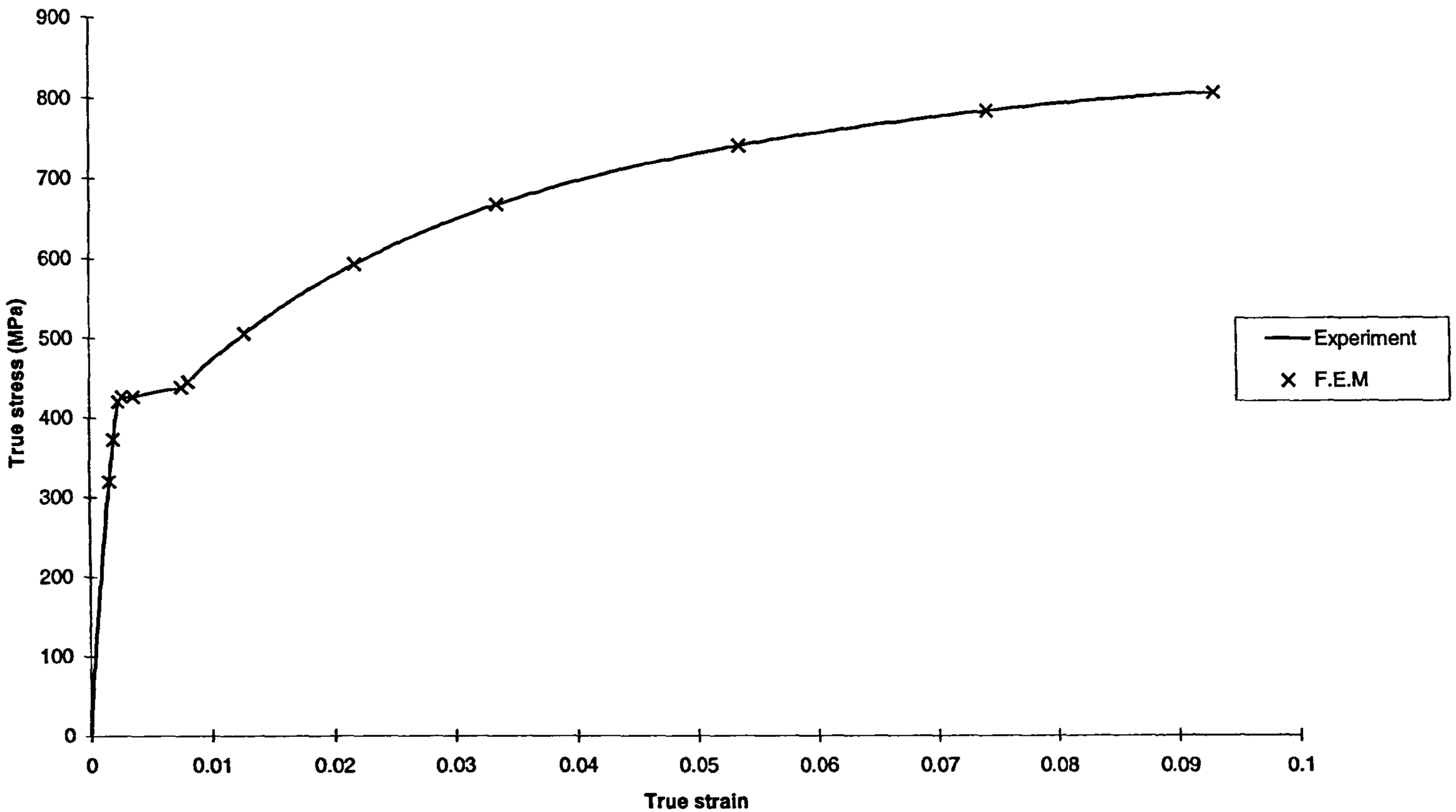

Figure 6.2 Material modelling used in the F.E for gauge steel

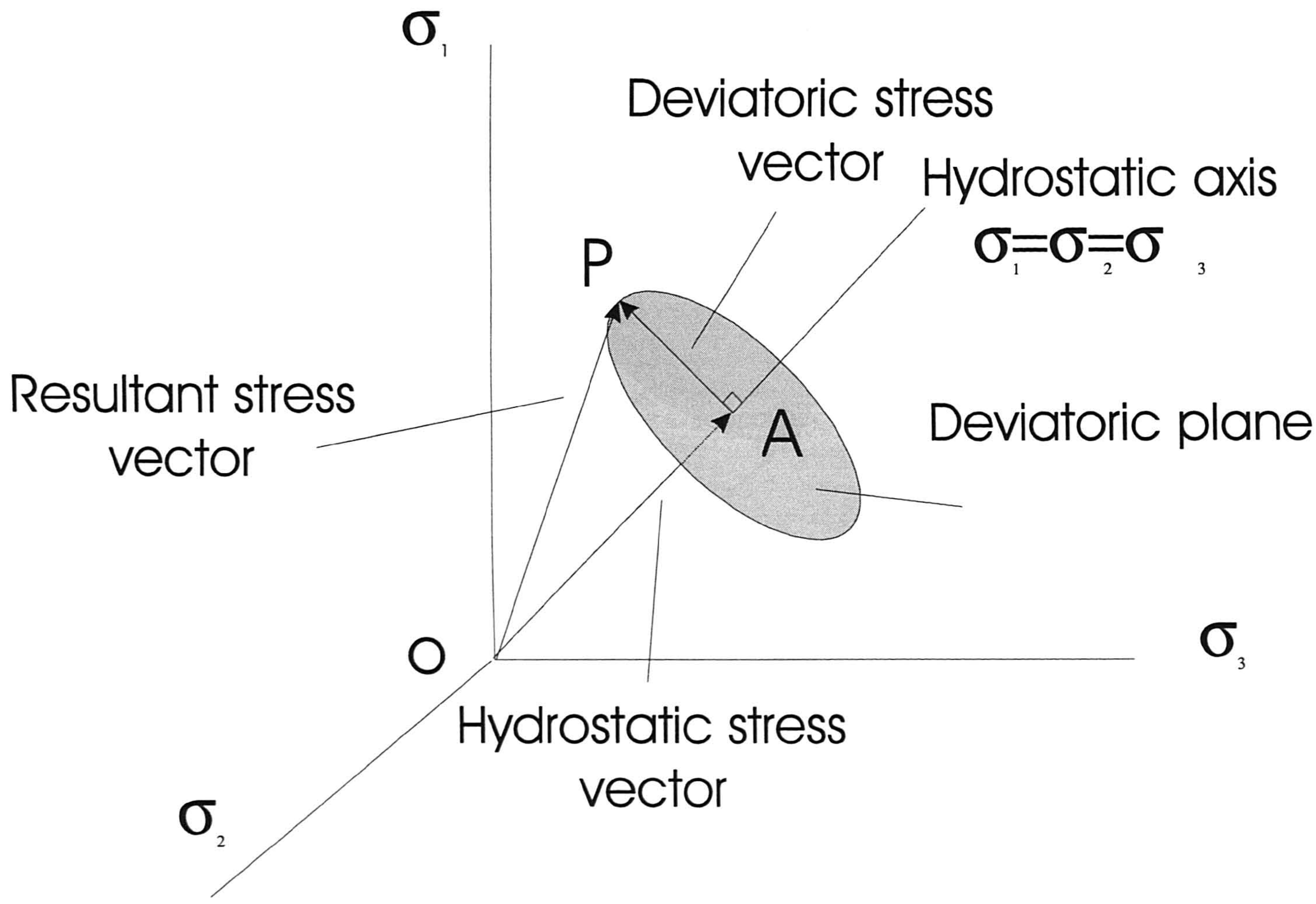

Figure 6.3 Principal stress space - representation of hydrostatic and deviatoric stress components

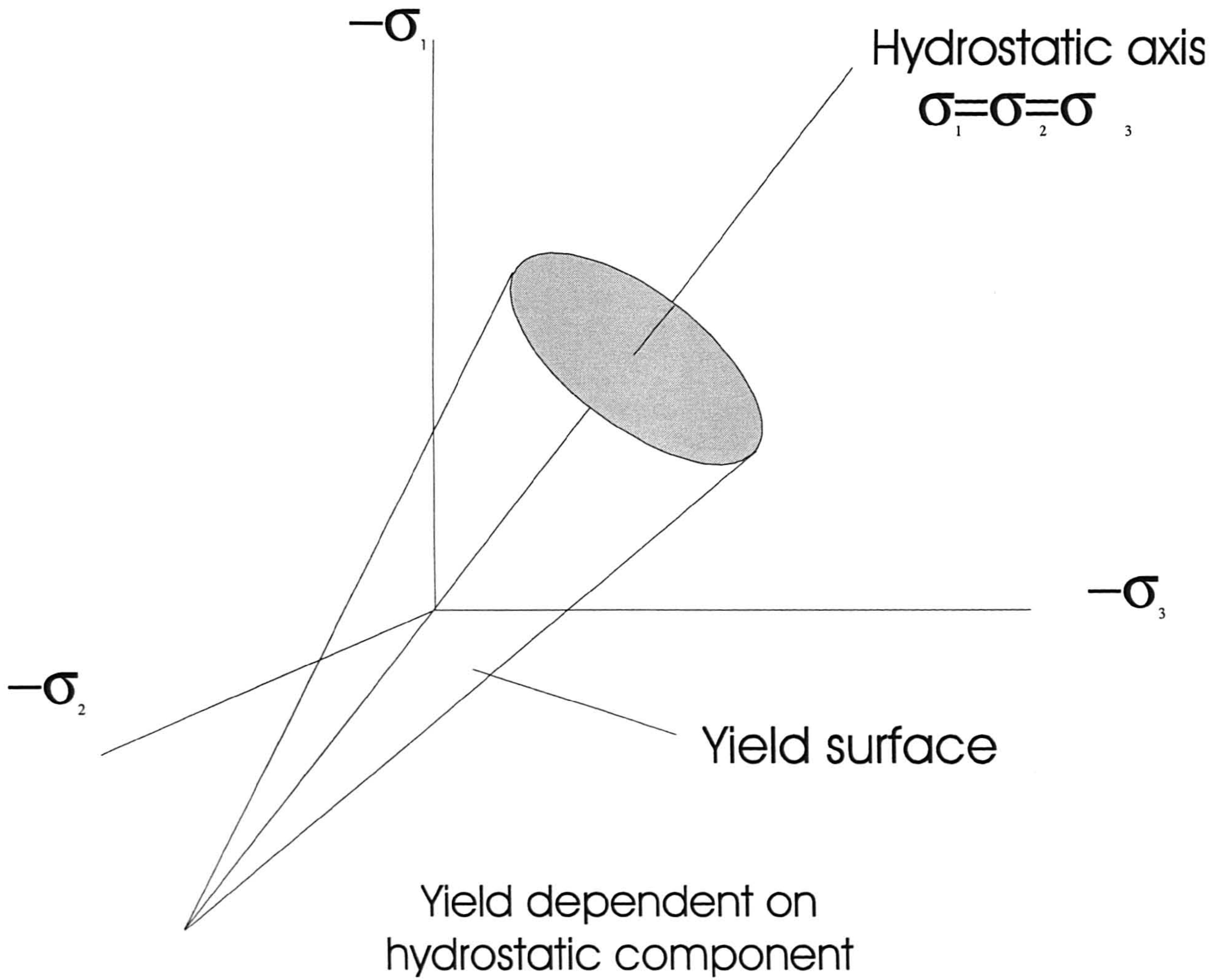

Figure 6.4 Yield surface representation in the principal stress space when there is dependence on the hydrostatic stress component

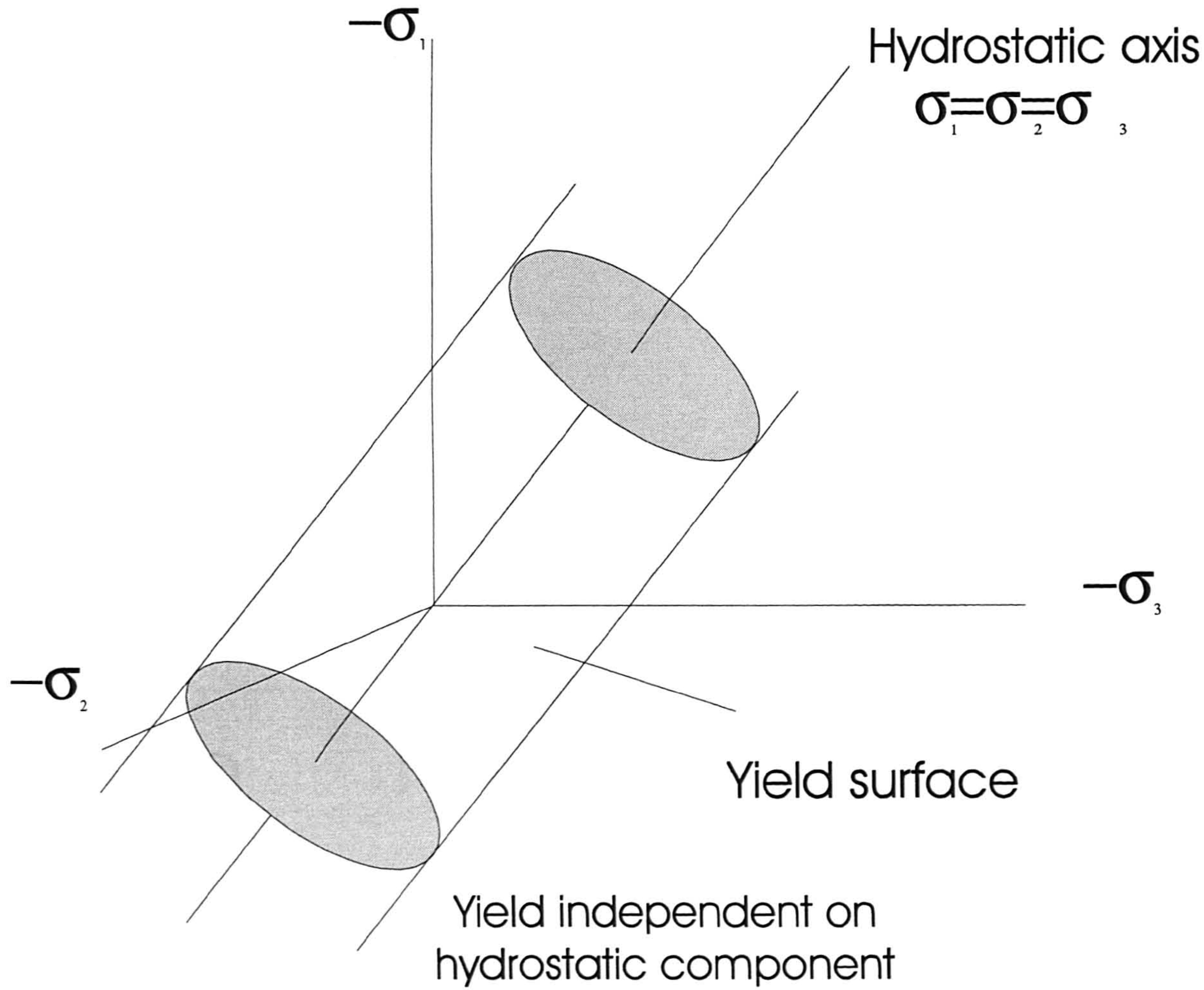

Figure 6.5 Yield surface representation in the principal stress space when there is independence on the hydrostatic stress component

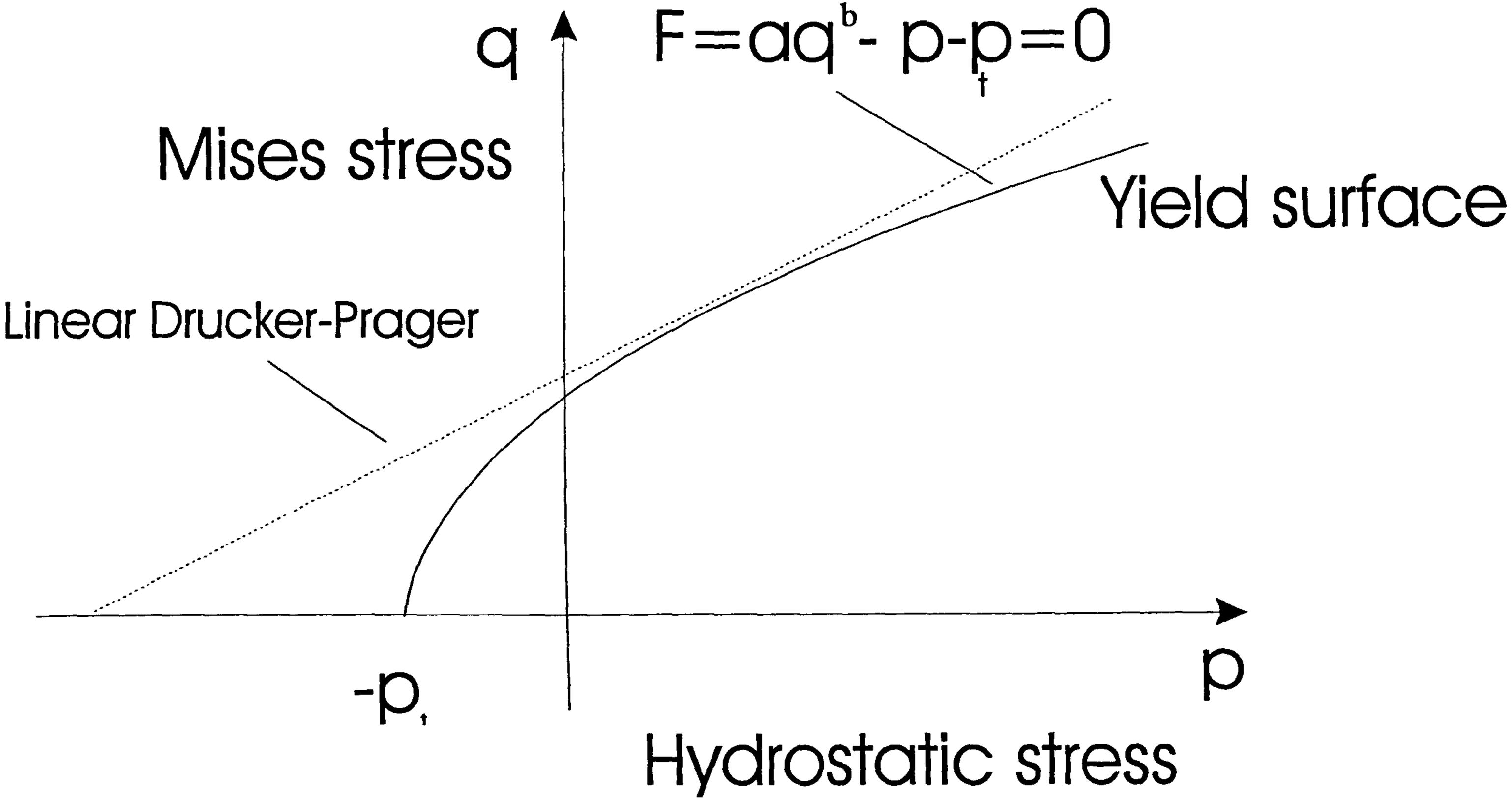

Figure 6.6 Representation of the yield surface in the meridional (p-q) plane

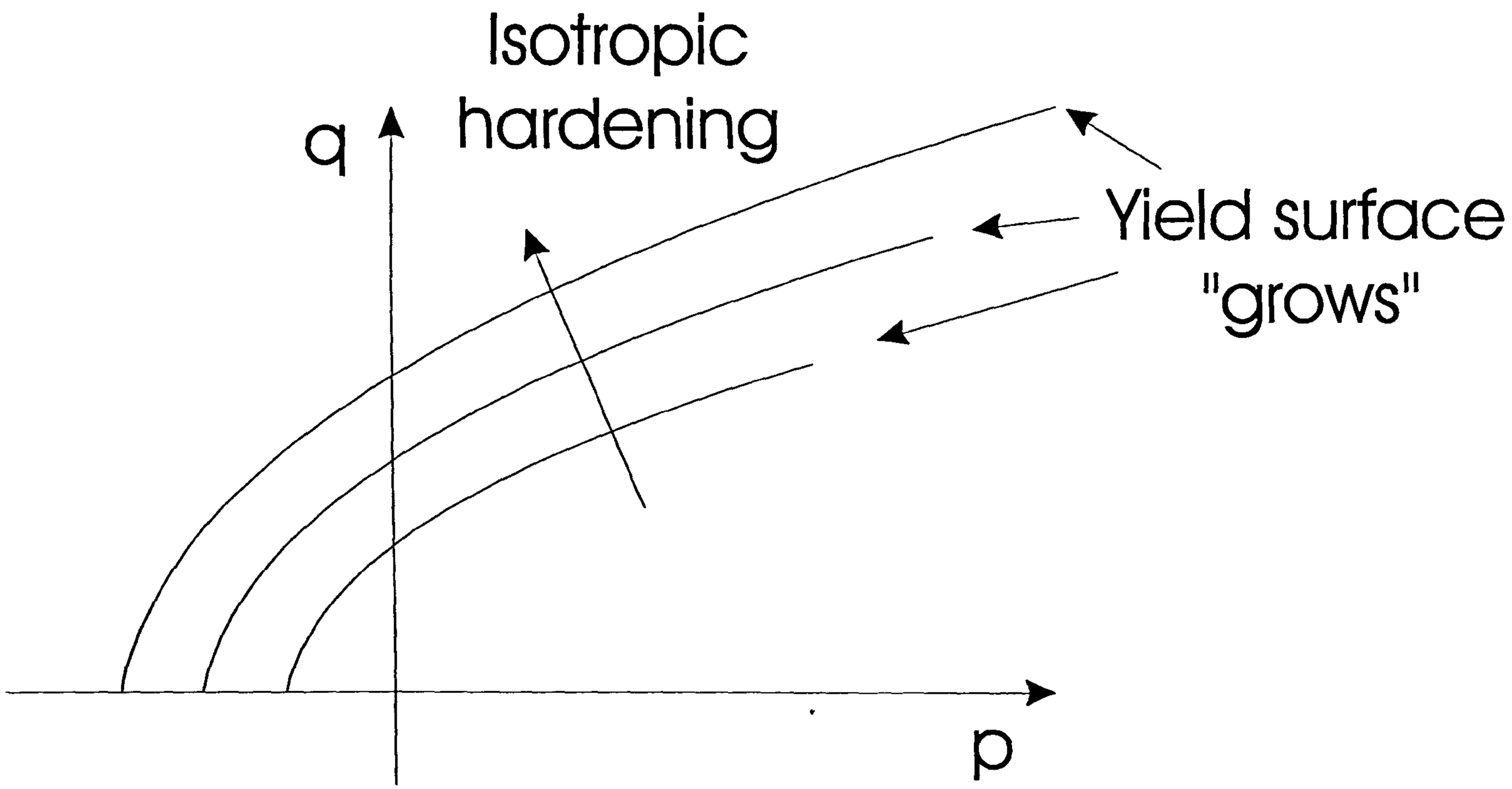

Figure 6.7 Representation of isotropic hardening for the case of the Raghava or exponent Drucker-Prager criteria

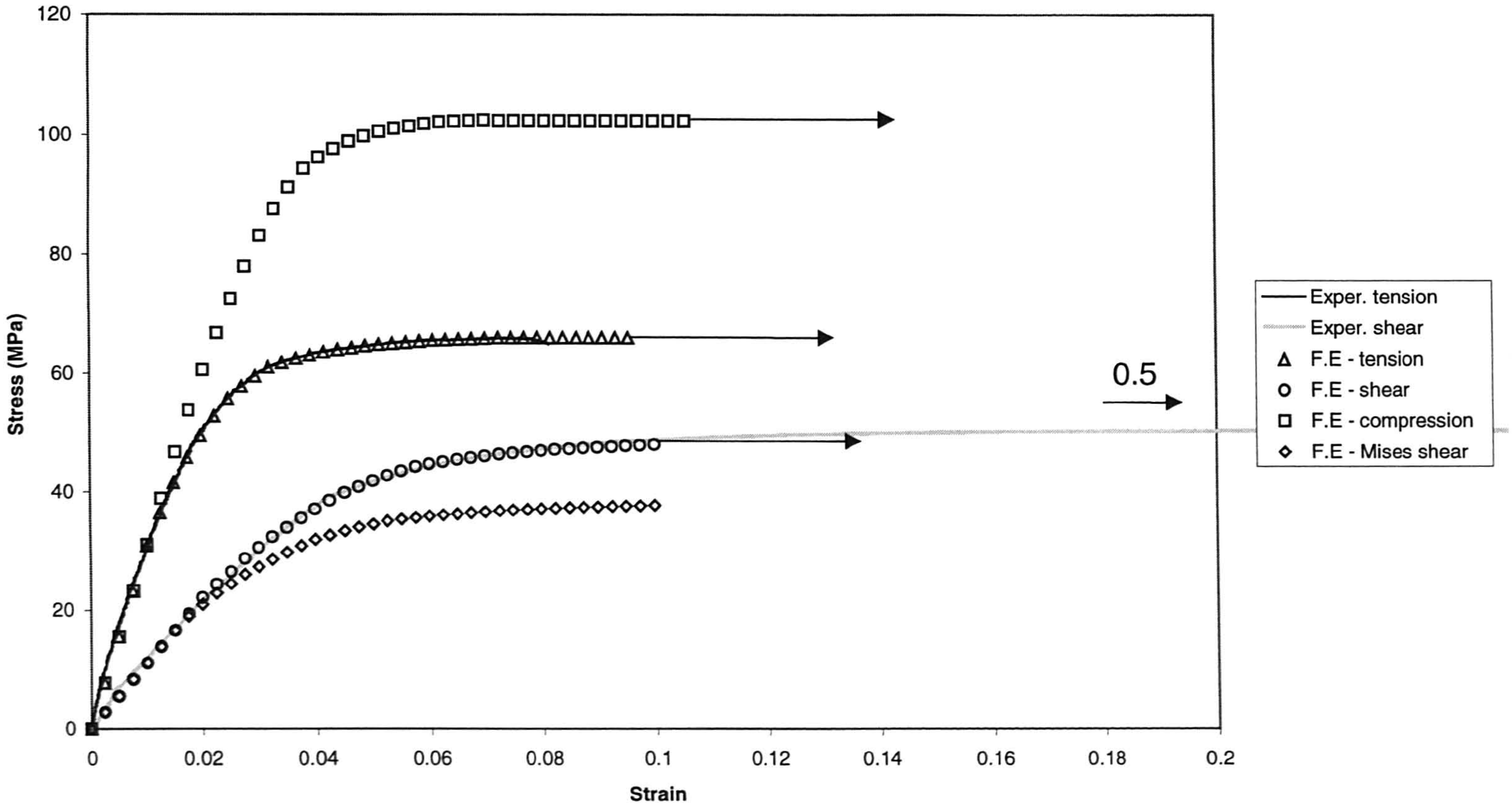

Figure 6.8 Verification of the Raghava material model used in the F.E for the EC 3448 adhesive

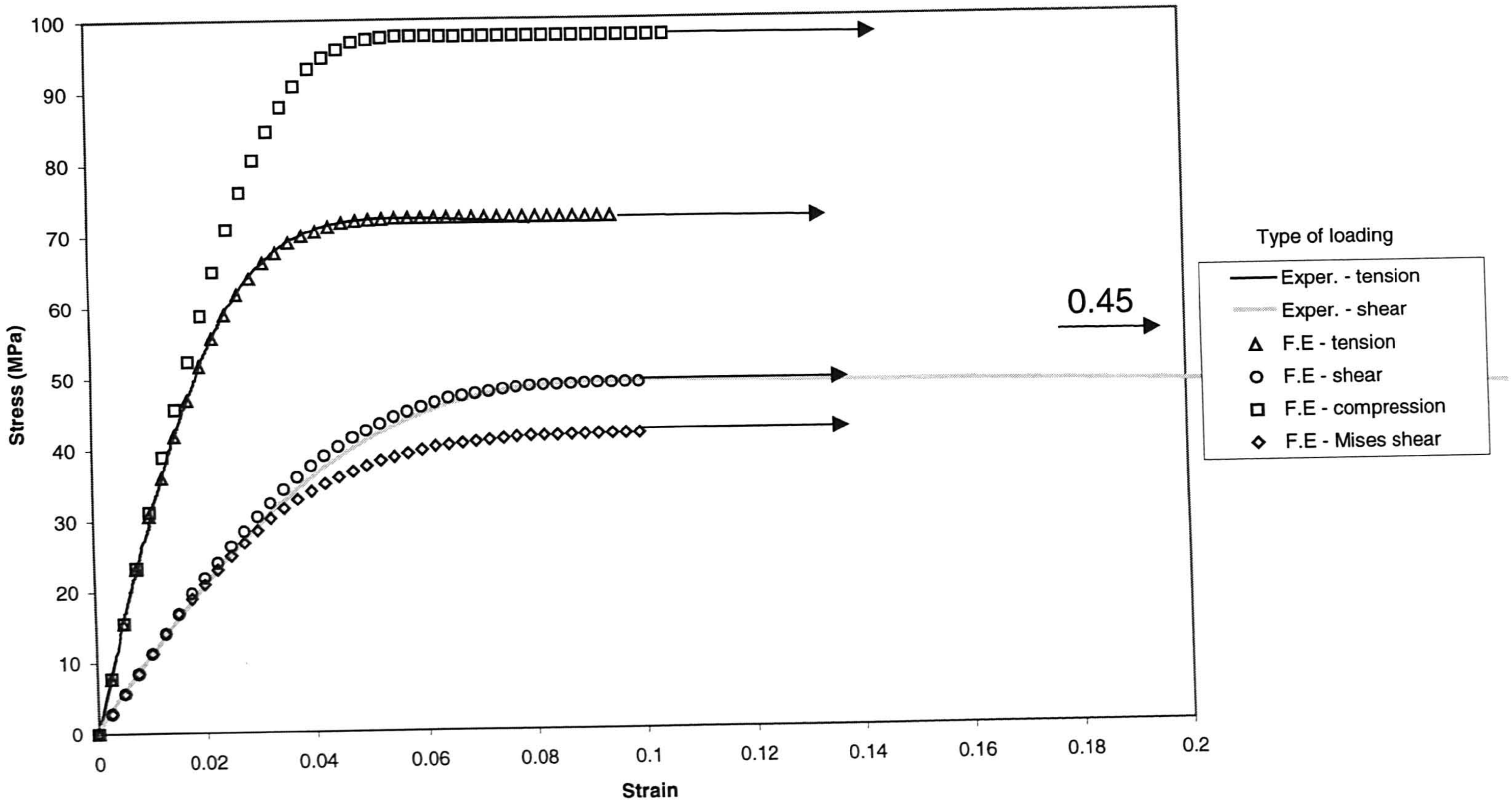

Figure 6.9 Verification of the Raghava material model used in the F.E for the AV 119 adhesive

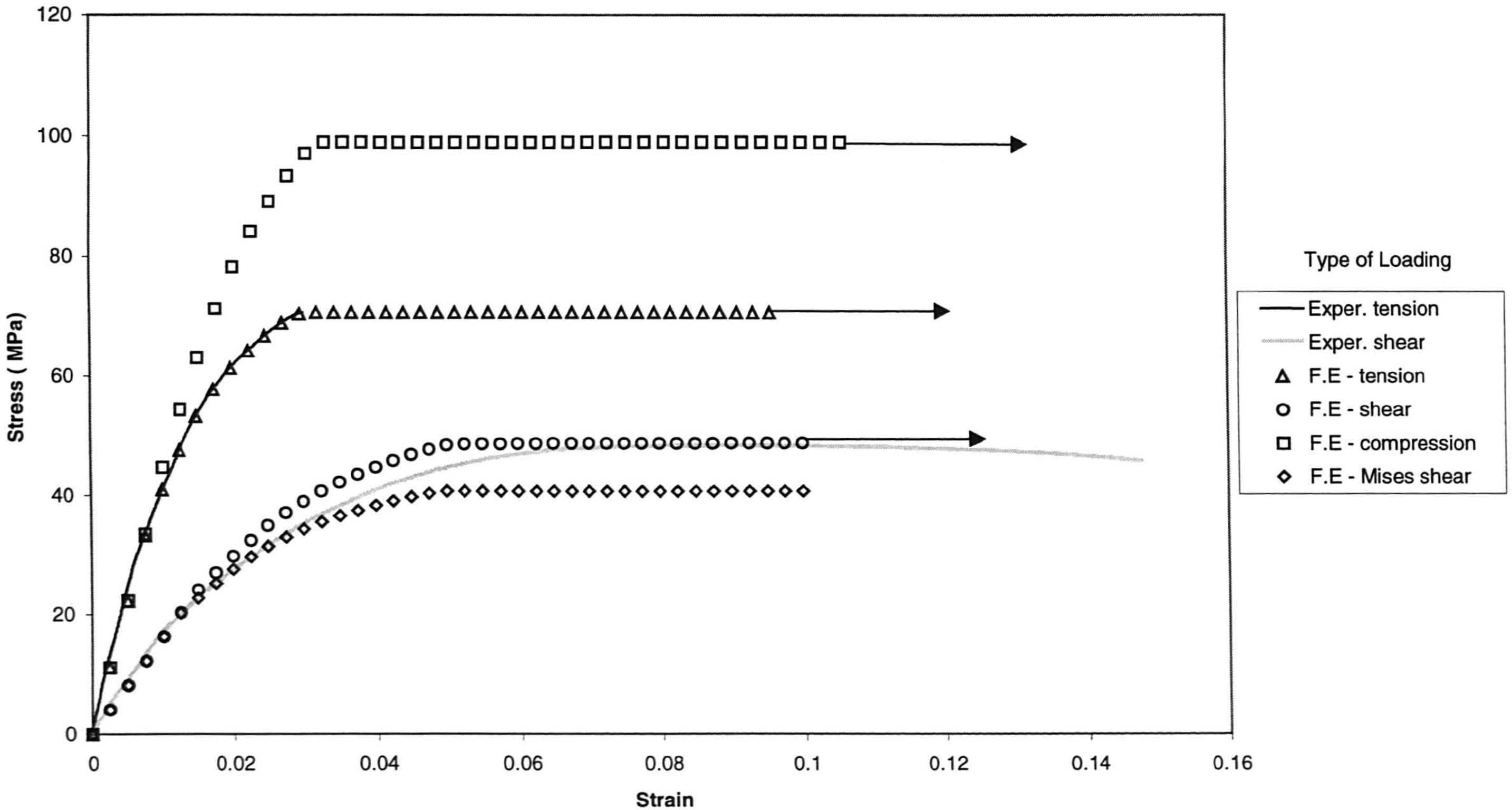

Figure 6.10 Verification of the Raghava material model used in the F.E for the ESP 110 adhesive

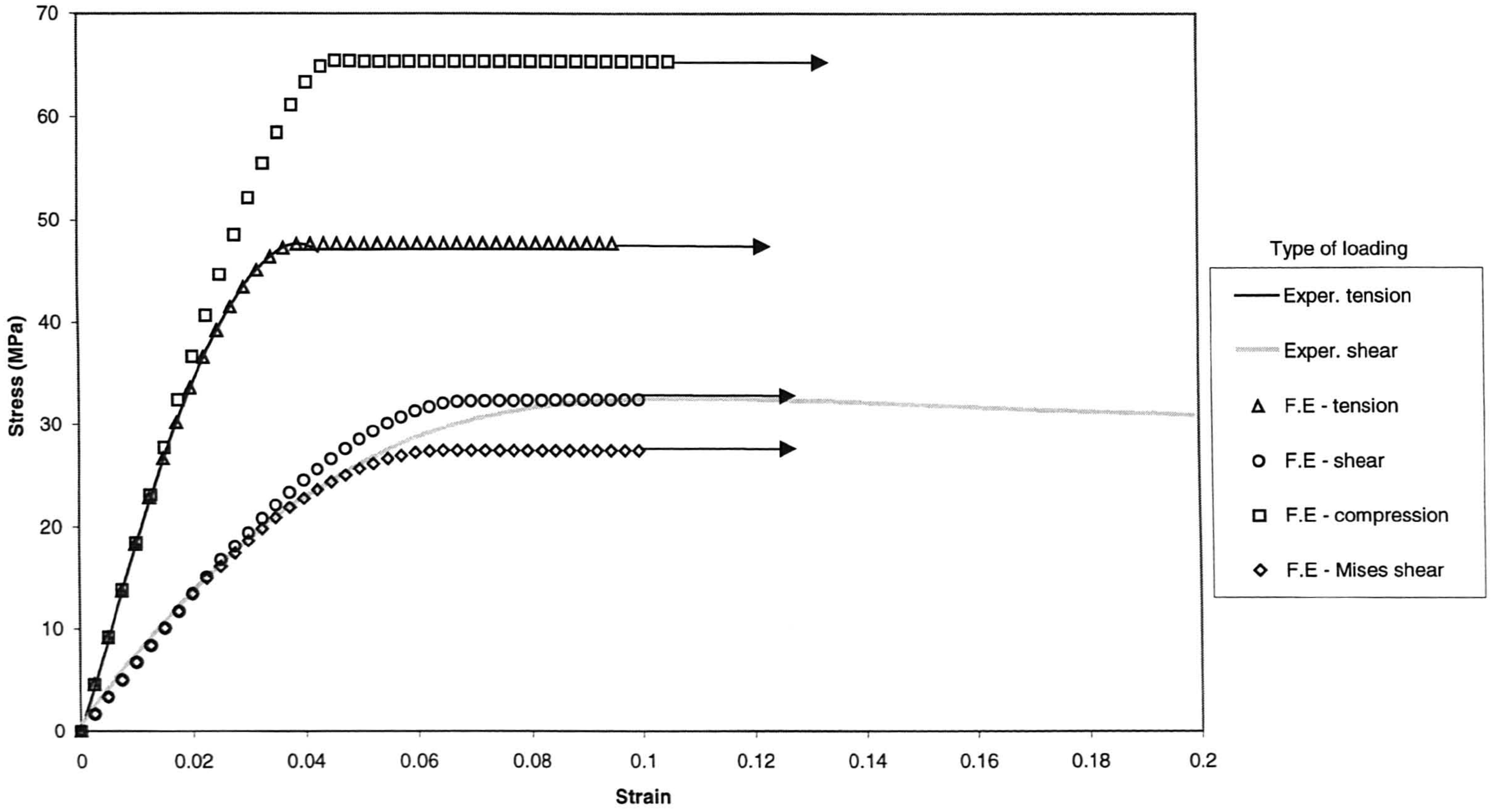

Figure 6.11 Verification of the Raghava material model used in the F.E for the MY753 adhesive

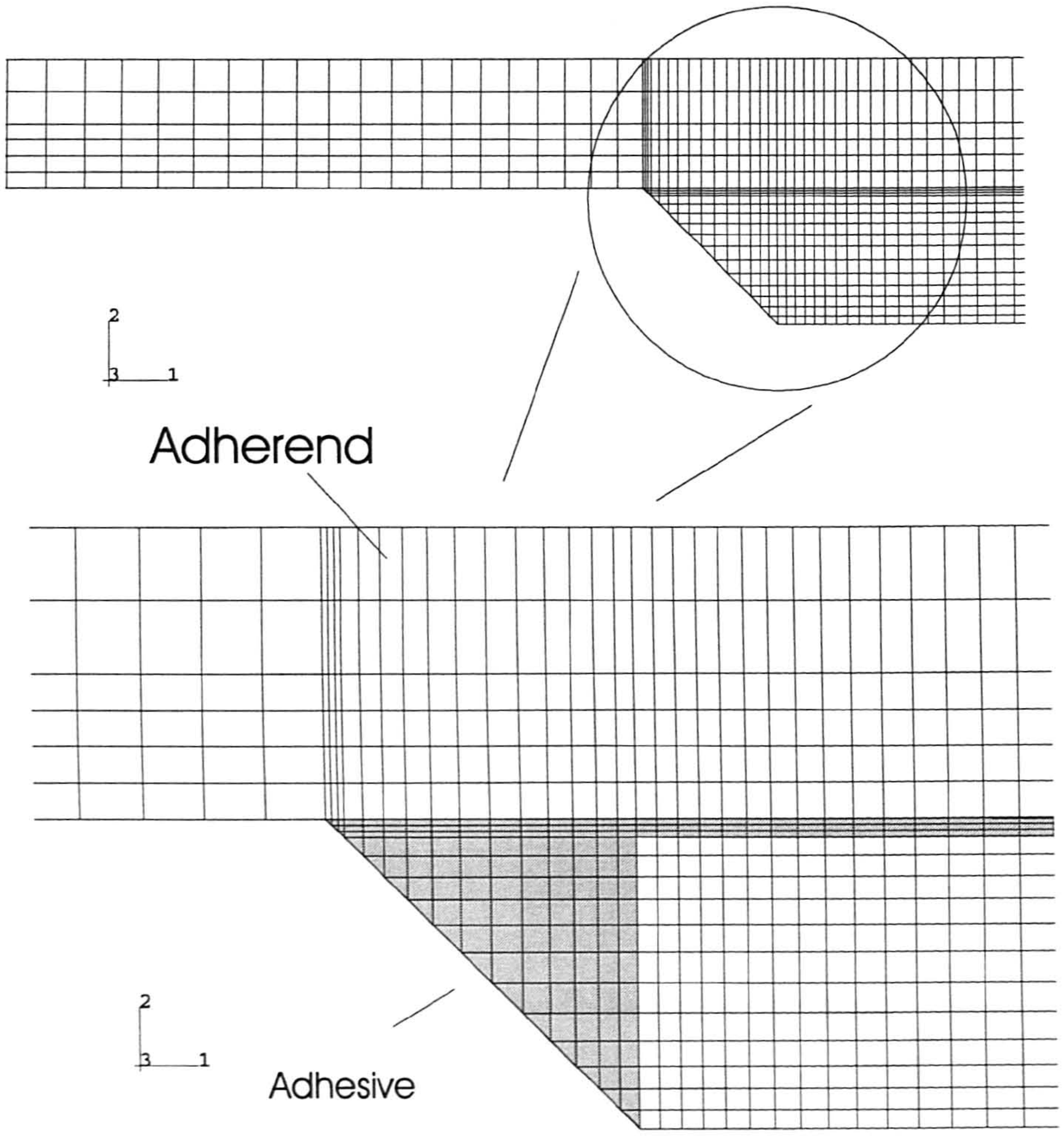

Figure 6.12 Detailed view of the finite element mesh used in the analyses

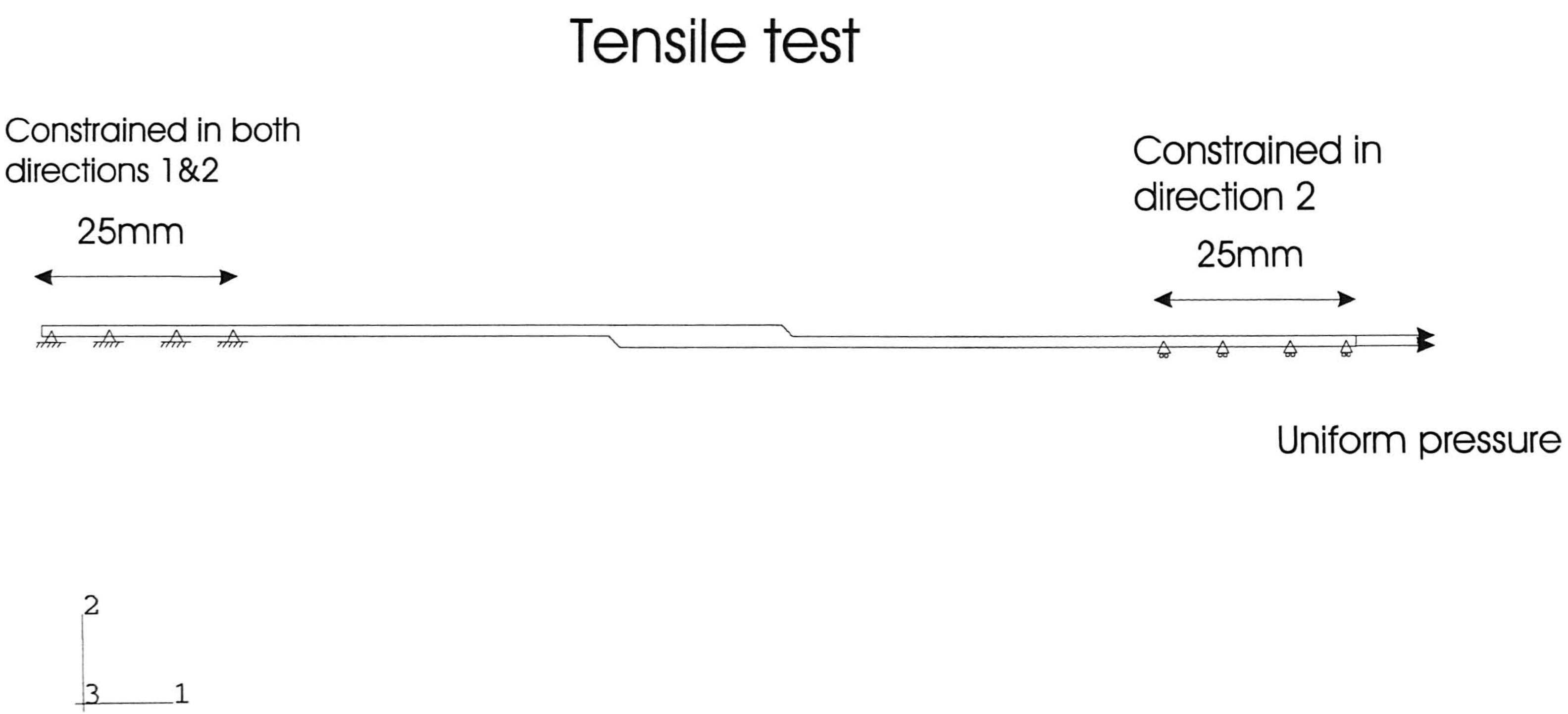

Figure 6.13 Boundary conditions in the finite element analysis - tensile loading

4 point bending test

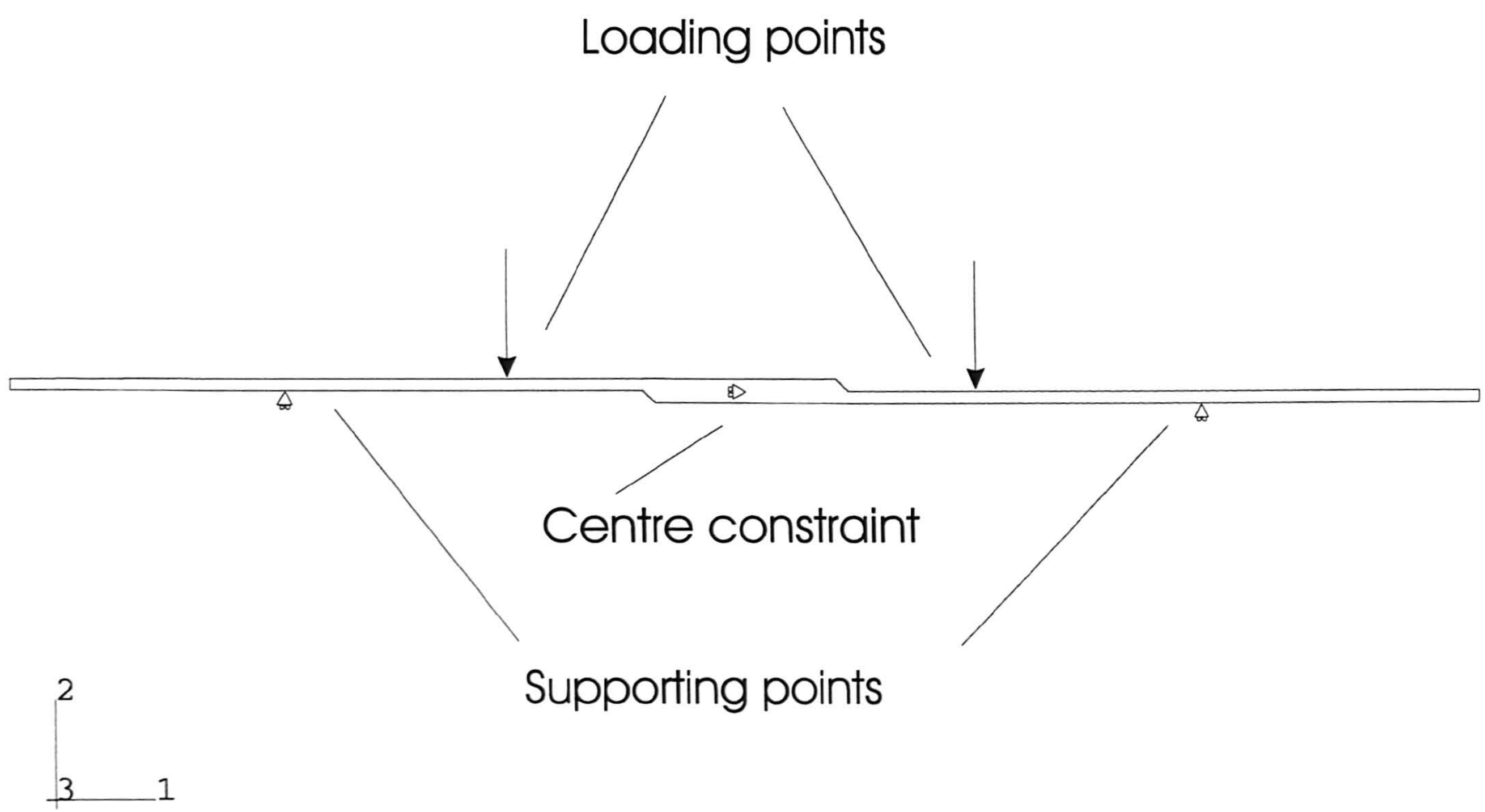

Figure 6.14 Boundary conditions in the finite element analysis - 4pt bend loading

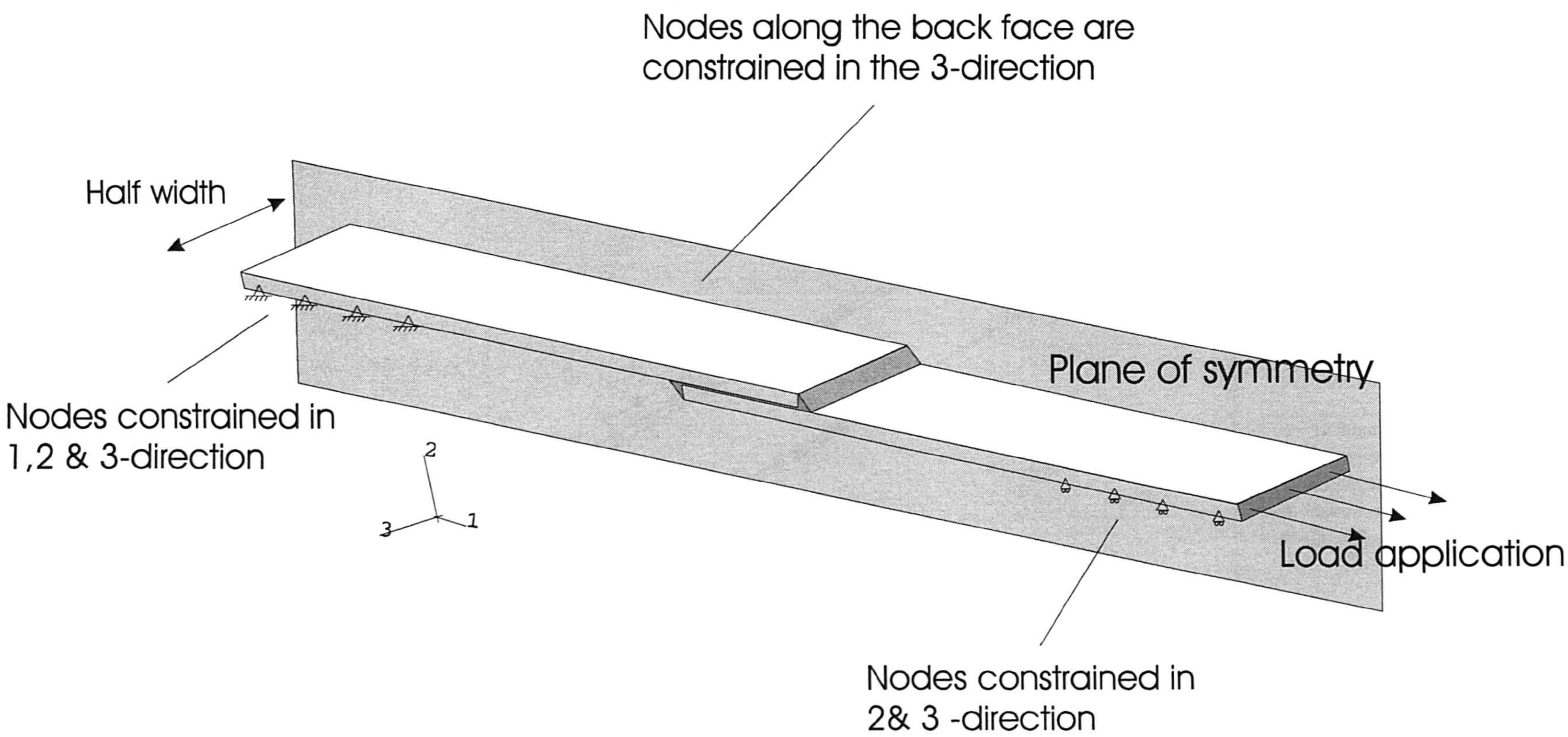

Figure 6.15 Boundary conditions in the 3-dimensional finite element analysis - tensile loading

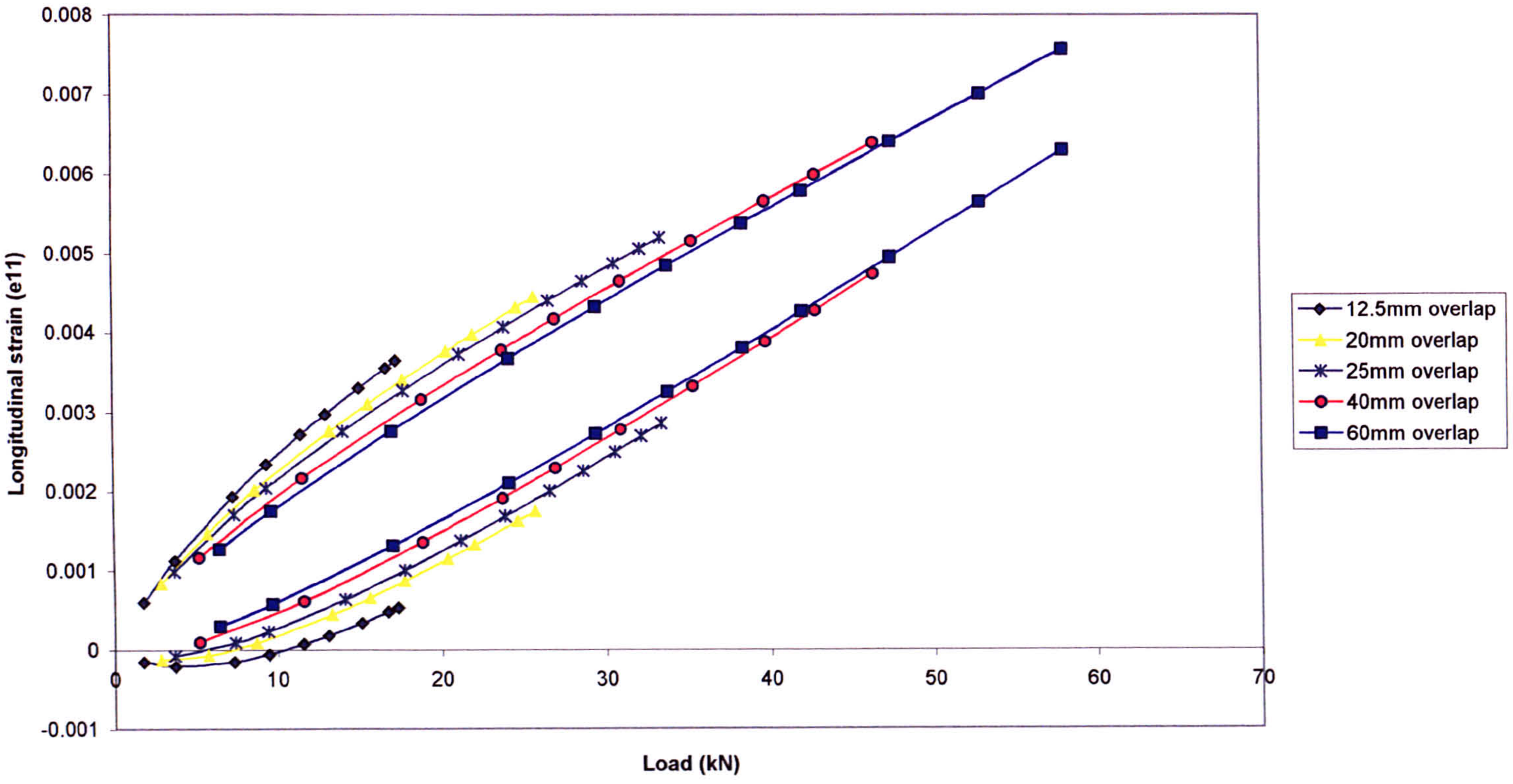

Figure 7.1 F.E prediction for the strain variation in the adherends for hard steel SLJs with EC 3448 adhesive and various overlap lengths under tensile loading

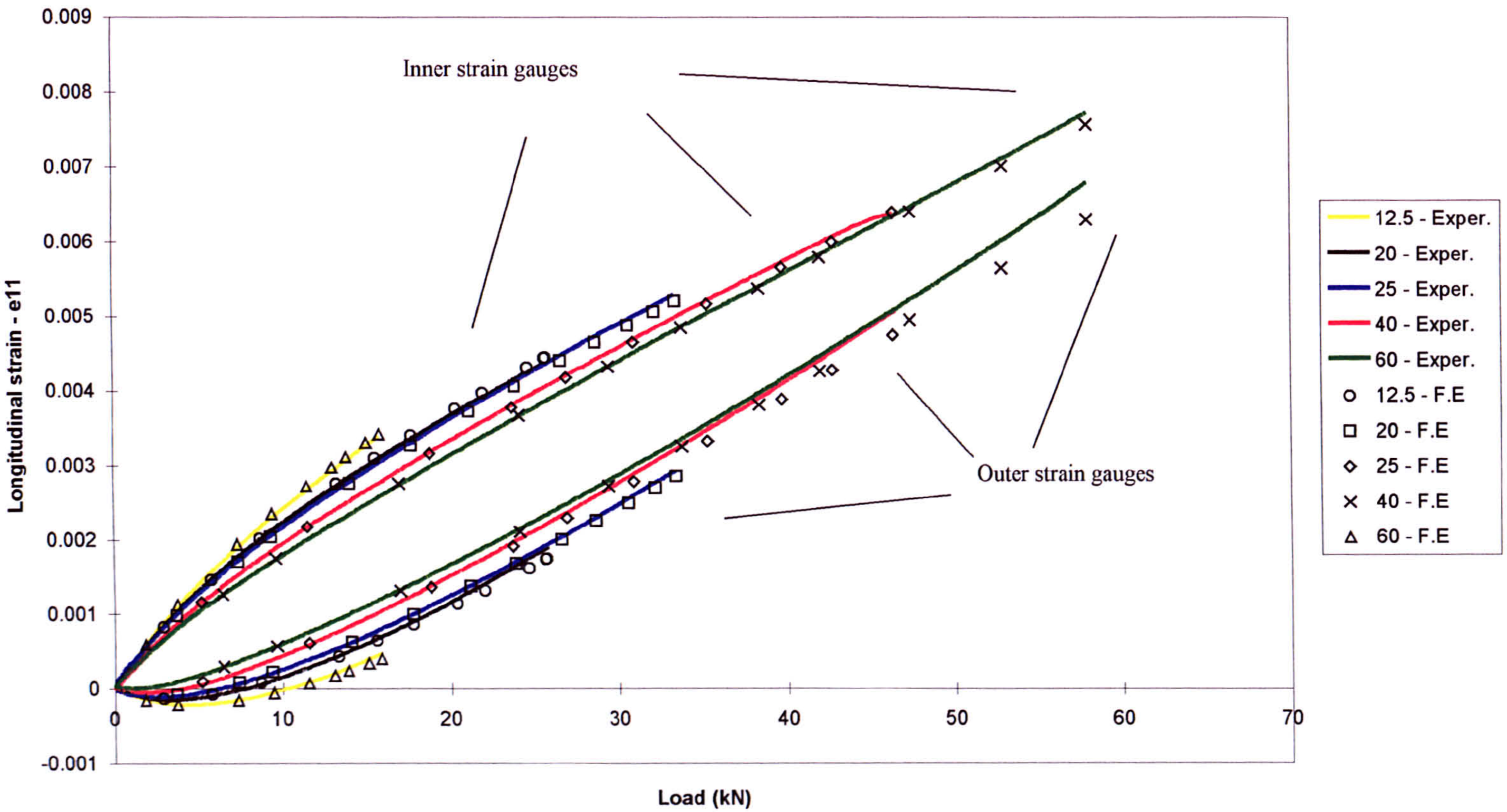

Figure 7.2 Experimental - F.E prediction correlation for the strain variation in the adherends for hard steel SLJs with EC 3448 adhesive and various overlap lengths under tensile loading

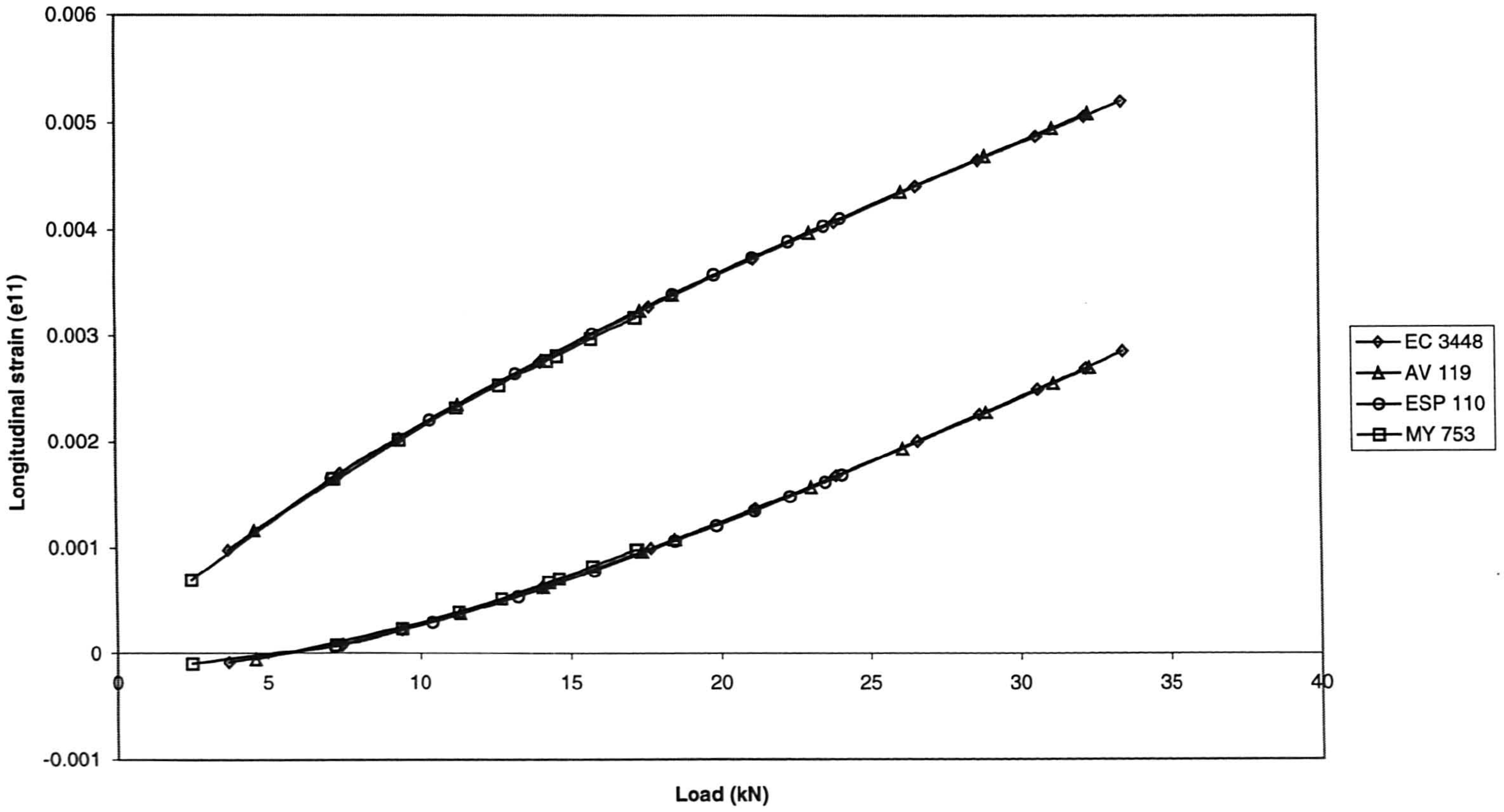

Figure 7.3 F.E prediction for the strain variation in the adherends for 25 mm overlap hard steel SLJs and various adhesives under tensile loading

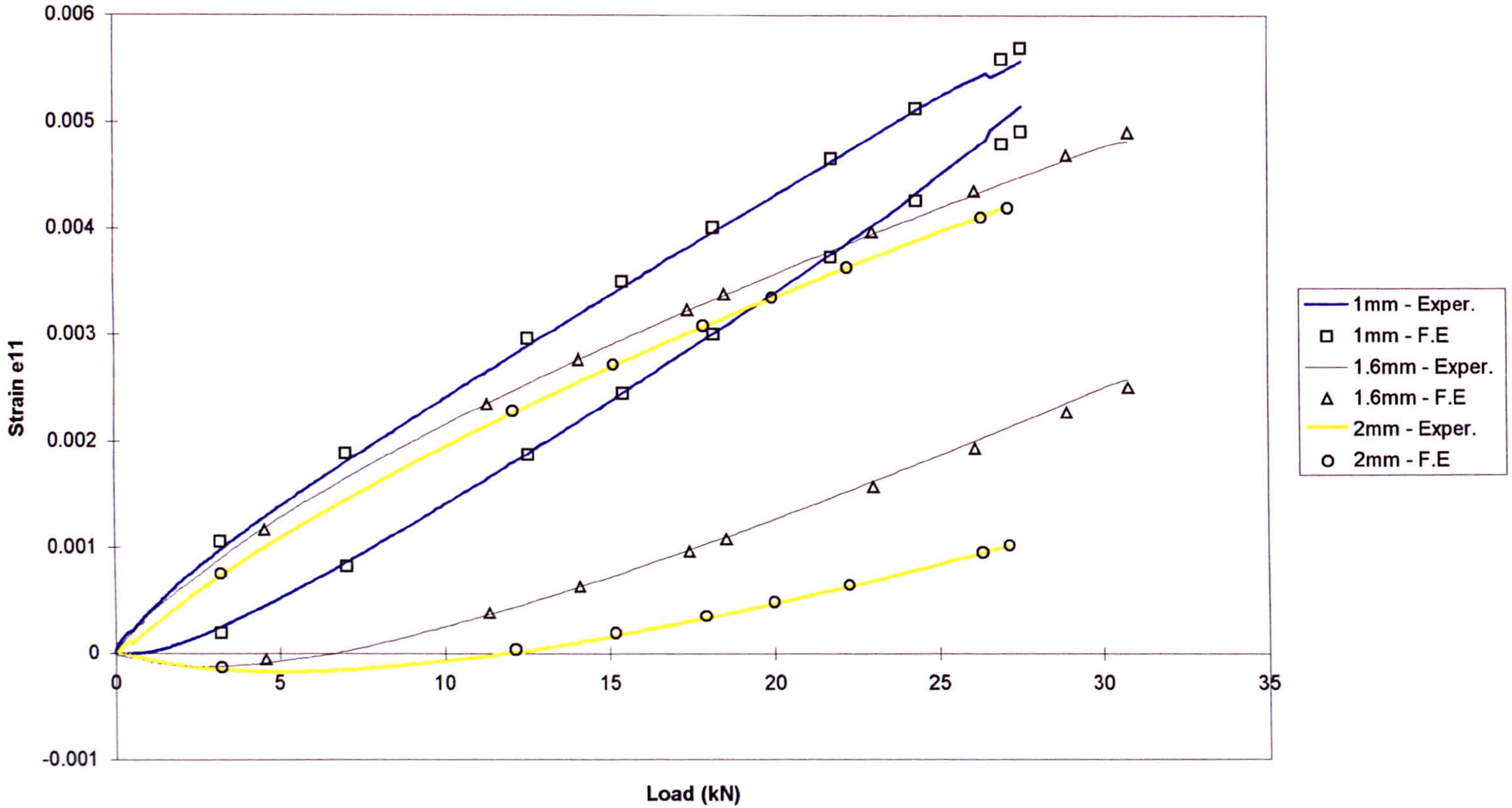

Figure 7.4 Experimental - F.E prediction correlation for the strain variation in the adherends for 25 mm overlap hard steel SLJs with AV 119 adhesive and various adherend thicknesses under tensile loading

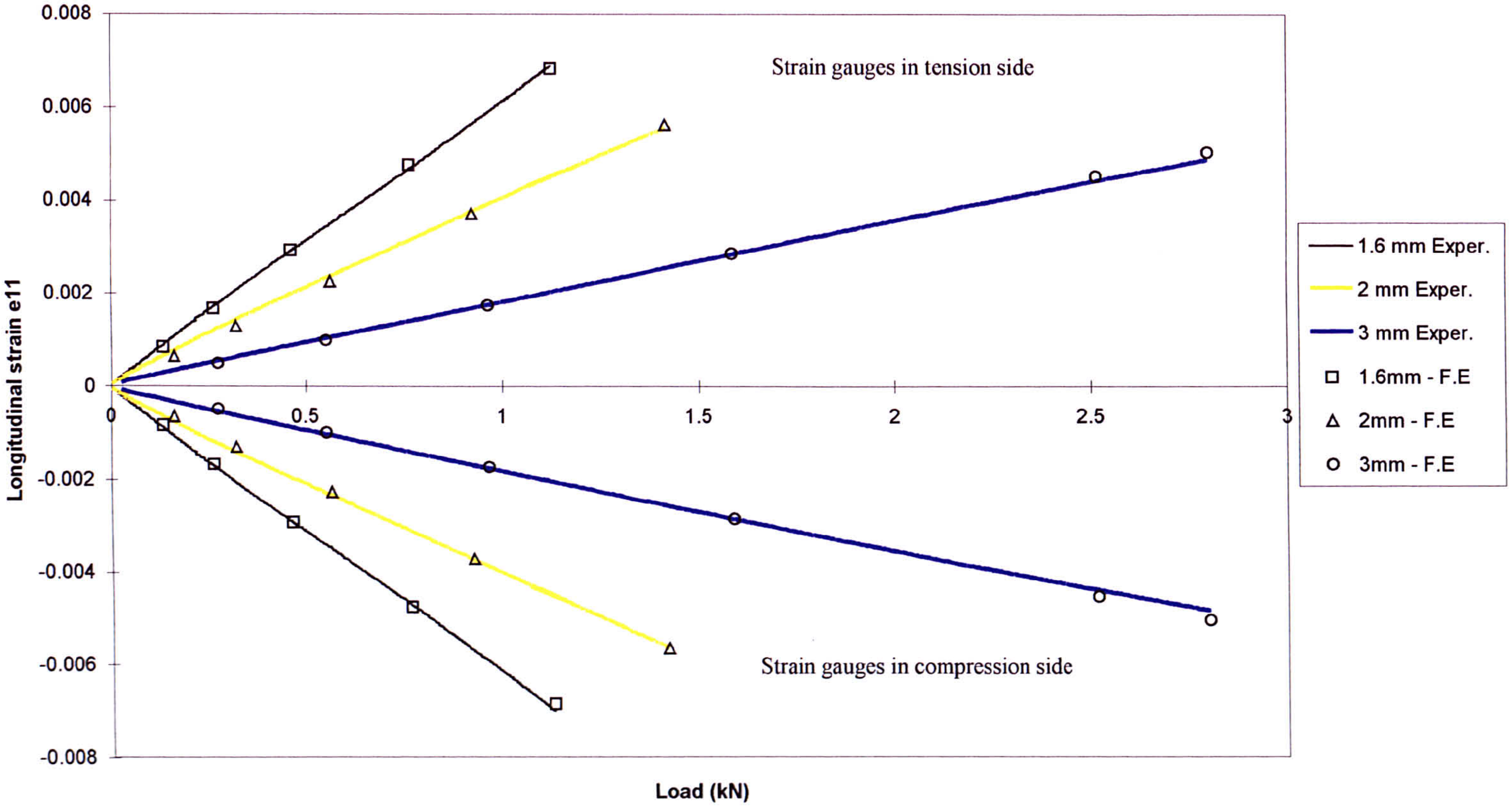

Figure 7.5 Experimental - F.E prediction correlation for the strain variation in the adherends for 25 mm overlap hard steel SLJs with AV 119 adhesive and various adherend thicknesses under 4 point bend loading

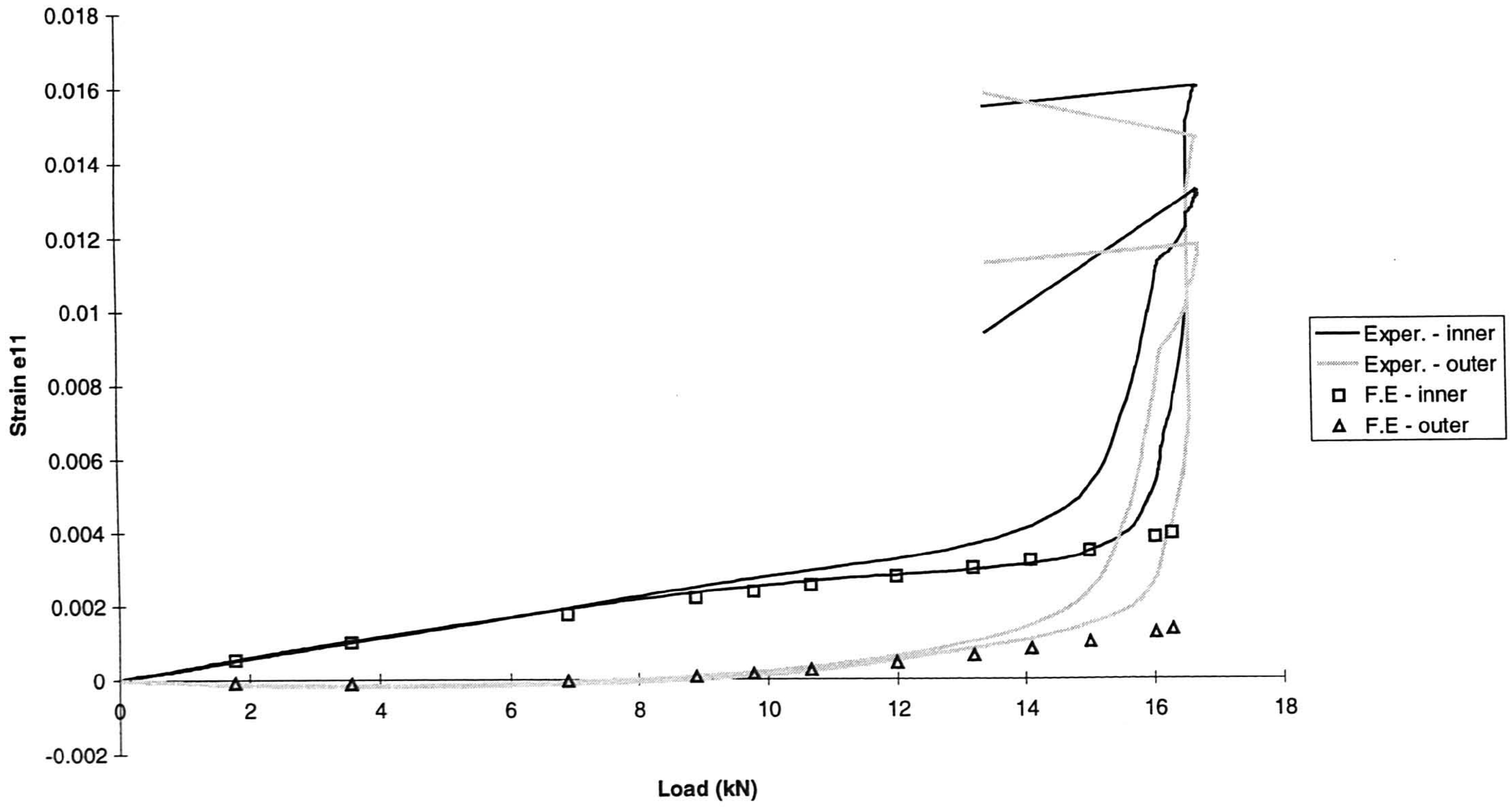

Figure 7.6 Experimental - F.E prediction correlation for the strain variation in the adherends for 12.5 mm overlap gauge steel SLJs with EC 3448 adhesive under tensile loading

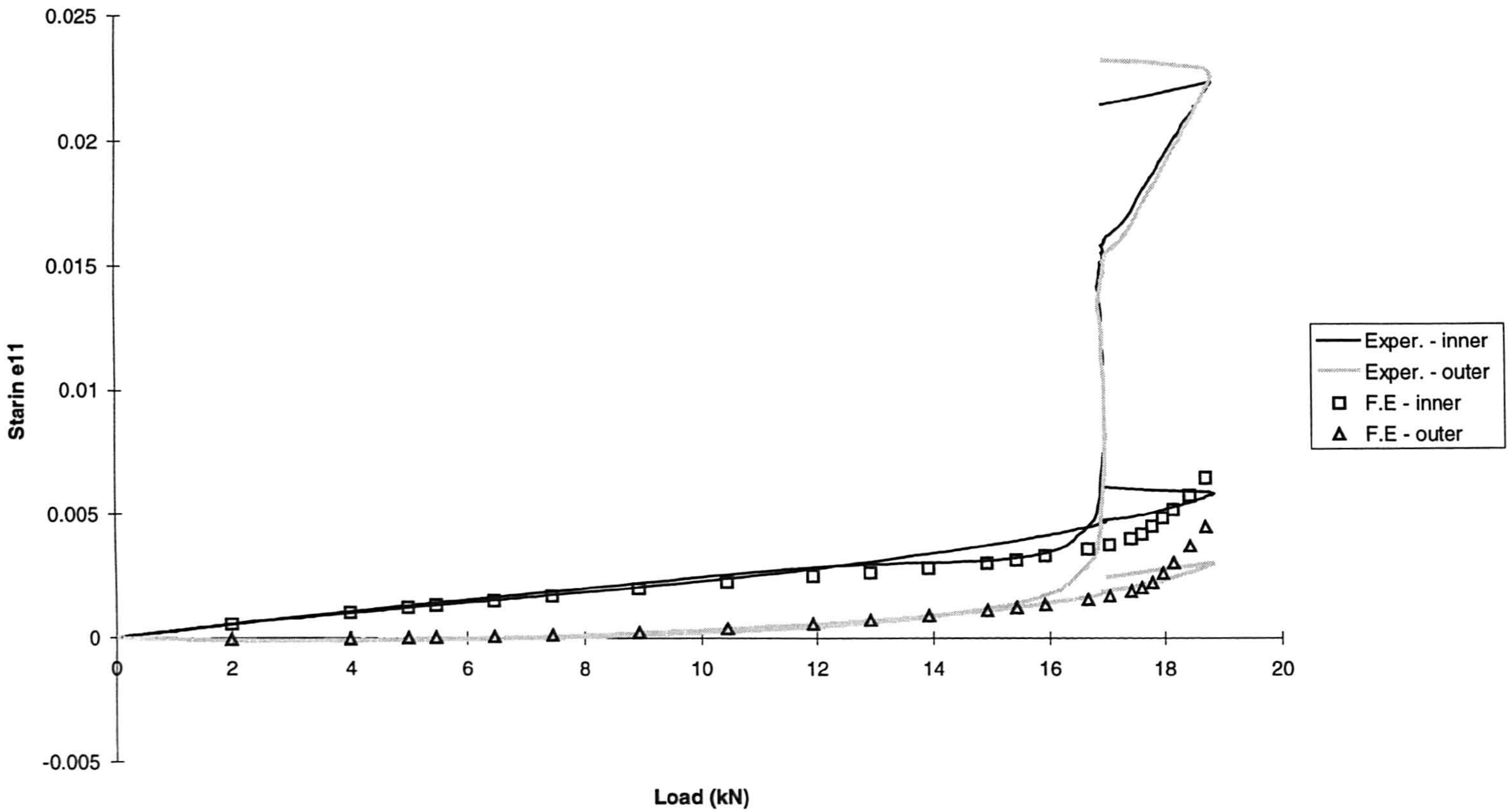

Figure 7.7 Experimental - F.E prediction correlation for the strain variation in the adherends for 20 mm overlap gauge steel SLJs with EC 3448 adhesive under tensile loading

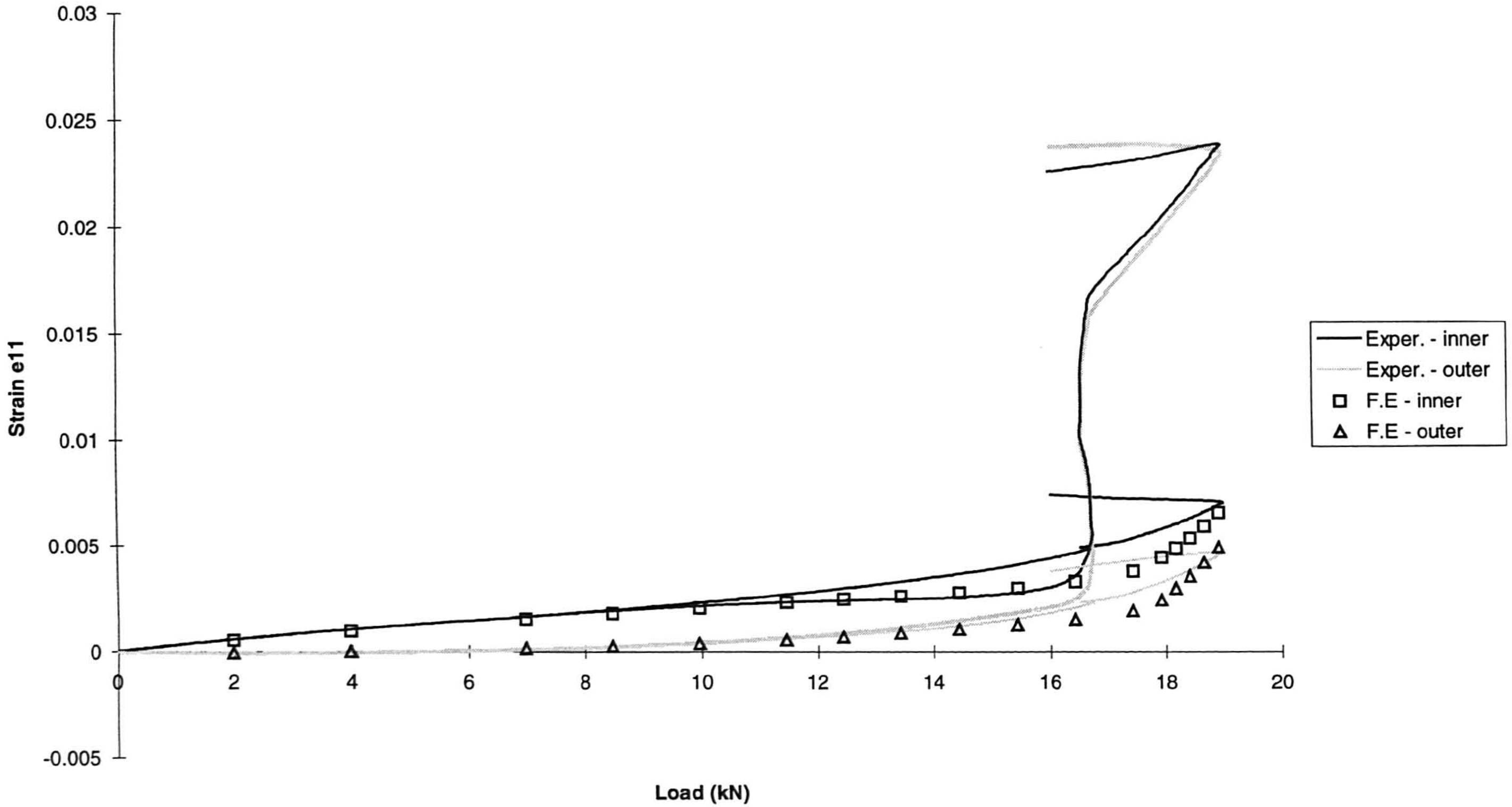

Figure 7.8 Experimental - F.E prediction correlation for the strain variation in the adherends for 25 mm overlap gauge steel SLJs with EC 3448 adhesive under tensile loading

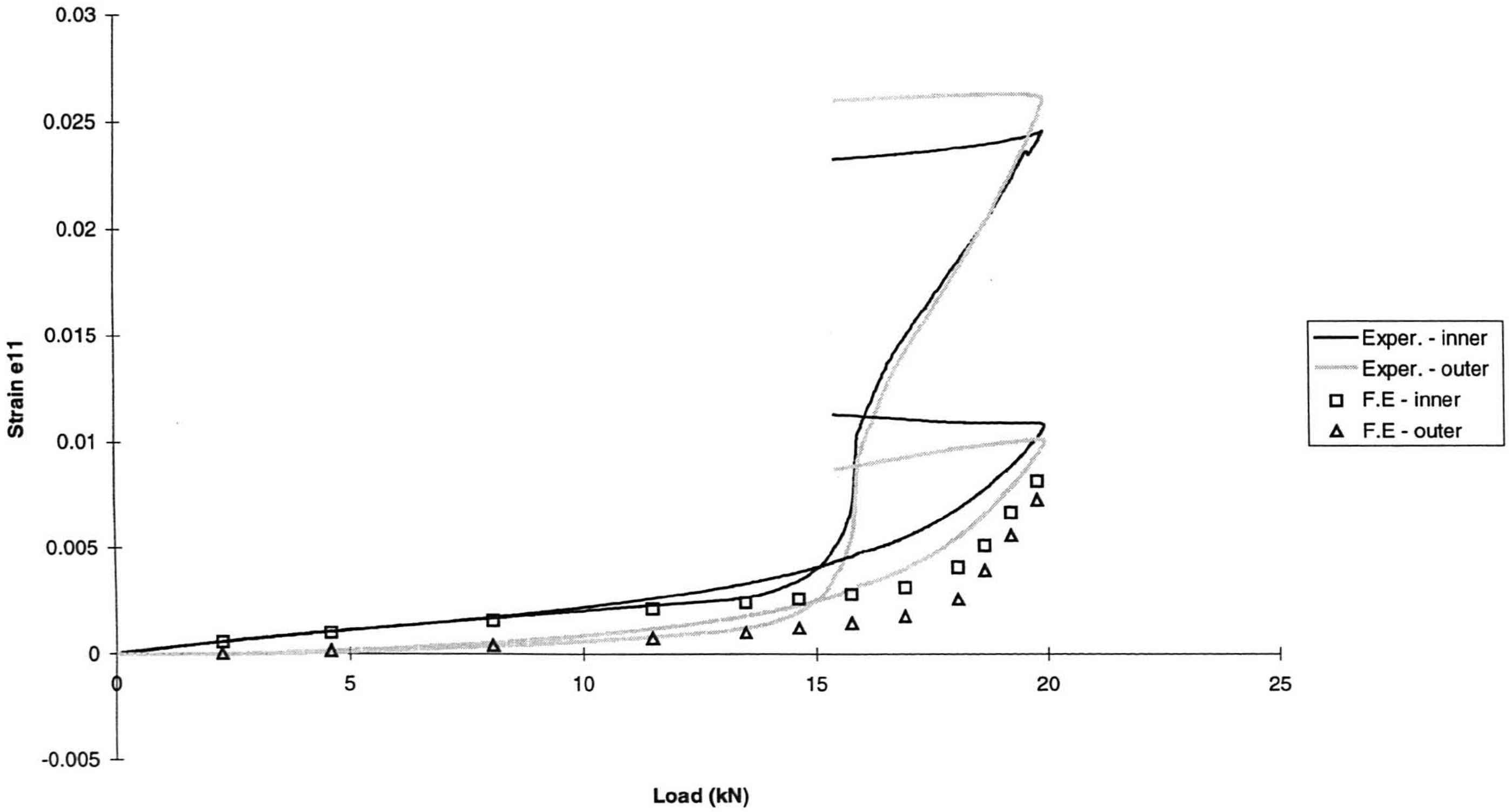

Figure 7.9 Experimental - F.E prediction correlation for the strain variation in the adherends for 40 mm overlap gauge steel SLJs with EC 3448 adhesive under tensile loading

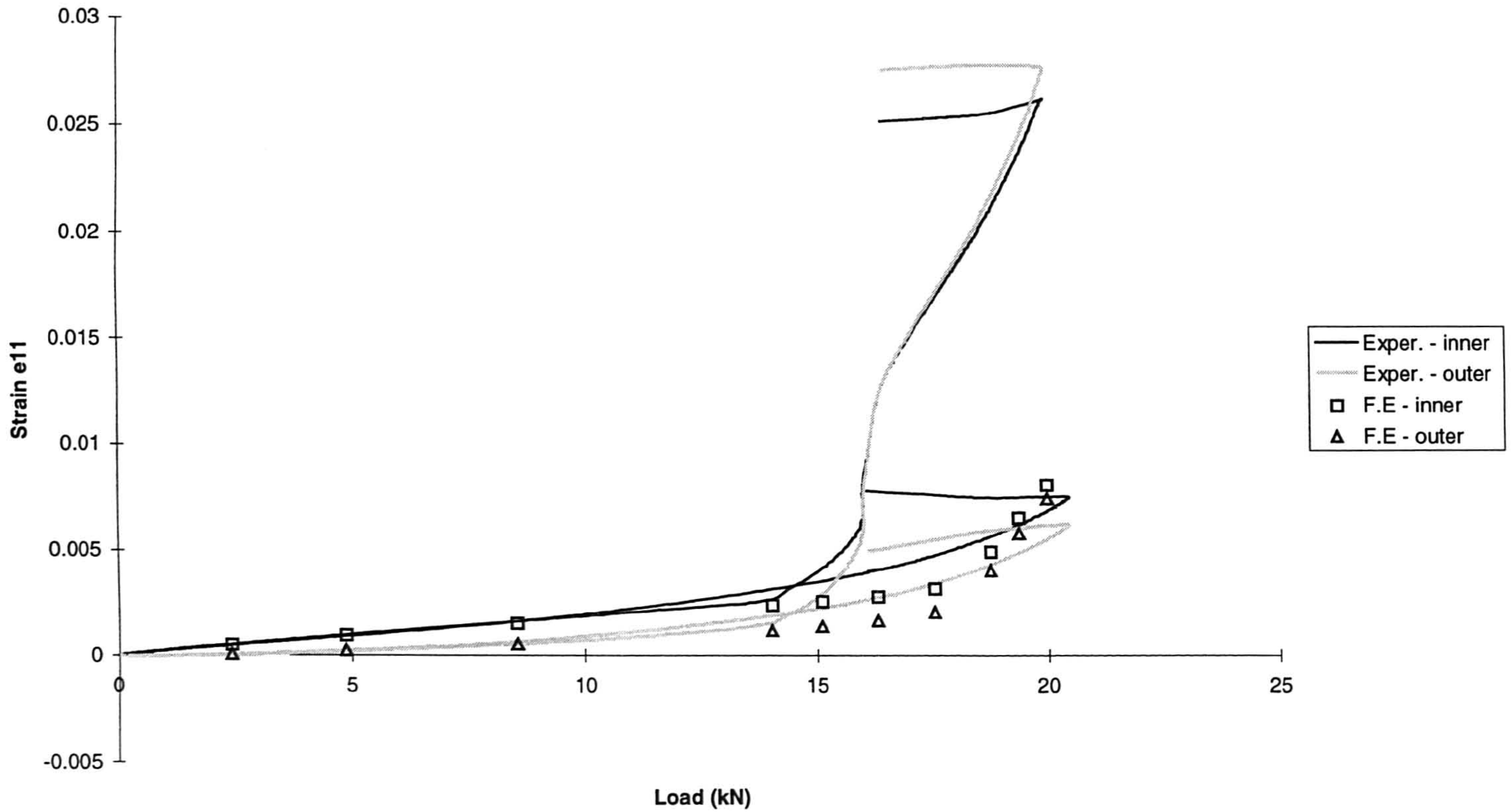

Figure 7.10 Experimental - F.E prediction correlation for the strain variation in the adherends for 60 mm overlap gauge steel SLJs with EC 3448 adhesive under tensile loading

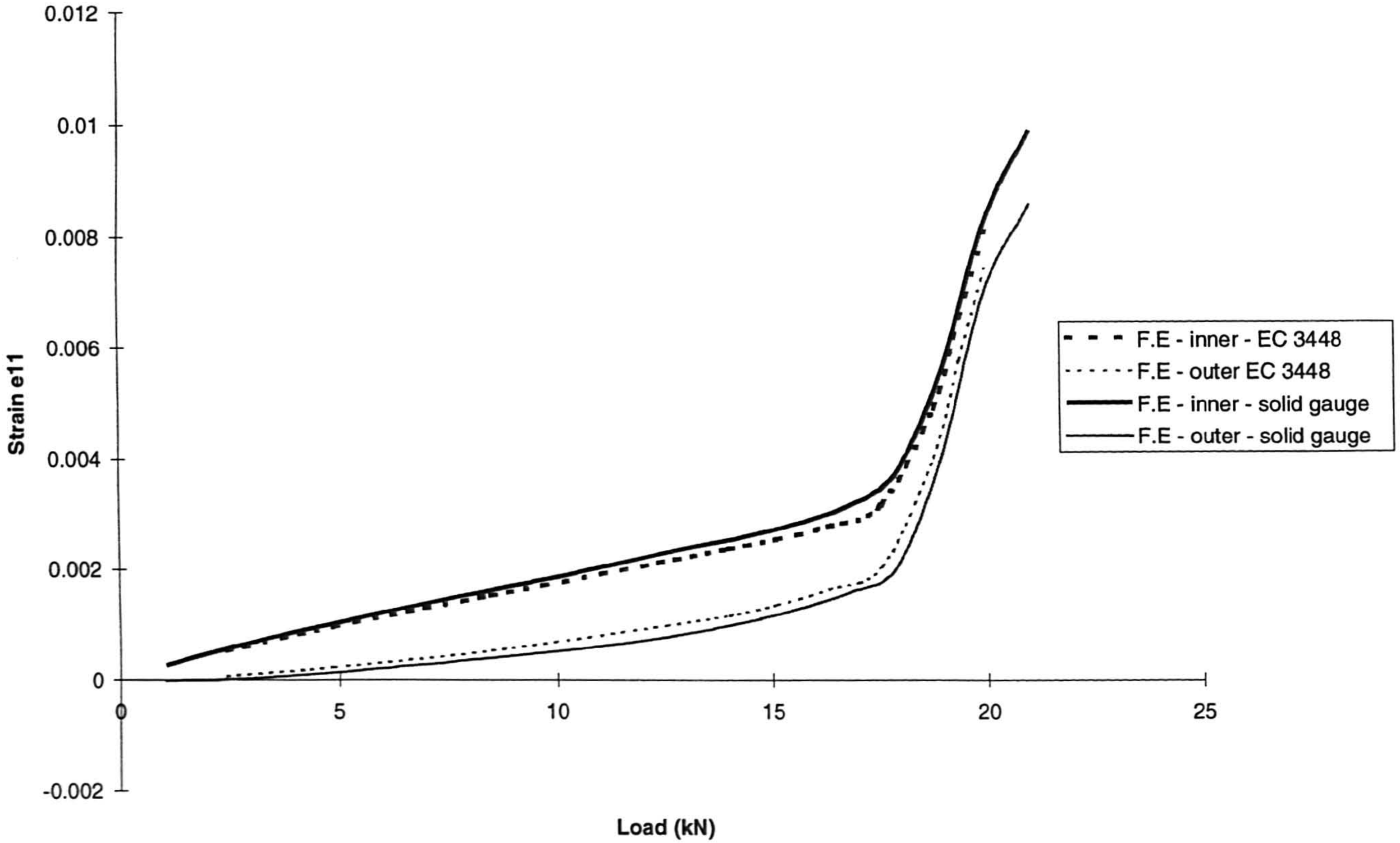

Figure 7.11 F.E prediction comparison of the strain variation in the adherends for 60 mm overlap gauge steel SLJs between EC 3448 adhesive and "Solid gauge" joint under tensile loading

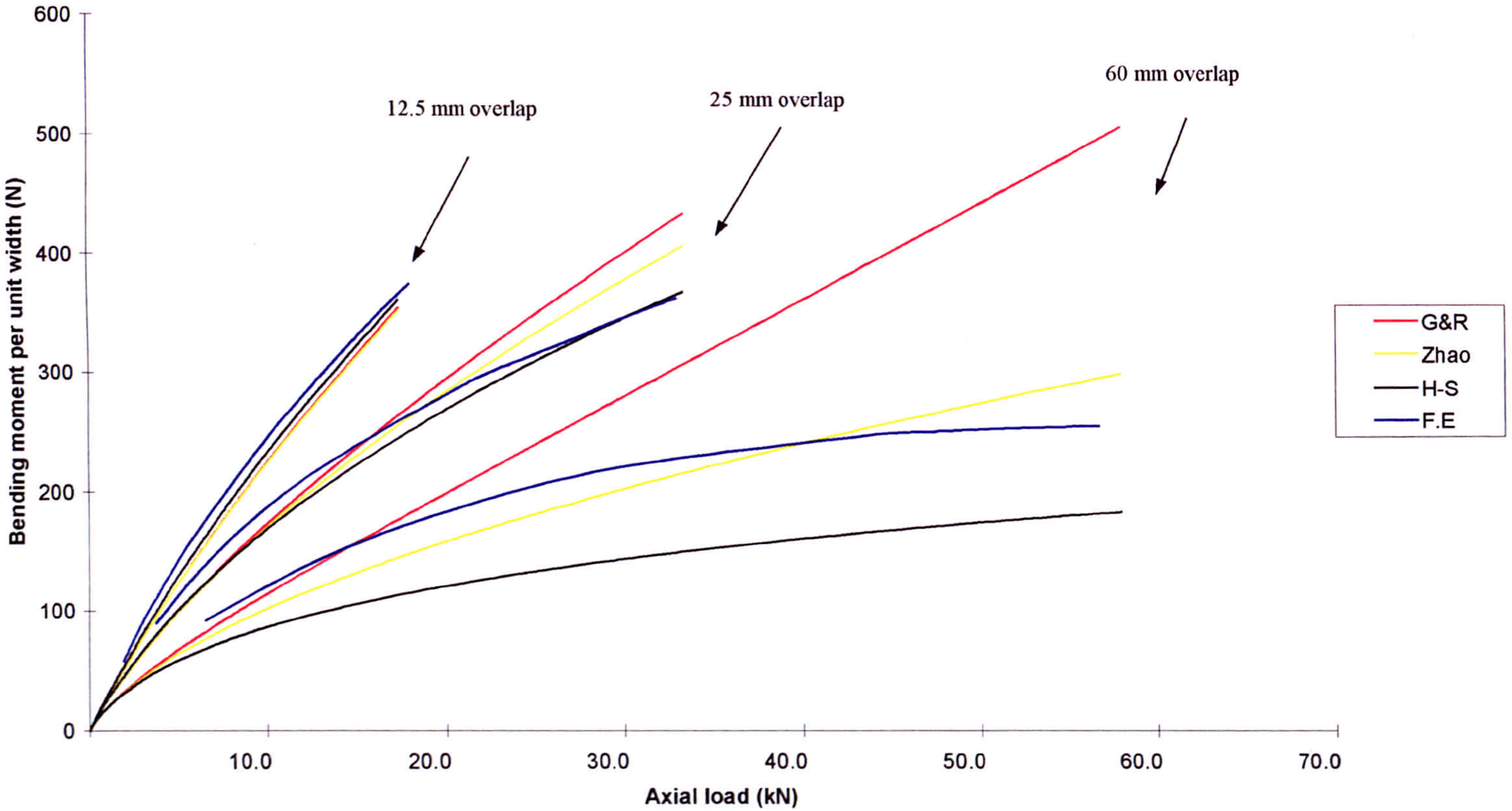

Figure 7.12 Comparison of bending moment variation at the overlap edges for 1.6 mm thick hard steel adherend SLJs with AV 119 adhesive and various overlap lengths between F.E analysis and other analytical solutions

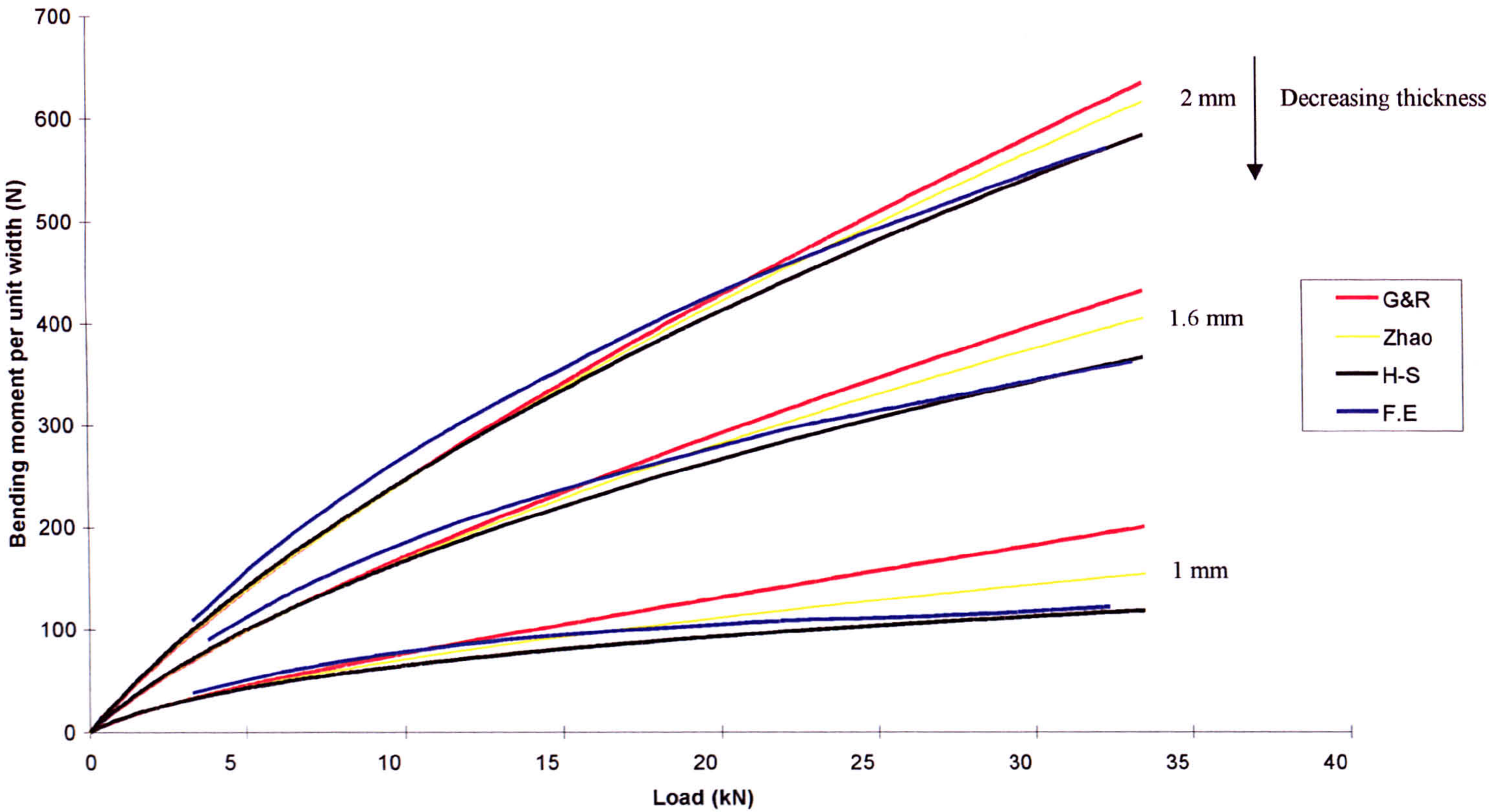

Figure 7.13 Comparison of bending moment variation at the overlap edges for 25 mm overlap hard steel SLJs with AV 119 adhesive and various adherend thicknesses between F.E analysis and other analytical solutions

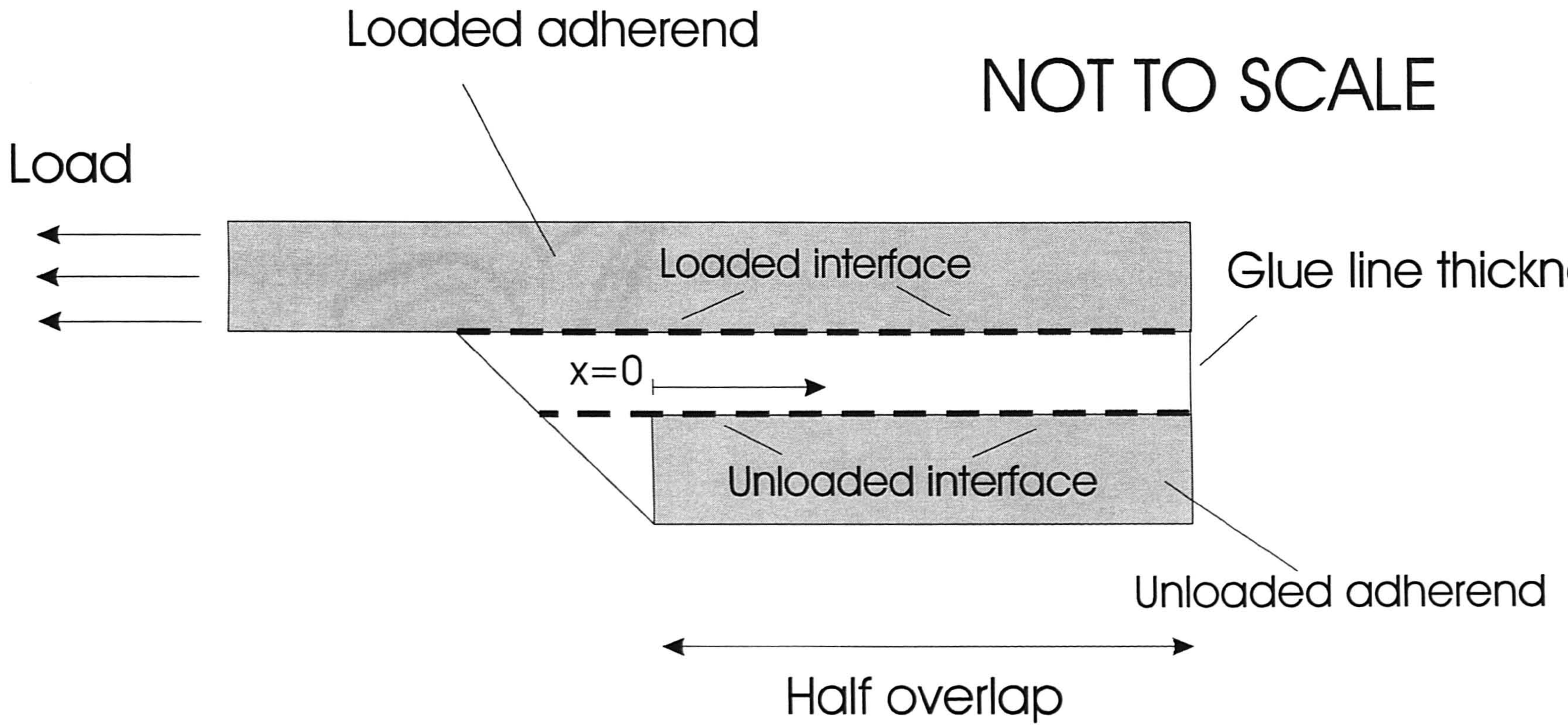

Figure 7.14 Definition of interfaces for plotting of F.E results

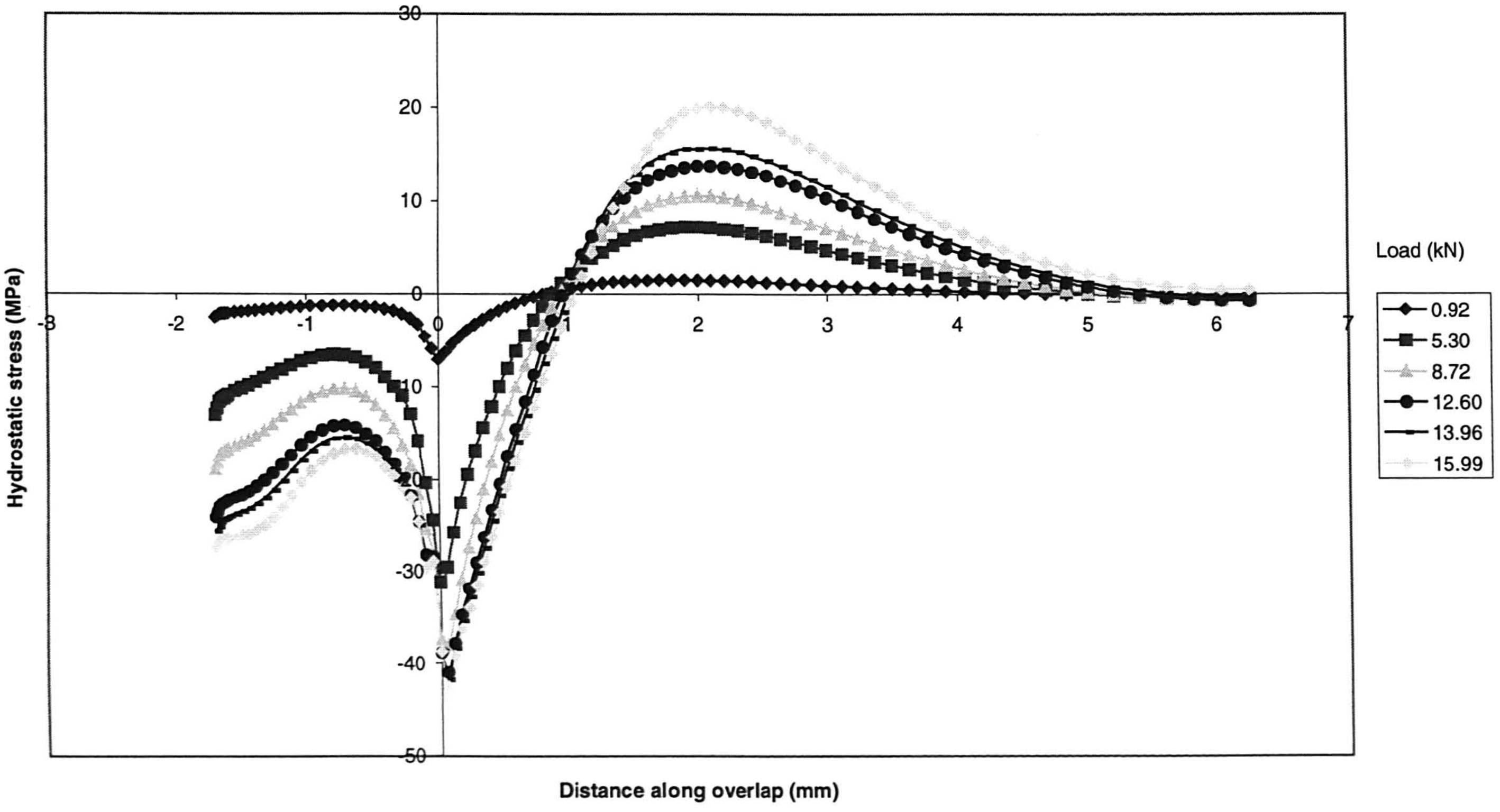

Figure 7.15 Variation of hydrostatic stress along the overlap length for the loaded interface - hard steel - AV 119 adhesive - 12.5 mm overlap - 1.6 mm thick adherends - tensile loading

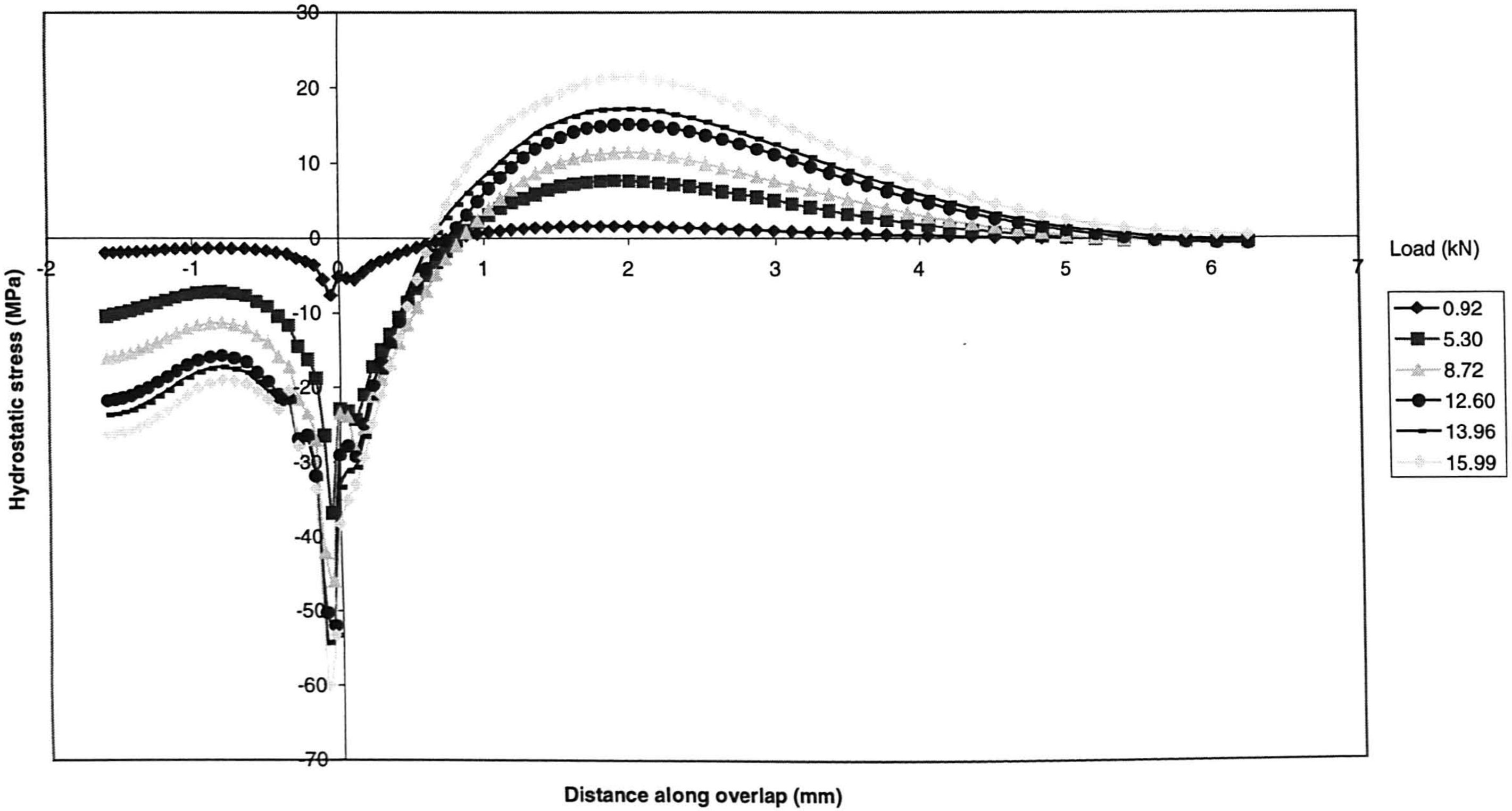

Figure 7.16 Variation of hydrostatic stress along the overlap length for the unloaded interface - hard steel - AV 119 adhesive - 12.5 mm overlap - 1.6 mm thick adherends - tensile loading

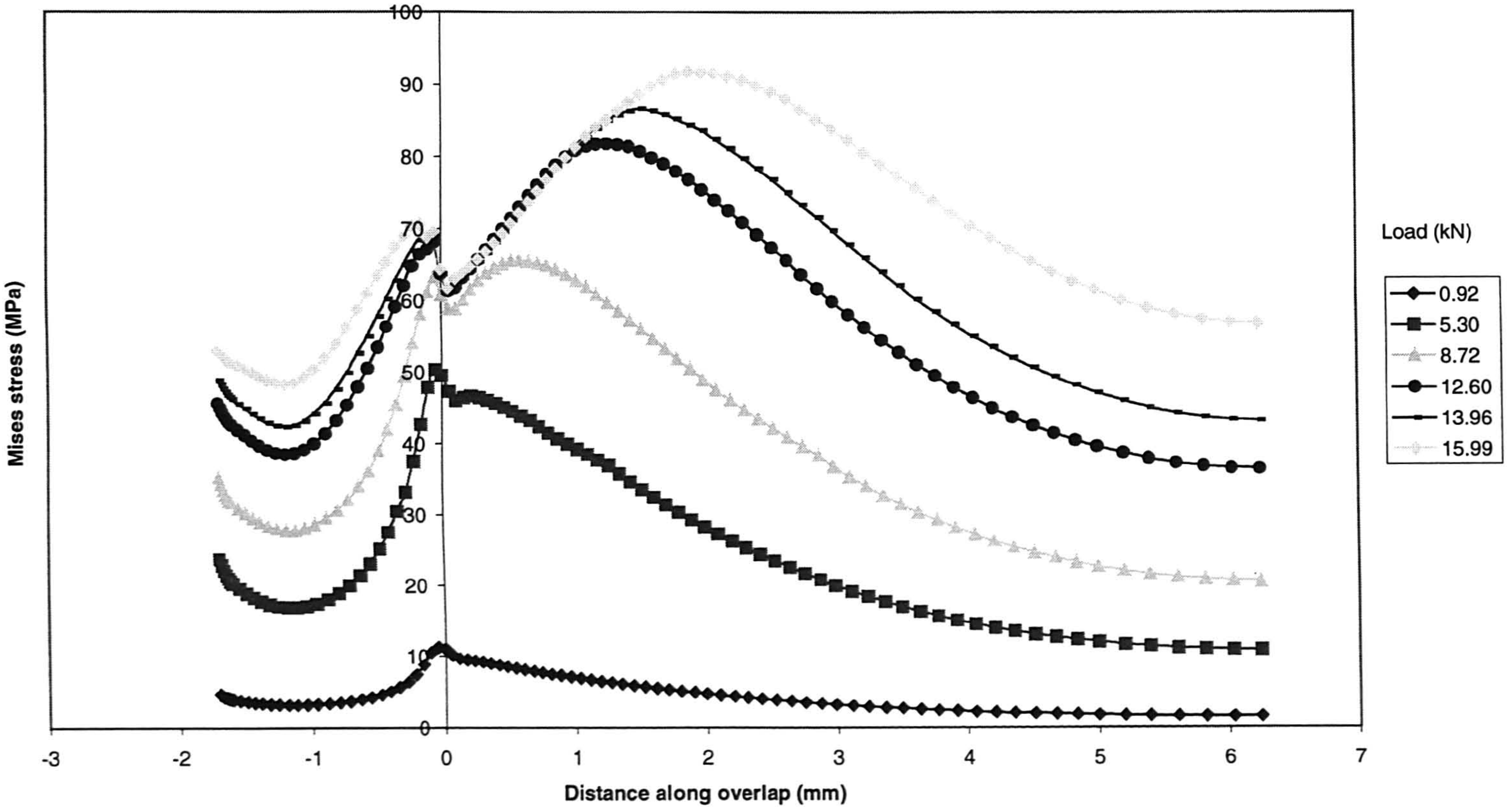

Figure 7.17 Variation of Mises stress along the overlap length for the loaded interface - hard steel - AV 119 adhesive - 12.5 mm overlap - 1.6 mm thick adherends - tensile loading

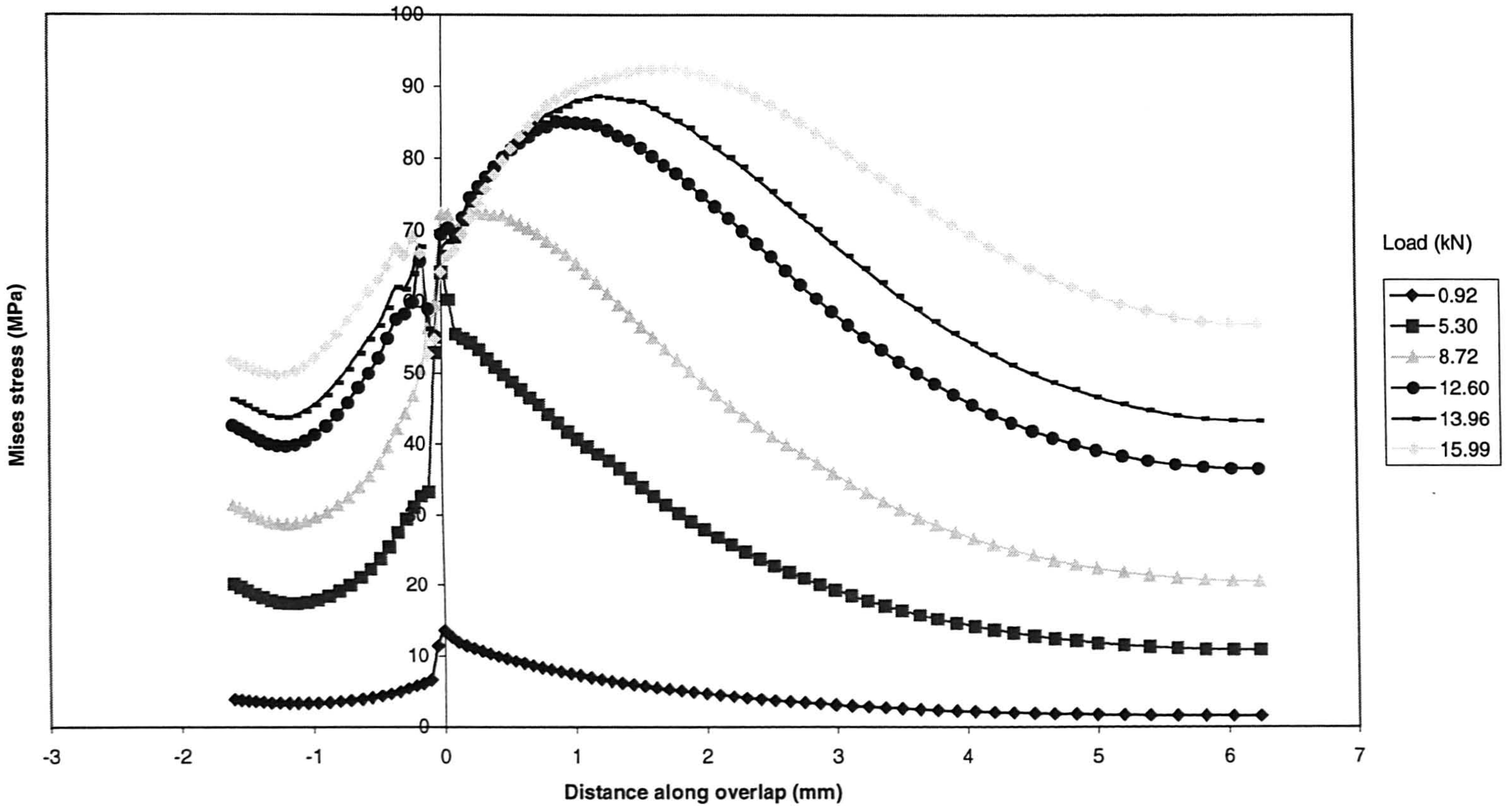

Figure 7.18 Variation of Mises stress along the overlap length for the unloaded interface - hard steel - AV 119 adhesive - 12.5 mm overlap - 1.6 mm thick adherends - tensile loading

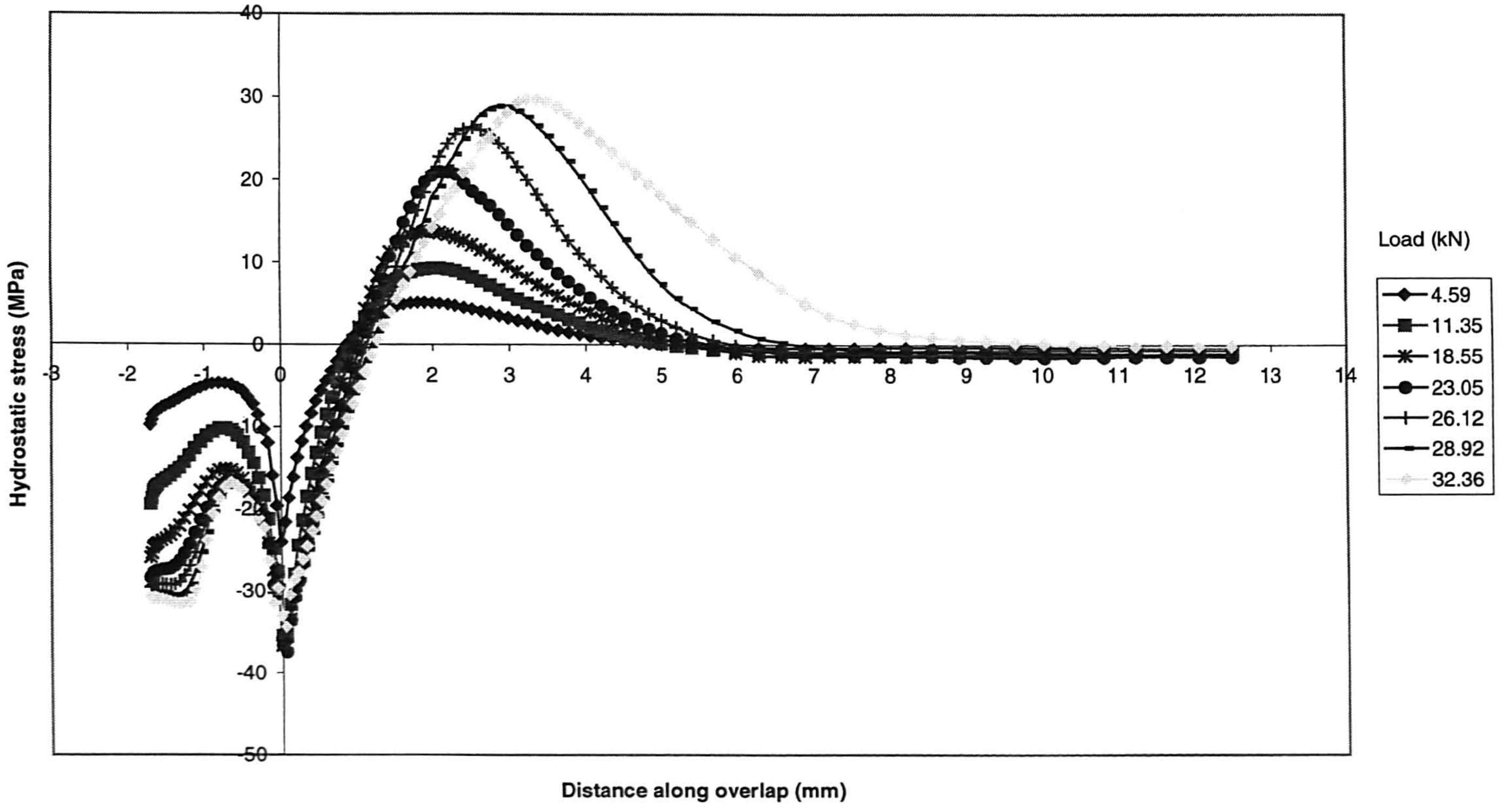

Figure 7.19 Variation of hydrostatic stress along the overlap length for the loaded interface - hard steel - AV 119 adhesive - 25 mm overlap - 1.6 mm thick adherends - tensile loading

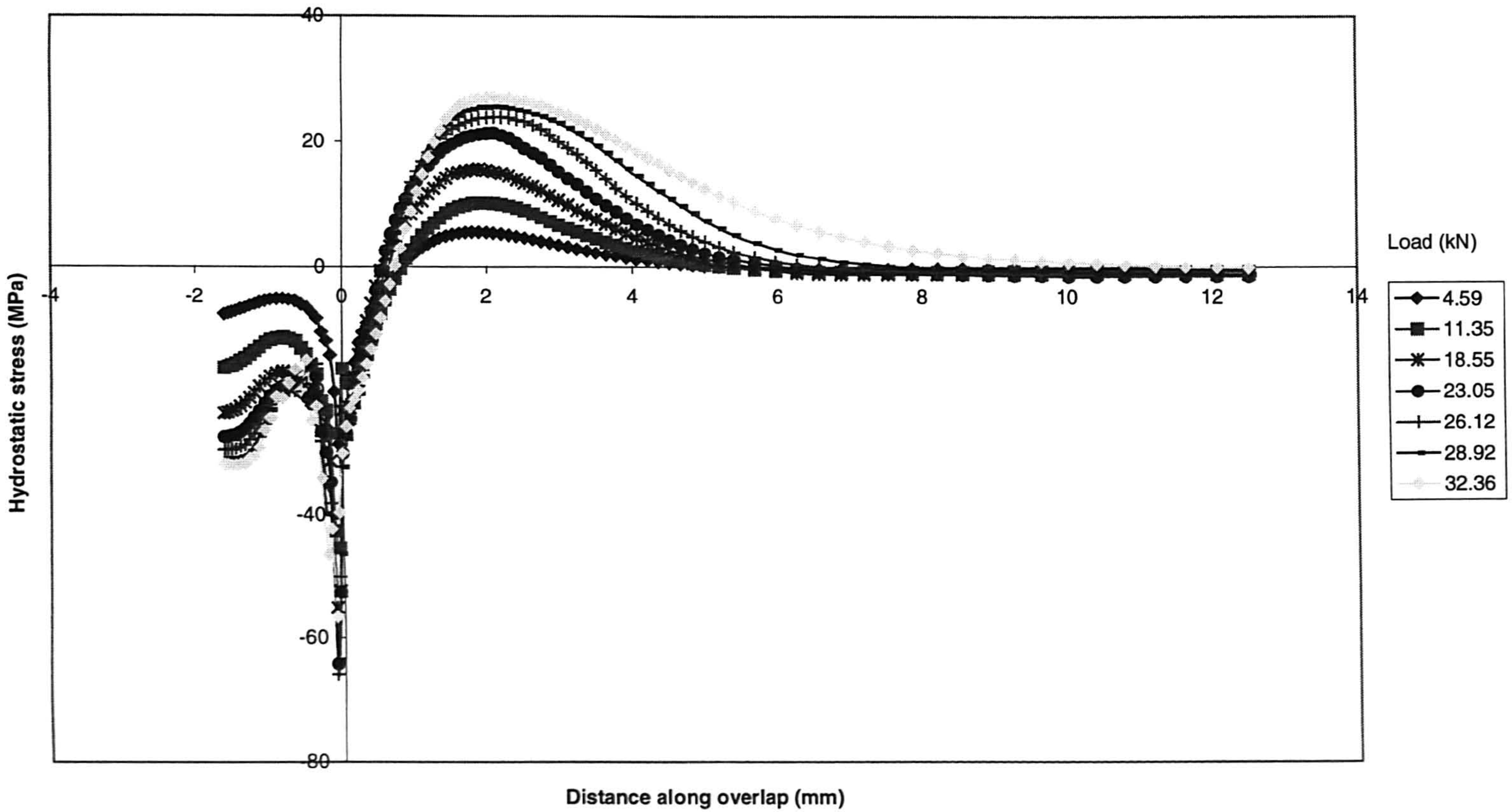

Figure 7.20 Variation of hydrostatic stress along the overlap length for the unloaded interface - hard steel - AV 119 adhesive - 25 mm overlap - 1.6 mm thick adherends - tensile loading

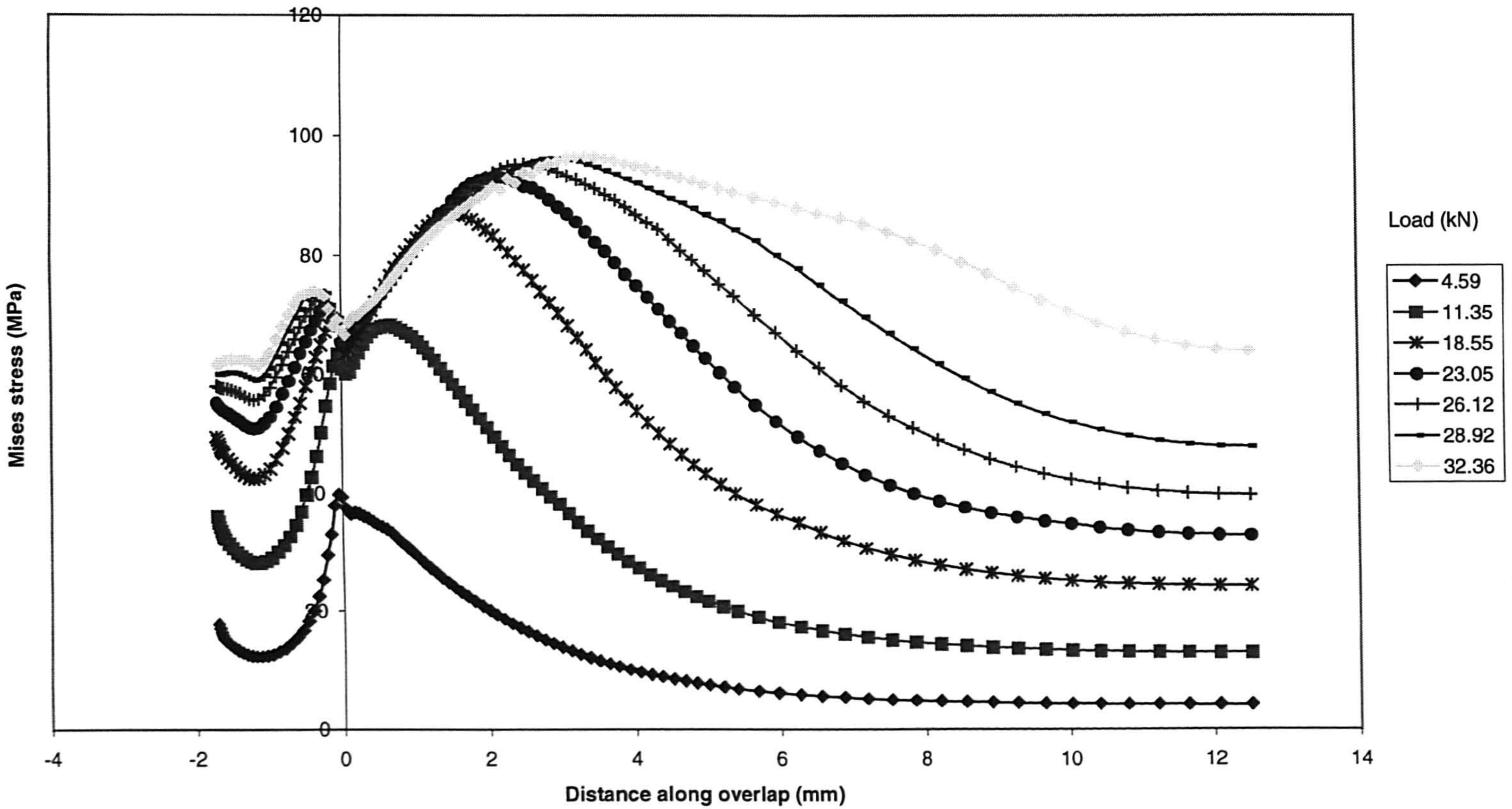

Figure 7.21 Variation of Mises stress along the overlap length for the loaded interface - hard steel - AV 119 adhesive - 25 mm overlap - 1.6 mm thick adherends - tensile loading

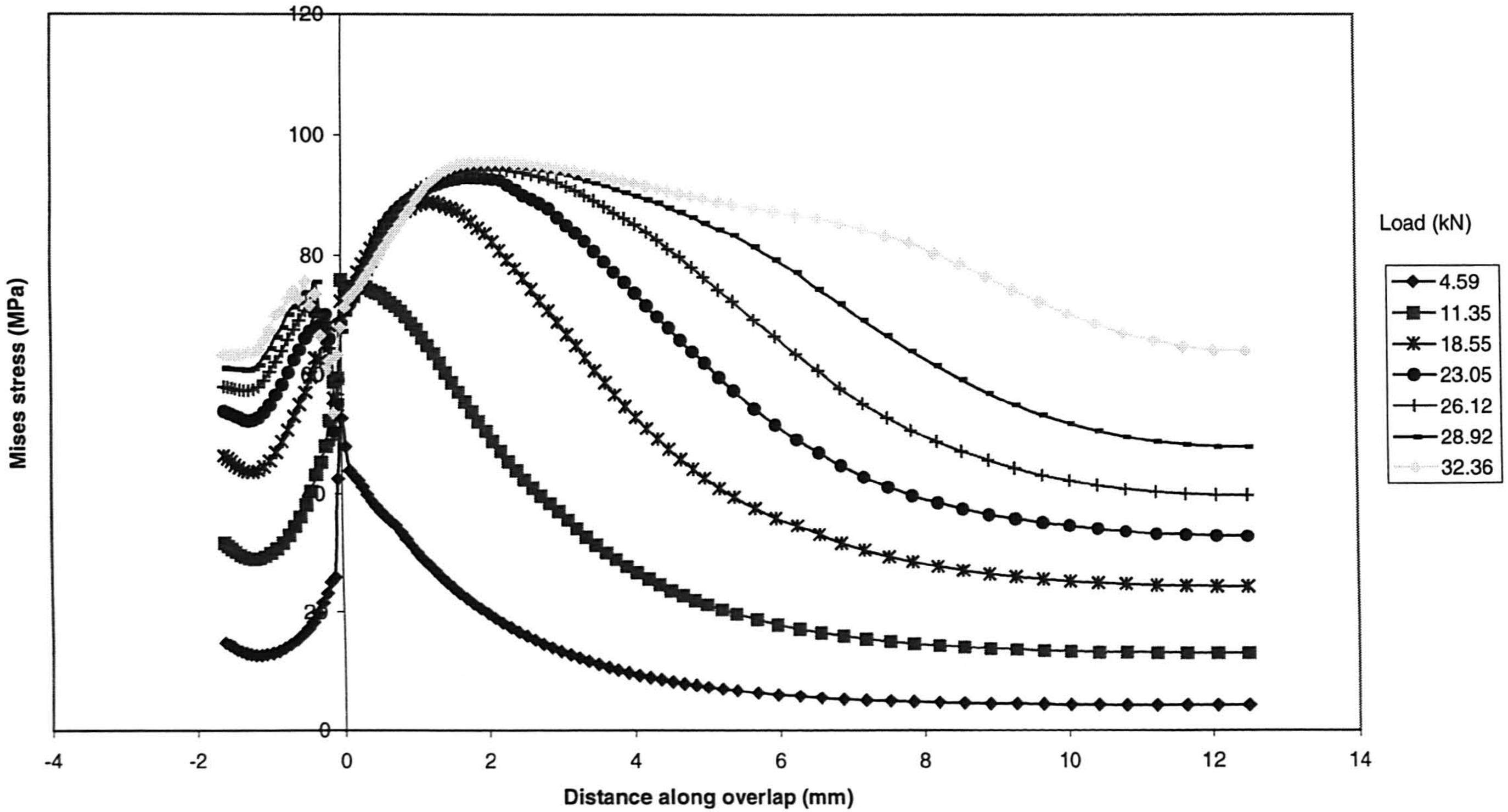

Figure 7.22 Variation of Mises stress along the overlap length for the unloaded interface - hard steel - AV 119 adhesive - 25 mm overlap - 1.6 mm thick adherends - tensile loading

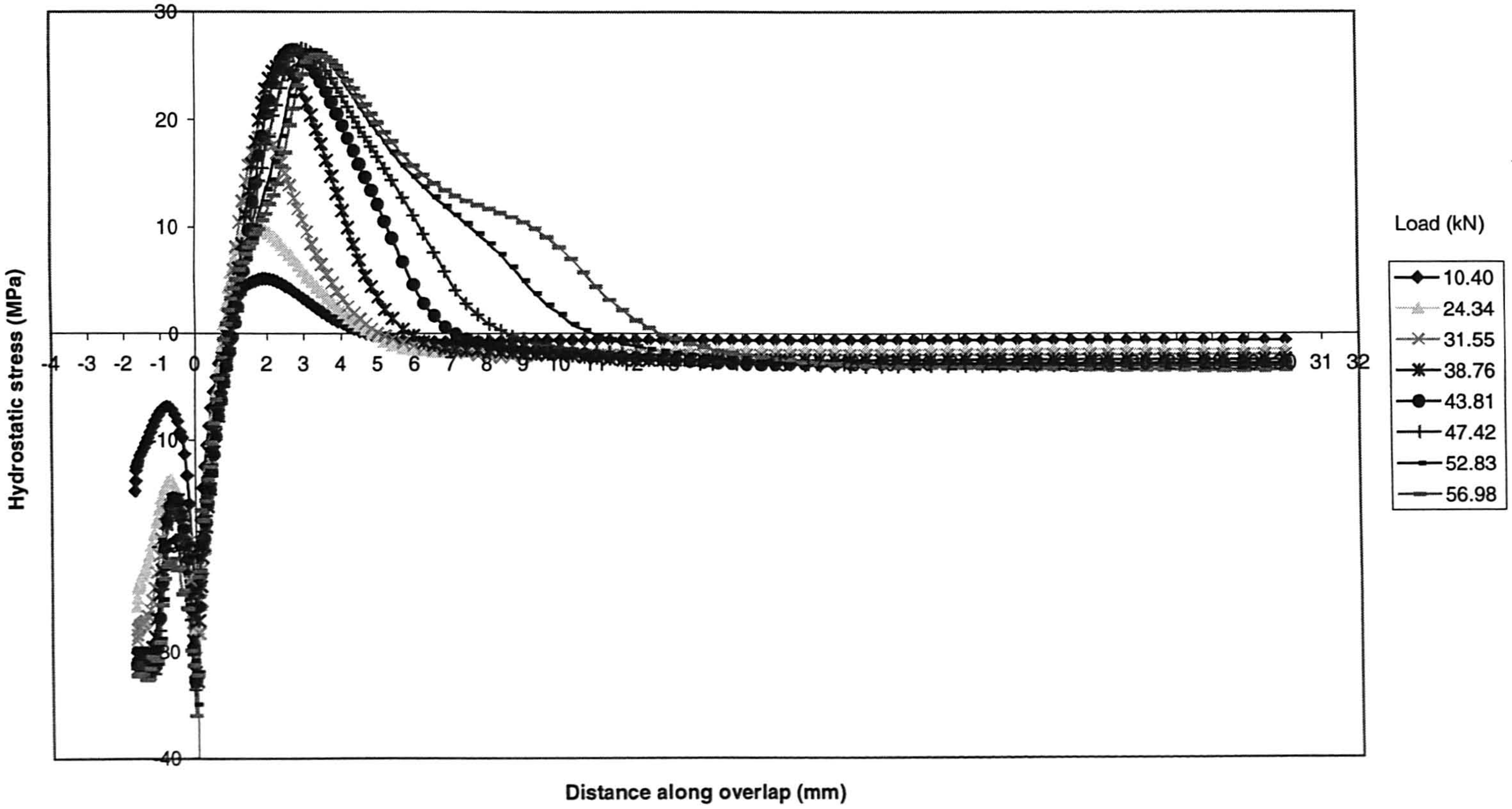

Figure 7.23 Variation of hydrostatic stress along the overlap length for the loaded interface - hard steel - AV 119 adhesive - 60 mm overlap - 1.6 mm thick adherends - tensile loading

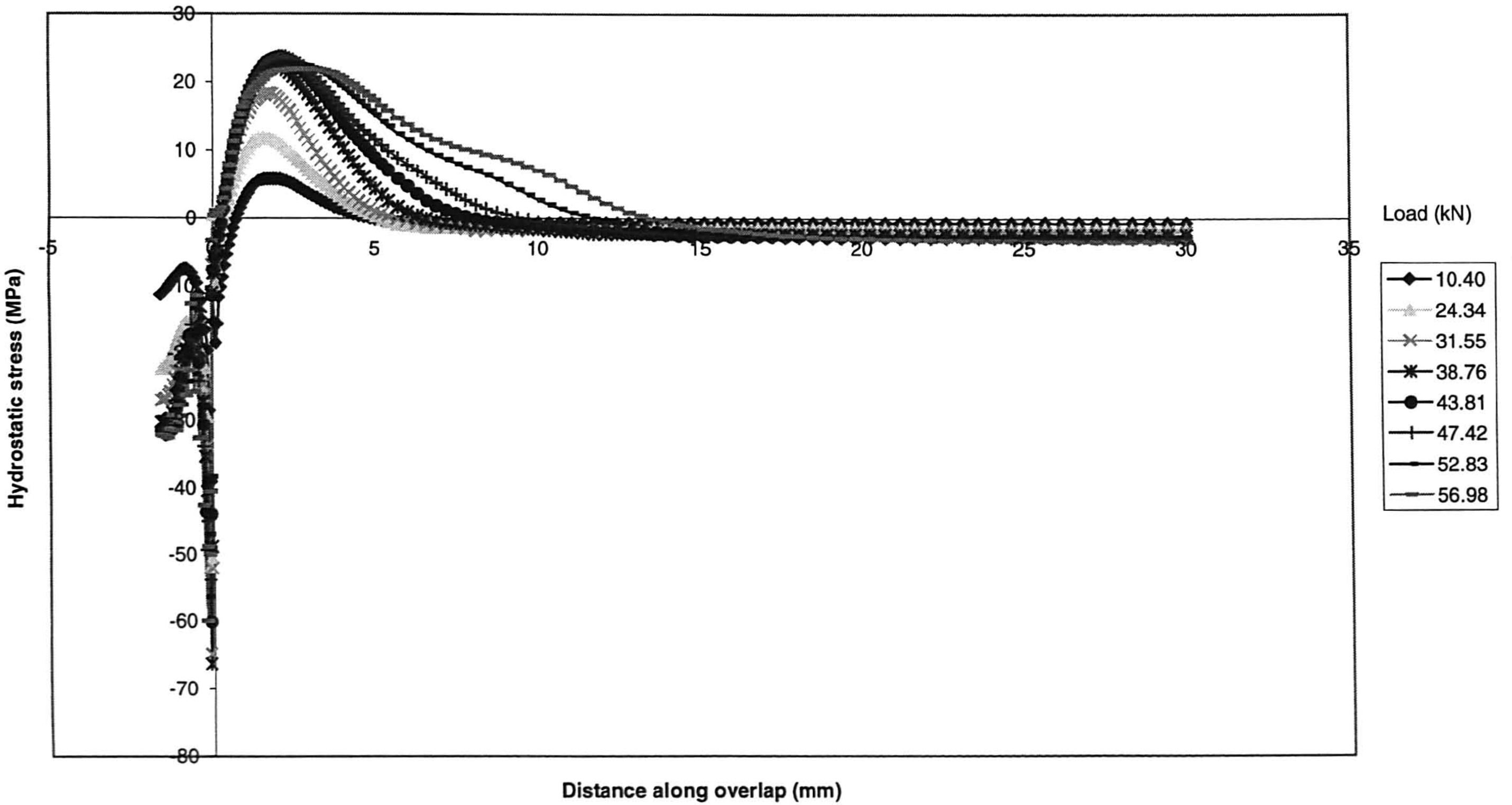

Figure 7.24 Variation of hydrostatic stress along the overlap length for the unloaded interface - hard steel - AV 119 adhesive - 60 mm overlap - 1.6 mm thick adherends - tensile loading

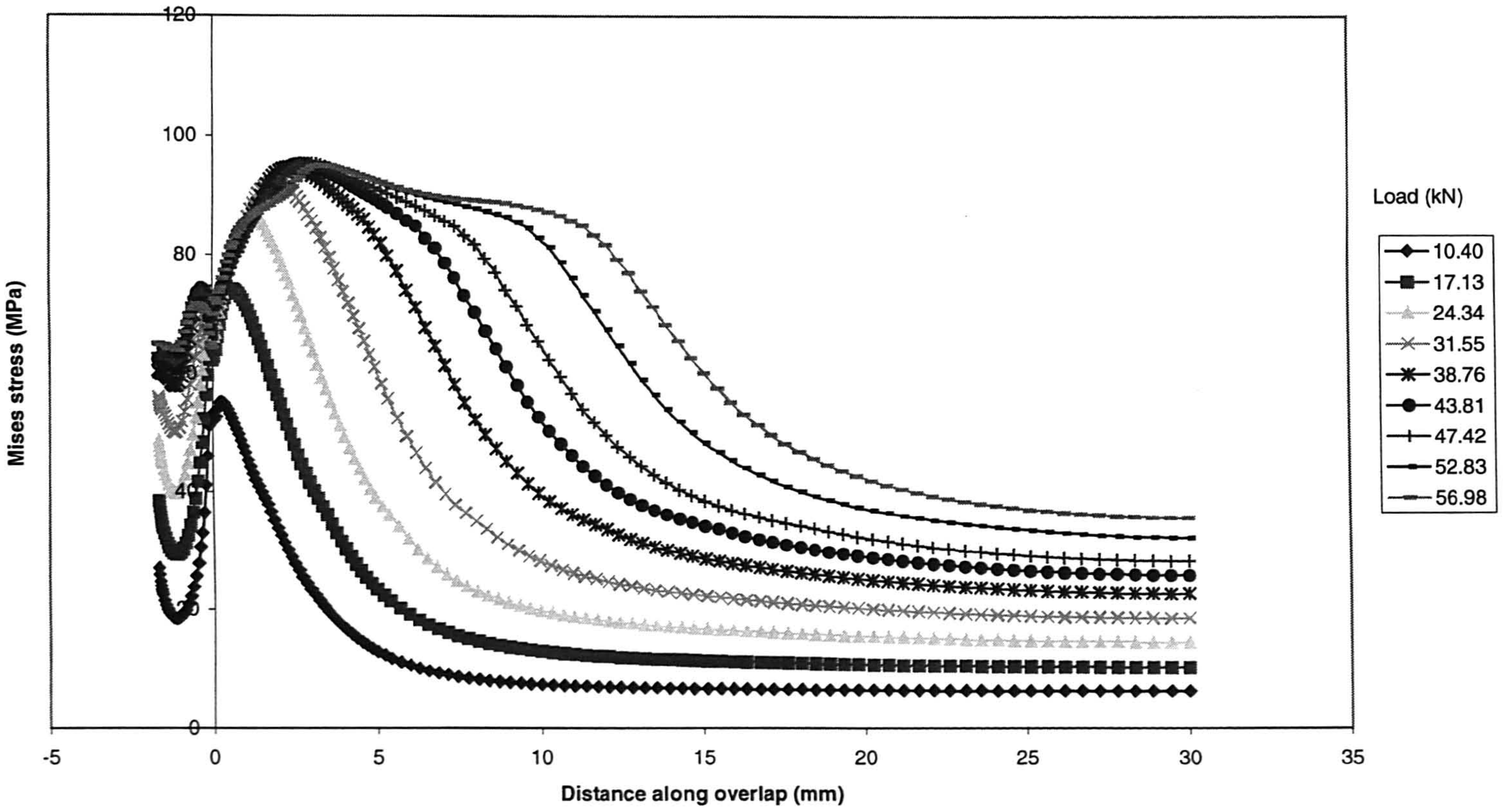

Figure 7.25 Variation of Mises stress along the overlap length for the loaded interface - hard steel - AV 119 adhesive - 25 mm overlap - 1.6 mm thick adherends - tensile loading

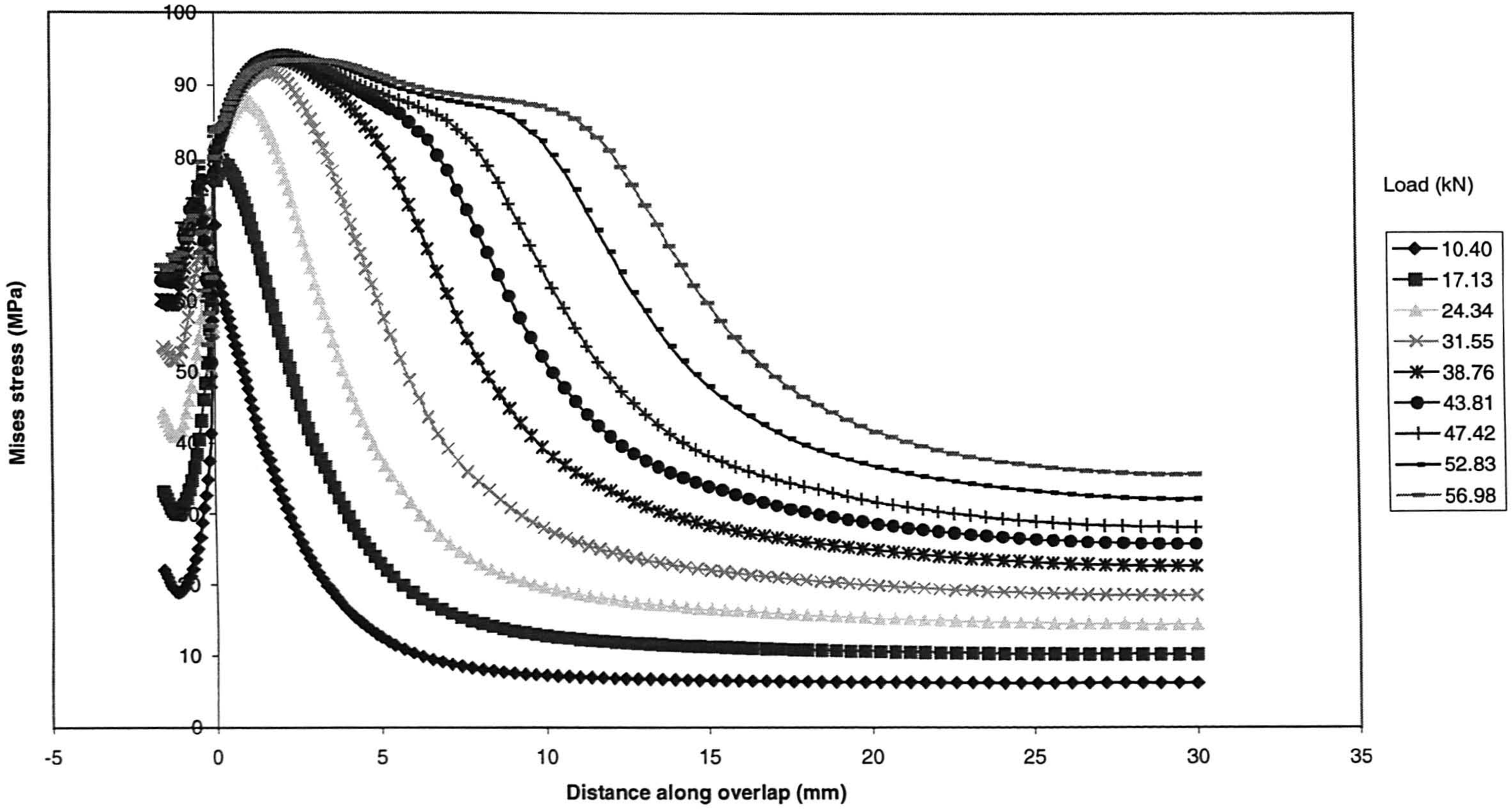

Figure 7.26 Variation of Mises stress along the overlap length for the unloaded interface - hard steel - AV 119 adhesive - 60 mm overlap - 1.6 mm thick adherends - tensile loading

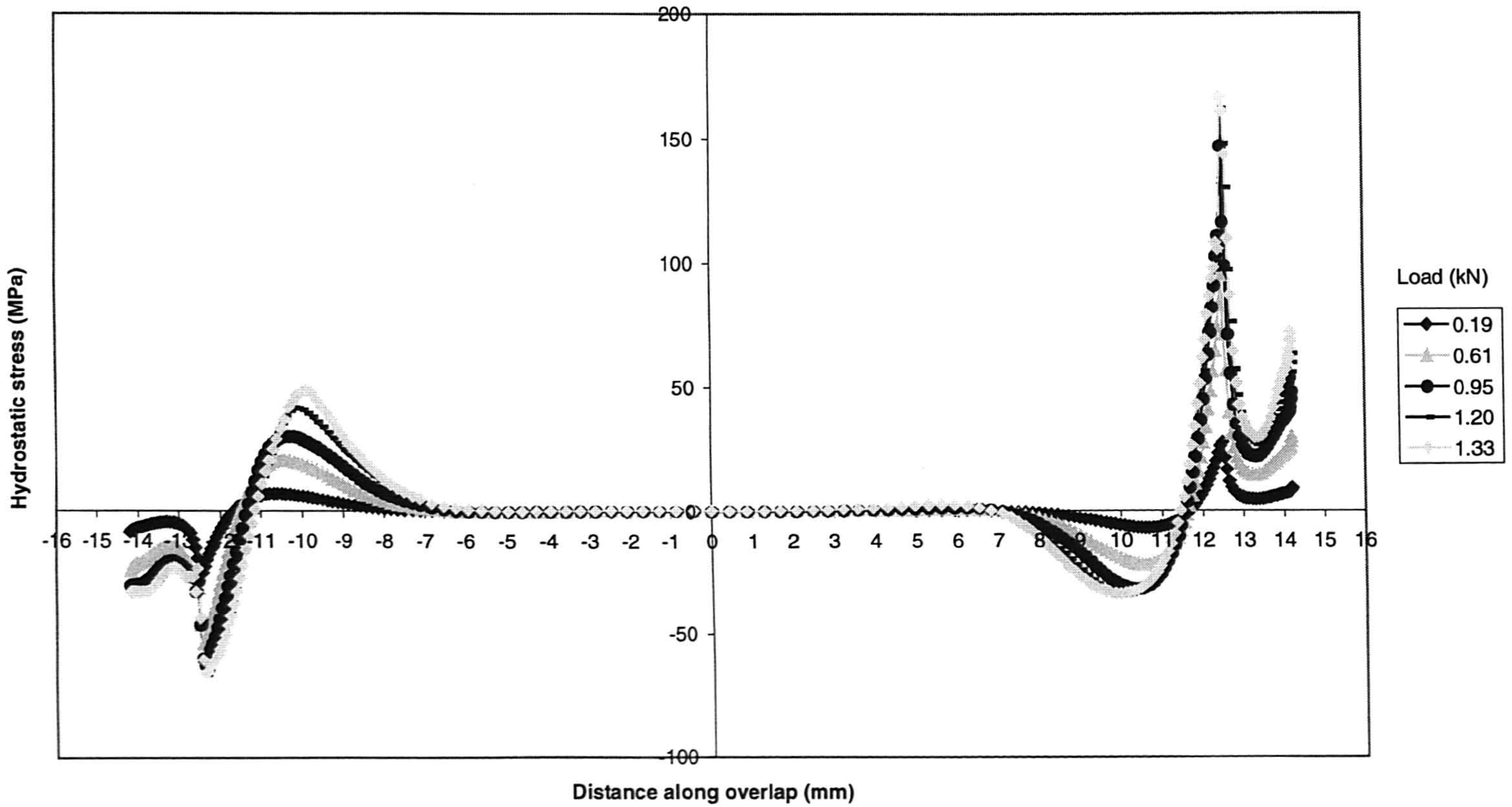

Figure 7.27 Variation of hydrostatic stress along the overlap length for the loaded interface - hard steel - AV 119 adhesive - 25 mm overlap - 1.6 mm thick adherends - 4 point bend loading

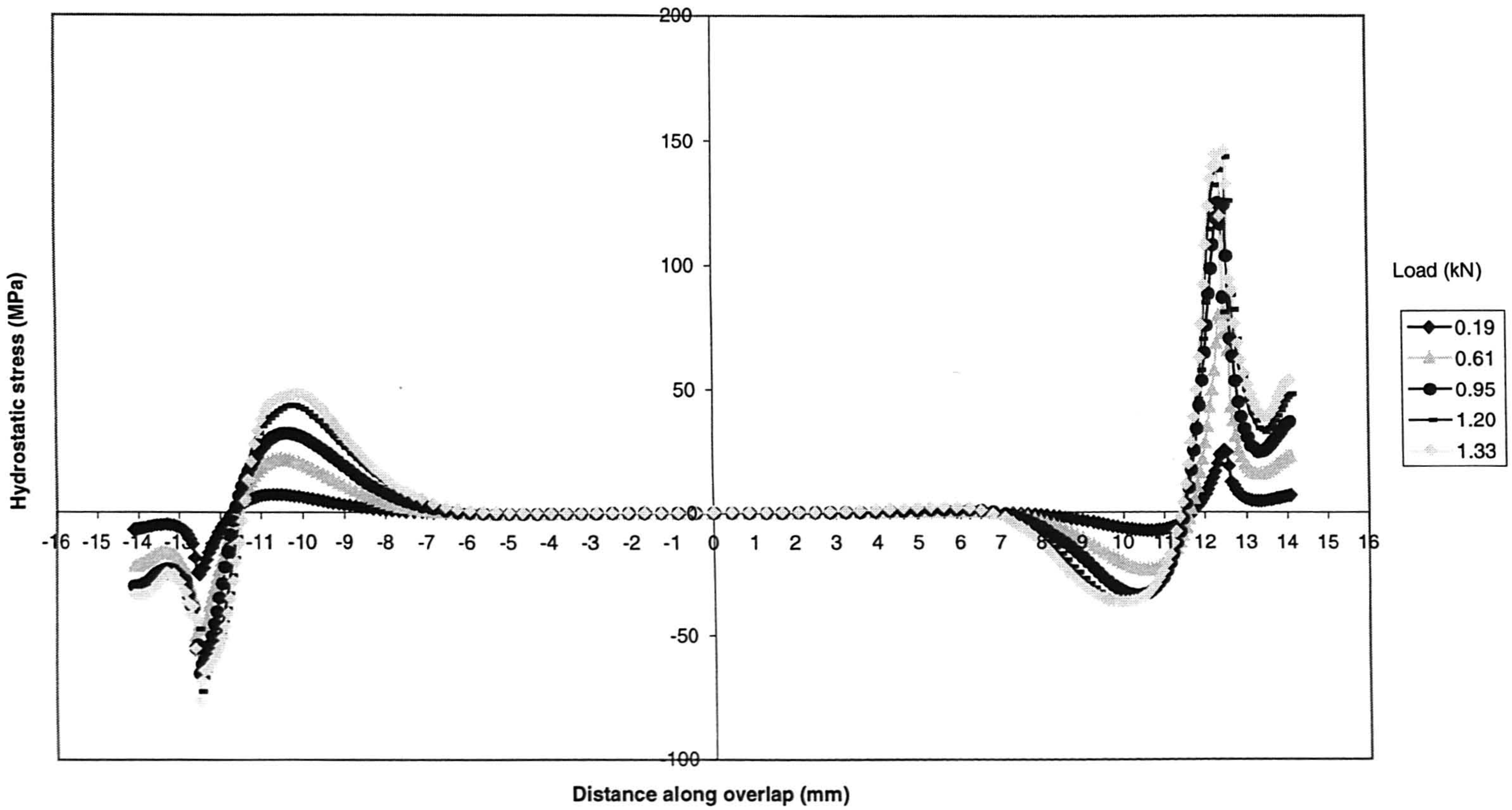

Figure 7.28 Variation of hydrostatic stress along the overlap length for the un loaded interface - hard steel - AV 119 adhesive - 25 mm overlap - 1.6 mm thick adherends - 4 point bend loading

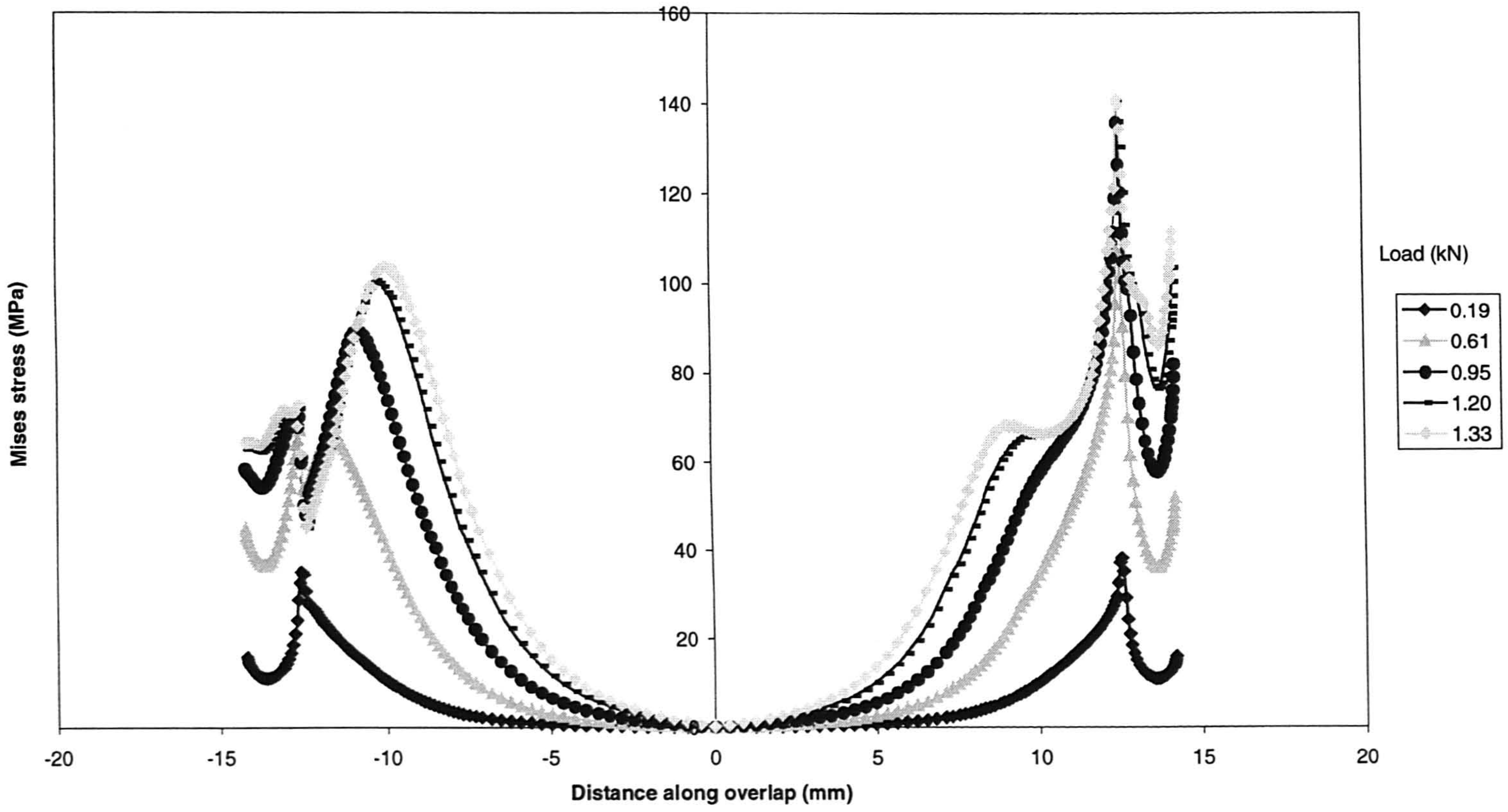

Figure 7.29 Variation of Mises stress along the overlap length for the loaded interface - hard steel - AV 119 adhesive - 25 mm overlap - 1.6 mm thick adherends - 4 point bend loading

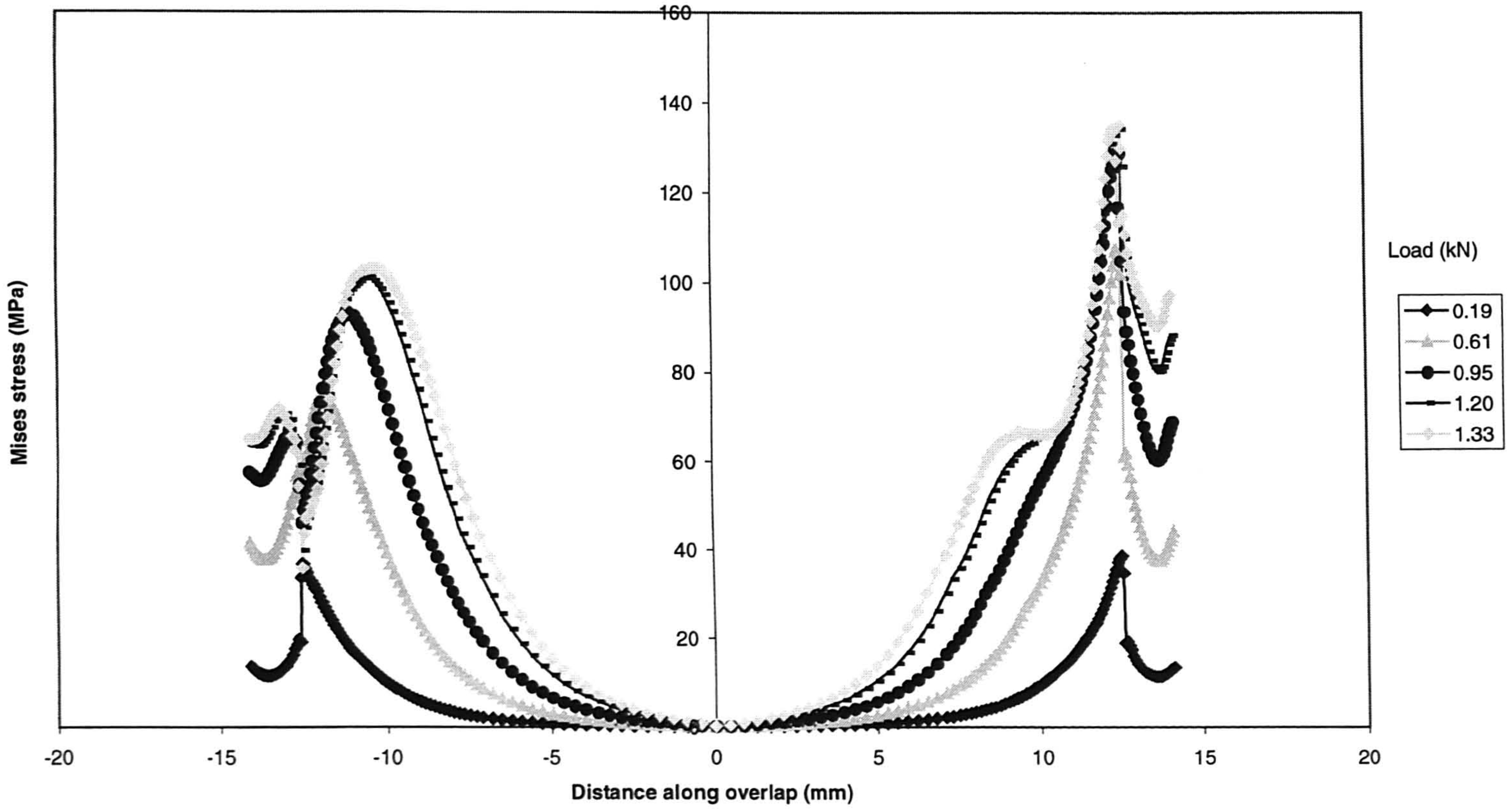

Figure 7.30 Variation of Mises stress along the overlap length for the un loaded interface - hard steel - AV 119 adhesive - 25 mm overlap - 1.6 mm thick adherends - 4 point bend loading

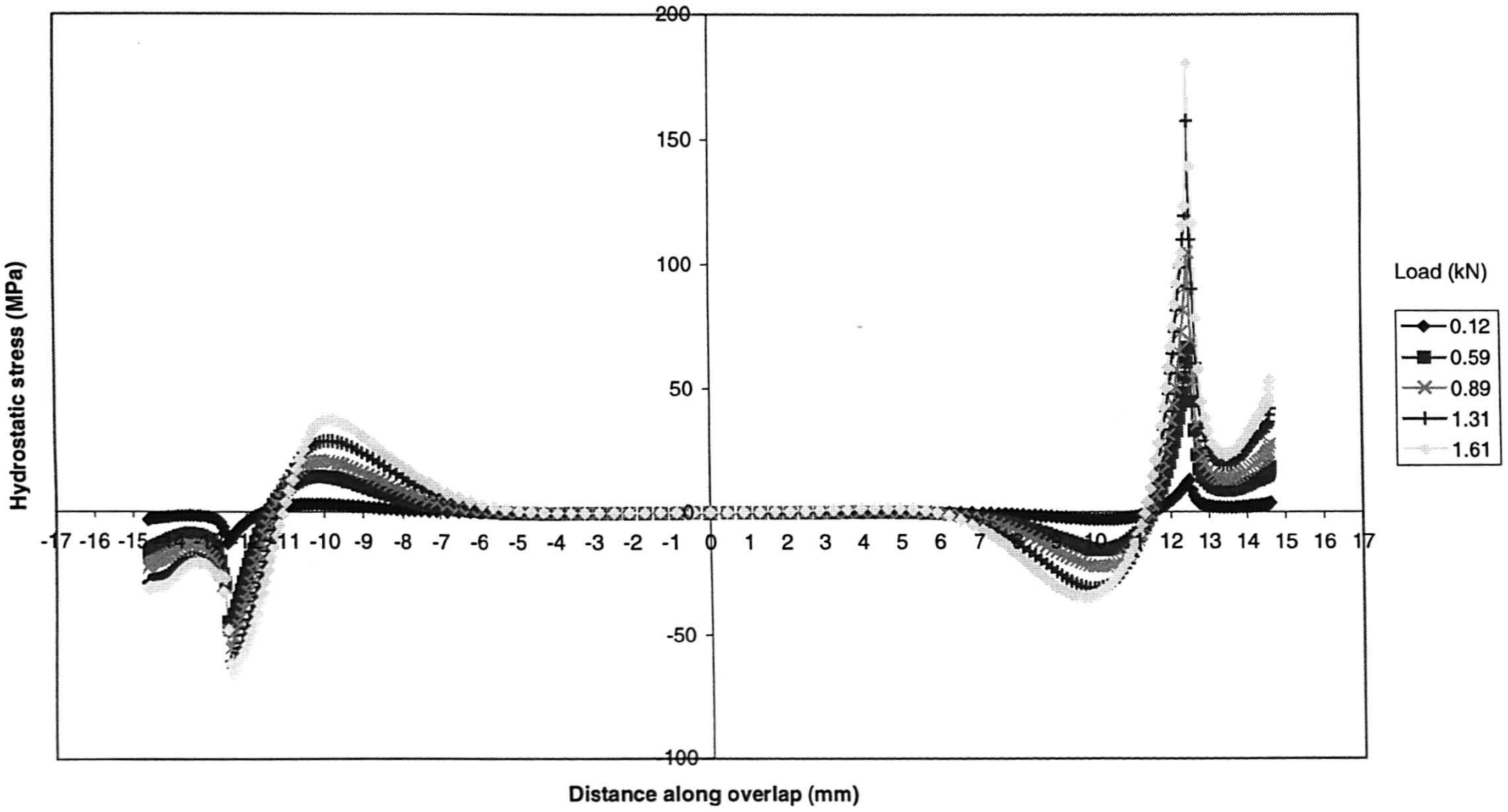

Figure 7.31 Variation of hydrostatic stress along the overlap length for the loaded interface - hard steel - AV 119 adhesive - 25 mm overlap - 2 mm thick adherends - 4 point bend loading

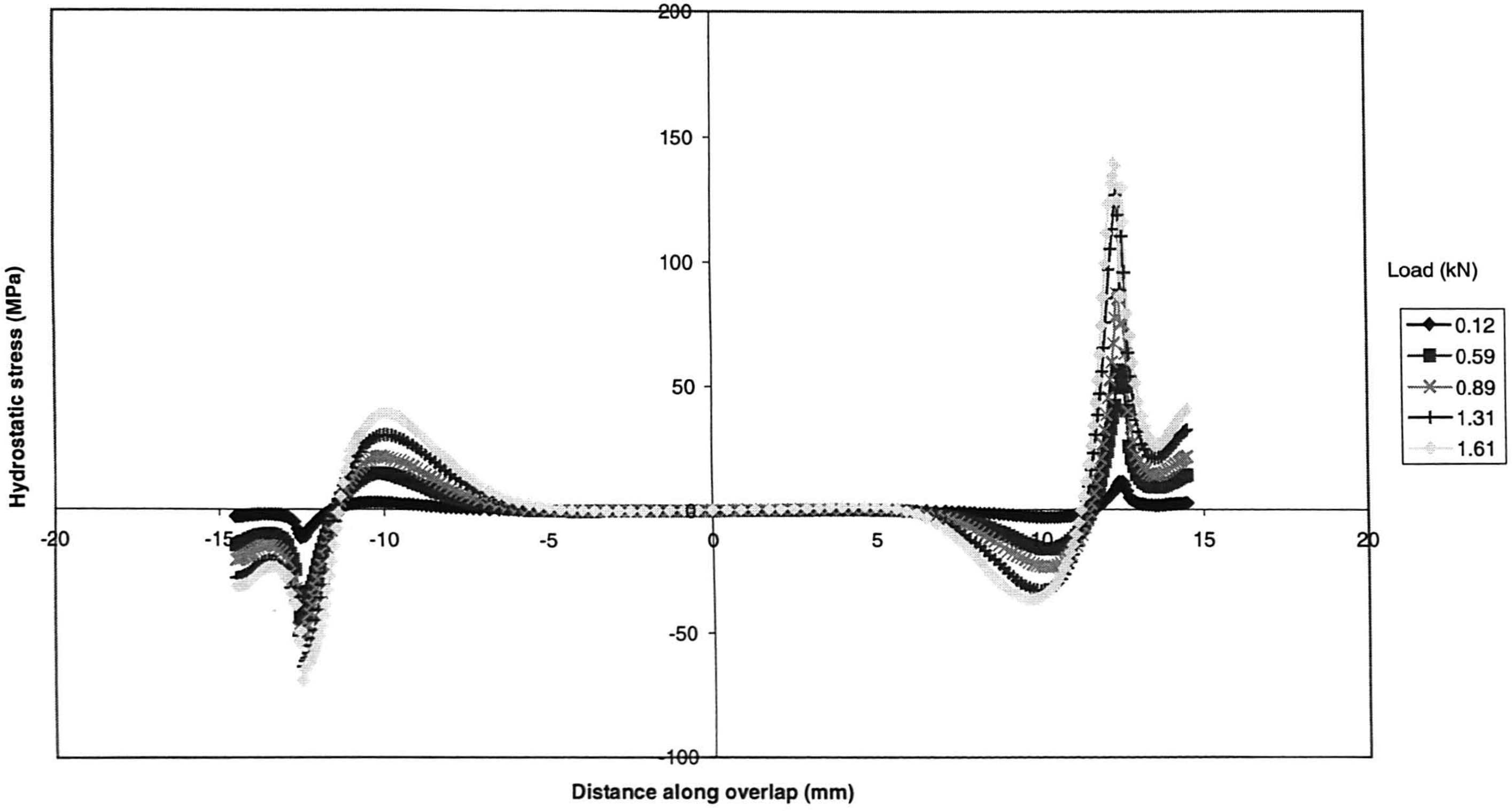

Figure 7.32 Variation of hydrostatic stress along the overlap length for the unloaded interface - hard steel - AV 119 adhesive - 25 mm overlap - 2 mm thick adherends - 4 point bend loading

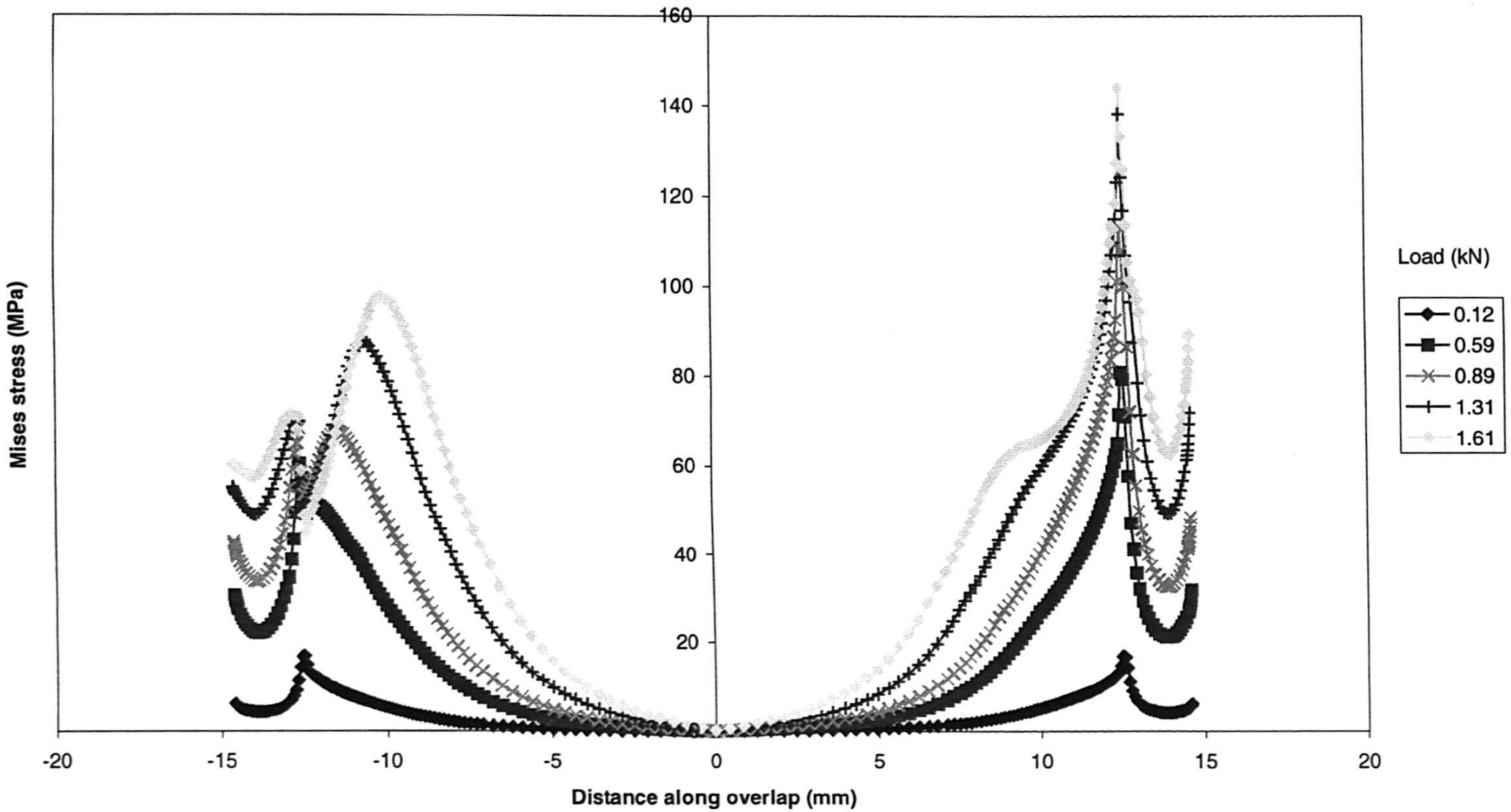

Figure 7.33 Variation of Mises stress along the overlap length for the loaded interface - hard steel - AV 119 adhesive - 25 mm overlap - 2 mm thick adherends - 4 point bend loading

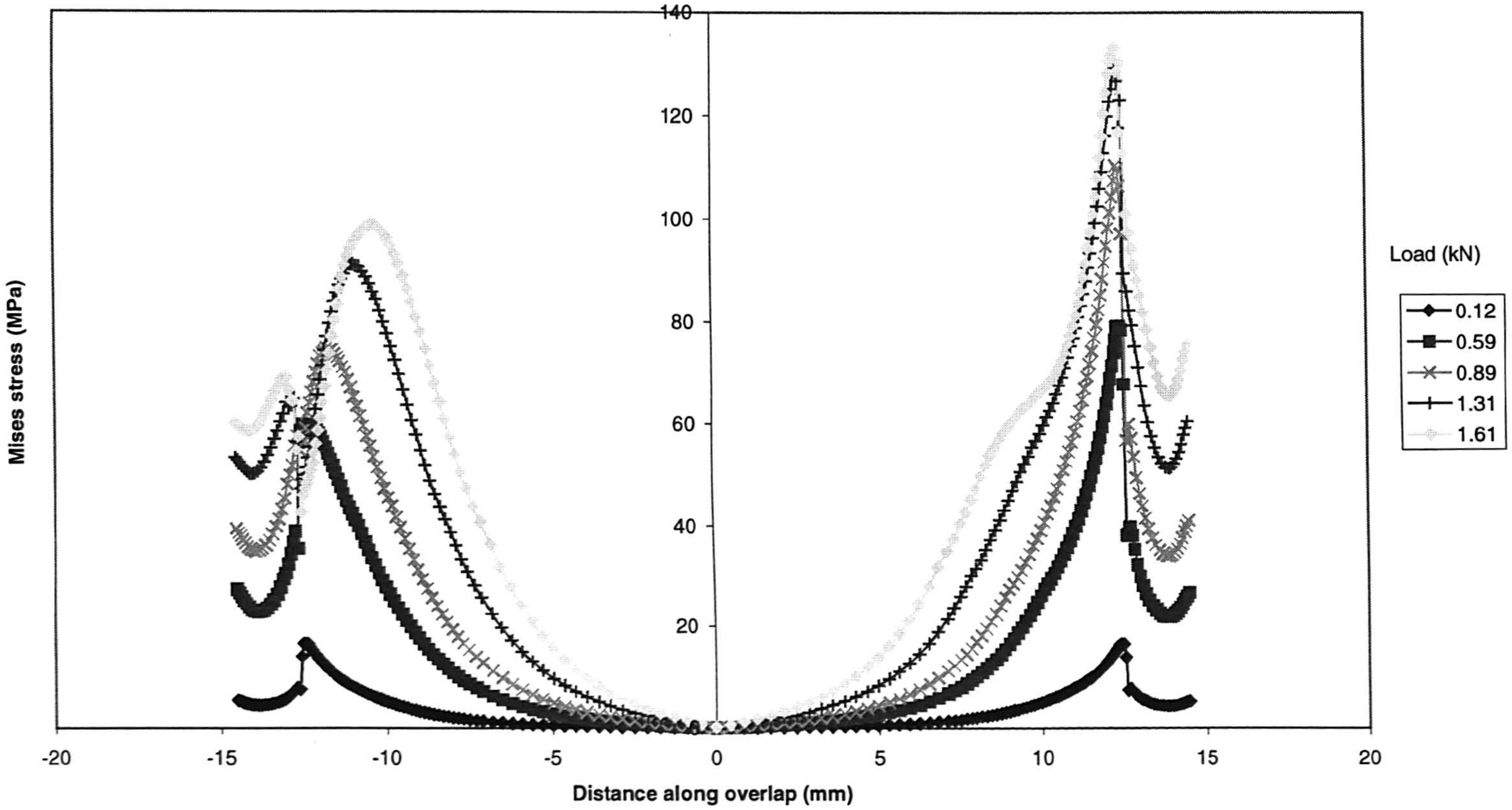

Figure 7.34 Variation of Mises stress along the overlap length for the unloaded interface - hard steel - AV 119 adhesive - 25 mm overlap - 2 mm thick adherends - 4 point bend loading

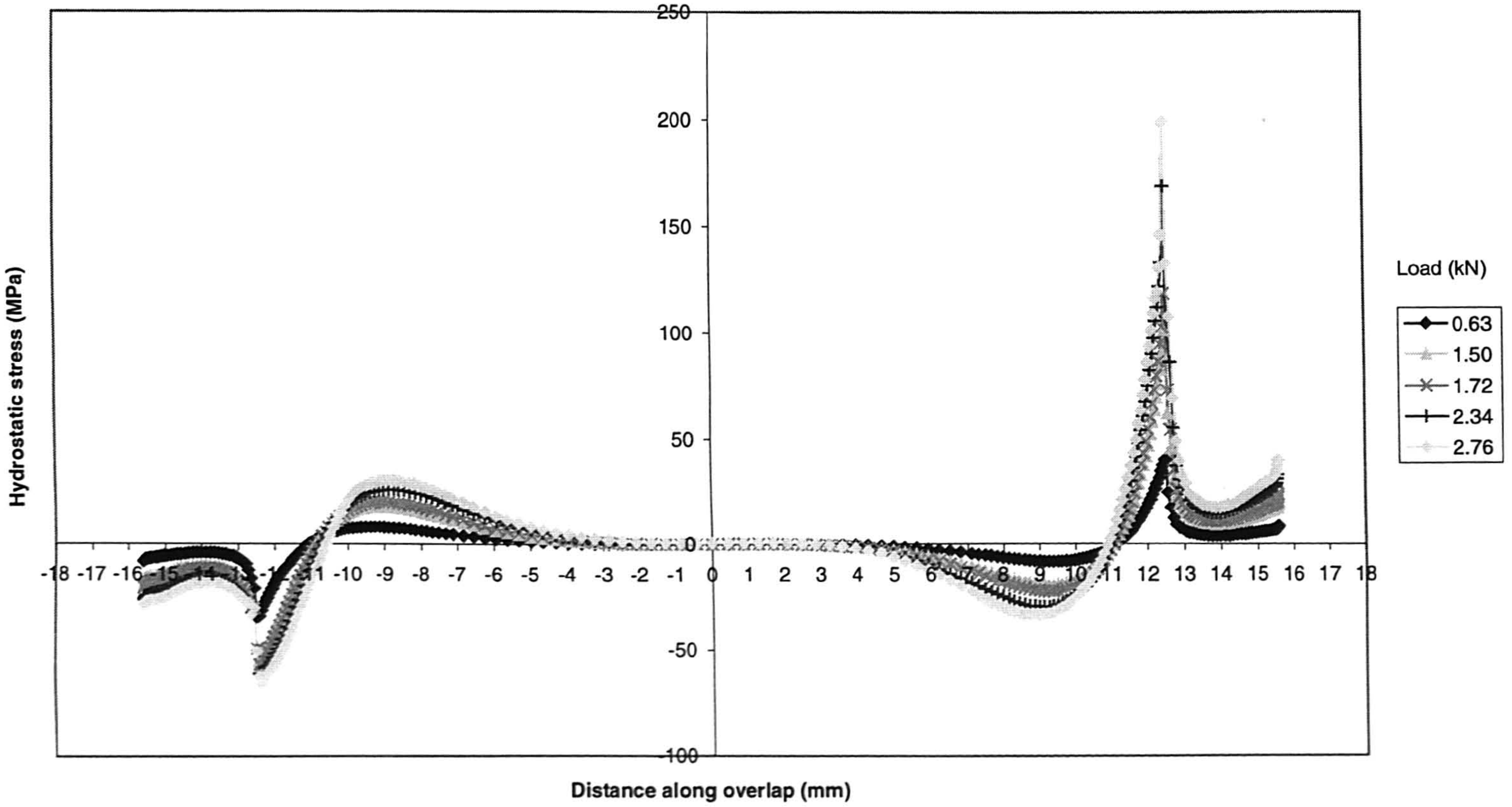

Figure 7.35 Variation of hydrostatic stress along the overlap length for the loaded interface - hard steel - AV 119 adhesive - 25 mm overlap - 3 mm thick adherends - 4 point bend loading

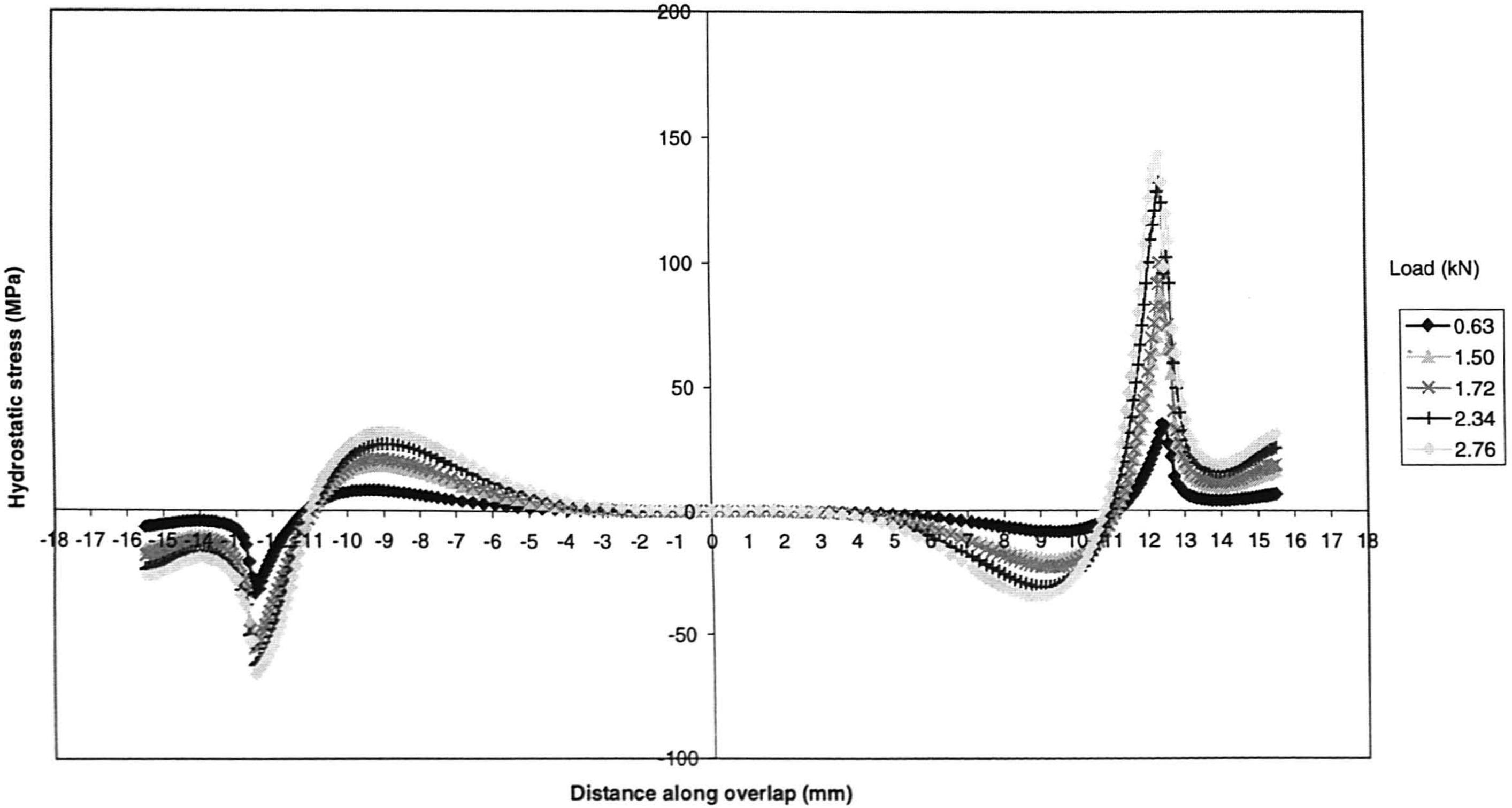

Figure 7.36 Variation of hydrostatic stress along the overlap length for the unloaded interface - hard steel - AV 119 adhesive - 25 mm overlap - 3 mm thick adherends - 4 point bend loading

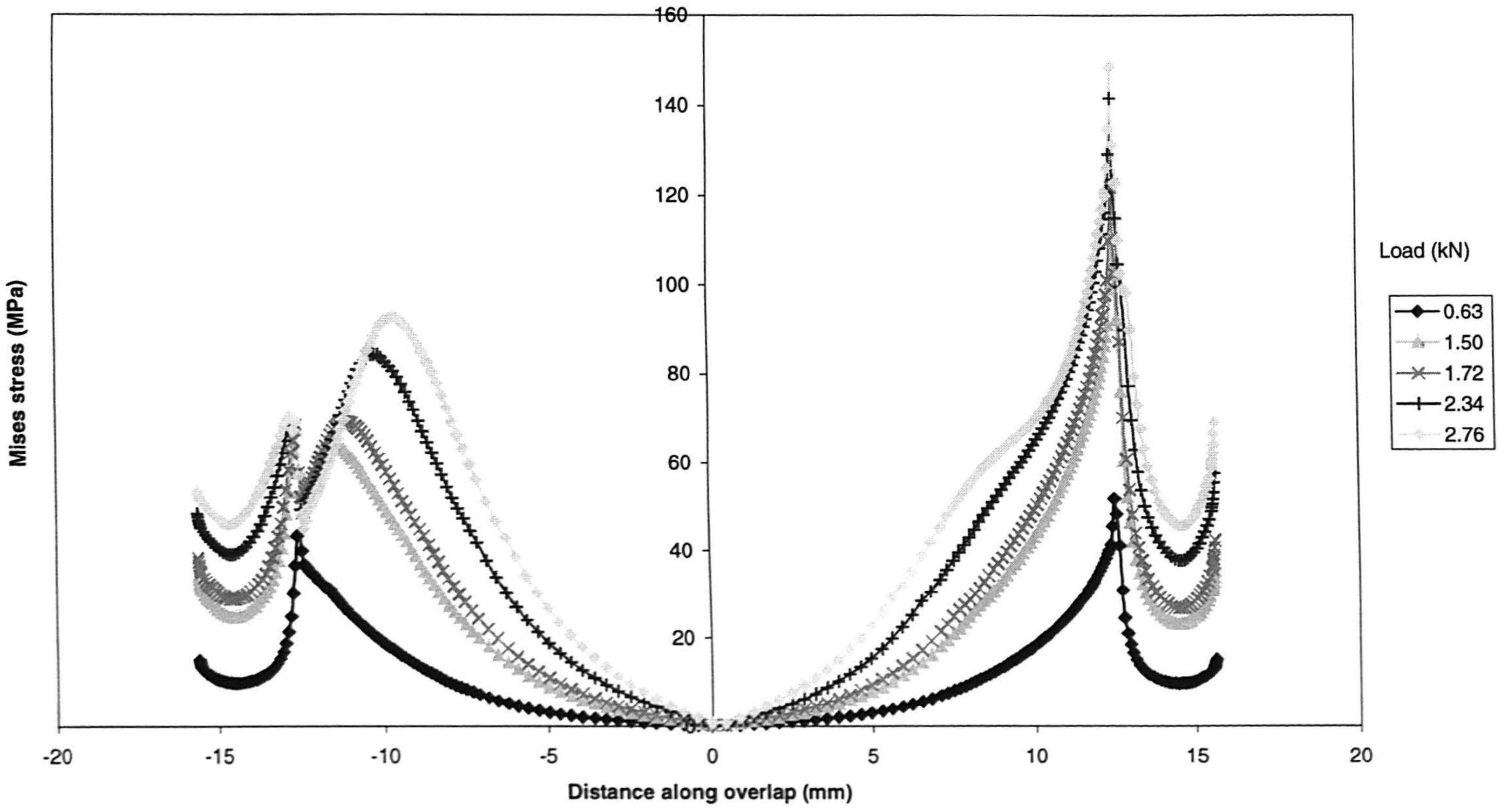

Figure 7.37 Variation of Mises stress along the overlap length for the loaded interface - hard steel - AV 119 adhesive - 25 mm overlap - 3 mm thick adherends - 4 point bend loading

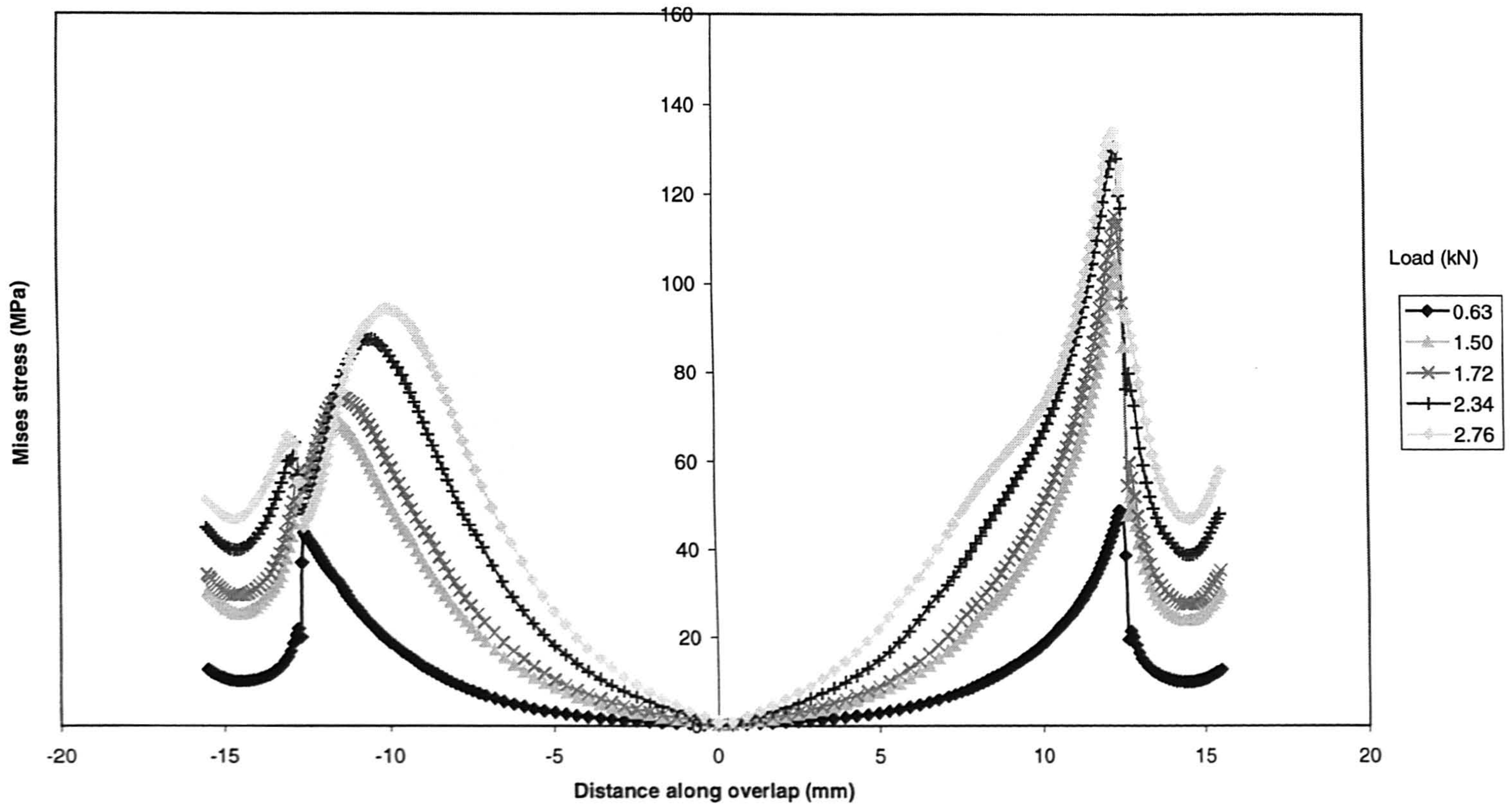

Figure 7.38 Variation of Mises stress along the overlap length for the unloaded interface - hard steel - AV 119 adhesive - 25 mm overlap - 3 mm thick adherends - 4 point bend loading

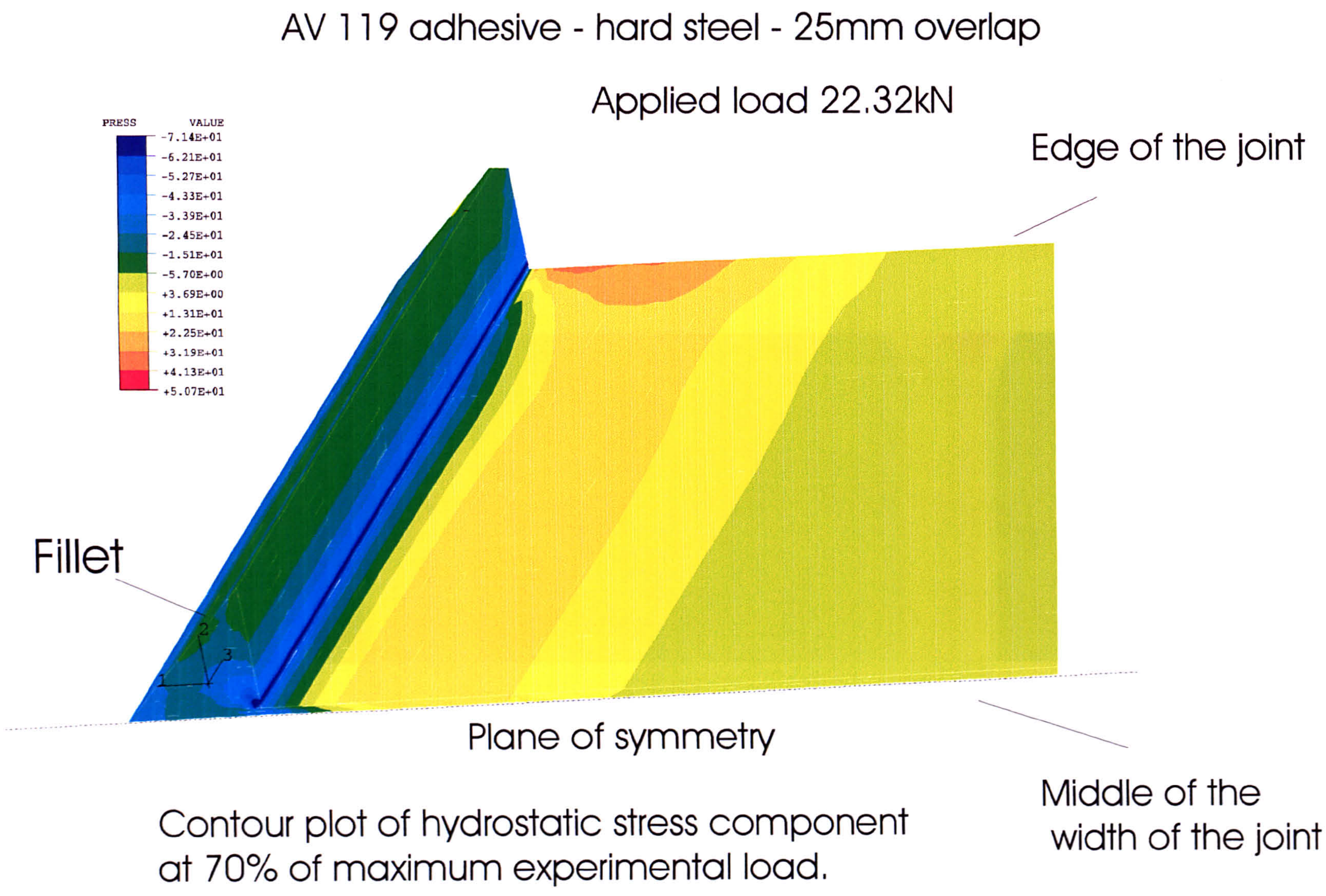

Figure 7.39 Contour plot of hydrostatic stress variation from 3-D F.E.analysis for 25 mm overlap hard steel AV 119 adhesive SLJs under tensile loading

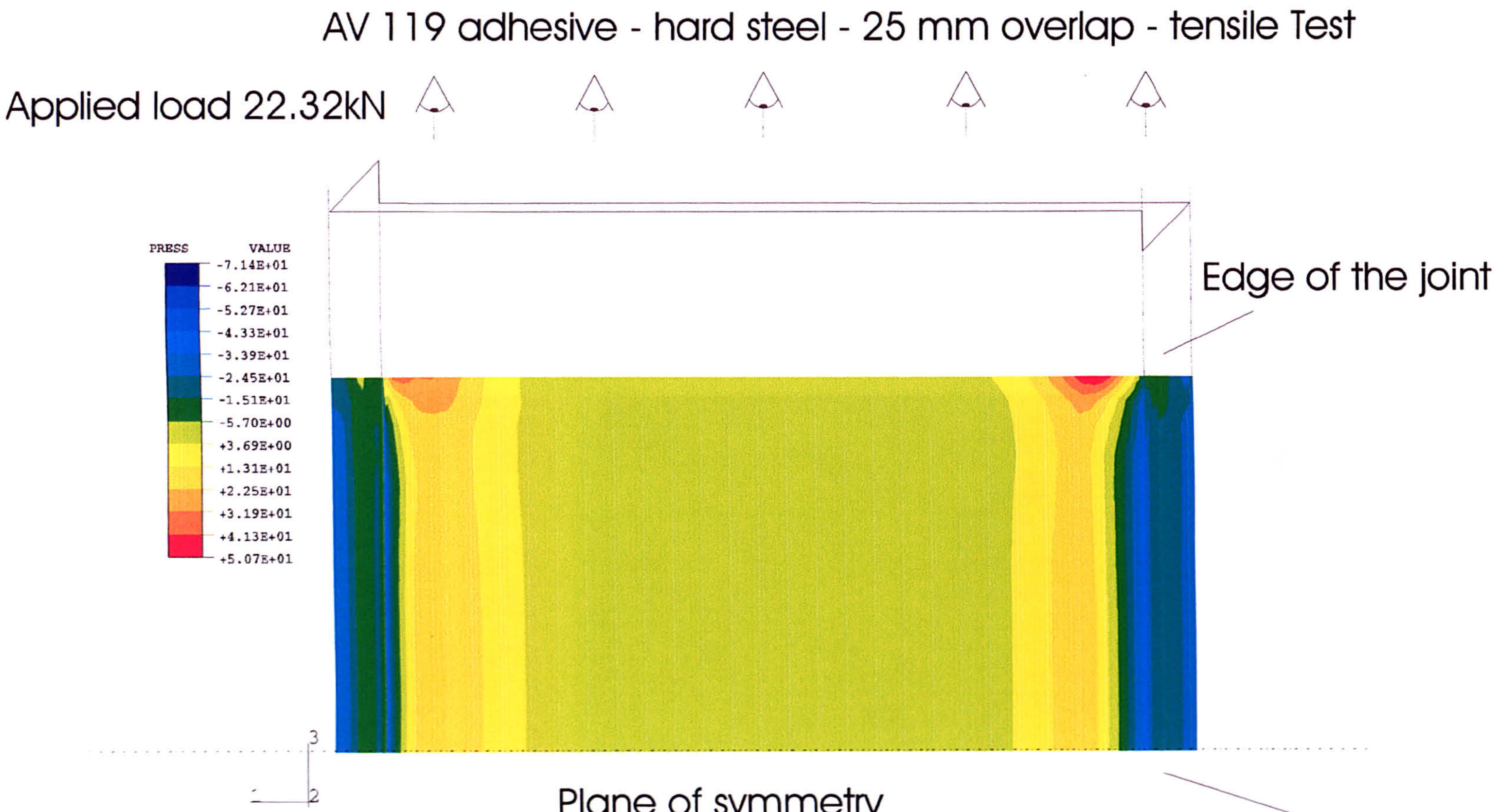

Figure 7.40 Contour plot of hydrostatic stress variation from 3-D F.E. analysis for 25 mm overlap hard steel AV 119 adhesive SLJs under tensile loading

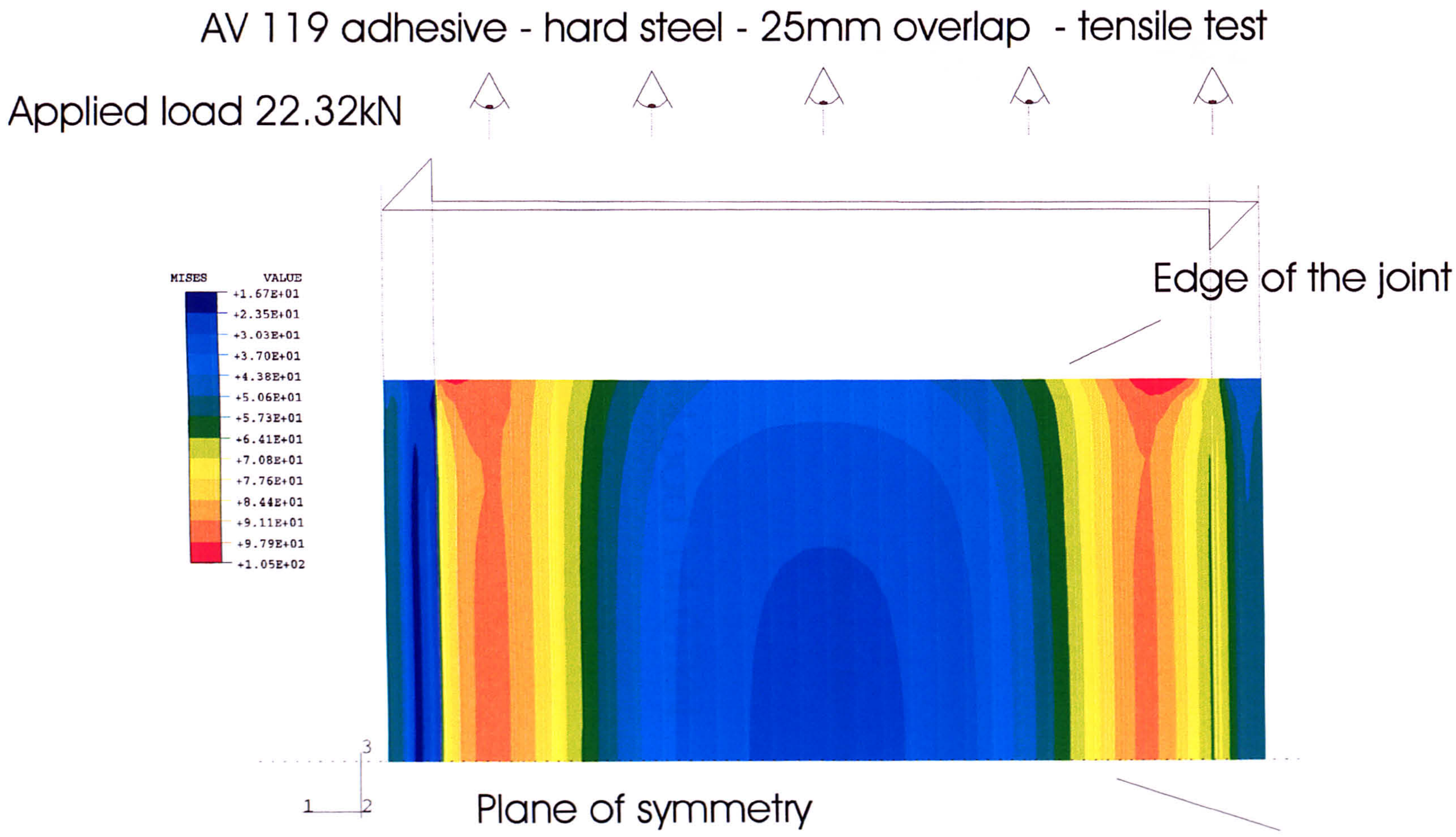

Figure 7.41 Contour plot of Mises stress variation from 3-D F.E. analysis for 25 mm overlap hard steel AV 119 adhesive SLJs under tensile loading

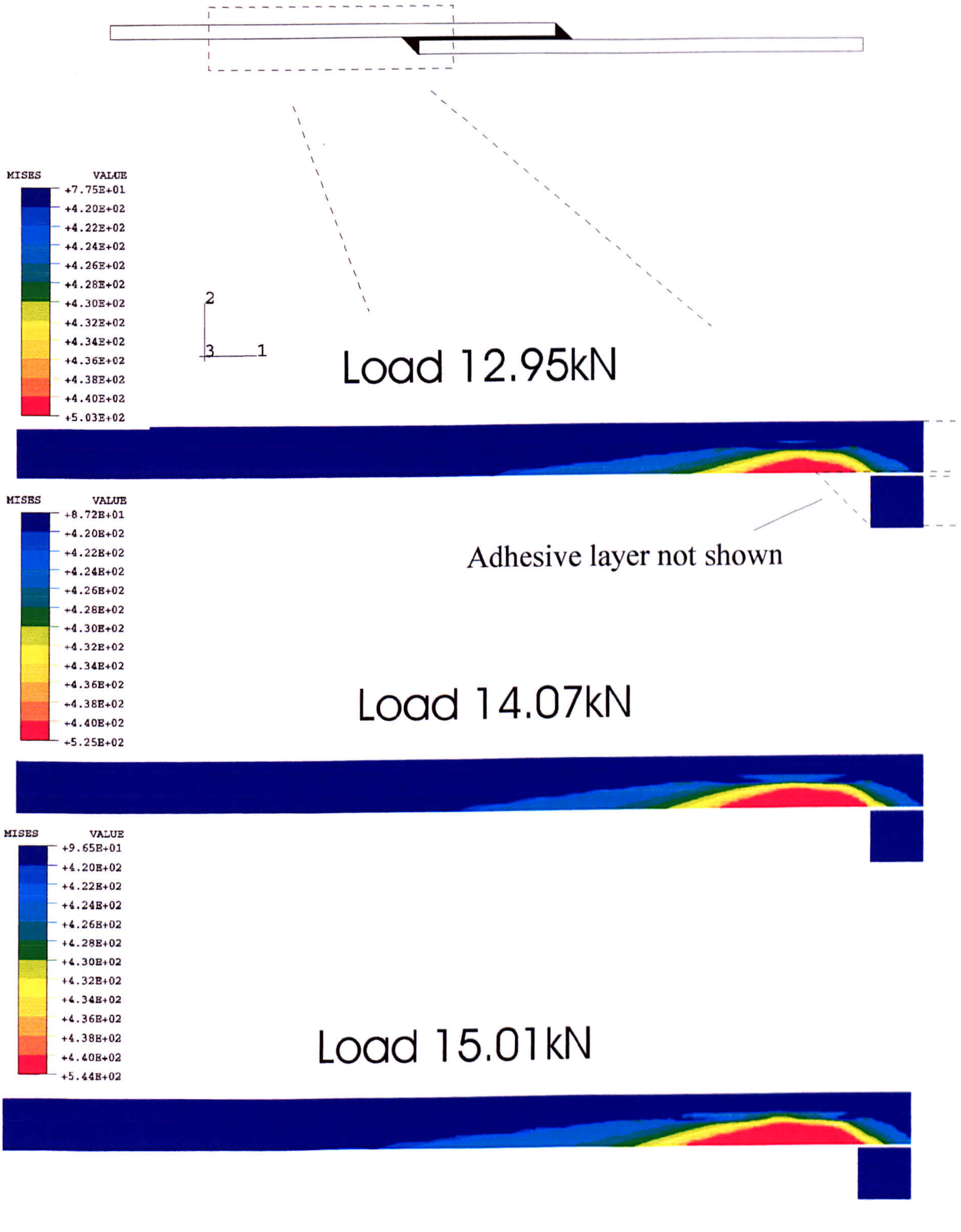

Figure 7.42 Contour plots of Mises stress variation in the adherends for 12.5 mm overlap, gauge steel, EC 3448 adhesive SLJ under tensile loading

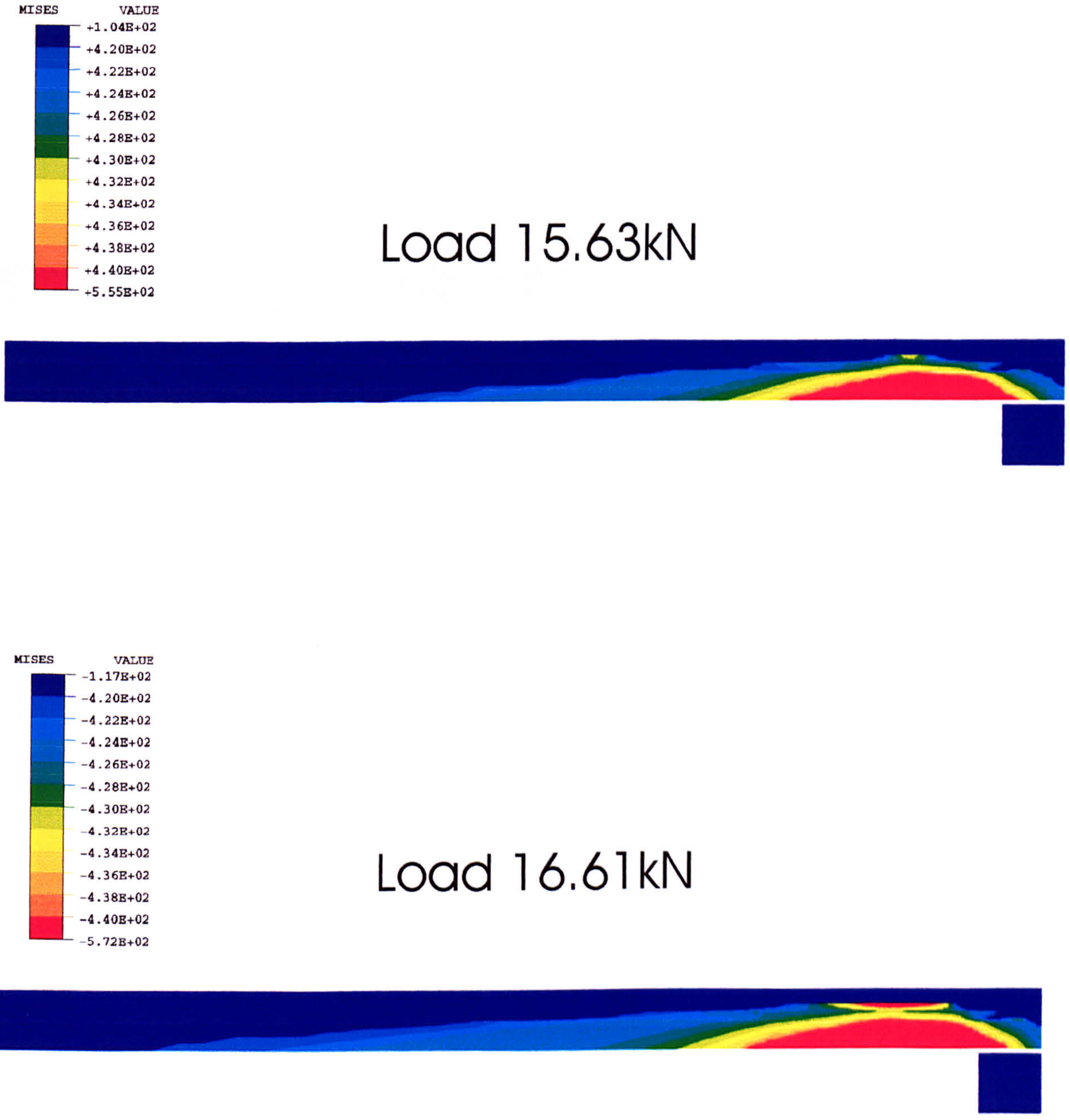

12.5 mm overlap - gauge steel - EC 3448 adhesive

Figure 7.42b Contour plots of Mises Stress variation in the adherends for 12.5 mm overlap, gauge steel, EC 3448 adhesive SLJ under tensile loading

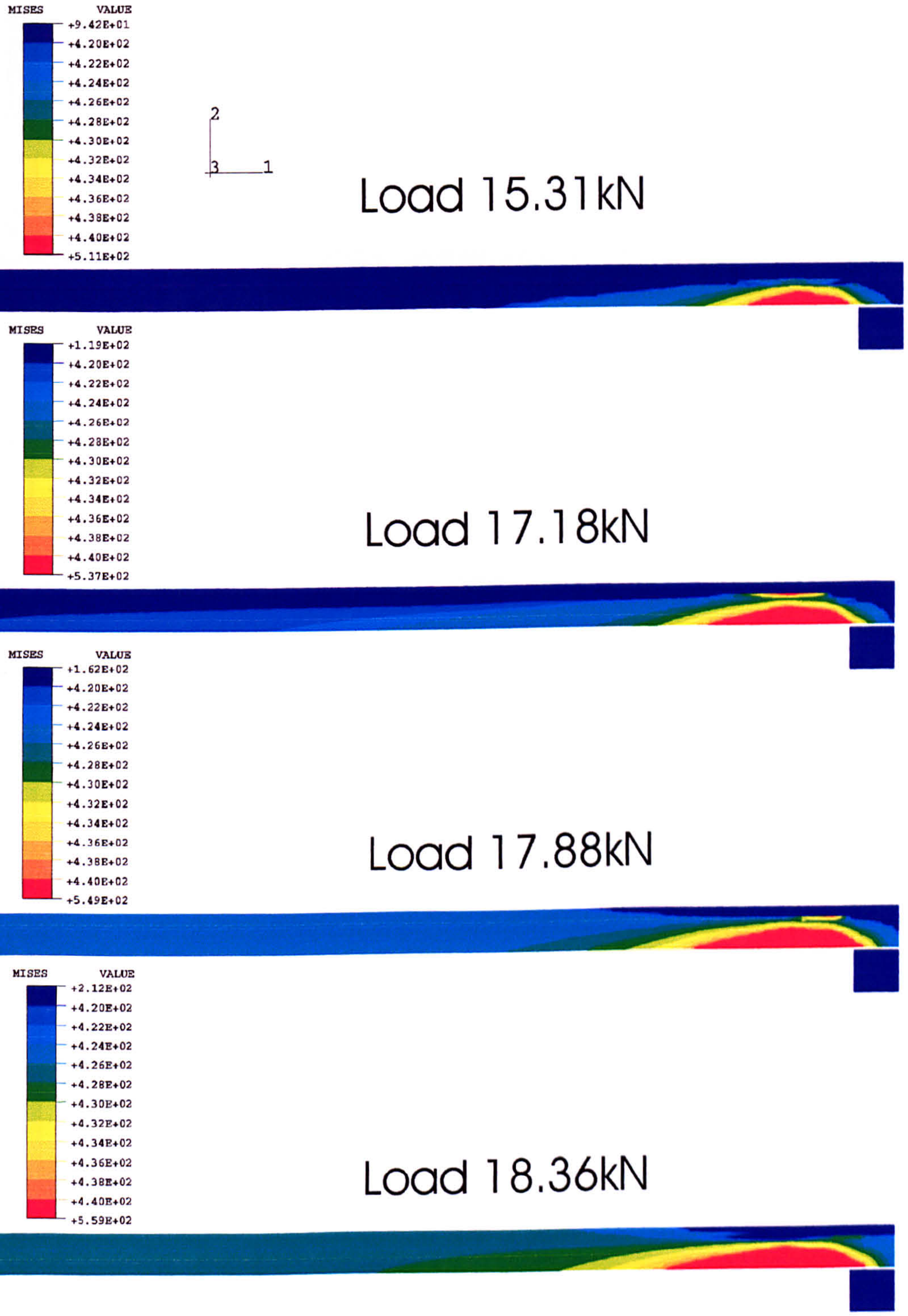

20 mm overlap - gauge steel - EC 3448 adhesive

Figure 7.43 Contour plots of Mises stress variation in the adherends for 20 mm overlap, gauge steel, EC 3448 adhesive SLJ under tensile loading

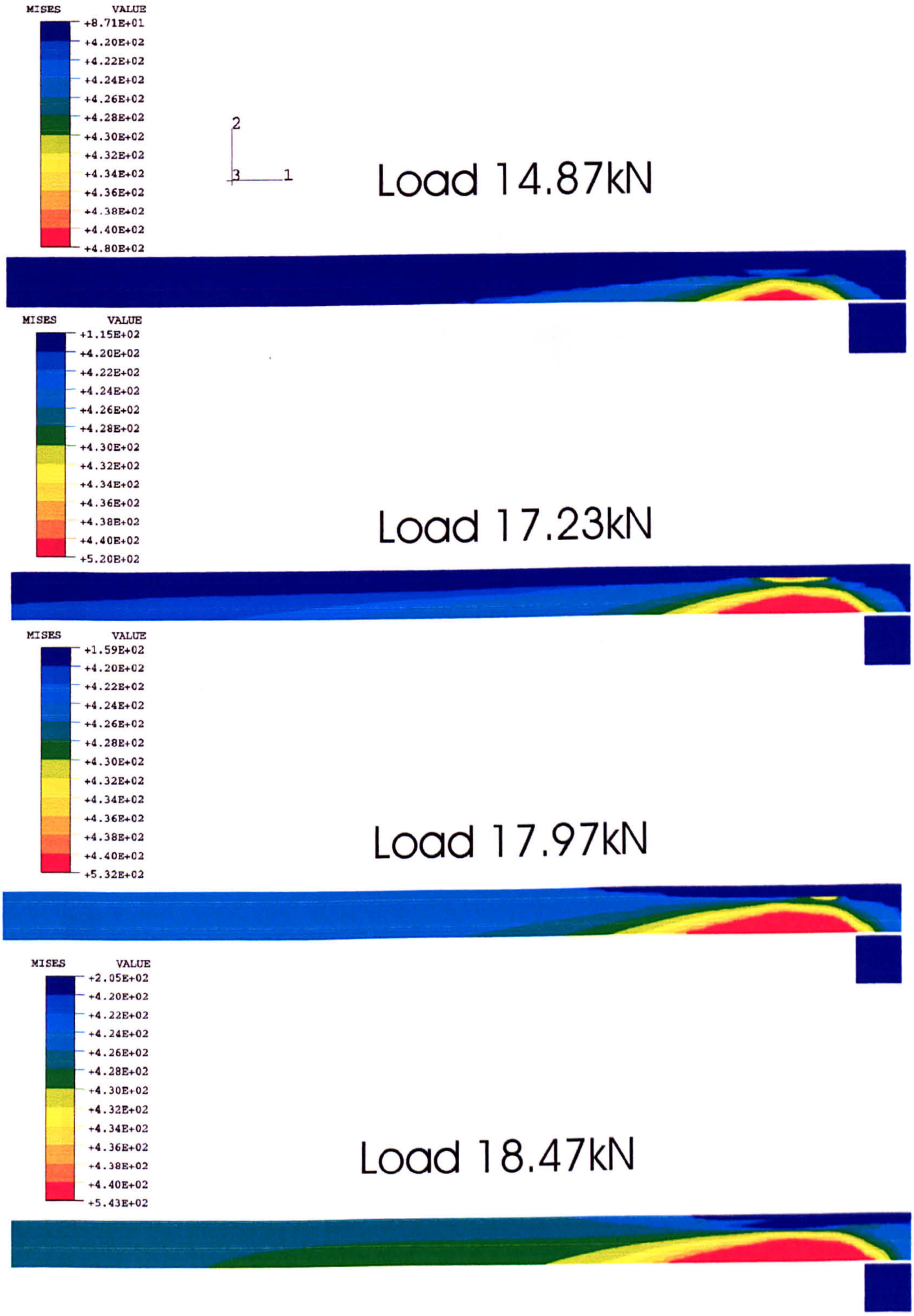

Figure 7.44 Contour plots of Mises stress variation in the adherends for 25 mm overlap, gauge steel, EC 3448 adhesive SLJ under tensile loading

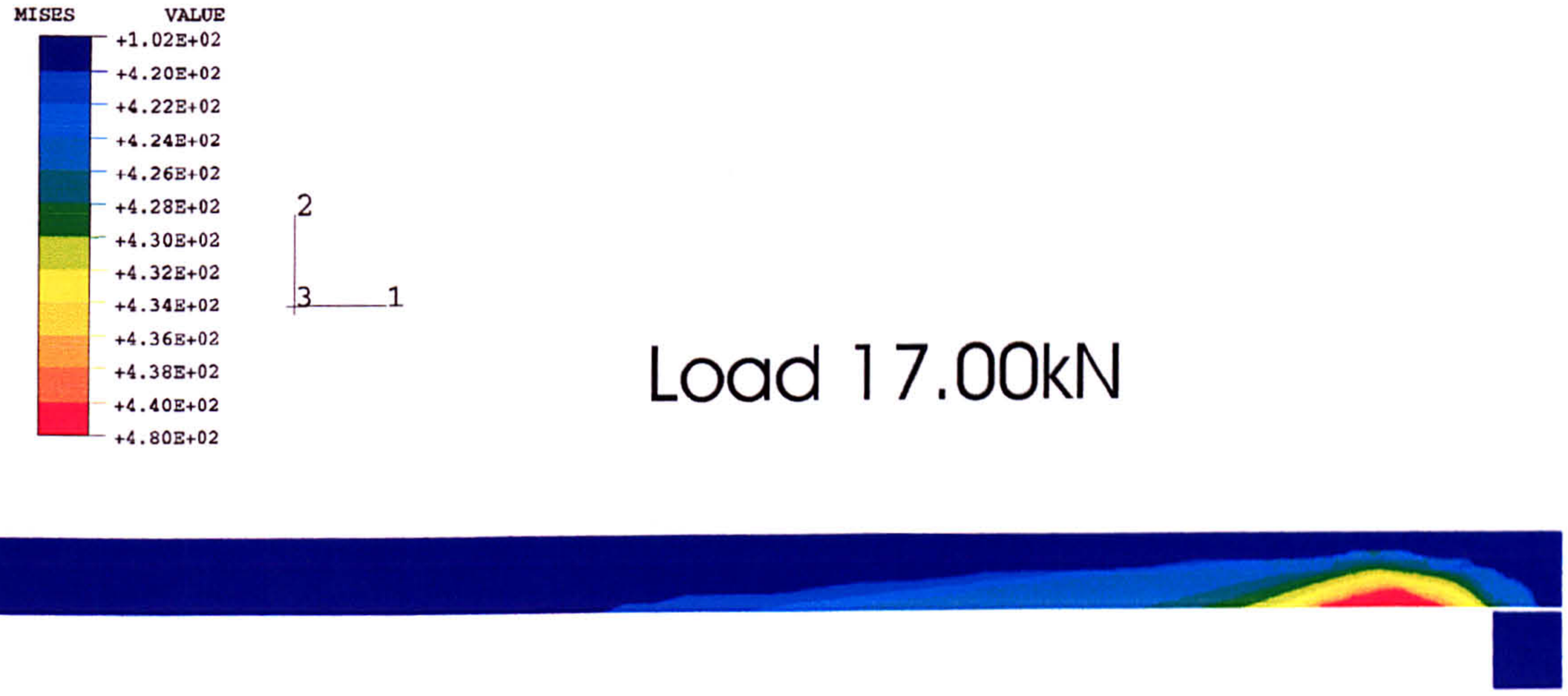

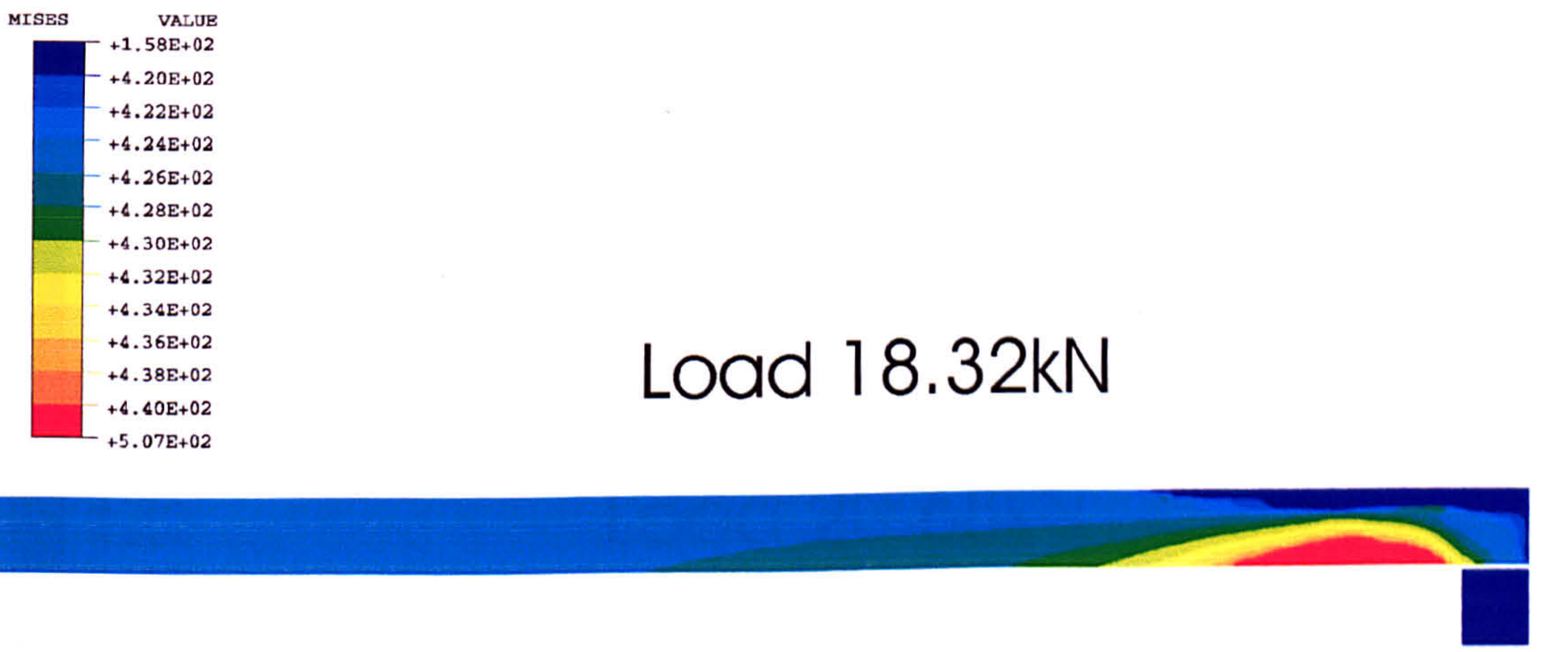

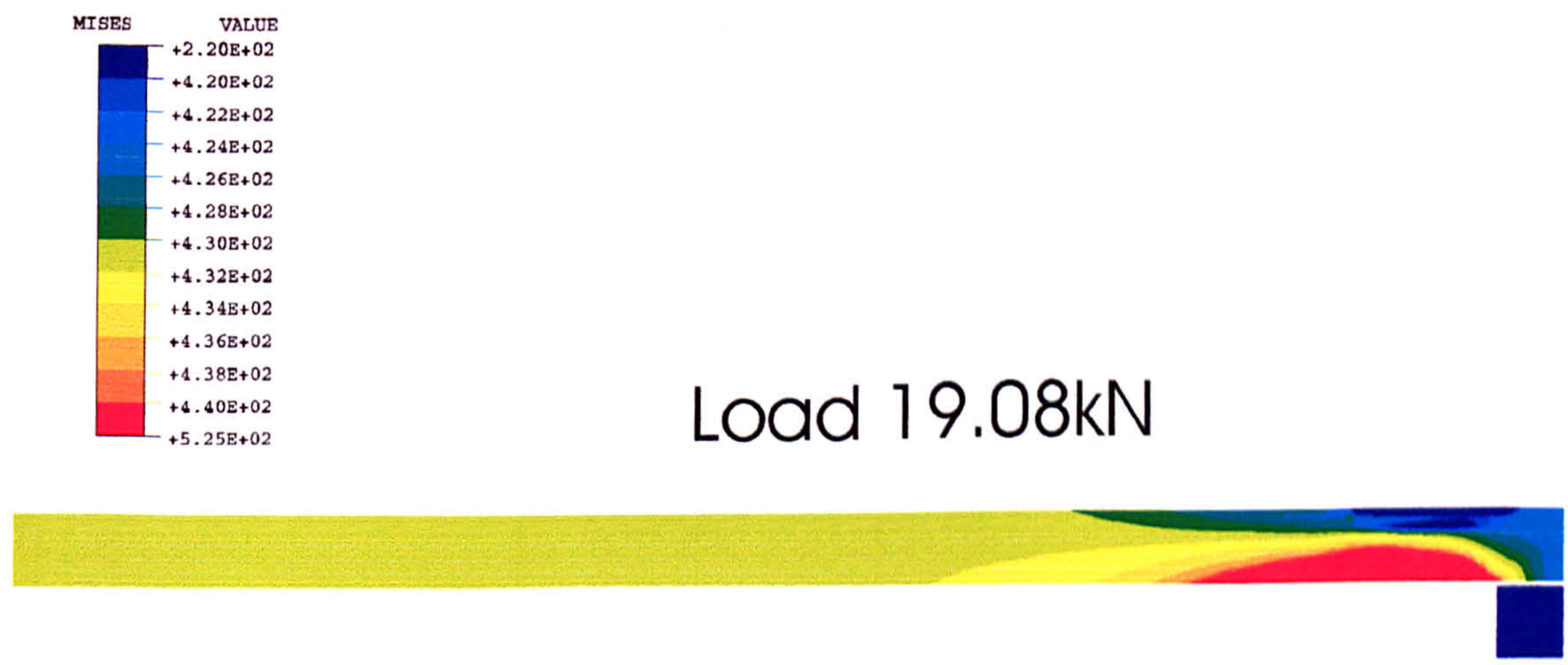

40 mm overlap - gauge steel - EC 3448 adhesive

Figure 7.45 Contour plots of Mises stress variation in the adherends for 40 mm overlap, gauge steel, EC 3448 adhesive SLJ under tensile loading

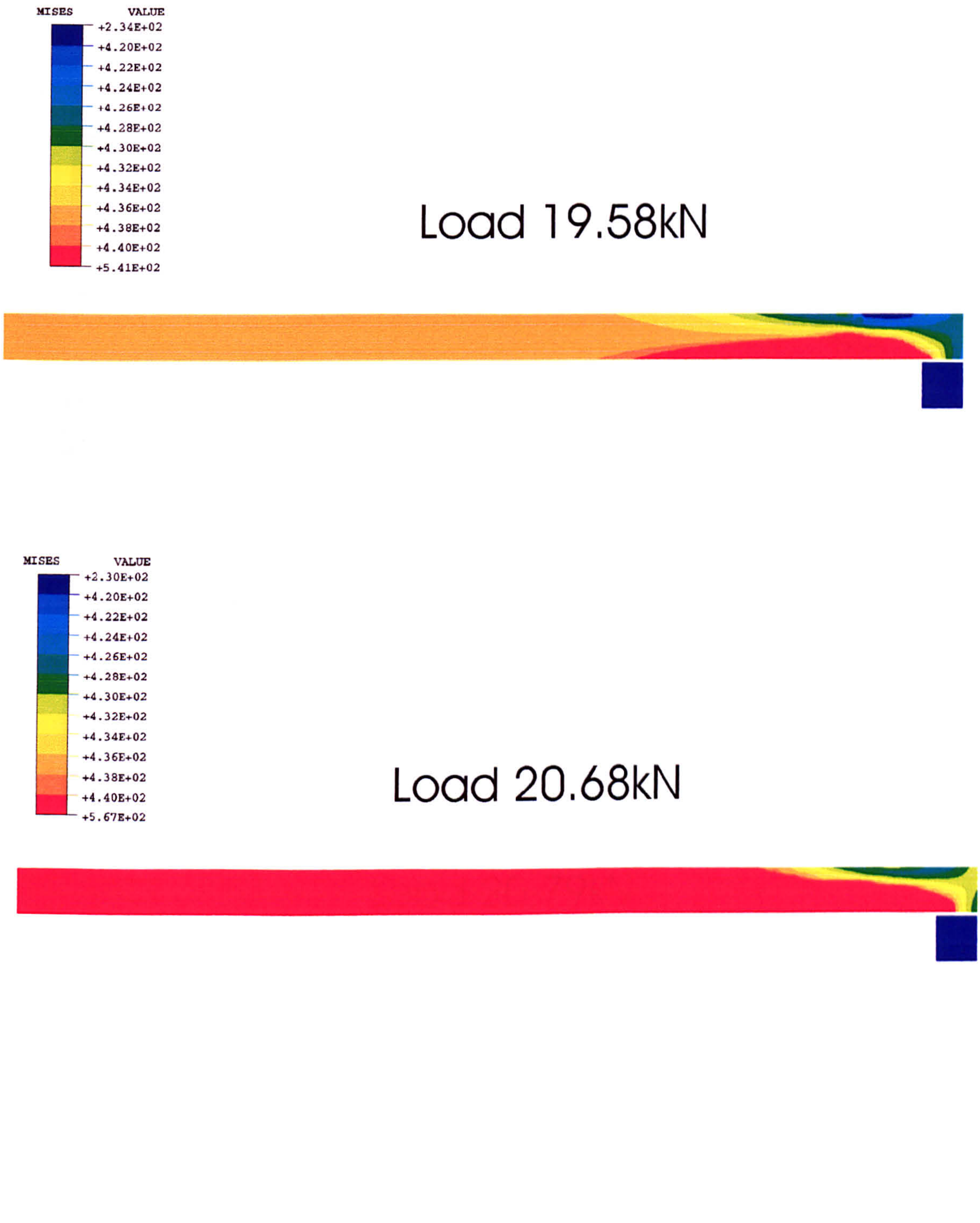

40 mm overlap - gauge steel - EC 3448 adhesive

Figure 7.45b Contour plots of Mises stress variation in the adherends for 40 mm overlap, gauge steel, EC 3448 adhesive SLJ under tensile loading

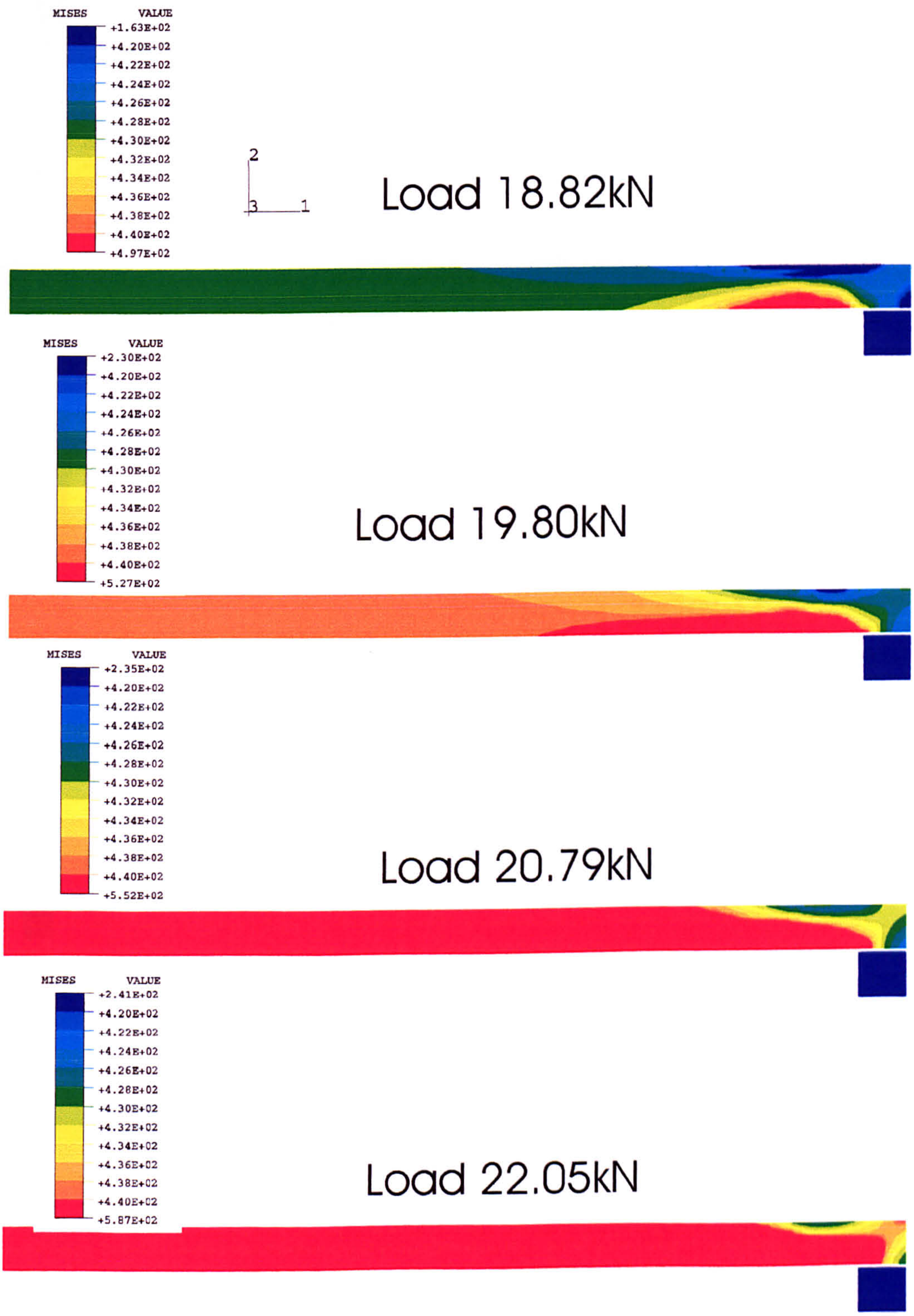

Figure 7.46 Contour plots of Mises stress variation in the adherends for 60 mm overlap, gauge steel, EC 3448 adhesive SLJ under tensile loading

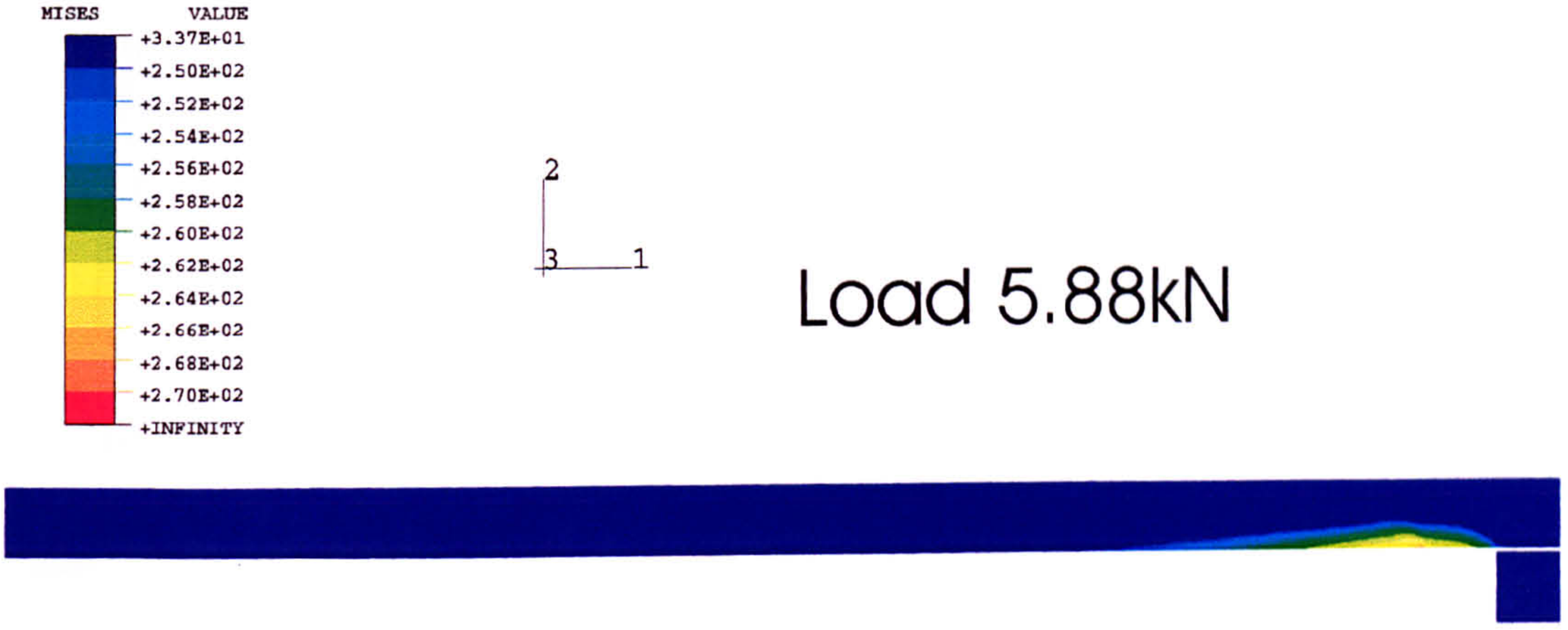

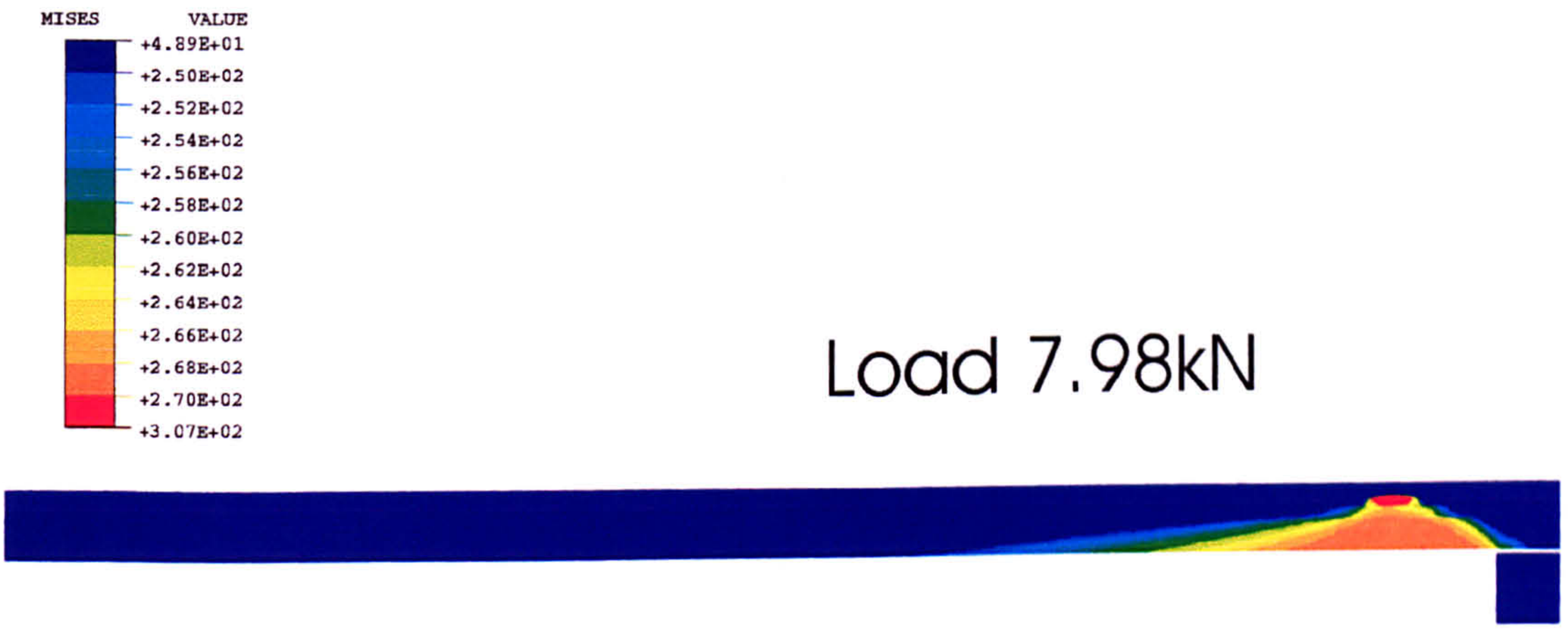

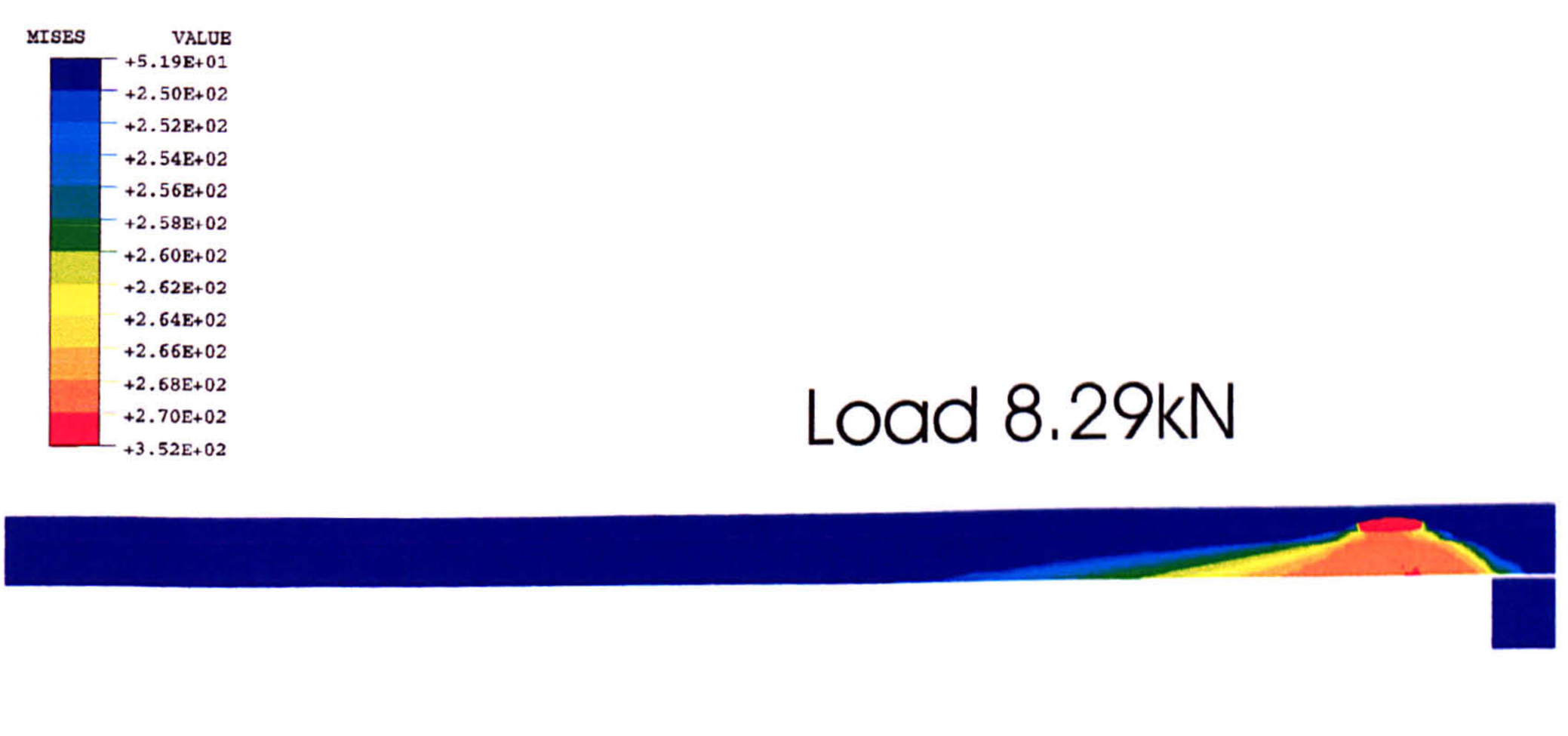

12.5 mm overlap - mild steel - AV 119 adhesive

Figure 7.47 Contour plots of Mises stress variation in the adherends for 12.5 mm overlap, mild steel, AV 119 adhesive SLJ under tensile loading

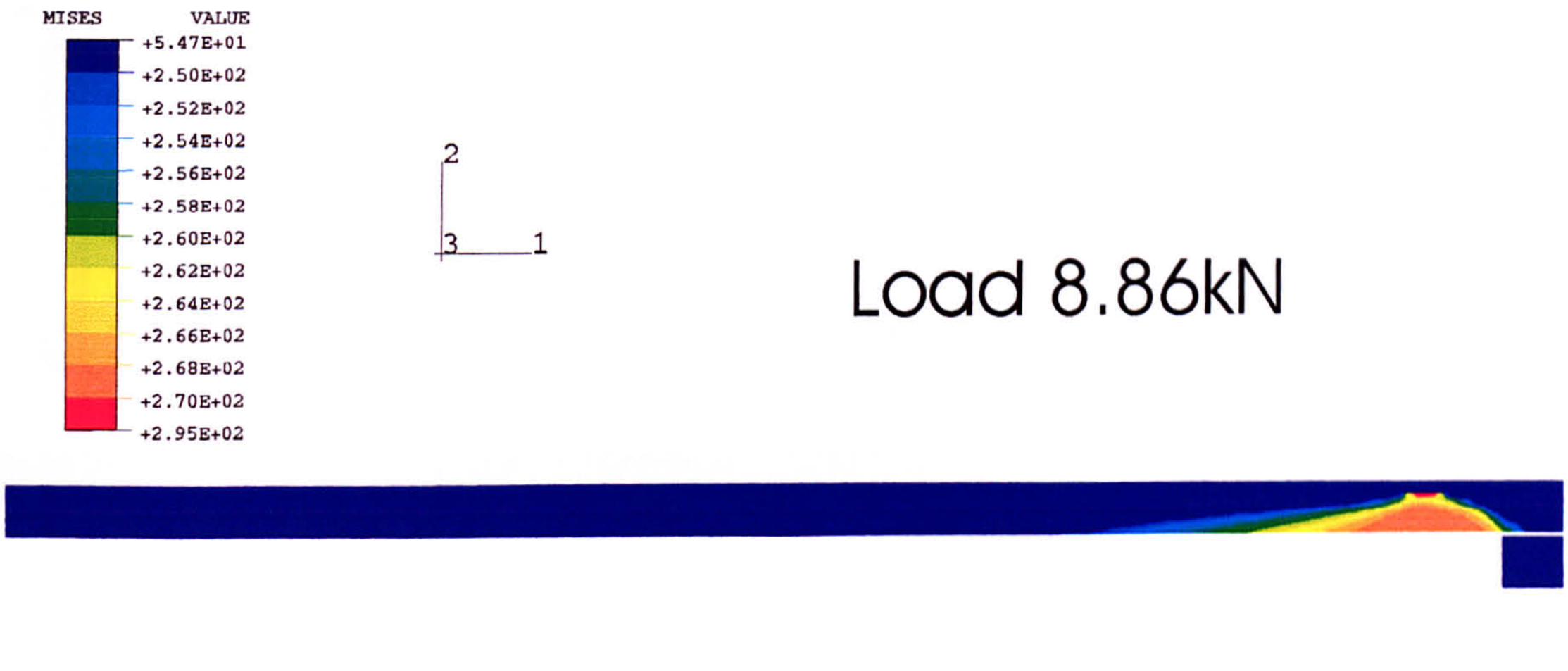

Figure 7.48 Contour plots of Mises stress variation in the adherends for 20 mm overlap, mild steel, AV 119 adhesive SLJ under tensile loading

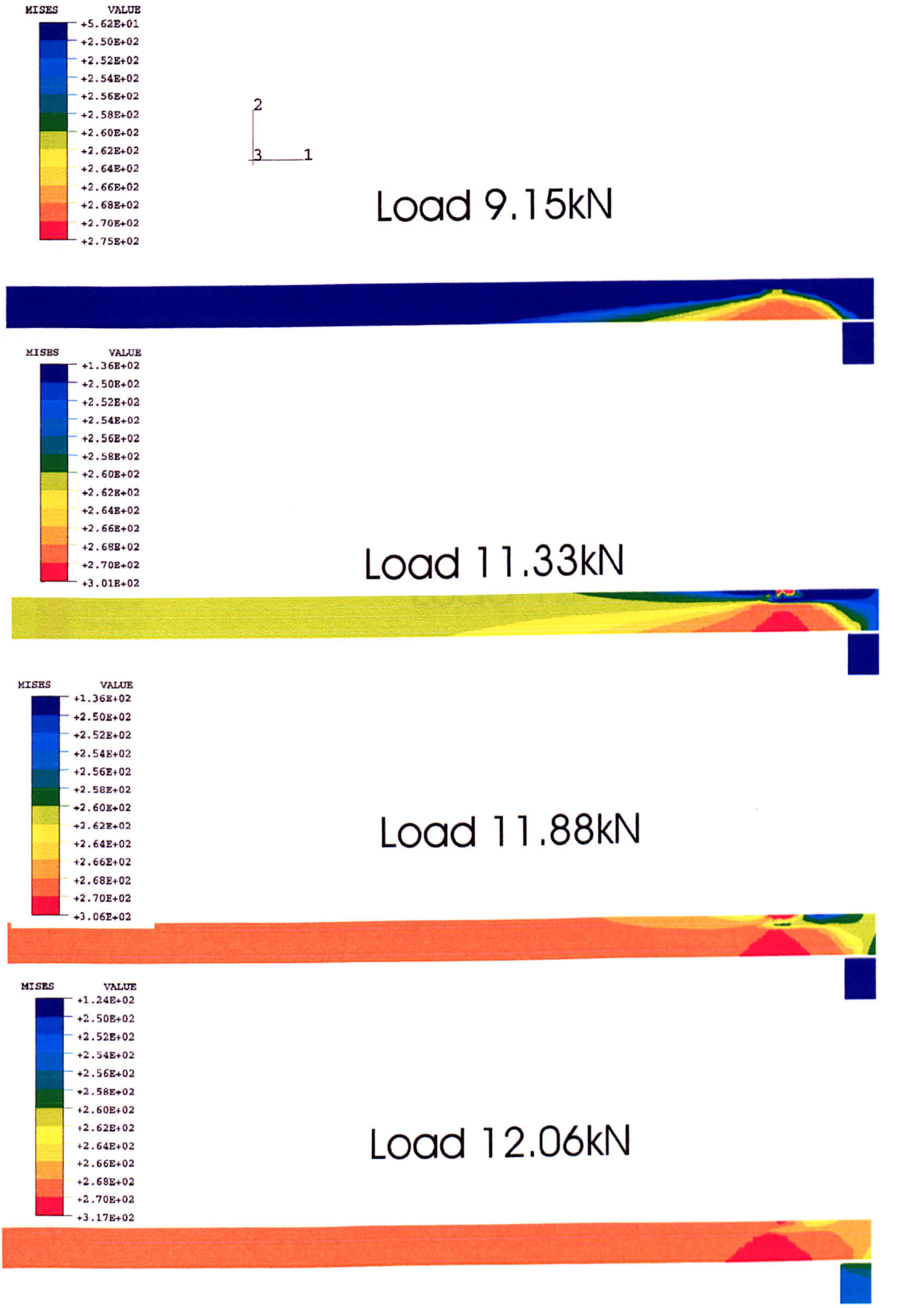

Figure 7.49 Contour plots of Mises stress variation in the adherends for 25 mm overlap, mild steel, AV 119 adhesive SLJ under tensile loading

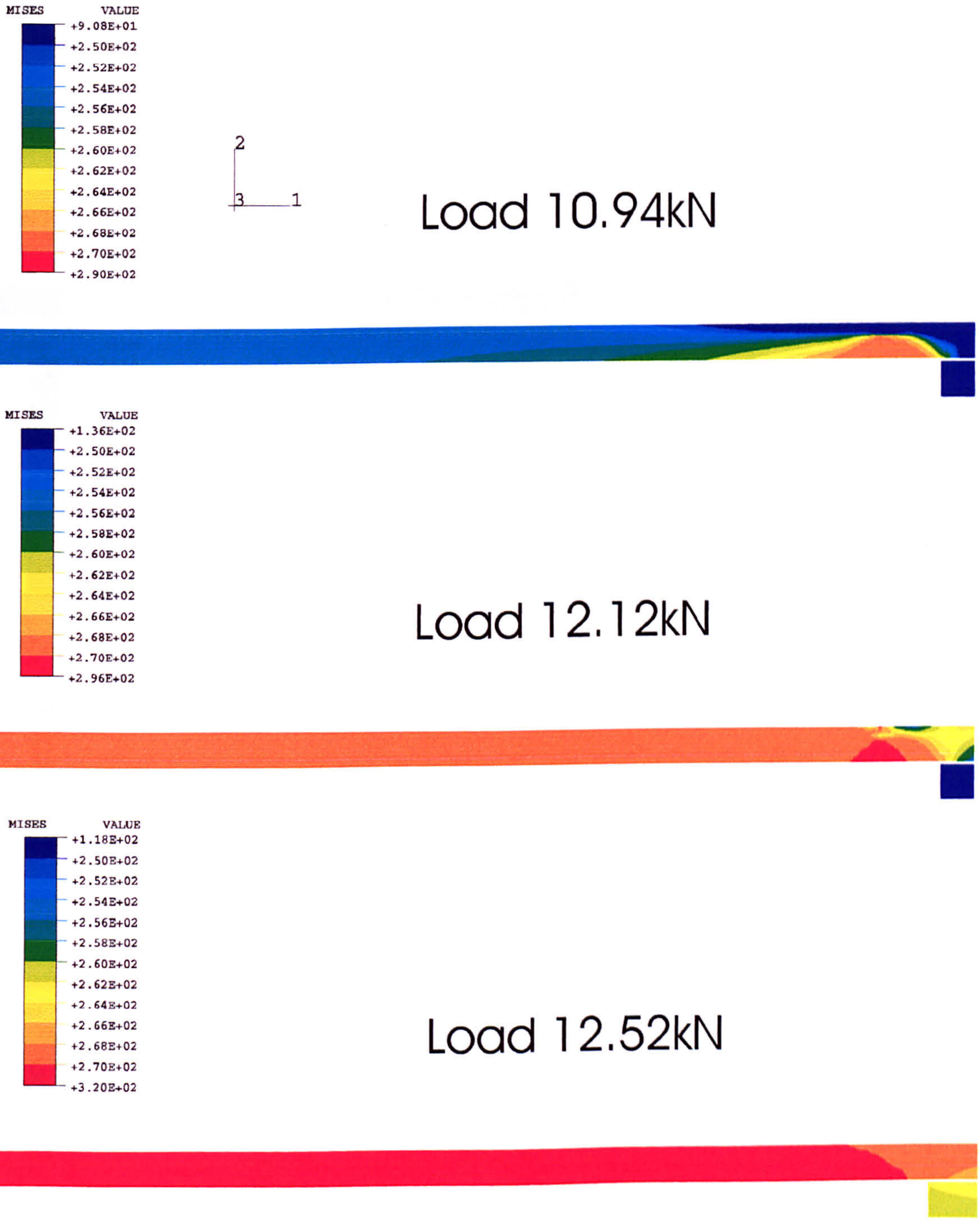

40 mm overlap - mild steel - AV 119 adhesive

Figure 7.50 Contour plots of Mises stress variation in the adherends for 40 mm overlap, mild steel, AV 119 adhesive SLJ under tensile loading

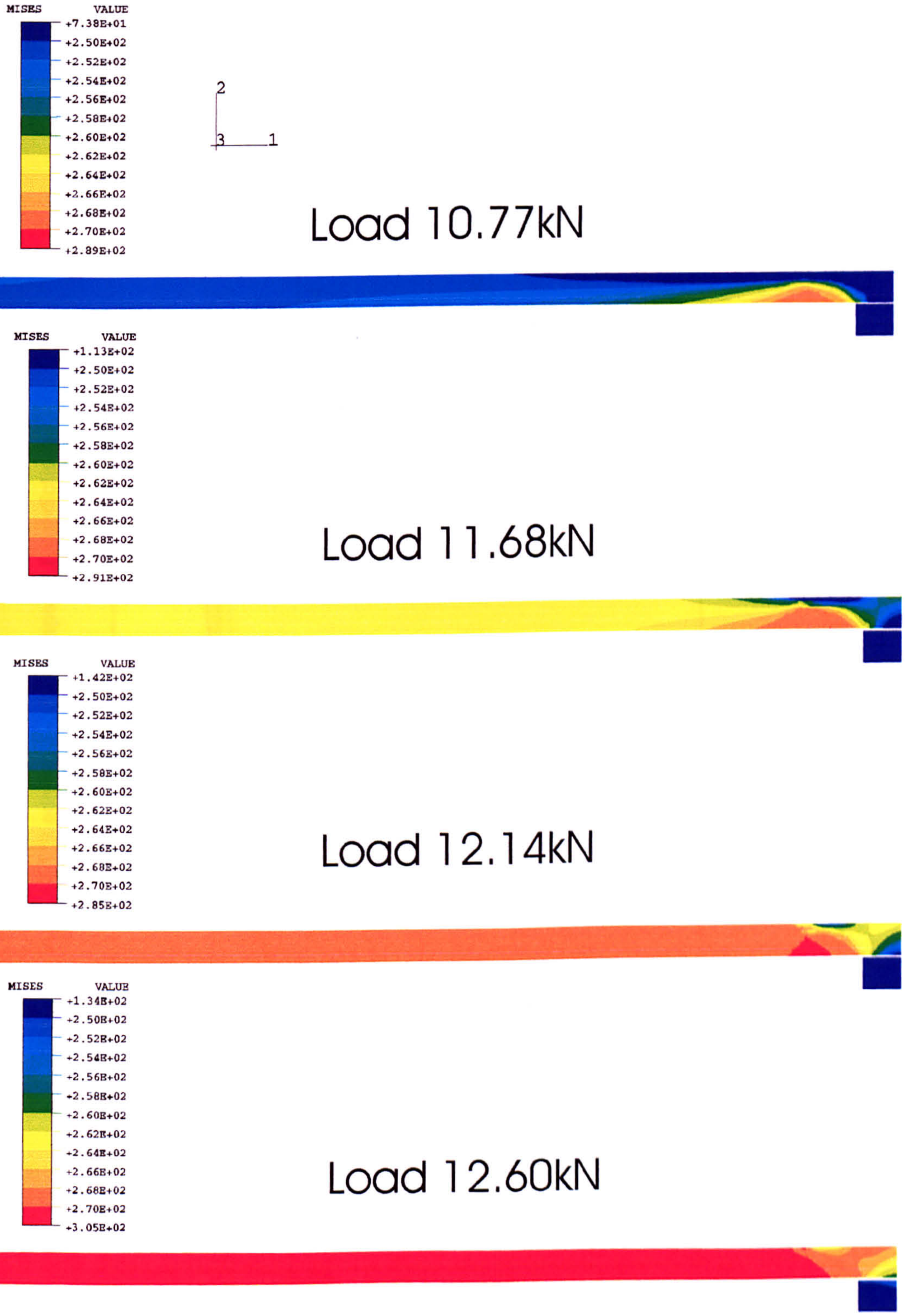

Figure 7.51 Contour plots of Mises stress variation in the adherends for 60 mm overlap, mild steel, AV 119 adhesive SLJ under tensile loading

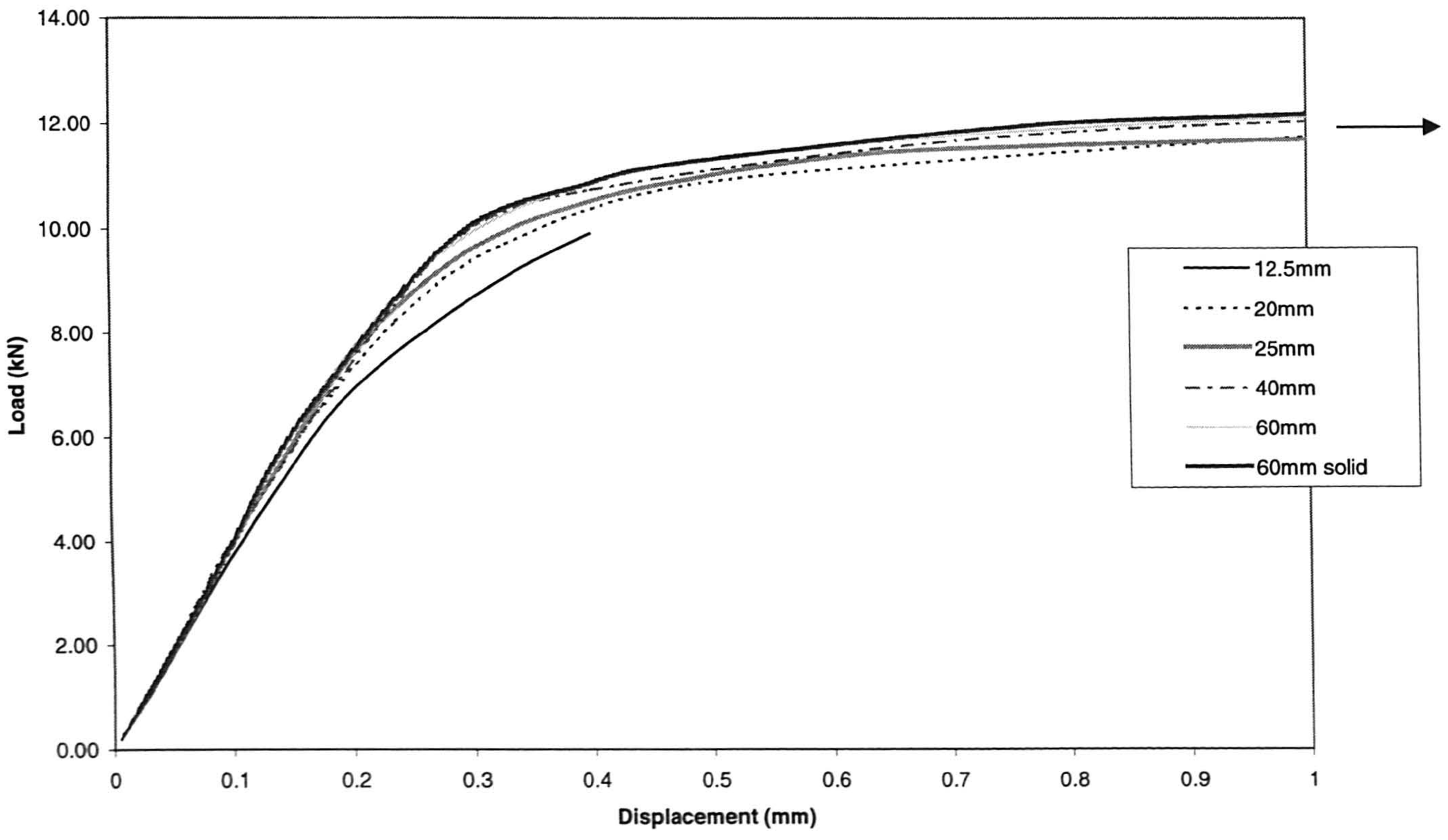

Figure 7.52 Load-displacement curves from F.E predictions for mild steel AV 119 adhesive SLJs for various overlaps under tensile loading

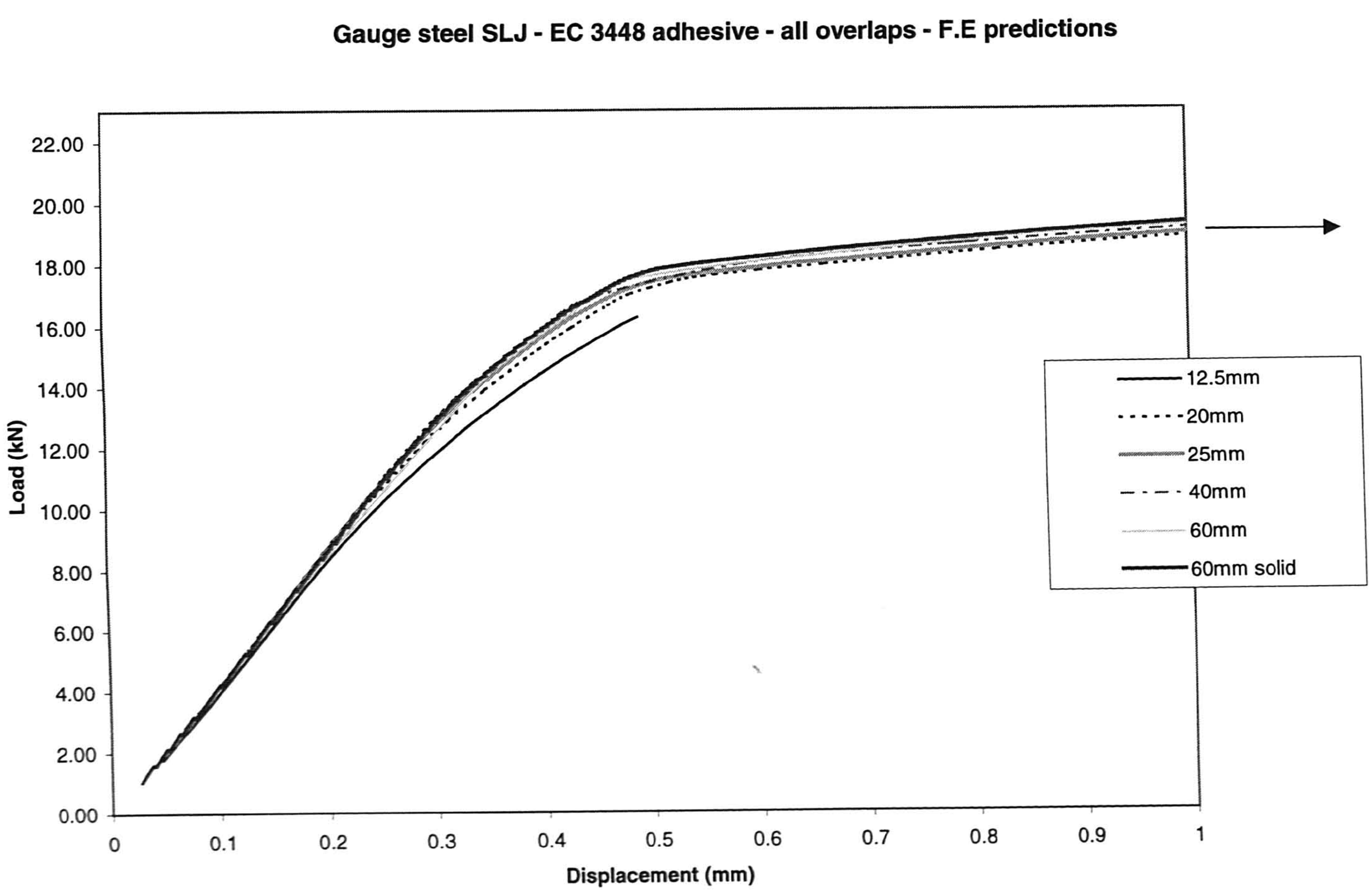

Figure 7.53 Load-displacement curves from F.E predictions for gauge steel EC 3448 adhesive SLJs for various overlaps under tensile loading

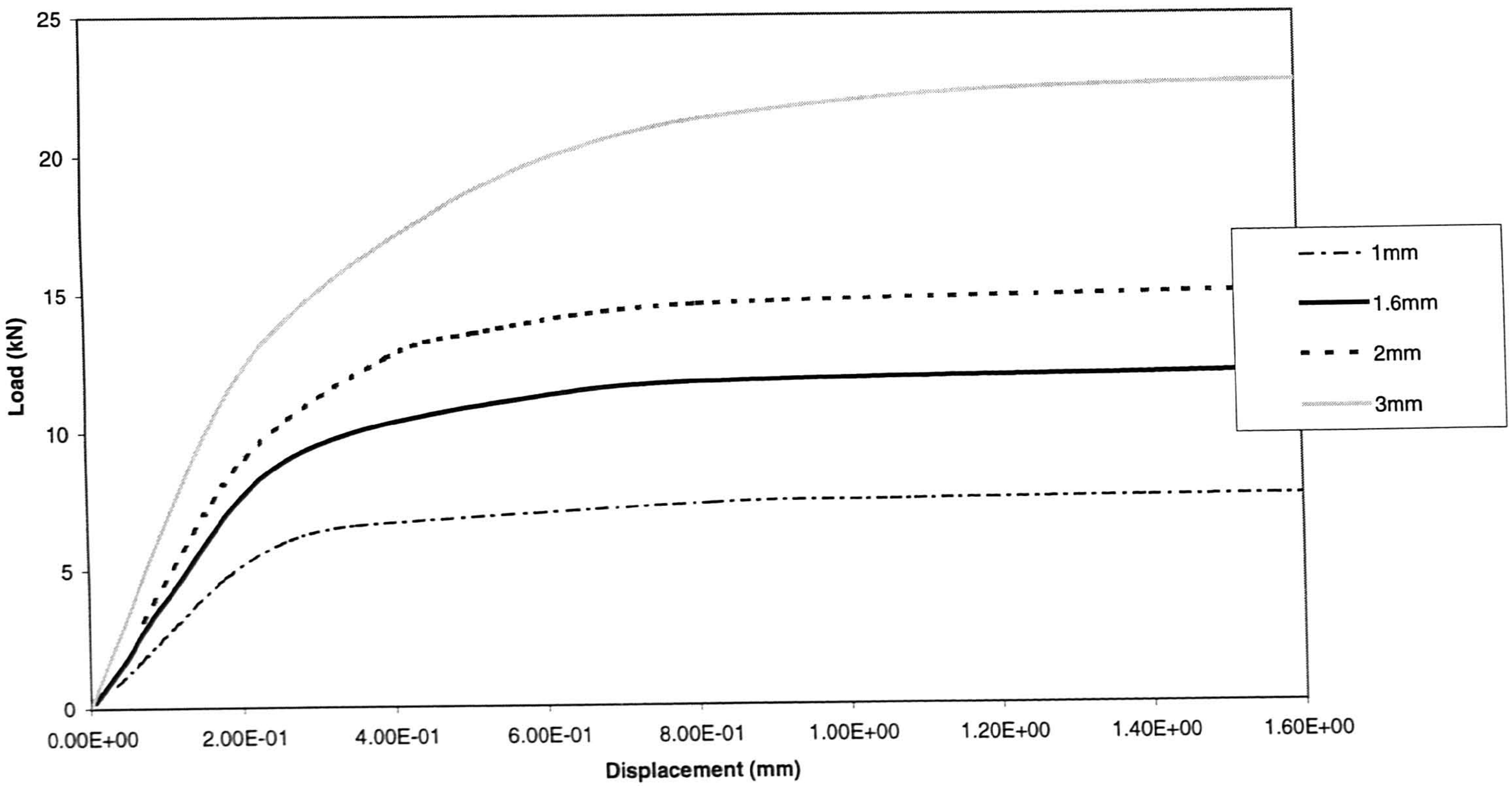

Figure 7.54 Load-displacement curves from F.E predictions for 25 mm overlap mild steel AV 119 adhesive SLJs for various adherend thicknesses under tensile loading

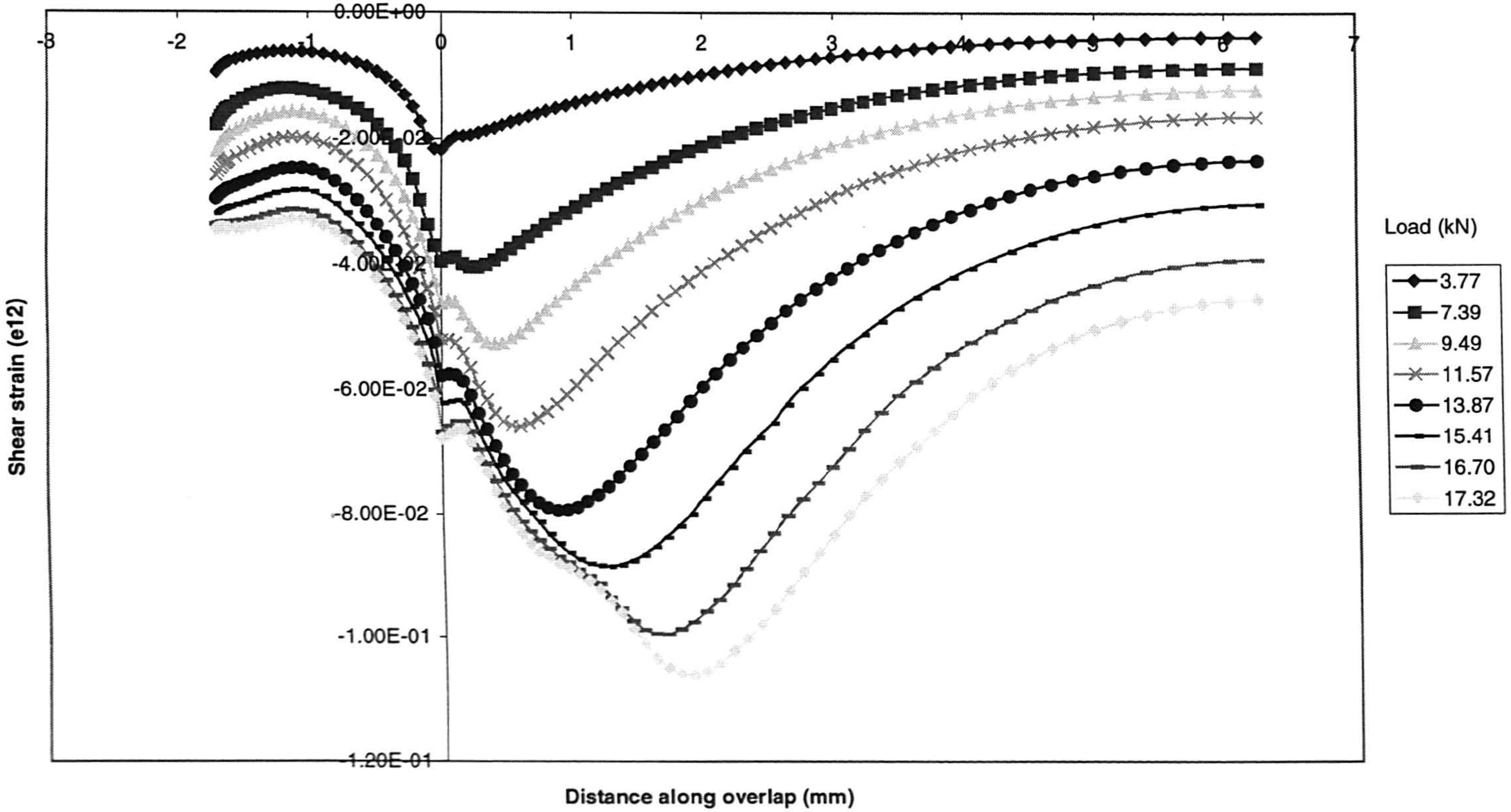

Figure 7.55 Variation of shear strain along the overlap length for the loaded interface - hard steel - EC 3448 adhesive - 12.5 mm overlap - 1.6 mm thick adherends - tensile loading

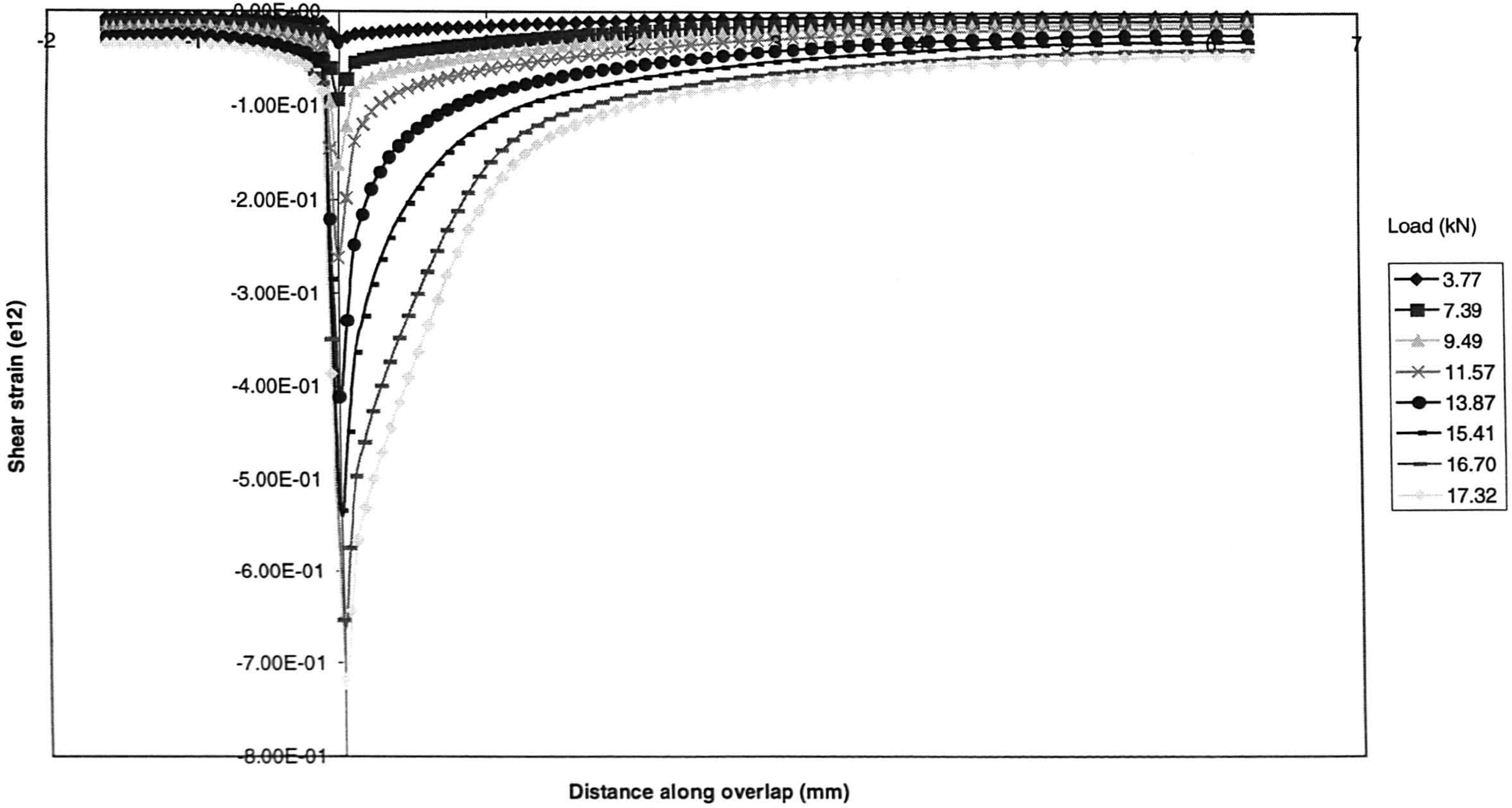

Figure 7.56 Variation of shear strain along the overlap length for the unloaded interface - hard steel - EC 3448 adhesive - 12.5 mm overlap - 1.6 mm thick adherends - tensile loading

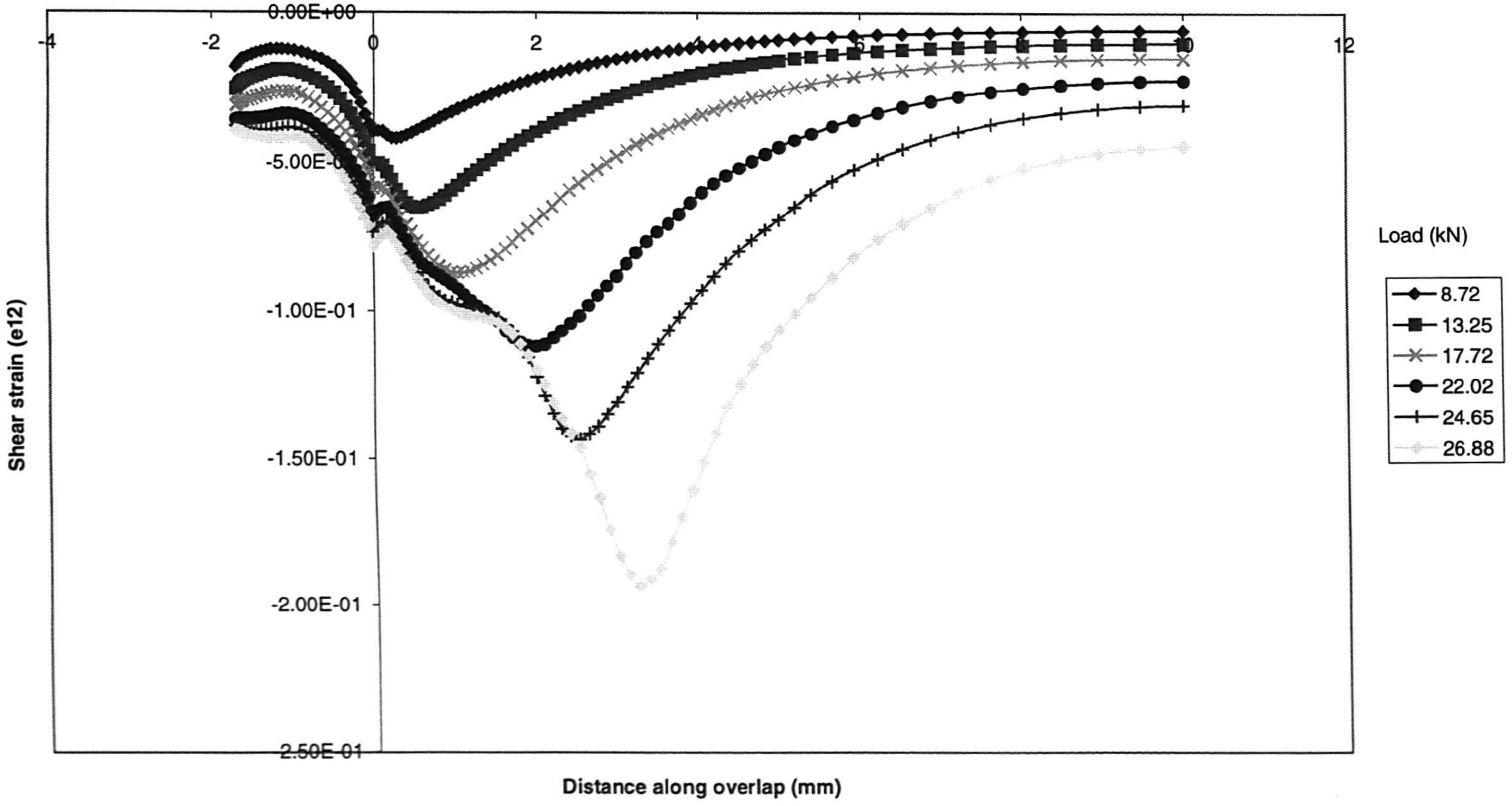

Figure 7.57 Variation of shear strain along the overlap length for the loaded interface - hard steel - EC 3448 adhesive - 20 mm overlap - 1.6 mm thick adherends - tensile loading

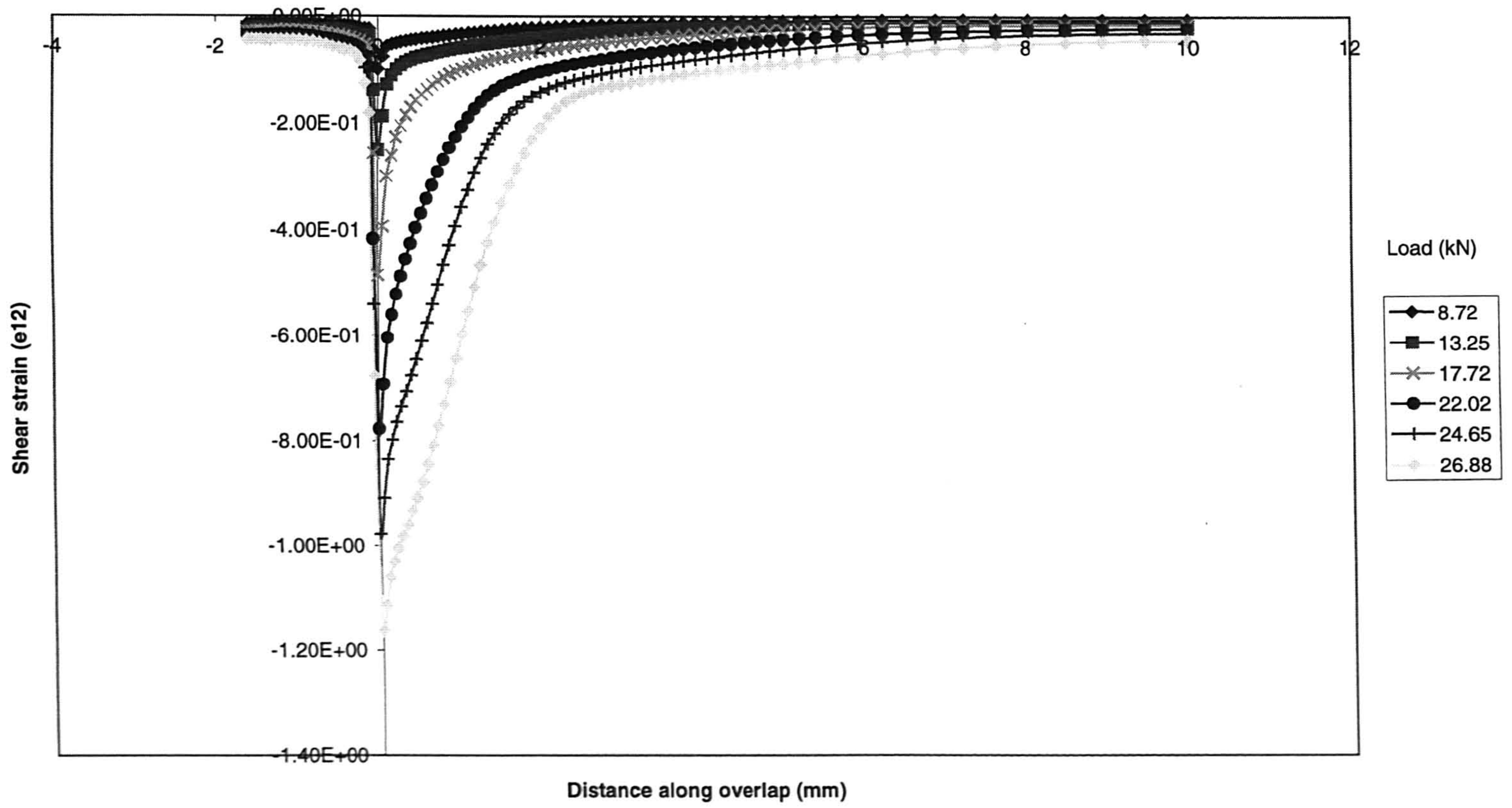

Figure 7.58 Variation of shear strain along the overlap length for the unloaded interface - Hard steel - EC 3448 adhesive - 20 mm overlap - 1.6 mm thick adherends - tensile loading

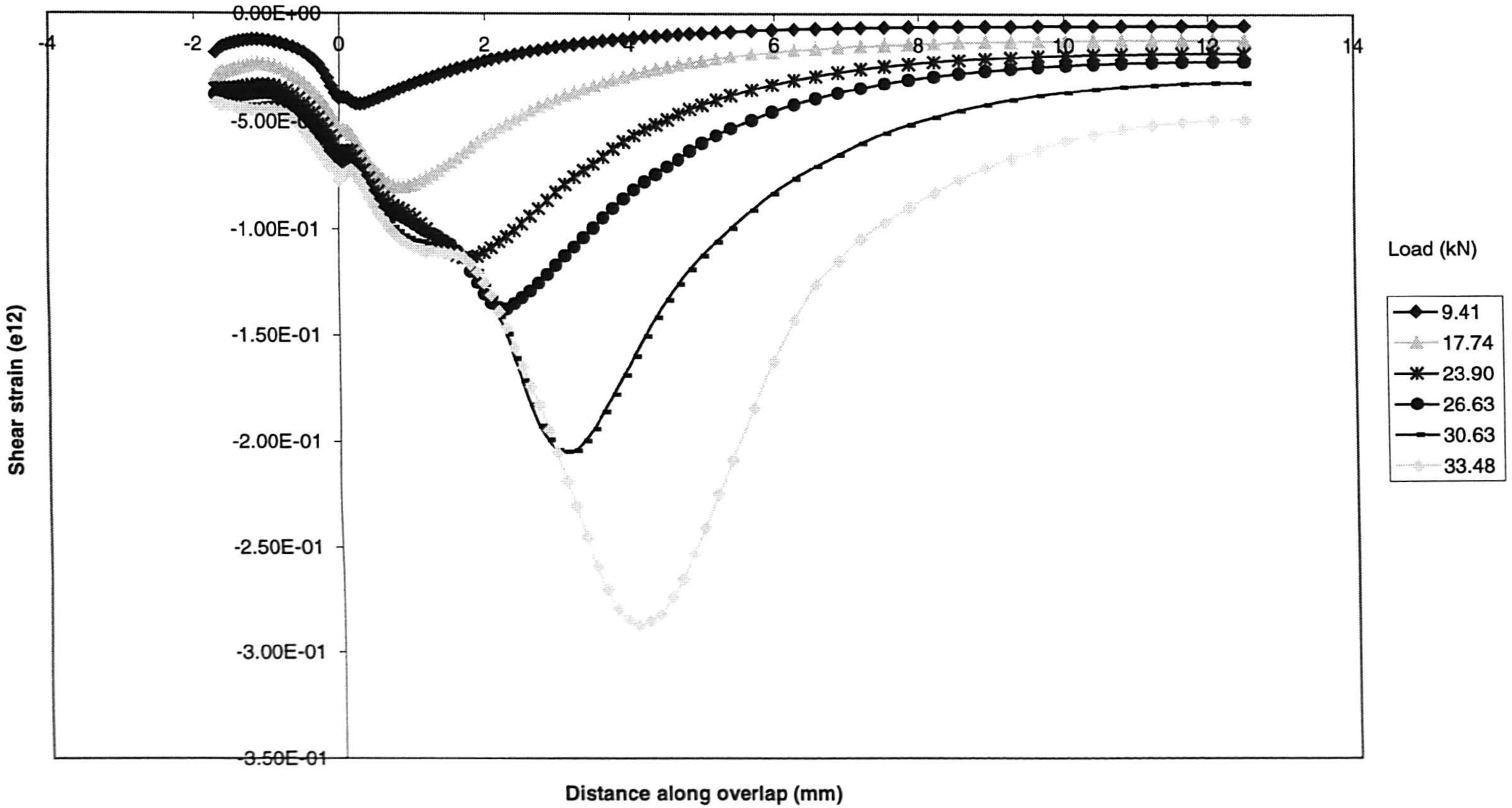

Figure 7.59 Variation of shear strain along the overlap length for the loaded interface - hard steel - EC 3448 adhesive - 25 mm overlap - 1.6 mm thick adherends - tensile loading

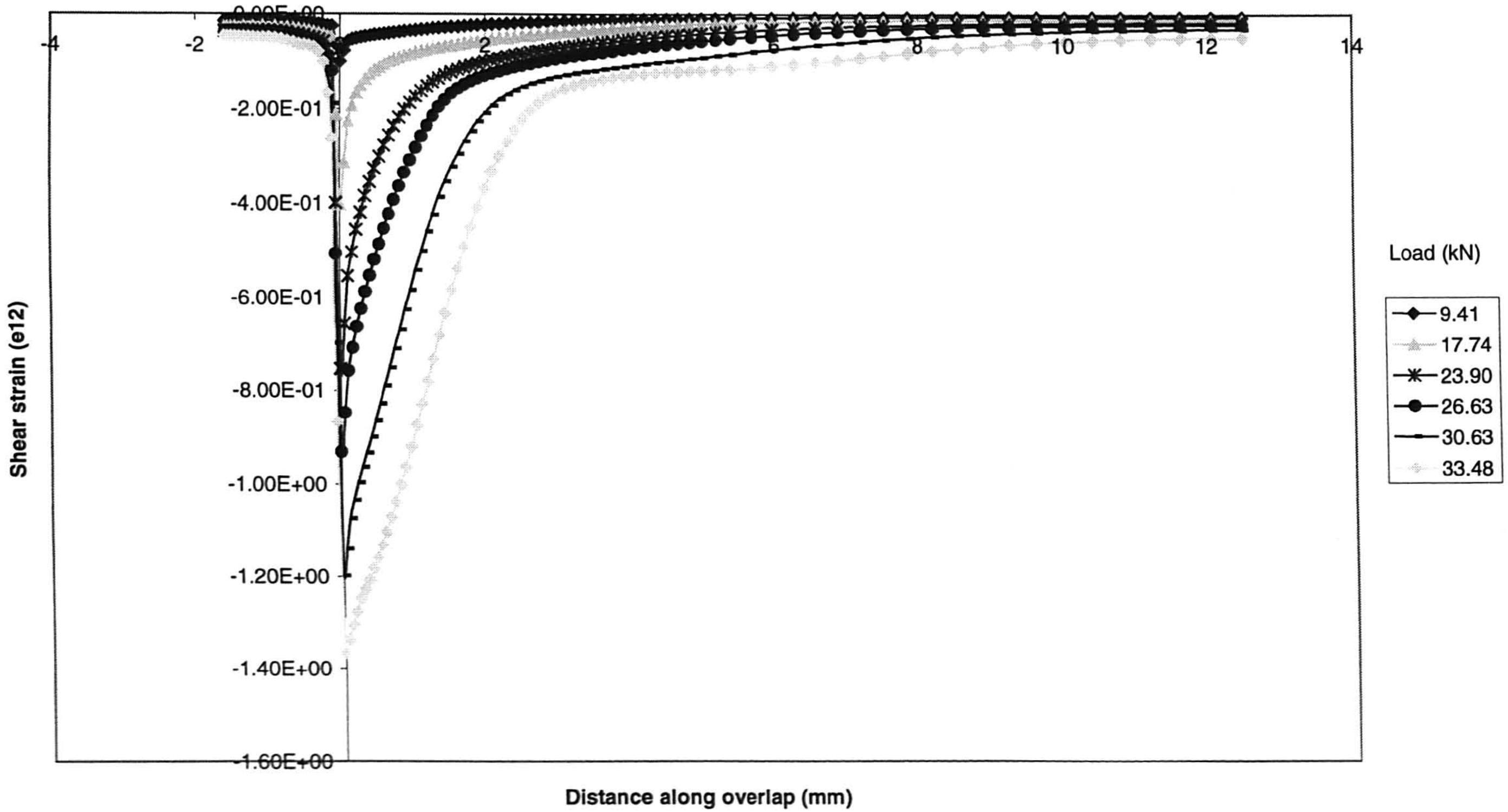

Figure 7.60 Variation of shear strain along the overlap length for the unloaded interface - hard steel - EC 3448 adhesive - 25 mm overlap - 1.6 mm thick adherends - tensile loading

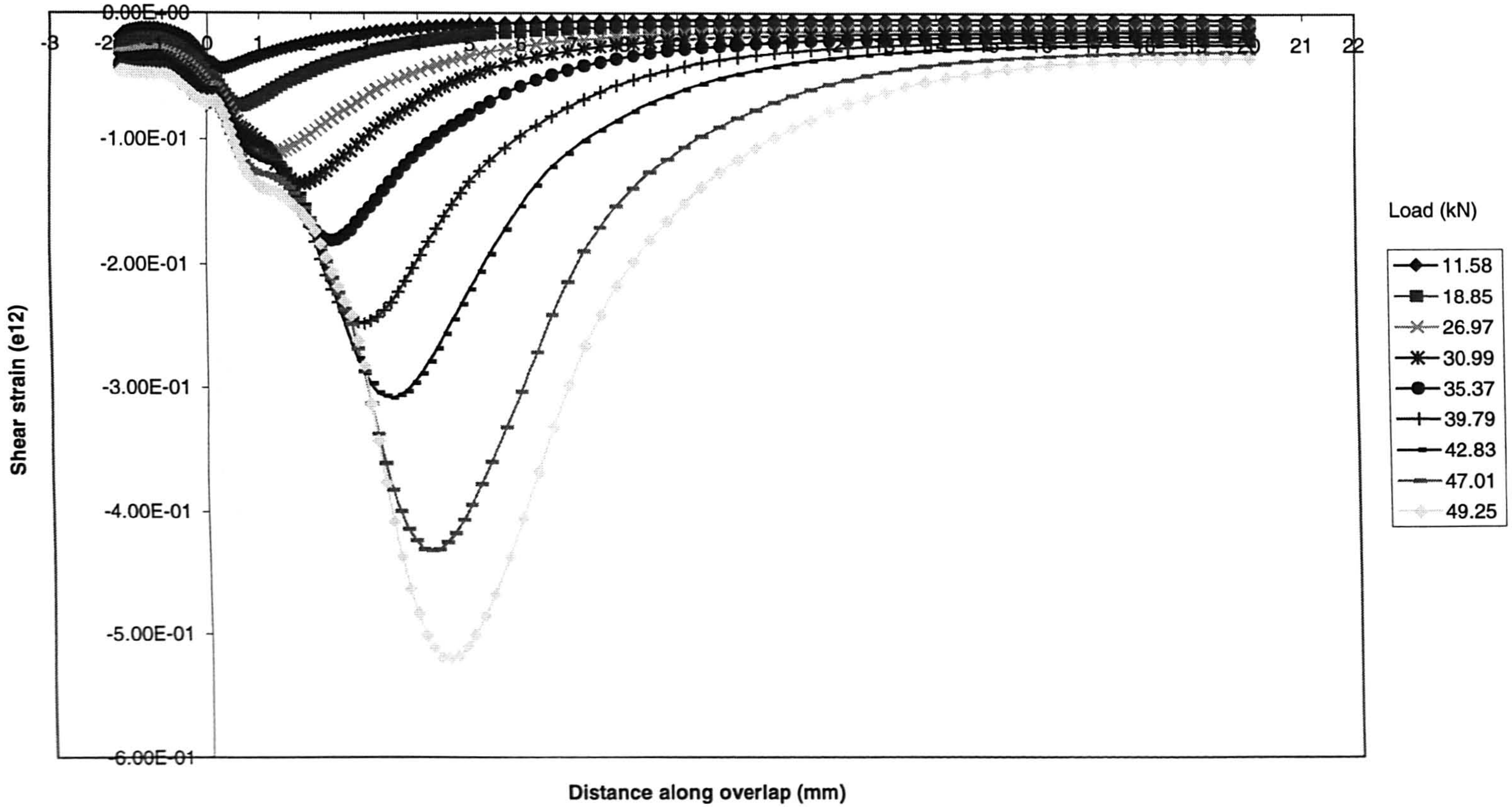

Figure 7.61 Variation of shear strain along the overlap length for the loaded interface - hard steel - EC 3448 adhesive - 40 mm overlap - 1.6 mm thick adherends - tensile loading

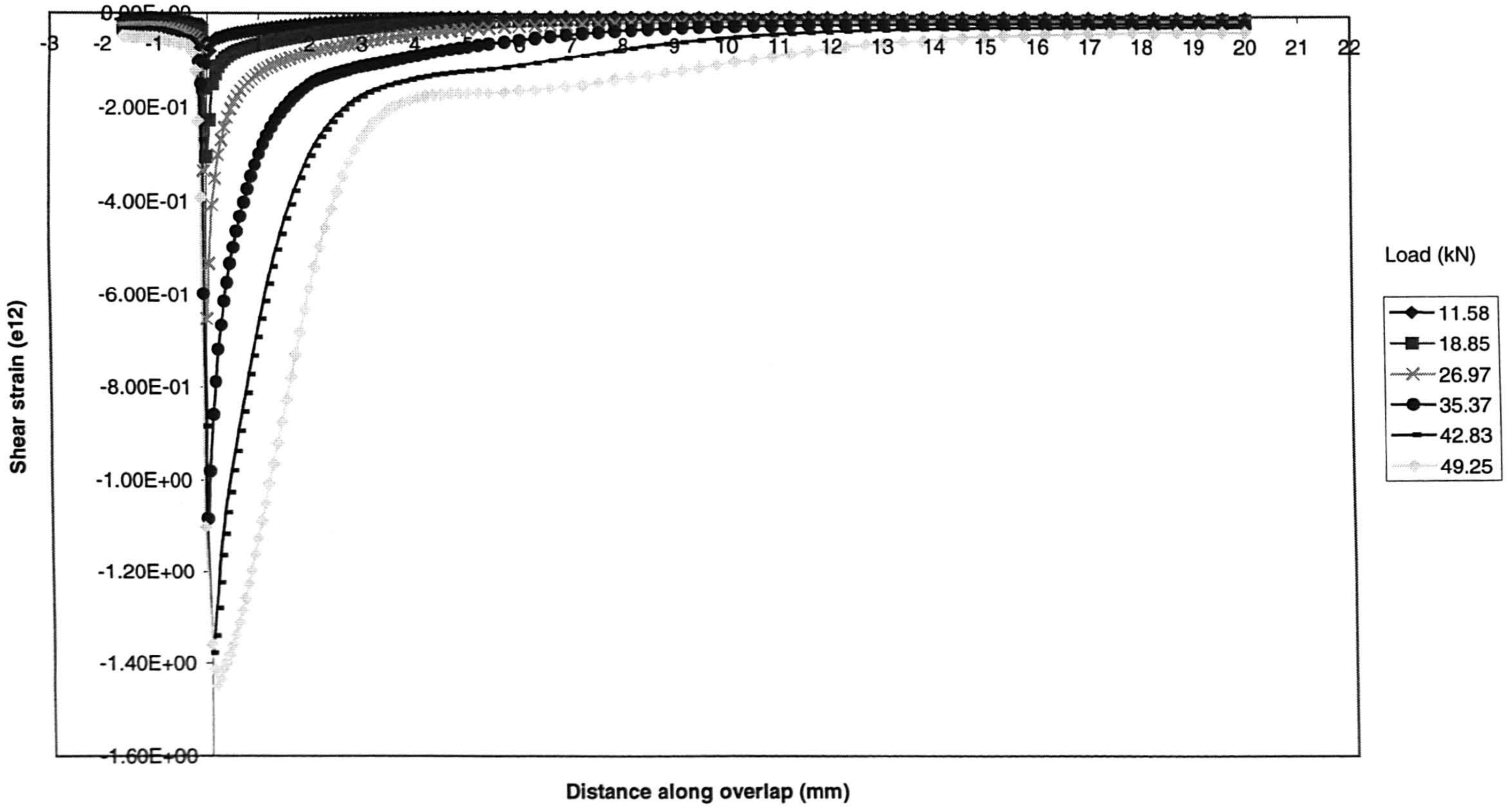

Figure 7.62 Variation of shear strain along the overlap length for the unloaded interface - hard steel - EC 3448 adhesive - 40 mm overlap - 1.6 mm thick adherends - tensile loading

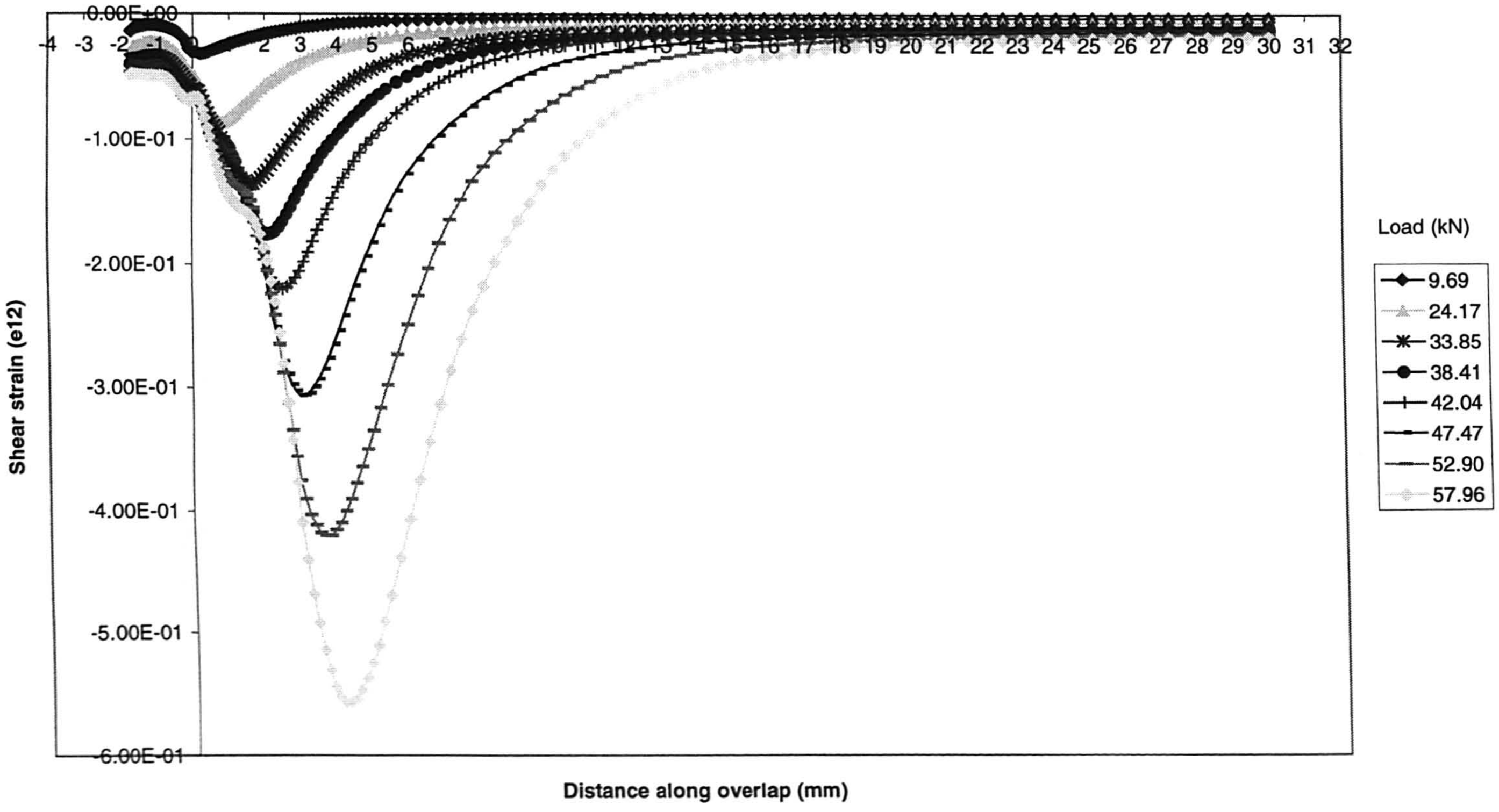

Figure 7.63 Variation of shear strain along the overlap length for the loaded interface - hard steel - EC 3448 adhesive - 60 mm overlap - 1.6 mm thick adherends - tensile loading

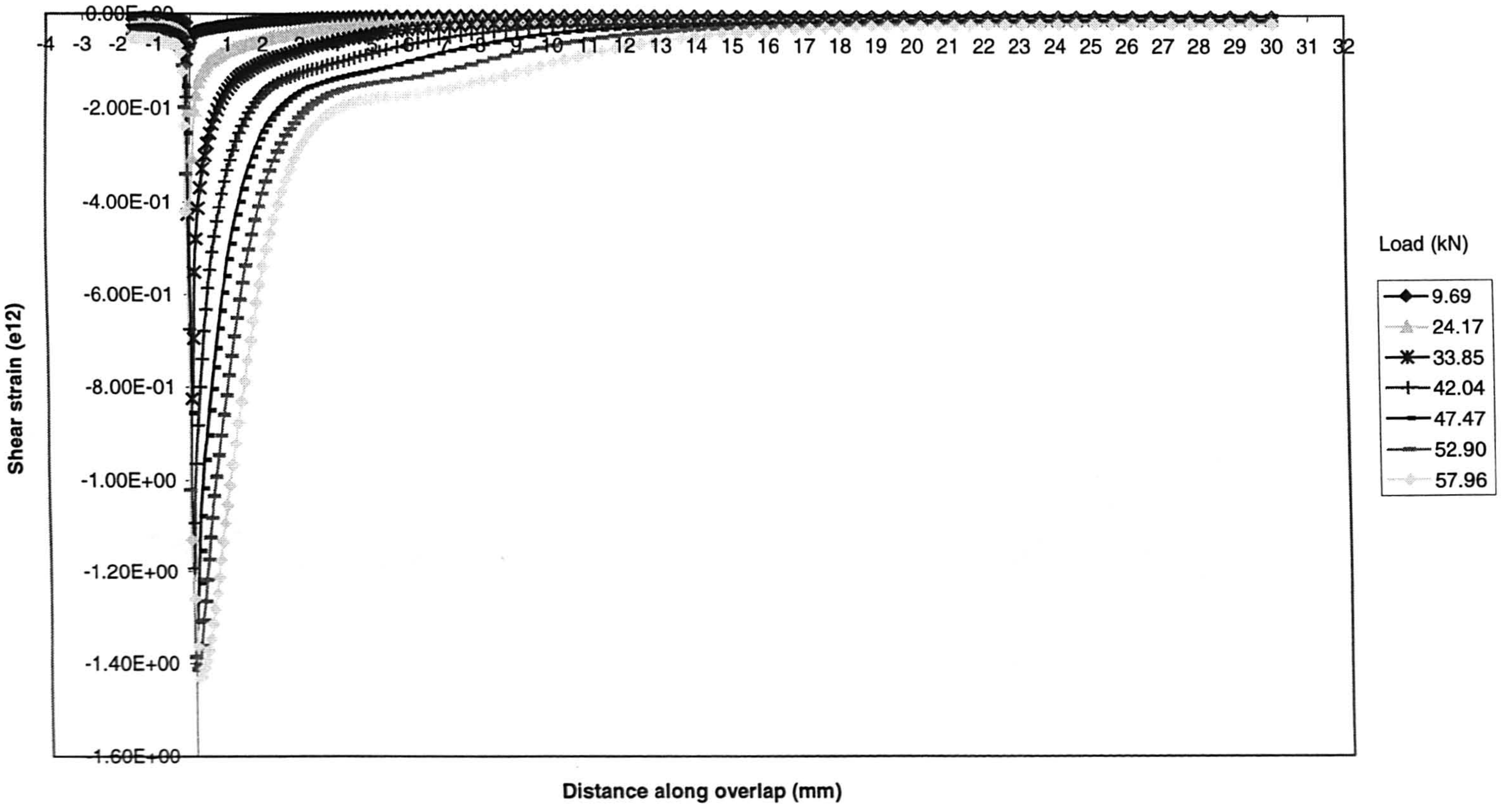

Figure 7.64 Variation of shear strain along the overlap length for the unloaded interface - hard steel - EC 3448 adhesive - 60 mm overlap - 1.6 mm thick adherends - tensile loading

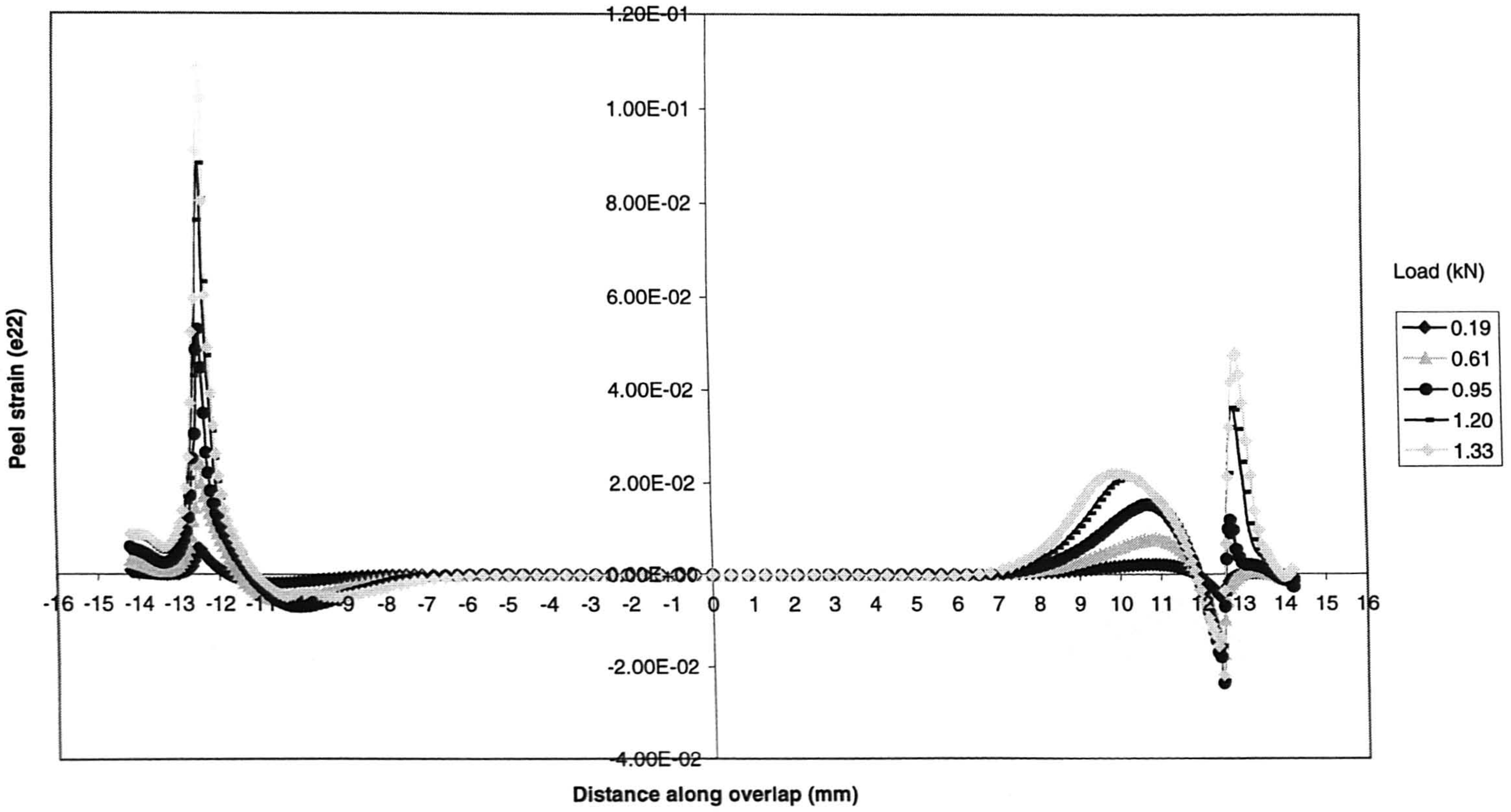

Figure 7.65 Variation of peel strain along the overlap length for the loaded interface - hard steel - AV 119 adhesive - 25 mm overlap - 1.6 mm thick adherends - 4 point bend loading

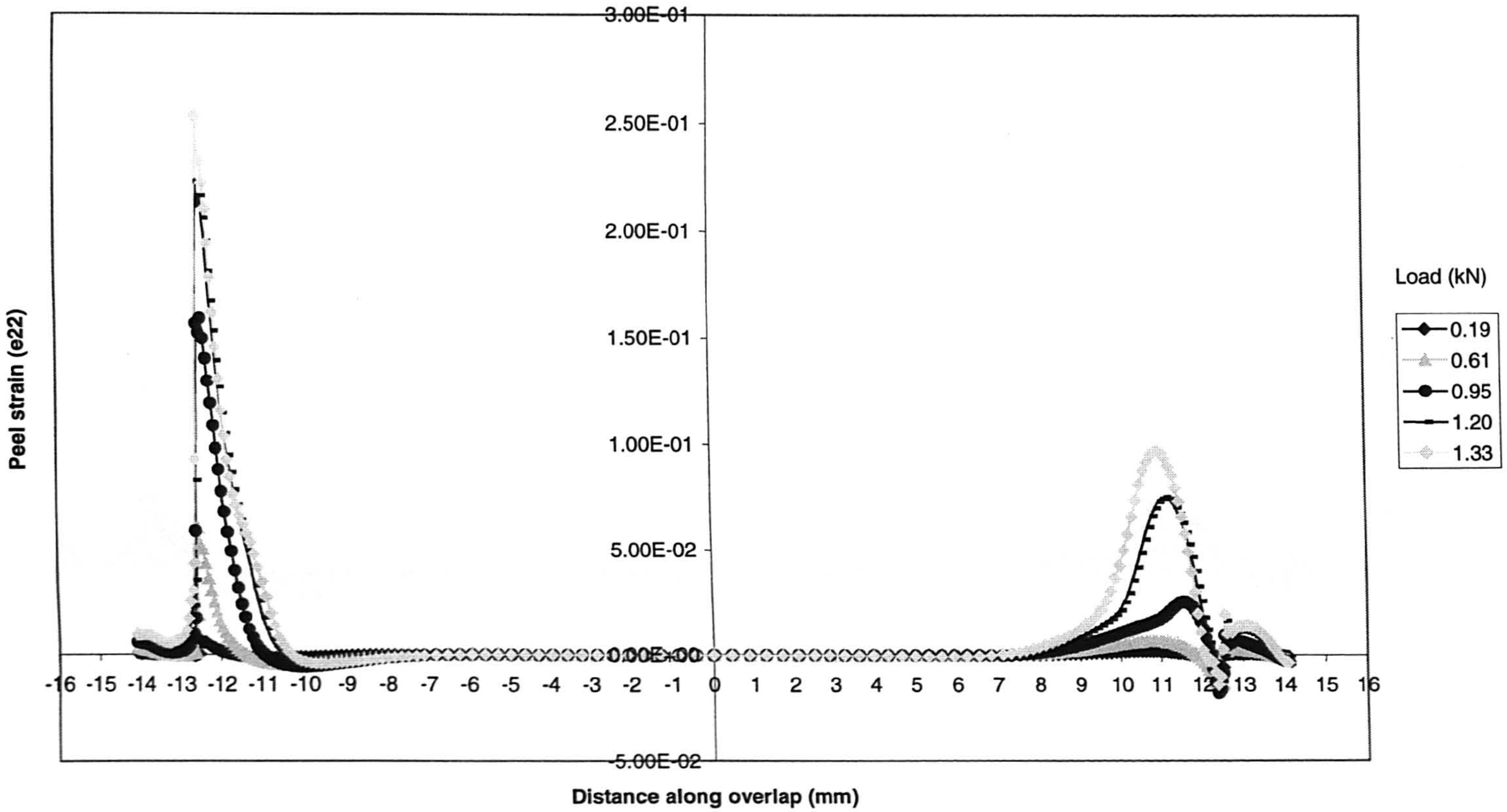

Figure 7.66 Variation of peel strain along the overlap length for the unloaded interface - hard steel - AV 119 adhesive - 25 mm overlap - 1.6 mm thick adherends - 4 point bend loading

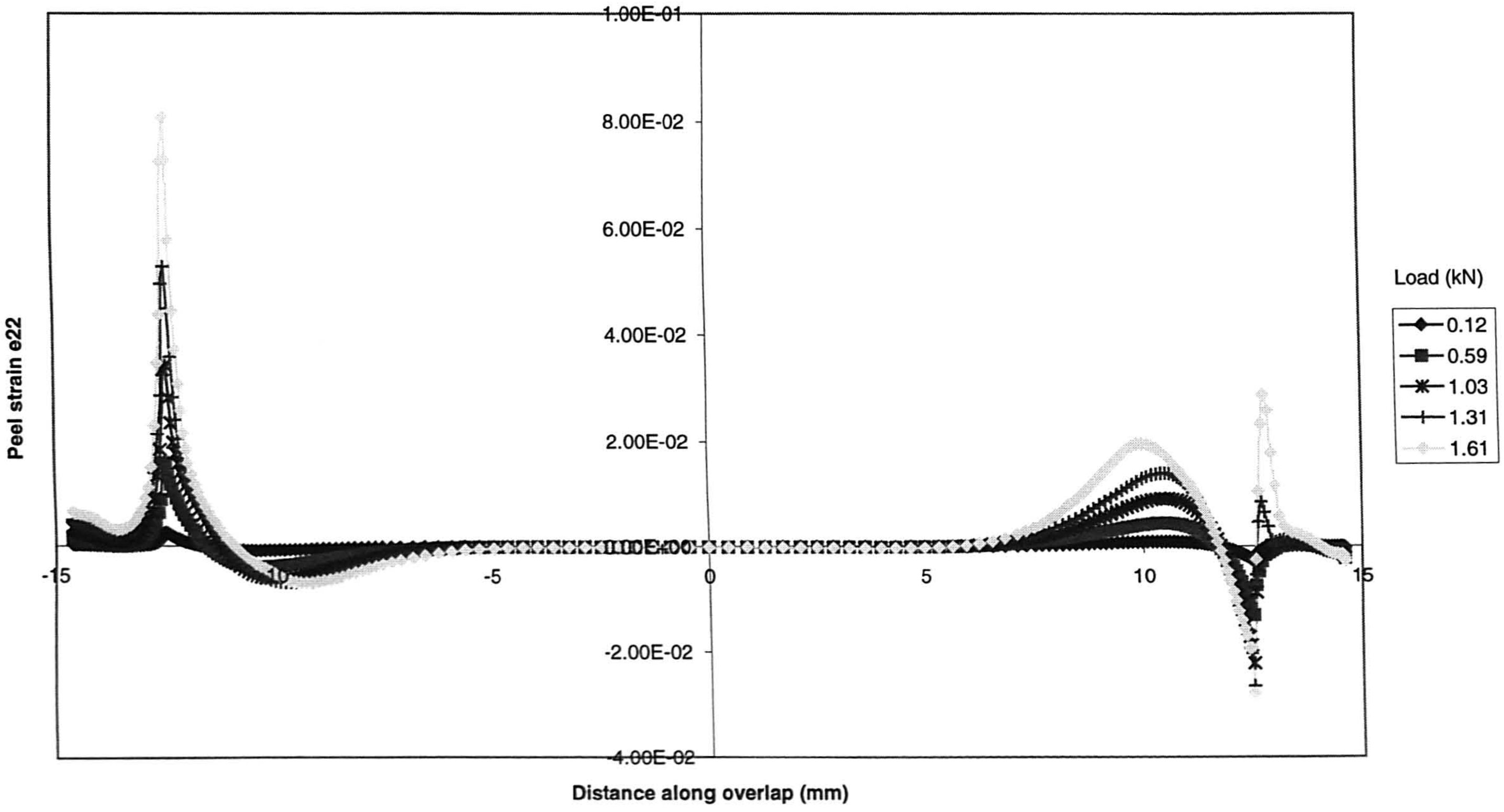

Figure 7.67 Variation of peel strain along the overlap length for the loaded interface - hard steel - AV 119 adhesive - 25 mm overlap - 2 mm thick adherends - 4 point bend loading

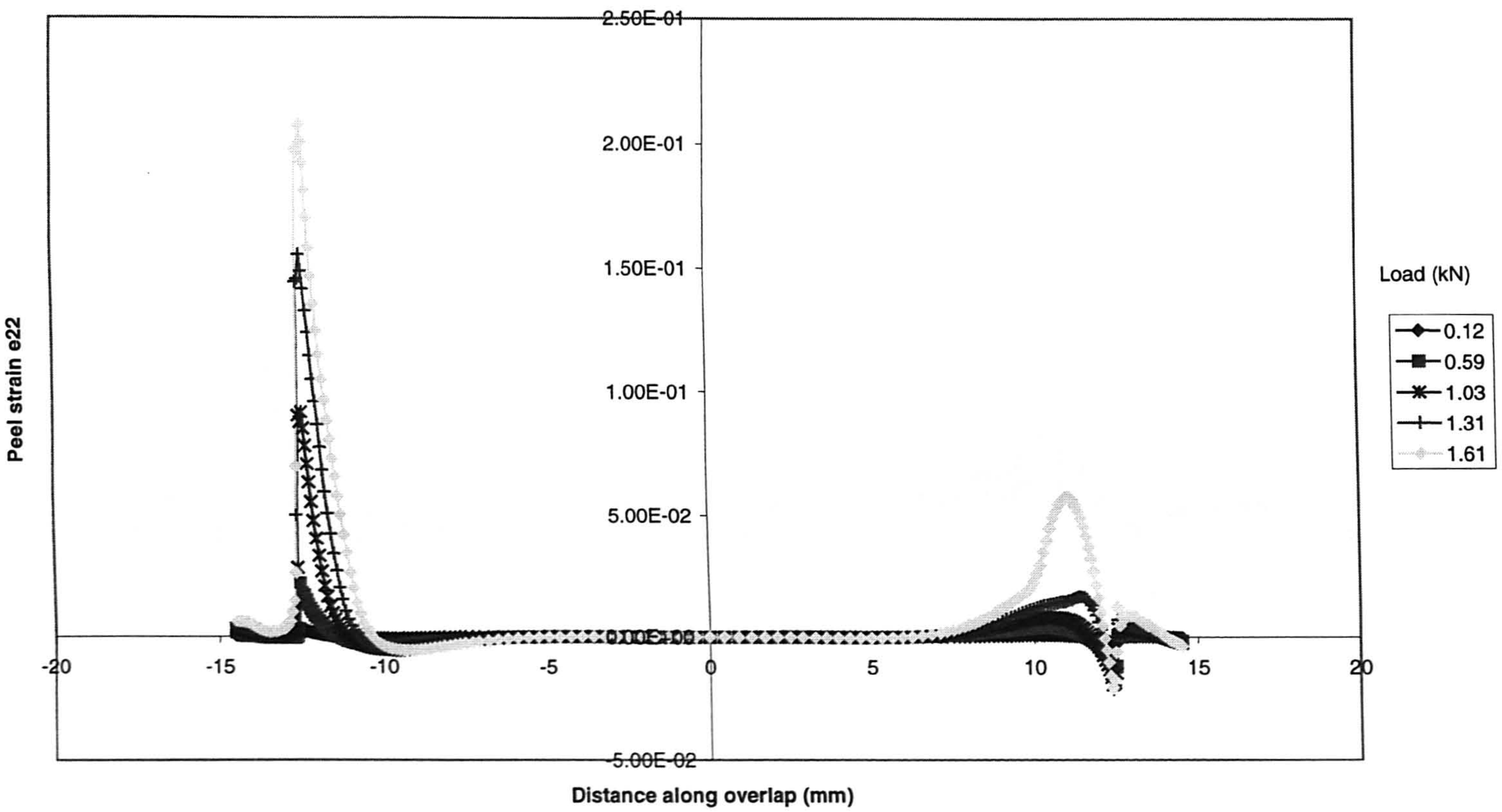

Figure 7.68 Variation of peel strain along the overlap length for the unloaded interface - hard steel - AV 119 adhesive - 25 mm overlap - 2 mm thick adherends - 4 point bend loading

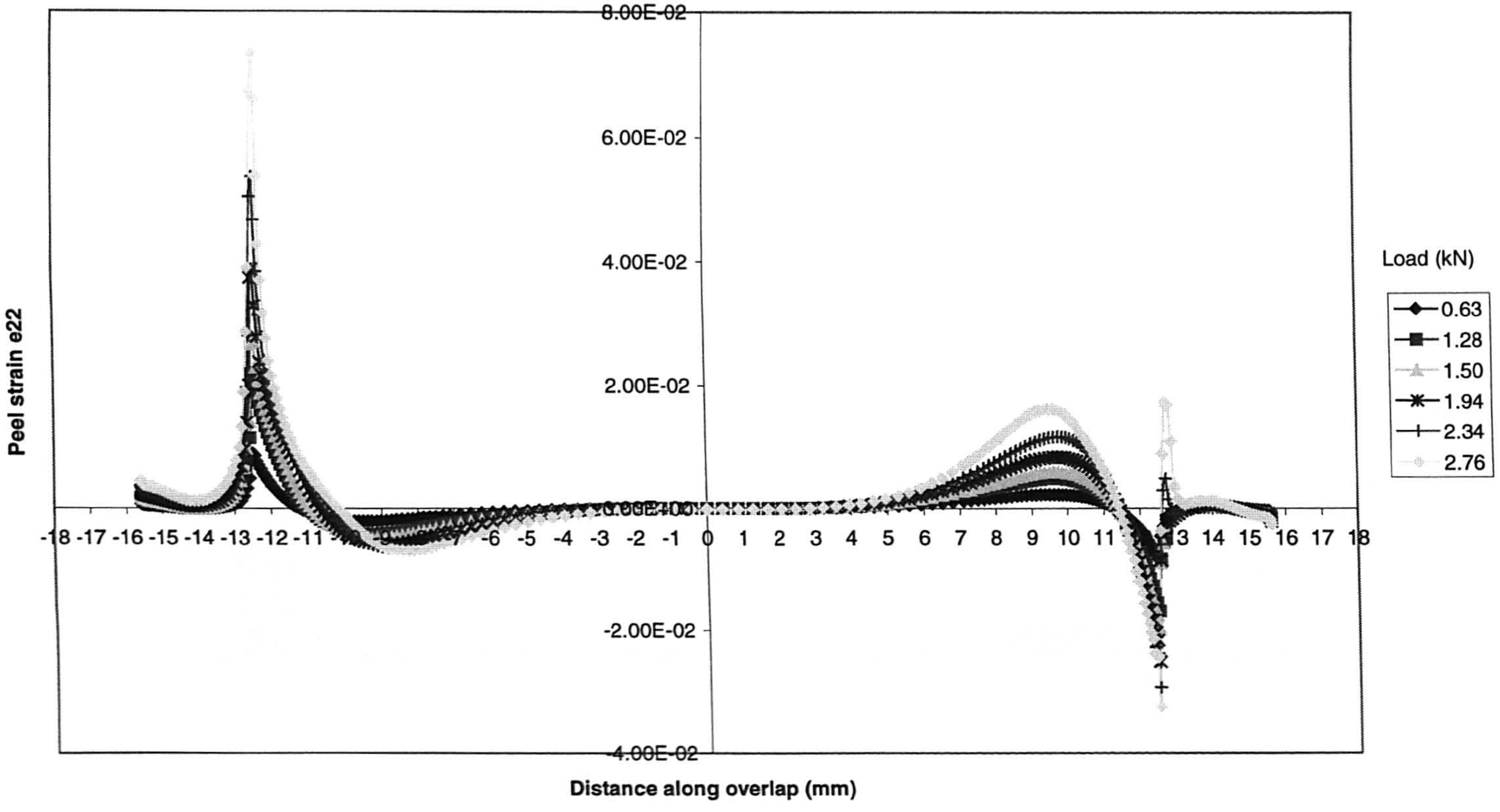

Figure 7.69 Variation of peel strain along the overlap length for the loaded interface - hard steel - AV 119 adhesive - 25 mm overlap - 3 mm thick adherends - 4 point bend loading

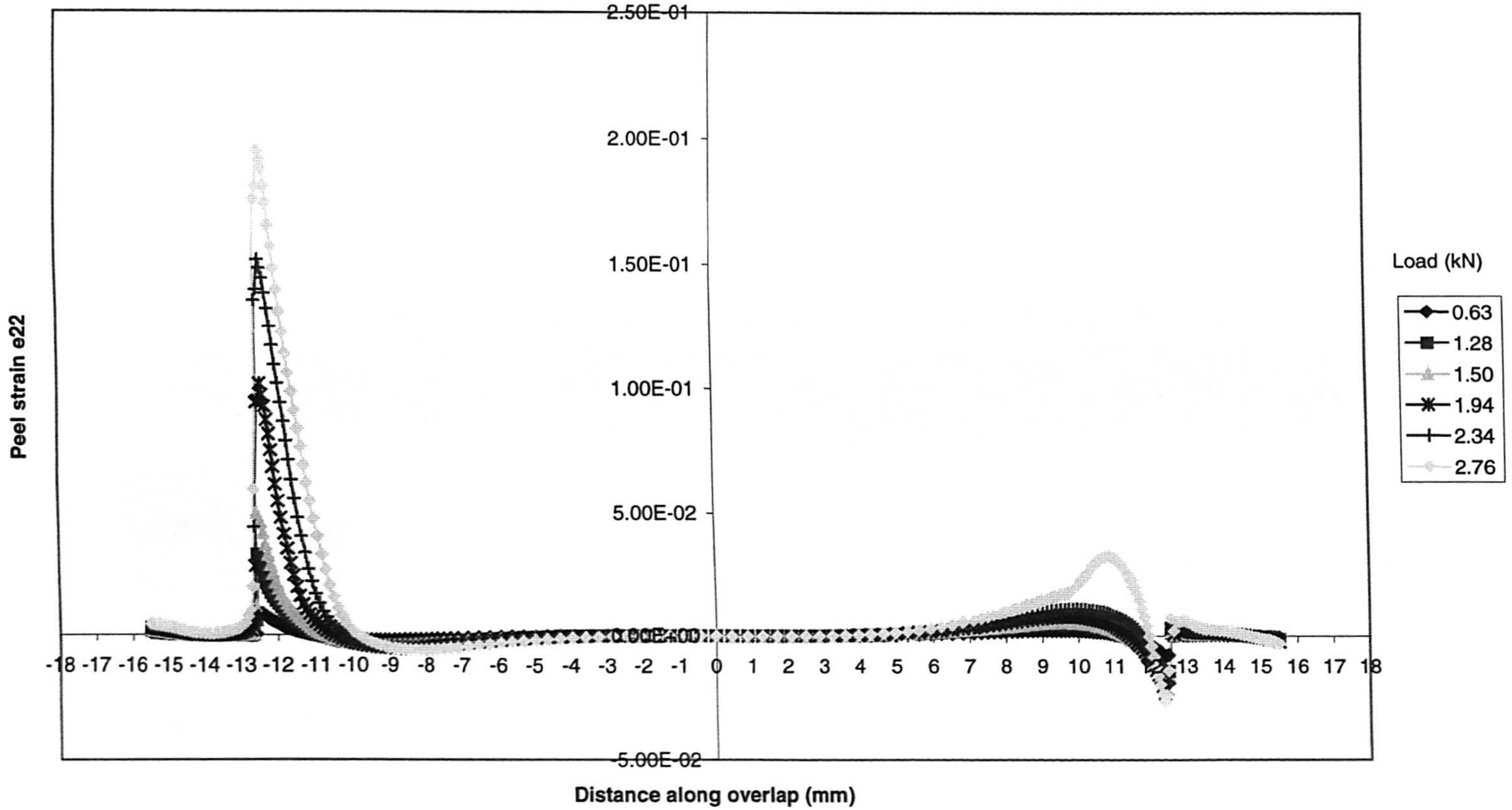

Figure 7.70 Variation of peel strain along the overlap length for the unloaded interface - hard steel - AV 119 adhesive - 25 mm overlap - 3 mm thick adherends - 4 point bend loading

25 mm overlap- hard steel - 1 mm thick adherends - AV 119 - tensile loading - 32.36kN load

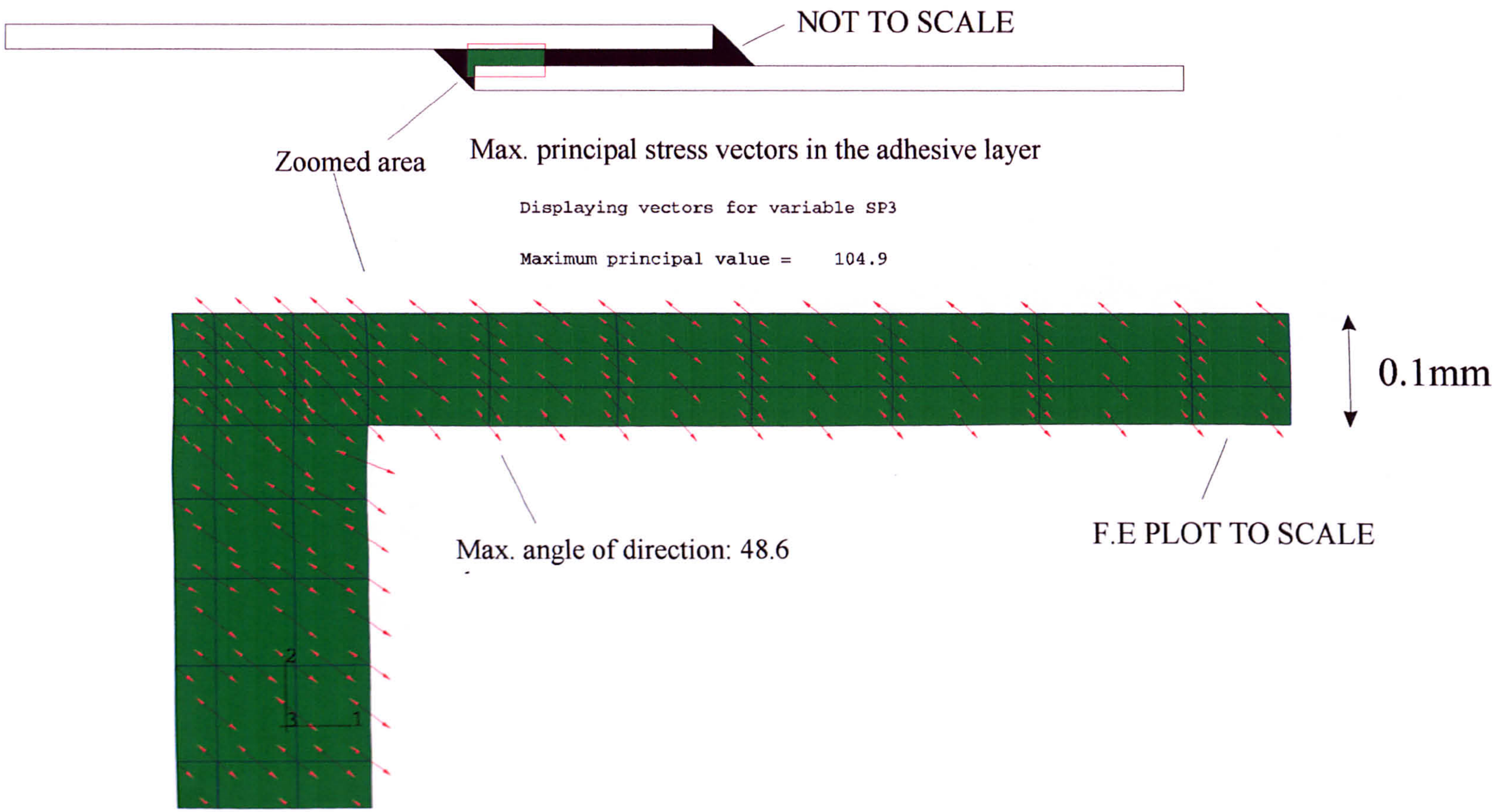

Figure 7.71 Maximum principal stress vectors in the adhesive layer for 25 mm overlap hard steel AV 119 SLJs - 1 mm thick adherends under tensile loading

25 mm overlap - hard steel - 1.6 mm thick adherends - AV 119 - tensile loading - 32.36kN

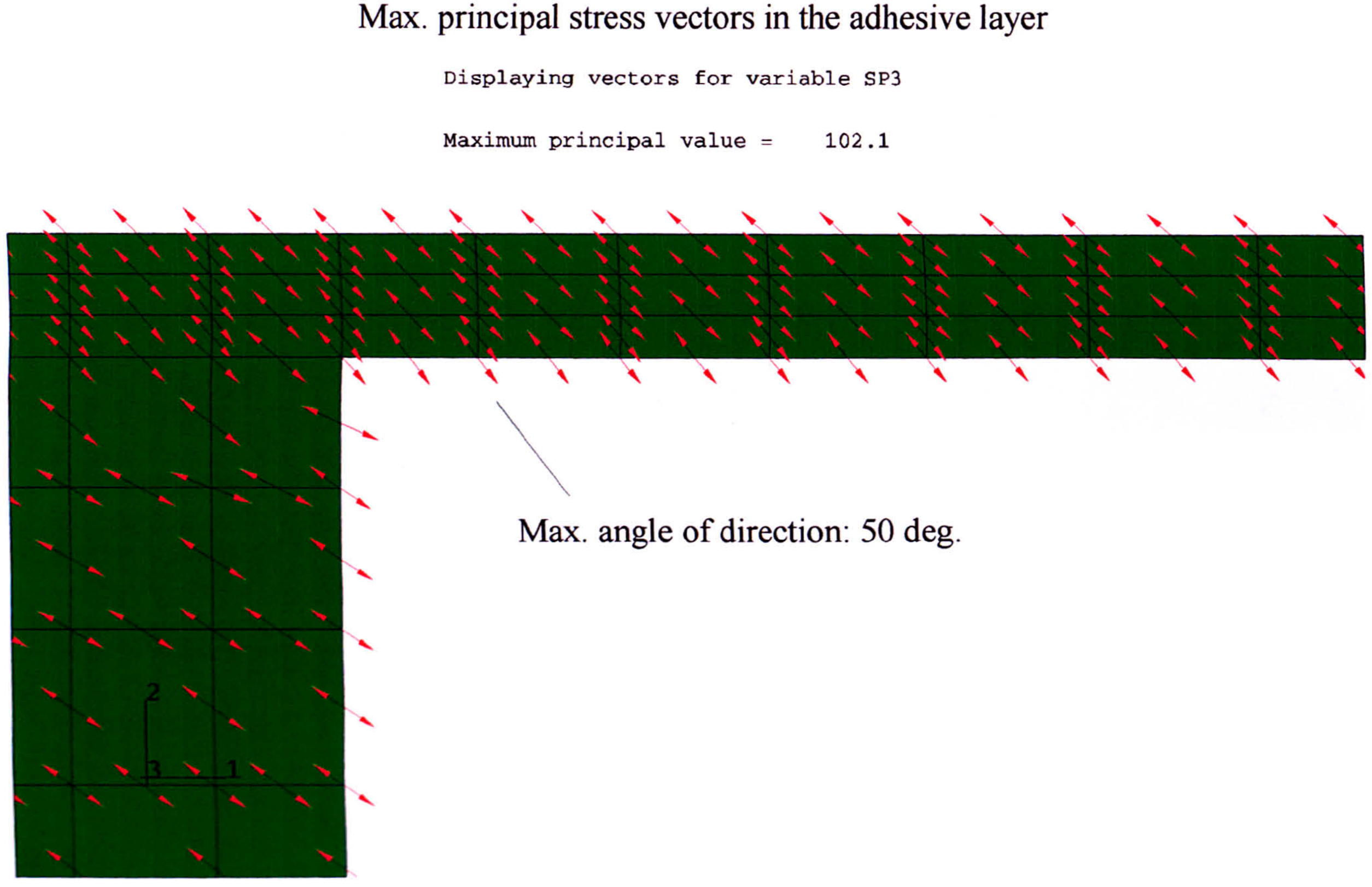

Figure 7.72 Maximum principal stress vectors in the adhesive layer for 25 mm overlap hard steel AV 119 SLJs - 1.6 mm thick adherends under tensile loading

25 mm overlap - hard steel - 2 mm thick adherends - AV 119 - tensile loading - 32.36kN

Max. principal stress vectors in the adhesive layer

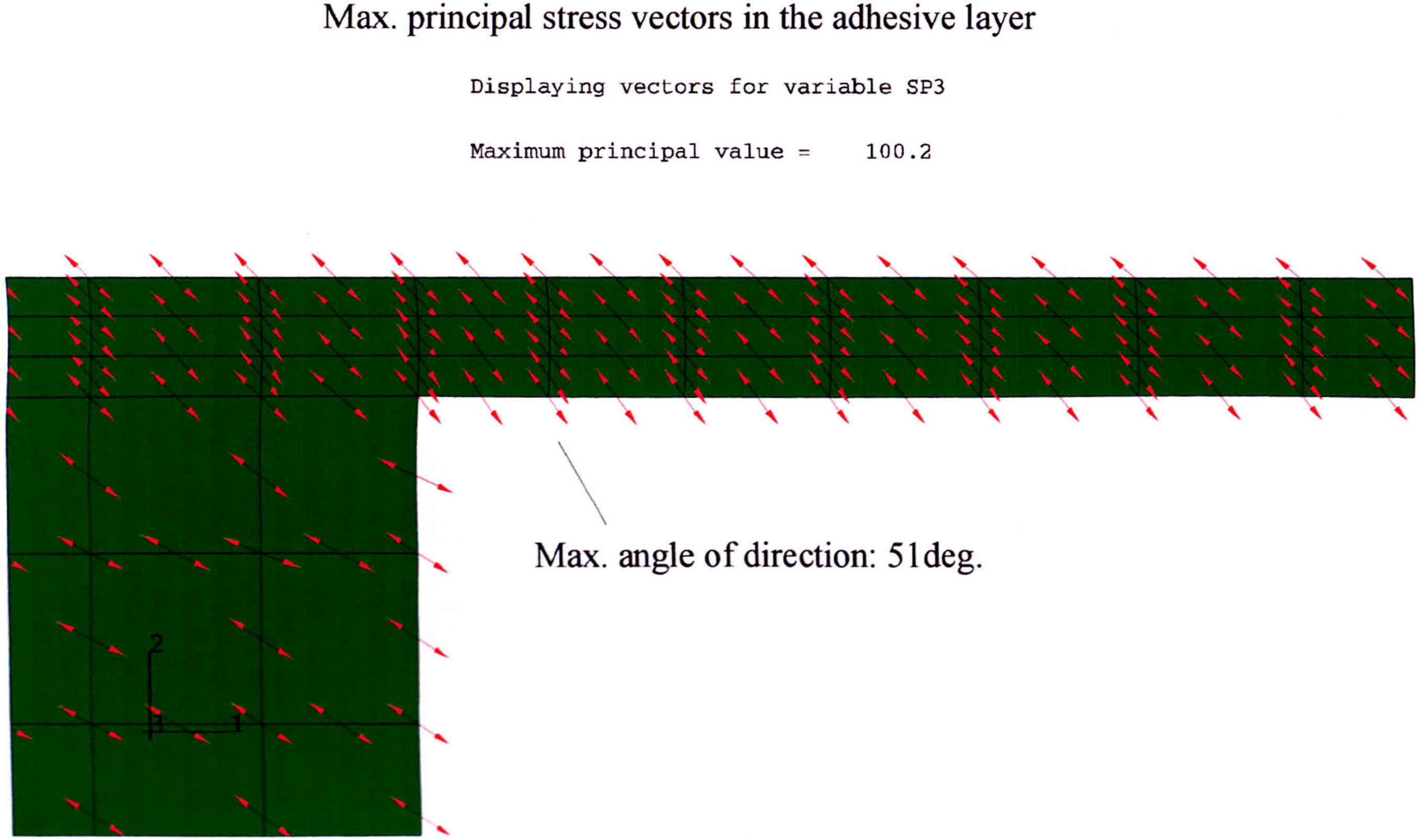

Figure 7.73 Maximum principal stress vectors in the adhesive layer for 25 mm overlap hard steel AV 119 SLJs - 2 mm thick adherends under tensile loading

25 mm overlap - hard steel - 1.6 mm thick adherends - AV 119 - 4pt bend test - 1.33kN load

Max. principal stress vectors in the adhesive layer

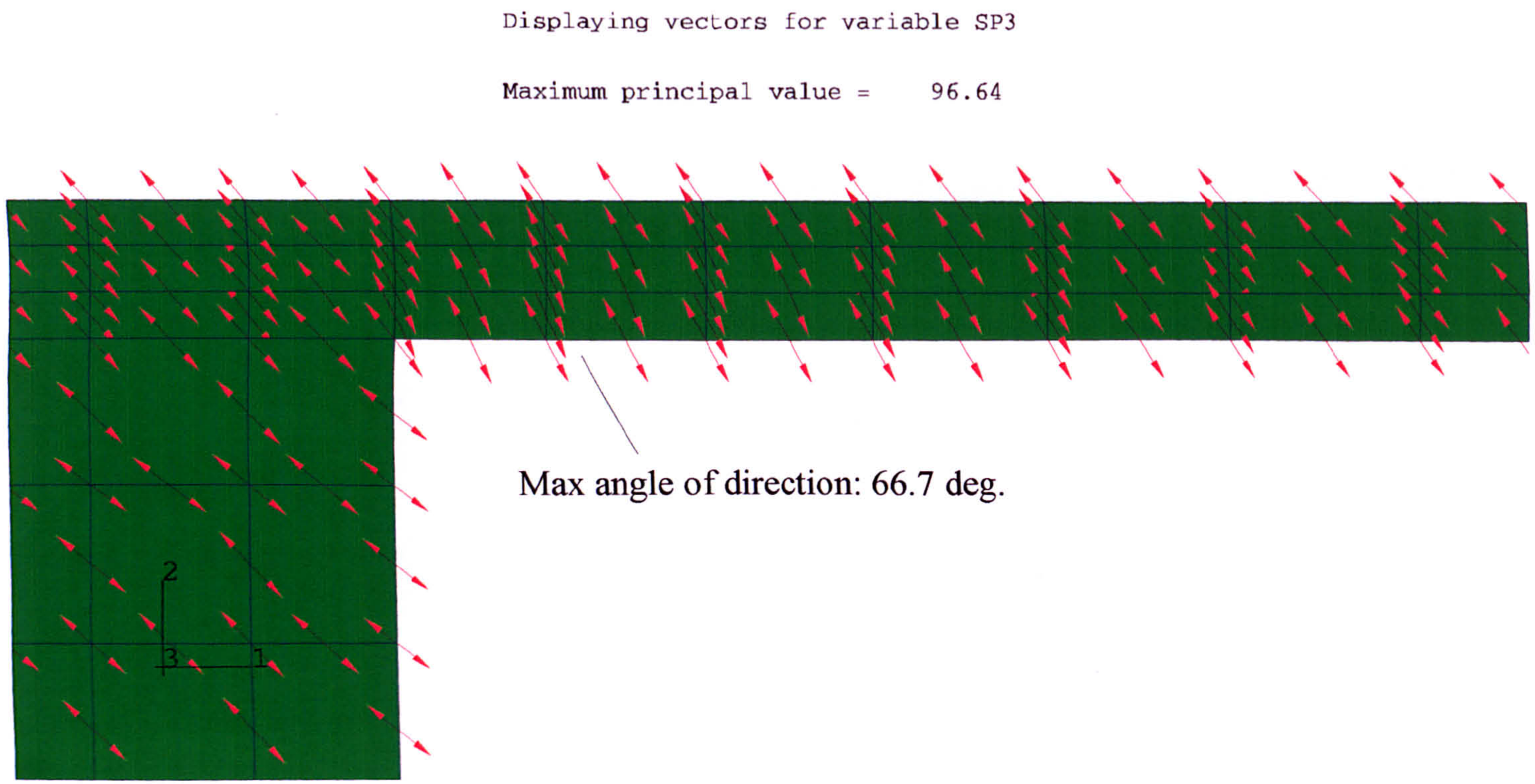

Figure 7.74 Maximum principal stress vectors in the adhesive layer for 25 mm overlap hard steel AV 119 SLJs - 1.6 mm thick adherends under 4 point bend loading

25 mm overlap - hard steel - 2 mm thick adherends - AV 119 - 4pt bend test - 1.61 kN load

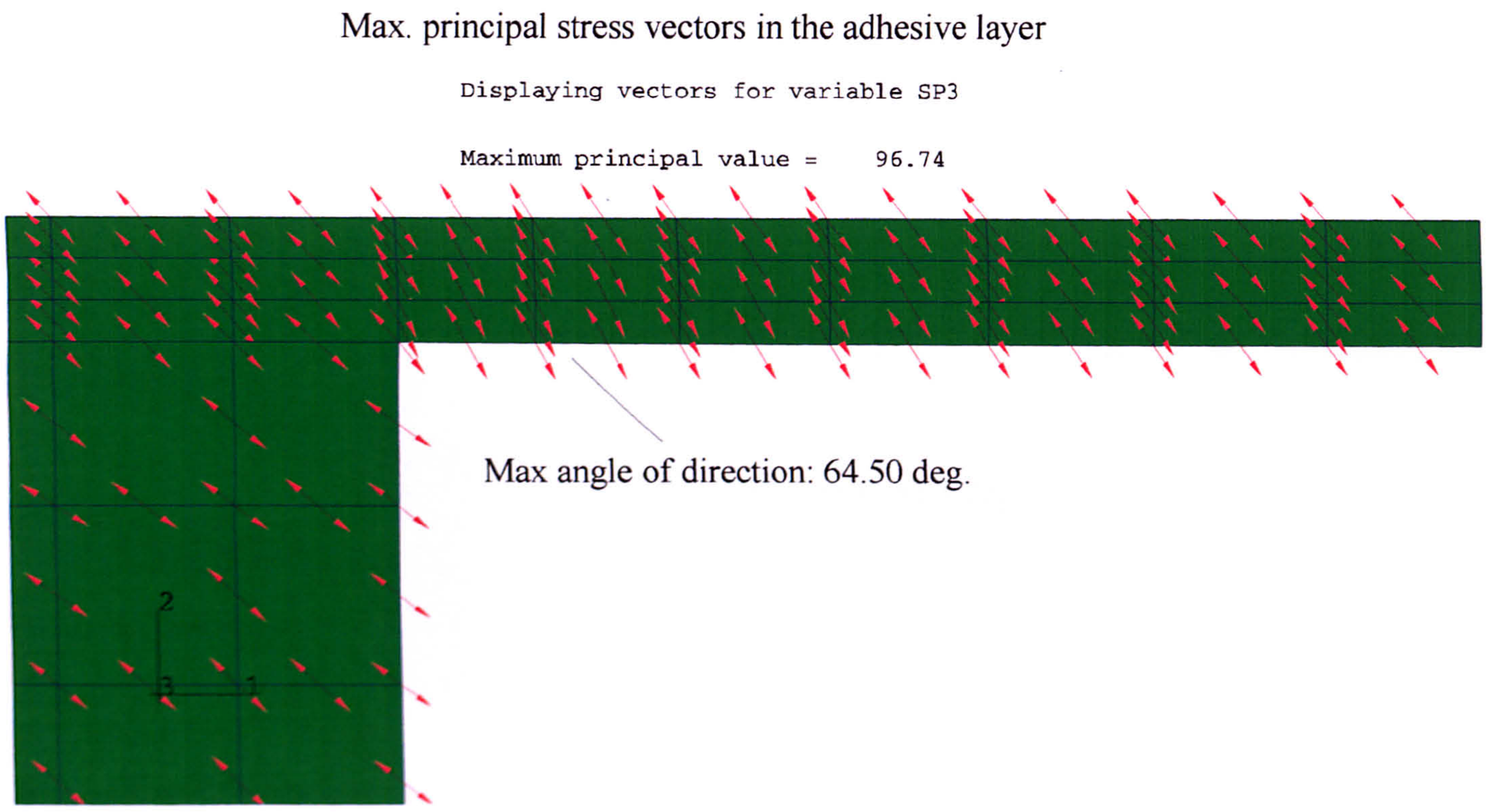

Figure 7.75 Maximum principal stress vectors in the adhesive layer for 25 mm overlap hard steel AV 119 SLJs - 2 mm thick adherends under 4 point bend loading

25 mm overlap - hard steel - 3mm thick adherends - AV 119 - 4pt bend test - 2.76kN load

Max. principal stress vectors in the adhesive layers

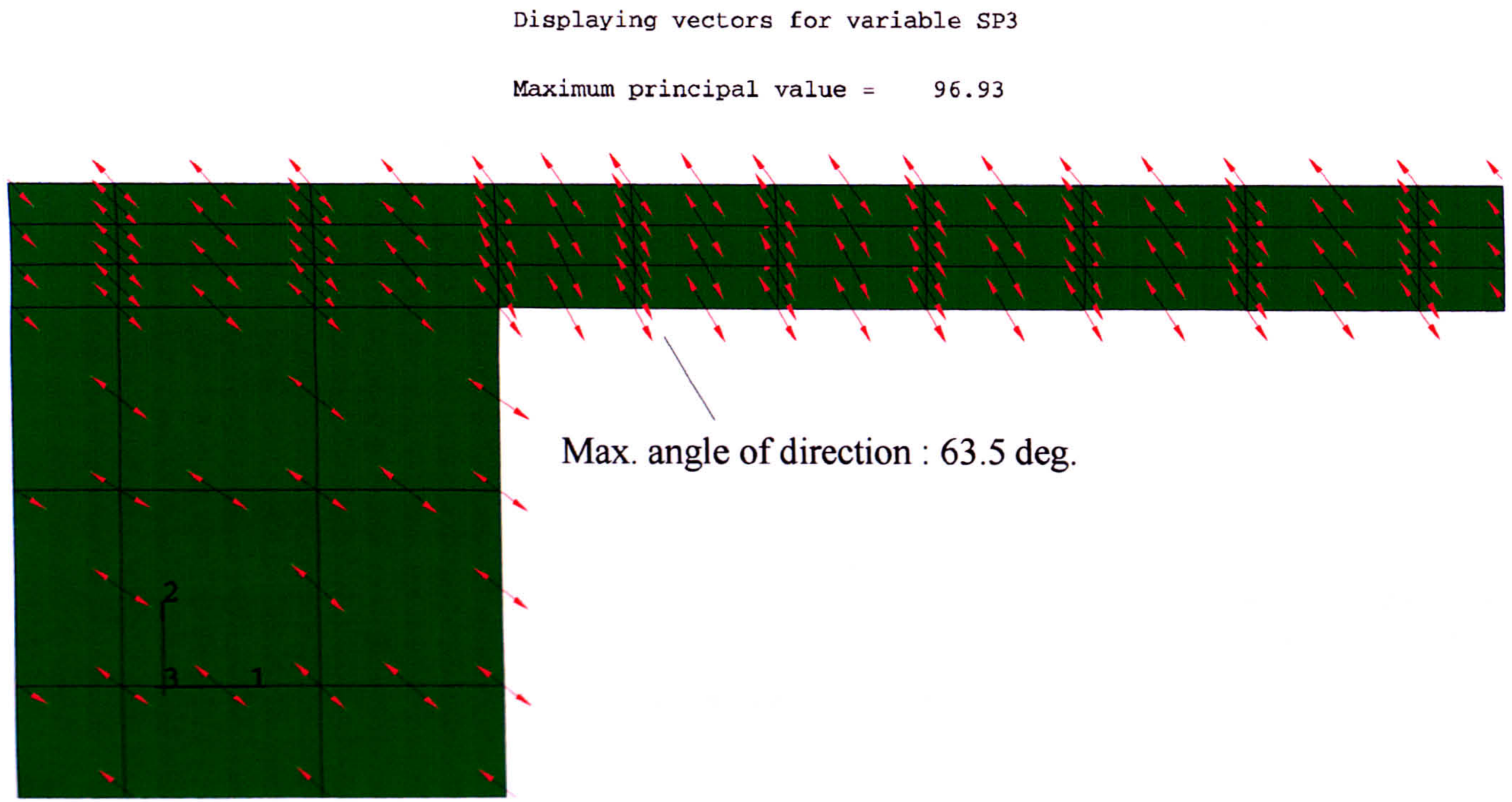

Figure 7.76 Maximum principal stress vectors in the adhesive layer for 25 mm overlap hard steel AV 119 SLJs - 3 mm thick adherends under 4 point bend loading

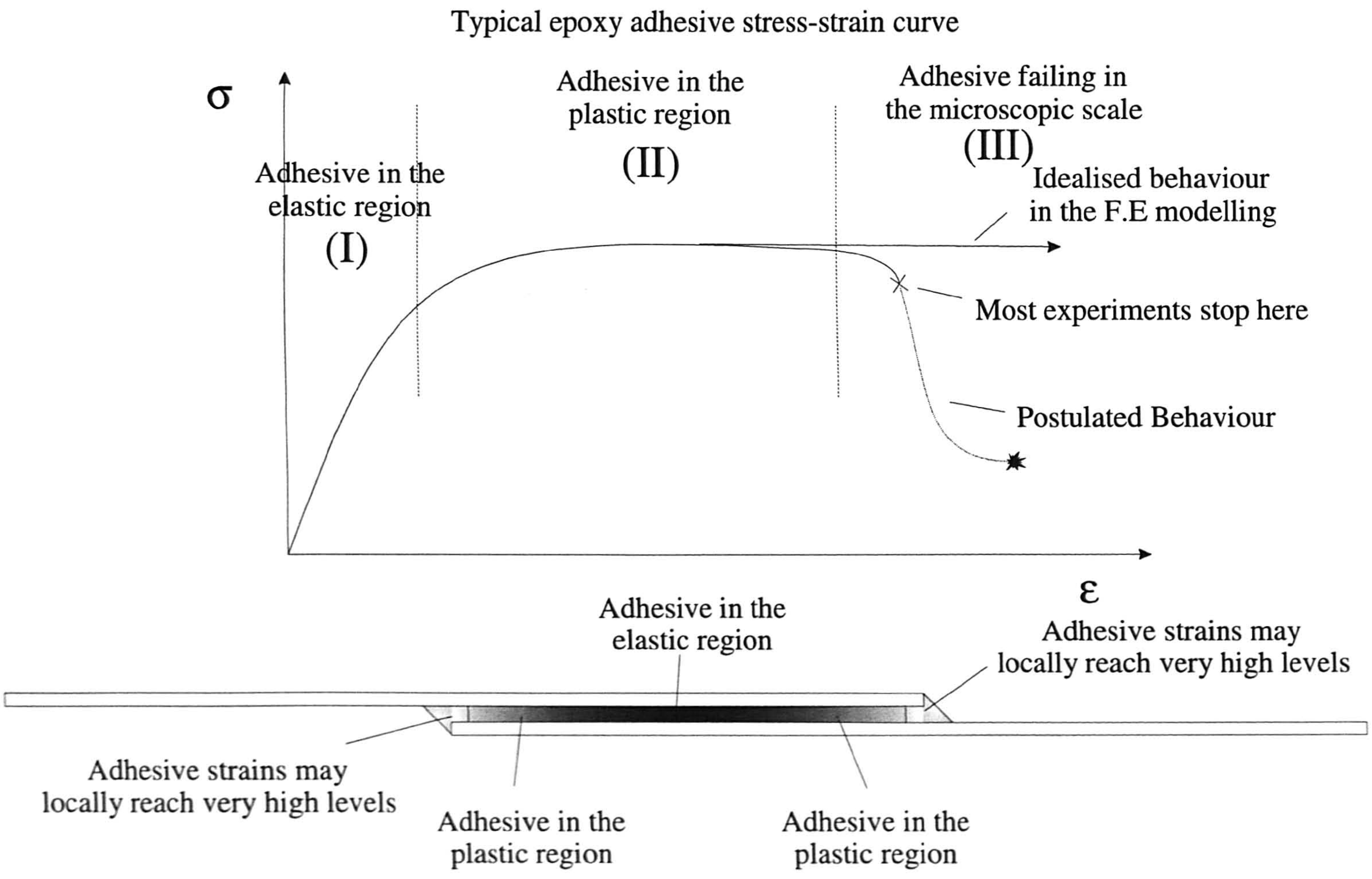

Figure 8.1 Typical behaviour of a structural adhesive in a SLJ along the overlap

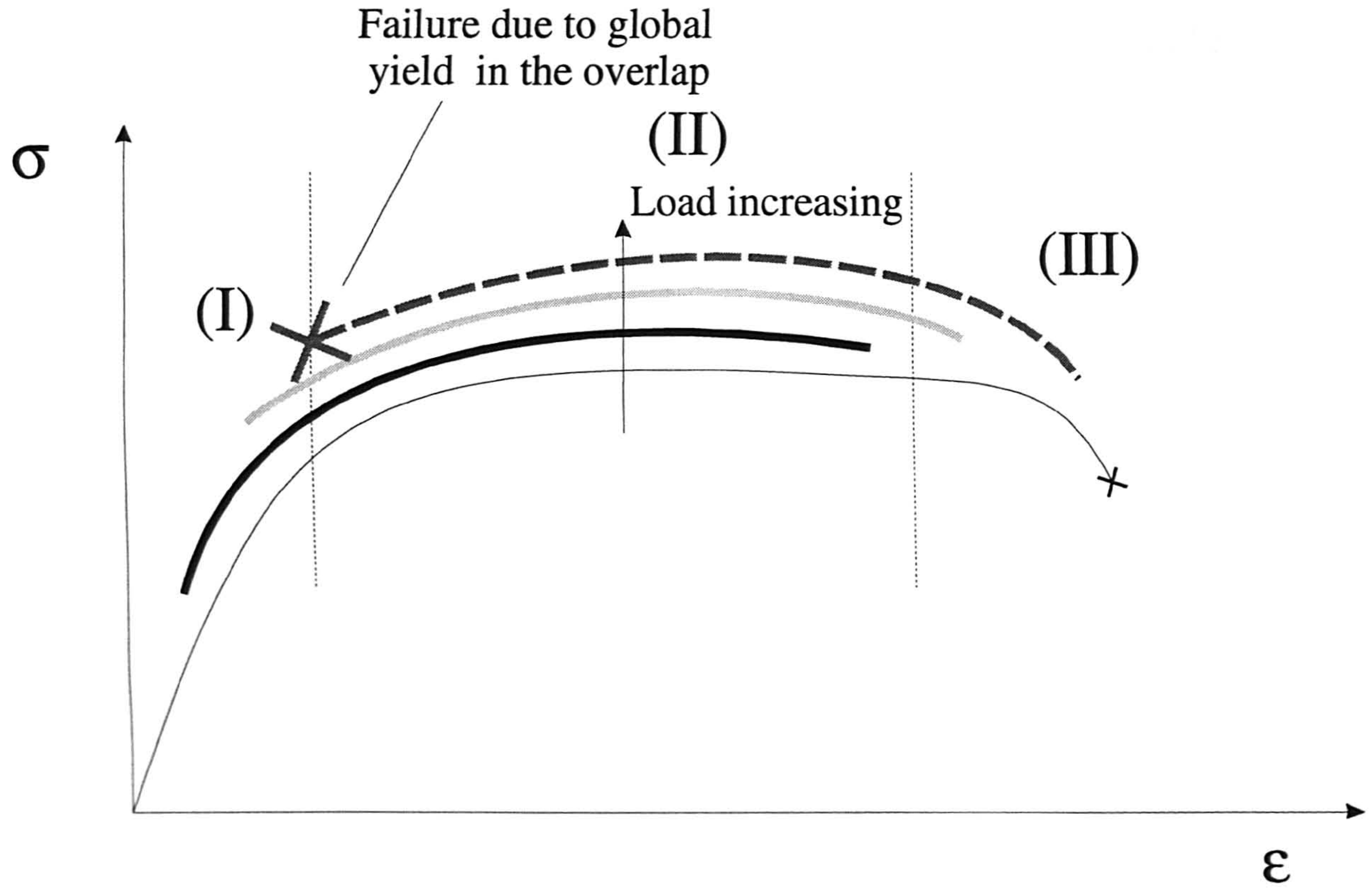

Failure load - failure due to global damage

High applied load - variable damage throughout the adhesive layer - all regions (I), (II)

Medium applied load - some of the adhesive in the elastic region (I) and some in the plastic region

Figure 8.2 Definition of damage is due to global failure in the adhesive layer

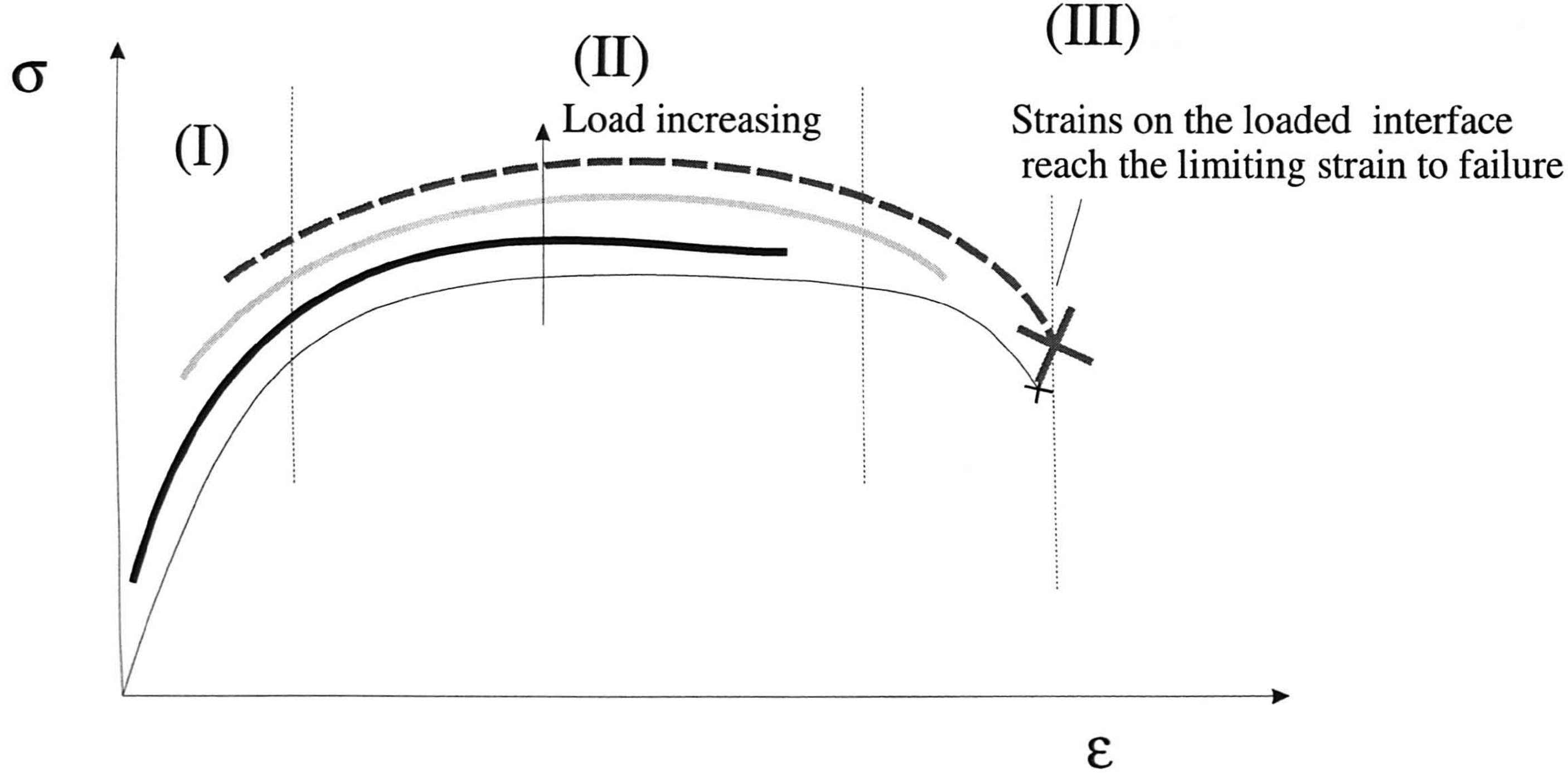

Failure load - failure due to local high strains

High applied load - variable damage throughout the adhesive layer - all regions (I), (II)

Medium applied load - some of the adhesive in the elastic region (I) and some in the plastic region

Figure 8.3 Definition of damage is due to local strains exceeding the limiting strain to failure

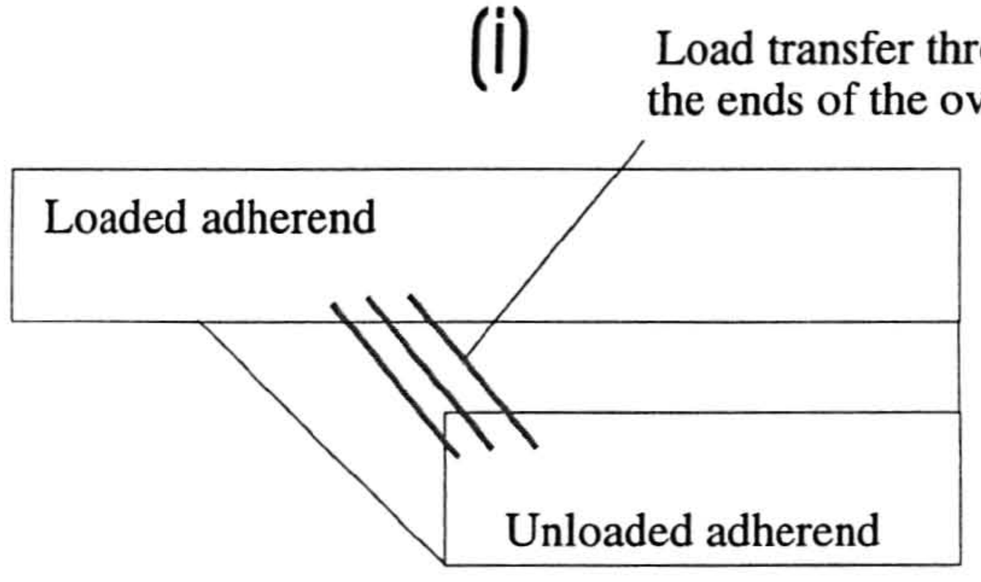

Low applied load, no damage in the adhesive

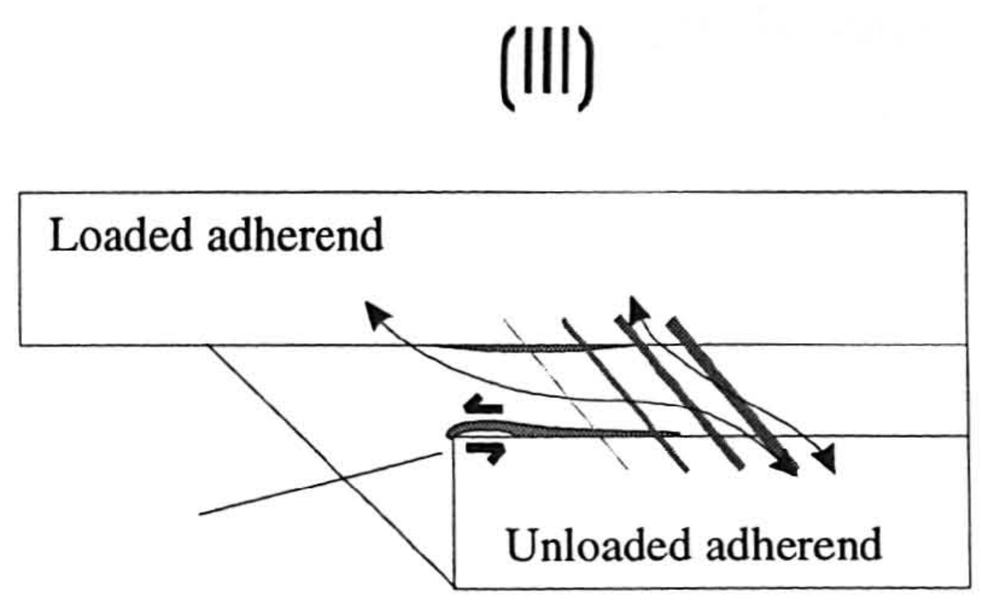

High applied load
Strains in the unloaded interface corner
exceeding adhesive critical limits (stress whitening, micro-voiding)
Strains in the loaded interface reaching critical levels

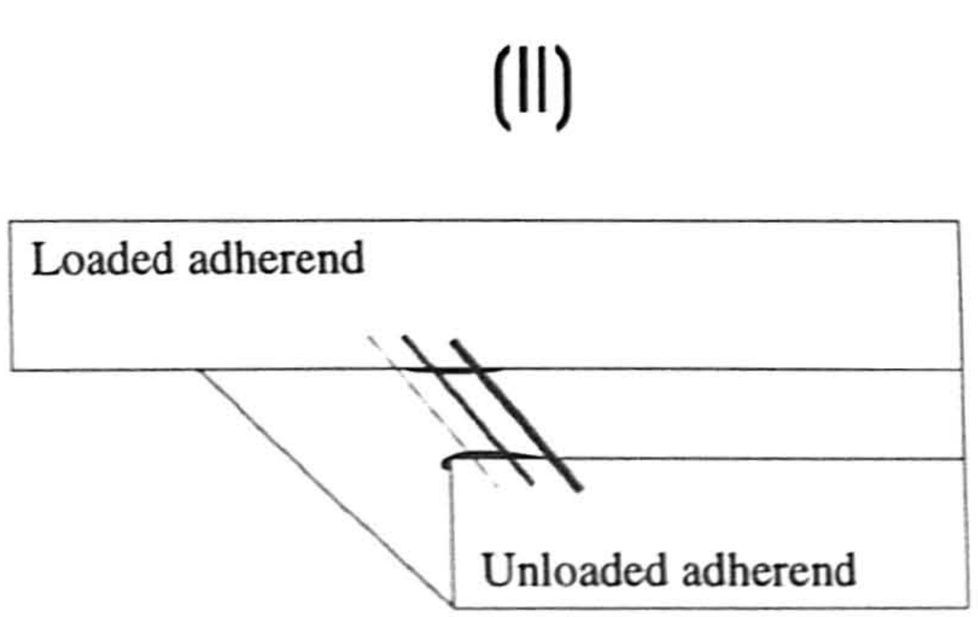

Medium applied load, some plasticity in the in the adhesive
especially around the unloaded interface corner

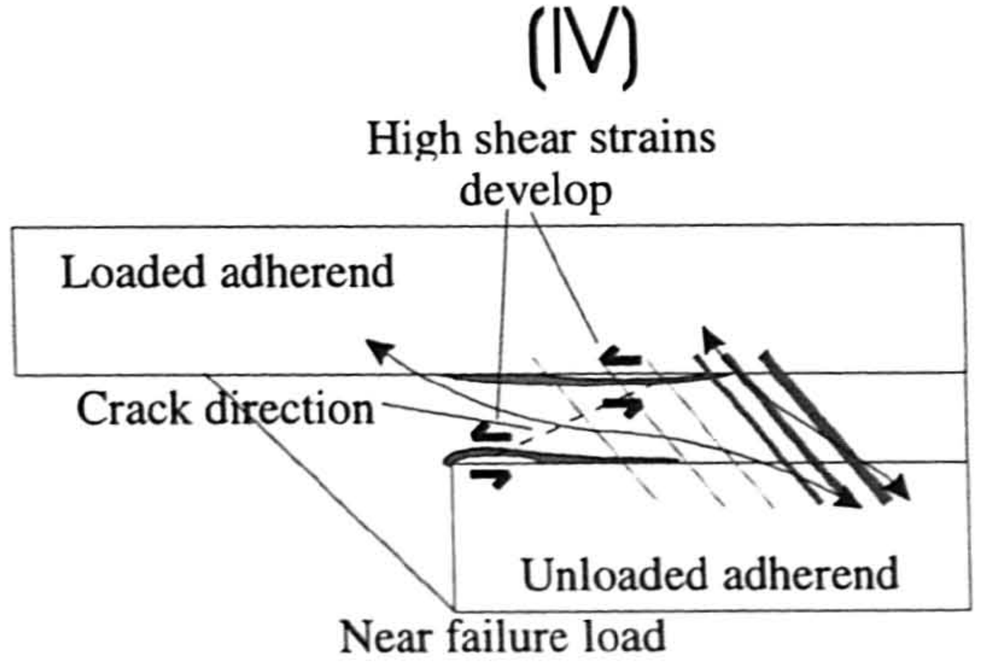

Near failure load
Strains in both interfaces exceeding adhesive critical limits
Immediate failure occurs

Figure 8.4 Illustration of load transfer around the overlap edges as the damage in the adhesive increases

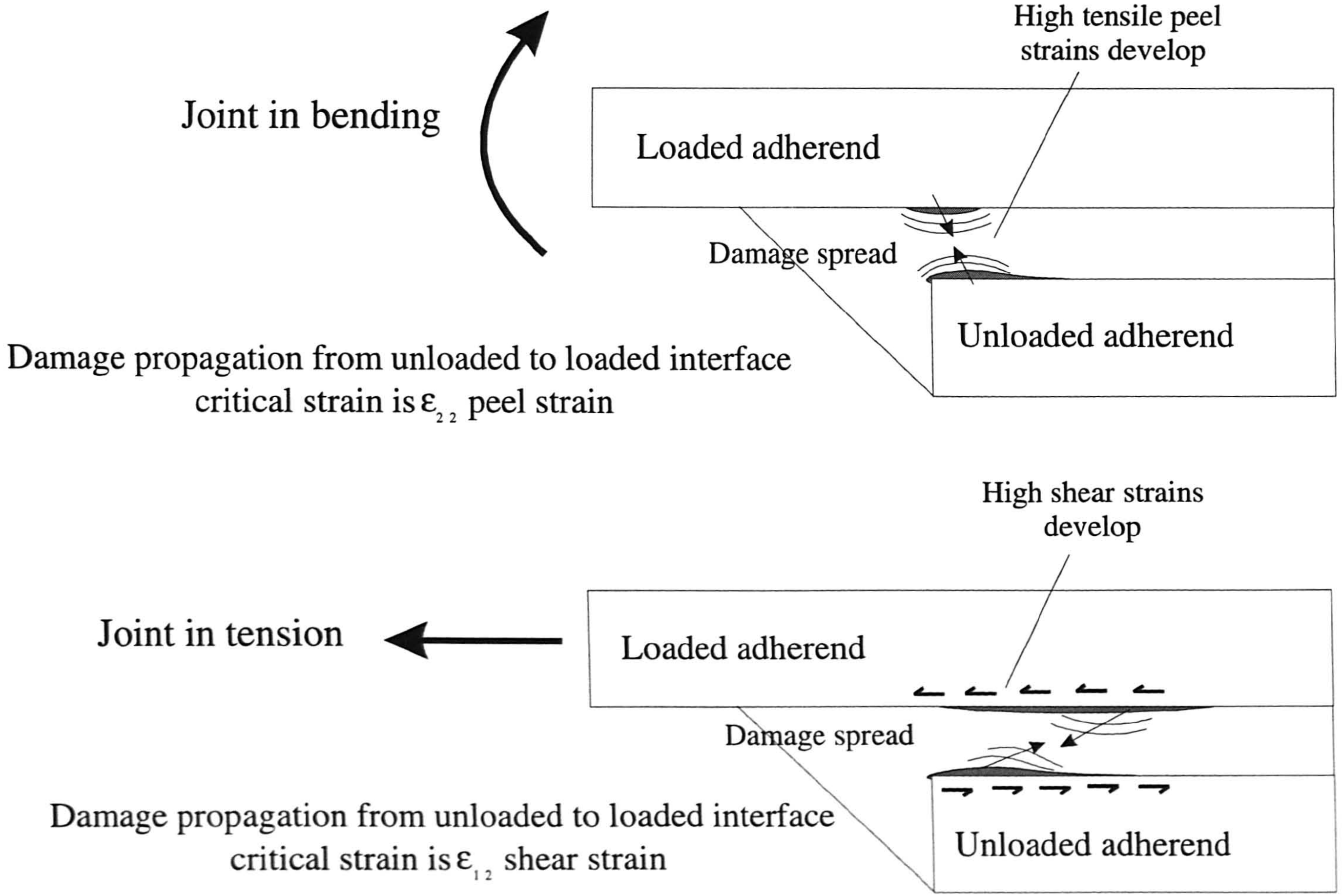

Figure 8.5 Illustration of damage propagation near the overlap ends for the case of a SLJ loaded in bending or tension

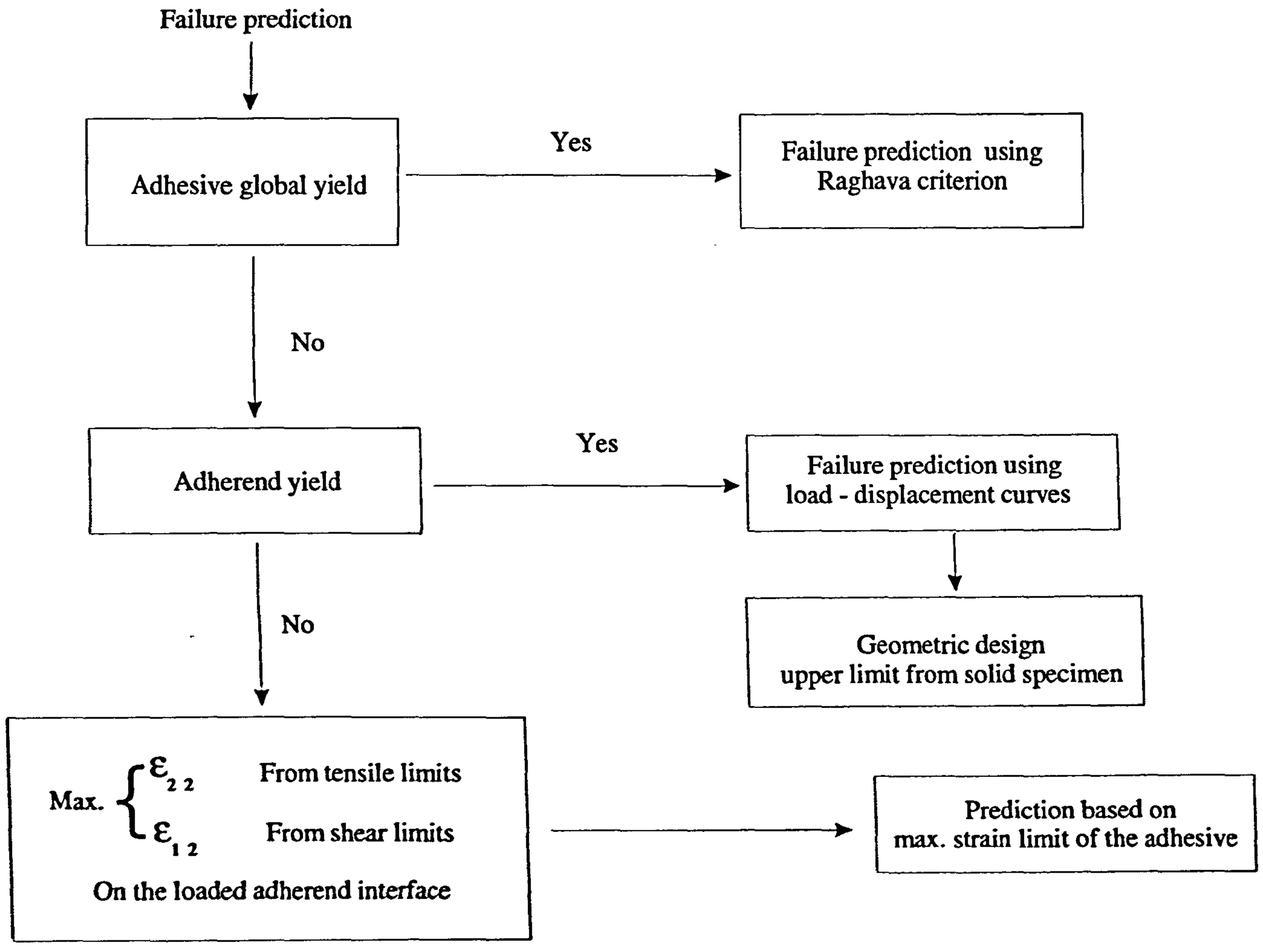

Figure 8.6 Failure Prediction Flow chart for bonded Joints

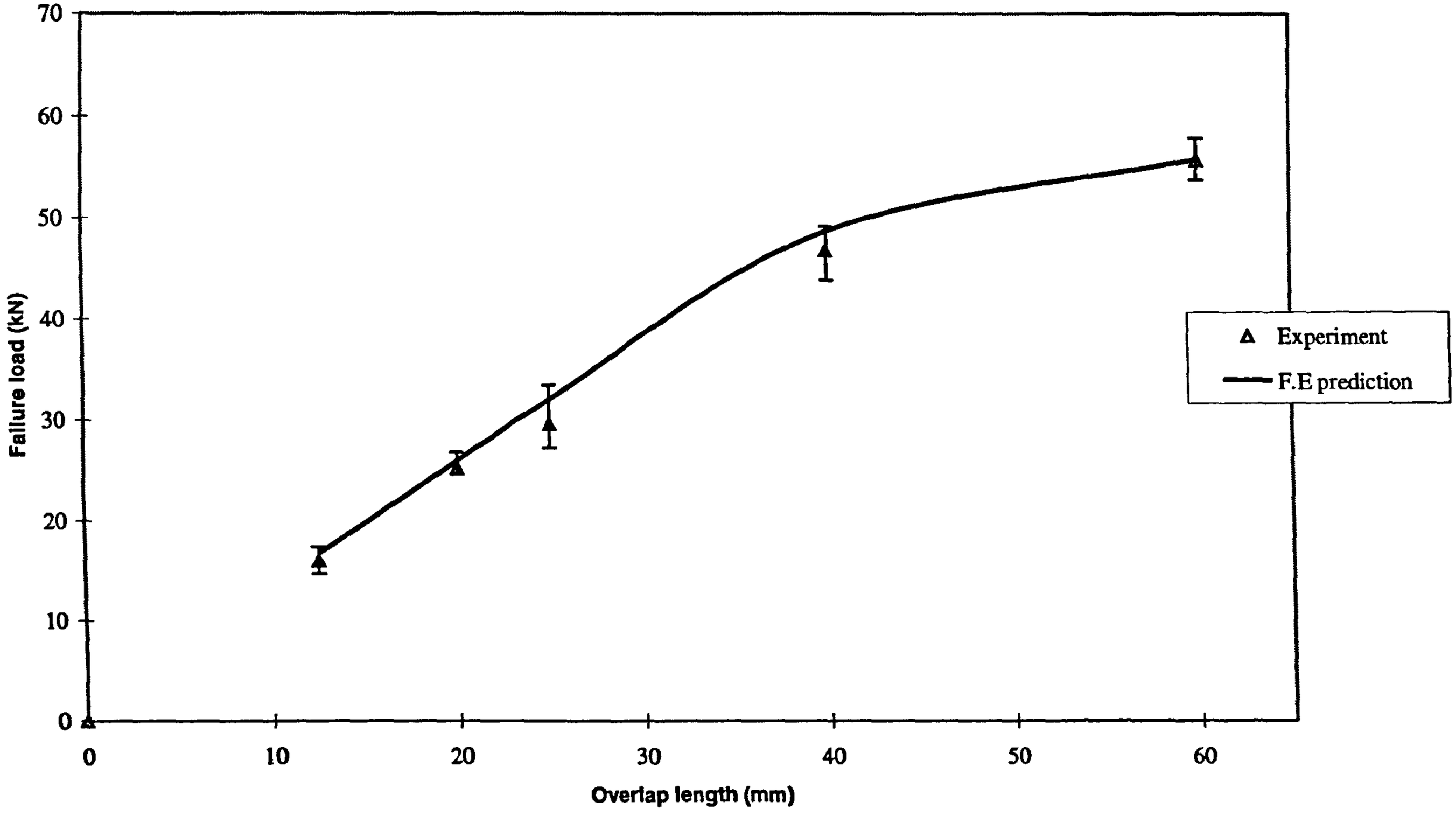

Figure 8.7 Experimental - F.E strength prediction correlation for hard steel SLJs with EC 3448 adhesive and various overlap lengths under tensile loading

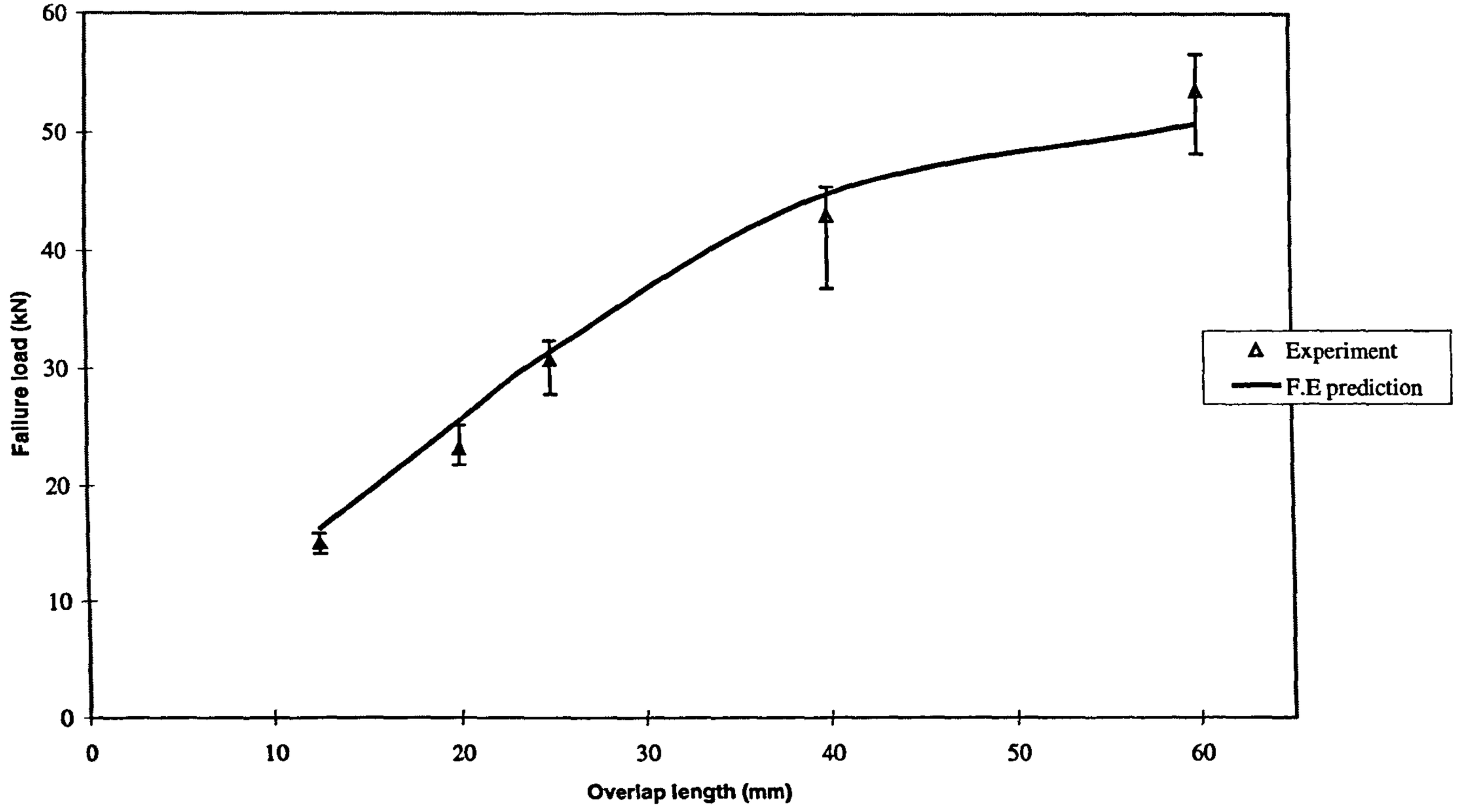

Figure 8.8 Experimental - F.E strength prediction correlation for hard steel SLJs with AV 119 adhesive and various overlap lengths under tensile loading

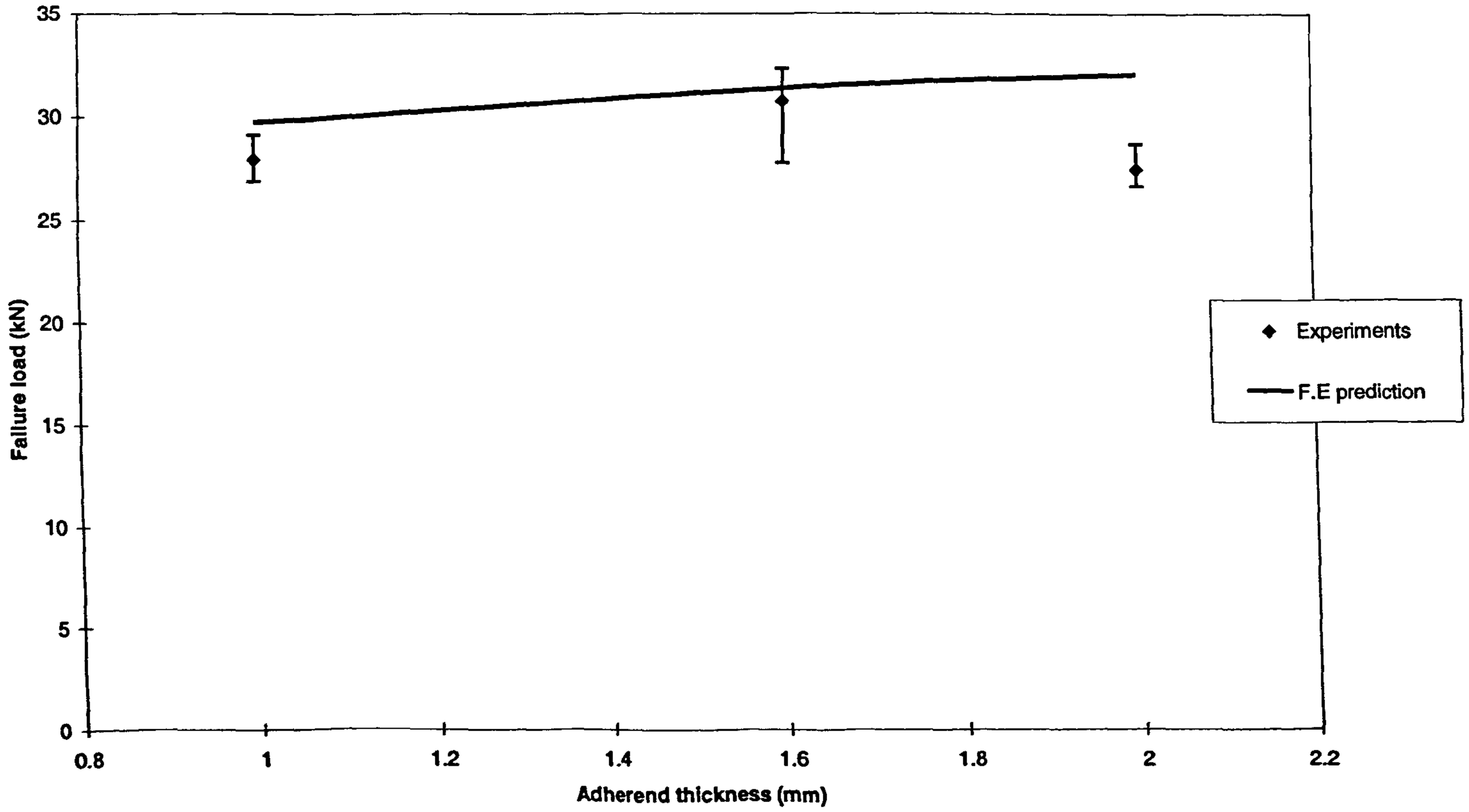

Figure 8.9 Experimental - F.E strength prediction correlation for 25mm overlap hard steel SLJs with AV 119 adhesive and various adherend thicknesses under tensile loading

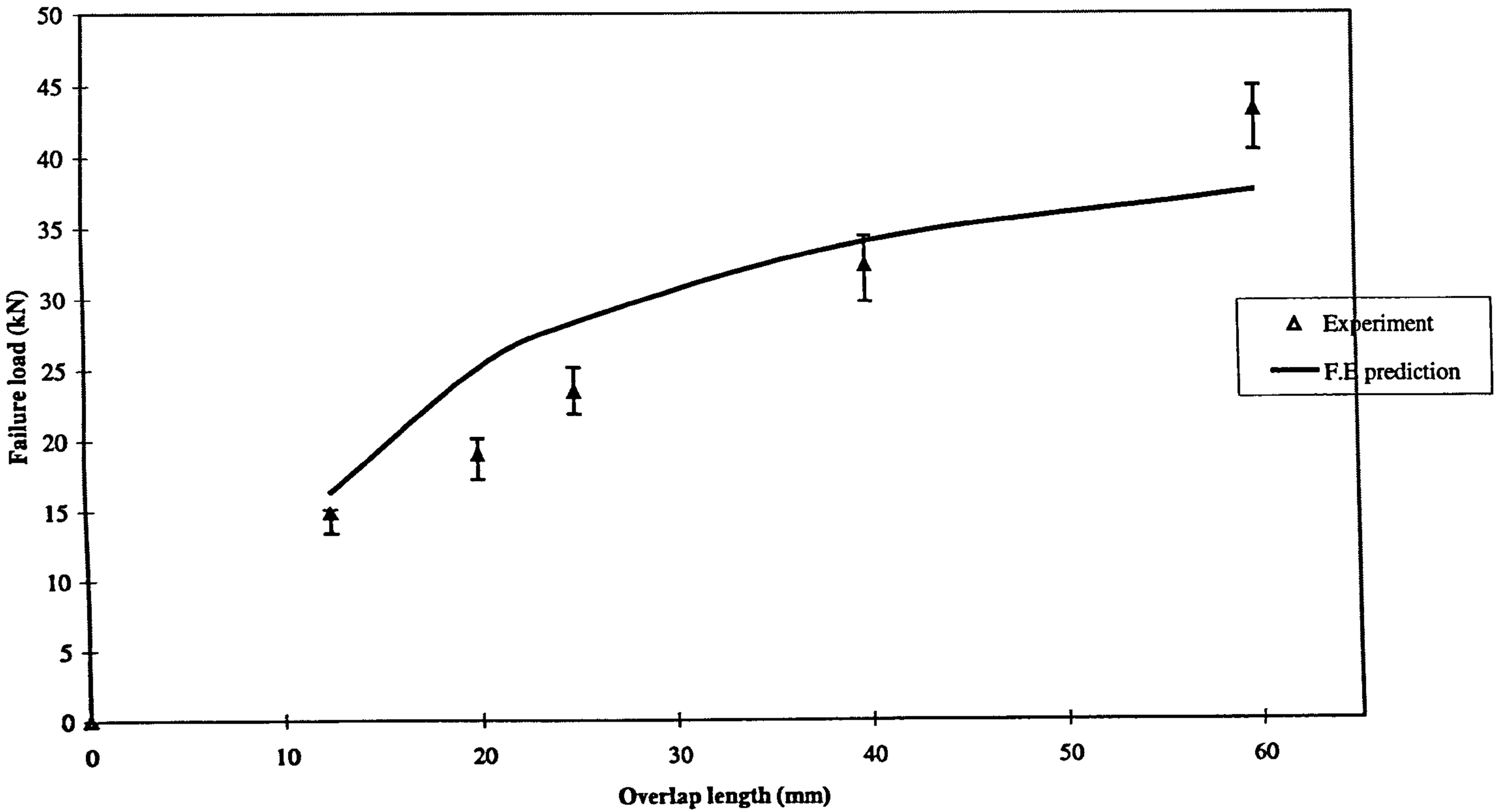

Figure 8.10 Experimental - F.E strength prediction correlation for hard steel SLJs with ESP 110 adhesive and various overlap lengths under tensile loading

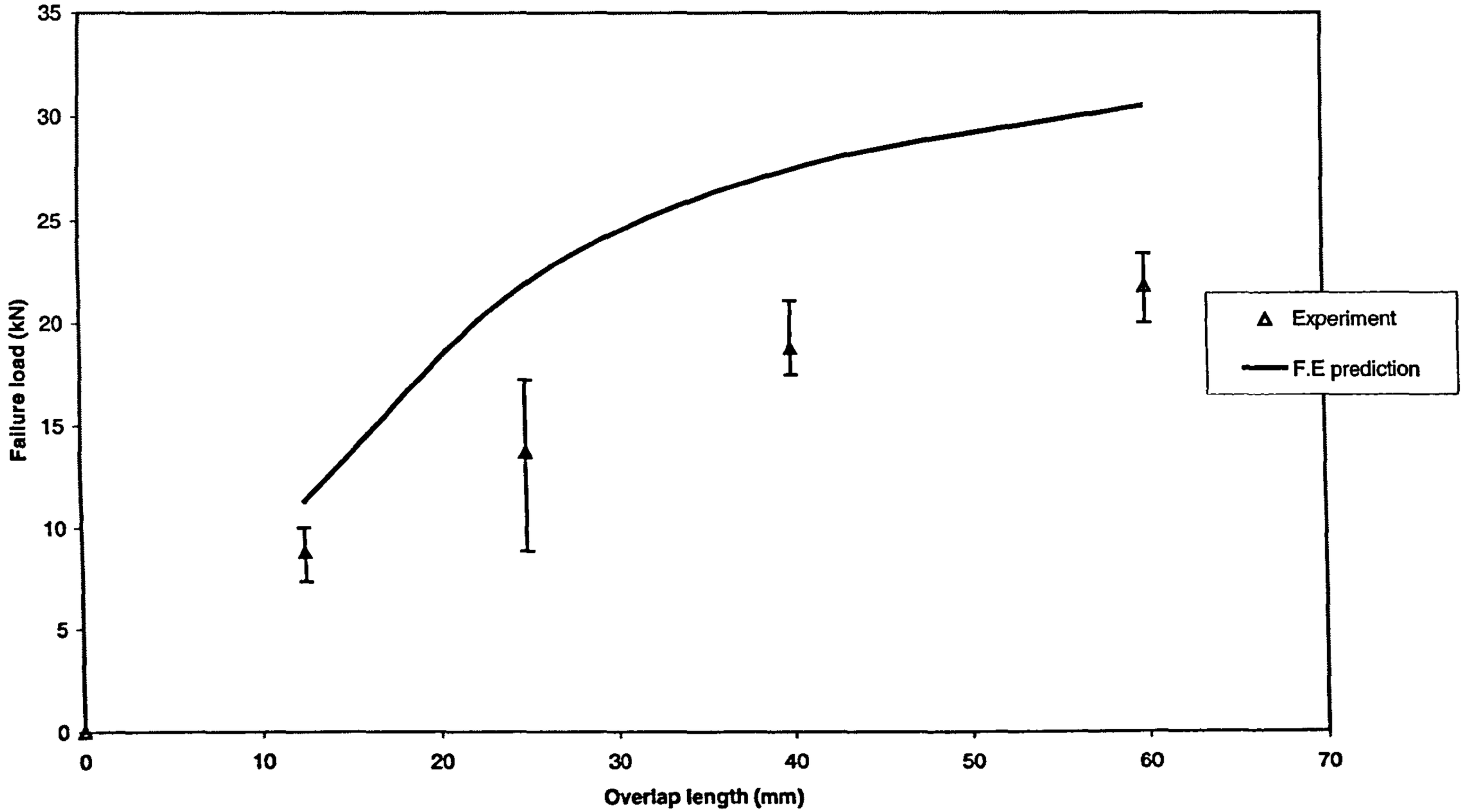

Figure 8.11 Experimental - F.E strength prediction correlation for hard steel SLJs with MY753 adhesive and various overlap lengths under tensile loading

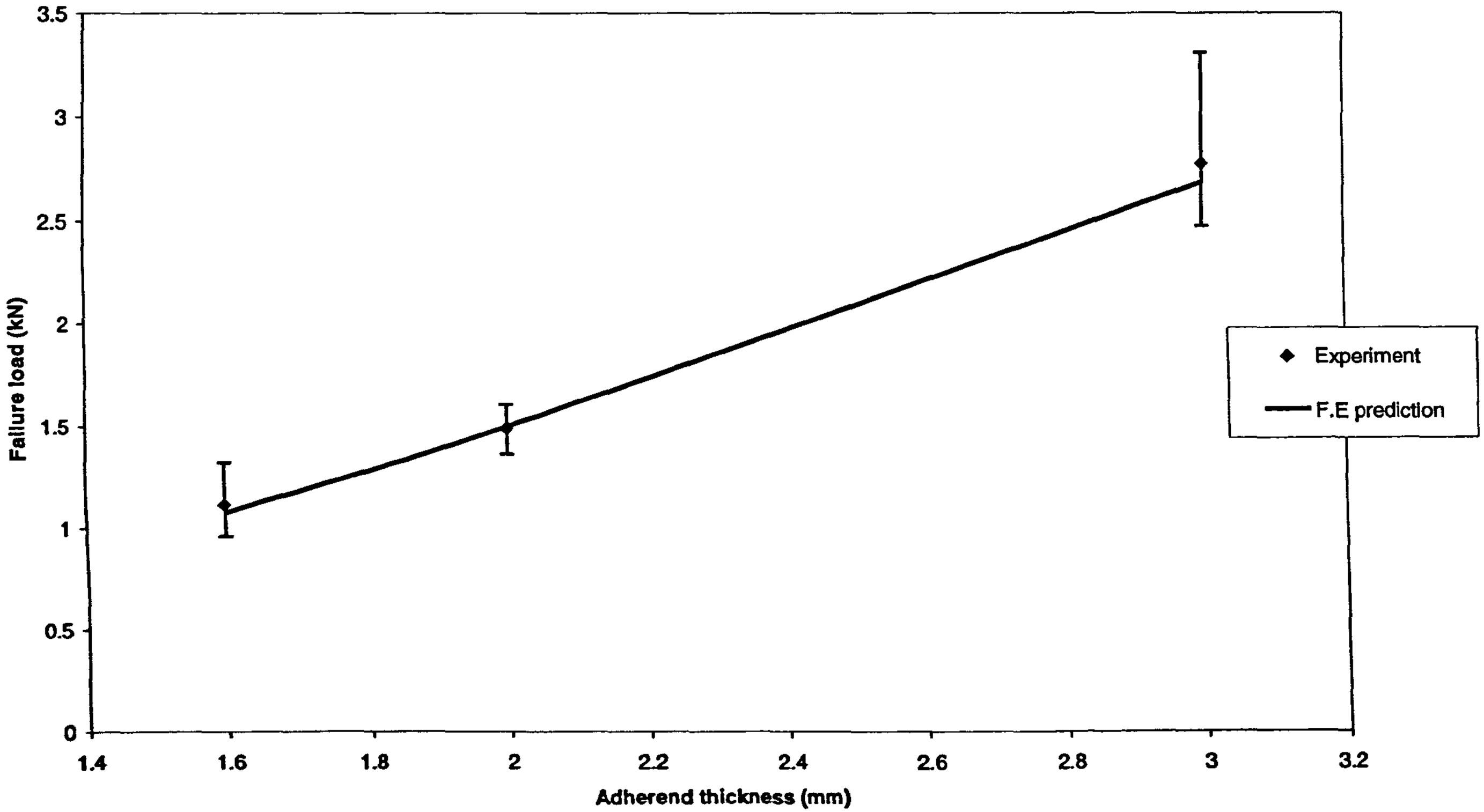

Figure 8.12 Experimental - F.E strength prediction correlation for 25mm overlap hard steel SLJs with AV 119 adhesive and various adherend thicknesses under 4 point bend loading

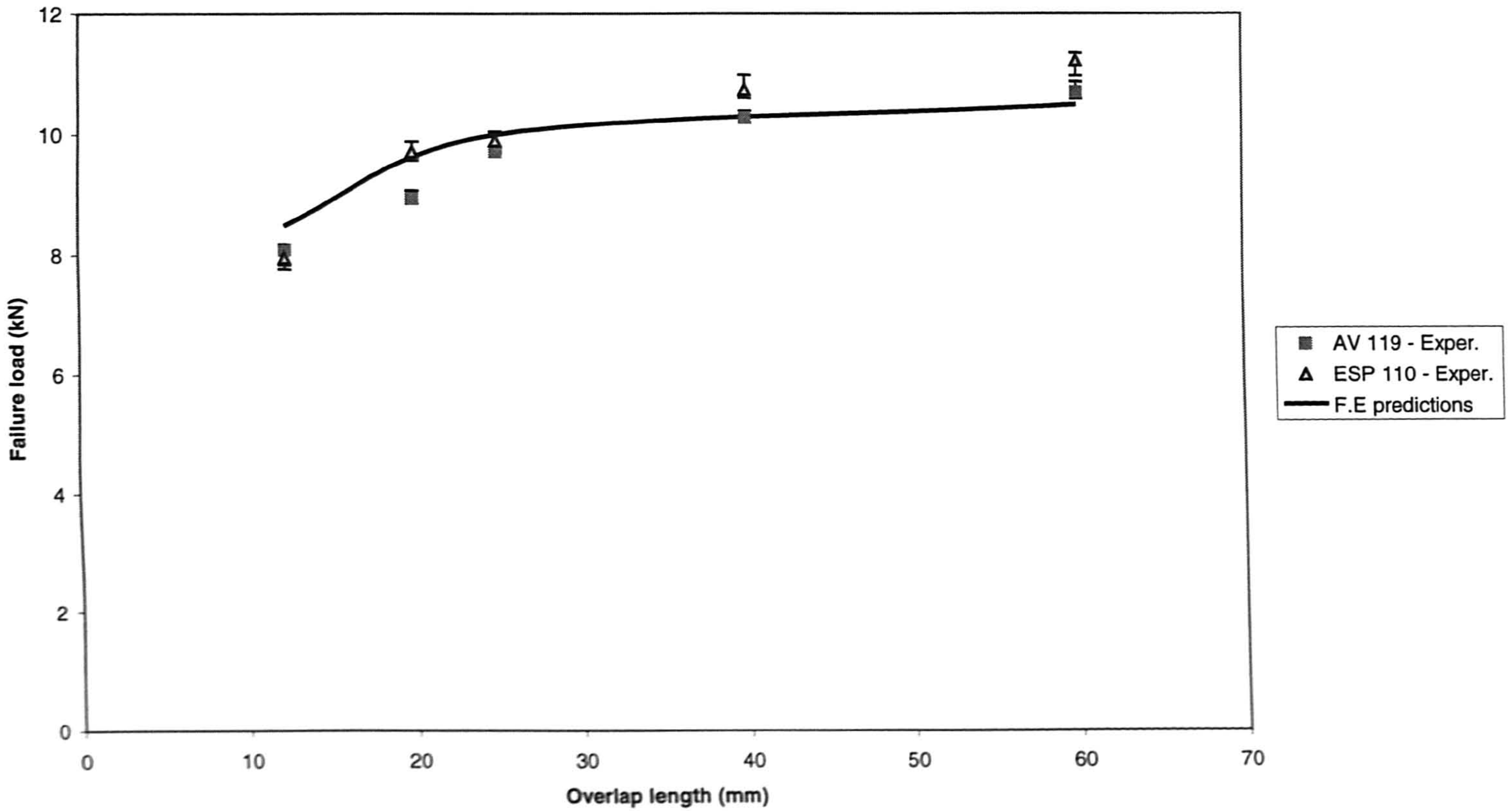

Figure 8.13 Experimental - F.E strength prediction correlation for mild steel SLJs with various adhesives and various overlap lengths under tensile loading

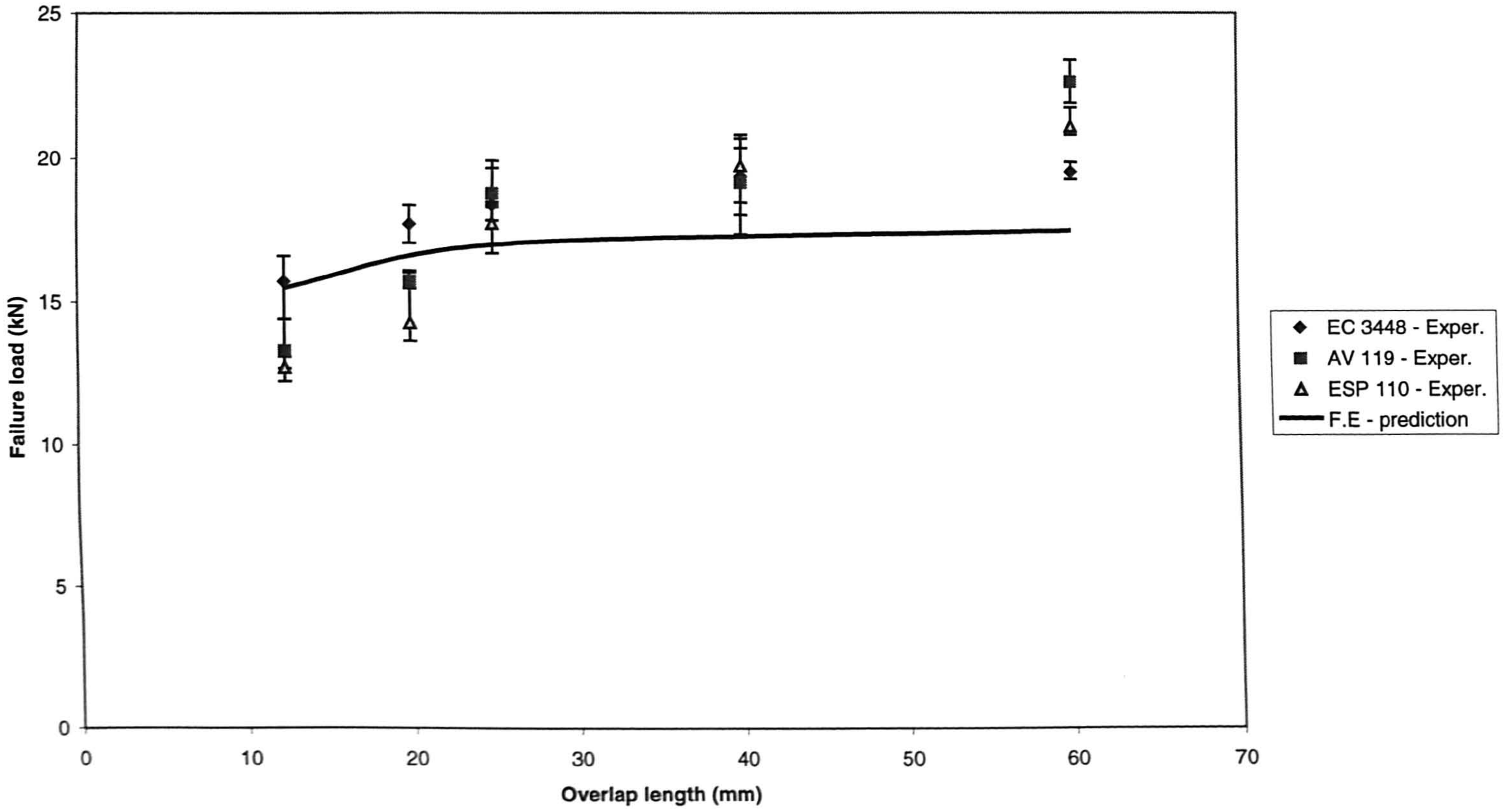

Figure 8.14 Experimental - F.E strength prediction correlation for gauge steel SLJs with various adhesives and various overlap lengths under tensile loading

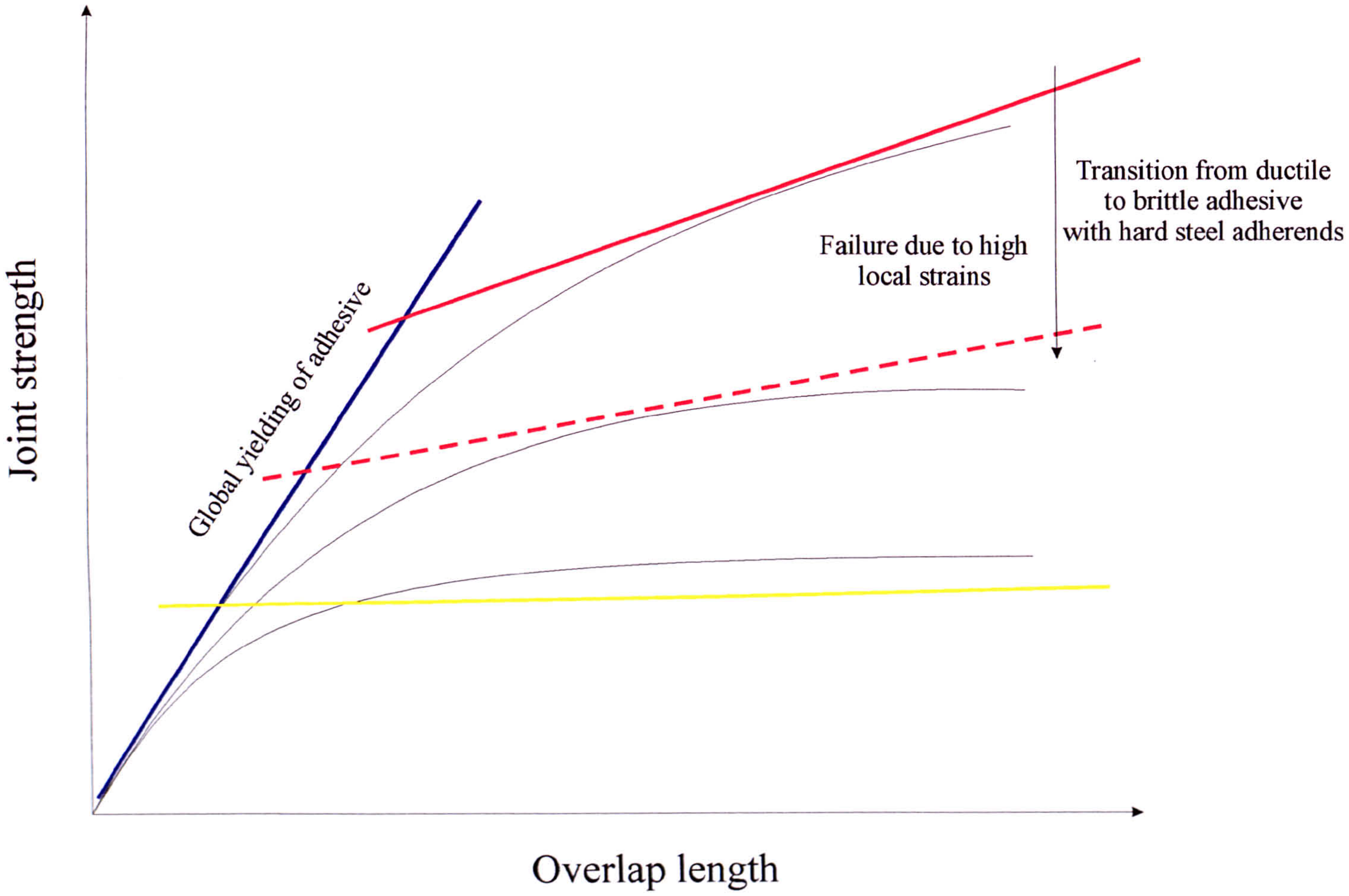

Figure 8.15 Design chart for strength prediction of bonded SLJs under tensile loading